



UNIVERSIDADE D  
COIMBRA

Carolina dos Santos Vertis

**IDENTIFICAÇÃO E MODELAÇÃO DE REDES DE  
REAÇÕES QUÍMICAS**

**Tese no âmbito do Doutoramento em Engenharia Química  
orientada pelo Professor Doutor Nuno Manuel Clemente de Oliveira e pelo  
Professor Doutor Fernando Pedro Martins Bernardo e apresentada ao  
Departamento de Engenharia Química da Faculdade de Ciências e Tecnologia  
da Universidade de Coimbra.**

Dezembro de 2021



Carolina dos Santos Vertis

# Identification and modeling of chemical reaction networks

A systematic methodology

Doctoral Thesis in Chemical Engineering  
presented to the Department of Chemical Engineering of the  
Faculty of Sciences and Technology of the University of Coimbra

**Supervisors:**

Professor Doctor Nuno Manuel Clemente de Oliveira  
and  
Professor Doctor Fernando Pedro Martins Bernardo

**Institution:**

Department of Chemical Engineering  
Faculty of Science and Technology of the University of Coimbra



UNIVERSIDADE D  
COIMBRA

December 2021



# Acknowledgments

Thanks to my supervisors, Prof. Nuno Oliveira and Prof. Fernando Bernardo.

Thanks to my friend Ricardo Rendall.

Financial support from CNPq — Conselho Nacional de Desenvolvimento Científico e Tecnológico, Brasil (scholarship 203592/2014-0) and PRODEQ — Associação Para o Desenvolvimento da Engenharia Química, Portugal, are gratefully acknowledged.

Now, last, but not least,

Thanks to my partner Fernando Ferreira.

To my family, with love...

*“Tu dás-me não apenas objetivo e direção,  
mas também tanta felicidade,  
que nunca poderia sentir-me insatisfeita com o  
presente infortunado que vivo nesse momento:  
tu dás-me esperança e a certeza do sucesso.”*

– Sigmund Schlomo Freud (1856-1939)



# Abstract

Kinetic models provide fundamental information about chemical systems, playing a fundamental role in the development of chemical products, and in the diagnosis and optimization of their respective processes. Despite their central role in Chemical Engineering, these models are sometimes derived based on a postulated set of reactions that supposedly explain observed transformations. One or more mechanistic models are usually suggested. However, the procedures adopted in this task can be based on heuristic aspects and qualitative analysis of the experimental data, producing results that might not be completely satisfactory (and questionable) from the points of view of the structural correctness (reaction network and corresponding kinetic expressions) and the precise/accurate description of the systems analyzed.

A systematic methodology is proposed in this thesis for the identification of mathematical models that describe the kinetics of chemical reactions from chemical species concentration data collected in batch experiments. The methodology contemplates 7 steps in which the construction of the model is carried out sequentially, allowing for greater certainty and precision about the identified model. The proposed methodology steps are: (i) experimental data treatment incorporating time-invariant relationships for continuous approximation of discrete data and accurate computation of species fluxes, (ii) data dimension analysis for determining model dimension and thorough understanding of the reaction system topology, (iii) determination of the reaction network superstructure incorporating time-invariant and energetic constraints, and factor analysis for structural model identification, (iv) enumeration of reaction networks using discrete optimization, (v) selection/identification of the network structure using experimental data, (vi) systematic kinetic modeling of the several reaction steps, and (vii) proposal of additional experiment tests based on the model information.

Through the incremental model development, the identification of the model structure is performed in an uncoupled manner, first elucidating the structure of the reaction network, and then the structures of the reaction kinetic expressions. Both structure identifications are supported by the differential method, in which linear optimization formulations are used to evaluate the rate of species concentration changes and reaction extents, ensuring the achievement of global optimal solutions. In the first case, from a superstructure of reaction networks, *all connections between species are explored*, guaranteeing that the

best reaction network (composed of an independent set of chemical reactions), describing observed changes in the composition of several species, is found. Regarding chemical reaction kinetics, the identification of the kinetic expressions is performed individually for each reaction step. From a superstructure of reaction kinetic expressions built based on first-principles laws and qualitative analysis of the computed reaction rate profiles, the reaction kinetic expression is identified taking into account the best compromise between fit to experimental data quality and model complexity, according to the Bayesian information criterion. Once the structural parts of the model have been identified, the nonlinear final adjustment of model parameters, supported by the integral method, is performed at the end of the methodology using nonlinear optimization, with the advantage of having as initial values for the parameters the ones obtained in the previous step of the methodology (based on the differential method). Thus, in the final phase, the optimal model parameters are obtained according to the maximum likelihood sense, in a simultaneous, bias-free, nonlinear regression procedure. The success of the model structure identification is dependent on good estimates of species fluxes and, consequently, reaction fluxes. For this, a robust data pre-processing method is proposed that incorporates time-invariant relationships as inter-profile constraints, increasing the data accuracy and leading to good fluxes estimates. However, when parts of the model are not satisfactorily identified, additional experimental tests are proposed to elucidate the complete structure of the reaction system under analysis.

The development of the proposed methodology is illustrated with the application to four case studies from the literature: the thermal isomerization of  $\alpha$ -pinene, the catalytic hydrogenation of succinic acid and maleic acid (two separated case studies), and the pharmaceutical case study from Pfizer company. On the basis of the results obtained, it can be concluded that: (i) a systematic model development is required for obtaining models with great confidence that are highly process descriptive and of lower complexity (simpler models) when compared to literature model proposals, (ii) experimental data with high uncertainty may compromise the complete identification of the model structure, requiring additional experiments for allowing a better description of the network structure, (iii) the use of energetic criteria to restrict the network superstructure enables a significant reduction in the number of generated networks, saving time and computational effort in the network synthesis step, (iv) the use of precedence constraints is required for generating consistently connected nonlinear reaction networks, (v) systematic methods for reaction kinetic modeling are essential for accurate model identification, avoiding excessive parameterization and obtaining narrow parameter confidence intervals, (vi) the use of time-invariant relationships in the data reconciliation procedure reduces the noise-to-signal ratio, and consequently increases model identifiability, and (vii) the incorporation of experimental data in the network generation phase to identify plausible structures reduce the number of alternative model candidates to be further analyzed, but at the cost of losing the incremental development of the model.

The main contributions of this thesis are: (i) a novel method of data reconciliation, where



data approximation is achieved with great accuracy by the incorporation of time-invariant relationships, (ii) mixed-integer linear programming formulations conceived to generate connected linear and nonlinear reaction networks (using precedence constraints), which can be applied to any process synthesis problem described by graphs, (iii) a systematic method for individual reaction kinetic modeling that follows a superstructure-based strategy, enabling the obtainment of parsimonious models, (iv) a methodology for validation of reaction invariants and determination of the data invariant space dimension, and (v) a method for building superstructures of reaction networks considering reaction invariant relationships, energetic criteria, and the checking the consistency of the model with the experimental data. In summary, the proposed methodology is able to identify robust models taking full advantage of experimental data and various optimization techniques. The obtained model increases process knowledge and facilitates process design, scale-up, monitoring, control, and optimization, which, naturally, may be used for improving safety, quality, productivity, and revenues of industrial processes.

**Keywords:** reaction networks, kinetic modeling, chemical reaction, network synthesis, experimental data treatment.



# Resumo

Os modelos cinéticos fornecem informações fundamentais sobre os sistemas químicos, desempenhando um papel essencial no desenvolvimento de produtos químicos, bem como no diagnóstico e otimização dos respectivos processos. Apesar de seu papel central na Engenharia Química, esses modelos às vezes são construídos com base num conjunto postulado de reações que supostamente explicam transformações observadas. Normalmente, são sugeridos um ou mais modelos mecanísticos. No entanto, os procedimentos adotados nesta tarefa podem ser baseados em aspectos heurísticos e análise qualitativa dos dados experimentais, produzindo resultados que podem não ser completamente satisfatórios (e questionáveis) do ponto de vista da estrutura do modelo (rede de reações e correspondentes expressões cinéticas) e da descrição precisa/fiável dos sistemas analisados.

Um método sistemático é proposto nesta Tese para a identificação de modelos matemáticos que descrevem a cinética das reações químicas a partir de dados de concentração recolhidos em experiências em regime descontínuo. A metodologia contempla 7 etapas nas quais a construção do modelo é realizada de forma sequencial, permitindo maior certeza e precisão sobre o modelo identificado. As etapas propostas da metodologia são: (i) tratamento de dados experimentais incorporando relações invariantes no tempo para aproximação contínua de dados discretos e computação precisa de fluxos de espécies, (ii) análise de dimensão de dados para determinar a dimensão do modelo e obter uma compreensão completa da topologia do sistema de reação, (iii) determinação da superestrutura da rede de reação incorporando restrições energéticas e invariantes no tempo e análise fatorial para identificação do modelo estrutural, (iv) enumeração de redes de reação usando otimização discreta, (v) seleção/identificação da estrutura da rede usando dados experimentais, (vi) sistemática modelagem da cinética da reação, e (vii) propostas de experimentos adicionais com base nas informações obtidas através do modelo identificado.

Através do desenvolvimento do modelo incremental, a identificação da estrutura do modelo é realizada de forma desacoplada, sendo primeiramente elucidada a estrutura da rede de reação e, a seguir, a estrutura da expressão cinética de cada passo reacional. Ambas as identificações estruturais são suportadas pelo método diferencial, no qual abordagens de otimização linear fazem parte do problema de avaliação de *fluxos de espécies e reações*, assegurando a obtenção de soluções ótimas globais. No primeiro caso, a partir de uma

superestrutura de redes de reação, *todas as conexões entre as espécies são exploradas*, garantindo que a melhor rede de reação (composta por um conjunto linearmente independente de reações químicas), que descreve as mudanças na composição de espécies observadas, seja encontrada. Em relação à cinética da reação química, a identificação das expressões cinéticas é realizada individualmente para cada componente da rede. A partir de uma superestrutura de expressões cinéticas, construída com base em leis de primeiros princípios e análise qualitativa dos perfis de fluxo de reação observados, a expressão cinética é identificada apresentando o melhor compromisso entre qualidade de ajuste aos dados e complexidade do modelo, de acordo com o critério de informação Bayesiano. Uma vez identificadas as partes estruturais do modelo, o ajuste final não linear dos parâmetros do modelo, suportado pelo método integral, é realizado no final da metodologia utilizando otimização não linear, com a vantagem de usar como valores iniciais para os parâmetros aqueles obtidos na etapa anterior da metodologia (com base no método diferencial). O sucesso da identificação da estrutura do modelo depende de boas estimativas dos fluxos de espécies e, conseqüentemente, dos fluxos de reação. Para isso, é proposto um método robusto de aproximação de dados que incorpora relações invariantes no tempo como restrições entre perfis, aumentando a precisão dos dados e levando a boas estimativas de fluxos. No entanto, quando partes do modelo não são identificadas de forma satisfatória, testes experimentais adicionais são propostos para elucidar a estrutura completa do modelo em análise.

O desenvolvimento da metodologia proposta é ilustrado com a aplicação a quatro casos de estudo a partir da literatura: a isomerização térmica de  $\alpha$ -pineno, as hidrogenações catalíticas de ácido succínico e ácido maleico (dois estudos de caso separados) e o estudo de caso farmacêutico da empresa Pfizer. Com base nos resultados obtidos, pode-se concluir que: (i) é necessário o sistemático desenvolvimento de um modelo para a obtenção de modelos com grande confiança, altamente descritivos do processo e de menor complexidade (modelos mais simples) quando comparados às propostas de modelos da literatura, (ii) dados experimentais com elevada incerteza podem comprometer a identificação completa da estrutura do modelo, exigindo experimentos adicionais para permitir uma melhor descrição da estrutura da rede, (iii) o uso de critérios energéticos para restringir a superestrutura da rede possibilita uma redução significativa do número de redes geradas, economizando tempo e esforço computacional na etapa de síntese da rede, (iv) o uso de restrições de precedência é necessário para gerar redes de reação não lineares que apresentam uma estrutura conexa consistente, (v) métodos sistemáticos para modelagem da cinética de reação são fundamentais para a identificação precisa do modelo, por forma a evitar a parametrização excessiva e a obter intervalos de confiança estreitos de parâmetros do modelo, (vi) o uso de relações invariantes no tempo no procedimento de reconciliação de dados reduz o rácio ruído-sinal e, conseqüentemente, aumenta a identificabilidade do modelo, e (vii) a incorporação de dados experimentais na fase de geração da rede para identificar estruturas plausíveis reduz o número de candidatos a modelos alternativos a serem analisados posteriormente, mas ao custo de perder o desenvolvimento incremental

do modelo.

As principais contribuições desta tese são: (i) um novo método de reconciliação de dados, onde a aproximação de dados é obtida com grande precisão pela incorporação de relações invariantes no tempo, (ii) formulações de programação linear inteira mista concebidas para gerar redes de reação lineares e não lineares (usando restrições de precedência), que podem ser aplicadas a qualquer problema de síntese de processo descrito por grafos, (iii) um método sistemático para modelagem individual da cinética da reação com base numa superestrutura previamente definida, permitindo a obtenção de modelos parcimoniosos, (iv) uma metodologia para validação de invariantes de reação e determinação da dimensão do espaço das invariantes a partir de dados experimentais, e (v) um método para construir superestruturas de redes de reação considerando relações invariantes de reação, critérios energéticos e a verificação da consistência do modelo com os dados experimentais. Em resumo, a metodologia proposta é capaz de identificar modelos robustos aproveitando ao máximo os dados experimentais e várias técnicas de otimização. O modelo obtido aumenta o conhecimento do processo e facilita o projeto, dimensionamento, monitorização, controlo e optimização do processo, o que, naturalmente, pode ser usado para melhorar a segurança, a qualidade, a produtividade e as receitas de processos industriais.

**Palavras-chave:** redes reacionais, modelação cinética, reação química, síntese de redes, tratamento de dados experimentais.



# Contents

<b>Acknowledgments</b>	<b>iii</b>
<b>Abstract</b>	<b>v</b>
<b>Resumo</b>	<b>ix</b>
<b>Table of Contents</b>	<b>xiii</b>
<b>List of Figures</b>	<b>xix</b>
<b>List of Tables</b>	<b>xxiii</b>
<b>Nomenclature</b>	<b>xxv</b>
<b>1 Introduction</b>	<b>1</b>
1.1 Motivation . . . . .	1
1.2 Objectives . . . . .	6
1.3 Thesis contributions . . . . .	10
1.4 Thesis organization . . . . .	15
1.5 Case studies considered . . . . .	17
1.5.1 Thermal isomerization of $\alpha$ -pinene . . . . .	17
1.5.2 Catalytic hydrogenation of succinic acid . . . . .	19
1.5.3 Catalytic hydrogenation of maleic acid . . . . .	20
1.5.4 Pfizer case study . . . . .	21
Bibliography . . . . .	22
<b>2 Theoretical Background &amp; Terminology</b>	<b>27</b>
2.1 Introductory basic concepts . . . . .	28
2.1.1 Graph representation of reaction networks . . . . .	29
2.1.2 Linear and nonlinear reaction networks . . . . .	30
2.1.3 Theory of steady-state chemical reactions . . . . .	31
2.2 The stoichiometric matrix properties . . . . .	39
2.2.1 The stoichiometric matrix . . . . .	40
2.2.2 The fundamental subspaces of the stoichiometric matrix . . . . .	41
2.2.3 The Singular Value Decomposition of $\mathbf{N}$ . . . . .	47

2.3	Reaction invariants and linear system of equations in chemical reaction systems . . . . .	52
2.3.1	Reaction invariants . . . . .	52
2.3.2	The invariant relationships and the stoichiometric matrix . . . . .	54
2.3.3	Representative and non-representative species . . . . .	57
2.3.4	Species map and reaction-invariant relationships . . . . .	59
2.3.5	Degrees of freedom and reaction-invariant relationships . . . . .	60
2.3.6	Time-invariant relationships in experimental data . . . . .	64
2.4	Mass balances as linear systems of equations . . . . .	65
2.4.1	Characterizing systems of linear equations . . . . .	66
2.4.2	SVD for solving linear system of equations . . . . .	67
2.5	Data reconciliation incorporating time invariants . . . . .	68
2.6	Final remarks . . . . .	69
	Bibliography . . . . .	70
<b>3</b>	<b>State of the Art</b>	<b>73</b>
3.1	Modeling the dynamics of chemical reaction systems using experimental data	74
3.1.1	Simultaneous method . . . . .	74
3.1.2	Incremental method . . . . .	75
3.1.3	Target factor analysis . . . . .	77
3.1.4	Inverse problems for identifying reaction networks . . . . .	80
3.2	Systematic generation and selection of reaction networks . . . . .	89
3.2.1	Metabolic reaction networks . . . . .	89
3.2.2	Generation of reaction mechanisms using a global reaction . . . . .	99
3.2.3	Generation of reaction networks via optimization . . . . .	106
3.3	Synthesis of graphs . . . . .	107
3.3.1	Spanning trees . . . . .	108
3.3.2	Elementary shortest path and travel salesman problems . . . . .	109
3.4	Data treatment and parameter identifiability . . . . .	113
3.4.1	Parameter identifiability . . . . .	113
3.5	Discussion of existing reaction modeling approaches . . . . .	114
3.5.1	Reaction network identification . . . . .	115
3.5.2	Reaction network generation . . . . .	116
	Bibliography . . . . .	117
<b>4</b>	<b>Methodology Description</b>	<b>127</b>
<b>5</b>	<b>Step 1 — Data Pre-processing</b>	<b>133</b>
5.1	Step 1 motivation . . . . .	134
5.2	Regularization methods . . . . .	135
5.2.1	Filter-based approaches . . . . .	136
5.2.2	Tikhonov regularization . . . . .	137



5.2.3	Sparse regression using MILP	138
5.2.4	Smoothing splines	139
5.2.5	Dynamic Response Surface Methodology with additional constraints	143
5.2.6	Comparative analysis of regularization methods	145
5.3	Continuous approximation of concentration data	146
5.3.1	Orthogonal Collocation on Finite Elements	147
5.3.2	Step 1 formulation	147
5.3.3	Step 1 flowchart	151
5.3.4	Application example	151
	Bibliography	155
<b>6</b>	<b>Step 2 — Data Dimensionality Analysis</b>	<b>159</b>
6.1	Introduction and chapter's organization	160
6.2	Step 2 overview	161
6.3	Effect of noise in the singular values and replicated experiments	162
6.4	Determining the model dimension using singular value analysis with empirical and heuristic approaches	170
6.4.1	Scree test	171
6.4.2	Fractional variances test	171
6.4.3	Kaiser test and auto-scaling operation	173
6.4.4	Conclusion on the basis of the results obtained	175
6.5	Determining the variant space of data by theoretical approaches	175
6.5.1	Malinowski test	176
6.5.2	Cross-validation	181
6.5.3	Hard-thresholding	186
6.6	Determining the invariant data space using optimization	187
6.6.1	Methodology for evaluating reaction-invariant relationships	187
6.6.2	Methodology for evaluating time-invariant relationships	188
6.6.3	Application example, discussion of the results obtained and conclusion about the proposed method	190
6.7	Comparative analysis of the applied methods	193
	Bibliography	195
<b>7</b>	<b>Step 3 — Superstructure of the Reaction Network</b>	<b>197</b>
7.1	Step 3 overview	198
7.2	Generation of chemical reactions	199
7.2.1	MILP formulation	201
7.2.2	Application example — chemical reaction generation	203
7.3	Target factor analysis (TFA)	205
7.3.1	TFA critical analysis	207
7.3.2	Application example	209
7.4	Incorporation of thermodynamic feasibility criteria	210

7.4.1	Application example — elucidating the energetically feasible reaction direction	212
	Bibliography	213
<b>8</b>	<b>Step 4 — Generation of Reaction Networks</b>	<b>217</b>
8.1	Step 4 contextualization	218
8.2	Network complexity and related terminology	220
8.3	Sets and common constraints in network generation problems	225
8.3.1	Defining sets	226
8.3.2	Common constraints	226
8.4	Linear reaction networks	227
8.4.1	Structural flux analysis (SFA)	229
8.5	Nonlinear reaction networks	234
8.5.1	Enumeration of reaction networks using ordering constraints	235
8.5.2	Enumeration of reaction networks using a tree of states	243
8.6	MILP formulations comparison	247
	Bibliography	252
<b>9</b>	<b>Step 5 — Plausible Reaction Networks</b>	<b>255</b>
9.1	Step 5 overview	256
9.2	Reaction rate estimation	257
9.3	Selection of plausible reaction networks	258
9.3.1	Application example	259
9.4	Implicit generation of reaction networks	261
9.4.1	Implicit generation of plausible reaction networks	262
9.4.2	Implicit generation of plausible reaction networks with simultaneous kinetic model identification	266
<b>10</b>	<b>Step 6 — Reaction Kinetic Modeling</b>	<b>269</b>
10.1	Step 6 overview	270
10.2	Methodology description	271
10.3	Application example	278
	Bibliography	280
<b>11</b>	<b>Case Studies</b>	<b>283</b>
11.1	Isothermal isomerization of $\alpha$ -pinene	284
11.1.1	Finding the model structure	285
11.1.2	Parameter correlation with temperature	290
11.1.3	Parameter fitting in comparison with the Stewart & Sørensen model	292
11.1.4	Parameter fitting in comparison with the Box et al. and Tjoa & Biegler models	295
11.2	Hydrogenation of maleic acid (MAC)	297
11.2.1	Finding the model structure	297

11.2.2	Parameter correlation with temperature	307
11.3	Pfizer case study	316
11.3.1	Data reconciliation	316
11.3.2	Analysis of time invariants	325
11.3.3	Evaluating the use of invariants in data reconciliation to increase model identifiability	326
11.3.4	Identifying the true network	332
11.3.5	Reaction kinetic expressions	337
11.3.6	Parameter correlation with temperature	341
	Bibliography	342
<b>12</b>	<b>Conclusions and Possible Extensions</b>	<b>347</b>
12.1	Main methodology attributes and contributions	347
12.2	Conclusions related to the case studies	349
12.3	Possible extensions of the methodology	351
<b>I</b>	<b>Basic Concepts</b>	<b>353</b>
I.1	Singular Value Decomposition	353
I.2	Orthogonal projection	356
I.3	Singular values and eigenvalues — what they mean and how they are related	358
	Bibliography	361
<b>II</b>	<b>Generation of reaction networks without using MILP</b>	<b>363</b>
II.1	Recursive algorithm to generate the tree of states	363
II.1.1	Pseudo-code	365
II.1.2	Example	365
II.2	Another application example	366
II.2.1	Toluene case study	366
	Bibliography	368



# List of Figures

1.1	Traditional method flowchart for modeling chemical reaction systems. . . . .	3
1.2	Superstructure of the reactor network . . . . .	15
1.3	Reaction network proposed by Fuguitt and Hawkins (1945) . . . . .	18
1.4	Reaction network proposed by Deshpande et al. (2002) . . . . .	19
1.5	Reaction network proposed by Chaudhari et al. (2003). . . . .	20
1.6	Pfizer reaction network. . . . .	21
2.1	Representation of a reaction network using the corresponding graph . . . . .	29
2.2	Linear and nonlinear reaction network graphs . . . . .	31
2.3	Reaction Horiuti numbers, example 1 . . . . .	33
2.4	Reaction Horiuti numbers, example 2 . . . . .	34
2.5	Reaction Horiuti numbers, example 3 . . . . .	34
2.6	Reaction Horiuti numbers, example 4 . . . . .	34
2.7	Reaction Horiuti numbers, example 5 . . . . .	36
2.8	Reaction Horiuti numbers, example 6 . . . . .	37
2.9	Reaction Horiuti numbers, example 7 . . . . .	38
2.10	Schematic representation of the stoichiometric matrix . . . . .	40
2.11	Reaction network with a redundant pathway and corresponding stoichiometric matrix. . . . .	44
2.12	Singular Value Decomposition of the stoichiometric matrix. . . . .	47
2.13	Characteristic subspaces interconnections of the stoichiometric matrix. . . . .	48
2.14	Null subspaces interconnections of the stoichiometric matrix. . . . .	48
2.15	Characteristic subspaces interconnections of the transposed stoichiometric matrix. . . . .	49
2.16	Null subspaces interconnections of the transposed stoichiometric matrix. . . . .	49
2.17	Time invariants analysis. . . . .	55
2.18	Reaction network graph with representative chemical species. . . . .	56
2.19	Time-invariant analysis and reaction network graph. . . . .	58
2.20	Invariant and stoichiometric matrices regarding the linear reaction network. . . . .	58
2.21	Species map (or species network), example 1. . . . .	59
2.22	Reaction system with a lower number of degrees of freedom. . . . .	61
2.23	Species map (or species network), example 2. . . . .	61
2.24	Convex conservation pool map, example 1 . . . . .	62
2.25	Convex conservation pool map, example 2 . . . . .	62

3.1	Schematic representation of the incremental identification . . . . .	77
3.2	Example of spanning tree. . . . .	108
3.3	ATSP formulations and their relationships. . . . .	111
4.1	Flowchart of the systematic methodology for the incremental development of chemical reaction models. . . . .	129
5.1	Orthogonal polynomials. . . . .	148
5.2	Step 1 flowchart. . . . .	152
5.3	Concentration data for the succinic acid system. . . . .	153
5.4	Concentration profiles for the succinic acid system. . . . .	154
5.5	Individual concentration profiles for the succinic acid system. . . . .	154
5.6	Concentration profiles with oscillatory behavior. . . . .	155
5.7	First derivative of species concentration profiles. . . . .	155
6.1	Step 2 flowchart. . . . .	163
6.2	Data distribution concerning a single species at a specific time instant. . .	164
6.3	Relative error of the singular values for a range of experiments. . . . .	167
6.4	Individual species profiles with true signal and average of noisy data. . . .	168
6.5	Representation of the entire dataset free of noise and the average of each noisy data in one thousand replicas. . . . .	169
6.6	Scree plots. . . . .	171
6.7	Fractional and cumulative variances. . . . .	172
6.8	Singular values analysis according to Kaiser's rule. . . . .	174
6.9	<i>F</i> -test diagram. . . . .	179
6.10	<i>F</i> -distributions for several dimensions of invariant pools. . . . .	180
6.11	PRESS-CV for LOO and <i>k</i> -fold cross-validation. . . . .	185
6.12	Singular values and optimal hard threshold. . . . .	186
7.1	Step 3 flowchart. . . . .	200
7.2	Linear superstructure of reaction networks. . . . .	204
7.3	Nonlinear reaction network superstructure. . . . .	205
7.4	Gibbs free energy change profiles. . . . .	214
7.5	Network superstructure with energetically feasible reaction directions. . .	215
8.1	Nonlinear reaction networks with <b>DI</b> = 0. . . . .	223
8.2	Nonlinear reaction networks with <b>DI</b> = 1. . . . .	224
8.3	Linear reaction networks with <b>n<sub>rp</sub></b> = 2, <b>DI</b> = 0 and <b>CI</b> = 1. . . . .	224
8.4	The set of nonlinear reaction networks with its subdivisions. . . . .	225
8.5	SFA in a linear network superstructure. . . . .	229
8.6	SFA in linear networks with <b>n<sub>rp</sub></b> = 1. . . . .	231
8.7	SFA in linear networks with <b>n<sub>rp</sub></b> = 2. . . . .	231
8.8	3 first reaction networks generated. . . . .	234
8.9	Graph representation of an inconsistent nonlinear reaction network. . . .	235

8.10	Nonlinear reaction network with a feasible cycle and its respective temporal scale of species production. . . . .	241
8.11	Superstructure of a linear reaction network with 4 representative species and 6 reversible chemical reactions. . . . .	243
8.12	Tree of states representing a linear network superstructure. . . . .	244
8.13	Comparison of formulations performance in the explicit enumeration of linear and nonlinear reaction networks. . . . .	250
8.14	Comparison of formulations performance in the explicit enumeration of linear reaction networks. . . . .	251
9.1	Step 5 flowchart. . . . .	257
9.2	Reaction networks ordered by the plausibility criterion. . . . .	260
9.3	Limited reaction network superstructure. . . . .	261
10.1	Condensed Step 6 flowchart. . . . .	271
10.2	Detailed Step 6 flowchart. . . . .	272
10.3	Net reaction rate plotted as a function of the reactant species. . . . .	273
10.4	Reaction rate $r_1$ as a function of AS concentration. . . . .	278
10.5	Adjusting the kinetic model for $r_1$ of the AS case study. . . . .	280
10.6	Homogeneous kinetics approximation of $r_1$ . . . . .	280
11.1	Reaction networks proposed in the literature and in this work. . . . .	285
11.2	Gibbs free energy variations associated with the individual reactions. . . . .	286
11.3	Linear superstructure with energetically feasible directions identified. . . . .	287
11.4	Reaction networks ordered by the plausibility criterion for AP case study. . . . .	287
11.5	Linear graph representation of plausible reaction networks. . . . .	288
11.6	Reaction network identified in Step 5 with 4 chemical reactions. . . . .	289
11.7	Simulation of the developed model in comparison with experimental data reported in Fuguitt and Hawkins (1945, 1947). . . . .	291
11.8	Simulation of the developed model in comparison with the model proposed by Stewart and Sørensen (1981). . . . .	293
11.9	Simulation of the developed model in comparison with the model proposed by Box et al. (1973); Tjoa and Biegler (1991). . . . .	296
11.10	Reconciled data for dataset T1 concerning the MAC case study. . . . .	298
11.11	Reaction network superstructure. . . . .	300
11.12	Plausible reaction networks for MAC case study. . . . .	300
11.13	Results from the differential method concerning to reaction network S13. . . . .	302
11.14	Results from the differential method concerning to reaction network S14. . . . .	303
11.15	Comparison of individual species concentration profiles from different models considering the integral method. . . . .	306
11.16	Comparison of reaction kinetic adsorption terms as a function of the initial reactant concentration. . . . .	307
11.17	Linear regression results for Arrhenius and van't Hoff parameters tuning. . . . .	309

11.18	S13LH1 model simulation. . . . .	311
11.19	S14LH1 model simulation. . . . .	312
11.20	S13LH2 model simulation. . . . .	313
11.21	S14LH2 model simulation. . . . .	314
11.22	Individual species concentration data. . . . .	317
11.23	A to E reconciled species profiles without shape constraints. . . . .	318
11.24	F to J reconciled species profiles without shape constraints. . . . .	319
11.25	A to E reconciled profiles with shape constraints. . . . .	321
11.26	F to J reconciled profiles with shape constraints. . . . .	322
11.27	Final data reconciliation results. . . . .	324
11.28	Reaction rates computed using datasets with 0, 1 and 2 invariants, first group of five. . . . .	329
11.29	Reaction rates computed using datasets with 0, 1 and 2 invariants, second group of five. . . . .	330
11.30	Reaction rates computed using datasets with 0, 1 and 2 invariants, third group of five. . . . .	331
11.31	Implicitly generated reaction network. . . . .	334
11.32	Reaction rates $r_1$ to $r_4$ as a function of reactant species concentration. . . . .	338
11.33	Reaction rates $r_5$ to $r_8$ as a function of reactant species concentration . . . . .	339
11.34	Individual species concentration profiles at 70 °C. . . . .	343
11.35	Individual species concentration profiles at 50 °C. . . . .	344
11.36	Individual species concentration profiles at 90 °C. . . . .	345
11.37	Species concentration profiles for every dataset. . . . .	346
I.1	Singular Value Decomposition and its economy format. . . . .	354
II.1	Recursive algorithm flowchart for the generation of consistent and linearly independent reaction networks. . . . .	364
II.2	Representation of the tree of states for the linear AS case study. . . . .	366
II.3	Reaction network proposed by Ardizzone et al. (2006). . . . .	366
II.4	Superstructure of networks for Toluene case study . . . . .	367
II.5	Reaction networks of Toluene case study. . . . .	368
II.6	Tree of states - Toluene case study. . . . .	368



# List of Tables

1.1	Objectives and tools of each step of the methodology. . . . .	9
3.1	Main characteristics that are critical in inverse methods for identifying reaction networks. . . . .	90
5.1	Main aspects of data regularization methods. . . . .	145
6.1	Results from the simulation of data with additive Gaussian noise considering several numbers of replicated experiments. . . . .	166
6.2	F-test results. . . . .	179
6.3	Main aspects of data dimension identification methods. . . . .	194
7.1	Listing of the obtained linear reactions. . . . .	204
7.2	Listing of the obtained nonlinear reactions. . . . .	205
7.3	List of chemical reactions, stoichiometric vectors and relative projection errors. . . . .	210
7.4	Thermodynamic data . . . . .	212
8.1	Problem dimension analysis for linear reaction networks with one initial reactant species. . . . .	233
8.2	Two branches of the tree concerning to the reaction networks (a) and (c) of Figure 8.1. . . . .	247
8.3	Formulations comparison in terms of number of variables and constraints. . . . .	248
8.4	Complete enumeration of linear and nonlinear reaction networks with $RI = 0$ concerning the AS case study. . . . .	249
8.5	Complete enumeration of linear reaction networks with $RI = 0$ concerning the AS case study. . . . .	251
9.1	Relative frequency of reactions in the most plausible reaction networks. . . . .	260
11.1	Stoichiometric coefficients and linear chemical reactions. . . . .	285
11.2	Thermodynamic data. . . . .	286
11.3	Optimal kinetic parameters. . . . .	289
11.4	Kinetic parameters tuned using data reported in Fuguitt and Hawkins (1945, 1947). . . . .	290
11.5	Optimal kinetic parameters. . . . .	292

11.6	Equivalent kinetic parameters adjusted by Stewart and Sørensen (1981).	294
11.7	Optimal parameter values associated with the developed model.	296
11.8	Optimal parameter values reported in Box et al. (1973) and Tjoa and Biegler (1991).	297
11.9	Target factor analysis.	299
11.10	List of stoichiometric balanced chemical reactions with negative standard Gibbs free energy changes at each experimental temperature.	299
11.11	Root mean square error in concentration data in comparison with the literature model.	304
11.12	Optimal kinetic parameters for datasets T1, T2 and T3.	304
11.13	Parameter values from linear regression.	308
11.14	CPU usage and objective function value.	310
11.15	Optimal parameter values for S13LH1 model.	311
11.16	Optimal parameter values for S14LH1 model.	312
11.17	Optimal parameter values for S13LH2 model.	313
11.18	Optimal parameter values for S14LH2 model.	314
11.19	Profiles trends from data analysis and respective implemented constraints.	320
11.20	Profiles trends from previous smooth procedure (2nd iteration) and respective implemented constraints.	323
11.21	Candidate invariant relationships of Pfizer case study.	325
11.22	Singular values comparison using data reconciled with 0, 1 and 2 time-invariant relationships.	326
11.23	TFA results comparison using data reconciled with 0, 1 and 2 time-invariant relationships.	327
11.24	List of generated chemical reactions with the corresponding TFA metrics.	333
11.25	List of kinetic expressions identified simultaneously with the reaction network.	335
11.26	True reaction network with corresponding reaction labels.	336
11.27	Optimal kinetic parameters for each dataset cluster.	340
11.28	Arrhenius parameter values, Pfizer.	342
12.1	Main characteristics and contributions of the thesis.	350
II.1	Stoichiometric coefficients of Toluene case study.	367

# Nomenclature

The matrices, vectors, scalars, and symbols definitions are generic to any chapter of the thesis unless otherwise indicated. The units of variables and parameters are indicated in the main text of the thesis.

## Matrices

Matrices are denoted by capital boldface latin or greek letters.

### *Latin letters*

- A** Atomic matrix [ $n_{el} \times n_{st}$ ] (Section 2.3.1); matrix of invariant relationships [ $n_{in_{li}} \times n_{sp}$ ] (Sections 2.3.2 to 2.3.6, 2.4, 2.5 and 5.3 and chapter 6).
- B** Matrix of positive coordinates of the Horiuti matrix [ $n_b \times n_{pa}$ ] (Section 2.1.3); a design matrix [ $n_{to} \times n_c$ ] (Section 3.1.4); a non-singular matrix [ $m \times n$ ] (Appendix I.2)
- C** Correlation matrix [ $n \times n$ ] (Appendix I.1)
- D** Data matrix in the reaction-variant form [ $n_{to} \times n_{st}$ ] (Section 2.3), [ $n_{to} \times n_{sp}$ ] (Sections 2.5, 3.1.4 and 6.5), Matrix of experimental data [ $m \times n$ ] (Appendix I.3)
- D<sub>Ξ</sub>** Matrix of cumulative changes of number of moles [ $n_{to} \times n_{sp}$ ] (Sections 2.5 and 7.3 and chapter 6)
- D<sub>R</sub>** Matrix of concentration derivatives [ $n_{to} \times n_{sp}$ ] (Sections 2.5 and 7.3 and chapter 6)
- E** Matrix of residues [ $n_{to} \times n_{sp}$ ] (Sections 3.1.4, 6.4 and 6.5.1), [ $m \times n$ ] (Appendix I.3); Matrix of noise [ $225 \times 10$ ] (Section 6.3)
- I** Identity matrix
- K** Matrix of kinetic parameters [ $n_c \times n_{sp}$ ] (Section 3.1.4); matrix obtained from *Reinsch* format of  $\mathbf{S}_\lambda$  [ $n \times n$ ] (Section 5.2)
- L** Matrix of lengths of projection [ $m \times n$ ] (Appendix I.3)
- M** Projection matrix [ $n_{sp} - 1 \times R$ ] (Section 6.5.2)
- N** Stoichiometric matrix [ $n_{rx} \times n_{st}$ ] or [ $n_{rx} \times n_{sp}$ ]; matrix of natural splines [ $n \times n$ ] (Section 5.2)
- P** Diagonal matrix of kinetic parameters [ $n_p \times n_p$ ] (Section 3.1.4)

- R** Reaction rate matrix [ $n_{\text{to}} \times n_{\text{rx}}$ ] (Section 2.3 and chapter 6), [ $n_{\text{to}} \times n_{\text{rx}_{\text{li}}}$ ] (Section 7.3)
- S<sub>λ</sub>** Positive semidefinite matrix [ $n \times n$ ] (Section 5.2.4)
- T** Score matrix [ $\frac{n_{\text{to}}}{n_k} \times R$ ] (Section 6.5.2)
- U** Orthonormal matrix from SVD [ $n_{\text{st}} \times n_{\text{st}}$ ] (Sections 2.2.3 and 2.4.2), [ $m \times m$ ] (Appendices I.1 and I.3) or [ $m \times R$ ] (Appendix I.1), [ $n_{\text{to}} - \frac{n_{\text{to}}}{n_k} \times n_{\text{to}} - \frac{n_{\text{to}}}{n_k}$ ] or [ $\frac{n_{\text{to}}}{n_k} \times R$ ] (Section 6.5.2)
- V** Orthonormal matrix from SVD (loading matrix) [ $n_{\text{rx}} \times n_{\text{rx}}$ ] (Sections 2.2.3 and 2.4.2), [ $n_{\text{in}_{\text{li}}} \times n$ ] (Section 2.5), [ $n \times n$ ] (Appendices I.1 to I.3) or [ $n \times R$ ] (Appendix I.1), [ $n_{\text{sp}} \times n_{\text{sp}}$ ] or [ $n_{\text{sp}} \times R$ ] or [ $n_{\text{sp}} - 1 \times R$ ] (Section 6.5.2), [ $n_{\text{sp}} \times n_{\text{sp}}$ ] (Sections 2.5 and 6.6.2)
- W** Matrix that spans the null space of **N** [ $n_{\text{st}} \times n_{\text{st}} - R$ ] (Section 2.2.2); diagonal matrix of weights [ $n \times n$ ] (Appendix I.3)
- X** Matrix that spans the left null space of **N** [ $n_{\text{rx}} \times n_{\text{rx}} - R$ ] (Section 2.2); predictor/design matrix [ $m \times n$ ] (Section 5.2); arbitrary matrix [ $m \times n$ ] (Appendix I.1)
- Y** Matrix of data/responses [ $m \times n$ ] (Appendix I.3); [ $n_{\text{to}} \times n_{\text{sp}}$ ] (Section 6.4)

### *Greek letters*

- Ξ** Matrix of reaction extents [ $n_{\text{to}} \times n_{\text{rx}}$ ] (Section 2.5 and chapter 6)
- Σ** Matrix of Horiuti vectors [ $n_{\text{rx}} \times n_{\text{pa}}$ ] (Section 2.1.3); Matrix of singular values [ $n_{\text{st}} \times n_{\text{rx}}$ ] or [ $R \times R$ ] (Section 2.2.3), [ $m \times n$ ] or [ $R \times R$ ] (Sections 2.4.2 and 5.2.2 and appendix I.1), [ $n \times n$ ], [ $m \times n$ ] or [ $R \times R$ ] (Appendix I.3), [ $R \times R$ ] or [ $n_{\text{in}_{\text{li}}} \times n_{\text{in}_{\text{li}}}$ ] (Section 6.5.1), [ $n_{\text{to}} - \frac{n_{\text{to}}}{n_k} \times n_{\text{sp}}$ ] or [ $R \times R$ ] (Section 6.5.2), [ $n_{\text{to}} \times n_{\text{sp}}$ ] (Section 7.3)
- Ω** Transposed basis for the null space of the stoichiometric matrix containing only intermediate species [ $n_{\text{rx}} \times n_b$ ] (Section 2.1.3)
- Ω<sub>N</sub>** Matrix of integrated squares of second derivatives of natural splines [ $n \times n$ ] (Section 5.2.4)

## Vectors

Vectors are denoted by small boldface latin or greek letters or symbols.

### *Latin letters*

- a** Vector of invariant relationships (row vector of **A**)
- b** Column vectors of **B**
- b<sub>in</sub>** Positive vector of conserved (integer) amounts
- c** Vector of species concentration [ $n_{\text{sp}} \times 1$ ] or [ $n_{\text{st}} \times 1$ ]
- c<sub>ref</sub>** Reference vector of species concentration

<b>d</b>	Column vector of <b>D</b>
<b>e</b>	Column vectors of <b>E</b> ; error of prediction [ $\frac{n_{\text{to}}}{n_k} \times 1$ ] (Section 6.5.2).
<b>k</b>	Column vector of <b>K</b>
<b>l</b>	Vector of lengths of projection (column of <b>L</b> )
<b>n</b>	Vector of species number of moles
<b>r</b>	Vector of instantaneous reaction rates (row vector of <b>R</b> )
<b>r<sub>dyn</sub></b>	Dynamic component vector of instantaneous reaction rates
<b>r<sub>ss</sub></b>	Steady-state component vector of instantaneous reaction rates
<b>u</b>	Column vector of <b>U</b>
<b>v</b>	Column vector of <b>V</b> ; any vector with real entries
<b>w</b>	Vector that lies to the null space of <b>N</b> ; vector that lies to the left null space of <b>B</b>
<b>x</b>	Vector that lies to the left null space of <b>N</b> ; any vector with real entries
<b>y</b>	Response vector (predicted function values)

*Greek letters*

<b><math>\alpha</math></b>	Vector of coordinates of the steady-state reaction rate component (Chapter 2)
<b><math>\beta</math></b>	Vector of positive coordinates of the Horiuti vector (Section 2.1.3); vector of coordinates of the dynamic reaction rate component (Section 2.2.2); vector of parameter estimates
<b><math>\gamma</math></b>	Vector of coordinates of the steady-state component of the concentration derivative vector
<b><math>\delta</math></b>	Vector of coordinates of the dynamic component of the concentration derivative vector
<b><math>\theta</math></b>	Vector of positive integer entries (Section 2.3); vector of parameters (Section 5.2)
<b><math>\mu</math></b>	Vector of means (Chapter 6); Vector of species chemical potentials
<b><math>\nu</math></b>	Stoichiometric vector, row vector of <b>N</b>
<b><math>\xi</math></b>	Vector of chemical reaction extents, row vector of <b><math>\Xi</math></b>
<b><math>\sigma</math></b>	Horiuti vector (Section 2.1.3); list of singular values (Chapter 6)
<b><math>\omega</math></b>	Transposed vector that represents the null space of the stoichiometric matrix containing only intermediate species

*Symbols*

<b>0</b>	Vector or matrix of appropriate dimension with all elements being 0
<b>1</b>	Vector or matrix of appropriate dimension with all elements being 1

## Scalars

Scalars are denoted by small or capital latin or greek letters or symbols.

### *Small latin letters*

$a$	Number of atoms of a chemical element; species activity (Section 7.4); polynomial coefficient (Section 5.3)
$b$	Positive scalar
$c$	Species concentration; cost parameter (Section 8.5.2)
$f$	Scalar function
$h$	Length of finite element
$k$	Reaction kinetic constant
$l$	Lagrange interpolating polynomial
$m$	Vector or matrix dimension; Number of data points (Section 10.2)
$n$	Vector or matrix dimension; Degrees of freedom (Section 10.2); Cardinal number of a given set (in subscript)
$n_b$	Number of paths of the route
$n_c$	Number of reactant complexes (possible reactant combinations)
$n_k$	Number of groups of data
$n_s$	Number of moles of species $s$
$n_p$	Number of kinetic parameters (diagonal terms of $\mathbf{P}$ )
$n_{to}$	Number of observations
$p$	Penalty term (smoothing factor)
$q$	Scalar that belongs to $\mathbb{R}$ ; binary variable
$r$	Reaction rate
$r_{neg}$	Negative reaction rate
$t$	Independent variable (time); position of node/species (Section 8.5.1)
$t_c$	Time constant
$v(0)$	Variance of the null space of data (variance of the pool of discarded components)
$v(0)^*$	Variance of the null space of data regarding the population (hypothesis test)
$v(R)$	Variance of the $R$ model component
$v(R)^*$	Variance of the $R$ model component regarding the population (hypothesis test)
$w$	Weight in the objective function
$x$	Independent variable; continuous variable respecting a conserved amount
$x_i$	Input factor; function knot
$x_j$	Collocation point (normalized)
$x_r$	Abscissa of the collocation point

$y$	Response variable (predicted function value); binary variable (Section 8.5)
$z$	Scalar that belongs to $\mathbb{R}$

*Capital latin letters*

$A_0$	Pre-exponential factor in Arrhenius equation
$C_p$	Heat capacity of species
$E_a$	Reaction activation energy
$F$	$F$ value (Fisher variance ratio)
$F_c$	Critical $F$ value
$G$	Gibbs free energy
$H$	Enthalpy free energy
$K$	Reaction adsorption constant
$M$	Scalar (upper bound)
$N$	Basis function (natural spline)
$P$	Pressure; Interpolating polynomial
$P_r$	Legendre polynomial
$R$	Universal gas constant; matrix rank number; model dimension
$S$	Entropy; polynomial
$T$	Temperature
$U$	Variable upper bound
$V$	Volume

*Greek letters*

$\alpha$	Kinetic parameter related to the reparametrization of Arrhenius equation (Chapter 10); coordinates of the steady-state reaction rate component vector (Chapter 2); surrogate variable in RLT-based formulation (Section 8.5.1)
$\beta$	Kinetic parameter related to the reparametrization of Arrhenius equation (Chapter 10); coordinates of the dynamic reaction rate component vector (Chapter 2); matrix dimension ratio (Section 6.5.3); surrogate variable in RLT-based formulation (Section 8.5.1)
$\beta_q$	Parametric function
$\gamma$	Activity coefficient (Chapter 7); coordinate of the steady-state component of the concentration derivative vector (Chapter 2); collinearity index (Section 3.4); scale factor (noise magnitude) (Section 6.5.3)
$\gamma_{q,r}$	Polynomial coefficient
$\delta$	Coordinate of the dynamic component of the concentration derivative vector (Chapter 2); weights in the objective function (Section 5.2)
$\epsilon$	Threshold value (Sections 6.6.2 and 9.3); noise value (Section 6.3)

$\theta$	Positive integer scalar (Section 2.3); parameter value; surrogate variable (Section 5.2.5); variable related to the reparametrization of van't Hoff equation (Chapter 10)
$\kappa$	Condition number of a matrix
$\lambda$	Penalization parameter / regularization factor; optimal hard threshold coefficient (Section 6.5.3)
$\mu$	Mean value (scalar) (Chapter 6); Species chemical potential
$\nu$	Stoichiometric coefficient
$\varrho$	Reaction rate of the pathway
$\sigma$	Horiuti number (Section 2.1.3); singular value; standard deviation (Section 6.3)
$\tau$	Independent variable related to time (Section 5.2.5); optimal hard threshold (Section 6.5.3); continuous variable that establishes a linear transformation (Section 6.6.2)
$\phi$	Objective function value; variable related to the reparametrization of van't Hoff equation (Chapter 10)
$\varphi$	Relative error of projection
$\chi$	Reactant conversion

## Symbols in teletype font

The symbols in teletype font can be variables, parameters and sets used for chemical reaction and network generation, and data treatment.

<code>ae</code>	Coefficient of product species (parameter to integer cut)
<code>ccpr</code>	Coefficient of product species (parameter to integer cut)
<code>ccrd</code>	Coefficient of reaction in the forward direction (parameter to integer cut)
<code>ccre</code>	Coefficient of reactant species (parameter to integer cut)
<code>ccri</code>	Coefficient of reaction in the reverse direction (parameter to integer cut)
<code>ccrx</code>	Coefficient of reaction in the solution (parameter to integer cut)
<code>CI</code>	Network complexity index
<code>CI<sub>max</sub></code>	Maximum network complexity index
<code>cp</code>	Set of collocation points
<code>cr</code>	Instantaneous chemical reaction rate
<code>DI</code>	Network dependency index
<code>DI<sub>max</sub></code>	Maximum network dependency index
<code>DI<sub>min</sub></code>	Minimum network dependency index
<code>ds</code>	Set of datasets
<code>dts</code>	Control set for mapping experimental temperature with dataset
<code>el</code>	Set of chemical elements (atoms)
<code>est</code>	Set of states (levels of a tree)
<code>exd</code>	Auxiliary set respect to: reactant, product, reaction (forward direction)



exi	Auxiliary set respect to: reactant, product, reaction (reverse direction)
F	Structural flux among network nodes
in	Set of invariant relationships
inA	Model parameter related to conserved quantities
irn	Integral of the negative reaction rate
it	Set of solutions
k	Kinetic parameter
km	Set of kinetic rate expressions
me	Set of measurement instants
ni <sub>s</sub>	Node incidence degree
ni <sub>li</sub>	Number of linearly independent time-invariant relationships
npr	Stoichiometric coefficient of product species
nre	Stoichiometric coefficient of reactant species
nrp	Number of initial reactant species
nrx	Number of chemical reactions
nrx <sub>li</sub>	Number of linearly independent chemical reactions
nrx <sub>li,max</sub>	Maximum number of linearly independent chemical reactions that a reaction network can present
nrx <sub>max</sub>	Maximum number of chemical reactions in the reaction network
nrx <sub>min</sub>	Minimum number of chemical reactions in the reaction network
nrx <sub>sup</sub>	Number of chemical reactions in the superstructure
nsp	Matrix of stoichiometric coefficients of product species
nsr	Matrix of stoichiometric coefficients of reactant species
ordrx	Ordering coefficient for the generation of chemical reactions
pa	Set of reaction pathways
pp	Set of representative product species
RI	Network redundancy index
rp	Set of representative initial reactants
rx	Set of chemical reactions
rxnl	Set of nonlinear chemical reactions
sd	Set of non-representative species
si	Set of intermediate species
sp	Set of representative species
ss	Supersource flux to the respective initial node
st	Set of chemical species
T	Theoretical time of species production
T <sub>min</sub>	Minimum theoretical time of species production
to	Set of observation times (sampling instants)

trn	Sum of the integrals of the negative reaction rates
ts	Set of experimental temperatures
yd	Binary variable for reaction in the forward direction {0,1}
yi	Binary variable for reaction in the reverse direction {0,1}
yj	Binary variable for the presence of a reaction at a level of the state tree {0,1}
ym	Assigns a kinetic expression to a chemical reaction {0,1}
yp	Binary variable for the species that is a product in the reaction in a given direction in the network {0,1}
ypr	Binary variable for the presence of species as a product in the reaction {0,1}
yr	Binary variable for the species that is a reactant in the reaction in a given direction in the network {0,1}
yre	Binary variable for the presence of species as a reactant in the reaction {0,1}
yrx	Binary variable for the presence of the reaction in the network {0,1}
ys	Binary variable for the presence of a species at a level of the state tree {0,1}
yt	Binary variable for the minimum theoretical time of species production {0,1}

## Abbreviations

ANOVA	Analysis of variance
AO	Allo-ocimene
AP	$\alpha$ -Pinene
AS	Succinic acid
ASP	Assignment problem
ATSP	Asymmetric travel salesman problem
BDO	1,4-Butanediol
BIC	Bayesian information criterion
BP	$\beta$ -Pyronene
BuOH	n-Butanol
CDF	Cumulative distribution function
CI	Confidence interval
COBRA	Constrained-based reconstruction and analysis
CPM	Critical path method
CPU	Central process unity
CSTR	Continuous stirred tank reactor
CV	Cross-validation
D	Dimer
DM	Differential method
DoE	Design of experiments

DPP	Data pre-processing
DRSM	Dynamic response surface methodology
EBA	Energetic balance analysis
EE	Empirical eigenvalues
ESPP	Elementary shortest path problem
FASP	Formulation based on assignment problem
FBA	Flux balance analysis
FMTZ	Formulation based on Miller-Tucker-Zemlin
FRLT	Formulation based on reformulation linearization technique
FSFA	Formulation based on structural flux analysis
GBL	$\gamma$ -Butyrolactone
IM	Integral method
IncTFA	Incremental target factor analysis
IP	Integer programming
LASSO	Least absolute shrinkage and selection operator
LD	Linearly dependent
LH	Langmuir-Hinshelwood
LI	Linearly independent
LIM	Limonene
LoESS	Locally estimated scatterplot smoothing
LoF	Lack-of-Fit
LOO	Leave-one-out
LP	Linear programming
MAC	Maleic acid
MCF	Multi-commodity flow
MFA	Metabolic flux analysis
MILP	Mixed-integer linear programming
MIP	Mixed-integer programming
MSE	Mean square error
MTZ	Miller-Tucker-Zemlin
NET	Network-embedded thermodynamic analysis
NMM	Numerical matrix method
NP	Non-deterministic polynomial-time
ODE	Ordinary differential equations
PC	Principal component
PDF	Probability density function
PRESS-CV	Predicted residual error sum of squares in cross validation
PrOH	n-Propanol

RE	Relative error [%]
RF	Relative frequency
RLT	Reformulation linearization technique
RMSE	Root mean square error
RRG	Reaction routes graphs
SCF	Single-commodity flow
SFA	Structural flux analysis
SSE	Sum of square error
STN	State task network
STFA	Structured target factor analysis
SVD	Singular value decomposition
TCF	Two-commodity flow
TE	Theoretical eigenvalues
TFA	Target factor analysis
THF	Tetrahydrofuran
TMFA	Thermodynamic-based metabolic flux analysis
TSP	Travel salesman problem
uFBA	Unsteady-state flux balance analysis

## Operators, spaces, and special functions

$\mathbb{N}$	Natural numbers space
$\mathbb{Z}$	Integer numbers space
$\mathbb{R}$	Real numbers space
$\text{col}(\cdot)$	Column space of a matrix
$\text{row}(\cdot)$	Row space of a matrix
$\text{leftNull}(\cdot)$	Left null space of a matrix
$\text{null}(\cdot)$	Right null space of a matrix
$\text{cov}(\cdot)$	Covariance matrix
$\text{mean}(\cdot)$	Mean
$\text{rank}(\cdot)$	Matrix rank of a matrix
$\text{std}(\cdot)$	Standard deviation
$\text{var}(\cdot)$	Variance
$\Delta$	Difference
$d$	Differential operator
$\text{SVD}(\cdot)$	Singular value decomposition of a matrix
$\text{proj}_{\mathbf{S}}\mathbf{v}$	Orthogonal projection of $\mathbf{v}$ in $\mathbf{S}$
$\equiv$	Definition,

$\Leftrightarrow$	Equivalence
$\perp$	Perpendicular, orthogonal complement
$\langle \cdot, \cdot \rangle$	Inner product
$\ \cdot\ _p$	p-norm of vectors and matrices
$\ \cdot\ $	Euclidean norm of vectors and matrices

## Subscripts

0	Initial value; data from invariant space (Section 6.5.1)
<i>ad</i>	Adsorption
<i>d</i>	Direct model component
<i>e</i>	Chemical element index
<i>f</i>	Final value; condition of formation of 1 mole of a substance (Section 7.4 and chapter 10)
<i>g</i>	Global chemical reaction (Section 2.1.3); experimental temperature index (Section 9.4.2)
<i>i</i>	Invariant relationship index; interval on time axis (approximating interval) index (Sections 5.3 and 9.4); inverse (direction) model component (Chapter 10)
<i>j</i>	Chemical reaction index; column vector index (Chapter 2); collocation point index (Sections 5.3 and 9.4)
<i>k</i>	Solution index; dataset index (Section 9.4)
<i>l</i>	Index of levels of the tree of states
<i>m</i>	Measurement instant index (Section 5.3); kinetic rate expression index (Section 9.4.2)
<i>p</i>	Reaction pathway index
<i>R</i>	Matrices using rate-based method or the matrix rank
<i>s</i>	Chemical species index
<i>t</i>	Time index
<i>v</i>	Reduced matrix or vector concerning to variant state variables
$\Xi$	Matrix using extent-based method

## Superscripts

*	A reduced matrix (Section 2.1.3); variable or parameter free of noise
$-k$	Train dataset in cross validatory procedures
+	Positive numbers; the Moore-Penrose pseudoinverse of a matrix
0	Data from invariant space (Section 6.5.1); standard condition
$\perp$	Orthogonal complement
T	Transpose of a vector or a matrix

$k$  Group of data (data subset); test dataset in cross validatory procedures

## Accents

$\hat{\mathbf{A}}$  Economy SVD format of a matrix (full rank matrix)

$\hat{\mathbf{a}}$  Response predicted variable; Parameter estimates

$\tilde{\mathbf{a}}$  Noisy variable

$\bar{\mathbf{a}}$  Average variable

$\mathbf{a}'$  Reconciled data; Autoscaled data

# Chapter 1

## Introduction

*“You know that I write slowly. This is chiefly because I am never satisfied until I have said as much as possible in a few words, and writing briefly takes far more time than writing at length.”*

– Carl Friedrich Gauss (1777–1855)

### Contents

---

1.1	Motivation . . . . .	1
1.2	Objectives . . . . .	6
1.3	Thesis contributions . . . . .	10
1.4	Thesis organization . . . . .	15
1.5	Case studies considered . . . . .	17
1.5.1	Thermal isomerization of $\alpha$ -pinene . . . . .	17
1.5.2	Catalytic hydrogenation of succinic acid . . . . .	19
1.5.3	Catalytic hydrogenation of maleic acid . . . . .	20
1.5.4	Pfizer case study . . . . .	21
	Bibliography . . . . .	22

---

### 1.1 Motivation

A chemical reaction network represents the inter-connections between species (or chemical components) in a reaction mixture through a series of parallel and/or consecutive chemical or biochemical reactions. These chemical components are products, or at least they make part of products, that are present in our daily lives such as organic compounds (alcohol, fuel additives, cleaning products, solvents, soaps, etc.), polymers, cosmetics, drugs,

vaccines, vitamins, and others. They are produced in small to large scales, depending on the case, involving chemical, pharmaceutical and biotechnological industries that can operate at batch, semi-batch and continuous conditions. Currently, due to market competition and high demand of chemical products, these industries need rapid and flexible process development at the minimum cost ensuring product quality specifications, safe manufacturing (production) processes, and fulfillment of rules for environment protection. For this purpose, reliable chemical reaction models can be used for monitoring, control, and optimization of industrial processes, allowing, for example, the maximization of the production of a target valuable chemical product, minimization of the production of undesirable products and pollutants, increase of process efficiency and/or improvement of products quality. Moreover, in the field of process design, chemical reaction models are used to determine optimal operating conditions and equipment dimensions that minimize energy and resources consumption and investment costs subjected to the satisfaction of product demand and other constraints of different nature such as physical, chemical, and environmental restrictions.

Modeling chemical reaction systems consists of the identification of the reaction network and the determination of its individual reaction kinetic expressions. Traditionally, the modeling of chemical reaction systems is of highly experimental nature, involving the qualitative and quantitative analysis of data collected essentially in the laboratory environment, using specialized knowledge. These models can be built based on a mechanistic and/or an empirical approach. In some cases, it is sought to obtain kinetic models of an empirical or purely regressive nature, *i.e.*, models with good ability to approximate a set of experimental data, but without the ability to explain them properly based on a reaction network (Côme, 1983; Nogueira et al., 2013). If industrial scale conditions are similar to those of the acquired data then the design and optimization of industrial units can be based on them. In this case, the risks inherent in forecasting by extrapolation (when this occurs), and the limitations in the interpretation of the results produced can be justified, given the greater speed and ease of obtaining them, in relation to a model with greater mechanistic support. However, in many other cases, it is preferable (or only practicable) to develop models with a mechanistic basis, due to the advantages of using these models, despite the effort associated with this task. Mechanistic models are based on *first-principles* that describe the state variables dynamics, such as concentration, temperature, and volume, through conservation and constitutive equations. The conservation equations are of differential nature such as molar balances, heat balances and continuity equation, while the constitutive equations are of algebraic nature such as equilibrium relationships and rate expressions. These equations include information regarding the reaction stoichiometry, enthalpy and rate, and system operating conditions such as initial conditions, material exchange terms and operational constraints (Amrhein, 1998; Bhatt, 2011).

Figure 1.1 illustrates the most common procedure for developing models of reaction systems. Starting with the identification of the species present in the reaction mixture, from a



set of theoretical knowledge about possible reactions and hypotheses of reaction networks that may explain the observed transformations, one or more mechanistic models of transformation of the species involved are postulated. [Katare et al. \(2004\)](#) describe this process as “an art practiced by chemists and chemical engineers”, given the use of heuristics and flexible rules, essential for the generation of plausible solutions. The mechanisms (reaction networks) produced are used to generate one (or more) compatible kinetic model(s), with unknown parameters, using a statistical regression procedure to approximate the predictions of the models to the available kinetic data. Depending on the quality of the predictions obtained, and the number of kinetic models under consideration, this procedure can be repeated and adapted, until a single satisfactory model is obtained, capable of adequately describing the set of available experimental data. Obviously, when the number of reactions and/or chemical species is not small, this procedure is impractical, and its automation is highly desirable.

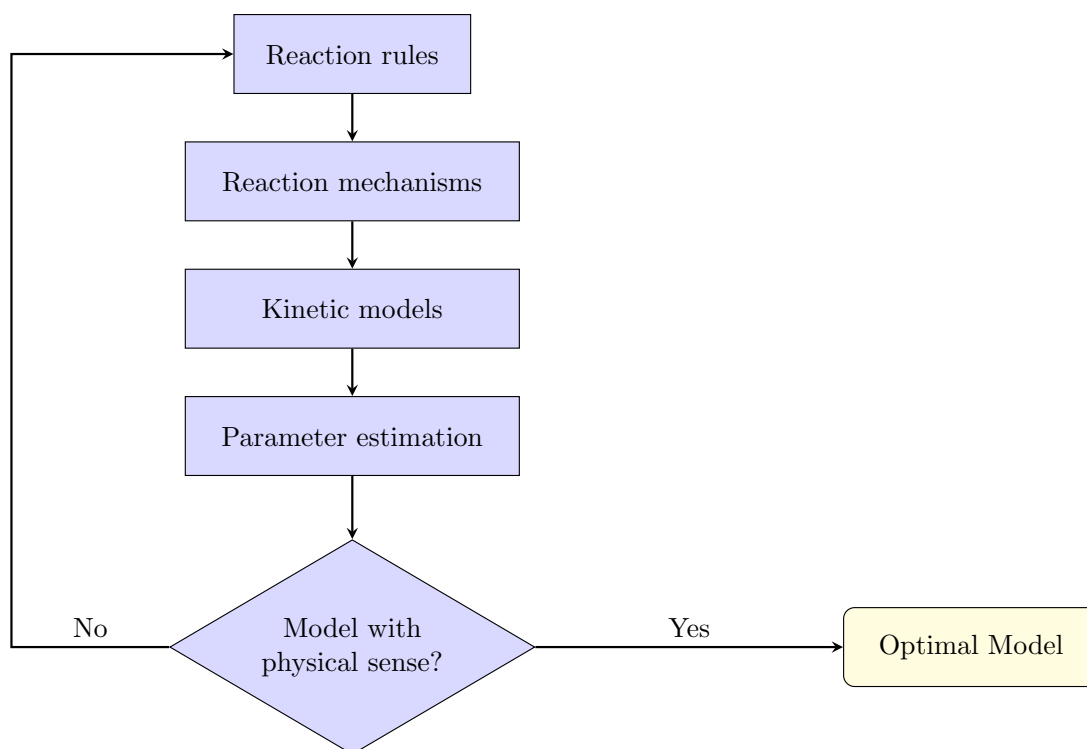


**Figure 1.1** Traditional method flowchart for modeling chemical reaction systems ([Katare et al., 2004](#)).

In addition to this need, postulated reaction steps often based on previous knowledge can also limit the quality of the results obtained. For example, following the procedure represented in [Figure 1.1](#), and given the solutions found through this method, there may be other models that are equally plausible (*i.e.*, with equivalent quality of explanation of the experimental data), which are not considered, due to the establishment (involuntary, sometimes) of analogies with other reaction systems previously analyzed. In other situations, it is the high number of possible reaction combinations that makes it difficult

to suggest all viable alternatives. In any of these scenarios, it becomes quite difficult to guarantee that the kinetic model obtained at the end of this task corresponds effectively to the best model. Considering the potential use of the kinetic models found, and their pivotal role, for example, in improving the performance of the industrial processes in question, the need to develop more systematic methodologies for the identification of reaction networks and obtaining the corresponding kinetic models is evident.

Despite the importance of this task, and some previous work carried out in this area, a generic and well-structured approach to the development of kinetic models is not currently available as an usual work tool in the field of industrial chemical kinetics. Chapter 3 presents a bibliographic review of several previous developments in this area, describing some of the main current scientific and practical challenges. “More systematic” methods of identifying chemical reaction models are discussed, however, with many limitations in their applications.

Furthermore, data collected during laboratory batch experiments is often scarce due to associated costs. In some cases, measuring specific chemical components is difficult, presenting a great uncertainty related to analytical techniques used and other sources of uncertainty. As a result, modelers have to manage irregular (incomplete and sparse), inaccurate and scarce sets of data, that can often compromise the modeling task.

Therefore, it is necessary to deal with the following problems to meet industrial goals based on available experimental data and prior knowledge regarding similar reaction systems:

- (P1) Use of efficient data pre-processing methods,
- (P2) Identify key directions of species compositional change,
- (P3) Build first-principles models using systematic and incremental approaches,
- (P4) Design experiments to discriminate between competitive models,
- (P5) Monitor, control and optimize reaction systems.

Problem P1 concerns the use of data regularization and reconciliation methods for data treatment, allowing the identification of the reaction model with more confidence. This step may be crucial for the model identification accomplishment by means of incremental methodologies, where good estimates of rates of species concentration change are required. Problems P2 and P3 are much more facilitated when handling good results from P1.

In the traditional approach of modeling chemical reaction systems, it is common to deal with overparameterized models containing a model dimension greater than the necessary, resulting in data overfitting. In other cases, additional model components may be linearly dependent chemical reactions that can be discarded, since, in general, they do not significantly contribute to the system dynamics. The model parameters are generally adjusted in a simultaneous and nonlinear regression procedure, consisting of a local optimal solution that is very sensitive to initial parameter estimates. This procedure may lead to

a mistaken interpretation of the reaction system using the probably incorrect obtained model. In these cases, at least, the structure of the model is questionable since no systematic method is verified for the network and kinetic expressions proposals and neither for the parameters initial estimates. In order to avoid this situation, Problems P2 and P3 must be considered.

P2 consists of finding the key directions of mass transformation that are observed from experimental data, corresponding to the number of linearly independent model components, *i.e.*, the required model dimension observed from data. P1 and P2 enable the segregated identification of the reaction network of the kinetic expressions in P3, ensuring optimal global solutions and good parameter estimates.

Thus, in P3, the development of mathematical models that describe the dynamic behavior of reaction systems is carried out through sequential steps where parts of the model are gradually elucidated with increasing complexity based on results coming from the solution of P1 and P2. Solutions of Problems P1 to P3 help to perform computer simulations under different scenarios and reduce costs and time in the laboratory, resulting in a faster process development.

The P4 problem becomes increasingly important in the sense that one wants to avoid costs, time and efforts in experimental tests that do not bring effective information, and therefore, more and more systematic and optimized methods of experiment proposals are needed to bring light over indiscriminate model components by providing elucidating data. The solutions to Problems P1 to P4 also help in the development of effective methods to solve Problem P5. The solution for P5 is essential to improve quality, safety and efficiency of the production process and environmental protection.

Once the advantages of using systematic methods for kinetic models development are evident, and in order to meet the previous described challenges, dealing with Problems P1–P5, this dissertation presents an incremental and systematic methodology for modeling chemical reaction systems in which first-principles models are built in sequential steps, based on a set of experimental data typically corresponding to concentration profiles of different species, collected during experimental tests carried out in a transient state. Along the proposed incremental steps, parts of the models are individually elucidated allowing the decoupled identification of the reaction network and the reaction kinetic expressions. In this systematic approach, the complete space of reaction network structures composed by linearly independent chemical reactions is explored, ensuring the selection of the most plausible ones according to experimental data. The developed methodology leads to a high certainty level in the reaction network identification, in contrast with the traditional method where the identification of the best model structure is not guaranteed given available data.

## 1.2 Objectives

This dissertation presents a systematic methodology that defines an integral approach to the modeling of chemical reaction systems covering the Problems P1 to P4 described above, leading to accurate models that can be successfully used in P5. The methodology aims at an incremental model development and is organized in 7 steps. Each step has its own characteristic problems and particular objectives often requiring a high level of knowledge on specific topics. However, in this work, an attempt was made to delve into the most relevant and descriptive aspects of each step without losing the global view of the methodology, *i.e.*, always seeking to assess the significant influence related to the gain in further deepening/detailing a specific aspect in relation to the methodology as a whole.

Many topics and tools of process system engineering and more generally of applied mathematics are handled, including data reconciliation, linear algebra, vectorial space analysis, graph theory, network synthesis problems, operations research problems (scheduling, assignment, shortest and longest paths, spanning trees, etc.), discrete and continuous (global) optimization, combinatorial problems, systems of differential and algebraic equations, model identifiability and parameter estimation, design of experiments for model discrimination, data space characterization/mapping, optimal parameter fitting.

The main objectives of each methodology step are:

**Step 1** Recreating continuous and smooth species concentration profiles to produce good estimates of their time derivatives is the main objective of the first methodology step. To achieve this objective, the processing of experimental data is carried out simultaneously with the identification and incorporation of time-invariant restrictions in a data smoothing procedure that, due to the imposed conservation relationships, guarantees more certainty in the reconciled data. In addition, the smoothness of the obtained profiles is ensured by shape restrictions that are observed from the profiles trends. The continuous approximation of concentration data is critical for the entire model development, since the structural parts of the model are identified on the basis of species concentration derivatives and/or cumulative changes of number of moles.

**Step 2** The identification of the model dimension is the principal objective of the second step of the methodology. To attend this goal, the identification of the data variant space, composed by key directions of species compositional changes, must be performed through the use of data analysis techniques. The achievement of this objective allows (i) saving time and effort in the generation of reaction network structures, since the correct dimension of the network will be known, excluding the need to generate structures of different dimensions, (ii) the validation/assessment of target stoichiometric vectors through the evaluation of projection errors in the data variant space identified using target factor analysis (TFA), and (iii) a complete understanding of the reaction system, assisting in the task of identifying and validat-

ing variants and invariants of the chemical system (Waller and Makila, 1981). The terminology related to the variant and invariant data spaces is defined in Section 2.4.

**Step 3** The main objective of this step is to generate the reaction network superstructure, *i.e.*, identify all possible chemical reactions that are plausible to occur between the observed species in the chemical system. This network superstructure must contain all the possibilities, but exclude the options that would not be plausible. Otherwise, in the next step, in which a problem of a combinatorial nature is to be solved, the number of solutions may explode with the number of chemical reactions considered. This step must be (i) systematic, ensuring a *complete* and *unique* description of the reactions among chemical species, avoiding repeated solutions, (ii) generic, *i.e.*, it can be applied to *any* chemical system, and (iii) flexible, in the sense that heuristic criteria and knowledge about the chemical system under analysis can also, and should, be incorporated in this phase. To obtain the complete list of possible chemical reactions, invariant constraints that obey stoichiometric criteria and other restrictions (*e.g.*, limits on the number of reactive molecules in an elementary reaction) are included in a mixed-integer linear programming (MILP) formulation that is solved iteratively by the addition of integer cuts in an optimization procedure. The generated chemical reactions must be validated according to experimental data by evaluating if they lie in the previously identified linear space of key compositional changes (data variant space) using TFA (Bonvin and Rippin, 1990; Amrhein et al., 1999; Georgakis and Lin, 2005). Moreover, in order to limit the number of reactions in the network superstructure (further decreasing the number of feasible reaction networks), a thermodynamic analysis of the reaction system should be considered. In this sense the identification of the individual reaction direction, in which the net reaction flux is feasible to occur, is performed by computing the Gibbs free energy change of the reaction (Fishtik et al., 1999; Fishtik and Datta, 2000).

**Step 4** The main objective of the fourth step is to generate all consistent network structures that link all observed species with a fixed number of a linearly independent set of chemical reactions from the reaction network superstructure. It consists of a combinatorial discrete optimization problem in which chemical reactions are assigned, satisfying linear constraints that ensure the network connectivity with a controlled number of chemical reactions. Transportation scheduling problems, the concept of state task networks, and the classical assignment problems are reference for the developed MILP formulations in this dissertation (Gavish and Graves, 1978; Miller et al., 1960; Sherali and Adams, 1990; Kondili et al., 1993; Shah et al., 1993; Maravelias and Grossmann, 2003; Floudas and Lin, 2005). Through the proposed MILP formulations, the reaction networks can be generated with (i) different complexities, (ii) more than one initial reactant species, and (iii) parallel and series reaction pathways. In order to enumerate all feasible structures composed by linearly independent chemical reactions, integer cut equations are considered. In this task, it is not necessary to postulate the kinetic laws that describe the different re-

action steps. This fact greatly simplifies the Step 3 implementation and the phased organization of the model development methodology.

**Step 5** The main objective of the fifth step is to select the most plausible reaction networks previously generated, according to experimental data. At the end of this selection step, the reaction networks are ordered in decreasing order of plausibility, eliminating most of the analyzed structures. This task is carried out using linear optimization in a constrained data regression problem that consists of minimizing the error in the species mass balances (linear system of algebraic equations) constrained to present non-negative reaction rates (positive variables). When the study involves many species and the number of reactions generated is very high, it is possible to consider the combination of the steps of generating and selecting reaction networks, by imposing acceptance limits on their plausibility; this corresponds to the implicit generation of the reaction networks to be considered. At the end of this stage, the number of reaction networks classified as plausible can be further reduced by suggesting extra experimental tests, designed specifically to discriminate the interpretive capabilities of the various candidate reaction networks.

**Step 6** The main objectives of Step 6 of the methodology are to identify the best reaction kinetic expression for each chemical reaction and determine the optimal parameter estimates. To perform these tasks optimization tools are required to solve linear and nonlinear regression problems with single and multi-responses. Moreover the Bayesian information criterion (BIC) is used to identify the best compromise between data agreement and number of parameters of the model. Here the observation of the reaction rate curves as a function of the concentrations of the reactant species allows the suggestion of several qualitative aspects that should be incorporated in these expressions, such as reversible kinetic laws, with monotonous behavior (or not), and other limitations (*e.g.*, limits adsorption, inhibition due to the presence of other species, etc.). This phase is also considered as a refinement of the selection of reaction networks since the structures that do not show a good correlation of reaction rates with respective reactant species may be eliminated.

**Step 7** The proposals of additional experiments that can be able to elucidate identification problems during Steps 1, 2, 5 and 6 of the developed methodology is the main objective of Step 7. These experimental proposals are supported on the results obtained from the application of each step of the methodology, where specific information may be required for elucidating certain aspects related to the step objective.

The objectives described above and the tools used to achieve them are summarized in Table 1.1.

**Table 1.1** Steps of the methodology proposed in this dissertation for the development of chemical reaction models with the corresponding objectives and tools. There is also an indication of whether kinetic knowledge is necessary or not.

	Objectives in this study	Tools used
<b>Step 1</b> <sup>(a)</sup> : Data processing	Regularization of data. Increase data certainty. Smooth profiles: $c(t)$ and $dc(t)/dt$	Orthogonal collocation on finite elements with shape and time-invariant constraints.
<b>Step 2</b> <sup>(a)</sup> : Data analysis	Determination of data variant and invariant spaces. Identify the network dimension.	Singular Value Decomposition. Parametric and non-parametric tests (PRESS-CV, $F$ -test, etc.).
<b>Step 3</b> <sup>(a)</sup> : Network super-structure generation	Generate stoichiometric balanced chemical reactions. Validate reaction vectors. Identify feasible net reaction flux directions.	MILP optimization. Integer cuts. Projection error (TFA). Gibbs free energy change of the chemical reaction.
<b>Step 4</b> <sup>(a)</sup> : Reaction network generation	Generate feasible and consistent structures that link all observed species with linearly independent reactions.	MILP formulation. Combinatorial optimization. Precedence constraints. Integer cuts.
<b>Step 5</b> <sup>(a)</sup> : Network identification	Selection of plausible network structures. Identify the reaction network.	Linear optimization. Solve species mass balances with positive reaction rates constraints.
<b>Step 6</b> : Kinetic modeling	Identify the kinetic expression for each individual reaction. Good parameter estimates. Simultaneous fit (bias-free). Tight parameter confidence intervals.	Linear optimization. Differential method and BIC (rate-based approach). Nonlinear optimization. Integral method.
<b>Step 7</b> : Design of experiments	Additional experiments proposals. Elucidation of uncertain model components.	Candidate models results. Knowledge acquired during Steps 1 to 5.

(a) No knowledge of reaction kinetics.

### 1.3 Thesis contributions

The next list of bullets presents the main aspects and contributions of the proposed methodology:

- The processing of data until obtaining the reaction kinetic model is divided into individual tasks, which must be applied sequentially. Each step produces a component of the model that is incrementally incorporated in the next step, or generates information that conditions the particular models considered in the subsequent steps. This means that during the application of the proposed methodology, the next step is only considered after elucidating a certain aspect regarding the description of the reaction system. The successful completion of the last stage ensures that *all plausible models* for the system in question have been considered and analyzed. In comparison to the traditional and other incremental approaches, the proposed methodology contains much more steps for model identification and guarantees that the best model has been identified. In 2015, an initial proposal of the systematic methodology was presented in an international conference of process system engineering (Vertis et al., 2015b). In this paper, our first developed formulation to generate reaction networks is also presented on the basis of graph-theoretical analysis, in which node balances ensure the obtainment of connected networks using structural reaction fluxes.
- The identification of the system's conserved amounts is performed based on system-theoretical and data analyses. On the former, the molecular formulas of observed species are evaluated in terms of conserved chemical elements and/or moieties in stoichiometric balanced chemical reactions, while on the latter, the null space of the species compositional changes is considered in order to find the time-invariant relationships that are presented in data regarding the reaction chemical system in question. The identification and incorporation of these time-invariant constraints during data processing is essential for a successful model development, since the reconciled data have less uncertainty associated, allowing for a more reliable and accurate elucidation of the structure of the reaction network. The identification of the data invariant space helps in identifying the data variant space, and therefore, it has direct implication in (i) well-determining the number of chemical reactions in the network (the data variant space dimension), and (ii) well-characterizing the linear space of key compositional changes by finding a plausible basis that spans the data variant space (which is the same space that the stoichiometric matrix may span). Therefore, time-invariant relationships are valuable information for model development and their identification is addressed in the methodology proposed in this dissertation. In contrast, in the traditional method and several data processing methods, no concern has been shown related to identifying time-invariant relationships in the context of modeling reaction kinetic systems.
- The validation/assessment of the chemical reactions that compose the reaction net-



work superstructure is performed after the obtainment of the entire list of stoichiometrically balanced reaction vectors, and using the previously identified data variant space. However, one could consider to perform these sequential procedures in a single simultaneous task when considering the incorporation of experimental data in the formulation to enumerate chemical reactions, for example, by imposing a threshold for the acceptance of target reaction vectors that show small errors of projection in the data variant space. In this case, difficulties may arise in defining the threshold value since it is hard to predict reliably how much of the original data uncertainty propagates to the data variant space characterization. In addition, it is not intended to exclude target vectors that present poor projections, but rather to evaluate and identify them as potential components of the model that can be a source of uncertainty in the adjustment of parameters, since they can be required to explain the formation of, for example, residual species. Consequently, the reaction vectors assessment according to data (using TFA) is separately carried out from their generation in order to attend these needs. A major contribution to the results arising from the application of TFA is achieved in this dissertation through the use of time-invariant constraints in data reconciliation and in the enumeration of reactions that satisfy these system invariants. The use of invariant constraints allows to obtain reduced projection errors of target vectors in the variant space of data, thus increasing the identifiability of the reaction model on the basis of the reconciled data. In Section 11.3.2, this is demonstrated through the application of the developed methodology to a pharmaceutical case study. This same case study was the subject of previous publications in which the intended objective was also to increase the identifiability of the model, measured by TFA results, using a different method of data processing that does not take into account the system's invariants (Santos-Marques et al., 2019; Dong et al., 2019a,b). With the incorporation of invariants in the data processing phase, we were able to obtain better results than those presented in the literature.

- Concerning the possibility of incorporating the identification of the energetically feasible reaction directions in the chemical reaction generation phase, the energetic constraints, and the physical property data required for their implementation, must be considered. This would result in a simultaneous approach that could present an advantage in generating all stoichiometrically consistent solutions with the energetically feasible direction by eliminating the subsequent filtering step. However, it can be negatively influenced by the uncertainty in the physical data used, which needs to be frequently estimated from other properties. Moreover, the nonlinear nature of the thermodynamic equations may require the use of nonlinear programming, while the remaining constraints are usually linear balance equations. For these reasons, the generation of chemical reactions is performed separately from the reaction energetic analysis in sequential procedures of the Step 3. The developed method for systematic generation of chemical reactions and reaction networks subject to

energetic constraints was published and presented in an international conference of process system engineering (Vertis et al., 2017). In addition, it should be noted that the reaction energetic analysis is well known and is usually applied in the literature in the context of the identification of metabolic networks (Kauffman et al., 2003; Qian et al., 2003; Beard et al., 2004; Qian and Beard, 2005; Orman et al., 2011; Ataman and Hatzimanikatis, 2015; Bordbar et al., 2017; Portela et al., 2019). In this dissertation, this analysis was used as an application tool, in which no additional contribution was developed in relation to what already exists in the literature. In this sense, in Chapter 7, the thermodynamic concepts that are behind the set of equations of the method are not deeply explored, presenting only its form of implementation and results obtained.

- Through the incremental model development, the identification of the reaction network structure is decoupled from its reaction kinetic expressions ensuring more certainty about the final model obtained. This segregated identification is supported on the differential method, in which the species mass fluxes (and the linear space that they span) are the basis for the structural model identification<sup>1</sup>. The reaction networks identified are composed by linearly independent reactions whose stoichiometric vectors represent the key directions of mass compositional changes. Therefore, for the accomplishment of the identification of the reaction network structure, it is crucial to have good estimates of concentration derivatives or cumulative changes of number of moles (data in the variant format) from the data processing step that incorporates time-invariant relationships. It will be shown, in this dissertation, that the identified plausible network defines a linear space in which all compositional change vectors lie in its positive orthant, since they are built by nonnegative coordinates that consist of positive net reaction fluxes. In 2016, the developed method for experimental data processing was published in an international conference, presenting a novel formulation of continuous approximation of time-concentration data that incorporates qualitative and quantitative constraints for the obtainment of smoothed and reconciled profiles, namely the species time-concentration and its first and second time-derivatives (Vertis et al., 2016a).
- The methodology guarantees that every plausible reaction network structure is analyzed through the exhaustive generation of consistent combinations of reaction vectors that link every observed species. This task consists of a constrained combinatorial optimization problem formulated as a MILP that incorporates assignment and precedence constraints. Differently of the traditional and other methods of modeling chemical reaction systems, in which no systematic tool is verified in the network structure proposals, the proposed methodology exhaustively explores the space of possible reaction networks and makes the most of the experimental data to select the most plausible structures.

---

<sup>1</sup>The terminology species and reaction fluxes is adopted in this thesis and its definition is presented in the introduction of Section 2.2.

- The implicit generation of reaction networks may be considered when the number of structures explicitly generated explodes, *i.e.*, in the presence of reaction network superstructures composed by more than a hundred chemical reactions. In this dissertation, one of the considered case studies exemplifies this situation in Section 11.3.4. Moreover, in 2016, the explicit and implicit generation of reaction networks was presented in an international conference of process system engineering (Vertis et al., 2016b). In this paper, two MILP formulations to generate reaction networks explicitly and implicitly are presented, with an illustrative case study of reduced dimension.
- The identification of the kinetic expression is performed individually for each chemical reaction. This identification is also supported on the differential method since the instantaneous reaction rate (a linear combination of concentration derivatives) regarding an individual chemical reaction defines the dependent variable that is correlated with the time-concentration of the respective reactant species. At this phase, the best tradeoff between quality of fit and model dimension is established by means of the minimum BIC value. It is important to note that the identification of the model is carried out using linear optimization with a guaranteed global optimal solution, albeit in a biased regression procedure.
- Simultaneous nonlinear regression is performed in the last phase of the methodology using the integral method. At this stage, the parts of the structural model (reaction network and kinetic expressions) are already identified, with good parameter estimates in hand. For the optimal adjustment of parameters, the original experimental data (with the associated original uncertainty) are considered in a bias-free approximation procedure in the sense of maximum likelihood, using the parameter estimates obtained previously as initial estimates. In this phase, the confidence intervals of the parameters and other statistical metrics are calculated, which may show satisfactory values/results, confirming that a robust and reliable model is obtained through the incremental and systematic methodology.
- Each task is entirely supported by the available experimental data, and if it cannot be applied conclusively, additional experimental data may be recommend. For example, more data can be required for help in (i) identifying the dimension of the data in the variant form and/or establishing the number of invariant relationships over time, (ii) discriminating plausible reaction network structures, thus elucidating the uncertain origin of residual species, and (iii) identifying the correct model from candidate kinetic expressions that have shown equal data-fitting performance. In this sense, the proposals of additional experiments are supported on the results obtained from the application of each step of the methodology. This aspect is an advantage over the usual methods of designing experiments that follow a data-based approach, where experiments are proposed in the absence of structural information of the system. Hence, through this model-based approach, it is expected that the

identification of the chemical reaction model is more effective and direct, requiring fewer experiments to elucidate the model and, consequently, saving time and costs. However, in this dissertation, no systematic method was developed for experiment proposals, and the automation of this task, based on candidate models in an integrated approach to systematic identification of chemical reaction models, is one of the suggestions for future work.

- In addition to the direct support of the various stages of this methodology in the available experimental data, a fundamental advantage of this approach is the complete avoidance of solving nonlinear optimization problems during the first stages of its application, where the fundamental knowledge about the structure of the reaction network is systematized. Thus, the need to solve nonlinear problems is postponed to the final stages of the methodology. This possibility contrasts sharply with the classic method of developing kinetic models previously described in Figure 1.1, where nonlinear regression is commonly adopted from the beginning, as a validation tool for the tested models against the basic experimental data. Given the relative frequency of the occurrence of multiple optimal locations in solving problems of estimation of kinetic parameters, this aspect of the methodology developed considerably facilitates the systematic development of mechanistic-based kinetic models.
- Although this dissertation does not present methods that cover the P5 problem, the optimal design of a reactor network was presented in an international chemical engineering conference (Vertis et al., 2015a). The optimal synthesis of the reactor network was based on a superstructure containing different possibilities for individual reactor units and their interconnection, including arrangements of individual units in series and/or parallel and different alternatives for feed distribution and stream mixing, division and re-circulation, see Figure 1.2. The design variables such as volume, number and type of reactors, stream interconnections and operating conditions were determined for optimal performance of the overall system, such as maximum selectivity and maximum revenues. The main reference works for this study development were (Balakrishna and Biegler, 1992; Schweiger and Floudas, 1999).

The objective of this work was to illustrate the importance of the availability of well-defined kinetic models, comprising the reaction network plus the kinetic description of each reaction component, in the optimal design of the corresponding reactor network. In this sense, the influence of different reaction models in the optimal reactor network design was studied, considering the chemical reaction model resulting from the application of the proposed methodology and two models of the same case study reported in the literature. In fact, for the considered case study, it was demonstrated that a better reaction network (including its kinetic parameters) could be found in relation to previous models proposed in the literature, and, as

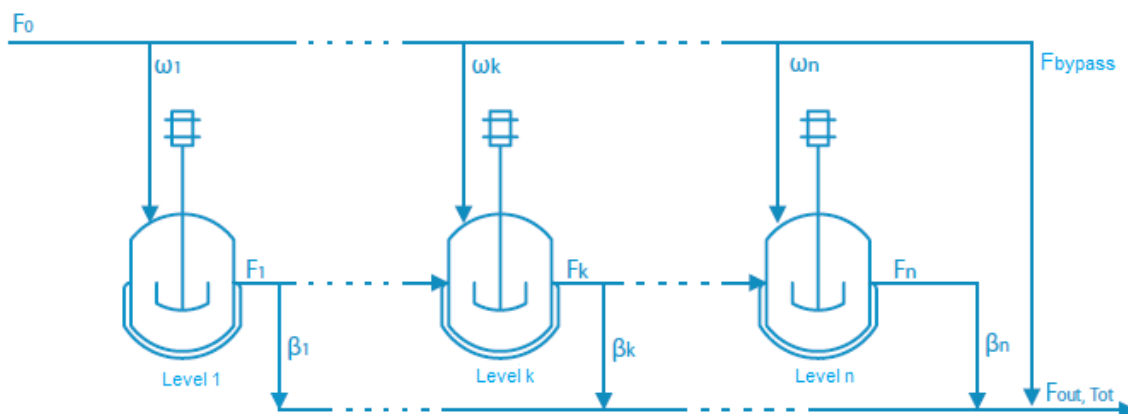


**Figure 1.2** Superstructure of the reactor network (Vertis et al., 2015a).

expected, it was shown that the kinetic model structure has great influence on the design of the corresponding optimal reactor network. The main novelty of this work is to integrate the synthesis of reaction models in the optimal equipment design, by combining (i) a systematic methodology for the development of kinetic models of complex reaction systems with (ii) a superstructure-optimization-based approach in the synthesis of reactor networks. Hence, a comprehensive method to model and design complex reaction systems was proposed, covering the Problem P5.

## 1.4 Thesis organization

*“The last thing one knows in constructing a work is what to put first.”*

– Blaise Pascal

The organization of this dissertation follows the steps of the proposed methodology. Every chapter concerning a given step contains (i) a brief introduction to the topic that will be presented, including the main literature references that have contributed to the step development, (ii) a systematization of the method that will be proposed, for a better guidance of its sequential tasks/sub-steps, and (iii) an example illustrating the application of the methodology step and also how its results contribute to the overall model development process. The examples studied are introduced in the next section.

Chapter 2 presents the fundamental theoretical concepts on which some of the steps of the methodology were based, including (i) base concepts and terminology related to reaction network representation as a graph and the theory of steady-state reactions, (ii) the analysis of the properties of the stoichiometric matrix in order to achieve a more complete understanding of the reaction network on the basis of linear algebra concepts, (iii) the meaning of time-invariant relationships in chemical reaction systems, addressing issues such as what they represent and how they can be used in linear systems of equations,

for example, for identifying subspace dimensions and reducing the model complexity, (iv) species mass balances and related issues, and finally, (v) data reconciliation in terms of orthogonal projection of data in particular matrices. Moreover the final remarks are presented at the end of this chapter.

Chapter 3 presents a bibliographic review embracing the various topics covered in this dissertation, including general methods for modeling chemical reaction systems and reaction network identification, and the description of networks structures through graphs and related problems.

Chapter 4 presents the methodology description including the schematic flowchart of the entire proposed methodology. From this chapter, those that follow correspond to each step of the methodology.

Chapter 5 considers the treatment/processing of experimental data. In this chapter, the Step 1 motivation is presented with a brief comparison of the differential and the integral methods of adjusting kinetic parameters, followed by the description of several data regularization methods for continuous (or quasi-continuous) approximation of concentration data and estimation of species concentration derivatives. The proposed method of approximating discrete data to continuous curves is also described, using orthogonal collocation on finite elements, with material conservation and qualitative shape constraints.

In Chapter 6 the data dimension analysis is addressed, containing the analysis of singular values and the use of empirical and heuristic methods for determining data dimensionality. A study of simulated noise in concentration data is considered to assess the behavior of singular values and determine the number of replicated experiments that is required for the identification of the model dimension, even in the presence of reaction extents that are comparable to the noise level. In addition, the application of several methods for determining the characteristic space of data in the variant form is considered. At the end of this chapter, a novel method for determining the data invariant space dimension is presented. This approach is focused on the characterization of the null space of noisy data through the use of linear optimization with binary variables to identify quantities with physical meaning that are conserved during the mass transformation in chemical reaction systems.

Chapter 7 describes the generation of the reaction network superstructure, including a brief description of the most relevant topics from literature that have contributed to the development of the Step 3. The description of the method for generating chemical reactions is presented in Section 7.2, followed by TFA application and reaction thermodynamics analysis, in Sections 7.3 and 7.4, respectively.

Chapter 8 presents the core of this dissertation: the generation of reaction networks (Step 4). In this chapter, the four MILP formulations developed in this work are presented and compared in terms of their performance.

In Chapter 9, the obtainment of reaction rate profiles from species concentration derivatives is described, presenting the metrics used to select/identify plausible reaction networks. Furthermore, the implicit generation of reaction networks is considered in Section 9.4, presenting the formulations for the obtainment of plausible structures with (i) positive reaction rates and (ii) established kinetic expressions.

In Chapter 10, the methodology proposed for reaction kinetic modeling is presented, including the identification of the structure of the kinetic expressions on the basis of the differential method, and the final parameter tuning using the integral method.

The main results obtained with the application of the systematic methodology for modeling chemical reaction systems to several case studies are presented in Chapter 11.

Finally, Chapter 12 presents concluding remarks and several future directions. For now, I can only wish for a pleasant reading of this thesis in the chapters that follow.

## 1.5 Case studies considered

The various features of the methodology proposed in this thesis are illustrated by the application to four case studies collected from the literature, with a moderate number of species. The first case consists of a traditional example in the context of the adjustment of kinetic parameters, the thermal isomerization of  $\alpha$ -pinene (Fuguitt, 1943; Fuguitt and Hawkins, 1945, 1947). The second case corresponds to a more recent example, involving more components, and consequently a greater number of reactions. This consists of the catalytic hydrogenation of succinic acid (Deshpande et al., 2002). The third case study is related to the previous case, presenting chemical species in common, although starting from another initial reactant. This consists of the catalytic hydrogenation of maleic acid (Chaudhari et al., 2003). Finally, the fourth is a pharmaceutical case study from Pfizer (Santos-Marques et al., 2019; Dong et al., 2019a,b). This last case is more challenging, as it contemplates greater (i) number of species with unknown molecular formula, (respecting the company's confidentiality agreements), and (ii) data base with 17 experiments varying initial and operating conditions.

### 1.5.1 Thermal isomerization of $\alpha$ -pinene

Fuguitt (1943) studied the thermal isomerization of  $\alpha$ -pinene in his doctoral thesis, later publishing two articles, one on the thermal isomerization of  $\alpha$ -pinene in liquid phase (Fuguitt and Hawkins, 1945), and the other on the kinetic study of the reactions involved, in two temperature ranges (Fuguitt and Hawkins, 1947).

This system comprises five chemical species:  $\alpha$ -pinene (AP), limonene (LIM), allo-ocimene (AO),  $\alpha$ - and  $\beta$ -pyronene (BP) and a dimer (D). The authors have suggested a reaction network, Figure 1.3, based on the interpretation of measured data in their experimental study, proposing that LIM and AO are formed simultaneously in parallel reactions and

that the component AO is decomposed into BP and D. [Box et al. \(1973\)](#) have also proposed the same reaction network for this chemical system.

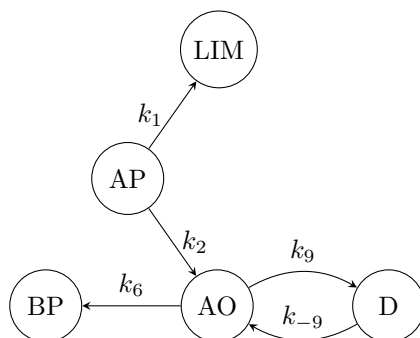


**Figure 1.3** Reaction network proposed by [Fuguitt and Hawkins \(1945\)](#).

In the experiments carried out by [Fuguitt and Hawkins \(1945\)](#), the reactions occurred very slowly (the total reaction time reported was approximately 25 days), and some difficulties related to the species measurements were also identified, especially for residual species such as BP and D. Two years later, the same authors published more data related to the previously reported experiments. These data refer to isothermal batch experiments with temperature range 189.5 — 285 °C, with pure initial reactant in liquid phase. They also considered the reaction kinetic modeling, presenting estimates for  $k_1$  and  $k_2$  at temperatures of 189.5 °C and 204.5 °C ([Fuguitt and Hawkins, 1947](#)).

Since BP and D are residual species, their origin in the network structure is hard to predict with great confidence. The authors commented that an additional experiment was carried out with the pure AO component, to identify the origins of BP and D formed, confirming the authors' initial hypothesis ([Fuguitt and Hawkins, 1945](#)). However, the data measurements of this experiment were not shown. Nonetheless, even considering these reactions as constituents of the network structure, there is still room to question the effective reaction network intrinsic to this chemical system. In this regard, the work developed will analyze the various possibilities of plausible reaction networks and identify whether any other reaction structure (associated with a kinetic model) can represent equally well (or even better) the available experimental data.

In addition to these initial kinetic studies, this reaction system has also been used in a significant number of studies to adjust kinetic parameters, considering concentration data registered in experiments carried out at constant temperature ([Box et al., 1973](#); [Stewart and Sørensen, 1981](#); [Tjoa and Biegler, 1991](#)). In this thesis the model is developed using a systematic methodology, and it is compared with the ones proposed in literature. However, for a well established comparison, the same data in each literature example is considered for parameter tuning. Section 11.1 presents (i) how the model structure was found and (ii) the parameter correlation with temperature. The identified model is compared with the models proposed by [Stewart and Sørensen \(1981\)](#) (and reviewed in [Stewart et al. \(1992\)](#)), [Box et al. \(1973\)](#) and [Tjoa and Biegler \(1991\)](#).



### 1.5.2 Catalytic hydrogenation of succinic acid

Deshpande et al. (2002) studied the hydrogenation reaction of succinic acid at the temperature of 523 K and at the pressure of 100 bar, in the presence of Ru-Co bi-metallic catalyst (1%), having proposed a reaction network with two alternative routes for the production of *n*-butanol (Figure 1.4). Therefore, this is a more complex case study presenting a greater number of chemical species and heterogeneous reaction kinetics.

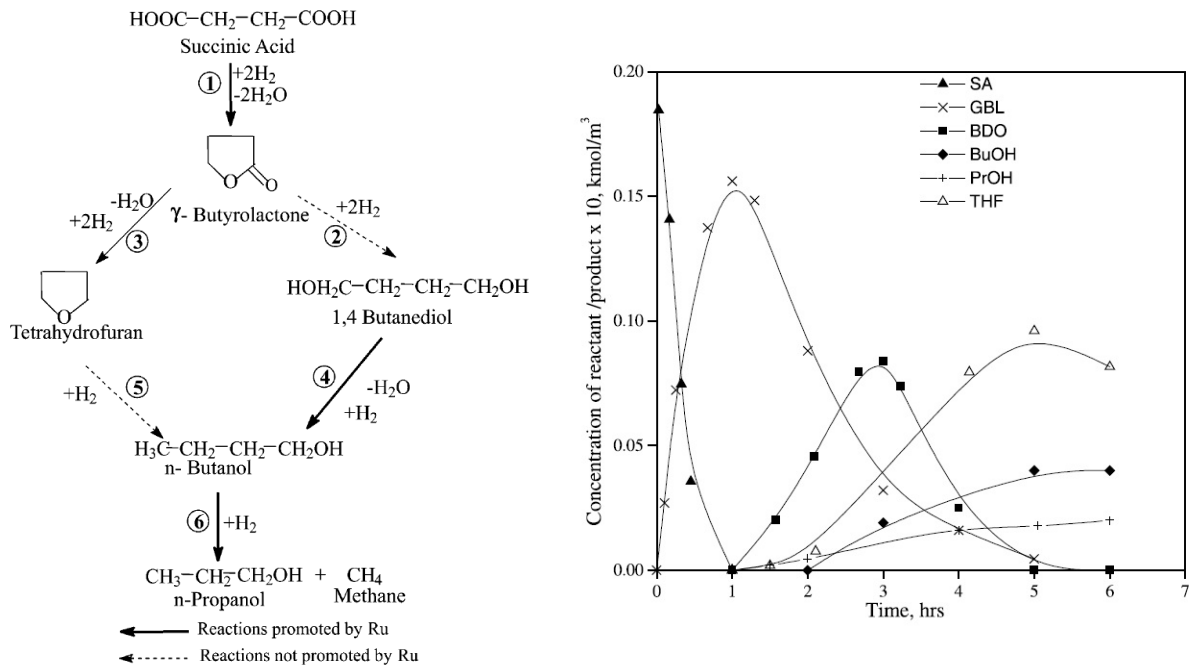


**Figure 1.4** Reaction network proposed by Deshpande et al. (2002) and respective experimental study of the hydrogenation reaction of succinic acid. Copyright (2021) by Elsevier.

In contrast to the AP case study, the AS case considers a system studied more recently in several publications. Experimental results regarding hydrogenation of succinic acid with different catalysts have been reported in several reaction environments, giving rise to products with high added value in the current market (Hong et al., 2011; Ly et al., 2012; Hong et al., 2012a,b). These articles present different hypotheses of reaction networks that allow the interpretation of the collected experimental data; this diversity can be attributed to the fact that different catalysts have been tested, which allow to activate different reaction paths in this system, as well as to the different operating conditions considered in each study.

In this dissertation the AS case study is used as an illustrative example that follows every methodology step, *i.e.*, it is considered in the end of every chapter regarding the methodology steps. In this example, hydrogenation chemical reactions are carried out from the initial reactant AS originating the main products 1,4-butanediol (BDO),  $\gamma$ -butyrolactone (GBL) and tetrahydrofuran (THF), and the residual components *n*-butanol

(BuOH) and *n*-propanol (PrOH).

### 1.5.3 Catalytic hydrogenation of maleic acid

Chaudhari et al. (2003) studied the hydrogenation of maleic acid (MAC) which is a precursor species that originates AS (the initial reactant of the previous case study). This case study contemplates five observed species: maleic acid (MAC), succinic acid (AS),  $\gamma$ -butyrolactone (GBL), tetrahydrofuran (THF) and *n*-butanol (BuOH). The experiments were carried out in a three phase, semi-batch slurry reactor at isobaric and isothermal conditions, over bimetallic Ru–Re/C catalyst. Three datasets are available at distinct temperatures: data T1 at 503 K, data T2 at 523 K, and T3 at 543 K; with the same experimental conditions: MAC initial concentration  $0.862 \text{ kmol m}^{-3}$ , catalyst loading  $50 \text{ kg m}^{-3}$  and total pressure 13.91 MPa. The aqueous phase is saturated with hydrogen, and Henry's law was used to compute the hydrogen concentration.

Chaudhari et al. (2003) proposed a reaction network composed by four linearly independent chemical reactions in series (Figure 1.5) with heterogeneous kinetic expressions based on Langmuir-Hinshelwood (LH) law, equation (1.1), where  $w$  is the catalyst mass concentration.

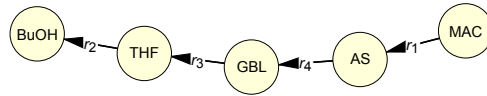


**Figure 1.5** Reaction network proposed by Chaudhari et al. (2003).

$$r_j = \frac{wH_2k_jc_{\text{react},j}}{(1 + K_{H_2}H_2 + K_{\text{MAC}}\text{MAC} + K_{\text{AS}}\text{AS} + K_{\text{GBL}}\text{GBL})^2}, \quad j = 1, \dots, 4. \quad (1.1)$$

The presence of strong reaction inhibition is detected in this case study by the first two reactant species adsorbed on the catalyst active sites. The reaction  $r_4$  only starts when the concentration of MAC approaches a small value and AS a maximum, and, that the subsequent hydrogenation reactions are initiated when AS reaches small concentration values.

In this dissertation the model proposed by Chaudhari et al. (2003) is questioned, and it is compared with other models obtained through the methodology application. This case study illustrates well the systematic method of identification of reaction kinetic expressions, where several species are considered as potential candidates to participate in the catalyst adsorption phenomenon. Furthermore, the correlation of kinetic parameters with temperature is also considered. The hydrogenation of MAC is addressed in Section 11.2.

### 1.5.4 Pfizer case study

The pharmaceutical case study from Pfizer company has been studied in the literature in three recent publications (Santos-Marques et al., 2019; Dong et al., 2019a,b). The chemical system involves 10 species, named as A, B, ..., J, linked through a network composed by 8 linearly independent chemical reactions, see Figure 1.6. No information about the reaction kinetic expressions and the chemical species involved were provided.

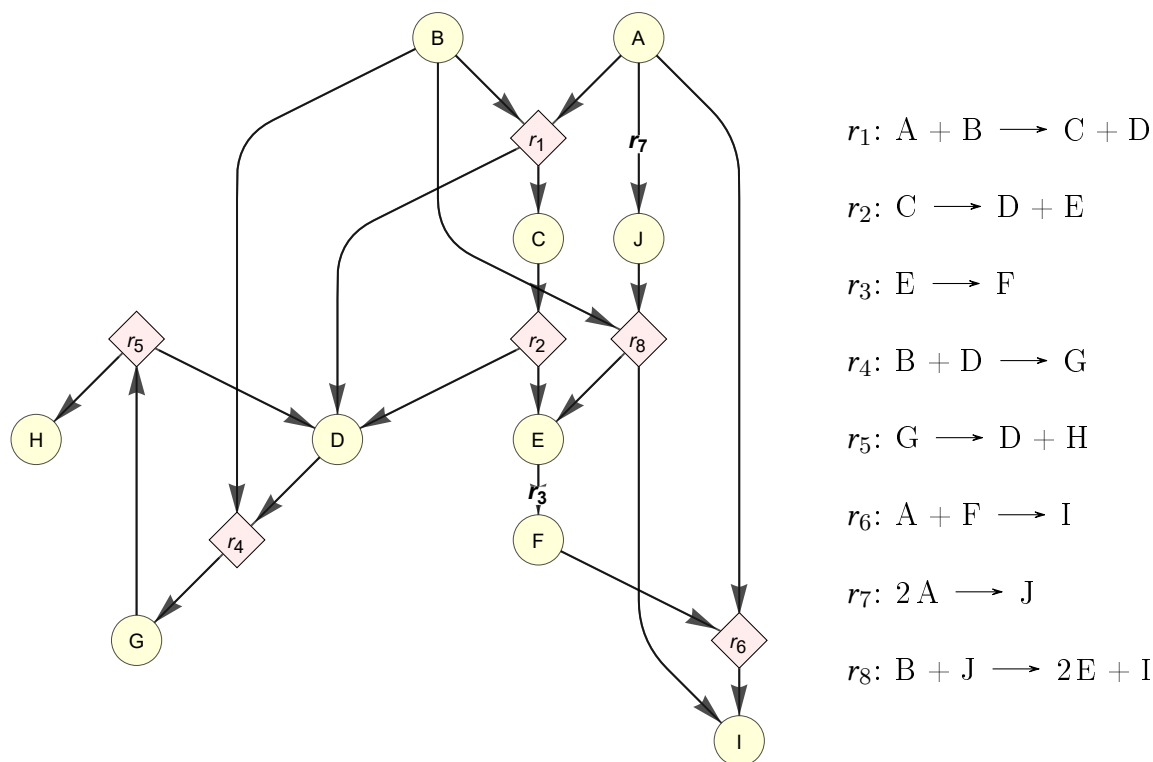


**Figure 1.6** Pfizer reaction network and corresponding list of chemical reactions.

In these studies the main objective was to validate/identify the known reaction network that describes the complex chemical system in a data-driven approach. For this purpose, 17 datasets were simulated considering several initial and experimental conditions determined by an optimal design of experiments approach. Posteriorly, Gaussian noise with zero mean and 0.005 standard deviation was added to data. It was shown that through the use of a data smoothing technique, namely dynamic response surface methodology with shape constraints, an improvement is achieved in the reaction network identification. In short, these authors presented a methodology for noisy data filtering to better elucidate the data variant space, discovering its dimension and an appropriate basis that characterizes this space.

In this thesis, the 17 datasets were considered to model the reaction kinetics from the known reaction network. In methodology Step 1, these data were reconciled regarding the system invariants established through the null space of the stoichiometric matrix. These invariants are essentials to well determine the data variant space since they support the

elucidation of the data dimension and increase the confidence in reconciled data, although the previous authors did not take into account these equality constraints. Moreover, the methods proposed for data dimensionality analyses in Step 2 are supported on this case study.

In addition, the information related to the known stoichiometry shown in Figure 1.6 was the basis for many studies of this thesis. For example, the assessment on the use of invariant constraints in the model identification task and the elucidation of reaction kinetic laws were performed considering the “true” (known) stoichiometry. However, an effort was also made to identify the true reaction network from the reconciled experimental data using implicit generation of reaction networks. In short, the Pfizer case study illustrates four main aspects of the proposed methodology: (i) the impact of the use of invariant relationships in data regularization procedures for model identification, (ii) a novel method proposal for determining the number of time-invariant relationships from noisy data, (iii) the implicit generation of reaction networks (including nonlinear networks), and (iv) the systematic methodology for kinetic model development, including parameter correlation with temperature. The Pfizer case study is addressed in Section 11.3.

## Bibliography

- Amrhein, M. (1998). *Reaction and flow variants/invariants for the analysis of chemical reaction data*. PhD thesis, EPFL, Lausanne.
- Amrhein, M., Srinivasan, B., and Bonvin, D. (1999). Target factor analysis of reaction data: use of data pre-treatment and reaction-invariant relationships. *Chemical Engineering Science*, 54(5):579–591.
- Ataman, M. and Hatzimanikatis, V. (2015). Heading in the right direction: thermodynamics-based network analysis and pathway engineering. *Current Opinion in Biotechnology*, 36:176–182. Pathway engineering.
- Balakrishna, S. and Biegler, L. T. (1992). Constructive targeting approaches for the synthesis of chemical reactor networks. *Industrial & Engineering Chemistry Research*, 31(1):300–312.
- Beard, D. A., Babson, E., Curtis, E., and Qian, H. (2004). Thermodynamic constraints for biochemical networks. *Journal of Theoretical Biology*, 228(3):327–333.
- Bhatt, N. P. (2011). *Extents of Reaction and Mass Transfer in the Analysis of Chemical Reaction Systems*. PhD thesis, EPFL, Lausanne.
- Bonvin, D. and Rippin, D. (1990). Target factor analysis for the identification of stoichiometric models. *Chemical Engineering Science*, 45(12):3417–3426.
- Bordbar, A., Yurkovich, J. T., Paglia, G., Rolfsson, O., Sigurjónsson, Ó. E., and Palsson, B. Ø. (2017). Elucidating dynamic metabolic physiology through network integration of quantitative time-course metabolomics. *Scientific reports*, 7:46249.

- Box, G., Hunter, W., MacGregor, J., and Erjavec, J. (1973). Some problems associated with the analysis of multiresponse data. *Technometrics*, 15(1):33–51.
- Chaudhari, R., Rode, C., Deshpande, R., Jaganathan, R., Leib, T., and Mills, P. (2003). Kinetics of hydrogenation of maleic acid in a batch slurry reactor using a bimetallic Ru–Re/C catalyst. *Chemical Engineering Science*, 58(3):627–632. 17th International Symposium of Chemical Reaction Engineering (IS CRE 17).
- Côme, G. (1983). Chapter 3 the use of computers in the analysis and simulation of complex reactions. In Bamford, C. and Tipper, C., editors, *Modern Methods in Kinetics*, volume 24 of *Comprehensive Chemical Kinetics*, pages 249–332. Elsevier.
- Deshpande, R., Buwa, V., Rode, C., Chaudhari, R., and Mills, P. (2002). Tailoring of activity and selectivity using bimetallic catalyst in hydrogenation of succinic acid. *Catalysis Communications*, 3(7):269–274.
- Dong, Y., Georgakis, C., Mustakis, J., Hawkins, J. M., Han, L., Wang, K., McMullen, J. P., Grosser, S. T., and Stone, K. (2019a). Constrained version of the dynamic response surface methodology for modeling pharmaceutical reactions. *Industrial & Engineering Chemistry Research*, 58(30):13611–13621.
- Dong, Y., Georgakis, C., Mustakis, J., Hawkins, J. M., Han, L., Wang, K., McMullen, J. P., Grosser, S. T., and Stone, K. (2019b). Stoichiometry identification of pharmaceutical reactions using the constrained dynamic response surface methodology. *AIChE Journal*, 65(11):e16726.
- Fishtik, I., Alexander, A., and Datta, R. (1999). Enumeration and discrimination of mechanisms in heterogeneous catalysis based on response reactions and unity bond index–quadratic exponential potential (UBI–QEP) method. *Surface science*, 430(1–3):1–17.
- Fishtik, I. and Datta, R. (2000). A thermodynamic approach to the systematic elucidation of unique reaction routes in catalytic reactions. *Chemical Engineering Science*, 55(19):4029–4043.
- Floudas, C. A. and Lin, X. (2005). Mixed integer linear programming in process scheduling: Modeling, algorithms, and applications. *Annals of Operations Research*, 139(1):131–162.
- Fuguitt, R. E. (1943). *Kinetics of Liquid Phase Thermal Isomerization of Alpha-Pinene*. PhD thesis, University of Florida.
- Fuguitt, R. E. and Hawkins, J. E. (1945). The liquid phase thermal isomerization of  $\alpha$ -pinene. *Journal of the American Chemical Society*, 67(2):242–245.
- Fuguitt, R. E. and Hawkins, J. E. (1947). Rate of the thermal isomerization of  $\alpha$ -pinene in the liquid phase. *Journal of the American Chemical Society*, 69(2):319–322.
- Gavish, B. and Graves, S. C. (1978). The travelling salesman problem and related problems. *Operations Research Center Working Papers*, 078(78).

- Georgakis, C. and Lin, R. (2005). Stoichiometric modeling of complex pharmaceutical reactions. In *Proceedings of the Annual AIChE meeting in Cincinnati, OH, November*.
- Hong, U. G., Lee, J., Hwang, S., and Song, I. K. (2011). Hydrogenation of succinic acid to  $\gamma$ -butyrolactone (GBL) over palladium-alumina composite catalyst prepared by a single-step sol-gel method. *Catalysis letters*, 141(2):332–338.
- Hong, U. G., Park, H. W., Lee, J., Hwang, S., and Song, I. K. (2012a). Hydrogenation of succinic acid to  $\gamma$ -butyrolactone (GBL) over ruthenium catalyst supported on surfactant-templated mesoporous carbon. *Journal of Industrial and Engineering Chemistry*, 18(1):462–468.
- Hong, U. G., Park, H. W., Lee, J., Hwang, S., Yi, J., and Song, I. K. (2012b). Hydrogenation of succinic acid to tetrahydrofuran (THF) over rhenium catalyst supported on  $\text{H}_2\text{SO}_4$ -treated mesoporous carbon. *Applied Catalysis A: General*, 415-416(0):141–148.
- Katare, S., Caruthers, J. M., Delgass, W. N., and Venkatasubramanian, V. (2004). An intelligent system for reaction kinetic modeling and catalyst design. *Industrial & Engineering Chemistry Research*, 43(14):3484–3512.
- Kauffman, K. J., Prakash, P., and Edwards, J. S. (2003). Advances in flux balance analysis. *Current Opinion in Biotechnology*, 14(5):491–496.
- Kondili, E., Pantelides, C. C., and Sargent, R. W. (1993). A general algorithm for short-term scheduling of batch operations — i. MILP formulation. *Computers & Chemical Engineering*, 17(2):211–227.
- Ly, B. K., Minh, D. P., Pinel, C., Besson, M., Tapin, B., Epron, F., and Especel, C. (2012). Effect of addition mode of re in bimetallic pd-re/tio 2 catalysts upon the selective aqueous-phase hydrogenation of succinic acid to 1, 4-butanediol. *Topics in Catalysis*, 55(7-10):466–473.
- Maravelias, C. T. and Grossmann, I. E. (2003). New general continuous-time state- task network formulation for short-term scheduling of multipurpose batch plants. *Industrial & engineering chemistry research*, 42(13):3056–3074.
- Miller, C. E., Tucker, A. E., and Zemlin, R. A. (1960). Integer programming formulation of traveling salesman problems. *J. ACM*, 7:326–329.
- Nogueira, A., Silva, D., Reis, M., and Baptista, C. (2013). Prediction of the by-products formation in the adiabatic industrial benzene nitration process. *Chemical Engineering Transactions*, 32:1249–1254.
- Orman, M. A., Berthiaume, F., Androulakis, I. P., and Ierapetritou, M. G. (2011). Advanced stoichiometric analysis of metabolic networks of mammalian systems. *Critical Reviews in Biomedical Engineering*, 39(6):511–534.
- Portela, R., Richelle, A., Dumas, P., and von Stosch, M. (2019). Time integrated flux analysis: Exploiting the concentration measurements directly for cost-effective metabolic network flux analysis. *Microorganisms*, 7(12):620.

- Qian, H. and Beard, D. A. (2005). Thermodynamics of stoichiometric biochemical networks in living systems far from equilibrium. *Biophysical Chemistry*, 114(2–3):213–220.
- Qian, H., Beard, D. A., and Liang, S.-d. (2003). Stoichiometric network theory for nonequilibrium biochemical systems. *European Journal of Biochemistry*, 270(3):415–421.
- Santos-Marques, J., Georgakis, C., Mustakis, J., and Hawkins, J. M. (2019). From dynamic response surface models to the identification of the reaction stoichiometry in a complex pharmaceutical case study. *AIChE Journal*, 65(4):1173–1185.
- Schweiger, C. A. and Floudas, C. A. (1999). Optimization framework for the synthesis of chemical reactor networks. *Industrial & Engineering Chemistry Research*, 38(3):744–766.
- Shah, N., Pantelides, C., and Sargent, R. (1993). A general algorithm for short-term scheduling of batch operations—ii. computational issues. *Computers & chemical engineering*, 17(2):229–244.
- Sherali, H. D. and Adams, W. P. (1990). A hierarchy of relaxations between the continuous and convex hull representations for zero-one programming problems. *SIAM Journal on Discrete Mathematics*, 3(3):411–430.
- Stewart, W. E., Caracotsios, M., and Sørensen, J. P. (1992). Parameter estimation from multiresponse data. *AIChE Journal*, 38(5):641–650.
- Stewart, W. E. and Sørensen, J. P. (1981). Bayesian estimation of common parameters from multiresponse data with missing observations. *Technometrics*, 23(2):131–141.
- Tjoa, I. B. and Biegler, L. T. (1991). Simultaneous solution and optimization strategies for parameter estimation of differential-algebraic equation systems. *Industrial & Engineering Chemistry Research*, 30(2):376–385.
- Vertis, C. S., Granjo, J. F. O., Oliveira, N. M. C., and Bernardo, F. P. (2017). Systematic generation of chemical reactions and reaction networks subject to energetic constraints. In Espuña, A., Graells, M., and Puigjaner, L., editors, *27th European Symposium on Computer Aided Process Engineering*, volume 39 of *Computer Aided Chemical Engineering*. Elsevier.
- Vertis, C. S., Oliveira, N. M., and Bernardo, F. P. (2015a). Influence of reaction models in the optimal design of reactor network systems. Oral presentation in 10th European Congress of Chemical Engineering, Nice, France.
- Vertis, C. S., Oliveira, N. M., and Bernardo, F. P. (2015b). Systematic development of kinetic models for systems described by linear reaction schemes. In Krist V. Gernaey, J. K. H. and Gani, R., editors, *12th International Symposium on Process Systems Engineering and 25th European Symposium on Computer Aided Process Engineering*, volume 37 of *Computer Aided Chemical Engineering*, pages 647–652. Elsevier.
- Vertis, C. S., Oliveira, N. M., and Bernardo, F. P. (2016a). Constrained smoothing of experimental data in the identification of kinetic models. In Kravanja, Z. and Bogataj, M.,

- editors, *26th European Symposium on Computer Aided Process Engineering*, volume 38 of *Computer Aided Chemical Engineering*, pages 2121–2126. Elsevier.
- Vertis, C. S., Oliveira, N. M., and Bernardo, F. P. (2016b). Explicit and implicit generation of chemical reaction networks through discrete structural optimization. In *7th International Symposium on Design, Operation and Control of Chemical Processes*. PSE Asia. <http://www.pse143.org/PSEAsiaTokyo/>.
- Waller, K. V. and Makila, P. M. (1981). Chemical reaction invariants and variants and their use in reactor modeling, simulation, and control. *Industrial & Engineering Chemistry Process Design and Development*, 20(1):1–11.



# Chapter 2

## Theoretical Background & Terminology

*“We are drowning in information and starving for knowledge.”*

– Rutherford D. Roger

### Contents

---

2.1	Introductory basic concepts . . . . .	28
2.1.1	Graph representation of reaction networks . . . . .	29
2.1.2	Linear and nonlinear reaction networks . . . . .	30
2.1.3	Theory of steady-state chemical reactions . . . . .	31
2.2	The stoichiometric matrix properties . . . . .	39
2.2.1	The stoichiometric matrix . . . . .	40
2.2.2	The fundamental subspaces of the stoichiometric matrix . . . . .	41
2.2.3	The Singular Value Decomposition of $\mathbf{N}$ . . . . .	47
2.3	Reaction invariants and linear system of equations in chemical reaction systems . . . . .	52
2.3.1	Reaction invariants . . . . .	52
2.3.2	The invariant relationships and the stoichiometric matrix . . . . .	54
2.3.3	Representative and non-representative species . . . . .	57
2.3.4	Species map and reaction-invariant relationships . . . . .	59
2.3.5	Degrees of freedom and reaction-invariant relationships . . . . .	60
2.3.6	Time-invariant relationships in experimental data . . . . .	64
2.4	Mass balances as linear systems of equations . . . . .	65
2.4.1	Characterizing systems of linear equations . . . . .	66
2.4.2	SVD for solving linear system of equations . . . . .	67
2.5	Data reconciliation incorporating time invariants . . . . .	68

2.6 Final remarks . . . . .	69
Bibliography . . . . .	70

---

This chapter presents fundamental concepts that support the development of several steps of the proposed methodology. The theoretical background is organized in four main sections. Section 2.1 presents introductory basic concepts and terminologies related to the reaction network representation as a graph, including the theory of steady-state reactions and the stoichiometric number. Section 2.2 consists of the analysis of the stoichiometric matrix properties, presenting its fundamental topological properties and discussing how these properties can be used to obtain a more thorough understanding of the reaction network that it represents. These properties are contained in the four fundamental subspaces associated with a matrix. Section 2.3 presents the meaning of time-invariant relationships in chemical reaction systems, *i.e.*, what they represent and how they can be used in linear system of equations, for example, for identifying subspace dimensions and reducing the model complexity, among other issues. In Section 2.4 the species mass balances are classified as types of linear systems of equations, discussing methods to solve them. Section 2.5 presents how experimental data can be reconciled using time-invariant constraints. Finally, Section 2.6 presents final remarks of the thesis theoretical background.

## 2.1 Introductory basic concepts

*“There is nothing more practical than a good theory.”*

– Kurt Lewin

A *reaction system* is defined here as the environment comprising the reaction bulk and the chemical species involved. It is considered that its complete description is made through the listing of the species present, the set of chemical reactions that take place, and the description of the kinetic laws corresponding to each chemical reaction.

The reaction system can be described through *elementary* and or *complex* chemical reactions. According to the definition given in the *IUPAC Gold Book* (McNaught and Wilkinson, 1997) the elementary reactions are defined as:

*“A reaction for which no reaction intermediates have been detected or need to be postulated in order to describe the chemical reaction on a molecular scale. An elementary reaction is assumed to occur in a single step and to pass through a single transition state.”*

On the other hand, complex chemical reactions involve the meeting of more than one species, containing intermediates as participants, that in general can be observed in experimental tests. The complex reactions can be the sum of elementary steps, resulting in chemical reactions where more than one products are formed from the same reactants or

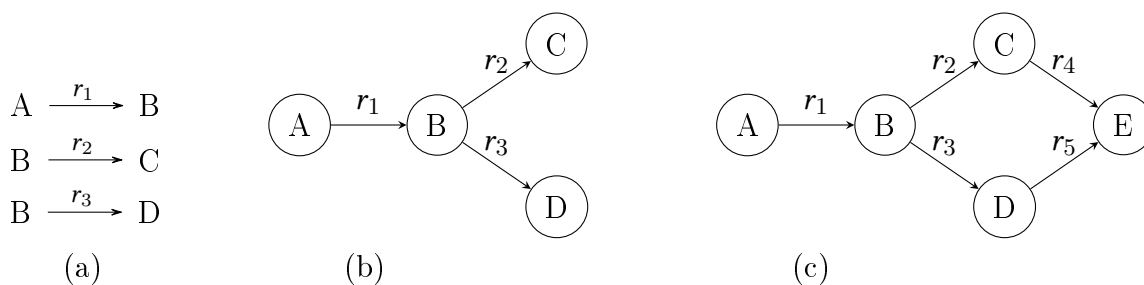


**Figure 2.1** (a) Representation of a reaction network using the corresponding graph (b). In (c) it is represented a reaction network with a redundant reaction pathway that forms species E.

different reactants produce the same products (Shahzad and Sultan, 2018). Hence, any complex chemical reaction can be described by a set of elementary reactions.

According to Marin and Yablonsky (2011) an elementary reaction is classified as unimolecular when it involves only one reactant molecule ( $A \rightarrow B$ ), in this case it is also named as a first order reaction. In cases where two molecules make part of the reaction (*e.g.*,  $A + B \rightarrow C$  or  $2A \rightarrow B$ ), the elementary reaction is classified as bimolecular or second order chemical reaction. If three molecules are involved ( $2A + B \rightarrow C$  or  $3A \rightarrow B$ ), the reaction is named as trimolecular or of third order. This last case rarely occur since it is improbable the simultaneous interaction of three (or more) reactant molecules in a single step.

In this context, the concept of *reaction mechanism* is defined as the reaction structure that contains only elementary steps, *i.e.*, elementary reactions. Wrongly, *reaction schemes*, or analogously *reaction networks*, are called mechanisms when those are formed not exclusively by elementary reactions, but include also complex chemical reactions. Temkin et al. (1996) defines the reaction network as a structure composed by several consecutive chemical reactions (elementary or not). The representation of reaction networks can be chosen for several reasons, for example in order to reduce the total number of reaction steps required, or to simplify the structural representation thus excluding species components that are not easily observed, such as radicals. Hence, reaction network is a more adequate designation to the description of a reaction system with complex chemical reactions; it is perhaps the representation most used in industrial chemical kinetics. Reaction network is the designation adopted in this document.

### 2.1.1 Graph representation of reaction networks

According to Temkin et al. (1996) a reaction network can be naturally represented through a *graph*, which elucidates several chemical species transformations from the initial reactant(s) to one or more desired final products, passing through different intermediate species (Figure 2.1).

In the area of Discrete Mathematics, a network (or graph) is composed of a set of *nodes*

(vertices) interconnected by *arcs* (edges). Usually nodes represent states, and arcs correspond to events. The arcs are classified as *directed* and *undirected*; a directed arc allows only the path in a given direction, while in an undirected arc the two directions of route are allowed. Hence, a reaction network can be represented through the respective graph, where nodes correspond to chemical species and arcs to chemical reactions (Temkin et al., 1996). The reaction network is always *connected*, *i.e.*, it corresponds to a connected graph. This connectivity characteristic is essential to the generation of alternative reaction networks<sup>1</sup>. It is said that a reaction network contains a *cyclic pathway* when it is possible to identify a finite set of arcs containing the same start and finish node. When the arcs represent reactions of catalytic nature, this set is called a *catalytic cycle* (Marin and Yablonsky, 2011).

Another extensively used terminology is the classification of species according to the location of the nodes in the corresponding network. The source node(s) as well as the destination node(s) are classified as *terminal* chemical species; an intermediate node in the network corresponds to an *intermediate* species. According to Marin and Yablonsky (2011) this division between species is clear, since intermediate species do not appear in the *global reaction*. The global reaction is obtained from the sum of weighted stoichiometric vectors in relation to the chemical reactions in the network. These weights are determined so that the intermediate species are not part of the set of terminal species that make up the overall reaction<sup>2</sup>.

### 2.1.2 Linear and nonlinear reaction networks

Although the previous representation in Figure 2.1 seems quite generic, it is not enough to represent all common reaction networks. The reaction networks can also be classified according to the structural nature of the constituent chemical reactions, as *linear* and *nonlinear*. In linear reaction networks each reaction has only one molecule of reactant and one of product species (Temkin et al., 1996). More generally, linear reactions involve the mass transformation between two species, while nonlinear reactions occur between more than two species. Nonlinear reaction networks have at least one nonlinear chemical reaction.

In linear networks, an arc connects two nodes only, *i.e.*, an arc has a source node and a destination node. This allows the representation of linear kinetic mechanisms such as reactions catalyzed by enzymes, which may be reversible or not. Typical examples of linear mechanisms are the Michaelis Menten mechanism, the water-gas shift reaction or the Temkin-Boudart mechanism, some liquid-phase hydrogenation mechanisms, isomerization reactions, and others (Marin and Yablonsky, 2011).

---

<sup>1</sup>This topic is considered in more detail in Section 3.3 and Chapter 8 regarding the generation of graphs and reaction networks, respectively.

<sup>2</sup>The concept of global reaction is widely used in the literature by different authors. It will be further explored in Section 3.2, where the description of methods for generating reaction networks is addressed.

More complex reaction networks that involve reactions combining two or more chemical species (therefore nonlinear), *e.g.*,  $A + B \longrightarrow C$  or  $C \longrightarrow D + E$ , cannot, in general, be represented by linear networks. Instead, *bipartite graphs* are a possible representation tool. In this type of graph, the nodes are divided into two non-equivalent subsets: one subset regarding chemical species and the other corresponding to *reaction events* (Yablonsky et al., 1991; Temkin et al., 1996).

Figure 2.2 illustrates two structures composed by 4 chemical species (circular nodes), in which (a) represents a linear reaction network composed by 3 chemical reactions (arcs) with a reversible one ( $r_3$ ), while in (b) a nonlinear reaction network with 2 chemical reactions is shown. Here, the reaction network is represented by a bipartite graph where the reaction event node ( $\diamond$ ) is used to linearize the representation of the nonlinear reaction  $r_1$ . Therefore, in a nonlinear reaction network represented by a bipartite graph, the number of arcs does not anymore correspond to the number of chemical reactions, as it happens in linear reaction networks. Also, for the representation of reversible nonlinear reactions, a curved line segment is used to indicate the group of species belonging to the same reaction side:

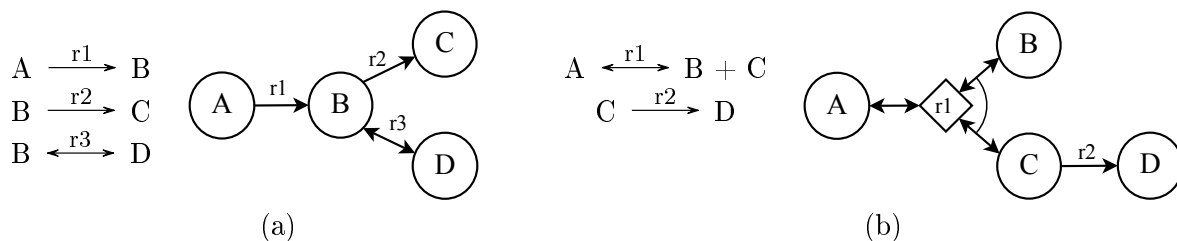


**Figure 2.2** Graph representations of (a) linear and (b) nonlinear reaction networks.

The same linear graph representation can be used to structurally describe *pseudo-linear* reaction networks. These (pseudo)-linear networks contain at least one reaction where the stoichiometric coefficient of the single reactant species is greater than one. This means that, in addition to unimolecular reactions, bi- or tri- molecular reactions make part of this network, but with reactant molecules of the same component, *e.g.*,  $2A \longrightarrow B$  is a bimolecular pseudo-linear chemical reaction which rate is probably described by a second order kinetic law. For example, suppose that the linear network represented in Figure 2.2(a) contains instead of  $r_3$ :  $B \longleftrightarrow D$  the pseudo-linear reaction  $r'_3$ :  $2B \longleftrightarrow D$ . The same linear graph representation is correct. In order to simplify the nomenclature, we will refer to pseudo-linear reaction networks as linear reaction networks, making a distinction among them when it is required.

### 2.1.3 Theory of steady-state chemical reactions

A chemical reaction is considered at steady state if the concentrations of every species in that reaction do not change in time. Evidently, this is possible only in an open system

such as a tubular reactor or a circulation flow system (Temkin, 1979). In steady-state, the concentration of an intermediate species does not change in time because the sum of rates of formation of this species is equal to the sum of rates of its consumption. The theory of steady-state chemical reactions can be very useful for model reduction. It involves a linear transformation of the original system, resulting in a reduced system (with smaller degrees of freedom) by eliminating intermediate species.

In this section the number of Horiuti is introduced (Horiuti and Nakamura, 1957). This is related to the definition of global chemical reactions, as it will be presented below. In fact, the theory of steady-state chemical reactions involves the concept of global reaction (and thus the Horiuti numbers) for determining the number of linearly independent reaction routes (or pathways) between terminal species (Horiuti, 1973; Temkin, 1979). In turn, reaction pathways can be decomposed into extreme paths, (or more broadly into paths of route (Yablonsky et al., 1991), or basic routes (Temkin, 1979)).

Furthermore, the concept of reaction pathways (which will be presented below) can be very useful for network synthesis, and it does not differ much from the concept used for metabolic network synthesis, despite the fact that it has different nomenclature and application contexts. Moreover it also not differs from the idea behind graph synthesis methods. These similarities between methods for generating network structures will be discussed in the state-of-the-art chapter.

The next section links the concepts of (i) the number of linearly (in)dependent chemical reactions, (ii) the number of reaction pathways, (iii) the number of Horiuti vectors, (iv) the type of network structure (linear and nonlinear) and (iv) the number of Horiuti (scalar).

### **Horiuti number, stoichiometric vector, stoichiometric matrix, global reaction, reaction pathways and network structure**

In the 1950s, the Japanese physical chemist Horiuti formulated a theory of steady-state reactions, using concepts from graph theory. Horiuti introduced the concept of *stoichiometric number*. This is the number of times each reaction step in a reaction network must be multiplied to cancel out the presence of intermediate species in the global reaction (Horiuti and Nakamura, 1957). Yablonsky et al. (1991) preferred to call this stoichiometric number as *Horiuti number*, since the original name can induce to mistake, confounding with the number of reagent molecules taking part in the reaction<sup>3</sup>. The latter, in turn, is the stoichiometric coefficient  $\nu_{s,j}$  of the species  $s \in \text{st}$  and reaction  $j \in \text{rx}$ , where  $\text{st}$  and  $\text{rx}$  are, respectively, the sets of species and reactions that compose the network. Every reaction  $j \in \text{rx}$  has its correspondent stoichiometric vector  $\boldsymbol{\nu}_j \in \mathbb{Z}^{n_{\text{st}}}$ , and the set of stoichiometric vectors establishes the rows of the stoichiometric matrix  $\mathbf{N} \in \mathbb{Z}^{n_{\text{rx}} \times n_{\text{st}}}$ , where  $n_{\text{rx}}$  and  $n_{\text{st}}$  are the cardinals of the respective sets. Therefore, the sum of every stoichiometric vector multiplied by its respective Horiuti number, the scalar  $\sigma_j$ , results in

---

<sup>3</sup>The nomenclature adopted for stoichiometric number, during this document, is also Horiuti number.

the global reaction, free of intermediate species, such that:

$$\sum_j \sigma_j \nu_j = \nu_g \quad \Leftrightarrow \quad \mathbf{N}^T \cdot \boldsymbol{\sigma} = \nu_g \quad (2.1)$$

where  $\boldsymbol{\sigma} \in \mathbb{N}^{n_{rx}}$  is the vector of Horiuti numbers, and  $\nu_g \in \mathbb{Z}^{n_{st}}$  is the stoichiometric vector of the global chemical reaction. Hence the global reaction is a linear combination of the basic column vectors of the transposed stoichiometric matrix, and the Horiuti numbers are its positive coordinates in that basis.

A network without alternative reaction pathways, also known as a *single route* network, has an unique scalar  $\sigma_j$  for every reaction  $j \in rx$ , *i.e.*, it has a single vector  $\boldsymbol{\sigma}$ . This implies that this set  $rx$  is necessarily linearly independent, or in other words, the matrix  $\mathbf{N}$  has full (row) rank. When  $rx$  is a linearly dependent set, *e.g.*, as in the example in Figure 2.1c, more than one viable route between terminal species is possible. In this case, it becomes necessary to define more than one Horiuti number for every reaction present, each referring to the reaction pathway  $p \in pa$  chosen to obtain the terminal products:

$$\mathbf{N}^T \cdot \boldsymbol{\sigma}_p = \nu_g, \quad p = 1, \dots, n_{pa} \quad (2.2)$$

where  $n_{pa}$  is the number of linearly independent pathways in the set  $pa$ . Hence every vector  $\boldsymbol{\sigma}_p, p = 1, \dots, n_{pa}$ , establishes a route of consecutive steps to form the global reaction.

The examples in Figures 2.3 and 2.4 represent two different linear reaction networks, one with two and the other with four chemical reactions, but both networks have the same global reaction. The  $\sigma_{j,p}$  is the Horiuti number of reaction  $j = 1, \dots, n_{rx}$  in the pathway  $p = 1, \dots, n_{pa}$ .

Reaction	$r_j$	$\sigma_j$
A $\longrightarrow$ B	1	1
B $\longrightarrow$ C	2	1
Global reaction:	A $\longrightarrow$ C	

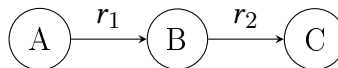


**Figure 2.3** Reaction Horiuti numbers in a linear network composed by a linearly independent set of reactions.

Networks strictly composed by linear reactions, as in the examples above, present only 0 or 1  $\sigma$  values, resulting in global reactions with the same number of moles in both reactant and product sides. In the case of networks with pseudo-linear reactions (as discussed in Section 2.1.2), the Horiuti numbers can be greater than one. Figure 2.5 illustrates such a case, namely of a reaction network with two pseudo-linear reactions ( $r_2$  and  $r_4$ ) that has the same graph representation of Figure 2.4, but different  $\sigma$  values and global reaction.

For linear and pseudo-linear reaction networks presenting linear graphs with more than one incident arc in a node, such as in Figures 2.4 and 2.5, the set of chemical reactions

Reaction	$r_j$	$\sigma_{j,1}$	$\sigma_{j,2}$
$A \rightarrow B$	1	1	0
$B \rightarrow C$	2	1	0
$A \rightarrow D$	3	0	1
$D \rightarrow C$	4	0	1
Global reaction:	$A \rightarrow C$		

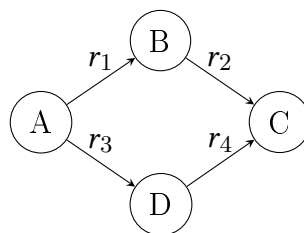


**Figure 2.4** Reaction Horiuti numbers in a linear network composed by a linearly dependent set of reactions. In fact the global reaction can be described by two different pathways:  $A \rightarrow B \rightarrow C$  and  $A \rightarrow D \rightarrow C$ .

Reaction	$r_j$	$\sigma_{j,1}$	$\sigma_{j,2}$
$A \rightarrow B$	1	2	0
$2B \rightarrow C$	2	1	0
$A \rightarrow D$	3	0	2
$2D \rightarrow C$	4	0	1
Global reaction:	$2A \rightarrow C$		

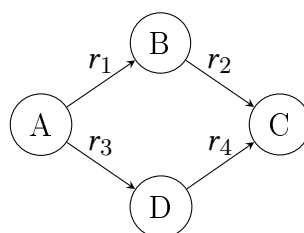


**Figure 2.5** Reaction Horiuti numbers in a pseudo-linear network composed by four chemical reactions configuring a linearly dependent set.

is always linearly dependent, (more than one pathway between terminal nodes exists). On the other hand, for nonlinear reaction networks, it is possible to have more than one incident arc in a given node with a linearly independent set of chemical reactions, and thus, these networks are single route networks (or single pathways) having a single Horiuti vector. Hence the number of incident arcs in a node does not establish the number of existing pathways in a given network, however, the number of linear dependencies in the stoichiometric matrix does. Figure 2.6 shows a nonlinear reaction network with two incidences in node D through reactions  $r_2$  and  $r_4$ , although presenting a linearly independent set of chemical reactions.

Reaction	$r_j$	$\sigma_j$
$A \rightarrow B$	1	2
$2B \rightarrow D + E$	2	1
$A \rightarrow C$	3	1
$C \rightarrow D$	4	1
Global reaction:	$3A \rightarrow 2D + E$	

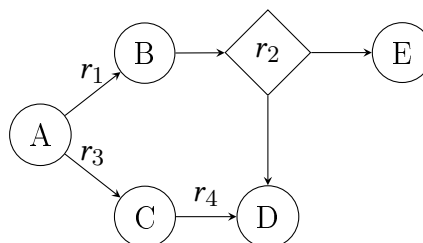


**Figure 2.6** Reaction Horiuti numbers in a nonlinear reaction network with a single pathway.



### Reaction rates based on the Horiuti numbers

When the formation of a molecule in one of the steps is compensated by its consumption in the other step, the steady-state reaction process is realized. The complete compensation for the formation and consumption of intermediates does signify the completion of a pathway along some reaction network (Yablonsky et al., 1991). Considering that concept of reaction pathway, the rate of a steady-state reaction is determined by the rates along the routes, such that

$$\mathbf{r} = \sum_{p=1}^{n_{pa}} \boldsymbol{\sigma}_p \varrho_p \quad (2.3)$$

where  $\mathbf{r} \in \mathbb{R}_+^{n_{rx}}$  is the vector of reaction rates and  $\varrho_p$  is the steady rate (scalar) of the pathway  $p = 1, \dots, n_{pa}$ . Hence the original rates are a linear combination of the rates of the routes, at steady conditions.

The mass balance equations for only intermediate species are established by

$$\begin{aligned} \mathbf{N}^{*T} \cdot \mathbf{r} &= \\ \mathbf{N}^{*T} \cdot (\boldsymbol{\Sigma} \cdot \boldsymbol{\varrho}) &= \mathbf{0} \end{aligned} \quad (2.4)$$

where  $\mathbf{N}^* \in \mathbb{Z}^{n_{rx} \times n_{si}}$  has the columns  $s = 1, \dots, n_{si}$  of the stoichiometric matrix  $\mathbf{N}$  respecting to the intermediate species  $s \in \mathbf{si}$ ,  $\mathbf{si}$  is the set of intermediate species,  $n_{si}$  is the cardinal of  $\mathbf{si}$  (thus  $\mathbf{si} \subset \mathbf{st}$  and  $n_{si} \leq n_{st} - 2$ ),  $\boldsymbol{\Sigma} \in \mathbb{N}^{n_{rx} \times n_{pa}}$  is the matrix of Horiuti vectors (or reaction pathways) with  $\boldsymbol{\sigma}_p, p = 1, \dots, n_{pa}$  column vectors, and  $\boldsymbol{\varrho} \in \mathbb{R}^{n_{pa}}$  is the vector of the rates of the routes/pathways.

The last equation demonstrates in fact that in each route the intermediate species are canceled since

$$\mathbf{N}^{*T} \cdot \boldsymbol{\sigma}_p = \mathbf{0}, \quad p = 1, \dots, n_{pa} \quad (2.5)$$

Thus, every pathway (Horiuti vector) is the homogeneous solution of (2.5)<sup>4</sup>.

Hence every  $\boldsymbol{\sigma}_p$  for  $p = 1, \dots, n_{pa}$  lies in the null space of  $\mathbf{N}^{*T}$ , *i.e.*,  $\boldsymbol{\sigma}_p \in \text{null}(\mathbf{N}^{*T})$  for  $p = 1, \dots, n_{pa}$ . Therefore, determining the  $\text{null}(\mathbf{N}^{*T})$  is finding a basis for this space, where  $\boldsymbol{\sigma}_p$ , for  $p = 1, \dots, n_{pa}$ , is obtained through a linear combination of that basis, such that

$$\boldsymbol{\Omega}^T \cdot \boldsymbol{\beta}_p = \boldsymbol{\sigma}_p, \quad p = 1, \dots, n_{pa} \quad \Leftrightarrow \quad \boldsymbol{\Omega}^T \cdot \mathbf{B} = \boldsymbol{\Sigma} \quad (2.6)$$

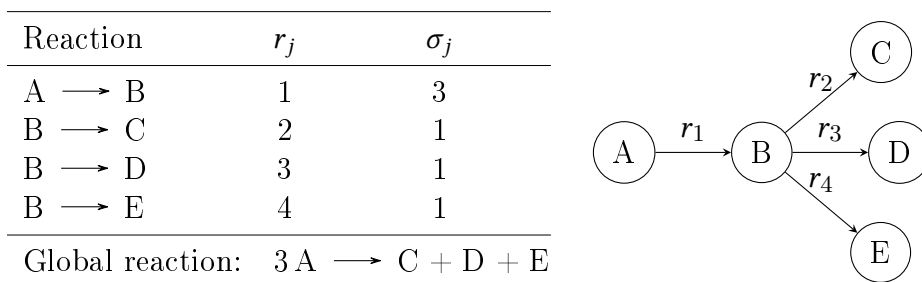
where  $\boldsymbol{\Omega}^T \in \mathbb{Z}^{n_{rx} \times n_b}$  is the matrix that represents the  $\text{null}(\mathbf{N}^{*T})$  of dimension  $n_b$ , *i.e.*, a basis for  $\text{null}(\mathbf{N}^{*T})$  formed by  $n_b$  linearly independent column vectors in  $\mathbb{Z}^{n_{rx}}$ , and  $\boldsymbol{\beta}_p \in \mathbb{R}_+^{n_b}$  is the vector of positive coordinates of  $\boldsymbol{\sigma}_p$  in that basis, for  $p = 1, \dots, n_{pa}$ . The  $\boldsymbol{\beta}_p, p = 1, \dots, n_{pa}$  vectors form the columns of  $\mathbf{B} \in \mathbb{R}_+^{n_b \times n_{pa}}$ .

---

<sup>4</sup>Notice that the Horiuti vector is determined to cancel the intermediate species in the global reaction, satisfying (2.2) and (2.5).

Actually,  $n_b$  represents the number of linearly independent basic paths that constitute sequences of arcs among terminal species, establishing fragments of the reaction network. Hence, when all fragments are simultaneously considered the entire network is established. Yablonsky et al. (1991) described the columns of  $\Omega^T$  as *paths of the route* (meaning fragments of the pathway). Therefore, the theory of steady-state reactions involves determining fragments of the network that are represented through vectors that lie in the null space of  $\mathbf{N}^{*T}$ .

In Figure 2.7, there are four chemical reactions (reaction steps) that form a single pathway,  $n_{pa} = 1$ , indicated by the single Horiuti vector  $\sigma$  that results in the global reaction.



$$\mathbf{N}^{*T} = \begin{bmatrix} r_1 & r_2 & r_3 & r_4 \\ 1 & -1 & -1 & -1 \end{bmatrix} \mathbf{B} \quad \mathbf{\Omega}^T = \begin{bmatrix} 1 & 1 & 1 \\ 0 & 0 & 1 \\ 0 & 1 & 0 \\ 1 & 0 & 0 \end{bmatrix} \begin{matrix} r_1 \\ r_2 \\ r_3 \\ r_4 \end{matrix} \quad \boldsymbol{\beta} = \begin{bmatrix} 1 \\ 1 \\ 1 \end{bmatrix} \begin{matrix} \text{(a)} \\ \text{(b)} \\ \text{(c)} \end{matrix} \quad \boldsymbol{\sigma} = \begin{bmatrix} 3 \\ 1 \\ 1 \\ 1 \end{bmatrix} \begin{matrix} r_1 \\ r_2 \\ r_3 \\ r_4 \end{matrix}$$

**Figure 2.7** Reaction Horiuti numbers, and related matrices, in a linear network composed by a linearly independent set of reactions, with only one intermediate species, B.

In fact, in Figure 2.7, the pathway is decomposed in three network fragments, (a) with  $r_1$  and  $r_4$ , (b) with  $r_1$  and  $r_3$ , and (c)  $r_1$  and  $r_2$ , indicated by the basic column vectors of  $\mathbf{\Omega}^T$ . These basic paths are represented through (a) A  $\longrightarrow$  B  $\longrightarrow$  E, (b) A  $\longrightarrow$  B  $\longrightarrow$  D, and (c) A  $\longrightarrow$  B  $\longrightarrow$  C. In steady state, the original reaction rates are a linear combination of the rates of the single route (left side of equation), as such as they are a linear combination of the rate of basic paths (a), (b) and (c), (right side of equation):

$$\begin{bmatrix} r_1 \\ r_2 \\ r_3 \\ r_4 \end{bmatrix} = \boldsymbol{\sigma} \varrho \quad \Leftrightarrow \quad \begin{bmatrix} r_1 \\ r_2 \\ r_3 \\ r_4 \end{bmatrix} = \mathbf{\Omega}^T \cdot \boldsymbol{\beta} \cdot \varrho = \mathbf{\Omega}^T \cdot \begin{bmatrix} r_a \\ r_b \\ r_c \end{bmatrix},$$

where  $r_a$ ,  $r_b$  and  $r_c$  are the rates of the basic paths (a), (b) and (c), respectively. Thus, establishing that: (i)  $r_1 = 3\varrho = r_a + r_b + r_c$ , (ii)  $r_2 = \varrho = r_c$ , (iii)  $r_3 = \varrho = r_b$ , and (iv)  $r_4 = \varrho = r_a$ . Therefore,  $r_1 = r_2 + r_3 + r_4$  in steady conditions.

Consequently, the paths along the non-basic routes composing a reaction are substituted

by equivalent paths along the basic routes. In fact, the pathway  $p \in \mathbf{pa}$  can be a non-basic route, which is a linear combination of the basic paths, and, as shown in the previous example, every reaction can be substituted by equivalent paths along the basic routes.

In order to study the cases where  $n_{\mathbf{pa}} > 1$ , consider an additional reaction in the network of Figure 2.7, for example  $r_5 : C \rightarrow D$ , that turns the system linearly dependent, as shown in Figure 2.8.

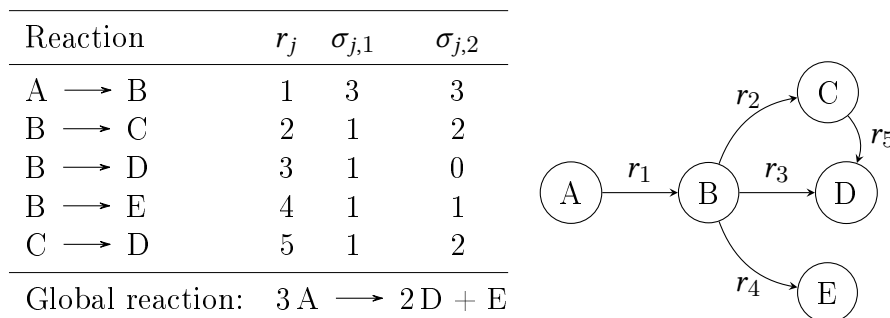


**Figure 2.8** Reaction Horiuti numbers in a linear network composed by a linearly dependent set of reactions, with two intermediate species, B and C.

With the addition of  $r_5$  to this chemical system, the basic paths are now (a)  $A \rightarrow B \rightarrow E$ , (b)  $A \rightarrow B \rightarrow D$ , and (c)  $A \rightarrow B \rightarrow C \rightarrow D$ . The reaction rates can be written as

$$\begin{bmatrix} r_1 \\ r_2 \\ r_3 \\ r_4 \\ r_5 \end{bmatrix} = \begin{bmatrix} 3 \\ 1 \\ 1 \\ 1 \end{bmatrix} \varrho_1 + \begin{bmatrix} 3 \\ 2 \\ 0 \\ 1 \\ 2 \end{bmatrix} \varrho_2 = \begin{bmatrix} 1 & 1 & 1 \\ 0 & 0 & 1 \\ 0 & 1 & 0 \\ 1 & 0 & 0 \\ 0 & 0 & 1 \end{bmatrix} \cdot \begin{bmatrix} 1 & 1 \\ 1 & 0 \\ 1 & 2 \end{bmatrix} \cdot \begin{bmatrix} \varrho_1 \\ \varrho_2 \end{bmatrix} = \begin{bmatrix} 1 & 1 & 1 \\ 0 & 0 & 1 \\ 0 & 1 & 0 \\ 1 & 0 & 0 \\ 0 & 0 & 1 \end{bmatrix} \cdot \begin{bmatrix} r_a \\ r_b \\ r_c \end{bmatrix}$$

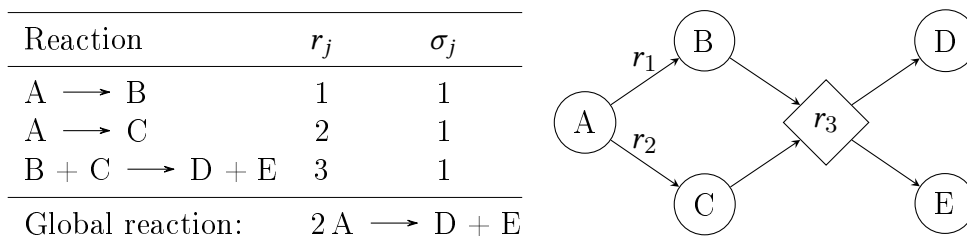
Thus, establishing that: (i)  $r_1 = 3(\varrho_1 + \varrho_2) = r_a + r_b + r_c$ , (ii)  $r_2 = \varrho_1 + 2\varrho_2 = r_c$ , (iii)  $r_3 = \varrho_1 = r_b$ , (iv)  $r_4 = \varrho_1 + \varrho_2 = r_a$ , and (v)  $r_5 = \varrho_1 + 2\varrho_2 = r_c$ . Therefore,  $r_1 = r_2 + r_3 + r_4$  and  $r_2 = r_5$  in steady conditions.

For nonlinear networks, the previous analysis is not as simple as it is for linear networks since more than one node is involved in a single (nonlinear) reaction step. However, if the abstraction of the nodes is considered and the concept of path is performed by imagining a sequence of events, it is possible to obtain an analogy with the analysis performed for linear networks. Let us consider the previous example in Figure 2.6, in which species B and C are intermediates, the matrices and vectors previously described assume these values:

$$\mathbf{N}^{*T} = \begin{array}{cccc} & r_1 & r_2 & r_3 & r_4 \\ \begin{array}{c} \text{B} \\ \text{C} \end{array} & \begin{bmatrix} 1 & -2 & 0 & 0 \\ 0 & 0 & 1 & -1 \end{bmatrix} & & & \end{array} \quad \mathbf{\Omega}^T = \begin{array}{cc} \text{(a)} & \text{(b)} \\ \begin{bmatrix} 0 & 2 \\ 0 & 1 \\ 1 & 0 \\ 1 & 0 \end{bmatrix} & \begin{array}{c} r_1 \\ r_2 \\ r_3 \\ r_4 \end{array} \end{array} \quad \boldsymbol{\beta} = \begin{array}{c} \begin{bmatrix} 1 \\ 1 \end{bmatrix} \\ \text{(a)} \\ \text{(b)} \end{array} \quad \boldsymbol{\sigma} = \begin{array}{c} \begin{bmatrix} 2 \\ 1 \\ 1 \\ 1 \end{bmatrix} \\ r_1 \\ r_2 \\ r_3 \\ r_4 \end{array}$$

Note that, differently of linear networks, the basis vectors of  $\mathbf{\Omega}^T$  present values superior than unity. The first column basis vector of  $\mathbf{\Omega}^T$ , represented by (a), contains the reaction  $r_3$  and  $r_4$ , establishing the path  $A \rightarrow C \rightarrow D$ ; and the column vector (b) establishes  $2A \rightarrow 2B \rightarrow D + E$ , concerning  $2r_1$  and  $r_2$ . The single pathway is, thus, established through the sum of both basic paths, resulting in the global reaction  $3A \rightarrow 2D + E$ .

In the example of a nonlinear network shown in Figure 2.9, there is a single basic vector that forms the single pathway,  $\boldsymbol{\sigma} = \boldsymbol{\omega}^T$ , where the symbol  $\boldsymbol{\omega}$  is used to indicate a row vector of  $\mathbf{\Omega}$ . Note that the first step of this pathway is related to  $r_1$  plus  $r_2$ , and the second to  $r_3$ . Once  $r_1$  and  $r_2$  occur in parallel reactions, the joining of both reaction components maintains the same rate of the slowest one, but, since there is steady condition, *i.e.*, B and C are intermediate species in which the rate of their production equals the consumption rate, these invariants are established:  $r_1 = r_2 = r_3 = \rho$ .



$$\mathbf{N}^{*T} = \begin{array}{ccc} & r_1 & r_2 & r_3 \\ \begin{array}{c} \text{B} \\ \text{C} \end{array} & \begin{bmatrix} 1 & 0 & -1 \\ 0 & 1 & -1 \end{bmatrix} & & \end{array} \quad \boldsymbol{\omega}^T = \begin{array}{c} \text{(a)} \\ \begin{bmatrix} 1 \\ 1 \\ 1 \end{bmatrix} \end{array} \begin{array}{c} r_1 \\ r_2 \\ r_3 \end{array} \quad \boldsymbol{\beta} = 1 \quad \boldsymbol{\sigma} = \begin{array}{c} \begin{bmatrix} 1 \\ 1 \\ 1 \end{bmatrix} \\ r_1 \\ r_2 \\ r_3 \end{array}$$

**Figure 2.9** Horiuti numbers and related matrices for a nonlinear network composed by a linearly independent set of reactions, with two intermediate species, B and C.

Yablonsky et al. (1991) wrote: “The application of the concept of *the rate along the basic route* provides a possibility of obtaining a new formulation for the quasi-stationary conditions in terms of the Horiuti theory which is different from the ordinary one, *i.e.*, *the formation of an intermediate is equal to that of its consumption*. Temkin called the equations obtained *the conditions for the stationarity of steps*.”

Pantea et al. (2014) studied the use of quasi-steady-state assumption for model reduction in chemical reaction systems operating at unsteady conditions. In this case the steady-

state assumption is adopted to eliminate highly reactive intermediate species and remove large rate constants that cannot be determined from concentration measurements. They demonstrated with examples that the classical model reduction method has the advantages of (i) allowing an easier model validation (since the reduced model covers species that are observed to greater extents), (ii) facilitating the estimation of parameters (since slower kinetics are presented in this reduced version of the model in contrast to the original model in which in practice the origin of intermediate species cannot be accurately identified), and (iii) avoiding numerical problems.

Although the theory of steady-state reaction systems described in this section is different from what we are interested in performing — modeling the dynamics of reaction systems, *i.e.*, finding networks that match unsteady-state conditions — the concepts covered by this theory are very useful in the task of generating feasible networks (connected and consistent structures) without the support of experimental data, but instead, considering structural fluxes in steady conditions, as it will be shown in later sections. Therefore, the identification of alternative reaction paths existing in a given reaction network constitutes a fundamental problem in the analysis of the corresponding kinetic models, which can be carried out either through the study of the properties of the corresponding network, or through the analysis of the algebraic properties of matrices that describe this network. Another possibility consists, for example, in the analysis of the stoichiometric matrix of the set of chemical reactions. This topic is considered in the next section.

## 2.2 The stoichiometric matrix properties

*“The stoichiometric matrix is so informative about physiological states that we must study its fundamental properties.”*

– John Doyle

This section describes the meaning of the spatial relationships between vectors in a linear system of equations, namely to understand the relationships between reaction fluxes and species fluxes through the linear transformation that the stoichiometric matrix represents. The concepts that emerge from this study are essential/fundamental for a complete understanding of the meaning of each component of a linear system of equations and how they can be decomposed/visualized in fundamental subspaces of a matrix, always having in view the interpretation of these properties to extract their physical meaning, allowing a better identification of chemical reaction systems.

Thus, these concepts will be necessary to understand: what (i) are invariant relationships in reaction systems, (ii) the steady state means and how these two concepts are related to network connectivity properties and representation of linear and nonlinear structures, (iii) the dynamic state represents and how this is related to the dynamic reaction component, as well as other concepts.

The terminology “flux” is widely used. Here, these quantities do not represent flow of species (per unit of area and time); instead they represent a rate of change, or simply a change through a specific network of connections, and hence they are more similar to flowrates. *Species fluxes* can be represented by cumulative changes of number of moles or concentration changes, the rate of molar changes or the concentration derivatives. They are response/dependent variables of the species mass balances, both in the rate- or the extent-based approaches. *Reaction fluxes* can be reaction rates (moles per time and per unit of volume or not) or reaction extents (moles). They are the unknown vectors (variables) in the species mass balances. Rate- and extent-based approaches are (approximately) equivalent, depending on the available data relating to a case study and the choice of the type of methods one wants to work with. In fact we want to correlate species fluxes with reaction fluxes in order to identify the reaction network.

### 2.2.1 The stoichiometric matrix

The stoichiometric matrix is the starting point for various mathematical analysis used to determine the properties of chemical reaction networks (Palsson, 2006b). It contains chemical and network (structural) information related to the rules of chemistry and reaction interconnections. As presented in Section 2.1.3, the stoichiometric matrix  $\mathbf{N} \in \mathbb{Z}^{n_{\text{rx}} \times n_{\text{st}}}$  is composed by integer coefficients consisting of the number of molecules participating in the reaction. This number is the stoichiometric coefficient  $\nu_{j,s}$  that assumes negative and positive values for reagent and product species  $s \in \text{st}$ , respectively, in the chemical reaction  $j \in \text{rx}$ . We define here  $\text{st}$  and  $\text{rx}$  as the sets of species and reactions, respectively, that compose the network, and,  $n_{\text{st}}$  and  $n_{\text{rx}}$  as their cardinals. Therefore, the stoichiometric matrix is composed by  $n_{\text{rx}}$  rows and  $n_{\text{st}}$  columns with  $n_{\text{rx}}n_{\text{st}}$  entries  $\nu_{j,s}$ . Figure 2.10 presents an schematic representation of the transposed stoichiometric matrix.

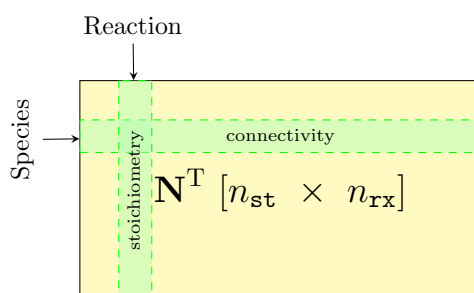


**Figure 2.10** Schematic representation of  $\mathbf{N}^T$ . Notice that every column  $j = 1, \dots, n_{\text{rx}}$  and every row  $s = 1, \dots, n_{\text{st}}$  contain, respectively, information related to the stoichiometry of species and to the connectivity of reactions.

As represented by the green lines in Figure 2.10, each column  $j \in \text{rx}$  describes a *reaction* that is constrained by the rules of chemistry, such as elemental balancing, thus establishing the stoichiometric relationships. Each row  $s \in \text{st}$  describes the reactions in which the *species*  $s$  participates and therefore how the reactions are interconnected, forming the

reaction network (Palsson, 2006b).

In batch chemical reaction systems, assumed to be of constant volume, the stoichiometric matrix represents a *linear transformation* of the instantaneous reaction flux vector  $\mathbf{r}(t) \in \mathbb{R}_+^{n_{rx}}$  to a vector of time derivatives of the species concentration vector  $\mathbf{c}(t) \in \mathbb{R}_+^{n_{st}}$ , establishing the dynamic mass balances:

$$\frac{d\mathbf{c}(t)}{dt} = \mathbf{N}^T \cdot \mathbf{r}(t) \quad \Leftrightarrow \quad \frac{d\mathbf{c}(t)}{dt} = \sum_{j=1}^{n_{rx}} \boldsymbol{\nu}_j r_j(t) \quad (2.7)$$

where  $\boldsymbol{\nu}_j \equiv \boldsymbol{\nu}_{*,j}$  is the column  $j$  of the transposed stoichiometric matrix, and  $r_j(t)$  the instantaneous reaction flux related to the reaction component  $j \in rx$ . In general  $\mathbf{r}(t)$  is a vector of variables of the previous function, thus, it belongs to the *codomain* while  $d\mathbf{c}(t)/dt$  to the *domain* of the linear transformation. Note that the stoichiometric matrix is a mathematical mapping operation.

The next section presents the four fundamental subspaces associated with the stoichiometric matrix and how we can mathematically define them and interpret their contents in (bio)chemical terms.

### 2.2.2 The fundamental subspaces of the stoichiometric matrix

There are four fundamental subspaces associated with  $\mathbf{N}^T$  that assume important roles in the chemical physical properties of the system, namely, the column and the row spaces, and, the left and the right null spaces. The column and row spaces of  $\mathbf{N}^T$  are spanned by the respective basic columns and basic rows of this matrix, *i.e.*, the ones that present pivot coefficients after a Gauss-Jordan decomposition (Meyer, 2000). The left and right null spaces are defined through any set of linearly independent vectors that satisfies, respectively, the next homogeneous systems of equations, such that

$$\mathbf{N} \cdot \mathbf{w}_k = \mathbf{0}, \quad k = 1, \dots, n_{st} - R \quad \text{and} \quad \mathbf{N}^T \cdot \mathbf{x}_k = \mathbf{0}, \quad k = 1, \dots, n_{rx} - R \quad (2.8)$$

where  $R$  is the matrix rank of  $\mathbf{N}$ , and,  $\mathbf{w}_k \in \mathbb{R}^{n_{st}}$  and  $\mathbf{x}_k \in \mathbb{R}^{n_{rx}}$  belong to the left and right null spaces of  $\mathbf{N}^T$ , respectively. Therefore, the dimensions of the left and right null spaces of  $\mathbf{N}^T$  are the differences among the number of rows (species) and  $R$ , and among the number of columns (chemical reactions) and  $R$ , respectively. These differences, *i.e.*, the left and the right null spaces dimensions, establish the number of linearly dependent relationships among species and chemical reactions, respectively. On the other hand,  $R$  represents the number of linearly independent relationships in both sets of chemical reactions (columns) and chemical species (rows), which all of them compose the reaction network.

The row and (right) null spaces are complementary and orthogonal with each other,

supporting information related to the set of chemical reactions, such that<sup>5</sup>:

$$n_{rx} = \dim\left(\text{null}\left(\mathbf{N}^T\right)\right) + \dim\left(\text{row}\left(\mathbf{N}^T\right)\right) \quad (2.9)$$

forming the place where  $\mathbf{r}(t) \in \mathbb{R}_+^{n_{rx}}$  belongs. In fact the reaction rate vector can be decomposed in two components:

$$\mathbf{r}(t) = \mathbf{r}_{ss}(t) + \mathbf{r}_{dyn}(t) \quad (2.10)$$

in which  $\mathbf{r}_{ss} \in \text{null}\left(\mathbf{N}^T\right)$  is related to the *steady-state* component and  $\mathbf{r}_{dyn} \in \text{row}\left(\mathbf{N}^T\right)$  with the *dynamic* component. Hence, both reaction components can be written as linear combinations of the respective basis vectors that form each space:

$$\mathbf{r}_{ss} = \sum_{k=1}^{n_{rx}-R} \mathbf{x}_k \alpha_k \quad \text{and} \quad \mathbf{r}_{dyn} = \sum_{s=1}^R \boldsymbol{\nu}_s \beta_s \quad (2.11)$$

where  $\alpha_k$  and  $\beta_s$  are, respectively, the coordinates of the steady-state and dynamic reaction components in the related bases  $\mathbf{x}_k$ ,  $k = 1, \dots, n_{rx} - R$  and  $\boldsymbol{\nu}_s \equiv \boldsymbol{\nu}_{s,*}$ ,  $s = 1, \dots, R$ , the basis vectors that span, respectively, the null and the row spaces of  $\mathbf{N}^T$ .

Therefore  $\text{null}\left(\mathbf{N}^T\right)$  contains all steady-state reaction flux components of interest for homeostatic states that occurs in several (bio) living systems and chemical systems that operates in steady conditions, while  $\text{row}\left(\mathbf{N}^T\right)$  embraces all dynamic reaction flux distributions and thermodynamic driving forces responsible to reaction activity changes (Palsson, 2006b).

On the other hand, the column and left null spaces, also complementary and orthogonal with each other, support information related to the set of species such that

$$n_{st} = \dim\left(\text{leftNull}\left(\mathbf{N}^T\right)\right) + \dim\left(\text{col}\left(\mathbf{N}^T\right)\right) \quad (2.12)$$

forming the required dimension of the concentration derivative vector,  $d\mathbf{c}(t)/dt \in \mathbb{R}^{n_{st}}$ , that belongs to this place. Similarly with the reaction rate vector, the concentration derivative vector can also be decomposed in two components

$$\frac{d\mathbf{c}(t)}{dt} = \frac{d\mathbf{c}(t)}{dt}_{ss} + \frac{d\mathbf{c}(t)}{dt}_{dyn} \quad (2.13)$$

in which the steady-state component  $d\mathbf{c}(t)/dt_{ss} \in \text{leftNull}\left(\mathbf{N}^T\right)$  and the dynamic  $d\mathbf{c}(t)/dt_{dyn} \in \text{col}\left(\mathbf{N}^T\right)$ . Therefore, both components constitute linear combinations of their respective

---

<sup>5</sup>From the typical linear algebra naming convention, null space refers to the right null space of an array. Therefore, the left null space always needs to be referred to as the left null space, while the right one does not, by convention.



bases:

$$\frac{dc(t)}{dt}_{ss} = \sum_{k=1}^{n_{st}-R} \mathbf{w}_k \gamma_k \quad \text{and} \quad \frac{dc(t)}{dt}_{dyn} = \sum_{j=1}^R \boldsymbol{\nu}_j \delta_j \quad (2.14)$$

where  $\gamma_k$  and  $\delta_j$  are the coordinates of the corresponding  $dc(t)/dt$  component in the related basis formed by  $\mathbf{w}_k, k = 1, \dots, n_{st} - R$ , and  $\boldsymbol{\nu}_j, j = 1, \dots, R$ , the basis vectors that span the left null and the column spaces of  $\mathbf{N}^T$ , respectively.

The leftNull( $\mathbf{N}^T$ ) addresses *conservation relationships* among chemical species during the reaction event, establishing *time or reaction invariants* of the chemical reaction system. This topic, invariants in chemical system, is discussed in more detail in the next section. On the other hand, the col( $\mathbf{N}^T$ ) contains all time derivatives of the species concentrations, presenting how the concentration states change in face of thermodynamic driving forces (Palsson, 2006b).

Therefore (2.7) can be rewritten as

$$\begin{aligned} \frac{dc(t)}{dt}_{ss} + \frac{dc(t)}{dt}_{dyn} &= \mathbf{N}^T \cdot (\mathbf{r}_{ss}(t) + \mathbf{r}_{dyn}(t)) \Leftrightarrow \\ \sum_{k=1}^{n_{st}-R} \mathbf{w}_k \gamma_k + \sum_{j=1}^R \boldsymbol{\nu}_j \delta_j &= \mathbf{N}^T \cdot \left( \sum_{k=1}^{n_{rx}-R} \mathbf{x}_k \alpha_k + \sum_{s=1}^R \boldsymbol{\nu}_s \beta_s \right) \Leftrightarrow \\ \mathbf{W} \cdot \boldsymbol{\gamma} + \mathbf{N}^T \cdot \boldsymbol{\delta} &= \mathbf{N}^T \cdot \mathbf{X} \cdot \boldsymbol{\alpha} + \mathbf{N}^T \cdot \mathbf{N} \cdot \boldsymbol{\beta} \end{aligned} \quad (2.15)$$

where  $\mathbf{W}[n_{st} \times n_{st} - R]$  is the matrix composed by column vectors  $\mathbf{w}_k$  that span the left null space of  $\mathbf{N}^T$ , and  $\boldsymbol{\gamma}$  and  $\boldsymbol{\delta}$  are the vectors of coordinates of the type  $\gamma_k$  and  $\delta_j$ , respectively; and  $\mathbf{X}[n_{rx} \times n_{rx} - R]$  is the matrix composed by the column vectors  $\mathbf{x}_k$  that span the null space of  $\mathbf{N}^T$ , and  $\boldsymbol{\alpha}$  and  $\boldsymbol{\beta}$  are the vectors of coordinates of the type  $\alpha_k$  and  $\beta_s$ , respectively.

Notice that:

- (i)  $\mathbf{W} \cdot \boldsymbol{\gamma} = \mathbf{0}[n_{st} \times 1]$ ,
- (ii)  $\delta_j = 0$  for every non basic column  $\boldsymbol{\nu}_j$  of  $\mathbf{N}^T$ , *i.e.*,  $j = R + 1, \dots, n_{rx}$ ,
- (iii)  $\mathbf{N}^T \cdot \mathbf{X} = \mathbf{0}[n_{rx} \times 1]$ , and
- (iv)  $\beta_s = 0$  for every non basic column  $\boldsymbol{\nu}_s$  of  $\mathbf{N}$ , *i.e.*,  $s = R + 1, \dots, n_{st}$ .

Therefore, the relation in (2.15) can be simplified to

$$\mathbf{N}^T \cdot \boldsymbol{\delta} = \mathbf{N}^T \cdot \mathbf{N} \cdot \boldsymbol{\beta} \quad (2.16)$$

where, it can be observed that

$$\boldsymbol{\delta} = \mathbf{N} \cdot \boldsymbol{\beta} \quad (2.17)$$

This last equation demonstrates that the vector of coordinates of the concentration derivative vector lie in the row space of the stoichiometric matrix. In fact, it is the  $\mathbf{r}_{\text{dyn}}$  in (2.11).

Thus, when considering the segregated analysis of the steady and the dynamic states, both components obey their respective linear transformations, such that:

$$\frac{d\mathbf{c}(t)}{dt}_{\text{ss}} = \mathbf{N}^T \cdot \mathbf{r}_{\text{ss}}(t) \quad \text{and} \quad \frac{d\mathbf{c}(t)}{dt}_{\text{dyn}} = \mathbf{N}^T \cdot \mathbf{r}_{\text{dyn}}(t) \quad (2.18)$$

where the component  $d\mathbf{c}(t)/dt_{\text{ss}}$  (the null vector with dimension  $n_{\text{st}}$ ) corresponds to the image of  $\mathbf{r}_{\text{ss}}(t)$  after the linear transformation in (2.18). Hence  $d\mathbf{c}(t)/dt = d\mathbf{c}(t)/dt_{\text{dyn}}$  and it is located in  $\text{col}(\mathbf{N}^T)$ . Although  $d\mathbf{c}(t)/dt_{\text{ss}} \in \mathbb{R}^{n_{\text{st}}}$  living in  $\text{leftNull}(\mathbf{N}^T)$ , it also belongs to  $\text{col}(\mathbf{N}^T)$ ; one of the necessary conditions of a given space is to own the null vector of its dimension (Meyer, 2000). Hence  $d\mathbf{c}(t)/dt_{\text{ss}}$  lives in the intersection of both column and left null spaces of  $\mathbf{N}^T$ , representing the origin dot.

Another way to view the previous description is to note that the null inner product is verified through

$$\langle \mathbf{w}_k, \boldsymbol{\nu}_j \rangle = 0, \quad k = 1, \dots, n_{\text{st}} - R \quad \text{and} \quad j = 1, \dots, n_{\text{rx}} \quad (2.19)$$

demonstrating the orthogonality among  $\text{leftNull}(\mathbf{N}^T)$  and  $\text{col}(\mathbf{N}^T)$ .

Moreover, the subspace  $\text{col}(\mathbf{N}^T)$  is limited (or bounded), *i.e.*, only a portion of this space is explored since the reaction fluxes  $r_j$  have a maximum value, *i.e.*,  $r_j \leq r_{j,\text{max}}$ , thus limiting the size of the time derivatives.

### Pedagogical example

Consider the following example in Figure 2.11 to illustrate the concepts that were introduced during this section. The system is composed by three species and three chemical reactions:



**Figure 2.11** Reaction network with a redundant pathway and corresponding stoichiometric matrix.

The three chemical reactions of Figure 2.11 form a linearly dependent set since one of them can be written as a linear combination of the others (for example:  $r_3 = r_1 + r_2$ ).

The vectors that satisfy the respective homogeneous system of equations in (2.8) are:

$$\mathbf{w} = z \begin{bmatrix} 1 \\ 1 \\ 1 \end{bmatrix} : z \in \mathbb{R} \quad \text{and} \quad \mathbf{x} = q \begin{bmatrix} 1 \\ 1 \\ -1 \end{bmatrix} : q \in \mathbb{R}$$

which span, respectively, the left and right null spaces of  $\mathbf{N}^T$ .

The first two columns and two rows span the column and the row spaces, respectively, of  $\mathbf{N}^T$ . Hence the four subspaces are given by:

$$\text{col}(\mathbf{N}^T) = \begin{bmatrix} -1 & 0 \\ 1 & -1 \\ 0 & 1 \end{bmatrix} \quad \text{row}(\mathbf{N}^T) = \begin{bmatrix} -1 & 1 \\ 0 & -1 \\ -1 & 0 \end{bmatrix} \quad \text{leftNull}(\mathbf{N}^T) = \begin{bmatrix} 1 \\ 1 \\ 1 \end{bmatrix} \quad \text{null}(\mathbf{N}^T) = \begin{bmatrix} 1 \\ 1 \\ -1 \end{bmatrix}$$

Assume, for example, that for a given instant  $t$  the concentration derivatives vector and the reaction rates vector are, respectively:

$$\frac{d\mathbf{c}(t)}{dt} = \begin{bmatrix} -4 \\ -1 \\ 5 \end{bmatrix} \quad \text{and} \quad \mathbf{r}(t) = \begin{bmatrix} 1 \\ 2 \\ 3 \end{bmatrix}$$

Thus one can verify that both equations in (2.11) hold:

$$\begin{bmatrix} \alpha \\ \alpha \\ -\alpha \end{bmatrix} = \begin{bmatrix} 1 \\ 1 \\ -1 \end{bmatrix} \cdot \alpha, \quad \forall \alpha \in \mathbb{R} \quad \text{and} \quad \begin{bmatrix} 1 \\ 2 \\ 3 \end{bmatrix} = \begin{bmatrix} -1 & 1 \\ 0 & -1 \\ -1 & 0 \end{bmatrix} \cdot \begin{bmatrix} 4 \\ 5 \end{bmatrix}$$

and the same for both equations in (2.14):

$$\begin{bmatrix} \gamma \\ \gamma \\ \gamma \end{bmatrix} = \begin{bmatrix} 1 \\ 1 \\ 1 \end{bmatrix} \cdot \gamma, \quad \forall \gamma \in \mathbb{R} \quad \text{and} \quad \begin{bmatrix} -4 \\ -1 \\ 5 \end{bmatrix} = \begin{bmatrix} -1 & 0 \\ 1 & -1 \\ 0 & 1 \end{bmatrix} \cdot \begin{bmatrix} -3 \\ -2 \end{bmatrix}$$

and (2.10) and (2.13) are, respectively, satisfied with  $\alpha = \gamma = 0$ :

$$\begin{bmatrix} 1 \\ 2 \\ 3 \end{bmatrix} = 0 \begin{bmatrix} 1 \\ 1 \\ -1 \end{bmatrix} + \begin{bmatrix} 1 \\ 2 \\ 3 \end{bmatrix} \quad \text{and} \quad \begin{bmatrix} -4 \\ -1 \\ 5 \end{bmatrix} = 0 \begin{bmatrix} 1 \\ 1 \\ 1 \end{bmatrix} + \begin{bmatrix} -4 \\ -1 \\ 5 \end{bmatrix}$$

However, if we consider the reaction rate vector as any solution that satisfies the under-

determined system of equations with this fixed  $dc(t)/dt$ , such that:

$$\begin{bmatrix} -4 \\ -1 \\ 5 \end{bmatrix} = \begin{bmatrix} -1 & 0 & -1 \\ 1 & -1 & 0 \\ 0 & 1 & 1 \end{bmatrix} \cdot \begin{bmatrix} 4-z \\ 5-z \\ z \end{bmatrix} \quad \text{with } 0 \leq z \leq 4$$

and consider (2.10) such that

$$\begin{bmatrix} 4-z \\ 5-z \\ z \end{bmatrix} = (3-z) \begin{bmatrix} 1 \\ 1 \\ -1 \end{bmatrix} + \begin{bmatrix} -1 & 0 \\ 1 & -1 \\ 0 & 1 \end{bmatrix} \cdot \begin{bmatrix} -3 \\ -2 \end{bmatrix}$$

it is notable that the degree of freedom  $z$  exists due to the existence of null  $(\mathbf{N}^T)$ .

Also, it is possible to verify from (2.15) that

$$\begin{bmatrix} -1 & 0 \\ 1 & -1 \\ 0 & 1 \end{bmatrix} \cdot \begin{bmatrix} \delta_1 \\ \delta_2 \end{bmatrix} = \begin{bmatrix} -1 & 0 & -1 \\ 1 & -1 & 0 \\ 0 & 1 & 1 \end{bmatrix} \cdot \begin{bmatrix} -1 & 1 \\ 0 & -1 \\ -1 & 0 \end{bmatrix} \cdot \begin{bmatrix} \beta_1 \\ \beta_2 \end{bmatrix}$$

where  $\delta_1 = -2\beta_1 + \beta_2$  and  $\delta_2 = -\beta_1 - \beta_2$ , with  $0 \geq \beta_2 \geq \beta_1$ . Note that this relationship

$$\boldsymbol{\delta} = \begin{bmatrix} -2 & 1 \\ -1 & -1 \end{bmatrix} \cdot \boldsymbol{\beta}$$

is valid only for these pair of basis that were chosen to represent  $\text{col}(\mathbf{N}^T)$  and  $\text{row}(\mathbf{N}^T)$ . Hence, naturally, the correlation among coordinates in each basis depends on the basis adopted.

Finally, notice that the left null space showed only a single conservation relationship among species A, B, C, indicating that they present the same, for example, amounts of carbon element, establishing an invariant among isomers molecules type. However, this example is a simple illustration about the stoichiometric spaces, where no information regarding the species molecular formula is provided. Notice that the orthogonality properties among left null and column spaces hold:

$$[1 \ 1 \ 1] \cdot \begin{bmatrix} -1 \\ 1 \\ 0 \end{bmatrix} = 0 \quad \text{and} \quad [1 \ 1 \ 1] \cdot \begin{bmatrix} 0 \\ -1 \\ 1 \end{bmatrix} = 0$$

as such as for null and row spaces:

$$[1 \ 1 \ -1] \cdot \begin{bmatrix} -1 \\ 0 \\ -1 \end{bmatrix} = 0 \quad \text{and} \quad [1 \ 1 \ -1] \cdot \begin{bmatrix} 1 \\ -1 \\ 0 \end{bmatrix} = 0$$

which is an obvious consequence since both null spaces are determined by solving their respective homogeneous system of equations, *i.e.*, the inner product is equivalent to a single equation of the homogeneous system of equations.

Although the complete description of the four subspaces of the stoichiometric matrix has been considered in this section, an additional analysis can be made showing the interconnection of the same subspaces using different bases that have particular characteristics: they are *orthonormal*, *i.e.*, they constitute a rotation of the previous bases in such a way that all vectors are orthogonal to each other, and also have the same unit length, ( $\ell_2$ -norm equal to one, unit vectors). This is the topic that follows next. An introduction about what is this technique and where it is used is presented in Appendix I.1.

### 2.2.3 The Singular Value Decomposition of $\mathbf{N}$

Unlike matrices that comprise experimental data with uncertain, sparse and incomplete measurements, the stoichiometric matrix  $\mathbf{N}$  is a “perfect” matrix with integer coefficients describing the structure of a reaction network. The Singular Value Decomposition (SVD) of  $\mathbf{N}^T$  is a particularly useful manner to obtain the basic information about the four fundamental subspaces of  $\mathbf{N}^T$  defined in the previous section, and thus it can be used to analyze network properties<sup>6</sup>.

The four fundamental spaces of  $\mathbf{N}^T$  are presented in Figure 2.12, where the columns of  $\mathbf{U}$  matrix represent  $\text{col}(\mathbf{N}^T)$  and  $\text{leftNull}(\mathbf{N}^T)$  through the purple and non colored areas, respectively, and the columns of  $\mathbf{V}$  matrix represent the  $\text{row}(\mathbf{N}^T)$  and  $\text{null}(\mathbf{N}^T)$  through the purple and non colored areas, respectively.

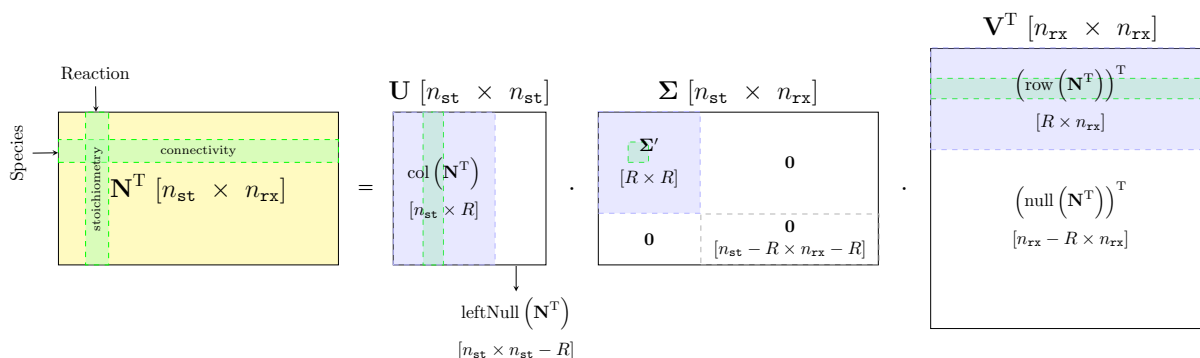


**Figure 2.12** Schematic representation of the SVD of  $\mathbf{N}^T$ .

Once the matrices  $\mathbf{U}$  and  $\mathbf{V}$  from SVD are orthonormal, the physical and chemical properties such as number of moles involved in each chemical reaction, mass conservation relationships, reaction rates, etc, are not easily (or directly) interpreted through the en-

<sup>6</sup>In the context of metabolic networks, they adopt the symbol  $\mathbf{S}$  for representing the transposed stoichiometric matrix ( $\mathbf{S} \equiv \mathbf{N}^T$ ). However, we follow the classic nomenclature using the symbol  $\mathbf{N}^T$ .

tries of these matrices. Hence orthonormal basis vectors are mathematically convenient, but not necessarily biologically or chemically meaningful (Palsson, 2015).

However, the first  $R$  columns of  $\mathbf{U}$  depict the stoichiometric relationships among species in every chemical reaction, analogous to a single column of  $\mathbf{N}^T$ , representing a single reaction. The corresponding column of  $\mathbf{V}$  presents the combination of the reaction fluxes that drive these stoichiometric relationships, thus, presenting the connectivity among chemical reactions in the network. Therefore the column space contains the direction of motion and the row space the drivers for motion. To compute the resulting dynamic states, one needs kinetic constants (Palsson, 2015).

Similarly with (I.5), the SVD of  $\mathbf{N}$  can be written as

$$\mathbf{N} \cdot \mathbf{U} = \mathbf{V} \cdot \Sigma \quad (2.20)$$

where the interrelationships of subspaces can be seen more easily. When separating the null spaces from columns and row spaces, it is clear to observe in Figure 2.13 that  $\mathbf{N}$  maps the  $\text{col}(\mathbf{N}^T)$  onto  $\text{row}(\mathbf{N}^T)$  scaled (stretched) by the corresponding  $\sigma$  value. On the other hand, the null spaces are also interconnected satisfying the same linear transformation in (2.20), see Figure 2.14.

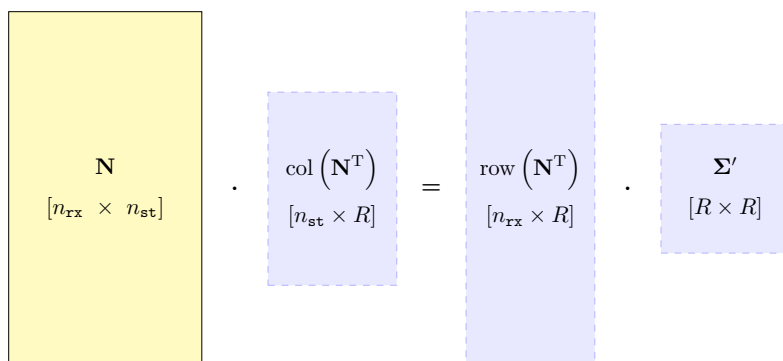


**Figure 2.13** Schematic representation of  $\text{SVD}(\mathbf{N})$  with its characteristic subspaces.

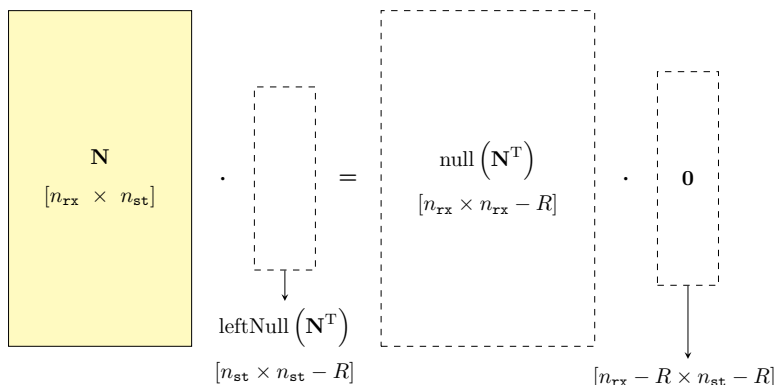


**Figure 2.14** Schematic representation of  $\text{SVD}(\mathbf{N})$  with its null spaces.

Similarly with (I.6), the next equation can be written as

$$\mathbf{N}^T \cdot \mathbf{V} = \mathbf{U} \cdot \Sigma \quad (2.21)$$

and not differently from previous observations,  $\mathbf{N}^T$  maps the row  $(\mathbf{N}^T)$  onto  $\text{col}(\mathbf{N}^T)$  stretched by the corresponding  $\sigma$  value, as shown in Figure 2.15.

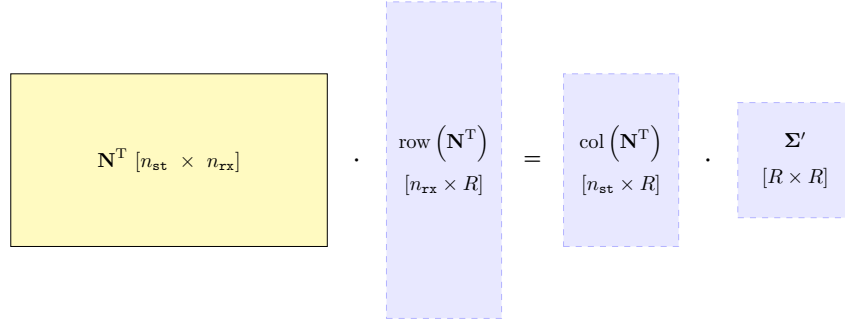


**Figure 2.15** Schematic representation of the  $\text{SVD}(\mathbf{N}^T)$  with its characteristics subspaces interconnections.

Which can also be schematized with regard to the linear transformation in (2.21) for null spaces, as presented in Figure 2.16.

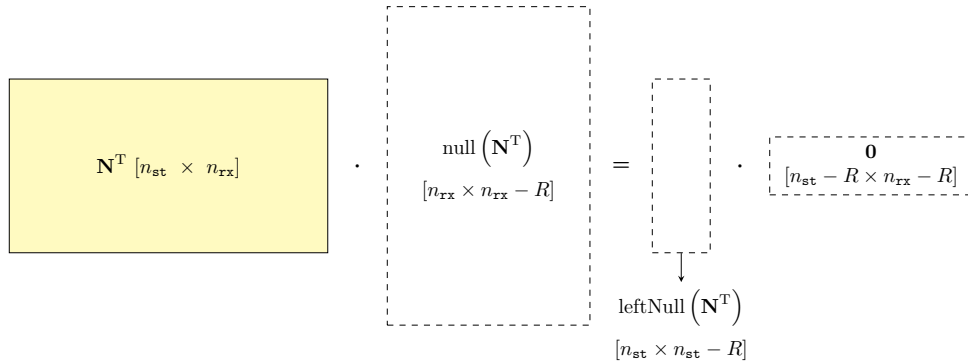


**Figure 2.16** Null spaces interconnection of  $\mathbf{N}^T$ .

Note that eqs. (I.5) and (I.6) represent only the part related to linearly independent sets of the column and row spaces of the stoichiometric matrix, *i.e.*, the ones showed in Figures 2.13 and 2.15, whereas eqs. (2.20) and (2.21) cover the four subspaces.

If we consider the first equation presented in this section, the dynamic balance in (2.7), with additional matrices operations the equation still satisfied as

$$\mathbf{U}^T \cdot \frac{d\mathbf{c}(t)}{dt} = \mathbf{U}^T \cdot \mathbf{N}^T \cdot \mathbf{V} \cdot \mathbf{V}^T \cdot \mathbf{r}(t) \quad \text{or} \quad \frac{d\mathbf{U}^T \cdot \mathbf{c}(t)}{dt} = \Sigma \cdot \mathbf{V}^T \cdot \mathbf{r}(t) \quad (2.22)$$

Therefore, the left singular vectors in  $\mathbf{U}$  form linear combinations of the concentration

variables and the right singular vectors in  $\mathbf{V}$  form linear combinations of the reaction fluxes. In fact every inner product of the component  $\mathbf{u}_i$  from  $\text{col}(\mathbf{N}^T)$  with the species concentration vector, *i.e.*,

$$\mathbf{u}_i^T \cdot \mathbf{c} = u_{i,1}c_1 + u_{i,2}c_2 + \dots + u_{i,n_{\text{st}}}c_{n_{\text{st}}} \quad (2.23)$$

is being uniquely moved by a linear combination of reaction fluxes in the row  $(\mathbf{N}^T)$ , such as

$$\mathbf{v}_i^T \cdot \mathbf{r} = v_{i,1}r_1 + v_{i,2}r_2 + \dots + v_{i,n_{\text{rx}}}r_{n_{\text{rx}}} \quad (2.24)$$

and the extent of this motion is given by  $\sigma_i$ .

An important feature of SVD is that the singular vectors are orthonormal to each other, and consequently each of the  $i$ th motions in eqs. (2.23) and (2.24) are, at maximum, structurally decoupled, *i.e.*, there is no correlation among the linear combinations of species concentration as such as among reaction flux linear combinations (Palsson, 2006b).

This concept defines *eigen-reactions* or *systemic reactions* as

$$\sum_{s \in u_{i,s} < 0}^{n_{\text{st}}} \mathbf{u}_{i,s} c_s \xrightleftharpoons[\sum_{j \in v_{i,j} < 0}^{n_{\text{rx}}} v_{i,j} r_j]{\sum_{j \in v_{i,j} > 0}^{n_{\text{rx}}} v_{i,j} r_j} \sum_{s \in u_{i,s} > 0}^{n_{\text{st}}} \mathbf{u}_{i,s} c_s, \quad i = 1, \dots, R \quad (2.25)$$

where the elements of  $\mathbf{u}_i$  are equivalent to *systemic stoichiometric coefficients* analogous to  $v_{s,j}$  in vectors  $\boldsymbol{\nu}_j$  that compose the columns of  $\mathbf{N}^T$ ; and the elements of  $\mathbf{v}_i$  are *systemic participation numbers*. Hence reactions with positive fluxes correspond to reactions driving the systemic reaction forward, while those with negative fluxes drive it in the reverse direction. The concept of systemic reactions has been used in the literature in the context of metabolic network identification for studying the systems biology of metabolism, describing the function of the metabolic network as a whole (Famili and Palsson, 2003b).

### Pedagogical example

Following the same pedagogical example previously presented in Figure 2.11, the SVD of  $\mathbf{N}^T$  leads to the following matrices:

$$\mathbf{U} = \frac{\sqrt{3}}{3} \begin{bmatrix} -\sqrt{2} & 0 & 1 \\ \frac{1}{\sqrt{2}} & -\sqrt{\frac{3}{2}} & 1 \\ \frac{1}{\sqrt{2}} & \sqrt{\frac{3}{2}} & 1 \end{bmatrix} \quad \mathbf{\Sigma} = \frac{\sqrt{3}}{3} \begin{bmatrix} 3 & 0 & 0 \\ 0 & 3 & 0 \\ 0 & 0 & 0 \end{bmatrix} \quad \mathbf{V}^T = \frac{\sqrt{3}}{3} \begin{bmatrix} \sqrt{\frac{3}{2}} & 0 & \sqrt{\frac{3}{2}} \\ -\frac{1}{\sqrt{2}} & \sqrt{2} & \frac{1}{\sqrt{2}} \\ -1 & -1 & 1 \end{bmatrix}$$

Notice that both  $\mathbf{U}$  and  $\mathbf{V}$  have full rank, but  $\mathbf{\Sigma}$  is singular (rank-deficient) with only two linearly independent vectors. Hence the rank of  $\mathbf{N}$  is two. The four orthonormal



subspaces are represented in  $\mathbf{U}$  and  $\mathbf{V}$  where

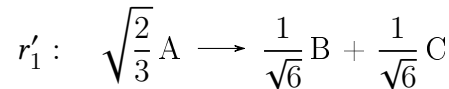
$$\text{col}(\mathbf{N}^T) = \frac{\sqrt{3}}{3} \begin{bmatrix} -\sqrt{2} & 0 \\ \frac{1}{\sqrt{2}} & -\sqrt{\frac{3}{2}} \\ \frac{1}{\sqrt{2}} & \sqrt{\frac{3}{2}} \end{bmatrix} \quad \text{leftNull}(\mathbf{N}^T) = \frac{\sqrt{3}}{3} \begin{bmatrix} 1 \\ 1 \\ 1 \end{bmatrix}$$

$$\text{row}(\mathbf{N}^T) = \frac{\sqrt{3}}{3} \begin{bmatrix} \sqrt{\frac{3}{2}} & -\frac{1}{\sqrt{2}} \\ 0 & \sqrt{2} \\ \sqrt{\frac{3}{2}} & \frac{1}{\sqrt{2}} \end{bmatrix} \quad \text{null}(\mathbf{N}^T) = \frac{\sqrt{3}}{3} \begin{bmatrix} -1 \\ -1 \\ 1 \end{bmatrix}$$

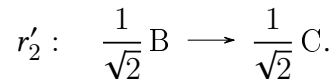
It is simple to verify that the same concentration derivative and reaction flux vectors can be written as a linear combination of the corresponding orthonormal basis:

$$\begin{bmatrix} -4 \\ -1 \\ 5 \end{bmatrix} = \text{col}(\mathbf{N}^T) \cdot \begin{bmatrix} 2\sqrt{6} \\ 3\sqrt{2} \end{bmatrix} \quad \text{and} \quad \begin{bmatrix} 1 \\ 2 \\ 3 \end{bmatrix} = \text{row}(\mathbf{N}^T) \cdot \begin{bmatrix} 2\sqrt{2} \\ \sqrt{6} \end{bmatrix}$$

The chemical reactions  $r_1$  and  $r_2$  of Figure 2.11 are written equivalently by the two columns of  $\mathbf{U}$ , such that



and



The reaction rates in this orthonormal basis are

$$r'_1 = \frac{1}{\sqrt{2}} r_1 + \frac{1}{\sqrt{2}} r_3$$

and

$$r'_2 = -\frac{1}{\sqrt{6}} r_1 + \sqrt{\frac{2}{3}} r_2 + \frac{1}{\sqrt{6}} r_3$$

using the first two columns of  $\mathbf{V}$ .

Notice that the original stoichiometric proportions are maintained in this orthonormal basis, although it is harder to interpret. Therefore, the choice of bases for the four fundamental subspaces becomes important since it influences the phenomenological interpretation.

Considering the relation in (2.22) and the orthonormal matrices of  $\text{SVD}(\mathbf{N}^T)$  the mass

balance is written as

$$\begin{bmatrix} -\sqrt{2} & \frac{1}{\sqrt{2}} & \frac{1}{\sqrt{2}} \\ 0 & -\sqrt{\frac{3}{2}} & \sqrt{\frac{3}{2}} \\ 1 & 1 & 1 \end{bmatrix} \cdot \begin{bmatrix} -4 \\ -1 \\ 5 \end{bmatrix} = \begin{bmatrix} \sqrt{3} & 0 & 0 \\ 0 & \sqrt{3} & 0 \\ 0 & 0 & 0 \end{bmatrix} \cdot \begin{bmatrix} \sqrt{\frac{3}{2}} & 0 & \sqrt{\frac{3}{2}} \\ -\frac{1}{\sqrt{2}} & \sqrt{2} & \frac{1}{\sqrt{2}} \\ -1 & -1 & 1 \end{bmatrix} \cdot \begin{bmatrix} 1 \\ 2 \\ 3 \end{bmatrix}$$

where the scalar  $\sqrt{3}/3$  is excluded. The components related to  $\text{leftNull}(\mathbf{N}^T) = (1,1,1)$  and  $\text{null}(\mathbf{N}^T) = (-1, -1, 1)$  could be excluded satisfying equally the previous relationship in an economy SVD format.

The SVD of the stoichiometric matrix is not only a useful tool to identify the four associated fundamental subspaces, but this technique is also widely used for data analysis. When considering its application to the matrix of data, it enables the finding of principal features that contribute most to data variance, allowing thus, the model reduction when identifying its complexity (dimension) required to explain the observable data changes. This is a fundamental problem of data-driven modeling techniques for the obtainment of any empirical model in the field of machine learning and artificial intelligence. However, the SVD (and the data analysis over its results) can also be used in the field of deterministic modeling, taking the advantage of characterizing the data space and determining the dimension of this space for building a model based on first principles. This is the approach adopted in this thesis, where the SVD of data is considered in the methodology Step 2, described in Chapter 6.

## 2.3 Reaction invariants and linear system of equations in chemical reaction systems

This section presents several concepts and terminology related to reaction network synthesis and analysis that are crucial for understanding structural characteristics of chemical reaction systems. For this, several concepts of linear algebra introduced in Section 2.2 are required. The catalytic hydrogenation of succinic acid is taken as an illustrative example during this section.

### 2.3.1 Reaction invariants

The modeling task involves the quantitative description of the system under analysis, requiring the establishment of system invariants. The invariants are conserved quantities that can be observed in any closed system, they are mathematically represented through equality equations that decrease the freedom degrees number (Flockerzi et al., 2007; Gadewar et al., 2001, 2005; Madron and Veverka, 1991).

Consisting in an invariant phenomenon of closed reaction systems, the mass conserva-

tion extends to conserve the number of atoms of each chemical element. Thus, a closed chemical reaction system may be described through a set of equations of the form

$$\sum_{s=1}^{n_{\text{st}}} a_{e,s} n_s = b_e; \quad e = 1, \dots, n_{\text{el}} \quad (2.26)$$

where  $a_{e,s}$  is the number of atoms respected to the element  $e$  in the species molecule  $s$ ,  $n_s$  is the number of moles of the species  $s$ , and,  $b_e$ , an invariant, is the fixed number of moles respected to the element  $e$  in the system. The quantities  $n_{\text{el}}$  and  $n_{\text{st}}$  are, respectively, the cardinal numbers of chemical elements  $e \in \text{el}$  and species  $s \in \text{st}$  sets. Alternatively, (2.26) can be written in terms of the differential moles number

$$\sum_{s=1}^{n_{\text{st}}} a_{e,s} dn_s = 0; \quad e = 1, \dots, n_{\text{el}} \quad (2.27)$$

where  $dn_s$  is the variation (delta) of the number of moles respected to species  $s$  between two chemical composition states (Smith and Missen, 1982). In matrix form the latter is

$$\mathbf{A} \cdot d\mathbf{n} = \mathbf{0} \quad (2.28)$$

where  $\mathbf{A} \in \mathbb{N}^{n_{\text{el}} \times n_{\text{st}}}$  is the *atomic matrix* of chemical species and  $d\mathbf{n} \in \mathbb{Z}^{n_{\text{st}}}$  is the vector of species stoichiometric coefficients in a single chemical reaction, thus a column vector of the transposed stoichiometric matrix.

From linear algebra, (2.28) consists of an *homogeneous system of equations*, and, determining its homogeneous space of solutions consists on finding a set of linearly independent vectors of  $d\mathbf{n}$  type, that span the (right) null space of  $\mathbf{A}$ , *i.e.*, a basis with dimension  $\text{nr}\chi_{\text{i}}$ . In this case, the number of degrees of freedom ( $\text{nr}\chi_{\text{i}}$ ) is easily computed by the difference between the variables number  $n_{\text{st}}$  and the number of independent equations (rank of  $\mathbf{A}$ ). This is the required number of additional relationships between the variables to determine any state of chemical composition, with zero degrees of freedom. These relationships can be derived from thermodynamic conditions, kinetic laws and analytical determinations (Smith and Missen, 1982). On the other hand, the rank of  $\mathbf{A}$  determines the dimension of the left null space of the transposed stoichiometric matrix, and its rows with pivot numbers constitute a basis for the invariant relationships in the chemical system. Therefore, the dimension of the row/column space of  $\mathbf{A}$  is the number of linearly independent invariant relationships,  $\text{nin}_{\text{i}}$ . Note that every row vector of  $\mathbf{A}$  belongs to the left null space of the transposed stoichiometric matrix, as it was previously presented in (2.8), on the left side.

However, beyond the total mass and the number of atoms of each chemical element, examples of additional invariants can be expressed through blocks of elements or molecular subunits (*e.g.*, carboxyl, hydroxyl, phosphate, benzyl groups, etc.), or chemical moieties (*e.g.*, pentose, purine, etc.) (Palsson, 2006b), kinetic parameters in reversible chemical

reactions that yield the equilibrium constants in particular reaction systems (Yablonsky et al., 2020), electric charge of ionic species, and additional relationships among chemical species that can be observed either through experimental data or the structure of the reaction network. Therefore, it makes more sense to refer  $\mathbf{A}$  as the *matrix of invariant relationships*, or simply *invariant matrix*, instead of *atomic matrix*, since it can present rows referring to others conserved properties than the number of atoms regarding to chemical elements among molecules, satisfying equally (2.28).

### 2.3.2 The invariant relationships and the stoichiometric matrix

In chemical reaction systems, since at least one conservative property must be verified (*e.g.*, the total mass of the reacting system), the left null space of the transposed stoichiometric matrix will always exist ( $n_{st} > \text{rank}(\mathbf{N}^T)$ ), and as such, the (right) null space of  $\mathbf{A}$  will always exist ( $n_{st} > \text{rank}(\mathbf{A})$ ). The null space of the invariant matrix and the left null space of the transposed stoichiometric matrix are related through

$$n_{st} - \dim(\text{leftNull}(\mathbf{N}^T)) = \dim(\text{null}(\mathbf{A})) \quad \Leftrightarrow \quad (2.29)$$

$$n_{st} - \text{nin}_{li} = \text{nr}_{xi}.$$

Observe that the greater is  $\text{rank}(\mathbf{N}^T)$  or the smaller is  $\dim(\text{leftNull}(\mathbf{N}^T))$ , the smaller is  $\text{rank}(\mathbf{A})$  or the greater is  $\dim(\text{null}(\mathbf{A}))$ , for a fixed number of species.

This section is developed around this discussion: the relationship between the number of linearly independent invariants and the number of linearly independent chemical reactions, trying to express in various ways the meaning of this relationship in terms of (i) the graph of the reaction network and (ii) the definition of species (groupings in subsets of species).

The next equations summarize previously presented concepts that will be needed to analyze the examples that will follow, making this discussion simpler:

- $\dim(\text{leftNull}(\mathbf{N}^T)) = n_{st} - \text{rank}(\mathbf{N}^T)$ ,
- $\dim(\text{null}(\mathbf{A})) = n_{st} - \text{rank}(\mathbf{A})$ ,
- $\text{rank}(\mathbf{A}) = \text{nin}_{li}$ , and
- $\text{rank}(\mathbf{N}^T) = \text{nr}_{xi}$ .

For example, the catalytic hydrogenation of succinic acid involves nine chemical components/species (with known molecular formula) in five chemical reactions. In Figure 2.17, a matrix of invariants is presented, where the first three rows are respected to chemical elements that make up the species molecules, formed namely by carbon, hydrogen and oxygen, and, the fourth (last) row concerns to an extra invariant relationship. This last invariant represents the conserved amount among molecules of the type  $C_4$  plus  $C_3$ , which

remains constant along the experiment, establishing that the number of moles given by AS + GBL + BDO + THF + BuOH + PrOH is unchanged. Notice that this last invariant relationship ensures that the presence of methane component is simultaneously verified with propanol, in the same rate of appearance.

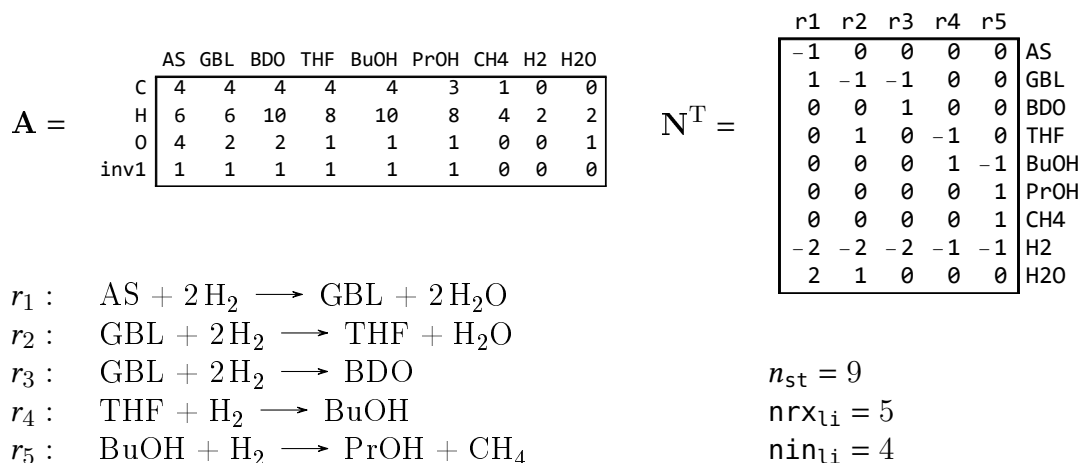


**Figure 2.17** On the upper left it is represented the invariant matrix, below it is located the list of chemical reactions, followed by its concerning transposed stoichiometric matrix and system characteristics.

Hence this system can be described through five linearly independent chemical reactions ( $nrx_{li} = 5$ ) that form a basis for  $\text{col}(\mathbf{N}^T)$  and  $\text{null}(\mathbf{A})$  in  $\mathbb{R}^9$  ( $n_{st} = 9$ ). Similarly, the matrix of invariants is composed by four linearly independent rows ( $nin_{li} = 4$ ) that form a basis for  $\text{row}(\mathbf{A})$  and  $\text{leftNull}(\mathbf{N}^T)$  in  $\mathbb{R}^9$ . Hence these space are complementary and orthogonal with each other, such that every inner product among  $\mathbf{A}$  rows and  $\mathbf{N}^T$  columns equals zero, *i.e.*,

$$\langle \mathbf{a}_{i,*}, \boldsymbol{\nu}_{*,j} \rangle = 0, \quad i = 1, \dots, nin_{li}, \quad j = 1, \dots, nrx_{li} \Leftrightarrow \text{row}(\mathbf{A}) \perp \text{col}(\mathbf{N}^T) \quad (2.30)$$

and their dimensions add up to  $n_{st}$ .

Observe that the matrix of invariants, namely its rows, span the left null space of  $\mathbf{N}^T$ , as such as, the columns of  $\mathbf{N}^T$  span the (right) null space of  $\mathbf{A}$ , or in another perspective, observe that the null vector (with dimension  $nrx_{li}$ ) is being written as linear combinations of the rows of  $\mathbf{N}^T$  through the coordinates vector  $\mathbf{a}_{i,*}$  such that

$$\sum_{s=1}^{n_{st}} a_{i,s} \boldsymbol{\nu}_{*,s} = \mathbf{0}, \quad i = 1, \dots, nin_{li} \Leftrightarrow \mathbf{A} \cdot \mathbf{N}^T = \mathbf{0} [nin_{li} \times nrx_{li}] \quad (2.31)$$

Thus, from another viewpoint, the invariant matrix can be described as a matrix of weights in such a way that species stoichiometric coefficients, multiplied by their respective weight, adds up to zero for every chemical reaction, establishing *reaction-invariant relationships*.

However, the five chemical reactions, in Figure 2.17, are structurally nonlinear involving more than one species in the reactant and/or in the product sides. In simultaneous they present a nonlinear reaction network which can be represented through a bipartite graph, see Figure 2.18(a). In certain cases, it is possible to *simplify* the nonlinear reaction network to linear by *omitting* some species (nodes) of the graph, like as shown in Figure 2.18(b).

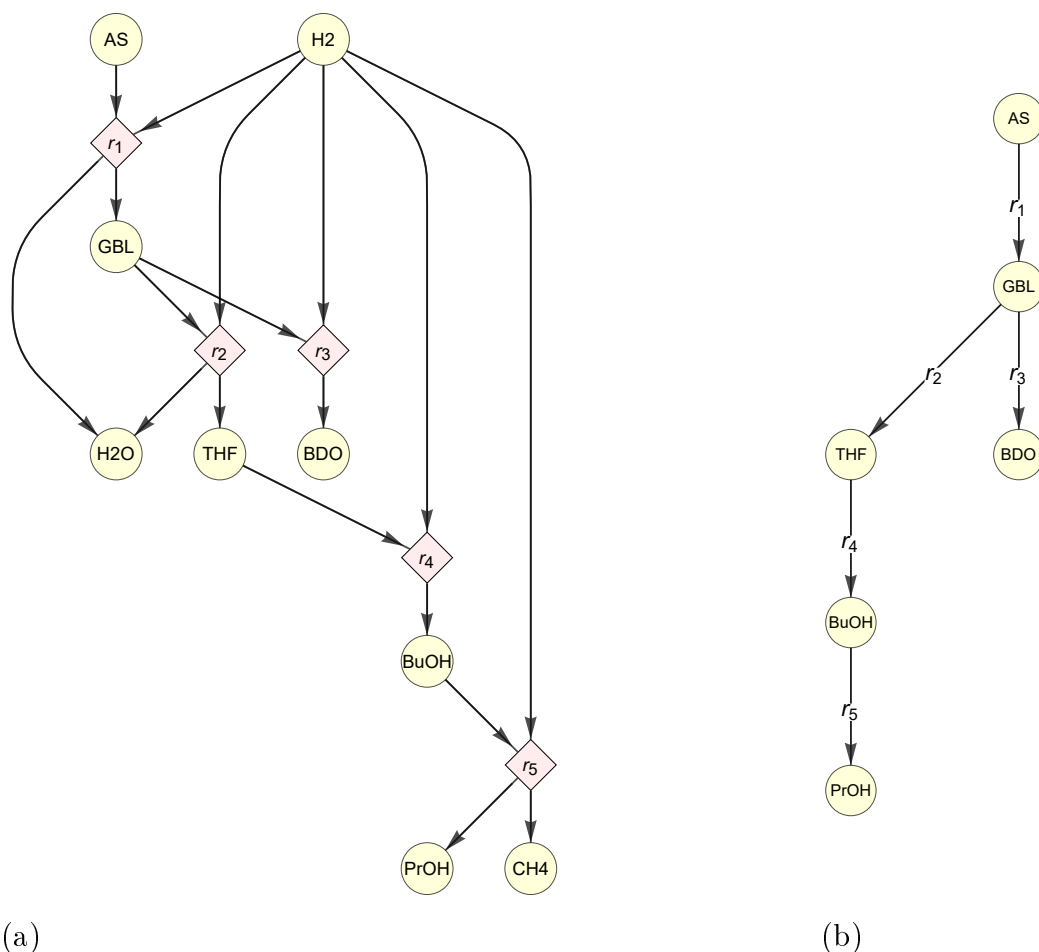


**Figure 2.18** Reaction network with five chemical reactions, described by (a) a nonlinear graph where *all* chemical species are representative (circular nodes), and (b) a linear graph with a smaller set of representative species.

The criterion to suppress or add one or more species in the graph representation must obey reaction-invariant relationships of the chemical system that are previously identified/observed, or establish *additional system invariants* for modeling purposes. Certain species can be omitted when the invariant relationships that they belong are excluded, as one chemical reaction can be unconsidered when there is an additional invariant relationship established, containing at least one of the species involved in that reaction. The next section presents several examples to clarify this topic.

### 2.3.3 Representative and non-representative species

For the purpose of establishing which species may be represented in a graph structure (reaction network graph), the set of species may be separated into two groups: (i) *representative species*, that are the ones represented by *nodes* in a graph, and (ii) *non-representative species*, those omitted in the reaction network representation in order to obtain a more straightforward graph eventually with a linear structure.

The non-representative species always constitute a set of linearly dependent species, *i.e.*, they correspond to non-pivotal columns of  $\mathbf{N}$ . On the other hand, the representative species concerns to pivotal columns of  $\mathbf{N}$  in addition to *at least one* linearly dependent species. This linear dependence appears in the set of representative species due to a fundamental network property: it must present a connected structure, and therefore, at least one invariant relationship must be written. For example, from Figure 2.17, the non-pivotal rows of  $\mathbf{N}^T$  concern to the last four rows (*i.e.*, PrOH, CH<sub>4</sub>, H<sub>2</sub> and H<sub>2</sub>O). Excluding these rows turns  $\mathbf{N}$  into a non-singular square matrix. This means that by excluding the contribution of these species in the reaction system, the null space of  $\mathbf{N}$  is excluded, (the invariant relationships are excluded). In a graph representation, this would result in a network with an open (free) arc where the arrow coming out of the BuOH is free, not pointing to any node. Hence PrOH cannot be excluded in the graph representation, and the system remains with one invariant quantity. On the other hand, observe that all the other linearly dependent species can be excluded by simplifying the nonlinear representation to a linear one, see Figure 2.18.

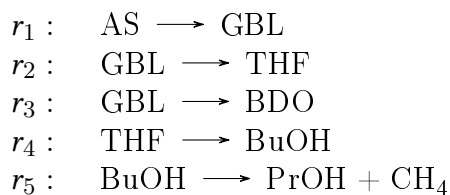
For example, the hydrogenation reaction of AS resulting in GBL and water,  $r_1$ :  $\text{AS} + 2\text{H}_2 \longrightarrow \text{GBL} + 2\text{H}_2\text{O}$ , that is represented by a linear graph when omitting the species H<sub>2</sub> and H<sub>2</sub>O resulting in  $\text{AS} \longrightarrow \text{GBL}$ . If the species H<sub>2</sub> and H<sub>2</sub>O are excluded from the set of representative species, the reaction-invariant relationships regarding these species are lost, resulting in the system presented in Figure 2.19. Note that it is still possible to observe the carbon conservation equation, since the CH<sub>4</sub> remains a representative species in this example.

However, there is no need to maintain both products of  $r_5$  since they present redundant information. Hence the reaction network in Figure 2.19 can be further simplified when excluding one of the  $r_5$  products, resulting in the linear network presented in Figure 2.18(b). The corresponding stoichiometric and reaction-invariant matrices of the linear network (Figure 2.18(b)) are presented in Figure 2.20, where only `inv1` remains valid.

In summary, whenever there is a nonlinear reaction involving more than one terminal species on either side of the reaction (independently if they are initial reactants or final products) one of the species can be considered non-representative, excluding it from the network (and from the stoichiometric and invariant matrices) and, consequently, vanishing/excluding the invariant relationship(s) that this species is part of. In this sense we are finally able to better define the representative species *as the ones that are required to*

$$\mathbf{A} = \begin{array}{c} \text{AS GBL BDO THF BuOH PrOH CH4} \\ \text{C} \\ \text{inv1} \end{array} \begin{array}{|c|c|c|c|c|c|c|} \hline 4 & 4 & 4 & 4 & 4 & 3 & 1 \\ \hline 1 & 1 & 1 & 1 & 1 & 1 & 0 \\ \hline \end{array}$$

$$\mathbf{N} = \begin{array}{c} \text{AS GBL BDO THF BuOH PrOH CH4} \\ r_1 \\ r_2 \\ r_3 \\ r_4 \\ r_5 \end{array} \begin{array}{|c|c|c|c|c|c|c|} \hline -1 & 1 & 0 & 0 & 0 & 0 & 0 \\ \hline 0 & -1 & 0 & 1 & 0 & 0 & 0 \\ \hline 0 & -1 & 1 & 0 & 0 & 0 & 0 \\ \hline 0 & 0 & 0 & -1 & 1 & 0 & 0 \\ \hline 0 & 0 & 0 & 0 & -1 & 1 & 1 \\ \hline \end{array}$$



$$n_{\text{st}} = 7 \quad n_{\text{rx}_{\text{li}}} = 5 \quad n_{\text{in}_{\text{li}}} = 2$$

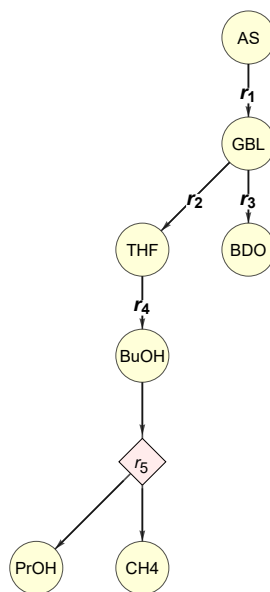


**Figure 2.19** Invariant and stoichiometric matrices and corresponding nonlinear reaction network.

$$\mathbf{A} = \begin{array}{c} \text{AS GBL BDO THF BuOH PrOH} \\ \text{inv1} \end{array} \begin{array}{|c|c|c|c|c|c|} \hline 1 & 1 & 1 & 1 & 1 & 1 \\ \hline \end{array}$$

$$n_{\text{rx}_{\text{li}}} = 5 \quad n_{\text{in}_{\text{li}}} = 1 \quad n_{\text{st}} = 6$$

$$\mathbf{N}^T = \begin{array}{c} r_1 \ r_2 \ r_3 \ r_4 \ r_5 \\ \begin{array}{|c|c|c|c|c|} \hline -1 & 0 & 0 & 0 & 0 \\ \hline 1 & -1 & -1 & 0 & 0 \\ \hline 0 & 0 & 1 & 0 & 0 \\ \hline 0 & 1 & 0 & -1 & 0 \\ \hline 0 & 0 & 0 & 1 & -1 \\ \hline 0 & 0 & 0 & 0 & 1 \\ \hline \end{array} \begin{array}{l} \text{AS} \\ \text{GBL} \\ \text{BDO} \\ \text{THF} \\ \text{BuOH} \\ \text{PrOH} \end{array} \end{array}$$

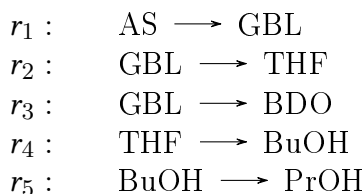


**Figure 2.20** Invariant and stoichiometric matrices regarding the linear reaction network presented in Figure 2.18(b).

*observe/determine invariant relationships* in chemical reaction systems. This definition is related with the graph representation of *species networks*, that is presented in the next section.

Furthermore, the partition of species in groups of representative and non-representative can be advantageous (i) when generating reaction networks, since less complex structures may be generated demanding a lower computational effort, and (ii) in the practical modeling task supported on experimental data, since, in general, not all species/components are measured during the experiment, and thus, the invariant relationships respecting all chemical elements cannot be verified using experimental data. Therefore, a useful criterion for establishing which species should be representative is: to select those that are measured and/or can be estimated. For example, consider the comparison of the systems in Figures 2.17 and 2.20, regarding the reaction networks (a) and (b) in Figure 2.18, re-



spectively. For the reduced system, the conserved amounts of chemical elements between molecules/species can no longer be verified. These invariants can only be verified when the non-representative species are measured during the experiment. However, the same invariant relationship related to the species carbon chain remains valid. The topic of evaluating time-invariant relationships from experimental data will be discussed in more detail in Section 2.3.6.

### 2.3.4 Species map and reaction-invariant relationships

The species map shows how chemical reactions are linked. It consists of an *open graph structure* that represents the transposed matrix that translates the reaction map<sup>7</sup>. Thus, the species map (or species network) is a transposition of the reaction map (or reaction network)<sup>8</sup>. When considering the *species map* instead of the *reaction map* in a graph, it can be observed how the fluxes of conserved entities travel in the network, see Figure 2.21. In an equation format, the species network graph is represented as a linear system of reaction mass balances, such that

$$\frac{d\mathbf{r}}{dt} = \mathbf{N} \cdot \mathbf{a}_i^T, \quad i = 1, \dots, n_{\text{rx}_i} \quad (2.32)$$

where no accumulation is verified in nodes  $r_j, j = 1, \dots, n_{\text{rx}_i}$ , such that  $d\mathbf{r}/dt = 0$ .

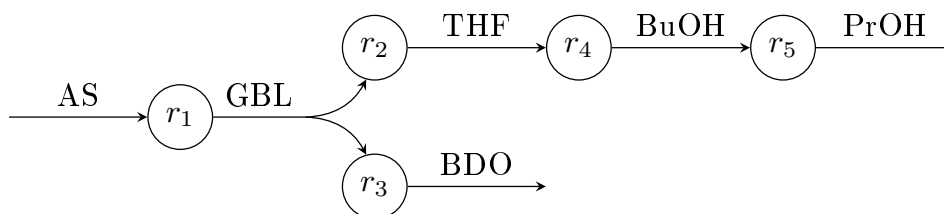


**Figure 2.21** Species map (or species network) corresponding to the transposed graph of Figure 2.18(b). In this case  $\mathbf{a}_1 = \mathbf{inv}1$  and  $\mathbf{N}$  is the stoichiometric matrix presented in Figure 2.20.

The reaction-invariant relationships can be represented by a convex basis that lies in the positive orthant of the linear space defined by chemical species (Palsson, 2006a). This basis is convex since any linear combination of its generation set of vectors is written with positive coordinates. This concept presents an (direct) analogy with *extreme pathways* in metabolic networks. This topic will be discussed in more detail in the state-of-the-art chapter, namely in Section 3.2.1.

<sup>7</sup>Note that it consists in the graph that represents the stoichiometric matrix (without being transposed); remember the concepts introduced in Figure 2.10.

<sup>8</sup>However, if the reaction network presents boundary fluxes (for example as is usual in metabolic networks), the species network will present a *closed structure* (without free-ended arcs).

Famili and Palsson (2003a) pioneered the concept of convex conservation pool maps, where the fluxes of reaction invariants can be seen in the species map graph, presenting fragments/piece-wises (or extreme pathways) of the species network. These fragmented paths regard to column vectors of the generating set of convex conservation space. They not necessarily form a linearly independent set of reaction-invariant relationships. In some cases, in order to define/verify the concept of *convex basis*, it is necessary to consider redundant paths, establishing invariant relations that are linear combinations of others, *i.e.*, the generating set of this convex space can present a number of vectors greater than  $n_{\text{inv}_{\text{li,max}}}$ .

The convex basis of reaction-invariant relationships concerning to the linear reaction system of Figure 2.20 has dimension one, and it is represented by the `inv1` column vector itself. In the next section a better example is presented for illustration of the concepts related to species map, extreme path of conserved relationships and convex space of concentration pools. This example is also related to the analysis of degrees of freedom, the topic that follows next.

### 2.3.5 Degrees of freedom and reaction-invariant relationships

The number of linearly independent chemical reactions in a reaction system consists of the number of degrees of freedom to solve the species mass balance as such in (2.7), or, in other words, the number of degrees of freedom corresponds to the number of linearly independent reaction vectors that solve the homogeneous system of equation

$$\mathbf{A} \cdot \mathbf{N}^T = \mathbf{0} \quad (2.33)$$

as previously mentioned in the beginning of the section.

So far, in all the examples analyzed until now, the number of representative species and the number of invariant relationships for a fixed number of chemical reactions have been varied, within the scope of a greater understanding of (i) how the representative species relate to the invariant relationships, and (ii) how the structure of the network can be simplified (removing nonlinearities) as a consequence of this relationship. Now that we know how these concepts work, always attending the relations in (2.33) and (2.29), let's consider varying the number of degrees of freedom to better understand the concept behind the *minimum* and the *maximum* number of linearly independent chemical reactions,  $n_{\text{rx}_{\text{min}}}$  and  $n_{\text{rx}_{\text{li,max}}}$ , respectively<sup>9</sup>.

For the same example, let's decrease the number of degrees of freedom in (2.33), maintaining a feasible reaction network structure. In Figure 2.22, the same reaction system is described through four linearly independent chemical reactions, where one of them con-

---

<sup>9</sup>The concepts of  $n_{\text{rx}_{\text{min}}}$  and  $n_{\text{rx}_{\text{li,max}}}$  that are introduced here are required during the thesis, specially in Step 4 of the methodology where the generation of reaction networks is considered. However, they will be re-called when necessary.

stitutes the sum of  $r_2$  and  $r_3$  of the previous example ( $r_6 = r_2 + r_3$ ). In this case, beyond the molar sum related to the representative species which remains verified as constant, an additional invariant relationship occurs, thus decreasing the degrees of freedom in (2.28). The row indicated by `inv2` establishes a nonlinear reaction structure; it sets that the weighted molar sum of three representative species is maintained constant following the proportion established.

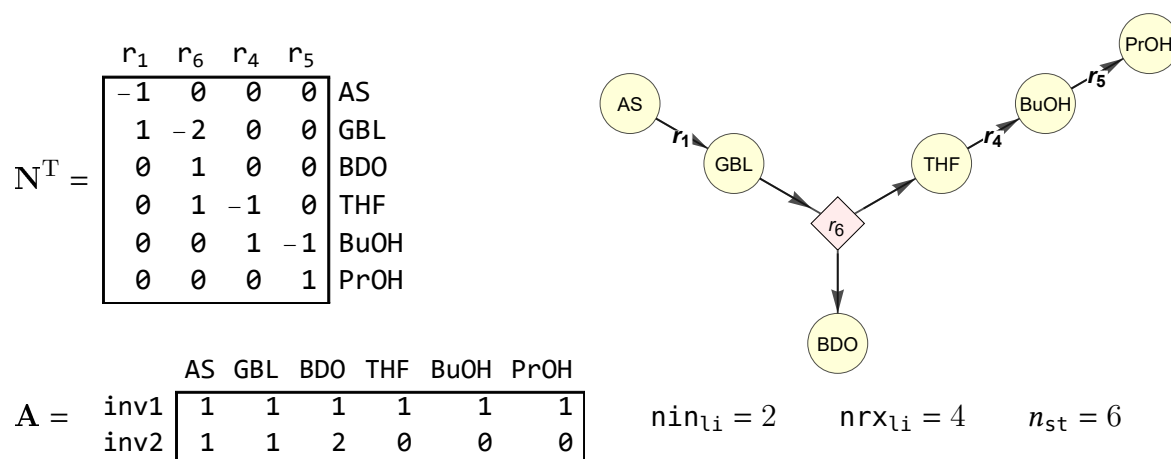


**Figure 2.22** Reduced reaction system with a lower number of degrees of freedom. The diamond node  $r_6$  in the bipartite graph corresponds to the sum of reactions  $r_2$  and  $r_3$ .

In order to understand the reaction invariants of this system let's consider the species map in Figure 2.23.

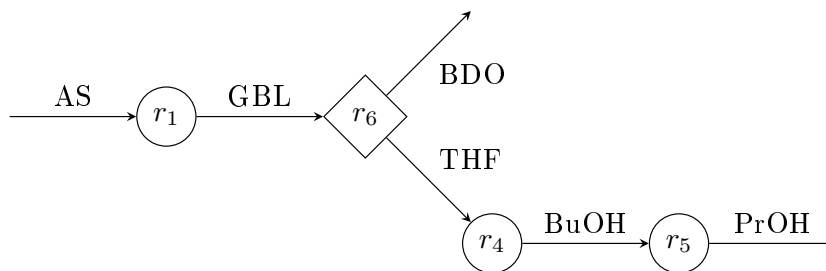


**Figure 2.23** Species map (or species network) corresponding to the transposed graph of Figure 2.22.

From the species map we can observe that there are two possible routes among chemical reactions for traveling quantities that establish conserved concentration pools, namely the routes represented by the red arcs in Figures 2.24 and 2.25. It can be observed that a convex conservation basis for this species map is given by

$$\mathbf{A} = \begin{array}{c} \text{AS} \quad \text{GBL} \quad \text{BDO} \quad \text{THF} \quad \text{BuOH} \quad \text{PrOH} \\ \left[ \begin{array}{cccccc} 1 & 1 & 2 & 0 & 0 & 0 \\ 1 & 1 & 0 & 2 & 2 & 2 \end{array} \right] \begin{array}{l} \text{inv2} \\ \text{inv3} \end{array} \end{array}$$

considering  $\mathbf{N}$  of Figure 2.22. Note that the invariant matrix given by the convex basis spans the same space of  $\mathbf{A}$  in Figure 2.22, since  $2\text{inv}1 = \text{inv}2 + \text{inv}3$ .

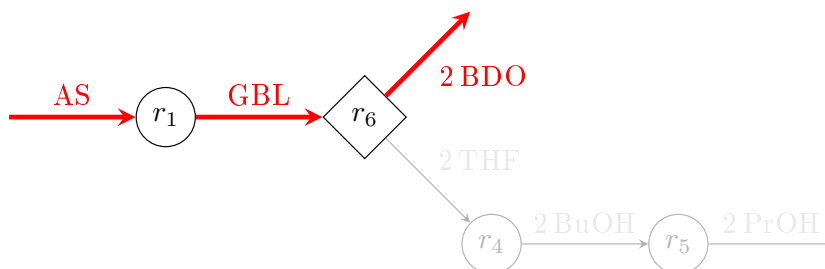


**Figure 2.24** Extreme path of conserved entities related to  $\text{inv}2$ , or convex conservation pool map.

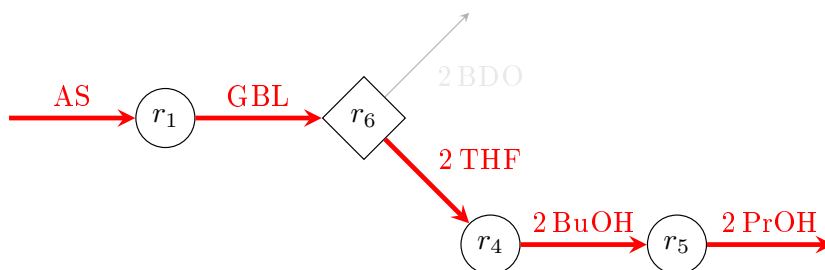


**Figure 2.25** Extreme path related to  $\text{inv}3$  (convex conservation pool map).

Therefore, every nonlinear reaction in a reaction network increase the number of paths/routes in a species map, presenting an associated convex conservation basis that can be interpreted in a convex conservation pool map. On the other hand, linear reaction networks when transposed to species maps maintain the same linear route of convex conservation pool map.

Moreover, note that one of the products of the nonlinear reaction  $r_6$  could be excluded in Figure 2.22, since they present redundant information (as such as the products of  $r_5$  in the example of Figure 2.19). This means that this system could be reduced to a linear format, by considering for example the BDO species as non-representative. In such situation only  $\text{inv}3$  would be verifiable.

Considering the example that has been analyzed during this section, it is observed that the *maximum* number of linearly independent chemical reactions that this system can support is five ( $\text{nr}x_{\text{li,max}} = 5$ ), whether linear or not. However, attending (2.29), it is possible to write lower and upper bounds above the variables for the example that has been followed, such that

$$\begin{aligned}
 [2 - 9] &= [1 - 5] + [1 - 5] \\
 n_{\text{st}} &= \text{nr}x_{\text{li}} + \text{nin}_{\text{li}}
 \end{aligned}
 \tag{2.34}$$

where we can play with the number of representative species  $n_{\text{st}}$  and, consequently, with

the number of invariants  $\text{nin}_{\text{li}}$ , in simultaneous with varying the number of degrees of freedom  $\text{nr}\mathbf{x}_{\text{li}}$ .

For the illustration of a concept, let us consider the hypothetical possibility in which species are omitted from the network until reaching the lowest limit in a fictitious situation where only two representative species exists connected by a single “linear” reaction that represents the weighted sum of all the others, with a single invariant relationship. In this case, hypothetically,  $\text{nr}\mathbf{x}_{\text{min}} = 1$  and  $\text{nin}_{\text{li}} = 1$ , requiring only two representative species. Clearly, this is a fictitious situation, as it has no physical meaning, *i.e.*, it would involve the meeting of too many molecules to get the final system maximally reduced, (reduced to the minimum). Note that the final linear reaction would be a simplification of the nonlinear global reaction, that is, the global reaction without redundant species.

Therefore, determining  $\text{nr}\mathbf{x}_{\text{min}}$  is concerned with establishing the maximum number of molecules involved on each side of the reaction, thus establishing the maximum complexity that is considered acceptable for nonlinear chemical reactions. In general, no more than tri-molecular chemical reactions occurs in reaction systems, being the most common situation the meeting of two reactant molecules in bio-chemical systems (Palsson, 2006c). From a structural point of view,  $\text{nr}\mathbf{x}_{\text{min}}$  is the minimum number of reactions that connects every representative species. Hence the key parameter for establishing  $\text{nr}\mathbf{x}_{\text{min}}$  is determining which are the representative species.

However, for this system  $\text{nr}\mathbf{x}_{\text{min}} = 4$  due to the establishment of acceptable upper bounds on the stoichiometric coefficients. This topic is discussed in more detail in Chapter 7. Hence the bounds presented in (2.33) can be updated to  $[5 - 9] = [4 - 5] + [1 - 5]$ .

On the other hand, when considering  $\text{nr}\mathbf{x}_{\text{li}} = \text{nr}\mathbf{x}_{\text{li,max}} = 5$ , it has been shown that  $1 \leq \text{nin}_{\text{li}} \leq 4$  from the analysis of the previous examples, and therefore,  $6 \leq n_{\text{st}} \leq 9$ . Note that if we had considered the possibility of species  $C_4$  segregate in  $4C_1$ , by considering methane as representative species with an independent production pathway, that is, the methane formation is independent of the propanol formation, the maximum degrees of freedom would be  $\text{nr}\mathbf{x}_{\text{li,max}} = 6$  with  $1 \leq \text{nin}_{\text{li}} \leq 3$ , and therefore,  $7 \leq n_{\text{st}} \leq 9$ .

In general, the  $\text{nr}\mathbf{x}_{\text{li,max}}$  is given by the number of representative species minus one (specially if the system is linear), or from the dimension of the null space of the reaction-invariant matrix regarding all (representative and non-representative) chemical species. Hence the  $\text{nr}\mathbf{x}_{\text{li,max}}$  comes from the number of species and the number of invariant relationships that can be written among them. In closed reaction networks (networks without free-ended arcs) composed by  $\text{nr}\mathbf{x}_{\text{li,max}}$ , there is no manner to increase the degrees of freedom, since it would hypothetically eliminate the presence of the  $\text{leftNull}(\mathbf{N}^T)$ , or in other words, it would ultimately violate the global mass conservation. Note that by adding linearly dependent chemical reactions (making  $\mathbf{N}^T$  rank-deficient, or singular), although increasing its number of columns, the number of degrees of freedom does not change in (2.33).

### 2.3.6 Time-invariant relationships in experimental data

Another perspective of conserved quantities in a closed system can be described by the species mass balances presented in (2.7), that implicitly ensure the presence of invariants since the following expression holds:

$$\mathbf{A} \cdot \frac{d\mathbf{c}(t)}{dt} = \mathbf{A} \cdot \mathbf{N}^T \cdot \mathbf{r}(t) = \mathbf{0} \quad (2.35)$$

It is clear that  $d\mathbf{c}(t)/dt$  and any column vector of the transposed stoichiometric matrix belong to the null space of  $\mathbf{A}$ . Hence  $\text{col}(\mathbf{N}^T) \equiv \text{null}(\mathbf{A})$ .

Similarly to the right side of (2.35) (where the conserved properties are established through the species stoichiometric coefficients multiplied by their respective weights, adding up to zero in every chemical reaction), on the left side of (2.35), each entry of the concentration derivatives vector multiplied by its respective (same) weight also adds up to zero, meaning that

$$\langle \mathbf{a}_{i,*}, \frac{d\mathbf{c}(t)}{dt} \rangle = 0, \quad i = 1, \dots, \text{nin}_{\mathbf{A}} \quad (2.36)$$

Since the previous equations are valid for every instant (or observation), they establish *time invariants* of the reaction system. Notice that

$$\mathbf{A} \cdot \frac{d\mathbf{c}(t)}{dt} \Leftrightarrow \frac{d\mathbf{A} \cdot \mathbf{c}(t)}{dt} \quad (2.37)$$

where

$$\mathbf{A} \cdot \mathbf{c}(t) = \boldsymbol{\theta} \quad (2.38)$$

with  $\boldsymbol{\theta}$  representing a vector of conserved quantities, *i.e.*, it defines the size of the *pools* established through the sum of weighted species concentrations. Palsson (2006b) explained the concept of concentration pools through invariant relationships saying that while there can be dynamic motion taking place in the column space of the transposed stoichiometric matrix along the stoichiometric (column) vectors, these motions do not change the total amount of mass in the time invariant pools.

Therefore, (2.38) define an *affine* hyperplane, that is, a plane that does not go through the origin. This is the place where the concentration vector  $\mathbf{c}(t)$  resides, named as the *concentration space*. Since species concentrations are nonnegative, a convex representation of the concentration space is useful through the establishment of a convex basis for the left null space of the transposed stoichiometric matrix, or in other words, establishing a convex basis for the row space of the invariant matrix, such as the one that we have been discussed in the previous sections.

The rows of  $\mathbf{A}$  have only zero or positive entries since it represents physical quantities of properties that are conserved among chemical species. Any vector inside of this convex

space (defined by the extreme vectors, edges of a cone with origin in the null dot) is a nonnegative vector written with positive coordinates in the basic columns. Consequently, and since  $\boldsymbol{\theta}$  is also nonnegative, every vector  $\mathbf{c}(t)$  is also nonnegative satisfying (2.38).

In order to use the same basis for both concentration space and the column space of the transposed stoichiometric matrix, the shifting of the concentration space to the origin is required. It is achieved using a reference concentration vector,  $\mathbf{c}_{\text{ref}}$ , that must verify the next two constraints

$$\langle \mathbf{c}_{\text{ref}}, \boldsymbol{\nu}_{*,j} \rangle = 0, \quad j = 1, \dots, n_{\text{rx}} \quad (2.39)$$

and

$$\langle (\mathbf{c}(t) - \mathbf{c}_{\text{ref}}), \mathbf{a}_{i,*} \rangle = 0, \quad i = 1, \dots, n_{\text{in}} \quad (2.40)$$

These constraints together give a unique solution for  $\mathbf{c}_{\text{ref}}$ . Note that  $\mathbf{c}_{\text{ref}}$  belongs to the left null of  $\mathbf{N}^T$  since from (2.39) it is established that  $\mathbf{N} \cdot \mathbf{c}_{\text{ref}} = \mathbf{0}$ . Similarly note that  $(\mathbf{c}(t) - \mathbf{c}_{\text{ref}})$  belongs to the null space of  $\mathbf{A}$ , since from (2.40) it is established that  $\mathbf{A} \cdot (\mathbf{c}(t) - \mathbf{c}_{\text{ref}}) = \mathbf{0}$ . In other words,  $\mathbf{c}_{\text{ref}}$  is a linear combination of the rows of  $\mathbf{A}$ , while  $(\mathbf{c}(t) - \mathbf{c}_{\text{ref}})$  can be written as a linear combination of the column space of the transposed stoichiometric matrix. Therefore, the concept of invariants applied directly in deltas of concentration data can be very useful for modeling chemical reaction systems, specially for identifying the  $\text{col}(\mathbf{N}^T)$  since the shifted concentration space spans that space.

In this section the subspaces associated with the stoichiometric matrix, the invariant matrix, and the experimental data matrix have been analyzed using mass balances. However, in the next section, we will continue to analyze mass balances but from a more practical perspective.

## 2.4 Mass balances as linear systems of equations

Considering the dynamics of an ideal chemical reaction system operating at batch conditions and free of uncertainties in its measurements, the species mass balance can be written as

$$\mathbf{D}_R = \mathbf{R} \cdot \mathbf{N} \quad (2.41)$$

where  $\mathbf{D}_R[n_{\text{to}} \times n_{\text{sp}}]$  is the matrix of concentration derivatives,  $\mathbf{R}[n_{\text{to}} \times n_{\text{rx}}]$  the matrix of reaction rates, and  $\mathbf{N}[n_{\text{rx}} \times n_{\text{sp}}]$ . Notice that (2.41) contains the same relation presented in (2.7), but in a transposed format and written for  $n_{\text{to}}$  observations. The subscript ‘‘R’’ indicates the mass balance in the rate-based format, describing instantaneous rates of species molar changes for a constant volume of mixture.

The previous equations can be written in terms of the differential number of moles, such that

$$\frac{d\mathbf{n}(t)}{dt} = \mathbf{N}^T \cdot \mathbf{r}(t)V \quad (2.42)$$

where  $V$  is the reaction mixture volume, generally assumed constant in batch systems.

Clearly,  $\mathbf{n}(t) = \mathbf{c}(t)V$ . Hence  $d\mathbf{n}(t)/dt \in \mathbb{R}^{n_{sp}}$  is the instantaneous rate of molar changes (*e.g.*, in  $\text{mol s}^{-1}$ ), and  $\mathbf{r}(t) \in \mathbb{R}_+^{n_{rx}}$  is the vector of instantaneous reaction rates (*e.g.*, in  $\text{mol m}^{-3} \text{s}^{-1}$  with  $V$  in  $\text{m}^3$ ).

Instead of considering instantaneous rates, the mass balances can be written in cumulative terms by considering the effective number of reacted and produced moles, such as:

$$\Delta\mathbf{n}(t) = \mathbf{N}^T \cdot \boldsymbol{\xi}(t) \quad (2.43)$$

where  $\Delta\mathbf{n}(t)[n_{sp} \times 1]$  is the cumulative changes of number of moles and  $\boldsymbol{\xi}(t)[n_{rx} \times 1]$  the reaction extents. Notice that

$$\Delta\mathbf{n}(t) = \mathbf{n}(t) - \mathbf{n}(0) \quad (2.44)$$

where  $\mathbf{n}(t)$  and  $\mathbf{n}(0)$  are the vectors of species number of moles in a given instant  $t$  and in the beginning of the experiment ( $t = 0$ ), respectively.

The reaction extents are related to the reaction rates through

$$\boldsymbol{\xi}(t) = V \int_0^t \mathbf{r}(t) dt \quad (2.45)$$

The mass balances in (2.43) can also be written in the matrix format, such as

$$\mathbf{D}_\Xi = \Xi \cdot \mathbf{N} \quad (2.46)$$

where  $\mathbf{D}_\Xi[n_{to} \times n_{sp}]$  is the matrix of cumulative molar changes and  $\Xi[n_{to} \times n_{rx}]$  the matrix of reaction extents. The subscript “ $\Xi$ ” indicates the mass balance in the extent-based format, describing cumulative species molar changes for a constant volume of mixture.

Hereafter, the subscripts “R” and “ $\Xi$ ” of  $\mathbf{D}$ , referring to mass balances in the rate- and extent-based methods, are omitted in the matrices that follow since every analysis that will be performed in  $\mathbf{D}$  is common for both data matrices. The matrix  $\mathbf{D}$  corresponds to the *data in the variant format*. The row space of  $\mathbf{D}$  is referred in the thesis as the *data variant space*, as well as the the null space of  $\mathbf{D}$  the *data invariant space*.

The selected  $n_{to}$  observations that form the rows of  $\mathbf{D}$  may be representative of the system dynamics. This means that the set of data points should be considered in appropriate time instants for increasing system identifiability.

### 2.4.1 Characterizing systems of linear equations

Linear systems of equations are classified primarily as *possible* or *impossible*. In possible linear systems, the response vectors lie in the column space of the design matrix, while in



impossible systems they do not.

The linear systems representing the species mass balances that have been analyzed until this moment have  $\text{rank}(\mathbf{D}) \leq \text{nr}\mathbf{x}_{\text{li}}$ <sup>10</sup>, meaning that they are all possible (there is no error in the closure of mass balances), as shown in eqs. (2.41) to (2.43). Two situations can be eligible in possible linear systems:

- $\mathbf{N}^T$  has full rank ( $n_{\text{rx}} = \text{nr}\mathbf{x}_{\text{li}}$ ). This means that no linearly dependent column in  $\mathbf{N}^T$  exists and thus  $\text{null}(\mathbf{N}^T) = \emptyset$ . Therefore, these systems are *perfectly determined*, *i.e.*, there exists a unique solution that satisfies the linear system.
- $\mathbf{N}^T$  is singular ( $n_{\text{rx}} > \text{nr}\mathbf{x}_{\text{li}}$ ). In this case,  $n_{\text{rx}} - \text{nr}\mathbf{x}_{\text{li}}$  linear dependencies in the columns of  $\mathbf{N}^T$  exist and therefore an infinite set of solutions satisfies these equations, *i.e.*, the system is *under-determined*.

On the other hand, impossible linear systems present  $\text{rank}(\mathbf{D}) > \text{nr}\mathbf{x}_{\text{li}}$ , meaning that it is impossible to write every response vector as a linear combination of the rows of  $\mathbf{N}$ . These systems are *over-determined*. In practice, dealing with data matrices corrupted with noise such that  $\text{row}(\mathbf{D}) \neq \text{row}(\mathbf{N})$  is the most common situation. This means that for at least a single instant  $t$  the response vector does not belong to  $\text{row}(\mathbf{N})$ , although probably it happens for all  $n_{\text{to}}$  instants.

The solutions of under- and over-determined linear systems of equations are obtained using additional criteria. An appropriate choice is minimization of the  $\ell_2$ -norm of (i) the solution vector in under-determined systems and (ii) the difference between the response vector and the model in over-determined systems, using the *least-squares* method.

However,  $n_{\text{st}} - \text{nr}\mathbf{x}_{\text{li}}$  redundant equations can be discarded from all these categories of linear systems without altering their solutions, since the invariant relationships presented in  $\text{leftNull}(\mathbf{N}^T)$  can be decoupled of the dynamic components that belong to  $\text{col}(\mathbf{N}^T)$ <sup>11</sup>.

## 2.4.2 SVD for solving linear system of equations

The SVD can be used to solve over-determined systems of equations, similarly to the least squares (without constraints) method, where the  $\ell_2$ -norm of the difference among  $\text{dc}(t)/\text{dt}$  and  $\mathbf{N}^T \cdot \mathbf{r}(t)$  is minimized for every  $k$  observation, *i.e.*,

$$\min \left\| \frac{\text{dc}(t)}{\text{dt}} - \mathbf{N}^T \cdot \mathbf{r}(t) \right\|_2 = \left\| \frac{\text{dc}(t)}{\text{dt}}^T \left( \mathbf{I}_{n_{\text{sp}}} - \hat{\mathbf{U}} \cdot \hat{\mathbf{U}}^T \right) \right\|_2 \quad \forall t \in [t_0, t_f] \quad (2.47)$$

<sup>10</sup>Remember that  $\text{nr}\mathbf{x}_{\text{li}} = \text{rank}(\mathbf{N})$ .

<sup>11</sup>In this case, (2.35) is no longer valid since the left null space of the transposed stoichiometric matrix (or the invariant relationships) has been excluded.

where  $\mathbf{I}_{n_{sp}}$  is the identity matrix with dimension  $n_{sp}$  and  $\hat{\mathbf{U}}$  is the orthonormal basis of  $\text{col}(\mathbf{N}^T)$  from the economy SVD of  $\mathbf{N}^T$ <sup>12</sup>. Hence, the row vector  $\text{dc}(t)/\text{dt}^T \cdot \hat{\mathbf{U}} \cdot \hat{\mathbf{U}}^T$  is the best projection of the concentration derivative (row) vector in row  $(\mathbf{N})$ , resulting in the lowest norm in (2.47). Every optimal solution regarding the instant  $t$  is thus computed through

$$\mathbf{r}(t)^T = \frac{\text{dc}(t)^T}{\text{dt}} \cdot \hat{\mathbf{U}} \cdot \hat{\Sigma}^{-1} \cdot \mathbf{V}^T, \quad \forall t \in [t_0, t_f] \quad (2.48)$$

where  $\hat{\mathbf{U}} \cdot \hat{\Sigma}^{-1} \cdot \mathbf{V}^T$  is the transposed Moore-Penrose inverse matrix of  $\mathbf{N}^T$ .

Observe that the solution obtained using SVD in (2.48), corresponds to the same solution using the least-squares method, although the objective function value SSE in the least squares is the square of the one in (2.47). However, these methods do not ensure positive reaction rates (unconstrained regression problems).

Moreover, both methods for solving over-determined linear systems of equations tend to overfit data, *i.e.*, the greater  $\text{nr}_{x_{li}}$  is, the lower the value of objective function will be until reach the dimension of the data variant space, turning the system perfectly determined with a null value of objective function.

## 2.5 Data reconciliation incorporating time invariants

In order to reduce the measurement noise, the closure of invariant balances must be forced when the species that respect the invariant relationships are measured, ensuring that

$$\tilde{\mathbf{D}}' \cdot \mathbf{A}^T = \mathbf{0} \quad (2.49)$$

where  $\tilde{\mathbf{D}}'[n_{t_0} \times n_{sp}]$  is the matrix of reconciled data in the variant format and  $\mathbf{A}[n_{in_{li}} \times n_{sp}]$ .

The reconciled data is obtained when considering the projection of the noisy data onto the null space of  $\mathbf{A}$ , such that

$$\tilde{\mathbf{D}}' = \tilde{\mathbf{D}} \cdot (\mathbf{I} - \mathbf{A}^+ \cdot \mathbf{A}) \quad (2.50)$$

where  $\tilde{\mathbf{D}}[n_{t_0} \times n_{sp}]$  is the matrix of noisy data and  $\mathbf{A}^+[n_{sp} \times n_{in_{li}}]$  is the Moore-Penrose pseudoinverse of  $\mathbf{A}$  that can be easily obtained when considering  $\text{SVD}(\mathbf{A})$ .

Using the  $\text{SVD}(\mathbf{A})$  and after some mathematical manipulation of (2.50), it is obtained

$$\tilde{\mathbf{D}}' = \tilde{\mathbf{D}} \cdot (\mathbf{I} - \hat{\mathbf{V}} \cdot \hat{\mathbf{V}}^T) \quad (2.51)$$

where  $\hat{\mathbf{V}}[n_{sp} \times n_{in_{li}}]$  is the orthonormal basis that describes the row space of  $\mathbf{A}$  with

---

<sup>12</sup>The economy SVD operation (Brunton and Kutz, 2019) is presented in Appendix I.1.

dimension  $\text{nin}_{\mathbf{I}}$ , *i.e.*, it corresponds to the first  $\text{nin}_{\mathbf{I}}$  rows of  $\mathbf{V}^T$ . Notice that the error of projection of the original data onto the row space of  $\mathbf{A}$  gives the projection of data onto the null space of  $\mathbf{A}$  (the row space of  $\mathbf{N}$ ). This property is easy to verify when considering the left multiplication of  $\mathbf{A}$  in the transposed format of (2.50), resulting in

$$\mathbf{A} \cdot \tilde{\mathbf{D}}'^T = \mathbf{A} \cdot \tilde{\mathbf{D}}^T - \mathbf{A} \cdot \mathbf{A}^+ \cdot \mathbf{A} \cdot \tilde{\mathbf{D}}^T \quad (2.52)$$

where  $\mathbf{A} \cdot \mathbf{A}^+ = \mathbf{I}$  and  $\mathbf{A} \cdot \tilde{\mathbf{D}}'^T = \mathbf{0}$  (as indicated by the transposed relation in (2.49)), Q.E.D.

Thus, this means that  $\tilde{\mathbf{D}}'$  is determined in the least squares sense, since it represents the smallest error of projection of data onto the null space of  $\mathbf{A}$ . However, notice that the systems in (2.49) are underdetermined with  $n_{\text{sp}} - \text{nin}_{\mathbf{I}}$  degrees of freedom for every system of equations.

In this thesis we satisfy (2.49) during the proposed method of data reconciliation in Step 1, but since we need the data to verify more criteria beyond its reconciliation, additional constraints must be considered. The least squares solutions obtained in (2.51) give the lowest euclidean norm of the trace of  $\tilde{\mathbf{D}}'$ . However, an infinite set of solutions with the same objective function value can be written, although only a restricted set of them is of interest. In the systematic methodology we are looking for  $\tilde{\mathbf{D}}'$  that lie in the positive orthant of  $\text{row}(\mathbf{N})$  (with positive coordinates in the basis  $\text{null}(\mathbf{A})$ ), presenting physical meaning. Moreover, we need  $\tilde{\mathbf{D}}'$  to present monotonous behaviors in time, with smooth and continuous temporal profiles. Thus the number of data points can be greater than the limited number of registers in experimental tests, resulting in a facilitated identification of the model.

Brendel et al. (2006) presented the data reconciliation procedure in (2.50), with  $\mathbf{A}$  corresponding to the atomic matrix in which every row is respected to a chemical element containing the corresponding number of atoms in each measured species. In this case, it is only possible to ensure every elemental balance when *all* chemical species are measured during the experiment.

## 2.6 Final remarks

In general, the stoichiometric matrix is unknown and, thus, the modeling task involves its identification from available data. The identification of the stoichiometric matrix passes through elucidating *both* row ( $\mathbf{D}$ ) and null ( $\mathbf{D}$ ), *i.e.*, the identification of the spaces where, respectively, the dynamic components and the invariant relationships lie in. Identifying such spaces is not an easy and straightforward task since data is typically noise-corrupted, sparse, and/or presents irregular structure due to scarce and/or grouped species measurements. All these difficulties can lead to a final model with high uncertainty associated and, in extreme cases, the model cannot be identified, requiring additional experimental

data. Therefore, there is a need for data pre-processing methods to reduce data uncertainty, incorporating time-invariant constraints and allowing greater modeling capability, that is, making the model structure and, consequently, its parameters identifiable with greater confidence. This is the approach adopted in Step 1 of the methodology, described in Chapter 5.

As target stoichiometric vectors can be validated by evaluating the projection error in the data variant space through target vector analysis (Bonvin and Rippin, 1990), similarly, target invariant vectors (*i.e.*, candidate rows of matrix  $\mathbf{A}$ ), can be validated by evaluating their projection in the data invariant space, when they present small projection errors. This means that these target vectors can be written as linear combinations of the respective spaces plus an epsilon (small error). However, the challenging tasks here are (i) determining these spaces dimensions  $\text{nr}_{\mathbf{I}_i}$  and  $\text{nin}_{\mathbf{I}_i}$  (and characterizing them) and (ii) determining this epsilon threshold in order to define the criterion to accept/neglect a candidate vector.

Quantifying the noise level in data, *i.e.*, determining the characteristic space of data by segregating signal and noise contributions, is a challenging task in the modeling field. Many methods that attend this problematic can be found in the literature, from more empirical approaches until more deterministic ones, including non-parametric and parametric tests (Wold, 1978; Malinowski, 1989; Gavish and Donoho, 2014). This thesis addresses a selection of suitable methods in this context, to apply them to experimental data from chemical reaction systems, leading to accurate results. These methods are described in Chapter 6.

Moreover, notice that the more species that are measured, the easier the task of identifying the model from the experimental data will be. This is because with, at the limit, *all* measured species, the complete set of invariant relationships may be elucidated. Hence, these time invariants must be imposed in the data reconciliation phase, thus reducing the uncertainty of the experimental point (*i.e.*, bringing the noisy point closer to the real/true point) and, consequently, increasing the model's identifiability (network structure and kinetic laws).

## Bibliography

- Bonvin, D. and Rippin, D. (1990). Target factor analysis for the identification of stoichiometric models. *Chemical Engineering Science*, 45(12):3417–3426.
- Brendel, M., Bonvin, D., and Marquardt, W. (2006). Incremental identification of kinetic models for homogeneous reaction systems. *Chemical Engineering Science*, 61(16):5404–5420.
- Brunton, S. and Kutz, J. (2019). *Data-Driven Science and Engineering: Machine Learning, Dynamical Systems, and Control*. Cambridge University Press.

- Famili, I. and Palsson, B. O. (2003a). The convex basis of the left null space of the stoichiometric matrix leads to the definition of metabolically meaningful pools. *Biophysical journal*, 85(1):16–26.
- Famili, I. and Palsson, B. O. (2003b). Systemic metabolic reactions are obtained by singular value decomposition of genome-scale stoichiometric matrices. *Journal of theoretical biology*, 224(1):87–96.
- Flockerzi, D., Bohmann, A., and Kienle, A. (2007). On the existence and computation of reaction invariants. *Chemical Engineering Science*, 62(17):4811–4816.
- Gadewar, S. B., Doherty, M. F., and Malone, M. F. (2001). A systematic method for reaction invariants and mole balances for complex chemistries. *Computers & Chemical Engineering*, 25(9–10):1199–1217.
- Gadewar, S. B., Schembecker, G., and Doherty, M. F. (2005). Selection of reference components in reaction invariants. *Chemical Engineering Science*, 60(24):7168–7171.
- Gavish, M. and Donoho, D. L. (2014). The optimal hard threshold for singular values is  $4/\sqrt{3}$ . *IEEE Transactions on Information Theory*, 60(8):5040–5053.
- Horiuti, J. (1973). Theory of reaction rates as based on the stoichiometric number concept. *Annals of the New York Academy of Sciences*, 213(1):5–30.
- Horiuti, J. and Nakamura, T. (1957). Stoichiometric number and the theory of steady reaction. *Zeitschrift für Physikalische Chemie*, 11(5\_6):358–365.
- Madron, F. and Veverka, V. (1991). Invariants of the chemical species balances of a reacting system. *Chemical Engineering Science*, 46(10):2633–2637.
- Malinowski, E. R. (1989). Statistical f-tests for abstract factor analysis and target testing. *Journal of Chemometrics*, 3(1):49–60.
- Marin, G. and Yablonsky, G. (2011). *Kinetics of Chemical Reactions*. Wiley.
- McNaught, A. D. and Wilkinson, A., editors (1997). *IUPAC the Gold Book*. Blackwell Scientific Publications, Oxford, 2nd ed. edition. Compendium of Chemical Terminology.
- Meyer, C. (2000). *Matrix Analysis and Applied Linear Algebra*. Society for Industrial and Applied Mathematics.
- Palsson, B. O. (2006a). The left null space of  $s$ . In *Systems Biology: Properties of Reconstructed Networks*, pages 154–169. Cambridge University Press.
- Palsson, B. O. (2006b). Part two: Mathematical representation of reconstructed networks. In *Systems Biology: Properties of Reconstructed Networks*, pages 87–176. Cambridge University Press.
- Palsson, B. O. (2006c). Systems biology: Properties of reconstructed networks. In *Systems Biology: Properties of Reconstructed Networks*, pages 12–25. Cambridge University Press.
- Palsson, B. O. (2015). Fundamental network properties. In *Systems Biology: Constraint-based Reconstruction and Analysis*, pages 184–203. Cambridge University Press.

- Pantea, C., Gupta, A., Rawlings, J. B., and Craciun, G. (2014). *The QSSA in Chemical Kinetics: As Taught and as Practiced*, pages 419–442. Springer Berlin Heidelberg, Berlin, Heidelberg.
- Shahzad, M. and Sultan, F. (2018). Complex reactions and dynamics. In Farrukh, M. A., editor, *Advanced Chemical Kinetics*, chapter 1. IntechOpen, Rijeka.
- Smith, W. and Missen, R. (1982). *Chemical reaction equilibrium analysis: theory and algorithms*. Wiley series in chemical engineering. Wiley.
- Temkin, M. (1979). The kinetics of some industrial heterogeneous catalytic reactions. In *Advances in Catalysis*, volume 28, pages 173–291. Elsevier.
- Temkin, O., Zeigarnik, A., and Bonchev, D. (1996). *Chemical Reaction Networks: A Graph-Theoretical Approach*. Taylor & Francis.
- Wold, S. (1978). Cross-validatory estimation of the number of components in factor and principal components models. *Technometrics*, 20(4):397–405.
- Yablonsky, G., Bykov, V., Elokhin, V., and Gorban, A. (1991). *Kinetic Models of Catalytic Reactions*. ISSN. Elsevier Science.
- Yablonsky, G. S., Branco, D., Marin, G. B., and Constales, D. (2020). New invariant expressions in chemical kinetics. *Entropy*, 22(3):373.

# Chapter 3

## State of the Art

*“The man who does not read good books  
has no advantage over the man who can’t read them.”*

– Mark Twain

### Contents

---

3.1	Modeling the dynamics of chemical reaction systems using experimental data . . . . .	74
3.1.1	Simultaneous method . . . . .	74
3.1.2	Incremental method . . . . .	75
3.1.3	Target factor analysis . . . . .	77
3.1.4	Inverse problems for identifying reaction networks . . . . .	80
3.2	Systematic generation and selection of reaction networks . . . . .	89
3.2.1	Metabolic reaction networks . . . . .	89
3.2.2	Generation of reaction mechanisms using a global reaction . . . . .	99
3.2.3	Generation of reaction networks via optimization . . . . .	106
3.3	Synthesis of graphs . . . . .	107
3.3.1	Spanning trees . . . . .	108
3.3.2	Elementary shortest path and travel salesman problems . . . . .	109
3.4	Data treatment and parameter identifiability . . . . .	113
3.4.1	Parameter identifiability . . . . .	113
3.5	Discussion of existing reaction modeling approaches . . . . .	114
3.5.1	Reaction network identification . . . . .	115
3.5.2	Reaction network generation . . . . .	116
	Bibliography . . . . .	117

---

This chapter presents the review of the literature addressing the main problems related to those considered in the various steps of the proposed methodology in this thesis, and also discusses alternative strategies for reaction systems modeling. This review makes it possible to highlight the innovative aspects of the new methodology, while providing a natural comparison between alternative approaches, evidencing their potential advantages and disadvantages.

Given the variety of topics covered, this literature review is divided into different parts. Section 3.1 introduces the main methods for modeling the dynamics of chemical reaction systems using experimental data. In Section 3.2, the methods of generating chemical reaction networks are presented, including metabolic networks and graph theoretical approaches. Once the structural description of reaction networks can be represented by graphs, the methods related to the synthesis of these graphs are considered in Section 3.3. In Section 3.4, some aspects of model parameter identifiability from experimental data are considered. Finally, Section 3.5 presents some additional notes on the approaches to identify reaction network models and a direct comparison between them and the methodology developed in this dissertation.

## 3.1 Modeling the dynamics of chemical reaction systems using experimental data

The modeling of chemical reaction kinetics involves the use of classical methods that support structural identification and parameter adjustment, such as the differential and the integral methods. Based on these fundamental methods several approaches can be found in the literature presenting distinct strategies to identify the reaction network, such as the adoption of an incremental development of the model where the different parts of the model are elucidated individually, or the use of simultaneous strategies where the overall model is obtained in a single procedure. During this section the description of model identification approaches supported on experimental data is considered.

This section is organized as follows: Sections 3.1.1 and 3.1.2 summarize the simultaneous and the incremental methods, respectively, presenting their main application advantages and drawbacks. Then, Section 3.1.3 introduces a data-driven technique that is complementary to the incremental method, named as target factor analysis. Finally, Section 3.1.4 describes simultaneous methods for identifying the reaction network, the reaction kinetic expressions and their parameters, using the differential method.

### 3.1.1 Simultaneous method

The simultaneous method is classified as “simultaneous or global identification” since all model levels are treated at once and model parameters are simultaneously estimated



via data regression (Brendel et al., 2006). Supported on the integral method, a system of postulated differential equations (species mass balances in a transient regime) is integrated to obtain a set of concentration expressions that are fitted to the experimental data by fine-tuning kinetic parameters. Parameters are optimized in the sense of the maximum likelihood, or according to other useful optimization criteria such as weighted least squares and Bayesian approaches (Bard et al., 1974).

The main advantage of this global method is its ability to handle complex structures with an arbitrary number of chemical reactions. On the down side, the parameter estimation is limited by eventual multiple local optima and the solution obtained may be sensitive to the initialization of variables and their bounds, depending on the solver adopted. Moreover, it can be computationally costly if the procedure is applied to several candidate reaction networks and kinetic expressions. Since every model component (and its parameters) is adjusted at once in this simultaneous procedure, it turns to be more difficult to identify the structural model mismatch of a specific model part, because residuals may be optimally distributed across several model components. Moreover, there is no systematic manner to propose good model candidates for the reaction network and kinetic expressions, and in this sense, the simultaneous method roughly approaches the traditional method, previously described in Figure 1.1, Section 1.1. Several integral methods are presented by Himmelblau et al. (1967) for simultaneous kinetic parameter tuning.

### 3.1.2 Incremental method

Unlike the simultaneous identification, the incremental method allows the decoupled identification of the reaction network of the kinetic expressions, resulting in more confidence in the identified model and its parameters. The identification of each chemical reaction model is performed individually, *i.e.*, the regression procedure is individually performed for every chemical reaction separately. Two distinct strategies can be found in the literature: one based on the differential method (Bardow and Marquardt, 2004; Marquardt, 2005; Brendel et al., 2006), and another based on the integral method (Bhatt et al., 2011, 2012; Srinivasan et al., 2012; Billeter et al., 2013; Rodrigues et al., 2018). The former is also called as a rate-based approach since the fitting procedure is performed on terms of reaction rates. Reaction rates are computed from the time-derivatives of the species observed concentrations, while the reaction rates are predicted by the kinetic expressions with their adjustable parameters. The approach based on the integral method is also known as extent-based approach, since reaction extents are used (instead of reaction rates) as a variable of the data regression optimization problem. In this case, reaction extents are computed from the concentration measurements and predicted through the integral of the reaction kinetic expressions.

Bhatt et al. (2012) concluded that the extent-based approach gives parameter estimates with tighter confidence intervals when compared to the rate-based. Although both approaches can lead to biased estimates, the bias may be reduced (i) by data regularization

in the rate-based approach, *e.g.*, using smoothing techniques to increase the precision on the numerical differentiation, and (ii) by efficient interpolation in the extent-based approach in order to have good numerical integration. In order to obtain statistically optimal parameters, [Bardow and Marquardt \(2004\)](#) and [Bhatt \(2011\)](#) proposed the use of simultaneous method in the last step of the incremental method.

A limitation of the incremental method, as it was proposed, is to solely handle systems composed by linearly independent chemical reactions. In order to directly calculate instantaneous reaction rates or extents, the number of linearly independent equations (species mass balances) must correspond to the number of variables (reaction rates or extents). Therefore, only reaction networks composed by a set of linearly independent chemical reactions can be identified. Another limitation is that, typically, the reaction network structure has to be postulated based on the modeler's expectation and know-how relative to the particular chemical system under study.

This dissertation presents a systematic method for modeling chemical reaction systems that approaches the original incremental method proposed by professor Marquardt and his students ([Marquardt, 2004](#); [Bardow and Marquardt, 2004](#); [Marquardt, 2005](#); [Brendel et al., 2006](#)). A scheme of the original incremental method is presented in [Figure 3.1](#), where the circled numbers represent: (1) the calculation of combined reaction and mass-transfer fluxes for each species, (2) the consideration of a reaction stoichiometry, (3) the estimation of reaction and mass-transfer rates (without assuming any kinetic structure), and finally (4) the identification of the kinetic law and parameter estimation, for each reaction path individually. The main similarities that can be highlighted are related to the incremental model identification itself, where (i) the identification task is split into a sequence of subproblems, (ii) the information available at a given step is used to refine the model in subsequent steps, and (iii) the entire structural model identification is supported on the differential method.

However, the methodology proposed in this thesis has several important distinctive features: (i) the systematic generation of candidate chemical reactions obeying to observed time invariants (that are previously detected through reaction data and system theoretical analyses), (ii) the exhaustive generation of reaction network structures with the required dimension to span the data variant space, ensuring that all feasible structures will be analyzed, (iii) the selection of the most plausible structures according to experimental data supported on the differential method, and (iv) a systematic identification of the reaction kinetic expressions using an inference criterion that establishes the best compromise between the model-data agreement and the number of parameters. At the end, the final parameter adjustment is performed simultaneously as proposed by [Bardow and Marquardt \(2004\)](#). Moreover, a special attention to the identification of time invariants and incorporation of them into the data reconciliation phase is carried out, allowing more certainty in every identification step.

The original incremental method schematized in [Figure 3.1](#) does not present a systematic

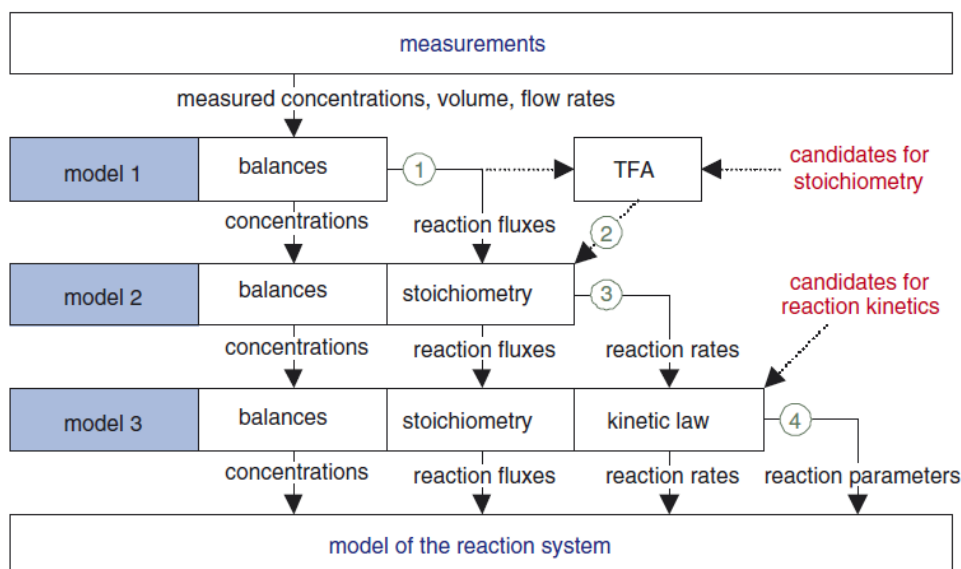


**Figure 3.1** Schematic representation of the incremental identification (rate-based approach) (Brendel et al., 2006). Here the authors use the term reaction fluxes to denote species concentration derivatives. Copyright (2021) by Elsevier.

manner to propose candidates for (i) stoichiometry, even validating hypotheses through the use of target factor analysis (TFA), and (ii) reaction kinetics, even considering individual reaction rate analyses. In this case, the validated stoichiometry may be questionable regarding the structure of the reaction network, with no guarantees of being the most appropriate. Consequently, the final model obtained can be, on the one hand, satisfactory but without certainty that it is the most appropriate, or, on the other hand, unsatisfactory, requiring more iterations of the method with other stoichiometry proposals. The next section addresses the topic TFA in the context of modeling chemical reaction systems.

### 3.1.3 Target factor analysis

Bonvin and Rippin (1990); Amrhein et al. (1999); Brendel et al. (2006); Bhatt (2011); Bhatt et al. (2012) proposed the use of a statistical technique, known as *target factor analysis* (TFA), to verify whether a given reaction network is reasonable in face of the available transient experimental data. The basic idea is to define a stoichiometric space given by measured data and then consecutively test if the stoichiometric vectors, corresponding to a postulated reaction network, lie in that space until a complete description of that space is obtained without linearly dependent vectors. The dimension of the data space corresponds to the number of linearly independent chemical reactions that is required in the network to explain the observed data. Several reaction networks, composed by the same number of linearly independent chemical reactions, constitute different bases that span the same system of coordinates, leading to the same description of the data space. Hence, there may be cases where several alternative reaction networks pass the

test. Therefore, to elucidate the reaction network one needs to consider in a subsequent stage kinetic laws describing the rate of each reaction step as a function of species concentration. Moreover, TFA cannot be directly applied to validate complex reaction networks composed by linearly dependent chemical reactions.

Some drawbacks of the TFA method are related to its dependence on the quality of experimental data and the *a priori* knowledge regarding the chemical system under study. In the case of data with noise, presenting high uncertainty related to concentration measurements, there are difficulties in determining the data variant linear space dimension and the projection error of stoichiometric vectors in that space (Prinz and Bonvin, 1994), thus leading to unreliable TFA results. Moreover, before applying TFA, the modeler must postulate a reaction network candidate (a target stoichiometry). In general, this proposal is based on prior knowledge of the chemical system and tends to be biased with the expectation of what is intended to happen, or typically is carried out on an *ad hoc* basis (Fotopoulos et al., 1994). Consequently, there may be cases where the proposed target vectors are far from being the intrinsic components of the system. In order to overcome these problems, the use of (i) data treatment methods for reducing the associated uncertainty, and (ii) systematic approaches for postulating target stoichiometries, is required. These are the approaches followed in this work, respectively in Steps 1 and 3 of the developed methodology. Thus, although there are some difficulties associated with TFA application, it is a useful tool to verify whether an individual chemical reaction is a potential candidate to explain the experimental data and it is therefore considered in this work. TFA is addressed in more detail in Section 7.3, where a critical analysis about its use is also presented.

Hamer (1989) pioneered the investigation of stoichiometries empirically derived from data analysis. In his work, the observed stoichiometric space is obtained using SVD of the matrix of data in the variant format, and, a rotation procedure of matrices is proposed in order to find meaningful stoichiometries from the orthonormal basis. Hence, through linear transformations of the abstract basis that approximately spans the data variant space, the author showed that it is possible to find a plausible network having meaningful reaction extents.

In the field of *tendency modeling* (Filippi-Bossy et al., 1989), a variation of TFA was proposed (Fotopoulos et al., 1994), named as *structured target factor analysis* (STFA). The main characteristics of tendency modeling is to develop low order, nonlinear and dynamic models that approximate the stoichiometric and kinetic models of a process using available process data along with fundamental knowledge of the process characteristics. In STFA, through the use of optimization, feasible stoichiometric vectors (targets) are determined by minimizing the distance between the target and its projection onto the observed stoichiometric space, considering specific elements of the target vector as variables of the optimization problem. Notice that, in contrast with the original TFA, STFA does not require any approximate *a priori* knowledge of the chemical reactions of the process.

Prinz and Bonvin (1994) have proposed the use of TFA in a sequential fashion in order to reduce the influence of measurement errors, named as *incremental target factor analysis* (IncTFA). In every iteration the contribution of an accepted target factor is excluded of the updated data projection matrix until complete identification of the network. This “exclusion” is performed by projecting experimental data onto the null space of the accepted target vector. This lower dimension matrix of experimental data is then used to perform TFA for the next candidate stoichiometric vector. With IncTFA application, a greater sensitivity for detecting small but relevant factors is achieved when compared to the original TFA procedure. Moreover, the authors have shown that the information extracted from singular value ratios helps in identifying the data dimension with more confidence. Singular values that respect to true model components (signal) increase with data space reduction, while noise model components remain at the same value, thereby allowing an improved estimate of the number of factors. However, there is no proposal for the establishment of the critical value for accepting/neglecting a target vector/factor, which must be empirically determined (Prinz and Bonvin, 1994).

Both Bonvin and Rippin (1990) and Prinz and Bonvin (1994) considered the use of TFA when *a priori* information about stoichiometric vectors is available. This information may be used to increase the identifiability of the remaining model parts (that are unknown) by excluding of the entire data space the contribution of the stoichiometric space formed by those known reaction vectors. Consequently, the remaining data space corresponds to unknown chemical reactions over which the TFA may be applied in order to completely identify the system stoichiometry.

Amrhein et al. (1999) have studied TFA and presented conditions for its application using experimental data in molar concentration units. The authors define the constructed data matrix for TFA application as the *data pre-treated to reaction-variant form*, since the contributions of the material exchange terms and the initial conditions are subtracted from the concentration terms, *i.e.*, the data matrix in the reaction-variant form contains the contributions of the maximum number of linearly independent chemical reactions exclusively. Notice that this definition is written for homogeneous reaction systems with inlet and outlet streams and varying density, since material exchange terms are presented in the material balance, and thus it encompasses the cases of batch, semi-batch and CSTR reactors. Necessary and sufficient conditions have been formulated for the acceptance of stoichiometric targets using reaction-invariant relationships. In cases in which not all chemical species are measured, a target vector can only be accepted if it lies in the row space of the data matrix, and (necessarily) if it is stoichiometrically balanced in the presence of the unmeasured species in the reaction vector. In this way, the following statement can be derived: as many reaction-invariant relationships are needed as there are unmeasured species, or in other words, the data (in the reaction-variant form) dimension must have the same dimension of the reaction network. The authors call this a necessary condition for accepting an uncompleted target that lies in the row space of data matrix in the reaction-variant form as a tool to remove ambiguities.

More recently, Santos-Marques et al. (2019) and Dong et al. (2019) have used TFA to identify/validate reaction stoichiometries from pre-treated data. The authors propose the use of dynamic response surface methodology (DRSM) for the obtainment of smoothed species concentration profiles from discrete and noisy data, and they conclude that this method have improved the identification of the true system stoichiometry from simulated noisy data, via TFA and incremental/sequential TFA, respectively.

Since the modeling of chemical reaction systems involves the reaction network identification, several methods to generate networks are described in the literature. The next section addresses some of these methods.

### 3.1.4 Inverse problems for identifying reaction networks

The identification of systems from observed data can be considered an inverse problem, since the causal factors that produced the set of observations are sought, starting with the observations (effects) and then identifying the model (causes). In the context of modeling chemical reaction systems, inverse problems appear on the basis of the differential method, where the species time concentration derivatives are used as reference data for model/system identification. In these cases, the established model is linear in its parameters, where time concentration derivatives are correlated with instantaneous concentration measurements of observed species that are consumed or produced over time. Hence, the species mass balances that constitute a set of ordinary differential equations (ODEs) are transformed into a set of algebraic equations when time concentration derivatives are previously computed. In the case of a batch chemical reaction system modeled with homogeneous reaction kinetics, the following set of linear systems of equations is obtained

$$\mathbf{D} = \mathbf{B} \cdot \mathbf{K} + \mathbf{E} \quad \Leftrightarrow \quad \frac{d\mathbf{c}_s}{dt} = \mathbf{B} \cdot \mathbf{k}_s + \mathbf{e}_s, \quad \forall s = 1, \dots, n_{sp} \quad (3.1)$$

where  $\mathbf{D}[n_{t0} \times n_{sp}]$  is the time concentration derivatives matrix with  $n_{t0}$  registers of  $n_{sp}$  chemical species, containing in its columns  $d\mathbf{c}_s/dt$ -type vectors,  $\mathbf{B}[n_{t0} \times n_c]$  is the design matrix composed by  $n_c$  reactant species (and/or complexes of reactant species) in its columns,  $\mathbf{K}[n_c \times n_{sp}]$  is the kinetic parameters matrix with  $\mathbf{k}_s, s = 1, \dots, n_{sp}$ , column vectors that are variables of the problem, and  $\mathbf{E}[n_{t0} \times n_{sp}]$  is the matrix of residuals between the observed data  $\mathbf{D}$  and the model  $\mathbf{BK}$ , composed by  $\mathbf{e}_s, s = 1, \dots, n_{sp}$ , column vectors.

Equation (3.1) can be written for any reaction kinetic expression for which the response variable varies linearly with the dependent variable (reactant concentration), even for approximation of nonlinear models that needs reparametrization to achieve a linear form. Moreover, notice that the interdependencies of the ODEs may be removed using reference concentration derivatives values, and thus enabling to estimate vectors  $\mathbf{k}_s$  separately for each  $s = 1, \dots, n_{sp}$ .

The solution  $\mathbf{k}_s$  obtained identifies the chemical reactions in which the species  $s$  is involved

with their respective mass action law. Therefore, from the analysis of the obtained  $\mathbf{K}$  it is possible to infer the species connections through the negative and positive signs of each kinetic parameter identifying the rates of species consumption and production, respectively, that are function of the respective reactant complex column of  $\mathbf{B}$ . In order to establish the system stoichiometry, the matrix  $\mathbf{K}$  can be decomposed in two matrices

$$\mathbf{K} = \mathbf{P} \cdot \mathbf{N} \quad (3.2)$$

where  $\mathbf{P}$  is a diagonal matrix composed by  $n_p$  kinetic parameters and  $\mathbf{N}$  is the stoichiometric matrix composed by  $n_p$  reaction components in its rows and  $n_{sp}$  chemical species in its columns.

Matrices  $\mathbf{K}$  and  $\mathbf{N}$  span the same row space with dimension inferior or equal to  $n_{sp}$ , and this subspace approaches the row space of  $\mathbf{D}$  as  $\mathbf{E}$  tends to zero. It is important to observe that through the use of matrix  $\mathbf{B}$  for kinetic parameters tuning, it is possible to adjust at most  $n_c$  variables (model parameters) when  $\mathbf{B}$  has full rank. When  $n_p$  is greater than  $n_{sp}$ , or more specifically, when  $n_p$  is greater than the matrix rank of  $\mathbf{D}$ , the resulting reaction network has redundant reaction pathways, whose instantaneous reaction fluxes can not be determined without establishing its reaction kinetics, since an underdetermined system of equations is in question. Therefore, (3.1) enables the adjustment of linearly dependent reaction network structures.

For example, consider a small chemical system composed by 3 chemical species connected by 3 chemical reactions with one reversible component:



The species mass balances are written as

$$\begin{bmatrix} | & | & | \\ A' & B' & C' \\ | & | & | \end{bmatrix} = \begin{bmatrix} | & | & | & | \\ A & B & B^2 & A^2 \\ | & | & | & | \end{bmatrix} \cdot \begin{bmatrix} -k_{1d} & k_{1d} & 0 \\ k_{1i} & -k_{1i} & 0 \\ 0 & -2k_2 & k_2 \\ -2k_3 & 0 & k_3 \end{bmatrix} \quad (3.4)$$

or equivalently

$$\begin{bmatrix} | & | & | \\ A' & B' & C' \\ | & | & | \end{bmatrix} = \begin{bmatrix} | & | & | & | \\ A & B & B^2 & A^2 \\ | & | & | & | \end{bmatrix} \cdot \begin{bmatrix} k_{1d} & 0 & 0 & 0 \\ 0 & k_{1i} & 0 & 0 \\ 0 & 0 & k_2 & 0 \\ 0 & 0 & 0 & k_3 \end{bmatrix} \cdot \begin{matrix} A & B & C \\ \begin{bmatrix} -1 & 1 & 0 \\ 1 & -1 & 0 \\ 0 & -2 & 1 \\ -2 & 0 & 1 \end{bmatrix} & \begin{matrix} r_{1d} \\ r_{1i} \\ r_2 \\ r_3 \end{matrix} \end{matrix} \quad (3.5)$$

where the last matrix is the stoichiometric matrix  $\mathbf{N}$  with matrix rank two, *i.e.*, only two linearly independent pathways can be seen in the network, as such as the the row space of  $\mathbf{D}$  has dimension two.

Hence, the general objective of these data approximation methods is to find the best correlations of time concentration derivatives (one for each observed species) as a linear function of reactant species concentration using experimental data and candidate reaction kinetics that are linear in their parameters, therefore identifying the kinetic expressions in simultaneous with the reaction network that is implicit in the set of the best correlations found. This problem is considered ill-posed since the computation of concentration derivatives amplify the uncertainty originally presented in concentration measurements, leading to identification problems. Therefore data regularization methods are required for increasing data accuracy and obtaining good estimates of its slopes.

However, in contrast with system identification approaches supported on the integral method, the inverse problem can be less computationally intensive, presenting global optimal solutions accordingly to the adopted linear optimization method, although with the presence of biased parameter estimates. As previously discussed in Section 3.1.1, the simultaneous approach to model chemical reaction systems supported by the integral method requires an intensive computational effort in the adjustment of kinetic parameters concerning to a previously postulated reaction model, where the ODEs are numerically solved as many times as necessary to find an optimal solution to the nonlinear regression problem, which in general is very sensitive to initial parameter estimates and often converges to local solutions, although free of bias.

On the other hand, in comparison with the incremental method (Section 3.1.2), although also supported on the species compositional changes information, the major difference appears on the coupling of the identification steps concerning to the reaction network and its reaction kinetics, while the incremental method decouples these two identification steps.

In the following paragraphs, two different approximation strategies for simultaneous identification of the reaction network and of the reaction kinetic expressions from the computation of concentration derivatives are discussed. At the end of this section, critical points are summarized pointing out some drawbacks and establishing a natural comparison with the work proposed in this dissertation.



### Numerical matrix method

The numerical matrix method (NMM) was firstly proposed by [Karnaukhov and Karnaukhova \(2003\)](#) for nonlinear dynamical system identification on the basis of the differential method. From the resolution of a set of linear systems of equations, the method is able to identify (i) the kinetic parameters, (ii) the kinetic expressions that govern the system dynamics, and (iii) the reaction network structure that links the chemical species (when it is unknown), explaining the observed compositional changes. For this purpose, it is assumed that no more than two molecules participate in a chemical reaction, establishing a superstructure of reaction kinetic expressions of homogeneous kinetic laws of zero, first and second orders. Consequently, the considered design matrix is composed by  $n_c = (n_{sp} + 2)(n_{sp} + 1)/2$  reactant complexes in its columns, including an unitary vector in order to cover reaction kinetics of zero order. For example, for a chemical system with two chemical species (*e.g.*, A and B), the design matrix would contain the following reactant complexes in its columns:  $\mathbf{B} = [1 \ A(t) \ B(t) \ A(t)^2 \ A(t)B(t) \ B(t)^2]$  with  $n_c = 6$ , and six kinetic parameters would be adjusted for each chemical species mass balance.

The objective function is given by the minimization of the  $l_2$ -norm of  $\mathbf{e}_s$  in (3.1) for species  $s = 1, \dots, n_{sp}$ . Therefore, every species mass balance is adjusted separately in an independent/individual linear regression procedure, and the presence of redundant chemical reactions can be verified after the obtainment of the entire set of  $n_{sp}$  optimal solutions (the  $\mathbf{K}$  matrix). Hence, NMM consists of least squares regression, where  $\mathbf{D}$  is orthogonally projected onto  $\mathbf{B}$  in order to get the best set of solutions  $\mathbf{K}$  in the least squares sense ([Karnaukhov and Karnaukhova, 2003](#); [Karnaukhov et al., 2005, 2007](#)), such that

$$\mathbf{B}^T \cdot \mathbf{B} \cdot \mathbf{K} = \mathbf{B}^T \cdot \mathbf{D} \quad \Leftrightarrow \quad \mathbf{B}^T \cdot \mathbf{B} \cdot \mathbf{k}_s = \mathbf{B}^T \cdot \frac{d\mathbf{c}_s}{dt}, \quad \forall s = 1, \dots, n_{sp} \quad (3.6)$$

Notice that the multiplication of  $\mathbf{B}^T$  in both equation sides consists of a linear transformation that turns the system (3.1) possible to be solved with null  $\mathbf{e}_s$  vector for  $s = 1, \dots, n_{sp}$ , since  $\mathbf{B}^T \mathbf{D}$  is a subset (it is contained) in  $\mathbf{B}^T \mathbf{B}$ . Consequently, the  $n_{sp}$  systems of equations in (3.6) are determined when  $\mathbf{B}$  has full rank (non-singular), and, in the opposite case, they are underdetermined when  $\mathbf{B}$  is singular. In general,  $\mathbf{B}$  is singular due to time-invariant characteristics of chemical reaction systems (at least the total mass is conserved). However, in order to turn the system completely identifiable, several datasets with different initial conditions must be considered for obtaining a global non-singular  $\mathbf{B}$  matrix in which holonomic constraints are broken ([Karnaukhov et al., 2007](#)).

Additionally, it may be observed that the matrix rank of  $\mathbf{B}$  is greater than or equal to the matrix rank of  $\mathbf{D}$ , and consequently, the matrix rank of  $\mathbf{B}^T \mathbf{D}$  is lower or equal to the rank of  $\mathbf{D}$ . When  $\mathbf{B}$  has full rank,  $\mathbf{B}^T \mathbf{D}$  and  $\mathbf{K}$  have the same matrix rank of  $\mathbf{D}$ , and  $\mathbf{K}$  corresponds to a basis rotation of  $\mathbf{B}^T \mathbf{D}$ . Hence, both the matrices  $\mathbf{B}^T \mathbf{D}$  and  $\mathbf{K}$  span the same row space with a dimension lower or equal to  $n_{sp}$ , as well as the rows of  $\mathbf{K}$  approximately span (at most) the same row space of  $\mathbf{D}$  ( $\text{row}(\mathbf{K}) \approx \text{row}(\mathbf{D})$ ).

As previously mentioned, the presence of a chemical reaction that links different species is identified when approximately the same  $k_{i,s}$  value (but with opposite sign) is obtained for the related  $s$  species mass balances. The authors establish that due to the presence of noise and numerical error approximations, the values of  $k$  that are lower than a threshold are assumed zero. [Karnaukhov et al. \(2007\)](#) assume that this threshold value must be empirically determined on the basis of noise level quantification in data. After obtaining  $\mathbf{K}$  in a first iteration through the solution of (3.6), a reduced system must be solved for increasing the precision of the method by considering only the columns of  $\mathbf{B}$  that are active, *i.e.*, by excluding entire columns of  $\mathbf{B}$  when the respective entire rows of  $\mathbf{K}$  converge to approximately zero. Moreover, when the stoichiometric matrix (or part of it) is known, the precision of the method for identifying kinetic expressions is increased presenting more accurate parameter estimates, since it effectively pairs up the reactant and product species for each known reaction, and therefore, the number of parameters to be estimated is much lower than that in the full superstructure of homogeneous kinetic laws of unknown chemical reactions ([Karnaukhov et al., 2005](#)).

The results obtained with NMM are extremely dependent on the accuracy of the concentration derivatives estimates which are performed using finite differences. Hence, a significant amount of data is needed to obtain (reasonably) reliable estimates of concentration derivatives, despite the presence of noise in the data. Furthermore, several datasets with different initial conditions are required to have a non-singular design matrix, which is a necessary condition for the method applicability. These constraints may be a limitation of the method applicability, specially for real case studies that present scarce measurements. In addition, the method can face numerical problems and problems related to aggregated parameters in the optimal solution that difficult the system identification. However, the major disadvantage of NMM is related to the presence of data noise in which the uncertainty associated with the concentration measurements is dragged (and in some cases it is amplified from the computation of concentration derivatives) to the model parameters, leading to an increased probability of overparameterization, and/or with the presence of poor parameter estimates.

The NMM can support larger problem sizes than those associated with bimolecular complexes, considering design matrices with larger reagent complexes, for example containing the combination of three reagent molecules. However, for kinetics of, at most, second order, the number of complexes increases with the square of the number of species, which may be (already) a limitation of the method, resulting in a combinatorial explosion for large case studies, such as for biochemical systems. Therefore, the presence of trimolecular complexes can easily lead to the combinatorial explosion of the problem, especially for large case studies.

Although the main characteristics of the method have been presented, an additional discussion is considered in Section 3.1.4 presenting a natural comparison with the work developed in this thesis. However, for closing this section we want to point out some

key issues that were not addressed by the authors of the NMM, thus, they still remain open, namely: (i) How many different initial conditions are needed in order to turn  $\mathbf{B}$  non-singular? (ii) Which initial concentration values should be chosen for decreasing the condition number of  $\mathbf{B}$ , *i.e.*, in order to turn the problem of NMM better conditioned? As suggestions for the NMM improvement, specially for problems that verify great amounts of noise in data, we advice the use of (i) data treatment techniques for increasing data precision and obtaining of good estimates of concentration derivatives before NMM application, and (ii) further methods for determining the best compromise between data agreement and model complexity (number of parameters) in order to avoid data overfitting, for example through the use of inference methods and/or cross validation. Next section addresses the identification of reaction networks using inference criterion.

### Identification of reaction networks using an inference criterion

Recently, on the basis of the differential method, an improved approach has been proposed to identify the reaction network using integer programming and inference criterion (Willis and von Stosch, 2016, 2017). These authors explored the use of MILP to perform linear sparse regression (parameter regularization) where the reaction network can be identified from the interpretation of the optimal kinetic parameter estimates that represent the best compromise between good approximation of the closure of every species mass balance in the differential form and model complexity, leading to an improved predictive performance when compared to ordinary least squares regression since overparameterization is avoided.

The objective function consists of the sum of two parcels concerning to the minimization of (i) the total absolute error between model's instantaneous concentration derivatives and the respective reference values ( $l_1$ -norm of absolute response residuals) plus (ii) the penalized  $l_0$ -norm of the kinetic parameters vector, *i.e.*, the cardinal number of active parameters. This penalization is considered using binary variables that assume unity when parameter estimates are different of zero and zero otherwise, and a regularization factor/weight that is determined using Bayesian information criterion (BIC) in a postponed phase. Hence, in sequential procedures, the parameter regularization is performed and the BIC is computed for a range of regularization factors, and therefore, the best model is identified when the lowest BIC is found. For more details, see Section 5.2.3.

Similar to the NMM previously described in Section 3.1.4, fine adjustment of parameters is supported in the calculation of concentration derivatives and in the establishment of a superstructure of the model that is linear in its parameters. This superstructure is composed by (i) homogeneous kinetic expressions dictated by uni- and bi-molecular chemical reactions (Willis and von Stosch, 2016), and (ii) empirical model components that can approximate to Monod and Michaelis-Menten kinetics in biochemical systems and heterogeneous kinetics in catalytic chemical system (Willis and von Stosch, 2017). In this last case, prior mathematical manipulation of the species mass balances is required for achieving substitute response variables that are written as a linear function of the

manipulated design matrix through the kinetic parameters (model reparameterization).

In contrast to NMM, through the sparse approximation strategy proposed in this approach, the overparameterization is avoided by dropping off irrelevant model components of the superstructure when related parameters converge to zero, instead of considering the best set of solutions in the least squares sense (with the presence of data overfitting and model overparameterization, see (3.6)). Moreover, Willis and von Stosch (2016) ensure the obtainment of balanced stoichiometries in the solution by pre-excluding infeasible species complexes of the superstructure, *i.e.*, combinations of reactant species that would lead to unbalanced chemical reactions, using the atomic matrix for checking elemental balances. In this way, they achieve a reduction in the number of complexes to be considered in the model's superstructure, thus reducing the size of the problem.

However, as much as this approach tries to avoid overparameterization of the model, there will always be a tendency towards overfitting of the data, especially in the presence of greater noise content. This means that additional model parameters can be verified in the solution to explain data components that are essentially noise. In addition, the resulting solution may present a network composed of a set linearly dependent on chemical reactions, since the number of linearly independent columns (representing the combinations of reactant species) in the design matrix is greater than the dimension of the variant space of the data (this being at most  $n_{sp} - 1$ , the maximum number of independent components, reaction fluxes, that conserve the total mass). Consequently, at most  $n_c$  model parameters can be adjusted in this procedure for a full rank  $\mathbf{B}$  matrix. However, this design matrix will always be poorly conditioned, since great correlation is verified between the species concentration measurements, in addition to the presence of noise.

The use of parametric model forms, such as rational polynomials (Willis and von Stosch, 2016) and smoothing splines (Willis and von Stosch, 2016, 2017), were considered to approximate data and extract the derivatives before applying the model identification method. Although the concentration derivatives are better estimated from approximated polynomial functions than from simple computation of finite differences, undesired oscillations in the smoothed profiles are observed in both works, concerning to different simulated case studies. These oscillations may lead to erroneous reference data that will interfere with the model identification. In contrast, when the reference data have appreciable bias (too much data regularization) or/and the measures are scarce, the optimal model structure found may not necessarily be validated by the available (original) data in a postponed model simulation. However, the smoothing splines method has its own implementation characteristics, presenting challenging issues for data smoothing from dynamic multi-response systems, such as for chemical reaction systems in which a smoothing factor must be determined for every individual species smoothing profile (establishing the amount of data regularization), where these last are related to each other by invariant relationships over time. This topic is addressed in Section 5.2.4. Although balanced stoichiometries are considered in the superstructure and the dimension of the model is

determined by the lowest BIC, no concern has been shown by the authors to identify invariant relationships of the system from data, and then use them for a better treatment of the data, or at least, to assess the dimension of the data space.

Willis and von Stosch (2016) were the pioneers in using MILP for reaction network and kinetic expression identification using experimental data, but, through this simultaneous approach, the obtainment of consistently connected networks<sup>1</sup> is not guaranteed<sup>2</sup>. For example, Willis and von Stosch (2017) found a solution with an inconsistency in the network in their case studies, and then, corrected it by imposing additional constraints in the optimization problem (by fixing some binary variables). This inconsistency was easy to identify and correct since there was no disturbance in the value of the BIC when the change/correction was made, however, the case study in question is of low dimension (five chemical species). For larger case studies presenting network inconsistencies, manual detection and correction can be a difficult problem to deal with, drastically interfering in the optimal condition of the solution found and, therefore, systematic approaches are necessary to avoid structural inconsistencies, especially in the presence of datasets with great uncertainty and residual species. In this dissertation, the use of MILP is also considered in the context of modeling reaction systems. In this case, the proposed computational approach concerns the generation of feasible structures for a fixed model dimension, without using experimental data, but, nevertheless, incorporating precedence restrictions between species that ensure the achievement of consistently connected networks, for more details see Chapter 8. Hence, the approach followed here considers the generation of feasible structures to then select the most plausible ones supported on experimental data, in sequential phases.

### Critical points

In summary, on the basis of the differential method (i) it is possible to convert the ODEs (species mass balances in the differential form) into an equivalent set of algebraic equations that can be independently solved through the previous estimation of concentration derivatives, and (ii) the set of solutions from every independent parameter estimation problem is theoretically sufficient to deduce the structure of the underlying model (simultaneous identification of the reaction network and kinetic expressions) through the use of a superstructure of kinetic expressions that are linear in their parameters. The main characteristics that are critical in both methods are summarized in Table 3.1.

As disadvantages, we must comment that, normally, this problem (i) is ill-posed (well known in the literature as the inverse problem), since small errors in the concentration measurements may be amplified in the computation of concentration derivatives, and (ii) presents a poorly conditioned design matrix that approaches the singularity. These facts

---

<sup>1</sup>A network/pathway in which the reaction fluxes consistently travel among species/nodes.

<sup>2</sup>The obtainment of connected structures is a concern addressed in the context of graph synthesis using graph theory. For more details, see Section 3.3. The same concern, including connectivity as well as consistency restrictions, is addressed in this thesis in the generation of reaction networks (Chapter 8).

can limit the applicability and success of the method, leading to the identification of mismatched models and/or with great uncertainty in the model parameters. In order to contour these problems, for item (i) data processing/regularization/treatment methods may be considered *a priori* to increase data accuracy and to enable good estimates of its derivatives (for more details see Chapter 5), and for item (ii) robust regression methods that are able to discard redundant information of the design matrix are required. Moreover, the presence of uncertainty in the data increases the probability of overparameterization, leading to the resultant model having components that essentially explain the noise of the data. Additionally, especially in cases of greater data noise content, the identified network structure can show inconsistencies and/or disconnected paths. In this sense, it is preferable a methodology that considers network properties as a restriction of the modeling problem, independently of, or simultaneous with, the ability to approximate the data.

The inference of network properties happens from the resulting model that is obtained with the parameterization of an ODE model structure *directly* from observed data, and therefore, this approach is highly dependent on the information contained in data, *i.e.*, it approaches an empirical model development, purely data-driven. In this sense, during this simultaneous identification (reaction network and kinetic expressions) the mechanistic support is diminished, it loses useful information that could be incrementally extracted when adopting a step-wise model development in which system's knowledge may be extracted from both theoretical and data analyses in every step-by-step model identification. For example: (i) the model dimension can be determined *a priori* from data analysis using parametric and non-parametric statistical tools/methods that enable the identification of the number of independent model components that is required to explain the observed compositional changes, consequently, avoiding overparameterization in the following steps of modeling, (ii) the presence of reaction inhibition can be observed from the analysis of reaction flux profiles, and candidate reaction kinetics can be suitably proposed based on qualitative analysis of profile shapes, mechanistic support and information related to the knowledge of the system. Also, in contrast with the incremental approach, it is not direct/easy to infer which reactions certainly belong to the network from the ones that are uncertain, in this simultaneous identification approach. These are examples of aspects that are incorporated in the methodology for incremental model development, addressed in this dissertation.

In this dissertation, we work analyzing the row space of  $\mathbf{D}$  for identifying the reaction network structure since  $\mathbf{D} = \mathbf{R} \cdot \mathbf{N} + \mathbf{E}$ , where both  $\mathbf{R}$  and  $\mathbf{N}$  are inferred/identified from  $\mathbf{D}$  without the need to establish reaction kinetic expressions. In this case, the identification of the reaction network structure is performed looking for linearly independent sets of plausible reaction fluxes with unknown reaction kinetic expressions. Hence, the network identification is decoupled from the reaction kinetics elucidation, and its structure is represented by a full row rank stoichiometric matrix  $\mathbf{N}$ . In contrast, the previously described inverse problems identify the reaction network from the analysis of  $\mathbf{K}$  (see (3.1)), simul-

taneously with the elucidation of reaction kinetics, enabling the adjustment of redundant reaction paths.

Moreover, when considering the kinetic modeling method presented in this dissertation, additional differences arise. Despite the similarity in considering a superstructure of kinetic expressions, the number of combinations (reactant complexes) considered here is much lower than in the proposed simultaneous approach since the reaction network is known at this methodology step, enabling the direct correlation of the reaction flux with the reactant species concentration(s). Therefore, instead of considering the simultaneous fit of several reaction fluxes for each species flux for an unknown reaction network, the kinetic expression identification is individually done for each reaction flux that represents a linear combination of the species fluxes. However, both methods can incorporate heterogeneous kinetic expressions that have nonlinear dependence on parameters and still remain a linear regression problem. This is possible through mathematical manipulation and changing variables in the objective function. The same procedure is performed in Step 6 of the methodology, when considering superstructures with Langmuir-Hinshelwood kinetics. For more details see Section 10.2.

## 3.2 Systematic generation and selection of reaction networks

*“Network reconstructions provide context for ‘content’.”*

– Mick Savage

The generation of alternative reaction networks is addressed in the literature under different contexts, including analysis of biological (metabolic) networks and chemical systems with catalytic and non-catalytic reactions. The generation of reaction networks based on optimization tools, graph theory, on linear algebra, and also in some cases taking into account the thermodynamic viability of the reactions in question, are considered here. Moreover, the methods related to the synthesis of metabolic networks are covered in this section, including the description of the concept of extreme pathways.

### 3.2.1 Metabolic reaction networks

The field of modeling biological reaction networks is challenging due to the complexity of these systems, presenting networks that contain a large number of degrees of freedom (more chemical reactions than metabolites). For example, a genome-scale metabolic network respected to an eukaryotic organism (yeast *Saccharomyces cerevisiae*), containing 1175 metabolic reactions and 584 metabolites, was reconstructed by (Förster et al., 2003). Modeling methods for metabolism reconstruction are based on constraints that

**Table 3.1** Critical characteristics of inverse methods for identifying reaction networks.

Critical characteristics	Commentary / Solution
Combinatorial problems <sup>(a)</sup> .	Decoupling the structural model identification for decreasing the number of potential candidate models.
Dependent of a superstructure of kinetic laws, which must be linear in its parameters.	This fact does not avoid the use of nonlinear kinetics such as heterogeneous ones, but this implies the need of model reparametrization which sometimes can lead to (more) poorly conditioned systems.
The design matrix is badly conditioned, approaching to the singularity.	Do not consider simultaneous identification, but instead, consider incremental identification.
The problems are ill-posed. (Small errors in concentration measurements represent large errors in concentration derivatives estimates).	Data regularization and data reconciliation (with time-invariants constraints) for increase data accuracy and compute good concentration derivatives estimates.
The resulting models present overparameterization, especially in the presence of significant data noise content.	Set the model dimension for a previously identified data variant space, and/or, consider robust sparse approximation methods.
The models, in general, present redundant reaction pathways.	Do not allow network redundancies.
It approaches a data-driven methodology, with few or none mechanistic support under consideration.	Incorporate mechanistic and empirical knowledge.
Can present network inconsistencies and/or disconnected paths.	Consider subtour elimination and precedence constraints.
Needs of establishment of a threshold to force the zero value of parameters.	It requires data analysis tools for noise quantification.
Present biased parameter estimates.	Requires a final iteration using the simultaneous/integral method with the identified model structure (reaction network and kinetic expressions) using the parameter estimates and original experimental data. Solution obtained free from bias, in the sense of maximum likelihood.

(a) It may face difficulties associated with the dimension of the case study, *i.e.*, larger case studies (greater number of species and candidate kinetic laws) lead to bigger superstructures of reaction kinetics.



systematically translate biochemical, genetic and genomic knowledge into a mathematical framework, thus allowing a mechanistic description of metabolic physiology (Bordbar et al., 2014a). It is assumed that living organisms operate with optimal functional states under the conditions they have evolved, and therefore functional states of networks may be predicted using constrained optimization (Palsson, 2015b). Most of related works in this field do not adjust kinetic parameters, but instead determine optimal reaction fluxes and feasible reaction networks that conduct to a maximum functional state (Jamshidi and Palsson, 2011). Famili and Palsson (2003a,b) have presented studies related to the metabolic networks using SVD and linear algebra for understanding physical meaningful properties of biological systems.

Typically, a superstructure of intra-cellular mechanisms is considered based on theoretical and mechanistic knowledge, containing a very large number of candidate pathways in which material fluxes can travel during intracellular processes. For modeling these complex systems, in general, many assumptions are required, starting by defining the system frontiers, and then assuming that this zone of the cell operates at steady or quasi-steady conditions under feasible boundary constraints. The existence of rate-controlled and/or equilibrium steps are other type of currently adopted assumptions. However, since many metabolites are (micro)molecules that cannot be measured in experimental tests, and the observed interactions between macromolecules often cannot be predicted through the adopted reaction network, model validation is a hard task. In general, validation occurs in terms of specific components productivity and feasible ranges for concentration ratios. Thiele and Palsson (2010) presents a protocol containing each step necessary to build a high-quality genome-scale metabolic reconstruction.

Two main constraint-based modeling approaches are distinguished in the literature: the metabolic flux analysis (MFA) and the flux balance analysis (FBA). In both approaches intracellular fluxes are constrained to operate at steady conditions, satisfying the stationary metabolites mass balances for a very large stoichiometric matrix describing a superstructure of reaction networks. The differences between these two methods arise in how these internal fluxes are determined. In MFA, fluxes are calculated by fitting extracellular rates measured experimentally. In this case the model must be simplified by excluding unobservable/residual or unidentifiable reaction components until a system with zero degrees of freedom is obtained (Wiechert, 2001). In FBA, a linear space of allowable flux distributions is determined by solving a linear optimization problem constrained to observed extracellular rates and upper and lower bounds on fluxes, for a given objective function, making it possible to predict, for example, the growth rate of an organism or the rate of production of a biotechnologically important metabolite (Orth et al., 2010). Therefore, the goal is to quantify the best metabolite concentrations and the optimal mass fluxes that travel in the metabolic network, thus determining the optimal mechanism that (i) minimizes the prediction error of extracellular rates in the case of MFA method, or (ii) maximizes the adopted objective function (*e.g.*, biomass or ATP production), in the case of FBA approach. Consequently, MFA is used for estimating reaction fluxes for biological

systems that can be measured in laboratory (experimental tests), whereas FBA is used for simulation studies (*in silico* predictions) for identifying genetic manipulations that can improve cell metabolisms and formulating novel hypotheses (Gianchandani et al., 2010).

Many authors have proposed the use of FBA using different formulations and strategies (Savinell and Palsson, 1992; Schilling et al., 1999, 2000a; Ibarra et al., 2002; Beard et al., 2002; Bordbar et al., 2014b). The formulation may be linear or not, depending on the established constraints, and it can contain binary variables to decide whether the path is present in the network. Kauffman et al. (2003) made an overview of the existent methods that use FBA presenting their chronological contributions. A comparison of modeling and analysis techniques for high-throughput data is found in the review by Bordbar et al. (2014a) about constraint-based metabolic models. Moreover, there is a toolbox available in the MATLAB software named as COBRA (constrained-based reconstruction and analysis) containing the main tools for biological networks reconstruction, including visualization of maps and data, FBA and related methods, and other reconstruction tools (Palsson, 2015b). For more information, see Becker et al. (2007) and Schellenberger et al. (2011).

To constrain even more the identification problem of biological reaction networks, the incorporation of thermodynamic restrictions is considered by several authors. In an optimization procedure, the optimal flux distributions are determined obeying simultaneously to boundary constraints established in FBA and additional energetic constraints. The main criterion consists of constraining the Gibbs free energy changes in all individual paths to be negative. Therefore, the optimal solutions obtained present (i) the concentrations of each metabolite at steady-state, and (ii) flux distributions with established net directions that are energetically feasible. The method of energetic balance analysis (EBA) was initially proposed by Beard et al. (2002), where a nonlinear optimization procedure is considered, with the imposition of negative free energy changes as nonlinear constraints of the problem. Obtained solutions have no guarantees to be global optimal, but the authors showed that the resulting feasible solution space is a subset of the space predicted by a traditional FBA. Qian et al. (2003) proposed a stoichiometric network theory for nonequilibrium biochemical systems based on EBA, establishing an analogy to Ohm's law in electrical circuits. Lately, Beard et al. (2004) formalized the conditions in which mass fluxes are energetically feasible to occur by means of linear algebra analysis. In this last case, the thermodynamic feasibility condition is valid not only for steady-state fluxes but also for transient ones. Moreover, the authors showed that flux vectors that are linear combinations of energetically feasible fluxes are not guaranteed to satisfy the thermodynamic constraints. The enunciated condition enables to eliminate unfeasible reaction cycles in metabolic reaction networks. Finally, Qian and Beard (2005) published a review of the method of incorporating thermodynamic constraints for steady-state and dynamic biochemical networks identification. Besides the elucidation of the reaction direction, the use of energetic criteria allows the estimation of how far from equilibrium the reactions in the network operate. Henry et al. (2007) proposed the use of MILP for identifying

biological networks using FBA and EBA, naming the method as thermodynamic-based metabolic flux analysis (TMFA). In this formulation (i) the nonlinear constraints of the EBA problem are written in a linear format by adopting as variable of the problem the logarithm of the metabolite concentrations (or activities); (ii) binary variables are used to identify the positive signs of the reaction fluxes and the direction in which these flux are energetically feasible. Moreover, the concentration ranges in which the fluxes are energetically feasible and the flux ranges in which the reaction Gibbs free energy change remains negative are also determined. [Ataman and Hatzimanikatis \(2015\)](#) made an overview of the existing methods of thermodynamic-based network analysis, differentiating three main approaches: the EBA, the TMFA and a third method named as network-embedded thermodynamic analysis (NET).

Although most of the previously described methods to generate reaction networks are not directly supported on experimental data, some of them use experimental data to evaluate the quality of the proposed model, by verifying the model simulation agreement with the data available (*e.g.*, [Henry et al. \(2007\)](#); [Edwards et al. \(2001\)](#)).

In contrast, the group of Professor Marquardt (pioneer in the incremental modeling strategy) adopted a step-wise method supported on experimental data to estimate kinetic parameters in metabolic networks ([Jia et al., 2012](#)). The optimization procedure enables the parameters adjustment for linearly independent and dependent chemical reactions in sequential steps, thus reducing the associated computational effort, but it is assumed that the reaction network is already identified.

The research group of Professor Grossmann also considered the problem of identifying metabolic networks using FBA, but in a more systematic approach in which all solutions that constitute extreme points with identical objective values are obtained through a recursive MILP formulation ([Lee et al., 2000](#)). This is achieved by reformulating the FBA problem in a canonical LP formulation using slack variables. The re-formulated problem presents only equality constraints and non-negative variables. In order to find multiple solutions, after obtaining the first solution, integer cuts are added to the formulation in every iteration, until all feasible solutions are found. With this approach, the authors have shown that the algorithm provides directions to additional experimental tests through the analysis of the multiple flux distribution alternatives.

Recently, [Portela et al. \(2019\)](#) propose the use of sparse regression using MILP for identifying metabolic reaction networks that balance sparseness of solutions (reduced number of reaction fluxes) against the data agreement (fit of extracellular compounds feedings). For this, the absolute error between molar quantities is considered, where the model counterpart is given by the integral of extracellular material balance at steady conditions. Therefore, the traditional MFA is transformed by using time-integrated reaction fluxes. Hence, it does not provide the rate at which the material is transformed for every time instance, but the (absolute) amount of material transformed by the pathways for a certain time span, identifying the relative use of pathways (or the total pathway usage for a

specified time interval).

### Extreme pathways

The concept of extreme pathways is very useful for understanding how a metabolism can work, since it enables the mathematical quantification of every feasible steady-state flux distribution, identifying their spacial and structural representation in terms of linear algebra and network topology, respectively. Any vector of steady-state reaction fluxes lies in a convex region that is inserted in the (right) null space of the transposed stoichiometric matrix (Schilling et al., 2000b). Remember from Section 2.2.2 that when the stoichiometric matrix is rank-deficient, it presents a (right) null space that corresponds to a linear combination of the stoichiometric vectors that add up to zero, resulting in a steady-state for the network (null response vector). The convex representation of the null space consists of a delimited region of the reaction flux space with a conical format, where the upper flux bounds establish hyperplanes that close the convex region and the lower flux bounds (fluxes are greater or equal to zero) establish the origin of the conical representation. The edges of this cone are the set of vectors that spans the convex space in a nonnegative fashion, and they correspond to extreme functions of the reaction network. They are thus called *extreme pathways* (Palsson, 2015a).

The extreme pathways are uniquely determined for a given reaction network superstructure, but their number can be greater than the dimension of the null space, configuring a generating set of positive steady fluxes. Therefore, any positive steady flux vector is written as a linear combination of the extreme pathways, but this combination can be not unique.

The problem of computing extreme pathways is of combinatorial nature, consisting of a NP-hard problem that has been solved using an algorithm that involves matrix operations (Schilling et al., 2000b; Bell and Palsson, 2005) and integer (linear) programming (Bordbar et al., 2014b). The number of extreme pathways grows faster than the number of species/components in a network, consisting of a problem that leads to large numbers of possible combinations. Bordbar et al. (2014b) proposed an algorithm (MINSPAN) to compute the minimal set of pathways, where the sparsest representation of the convex region is searched using a MILP formulation.

Famili and Palsson (2003a) made an analogy with extreme pathways, considering the convex space of the left null space of the stoichiometric matrix, where time-invariant relationships lie. These relationships establish *metabolic pools* (linear combination of metabolites concentration) whose total concentration does not change over time. The study of time invariants with physical meaning allows the identification of achievable states of the cell and their physiological interpretation.

### Dynamic metabolic flux analysis

In order to model batch and semi-batch biological reaction systems (*e.g.*, cell growth and intracellular metabolism with dynamics), dynamic metabolic flux analyses were proposed. In these approaches, the key concept passes through assume that the cell still work in steady-state conditions for intracellular processes, but these steady-states are function of several external conditions that vary in time. In practice, this means that the time-scale for process dynamics must be longer than the time-scale for intracellular metabolism to equilibrate with the extracellular environment ([Antoniewicz, 2013](#)). Therefore, in order to compute the intracellular fluxes that are dependent variables of time, whether using FBA or MFA methods, the task of computing extracellular dynamics is required. In this sense, it is assumed that every species/component that is measured during a batch (or semi-batch) experiment represents an external component responsible to determine an exchange flux that cross the boundary of the cell, and, on the other hand, the species that are unmeasured are part of the intracellular organism (inside of the boundaries) that operates at pseudo steady-states. The fluxes that cross these boundaries are therefore the ones that represent the process dynamics, and they must be computed using techniques that enables the quantification of the concentration slopes (time-concentration derivatives). Several works are proposed in the literature using different techniques for estimating the external species concentration derivatives (the fluxes that cross the boundaries). [Antoniewicz \(2013\)](#) and [Vercammen et al. \(2014\)](#) made a review of these works, presenting four main classes of methods which are based on (i) average fluxes, where time-concentration profiles are divided into phases and the average rates are calculated using finite differences, leading to average intracellular fluxes ([Lequeux et al., 2010](#)), (ii) time-resolved fluxes, where data smoothing or filtering procedures are used in order to obtain continuous approximation of data, and calculate instantaneous rates, leading to continuous intracellular fluxes over time ([Niklas et al., 2011](#)), (iii) piecewise flux dynamics, where the concentration of species are approximated by piecewise linear functions composed of continuous segments in the time domain, leading to segments of lines as flux function ([Leighty and Antoniewicz, 2011](#)), and finally, (iv) simulated dynamics, where the concentration of species are approximated by numerically integrated kinetic models that are previously proposed in a mechanistic basis, and using MFA in a hybrid approach (both static and dynamic analyses for flux estimation in a data regression procedure), resulting in simulated fluxes over time ([Yugi et al., 2005](#)). Notice that the last two classes of methods are derivative-free.

[Vercammen et al. \(2014\)](#) proposed the use of B-spline parameterization for dynamic metabolic flux modeling in a systematic methodology that establishes a sequence of non-linear dynamic optimization problems (involving orthogonal collocation, interior-point optimizer, Akaike model discrimination criterion and automatic differentiation). Through the use of B-splines of 2nd order, they ensure the obtainment of smooth intracellular fluxes, and in a simultaneous regression problem where all experimental data concerning to different measured species are fit together, the measure of goodness-of-fit can be assessed in a consistent way, differently of methods that use smoothing splines where in-

dividual fits are performed separately. Moreover, in simultaneous with the estimation of the reaction fluxes, the optimal choice of the basis that spans the null space of the stoichiometric matrix is considered during the sequential procedure, imposing that it must be orthonormal.

Bordbar et al. (2017) proposed the use of *unsteady-state flux balance analysis* (uFBA) for metabolic network reconstruction using experimental data. The technique uFBA combines (i) SVD of experimental data in a prior phase for identifying metabolic states that assume linear behavior with time and the respective duration of them (or instant of transition between them), and (ii) simple linear regression for predicting slopes of concentration profiles that will be used as bounds with 95% of confidence intervals for the estimation of reaction flux distributions for “dynamic systems”. It is assumed that in each state the concentration derivatives are constant for every measured species, *i.e.*, the instantaneous concentration of species varies linearly with time. Thus, the optimal distribution of fluxes can be determined for each identified state using FBA constrained to the boundary conditions defined by the concentration derivatives previously estimated. In ideal conditions the unmeasured species should present zero rates of consumption/production. However, when constraining these species to present null concentration derivatives, problems related to the overdetermination of the species mass balances occurs, and therefore, a relaxation of the problem is required by considering as variables the values of concentration derivatives that were set zero respecting to unmeasured species, thus increasing the number of degrees of freedom. The problem is solved as a MILP where the sparsest vector of concentration derivatives is searched subjected to attends the mass balance equations. The optimal solution identifies the network topology and the reaction flux distributions that best fit the measured data and most approximates to zero the species flux of unmeasured species, in a parsimonious criterion.

### Critical analysis

This section emphasizes the main characteristics of methods of metabolic network reconstruction previously described, establishing a comparison with the work proposed in this thesis for modeling chemical reaction systems. Next list of bullets summarizes this information.

- Metabolic reaction networks assume (quasi) steady-state conditions.

Reaction networks at steady, or quasi steady, condition present internal reaction fluxes that lead to zero rates of intermediate species consumption/production, *i.e.*, these species compositions do not change over time ( $dc/dt = 0$ ). In this thesis, the reaction network is identified using transient data for modeling chemical system dynamics, where species compositional changes are the basis for structural model identification. Perhaps this is the major difference between the methods for metabolic network reconstruction and the methodology proposed in this thesis for reaction network identification. Although, the reaction networks can be generated consid-

ering only structural criteria (without considering the experimental data directly in the formulation, *i.e.*, considering the explicit generation of reaction networks), their identification is only possible when using experimental data. Therefore, several steps of the methodology incorporate experimental data resulting in valuable information that are crucial to identify the structural model correctly, such as: (i) invariant relationships, (ii) network dimension, and (iii) determination of the data variant space. Differently, in metabolic networks, the structural proposals are identified when finding reaction flux distributions that lie in the invariant space of the reaction stoichiometry (the right null space of the transposed stoichiometric matrix), where positive fluxes build null vectors of concentration derivatives, and therefore, the convex space analysis makes sense.

Hence, the analysis of convex linear spaces is meaningful for chemical reaction systems that operate at steady regimes, presenting networks with (right) null spaces associated, *i.e.*, networks presenting structural redundancies (composed by a linearly dependent set of chemical reactions). In this dissertation, we are looking for reaction networks that describe the data variant space, *i.e.*, bases that define/span the data variant space, and therefore, are composed by a linearly independent set of chemical reactions.

In metabolic networks, the vector of reaction rates (the distribution of reaction fluxes) defines which are the chemical reactions (stoichiometric vectors) that make up the metabolic network, *i.e.*, those that are active when transforming matter among metabolites/species, at steady-state. Thus, the distribution of positive reaction fluxes identifies the metabolic network that operates in steady condition. The resulting network can be composed by reaction fluxes that require (i) a full description, or (ii) a partial description of the right null space of the network superstructure. On the former, the distribution of reaction fluxes is a linear combination of the entire set of basis vectors of the null space of the network superstructure, presenting certainly structural redundancies, while on the latter, it is a linear combination of a partial set of these basis vectors that can result in network with redundancies or not. On the other hand, in this work, we want to find the network that conduct to instantaneous distribution of fluxes whose respective stoichiometric vectors form a basis that span the row space of the compositional changes matrix, presenting network structures without redundancies.

- Positive reaction flux constraints are considered.

In this thesis, as such in methods for generating metabolic networks, the use of lower bounds for reaction flux computation (positive reaction rates) is considered. In this case, it defines the criterion used to select plausible reaction networks (plausible bases that define/span the data variant space, *i.e.*, the row space of  $\mathbf{D}$ ). On the other hand, in metabolic networks, the lower bounds of fluxes establish the origin of the conical representation of the convex space where every plausible flux distribution

lies.

- The theory of steady-state chemical reactions (Section 2.1.3) is present in metabolic networks.

Metabolic pathways are determined based on the null space of the superstructure of the stoichiometric matrix (containing boundary fluxes mapped in). The species that are associated with these boundary fluxes are the ones that form the terminal species in a global chemical reaction using the theory of steady-state in reaction mechanisms. On the other hand, the remaining species (*i.e.*, the intermediate species) are those whose consumption and production rates must be the same to verify stationary conditions and, therefore, to be canceled in the global reaction. Thus, the steady-state theory is applied to metabolic networks, but using different terminology, under a different context and with different methods to generate steady-state networks.

- Energetic criterion is used for identifying the reaction model in both works.

The use of energetic constraints for identifying the net reaction flux direction in which it is energetically feasible to occur (negative Gibbs free energy changes) can be considered in metabolic networks and it is considered in this dissertation. In the case of metabolic networks, the use of energetic criterion allows reducing the number of feasible solutions (steady flux distributions). In this work, it allows reducing the number of candidate chemical reactions that make up the network superstructure, thus, decreasing the number of feasible reaction networks to be generated.

- Metabolic networks also contain conserved properties regarding total mass of groups of species/metabolites.

As in this work, the identification of conserved relationships<sup>3</sup> brings to light the physiological processes of the cell (or in this case, it helps in the identification of the network topology for a better description of the system dynamics).

However, the techniques used for their identification are different. In metabolic networks, the identification of pools of species is carried out by left null space analysis of the superstructure stoichiometry times -1 (*i.e.*,  $\text{leftNull}(-\mathbf{N}_{\text{sup}}^T)$ ) (Famili and Pals-son, 2003a). This analysis establishes a direct analogy with extreme pathways since the identified relations that define the concentration pools lie in a convex space in which respective vectors are written as linear combinations of the basis vectors that define the convex space through positive coordinates. These positive coordinates establish meaningful molar proportions between metabolites and moieties or groups of molecules. In this dissertation, we work with both data- and theoretical-based

---

<sup>3</sup>In this work, the conserved relationships are called *time invariants*. However, this term adopts a broad (comprehensive) sense in metabolic networks, since the system itself operates in a time-invariant mode and, therefore, this term is not specifically designated to the conservation relations of mass and moieties, such as it's here in this work.



analyses for identifying concentration pools. On the one hand, through data analysis the conserved relationships are searched by assessing the left null space of the data matrix ( $\text{null}(\mathbf{D}^T)$ ). On the other hand, through stoichiometry (theoretical) analysis the conserved relationships are searched by assessing the null space of the atomic matrix ( $\text{null}(\mathbf{A})$ ).

### 3.2.2 Generation of reaction mechanisms using a global reaction

A different class of methods is based on the consideration of a known global (or overall) reaction and the linear combination of elementary reaction steps to produce that global reaction. As these methods manage elementary reactions, the resulting reaction network may be called a *mechanism* since it is more specific, also describing the mass transformation between non-observable species such as radicals. Once the concentrations of all intermediate species are assumed to be constant in steady-state mechanisms, the net rate of production of each intermediate is zero (Bertók and Fan, 2013). Hence, the analysis of steady-states of a chemical system can be aided by the identification of mechanisms responsible for overall reactions, from a set of elementary steps that involve the terminal species as well as reaction intermediates (Mavrovouniotis and Stephanopoulos, 1992).

A recent review (Bertók and Fan, 2013) distinguished two major approaches to generate reaction mechanisms subject to a global pre-specified reaction: one based on linear algebraic analysis and the other rooted in graph theory. In the first case (Happel and Sellers, 1982; Happel et al., 1990; Mavrovouniotis and Stephanopoulos, 1992; Mavrovouniotis, 1992, 1995), the goal is to find a basis able to generate all feasible mechanisms, obeying the global reaction, and in particular those with the maximum number of linearly independent reactions, also called direct or cycle-free mechanisms. The graph theoretic approach (Seo et al., 2001; Fan et al., 2002) is entirely different, it is rooted on a set of axioms of feasible mechanisms and combinatorially feasible mechanisms. It uses bipartite graphs and a combinatorial algorithm that was originally developed for the synthesis of process-networks using a network superstructure (Friedler et al., 1992). Moreover, a third approach to generate mechanisms concerning to a global chemical reaction can be found in the literature, where favorable catalytic reactions are identified through the energetic characteristics of surface reactions, *i.e.*, enthalpies of reaction and activation energies (Fishtik et al., 1999). The global mechanism has to be energetically favorable, even if some individual steps are not. This condition can be used for selecting the most energetically favorable mechanism.

The next sections address these three main methods of mechanisms generation supported on a global chemical reaction. However, in advance, a disadvantage of these methods of identification of steady-state mechanisms is the obtainment of networks that may not explain the formation of all species present in a *transient regime*. This happens due to the criterion used, which is summed up in combining the elementary steps so that the global reaction initially postulated is verified, without the commitment to describe the formation

and consumption of all intermediate species. Moreover, despite the potential advantages in using graph theoretic approaches, these methods have as their main disadvantage the difficulty in understanding the theory underlying this representation, which makes this methodology relatively little used, compared to other alternative approaches.

### Generation of reaction mechanisms via linear algebra

Since networks can be represented in matrix form under different ways, the study of the properties of these matrices can also provide alternative methods for the generation of alternative reaction networks. In this sense, a group of authors in the decade of 80's and beginnings of 90's have studied linear algebraic properties related to reaction system stoichiometry for the generation of reaction mechanisms from a list of elementary reactions (Happel and Sellers, 1982; Sellers, 1984; Happel et al., 1990; Otarod and Happel, 1992).

Happel and Sellers (1982) propose a combinatorial method of generating mechanisms starting from all elementary reactions, which can be considered both in the forward and in the reverse direction. Some proposed mechanisms are discarded based on thermodynamics or kinetic considerations. The validation of the mechanism depends on experimental data, but this step is not addressed by the authors. Each elementary reaction is written as a linear combination of the chemical species involved, just as each mechanism is also a linear combination of the elementary reactions involved. The set of all combinations of elementary reactions is classified as a linear space called a *mechanism space*; the set of all reactions constitutes another linear space called the *reaction space*, in which the dimension is defined by the maximum number of linearly independent elementary reactions<sup>4</sup>.

Happel et al. (1990) show that the matrix constituted by the stoichiometric coefficients provides a valid way to determine the overall number of linearly independent reactions in a chemical system. Mechanisms classified as *cycle-free* and/or *direct*, *i.e.*, composed by linearly independent set of chemical reactions/steps (and containing only elementary reactions), are manipulated. The property of directness in mechanisms means that they are irreducible in the sense that they cannot be separated into submechanisms, each of which produces the same overall reaction. Otarod and Happel (1992) define *direct mechanisms* as “the smallest possible physically distinct mechanisms for a chemical system. They cannot be shortened through elimination of a step or reduced to a combination of smaller submechanisms”. According to Mavrovouniotis and Stephanopoulos (1992), once all direct mechanisms have been identified, all other possible mechanisms must be seen as a linear combination of these direct mechanisms; these authors define a direct mechanism as: “to state that they are cycle-free; *i.e.*, the steps participating in a direct mechanism cannot be combined into a loop or cycle accomplishing in net transformation”.

---

<sup>4</sup>On the other hand, the set of all linear combinations of chemical elements can be called the species space; in turn the dimension of this space will be equal to the characteristic of the atomic matrix, *i.e.*, it corresponds to the number of independent species. The species space is contained in the reaction space, which in turn is contained in the mechanism space.

The problem of enumerating the direct mechanisms involves firstly generating all possible global reactions, and finally combining the elementary steps to obtain mechanisms that are free of cycles, composed of linearly independent reactions. For this purpose, an additional caution has to be considered: the set of global reactions must also be linearly independent; otherwise, the set of solutions obtained will not be unique, in addition to being direct. Thus arises the concept of direct overall reaction, this is the one with the characteristic that when removing some species from the initial overall reaction, the remaining overall reaction cannot be described by a new sub-network formed by linearly independent reactions; in other words, when removing a species from the direct overall reaction it becomes stoichiometrically inconsistent. The proposed algorithms are based on this combinatorial principle, in which elementary chemical reactions are combined to generate direct mechanisms, which are described by global/overall reactions that are also direct. For this purpose, species are previously divided into terminals and intermediates, linearly independent global reactions are determined based on reaction stoichiometry and linear algebra; to finally determine the sets of direct mechanisms that drive the respective direct global reactions.

[Sellers \(1984\)](#) proposed a combinatorial method for identifying mechanisms using linear algebraic analysis; the chemical reaction system is characterized by an integer matrix in which the incidence relationships between all chemical species and elementary reactions are expressed.

[Mavrovouniotis and Stephanopoulos \(1992\)](#) developed an algorithm, similar to the one proposed by [Happel and Sellers \(1982\)](#), to generate mechanisms. These authors state that this version of the algorithm corresponds to an elaboration of the original algorithm, since the obtained mechanisms are unique and non-redundant, being classified by these authors as *overall mechanisms*. An overall mechanism is defined as one that is described by a global reaction, *i.e.*, one that involves only terminal species, which can be obtained by the sum of all elementary reactions multiplied by their respective Horiuti numbers<sup>5</sup>. Like [Marin and Yablonsky \(2011\)](#), these authors begin by dividing the species  $a_j \in A$  in two subsets  $I = \{a_1, \dots, a_I\}$  referring to intermediate species and  $T = \{a_{I+1}, \dots, a_A\}$  referring to terminal species, where  $A = I \cup T$ . Each reaction is called a step, and the set of all these makes up the linear space  $S$ , such that  $S = \{s_1, \dots, s_S\}$ . So, each species  $a_j$  that is present in reaction  $s_i$  has a stoichiometric coefficient  $\alpha_{i,j}$ . The transformation that occurs through each reaction is seen as a linear application ( $R$ ), such that  $r_i = R(s_i) = \sum_{j=1}^A \alpha_{i,j} a_j$  obeying the rules of stoichiometry. A mechanism  $m_k \in M$ , where  $M$  is the space of mechanisms, is defined by  $m_k = \sum_{i=1}^S \sigma_{k,i} s_i$ . That is, the mechanism is also a linear combination of steps  $s_i \in S$ , where  $\sigma_{k,i}$  is the corresponding Horiuti number.

Once all these parameters are defined, the global reaction rate ( $r_k$ ) representing the global

---

<sup>5</sup>The Horiuti number is defined in Section 2.1.3

mechanism ( $m_k$ ) can be written as

$$r_k = R(m_k) = \sum_{j=1}^A \beta_{k,j} a_j = \sum_{j=1}^A \left( \sum_{i=1}^S \sigma_{k,i} \alpha_{i,j} \right) a_j$$

where  $\beta_{k,j} = \sum_{i=1}^S \sigma_{k,i} \alpha_{i,j}$ .

To obtain a global mechanism, the coefficient  $\beta_{k,j}$  has to be zero for all intermediate species

$$\text{Global mechanism } (m_k) \Leftrightarrow \beta_{k,j} = 0, \quad \forall j = 1, \dots, I$$

An additional constraint can be established considering the number of Horiuti, for obtaining direct mechanisms:

$$\text{Unidirectional mechanism } (m_k) \Leftrightarrow \sigma_{k,i} > 0, \quad \forall i = 1, \dots, S$$

When for a given step  $s_i$  of  $m_k$  the respective coefficient  $\sigma_{k,i} = 0$ , the mechanism is redundant, being called by these authors as *indirect mechanism*. When there are two pathways for the global reaction, *i.e.*, two subsets of linearly independent reactions, it defines the mechanism as *bidirectional*, yielding null coefficients of some  $\sigma_{k,i}$  on reaction paths. So, according to the definition of Mavrovouniotis (1992):

$$(\forall s_i, \exists \sigma_{k,i} = 0) \Leftrightarrow (m_k) \text{ Bidirectional mechanism}$$

The algorithm for generating mechanisms proposed by Happel and Sellers (1982) and refined by Mavrovouniotis and Stephanopoulos (1992) starts with several reaction mechanisms, initially constituted by only one reaction, chosen from the list of elementary reactions. As the iterative method is applied, new mechanisms subject to restrictions are generated, which in this case reflect the fact that unidirectional mechanisms are intended for the examples presented. Thus, possible combinations between mechanisms for the elimination of intermediate components in the global reaction (between the terminal species) are identified. The algorithm stops when there are no longer any intermediate species in a global reaction, and therefore, the obtained mechanism can be classified as a direct mechanism that attends a global reaction. Once the set of all possible direct mechanisms is obtained, those that are redundant and those that appear duplicated are identified and eliminated. Mavrovouniotis (1992) proposes that this phase of identification and elimination of redundant mechanisms is carried out as they are generated in each iteration, which allows considerable savings in computational effort, due to the smaller number of reaction combinations considered in this case.

### Generation of reaction mechanisms via graph theory

Methods based on graph theory follow a very different approach, considering a list of axioms for the generation of *combinatorially feasible reaction pathways* (T1 — T7) and *feasible reaction pathways* (R1 — R6), identifying steady-state mechanisms from a predefined/known global reaction. The mechanisms representation is in the form of bipartite graphs that are composed of horizontal bars and solid circles, respecting to elementary reactions and chemical species, respectively (Seo et al., 2001; Fan et al., 2002). These generation methods were inspired in formulations conceived to the synthesis of chemical processes, which were proposed by the same research group, same authors that follow the work of Prof. Friedler.

Friedler et al. (1992) were the pioneers of the application of graph theory, establishing algorithms for the synthesis of networks, applied to the synthesis of chemical processes. Similarly a list of axioms concerning process specifications is postulated. These authors considered operation units, raw materials, by-products, residues, and final products, using transformation, accumulation, and separation of matter throughout the process. The origin of the expression *P-graph* (process graph) has risen from this work, where the process is graphically represented through bipartite graphs, that represents the structure of the global process. Later, Friedler et al. (1993) proposed a method for generating the *maximum structure of the process*, called *superstructure of the process*, in which all possible structures are represented in the same graph.

Direct mechanisms are obtained by following the list below of 6 axioms regarding feasible reaction pathways (Fan et al., 2001, 2002; Seo et al., 2001; Barany et al., 2012; Bertók and Fan, 2013):

- R1: Each final product (target) species is fully produced by the reaction steps represented in the network.
- R2: Each starting reagent species (precursor) is totally consumed by the reaction steps represented in the network.
- R3: Each intermediate species produced by any reaction step is fully consumed by one or more reaction steps, and each intermediate species consumed by any reaction step is fully produced by one or more reaction steps.
- R4: All reaction steps are defined *a priori*.
- R5: The network representing the reaction pathway is acyclic.
- R6: At least one reaction step represented in the network activates a starting reagent (precursor).

A reaction pathway is combinatorially feasible if it satisfies the following 7 axioms (Fan et al., 2001, 2002, 2012; Seo et al., 2001; Barany et al., 2012; Bertók and Fan, 2013):

- T1: Each final product is represented in the network.

- T2: Each starting reagent is represented in the network.
- T3: Each reaction step is defined *a priori*.
- T4: All intermediate species represented in the network have at least one pathway leading to the final product of the global reaction.
- T5: All chemical species represented in the network must be a reactant or a product of at least one reaction step represented in the network.
- T6: A reactant of any elementary reaction represented in the network is an initial reactant if it is not produced by any reaction step represented in the network.
- T7: The network includes the reaction in only one direction (forward or reverse) of each elementary step represented in the network.

Based on these axioms, three algorithms were developed for the generation of chemical reaction networks. In published articles (Friedler et al., 1992, 1993; Fan et al., 2001, 2002), these algorithms are described in pseudo codes, in which the formulation is not presented explicitly, but the symbolic structure of the sequence of calculations is shown. The first algorithm addresses the generation of the superstructure of reactional pathways, containing exhaustively and exclusively combinatorially feasible structures; this algorithm is called: RPIMSG — reaction pathway identification maximum structure generation. The others respect the generation of reactional pathways, namely to generate the set of all combinatorially feasible reaction networks from the superstructure (RPISSG - reaction pathway identification solution structure generation), and, alternatively, to generate feasible reaction networks using back tracking (RPIPBT — reaction pathway identification pathway-back-tracking) (Fan et al., 2001, 2002; Seo et al., 2001; Barany et al., 2012; Bertók and Fan, 2013).

According to Barany et al. (2012), a P-graph (or a reaction network) is called a *structurally minimal reaction pathway* or an *independent reaction pathway* when it presents a feasible reaction pathway, and no subgraph can represent a feasible reaction pathway in it. This definition comes directly from the application of the axioms (R1)—(R6). Similarly, an independent reaction pathway corresponds to a network formed by linearly independent reactions (analogous concept of the method based on linear algebra referring to direct mechanisms). Barany et al. (2012), have mathematically demonstrated that *structurally minimal reaction pathways* are equivalent to *direct mechanisms*. In addition, Barany et al. (2013) have also demonstrated that *extreme pathways* (in which the conversion of primary inputs (substrates) into primary outputs (products) and thus contain exchange fluxes with the environment) are equivalent to *structurally minimal pathways*, or *direct mechanisms*.

There are many variations of algorithms that use graph theory. One possibility uses Petri nets (also known as P/T nets, or local nets (“*places*”)/transitions), a type of bipartite graph where nodes represent either places or transitions. In these networks the arcs describe the locations that are pre- and post-conditions for the various transitions. Other

authors use the theory of P-graphs for generating reaction network superstructures, to then consider FBA (Seo et al., 2001; Lee et al., 2005; Tick, 2007; Fan et al., 2012).

Seo et al. (2001) use a method based on the P-graph theory for the generation of complete superstructures of reaction networks, *i.e.*, maximum structures of minimum complexity, from a list of candidate elementary reactions. This method is applied to a traditional case study: the conversion of glucose to pyruvate, involving 14 elementary reactions. Later, these same authors propose a complementary identification of the multiple distribution of fluxes and metabolic routes in biological systems (Lee et al., 2005). The proposed approach integrates FBA, based on linear programming, and the previous graph theoretical method to determine alternative metabolic trajectories, some of which only manifest in appropriate environmental conditions. This study was applied to the *in silico Escherichia coli* model.

Fan et al. (2012) studied the catalytic hydrogenation of ethylene to produce ethane with a platinum catalyst. Two mechanisms were proposed, one composed of 7 elementary reactions involving competitive adsorption, and another composed of 8 elementary reactions with competitive and non-competitive adsorption. The motivation of this work was to demonstrate that, through exhaustive identification of routes using a method based on the P-graph theory, it is possible to model networks of complex reactions that involve two or more catalytic active sites. According to these authors, the method involving the P-graph theory is the most effective for exploring the structures of reaction networks, because it explores the structural information, together with elementary balances and reaction stoichiometry. The method also allows to obtain combinations of feasible routes, which they classify as more realistic solutions than feasible routes without cycles.

### Generation of reaction mechanisms considering energetic issues

In the context of catalytic reactions, Fishtik et al. (1999) generalize the approach of enumerating all possible mechanisms composed by catalytic reactions, with a view to their further discrimination, through an analysis of the energetic characteristics of the corresponding surface reactions (enthalpies of reaction and activation energies). This study is also based on the analysis of the properties of the corresponding stoichiometric matrix, and the various possible mechanisms are obtained by selecting an appropriate set of columns and rows that verify a particular algebraic criterion.

Later, in the field of microkinetics analysis, Fishtik et al. (2004a,b) proposed a systematic method to generate mechanisms given a set of elementary reactions, considering examples of both chemical and biological catalytic kinetics. In this case, the authors have combined methods to generate reaction networks that involve a global chemical reaction and energetic constraints. The mechanisms are obtained by a linear combination of these elementary reactions that satisfies a global reaction previously identified. The topology of the identified mechanisms are represented by Reaction Routes Graphs (RRG). For the discrimination of preferable routes in the complex mechanism, an analogy with electrical

networks using Kirchhoff's law is considered, where each elementary reaction is associated with an electrical resistance, the reaction rates are considered as currents and the affinities as voltages. A voltage source is considered between the terminal species (those involved in the global reaction) and the equivalent resistance offered by the global reaction results in a linear combination of the resistances offered by each elementary step. With this energetic analysis in the entire RRG, the redundant routes may be eliminated if they present greater resistance than the other via to arrive in the same node.

### 3.2.3 Generation of reaction networks via optimization

One of the areas where the generation of reaction networks has proved to be more important is that of biorefineries and the development of biofuels, taking into account the variety of possible routes and the large number of compounds that can be obtained. A fundamental problem in this area is the generation of reaction networks so as to maximize the use of raw materials and energy production, moving towards obtaining products that meet market needs, simultaneously solving the various aspects of product and process design (Pennaz, 2011; Voll and Marquardt, 2012; Marvin et al., 2013).

Pennaz (2011) makes use of a flux analysis in reaction networks to synthesize the optimal reaction network regarding a specific objective function. This method is first formulated as a LP problem, and later converted into a MILP through *integer cuts* that allow the generation of alternative solutions. In this way, all feasible possibilities of reaction networks from a reagent to a target product are listed. The optimal network is obtained based on thermodynamic, economic, security and heuristic factors. This author also proposes a graphical shortcut method based on chemical potentials for the formulation of reaction networks. In this method, chemical potential changes along the reaction network are used as a quick guide for the identification of feasible paths, as an alternative to stoichiometric enumeration of reactions and flux analysis in reaction networks. Pennaz (2011) applied the developed methodology to two case studies in the area of biorefineries. The first is a hypothetical case based on the conversion of biomass into liquid fuels. The second is a more elaborate case for obtaining the network of MTHF (2-methyl-tetrahydrofuran) synthesis from glucose and xylose.

Voll and Marquardt (2012) proposed an optimization method for reaction network synthesis concerning to biofuel production in biorefineries. This approach has similarities with FBA in metabolic networks, since the goal is to synthesize a reaction pathway (actually a plenty of them for further analysis) with an optimal flux distribution in steady-state conditions, considering several objective functions and subject to specific process constraints (the authors called this method as *reaction network flux analysis*). The generation of these pathways is done using a MILP formulation where the binary variables identify the reactions that make part of the optimal solution. Every feasible solution (with the same objective function, but with different steady flux distributions) is generated in a recursive formulation where the extreme bases can be found (Lee et al., 2000). Hence,



Voll and Marquardt (2012) proposed a systematic procedure where the objective function is first established, then feasible structures are generated based on flux analysis (linear optimization approach), to then consider the evaluation of nonlinear constraints (such as yields) and other network evaluation criteria for a fixed structure, to finally identify promising networks and tradeoffs between them.

Marvin et al. (2013) proposed a method of automated generation and optimal selection of the mixture of biofuels with gasoline through the synthesis of the corresponding reaction network. This approach allows the simultaneous identification of the desired product and of the corresponding synthesis route. Formulations of multi-objective optimization were considered, including criteria for minimizing energy and reaction-related costs, including catalyst-related costs.

In the literature, there are other optimization-based studies on the analysis of mass fluxes and determination of reaction pathways, according to the intended target. Several examples concern to metabolic networks reconstruction, which were previously described in Section 3.2.1, where the concept of mass fluxes is used to maximize, for example, the cell growth rate (Murabito et al., 2009).

### 3.3 Synthesis of graphs

Graph synthesis can be applied in completely different contexts, sharing a common feature: dealing with processes that can be represented by a connected structure that shows the relationships between nodes through their arcs. These nodes and arcs may represent completely different things, with different meanings. Consequently, the synthesis of graphs is largely used and there is a vast number of works in the literature. Some examples, apart from reaction network synthesis, are process synthesis and scheduling, transportation routes, computer networks and project scheduling.

Most of the problems of graph synthesis are related to the construction of *linear graphs*, in which only one type of node exists and two nodes are connected by only one arc. However, adaptation of the existing formulations can be done in order to enable generating more complex structures, namely nonlinear reaction networks. The general concern common to most methods for generating graphs is to ensure connectivity between all nodes, and formulations differ regarding this aspect.

A large number of methods for synthesis of graphs use integer programming, where binary variables define decisions such as selecting a path for the network from a previously defined superstructure. For example, for process synthesis and scheduling, MILP formulations and other variants (such as mixed-integer quadratic programming) has been used in the last decades (Grossmann, 1985; Achenie and Biegler, 1990; Floudas and Lin, 2005). On the other hand, other methods based on recursive algorithms can be found, where greedy strategies can be adopted during loop iterations (Jones et al., 2004).

However, for all of these graph synthesis methods, the problem starts by defining its domain or the superstructure of the network. The use of a superstructure for process synthesis and/or scheduling has been shown to be an effective tool in many applications (Achenie and Biegler, 1990). The superstructure must contain all possible alternatives of a potential topology of the process to which the optimal solution belongs. Adopting this approach to generate reaction networks defines a global model structure (that can be represented as a graph) containing all possible routes between chemical species and able to describe the observed compositional changes, obeying to stoichiometry and energetic criteria. This is the approach adopted in this work in Step 3, Chapter 7. In effect, it enables to systematize the generation of feasible reaction networks (exhaustively, or not), defining the space of optimal/feasible solutions.

In this section, the problems of generating graphs from a previously defined superstructure are addressed, including a brief description about iterative methods in Section 3.3.1, and a more detailed review about synthesis of graphs using discrete optimization in Section 3.3.2. Some of the methods presented in this last section were the basis for the development of three new formulations to generate reaction networks, in Chapter 8.

### 3.3.1 Spanning trees

A linear reaction network without redundant paths may be represented as a “*spanning tree*” (Chen et al., 2010), as illustrated in Figure 3.2. Therefore, algorithms to generate *spanning trees* can be directly applied to generate linear reaction networks only having linearly independent reactions. Iterative algorithms to construct spanning trees in graphs starting from a given node are known, with new visited nodes being done either in *depth* or in *width*. The basic idea is to obtain a structure that connects all nodes only once.

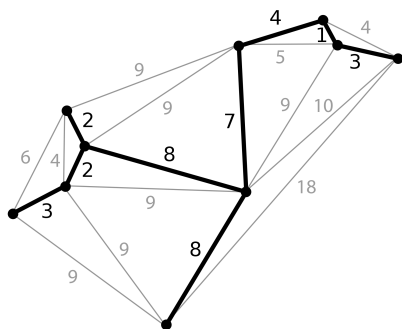


**Figure 3.2** Example of spanning tree (darker trace). The coefficients shown are arc lengths (weights) and the spanning tree is the one with the smallest total length — *minimum spanning tree* (Wikipedia, 2021).

There are several algorithms to enumerate all feasible spanning trees, whose basic components are: depth-first search, selective enumeration and testing, and arc exchanging (Gabow and Myers, 1978; Gabow et al., 1986; Kapoor and Ramesh, 1991, 1995). When

the first spanning tree is obtained, the next one will differ from the previous one by exchanging one arc in the network. This procedure is required until all different spanning trees are obtained. The computational effort required to generate spanning trees differs depending on the type of graph, which can be directed or undirected and/or weighted.

Given the importance of these representations in many applications, including discrete optimization and computer networks, these algorithms are relatively well known and can be adapted to exhaustively generate all possible spanning trees in a given graph. However, the number of possibilities increases exponentially with the number of existing nodes. For example, for a complete graph<sup>6</sup> with  $n$  vertices, Cayley's formula indicates that there are  $n^{n-2}$  possible distinct spanning trees (Gross and Yellen, 2005).

### 3.3.2 Elementary shortest path and travel salesman problems

A well known network generation problem is the elementary shortest path problem (ESPP), where a minimum-cost pathway between initial and terminal nodes is obtained, such that each node of a the network can only be visited once (Haouari et al., 2013). The path thus generated is classified as “elementary” and: (i) is cycle-free, (ii) does not necessarily contain all nodes of the network superstructure, and (iii) forms a sequence of nodes in series.

The travel salesman problem (TSP) is a variant of the ESPP, designed to find a circular pathway in which the salesman trajectory ends at the starting point, visiting every city once, thus establishing an Hamiltonian and elementary circuit. The problem is stated as a salesman that needs to visit a set of cities, each one once, and return to the starting city by traveling at minimum cost pathway (Miller et al., 1960; Dantzig et al., 1954, 1959). Note that it consists in determining a network where cities are represented by nodes and arcs represent the optimal trajectory selected between them. The network superstructure is represented by an undirected graph where the cost (or distance) is the same in both path directions. In Asymmetric TSP (ATSP) the path cost (or distance) can be different to node entry and exit in the same path, although the same goal is established: finding an Hamiltonian pathway with the lowest cost. The ATSP is represented by directed graphs, where the network superstructure presents arcs with established directions (arrows) between nodes. Notice that when a direction in the path is not allowed, its cost is  $\infty$ .

The main differences in TSP and ATSP when compared to ESPP are (i) all nodes in the superstructure must be covered in the network, and (ii) terminal and initial nodes are the same node. The network superstructure in ESPP can be directed or not, and also, in contrast with TSP, it can present negative path costs, thus, instead of paying cost for a path, some advantage may be got if the path is selected. Examples that can be found in the literature of ESPP with negative costs are related to column generation

---

<sup>6</sup>Containing all possible arcs between each pair of nodes.

algorithms, branch-and-price algorithms, currency exchange market, etc. (Ibrahim et al., 2009; Haouari et al., 2013; Taccari, 2015).

However, we will focus in problems where there is no negative cost in order to establish a parallelism between ESSP, TSP and ATSP formulations. All formulations look for cycle-free pathways during the node series trajectory, controlling the node incidence and/or the node outgoing through arcs. It is possible to easily transform one formulation into another when altering (i) the assignment constraints, and (ii) the terminal node. In TSP and ATSP the node incidence and outgoing, for every superstructure node, have to be strictly one, thus:

$$\sum_{j \neq i} y_{i,j} = \sum_{j \neq i} y_{j,i} = 1, \quad \forall i$$

where  $y_{i,j}$  is a binary variable that assumes the unity value when the path between nodes  $i$  and  $j$  is selected. Whereas in ESPP, only the node outgoing is restricted to be at most one:

$$\sum_{j \neq i} y_{i,j} \leq 1, \quad \forall i$$

Therefore, when considering only positive costs, adapting these assignment constraints adequately to the related problem, handling ESPP or TSP is the same.

In the last century, many authors have presented several ATSP, TSP and ESPP formulations differing, basically, with regard to the restrictions of eliminating *subtours*. Network subtours are disconnected paths (mostly circular isolated pathways) that still satisfy the basic assignment constraints in the absence of subtour elimination restrictions. These restrictions add complexity to the IP formulations increasing computational effort and sometimes limiting their application to small case studies with a restricted number of nodes. Basically these formulations can be divided (or grouped) according with the type of subtour elimination constraints adopted. Öncan et al. (2009) have grouped these formulations in five categories: (i) the exponential sized (ii) the sequential based, (iii) commodities flow based, (iv) time dependent, and (v) precedence variable based. In Figure 3.3 several ATSP formulations are shown, with their relative strength indicated by arrows, and group categories by colored circles. Öncan et al. (2009), in their review, have established new formulations comparisons; the results of their comparative study are indicated in the graph through dashed lines. The 24 formulations are represented through the surname initials of their original authors.

A plenty of journal articles were published comparing these formulations in terms of strength when considering (i) relaxation of binary variables facing LP problems, and (ii) polyhedral information. Formulations with additional variables can be compared considering their polyhedral projection into the original variables subspace without losing any integer solution. One formulation is said to be better face another when providing the larger relaxation value, *i.e.*, higher lowest bound in polyhedral convex region (Pataki, 2003; Öncan et al., 2009). Therefore, modelers seek to tighten the polyhedron representation of

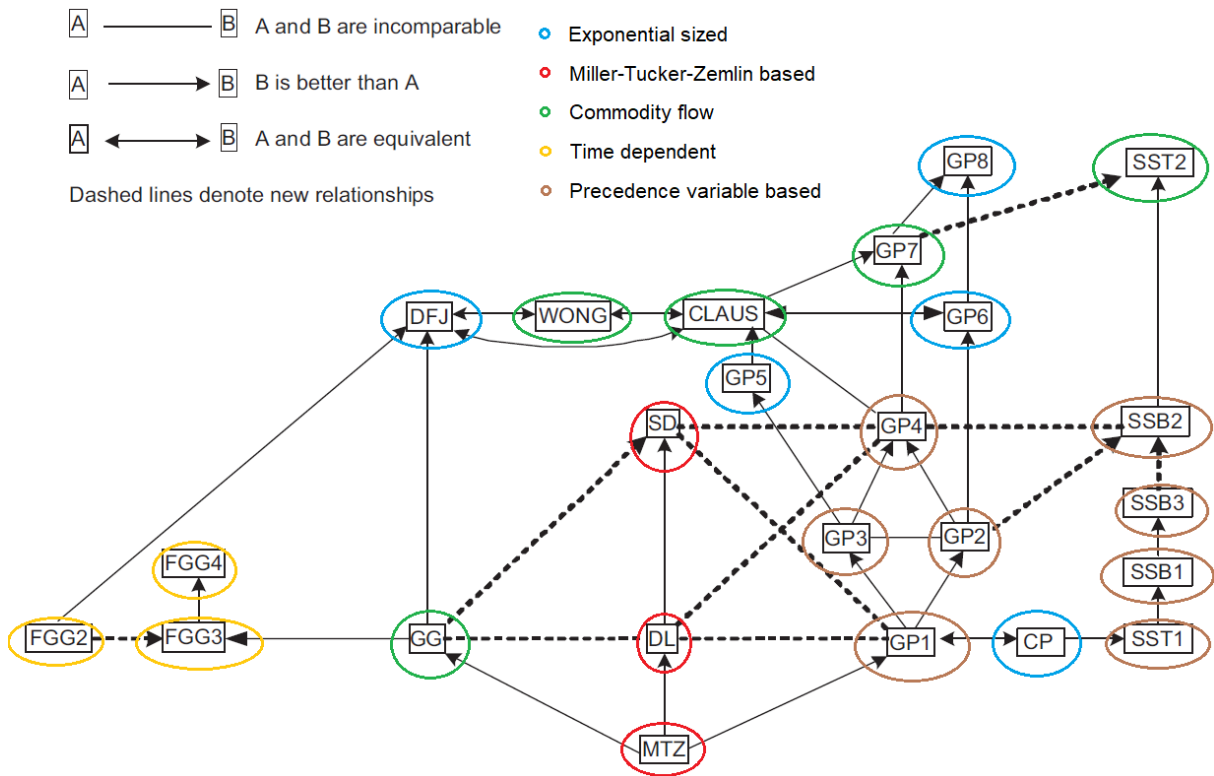


**Figure 3.3** ATSP formulations and their relationships (Öncan et al., 2009). The colors of the circles indicate the formulation category (group based). Copyright (2021) by Elsevier.

the initial formulation in order to increase the bounds produced by the linear programming relaxation that guides branching decisions. Commercial MIP solvers, such as CPLEX, during branch-and-bound-and-cut process focus on identifying cutting planes constraints after the first LP relaxation, to successively reduce the size of the feasible polyhedral region, thus providing better lower bounds (Sherali and Driscoll, 2002). The cutting planes are iteratively added until either an integral solution is found or it becomes impossible or too expensive to find another cutting plane. In the latter case, a traditional branch operation is performed and the search for cutting planes continues on the subproblems. For reference literature in the context of ATSP formulations comparison, we recommend the articles from Sherali and Adams (1990); Padberg and Sung (1991); Gouveia and Pires (1999); Sherali and Driscoll (2002); Pataki (2003); Sarin et al. (2005); Orman and Williams (2006); Öncan et al. (2009); Bektas and Gouveia (2014).

Pataki (2003) emphasize the importance in handling strong IP formulations in the field of combinatorial optimization in order to guarantee the achievement of optimal solutions in reasonable time and computational effort. Many network formulations available are weak, and comparing formulations through the number of variables and constraints, assuming that the one with lower number would be preferable is not an evidence of strength. A good evidence, thus, pass through evaluating the number of branch-and-bound nodes and

time required to solve them to optimality. This is the approach followed for the comparison of the developed formulations in Chapter 8. However, MIP commercial solvers, such as CPLEX, have the ability to reformulate weak formulations into strong ones by segregating the problem when considering additional inequalities constraints, thus assisting the optimal model convergence.

In the context of ATSP, Pataki (2003) proposed a sequential method that combined two formulation categories. In a first instance all possible subtours are encountered in a directed graph using exponential sized formulation, to later apply ordering constraints (using sequential based formulation) directly in these subtours, ensuring the nodes precedence and therefore eliminating these undesired isolated cycles. Through this sequential approach, it is significantly reduced (i) the number of branch-and-bound nodes, (ii) the relative gap of the objective function of the relaxed problem, thus assisting the solver to find an optimal integer solution, and (iii) in some cases the CPU usage.

Taccari (2016) also recommended sequential strategies to consider dynamic separation of subtour elimination constraints in order to decrease computational effort and allow handling larger-sized problems. This author advises the use of good primal heuristics and additional strong inequalities constraints in order to assist the solver convergence. However, when this separation procedure is not possible, he recommended the formulation category (iii), the commodity flow based.

The *commodities* problems are based on balanced structural flows that travel among nodes ensuring a connected structure. The single-commodity flow (SCF) formulation was originally presented by Gavish and Graves (1978), in the context of ATSP. These authors applied SCF for other related transportation problems, namely the Multi-TSP, the Delivery Problem, Multi-Terminal Delivery Problem, School Bus Problem, etc. Wong (1980) and Finke et al. (1984) presented, respectively, the multi- and two-commodity flow formulations, MCF and TCF. Few years later, Claus (1984) presented another MCF formulation. Langevin et al. (1990) established a comparison among them, where it was demonstrated that (i) TCF and SCF are equivalent, (ii) the latter MCF formulation is covered in the original one when half of the flow variables and their related constraints are eliminated, and (iii) the flow variables in SCF are an aggregation of the MCF.

The SCF formulation was adapted and applied to generate *linear reaction networks* with a controlled number of chemical reactions and a desired number of initial reactant species, *i.e.*, for any reaction network complexity with one or more initial reactants (Vertis et al., 2015). This formulation is presented in this dissertation in Section 8.4. Other new MILP formulation proposals presented in this work were inspired in the classical MTZ constraints, and adapted to generate nonlinear reaction networks. In this case, additional constraints are required in order to ensure precedence among nodes, avoiding network inconsistencies. For more details, see Section 8.5.

The formulations classified as precedence variable based could be potential candidates

to generate nonlinear structures. However, infeasible solutions presenting inconsistent network structures were allowed to be generated when testing these formulations (using the same constraints as they were proposed). However, additional precedence constraints can be considered to make them useful to our problem, at the price of weakening them due to the nature of these constraints. As well as precedence variable based formulations, many of the other formulations proposed in the literature were tested for the problem of generating reaction networks, but with no application success.

However, all these formulations are related to the generation of network structures without considering experimental data, this means that it concerns only about the feasible structural model part ensuring network connectivity in a consistent form, verifying species precedence. Clearly, after generating all feasible reaction networks they must be selected using experimental data. For this purpose methods for data treatment are required in order to increase data accuracy for structural model elucidation/identification.

## 3.4 Data treatment and parameter identifiability

The adjustment of kinetic parameters is a crucial step for the validation of kinetic models (including the reaction network), in the classical methodology of modeling chemical reaction systems. At this stage, statistical regression procedures are usually used, which in some cases may involve the formulation of specialized mathematical optimization problems (Duarte et al., 2008). Typical examples of these approaches are linear or nonlinear least squares and maximum likelihood formulations (Biegler, 2010). Before applying the regression procedure, it may still be necessary to treat/regularize the raw experimental data. The state of the art of the data treatment methods is presented in Section 5.2, where the Step 1 (data reconciliation) of the methodology is also addressed. However, a brief note on the identification of parameters from experimental data is made in the next section.

### 3.4.1 Parameter identifiability

During the systematic methodology for modeling chemical reaction systems (proposed in this thesis), the adjustment of reaction kinetic parameters is left to final step, after the identification of the reaction network structure. Therefore, the reaction rates can be individually correlated to reactant species concentrations in order to elucidate their respective kinetic expressions. This phase involves a series of linear regression procedures for predicting responses that are written as a linear combination of the columns of the design matrix through positive coordinates (kinetic parameters) in that basis. For more information, see Section 10.2. Hence, the model diagnostics can be done by assessing some properties of the design matrix regarding parameters identifiability. In this case, the design matrix corresponds to the Jacobian of the function to be fit in order to its parameters, *i.e.*, the sensitivity matrix. Thus, in order to ensure the identifiability of the model

parameters in relation to a set of experimental data, two aspects related to sensitivity matrix full rankness must be analyzed: the condition number and the collinearity index.

The singular values allows the computation of these metrics related to the condition of the problem in hands, such that

$$\kappa = \frac{\sigma_1}{\sigma_n} \quad \text{and} \quad \gamma = \frac{1}{\sigma_n} \quad (3.7)$$

where  $\kappa$  is the matrix condition number and  $\gamma$  the collinearity index.

While we look for well posed problems, in which  $\kappa$  is near to one (observe that an orthogonal matrix leads to this unity index) and  $\gamma \sim 10 - 100$  are expected. However, in real systems, specially without previous data treatment, it is hard to find. In general, in real systems, ill posed problems are faced due to the presence of nearly linear dependence between columns of the sensitivity matrix, or in other words, due to the presence of small singular values leading to an ill-conditioned system where the parameter vector is poorly identifiable (López C. et al., 2015).

In general, chemical reaction systems presents high correlation among variables since the reaction network links the species in a relation of dependence among them. Although this correlation exists, the presence of noise in concentration measurements also hinders the identification of model parameters, blurring the linear independence (or dependence) between the columns of the design matrix. Therefore, data treatment procedures, when increase data accuracy (*i.e.*, diminish the data noise content), increase the parameters identifiability, and consequently, the kinetic model elucidation, by improving the condition of the regression problems, *i.e.*, by decreasing  $\kappa$  and  $\gamma$  of the sensitivity matrix. This is the approach followed in this work, in which a data reconciliation method is proposed for increasing data accuracy in Step 1 (with subsequent data analysis in Step 2), thus improving structural model identifiability in both tasks: reaction network elucidation and kinetic expressions identification.

### 3.5 Discussion of existing reaction modeling approaches

A discussion of the reaction modeling approaches presented in this chapter is now considered and divided into three parts. The first part addresses how the reaction network is identified using experimental data. The second part is a critical comparison of the existing methods of network synthesis. Finally, in the third part, the main aspects that differentiate the proposed methodology from the approaches in the literature are pointed out.



### 3.5.1 Reaction network identification

In the simultaneous method of modeling chemical reaction systems, the kinetic parameters are tuned by fitting the model (obtained by numerical integration of a system of ODEs) to experimental concentration measurements, in a nonlinear regression procedure free of bias but subject to local optimal solutions. Therefore, the reaction network is identified when a satisfactory data-model agreement is obtained. There are two levels of concurrency in this approach: first, all kinetic parameters are simultaneously tuned in an unique approximation method, and second, the reaction network is identified simultaneously with the kinetic expressions that satisfactorily approximate the observed data. However, the method requires a network proposal prior to its application. This fact may result in the need to test different network structures until a reasonable fit is obtained (or not), resulting in a high computational effort. Moreover, tested networks are often biased by the modeler's expectations regarding the system behavior. Furthermore, as the method supports linear dependencies in the network structure, overparameterization may be present in the optimal solutions found, or in other cases data overfitting can occur in the presence of overdimensioned models.

On the other hand, the incremental method of modeling chemical reaction systems decouples parameter adjustments for each component of the model since concentration derivatives (or cumulative concentration changes) are previously calculated, enabling the interconnections between species to be broken in their respective mass balances. Therefore, for a given reaction network structure composed by a linearly independent set of reaction components, the kinetic parameters of each chemical reactions are estimated separately, through a (in general) linear regression. This can be done calculating reaction rates or reaction extents from observed data, depending on the incremental approach adopted (rate or extent-based, respectively). These problems are considered ill-posed since small errors in concentration measurements are amplified, resulting in poor parameter estimates. Prior data regularization may mitigate this problem.

Notice that there are two decoupling levels in the incremental method: first, the identification of the reaction network is decoupled from the parameter estimation, and second, the estimation of the kinetic parameters of each chemical reaction is carried out individually. However, the way in which the network identification is done may be criticized. This is due to the fact that when proposing the structure of the reaction network, either by using the TFA technique or in an *ad hoc* manner, the remaining potential structures are not systematically explored. Although the incremental method is more robust than the simultaneous method — due to the decoupled identification, resulting in greater confidence in the estimated parameters — it loses validity if the proposed structure is not the one that best describes the experimental data. As a result, and in both the simultaneous and the incremental strategies, errors may be masked at two levels: (i) at the level of the uncertain reaction network, and (ii) at the level of the established kinetic model.

In contrast, the third approach (presented in Section 3.1.4) is independent of reaction

network proposals. In this case the reaction network is identified simultaneously with the kinetic expressions, without the need of establishing its structure *a priori*, but through decoupled approximation of species fluxes that are written as linear combination of reaction fluxes whose parameters are tuned simultaneously. Therefore, each species compositional changes are predicted by a linear combination of reaction fluxes, which in turn vary linearly with the reactant complex (product of reagent concentrations), in an individual linear regression procedure. Based on the quality of these adjustments (and other criterion such as model complexity), the reaction network is identified. Thus, this approach presents an advantage against the other network identification methods since there is no need to establish network proposals. On the down side, the method tends to present overparameterization, with model components that explain essentially noise, which may be attenuated through prior data regularization and/or incorporation of techniques that balance model complexity against data fit agreement.

In short, the identification of stoichiometry is a critical task in the modeling of reaction systems, where the model that best describes the available experimental data must be identified, avoiding excessive parameterization. Despite previous contributions, there are still several limitations and room for a more systematic and well-structured approach. In particular, an approach that gradually incorporates the experimental data when evaluating and discriminating alternative reaction networks, and that goes through all possible solutions regarding the structures of kinetic models, ensuring that *all possibilities* have been analyzed and that the *best model* has been found. The methodology proposed in this dissertation attends these needs.

### 3.5.2 Reaction network generation

Regarding the theory of steady-state presented in the theoretical background (Section 2.1.3), parallelism can be established when considering the methods for the generation of reaction networks presented in this chapter, as they all present the same perspective of identification/modeling of the reaction network on the different context of applications:

- In metabolic networks, the network identification pass through the analysis of the null space of the stoichiometric matrix of the superstructure, including boundary reaction fluxes, in which a positive flux distribution can be verified in steady-state inside of the boundaries. In this way, an identified network presents terminal nodes that correspond to metabolites that receive or exclude boundary fluxes, and intermediate nodes that correspond to metabolites with equal consumption and production rates.

Moreover, the extreme pathways presenting external exchange fluxes with the environment can be directly compared to the extreme paths that compose the null space of the reduced stoichiometric matrix concerning to the intermediate species in the theory of steady-state chemical reactions.

- In direct mechanisms with their global chemical reactions, the network synthesis happens considering terminal species that are fixed (as such as the ones that receive/exclude boundary fluxes in metabolic networks) and intermediate species that are imposed to be canceled (presenting the same rate of production and consumption) to obtain the global mechanism, direct/free of cycles (verifying the steady conditions).
- In ESPP, the flux balance between intermediate nodes must verify null, while the starting and the exiting nodes (terminal nodes) present rates of -1 and 1, respectively (or vice-versa). In commodity formulations, the amount that is inserted in the starting node must be recovered in the sink node(s), while the intermediate nodes show a zero rate of accumulation.

Note that all these methods have the same principle: to obtain connected structures that link fixed terminal nodes from a graph superstructure, however, subject to the fulfillment of some specific restrictions for each case.

All these methods can be applied to generate linear reaction networks after some modifications, such as (i) transforming the final terminal nodes as variables of the problem (end product species are not previously determined) and (ii) imposing the production and consumption of all intermediates, forcing the generation of all observed species. This is the approach followed in this work for generating linear reaction networks. However, the generation of more complex structures as nonlinear networks needs additional constraints to ensure structural consistency. This is one of the novelties that this dissertation presents: MILP formulations capable of generating nonlinear network structures.

For a more detailed discussion of the main contributions of this thesis, see Section 1.3.

## Bibliography

- Achenie, L. and Biegler, L. (1990). A superstructure based approach to chemical reactor network synthesis. *Computers & chemical engineering*, 14(1):23–40.
- Amrhein, M., Srinivasan, B., and Bonvin, D. (1999). Target factor analysis of reaction data: use of data pre-treatment and reaction-invariant relationships. *Chemical Engineering Science*, 54(5):579–591.
- Antoniewicz, M. R. (2013). Dynamic metabolic flux analysis—tools for probing transient states of metabolic networks. *Current opinion in biotechnology*, 24(6):973–978.
- Ataman, M. and Hatzimanikatis, V. (2015). Heading in the right direction: thermodynamics-based network analysis and pathway engineering. *Current Opinion in Biotechnology*, 36:176–182. Pathway engineering.
- Barany, M., Bertok, B., Fan, L., and Friedler, F. (2013). Relationship between extreme

- pathways and structurally minimal pathways. *Bioprocess and Biosystems Engineering*, 36(9):1199–1203.
- Barany, M., Bertok, B., Imreh, C., Fan, L., and Friedler, F. (2012). On the equivalence of direct mechanisms and structurally minimal pathways. *Journal of Mathematical Chemistry*, 50(5):1347–1361.
- Bard, Y., Bard, J., and Bard, Y. (1974). *Nonlinear Parameter Estimation*. Academic Press.
- Bardow, A. and Marquardt, W. (2004). Incremental and simultaneous identification of reaction kinetics: methods and comparison. *Chemical Engineering Science*, 59(13):2673–2684.
- Beard, D. A., Babson, E., Curtis, E., and Qian, H. (2004). Thermodynamic constraints for biochemical networks. *Journal of Theoretical Biology*, 228(3):327–333.
- Beard, D. A., Liang, S.-d., and Qian, H. (2002). Energy balance for analysis of complex metabolic networks. *Biophysical journal*, 83(1):79–86.
- Becker, S. A., Feist, A. M., Mo, M. L., Hannum, G., Palsson, B. Ø., and Herrgard, M. J. (2007). Quantitative prediction of cellular metabolism with constraint-based models: the COBRA Toolbox. *Nature protocols*, 2(3):727.
- Bektaş, T. and Gouveia, L. (2014). Requiem for the miller–tucker–zemlin subtour elimination constraints? *European Journal of Operational Research*, 236(3):820–832.
- Bell, S. L. and Palsson, B. Ø. (2005). expa: a program for calculating extreme pathways in biochemical reaction networks. *Bioinformatics*, 21(8):1739–1740.
- Bertók, B. and Fan, L. T. (2013). Review of methods for catalytic reaction-pathway identification at steady state. *Current Opinion in Chemical Engineering*, 2(4):487–494. Biotechnology and bioprocess engineering / Process systems engineering.
- Bhatt, N., Amrhein, M., and Bonvin, D. (2011). Incremental identification of reaction and mass–transfer kinetics using the concept of extents. *Industrial & Engineering Chemistry Research*, 50(23):12960–12974.
- Bhatt, N., Kerimoglu, N., Amrhein, M., Marquardt, W., and Bonvin, D. (2012). Incremental identification of reaction systems—a comparison between rate-based and extent-based approaches. *Chemical Engineering Science*, 83(0):24–38. Mathematics in Chemical Kinetics and Engineering International Workshop 2011.
- Bhatt, N. P. (2011). *Extents of Reaction and Mass Transfer in the Analysis of Chemical Reaction Systems*. PhD thesis, EPFL, Lausanne.
- Biegler, L. (2010). *Nonlinear Programming: Concepts, Algorithms, and Applications to Chemical Processes*. Society for Industrial and Applied Mathematics, Philadelphia, PA.
- Billeter, J., Srinivasan, S., and Bonvin, D. (2013). Extent-based kinetic identification using spectroscopic measurements and multivariate calibration. *Analytica Chimica Acta*, 767(0):21–34.

- Bonvin, D. and Rippin, D. (1990). Target factor analysis for the identification of stoichiometric models. *Chemical Engineering Science*, 45(12):3417–3426.
- Bordbar, A., Monk, J. M., King, Z. A., and Palsson, B. Ø. (2014a). Constraint-based models predict metabolic and associated cellular functions. *Nature Reviews Genetics*, 15(2):107–120.
- Bordbar, A., Nagarajan, H., Lewis, N. E., Latif, H., Ebrahim, A., Federowicz, S., Schellenberger, J., and Palsson, B. Ø. (2014b). Minimal metabolic pathway structure is consistent with associated biomolecular interactions. *Molecular systems biology*, 10(7):737.
- Bordbar, A., Yurkovich, J. T., Paglia, G., Rolfsson, O., Sigurjónsson, Ó. E., and Palsson, B. Ø. (2017). Elucidating dynamic metabolic physiology through network integration of quantitative time-course metabolomics. *Scientific reports*, 7:46249.
- Brendel, M., Bonvin, D., and Marquardt, W. (2006). Incremental identification of kinetic models for homogeneous reaction systems. *Chemical Engineering Science*, 61(16):5404–5420.
- Chen, D., Batson, R., and Dang, Y. (2010). *Applied Integer Programming: Modeling and Solution*. Wiley.
- Claus, A. (1984). A new formulation for the travelling salesman problem. *SIAM Journal on Algebraic Discrete Methods*, 5(1):21–25.
- Dantzig, G., Fulkerson, R., and Johnson, S. (1954). Solution of a large-scale traveling-salesman problem. *Journal of the operations research society of America*, 2(4):393–410.
- Dantzig, G. B., Fulkerson, D. R., and Johnson, S. M. (1959). On a linear-programming, combinatorial approach to the traveling-salesman problem. *Operations Research*, 7(1):58–66.
- Dong, Y., Georgakis, C., Mustakis, J., Hawkins, J. M., Han, L., Wang, K., McMullen, J. P., Grosser, S. T., and Stone, K. (2019). Stoichiometry identification of pharmaceutical reactions using the constrained dynamic response surface methodology. *AIChE Journal*, 65(11):e16726.
- Duarte, B. P., Moura, M. J., Neves, F. J., and Oliveira, N. M. (2008). A mathematical programming framework for optimal model selection/validation of process data. In *Computer Aided Chemical Engineering*, volume 25, pages 343–348. Elsevier.
- Edwards, J. S., Ibarra, R. U., and Palsson, B. Ø. (2001). In silico predictions of escherichia coli metabolic capabilities are consistent with experimental data. *Nature biotechnology*, 19(2):125–130.
- Famili, I. and Palsson, B. O. (2003a). The convex basis of the left null space of the stoichiometric matrix leads to the definition of metabolically meaningful pools. *Biophysical journal*, 85(1):16–26.
- Famili, I. and Palsson, B. Ø. (2003b). Systemic metabolic reactions are obtained by singular value decomposition of genome-scale stoichiometric matrices. *Journal of theoretical*

*biology*, 224(1):87–96.

- Fan, L., Bertók, B., and Friedler, F. (2002). A graph-theoretic method to identify candidate mechanisms for deriving the rate law of a catalytic reaction. *Computers & Chemistry*, 26(3):265–292.
- Fan, L., Bertók, B., Friedler, F., and Shafie, S. (2001). Mechanisms of ammonia-synthesis reaction revisited with the aid of a novel graph-theoretic method of determining candidate mechanisms in deriving the rate law of a catalytic reaction. *Hungarian Journal of Industrial Chemistry*, 29(1):71–80.
- Fan, L. T., Lin, Y.-C., Shafie, S., Bertok, B., and Friedler, F. (2012). Exhaustive identification of feasible pathways of the reaction catalyzed by a catalyst with multiactive sites via a highly effective graph-theoretic algorithm: Application to ethylene hydrogenation. *Industrial & Engineering Chemistry Research*, 51(6):2548–2552.
- Filippi-Bossy, C., Bordet, J., Villermaux, J., Marchal-Brassely, S., and Georgakis, C. (1989). Batch reactor optimization by use of tendency models. *Computers & chemical engineering*, 13(1-2):35–47.
- Finke, G., Claus, A., and Gunn, E. (1984). A two-commodity network flow approach to the traveling salesman problem. *Congresses Numeration*, 41:167–178.
- Fishtik, I., Alexander, A., and Datta, R. (1999). Enumeration and discrimination of mechanisms in heterogeneous catalysis based on response reactions and unity bond index–quadratic exponential potential (UBI–QEP) method. *Surface science*, 430(1-3):1–17.
- Fishtik, I., Callaghan, C. A., and Datta, R. (2004a). Reaction route graphs. I. Theory and algorithm. *The Journal of Physical Chemistry B*, 108(18):5671–5682.
- Fishtik, I., Callaghan, C. A., and Datta, R. (2004b). Reaction route graphs. II. Examples of enzyme- and surface-catalyzed single overall reactions. *The Journal of Physical Chemistry B*, 108(18):5683–5697.
- Floudas, C. A. and Lin, X. (2005). Mixed integer linear programming in process scheduling: Modeling, algorithms, and applications. *Annals of Operations Research*, 139(1):131–162.
- Förster, J., Famili, I., Fu, P., Palsson, B. Ø., and Nielsen, J. (2003). Genome-scale reconstruction of the *saccharomyces cerevisiae* metabolic network. *Genome research*, 13(2):244–253.
- Fotopoulos, J., Georgakis, C., and Stenger, H. G. (1994). Structured target factor analysis for the stoichiometric modeling of batch reactors. In *Proceedings of 1994 American Control Conference - ACC '94*, volume 1, pages 495–499 vol.1.
- Friedler, F., Tarjan, K., Huang, Y., and Fan, L. (1992). Graph-theoretic approach to process synthesis: axioms and theorems. *Chemical Engineering Science*, 47(8):1973–1988.

- Friedler, F., Tarjan, K., Huang, Y., and Fan, L. (1993). Graph-theoretic approach to process synthesis: Polynomial algorithm for maximal structure generation. *Computers & Chemical Engineering*, 17(9):929–942.
- Gabow, H. N., Galil, Z., Spencer, T., and Tarjan, R. E. (1986). Efficient algorithms for finding minimum spanning trees in undirected and directed graphs. *Combinatorica*, 6(2):109–122.
- Gabow, H. N. and Myers, E. W. (1978). Finding all spanning trees of directed and undirected graphs. *SIAM Journal on Computing*, 7(3):280–287.
- Gavish, B. and Graves, S. C. (1978). The travelling salesman problem and related problems. *Operations Research Center Working Papers*, 078(78).
- Gianchandani, E. P., Chavali, A. K., and Papin, J. A. (2010). The application of flux balance analysis in systems biology. *Wiley Interdisciplinary Reviews: Systems Biology and Medicine*, 2(3):372–382.
- Gouveia, L. and Pires, J. M. (1999). The asymmetric travelling salesman problem and a reformulation of the miller–tucker–zemlin constraints. *European Journal of Operational Research*, 112(1):134–146.
- Gross, J. and Yellen, J. (2005). *Graph Theory and Its Applications, Second Edition*. Textbooks in Mathematics. Taylor & Francis.
- Grossmann, I. E. (1985). Mixed-integer programming approach for the synthesis of integrated process flowsheets. *Computers & chemical engineering*, 9(5):463–482.
- Hamer, J. W. (1989). Stoichiometric interpretation of multireaction data: application to fed-batch fermentation data. *Chemical Engineering Science*, 44(10):2363–2374.
- Haouari, M., Maculan, N., and Mrad, M. (2013). Enhanced compact models for the connected subgraph problem and for the shortest path problem in digraphs with negative cycles. *Computers & operations research*, 40(10):2485–2492.
- Happel, J. and Sellers, P. H. (1982). Multiple reaction mechanisms of catalysis. *Industrial & Engineering Chemistry Fundamentals*, 21(1):67–76.
- Happel, J., Sellers, P. H., and Otarod, M. (1990). Mechanistic study of chemical reaction systems. *Industrial & Engineering Chemistry Research*, 29(6):1057–1064.
- Henry, C. S., Broadbelt, L. J., and Hatzimanikatis, V. (2007). Thermodynamics-based metabolic flux analysis. *Biophysical Journal*, 92(5):1792–1805.
- Himmelblau, D., Jones, C., and Bischoff, K. (1967). Determination of rate constants for complex kinetics models. *Industrial & Engineering Chemistry Fundamentals*, 6(4):539–543.
- Ibarra, R. U., Edwards, J. S., and Palsson, B. Ø. (2002). Escherichia coli k-12 undergoes adaptive evolution to achieve in silico predicted optimal growth. *Nature*, 420(6912):186–189.
- Ibrahim, M., Maculan, N., and Minoux, M. (2009). A strong flow-based formulation for

- the shortest path problem in digraphs with negative cycles. *International Transactions in Operational Research*, 16(3):361–369.
- Jamshidi, N. and Palsson, B. Ø. (2011). Metabolic network dynamics: properties and principles. In *Understanding the Dynamics of Biological Systems*, pages 19–37. Springer.
- Jia, G., Stephanopoulos, G., and Gunawan, R. (2012). Incremental parameter estimation of kinetic metabolic network models. *BMC Systems Biology*, 6(1):142.
- Jones, N., Pevzner, P., and Pevzner, P. (2004). *An Introduction to Bioinformatics Algorithms*. A Bradford book. Bradford Books.
- Kapoor, S. and Ramesh, H. (1991). Algorithms for generating all spanning trees of undirected, directed and weighted graphs. In *Workshop on Algorithms and Data Structures*, pages 461–472. Springer.
- Kapoor, S. and Ramesh, H. (1995). Algorithms for enumerating all spanning trees of undirected and weighted graphs. *SIAM Journal on Computing*, 24(2):247–265.
- Karnaukhov, A. and Karnaukhova, E. (2003). Application of a new method of nonlinear dynamical system identification to biochemical problems. *Biochemistry (Moscow)*, 68(3):253–259.
- Karnaukhov, A., Karnaukhova, E., and Zarnitsina, V. (2005). Consideration of prior information and the type of experimental error in the identification method based on minimizing square residuals. *BIOPHYSICS-PERGAMON-C/C OF BIOFIZIKA*, 50(2):309–313.
- Karnaukhov, A. V., Karnaukhova, E. V., and Williamson, J. R. (2007). Numerical matrices method for nonlinear system identification and description of dynamics of biochemical reaction networks. *Biophysical Journal*, 92(10):3459–3473.
- Kauffman, K. J., Prakash, P., and Edwards, J. S. (2003). Advances in flux balance analysis. *Current Opinion in Biotechnology*, 14(5):491–496.
- Langevin, A., Soumis, F., and Desrosiers, J. (1990). Classification of travelling salesman problem formulations. *Operations Research Letters*, 9(2):127–132.
- Lee, D.-Y., Fan, L., Park, S., Lee, S. Y., Shafie, S., Bertók, B., and Friedler, F. (2005). Complementary identification of multiple flux distributions and multiple metabolic pathways. *Metabolic Engineering*, 7(3):182–200.
- Lee, S., Phalakornkule, C., Domach, M. M., and Grossmann, I. E. (2000). Recursive MILP model for finding all the alternate optima in LP models for metabolic networks. *Computers & Chemical Engineering*, 24(2-7):711–716.
- Leighty, R. W. and Antoniewicz, M. R. (2011). Dynamic metabolic flux analysis (DMFA): a framework for determining fluxes at metabolic non-steady state. *Metabolic engineering*, 13(6):745–755.
- Lequeux, G., Beauprez, J., Maertens, J., Van Horen, E., Soetaert, W., Vandamme, E., and Vanrolleghem, P. A. (2010). Dynamic metabolic flux analysis demonstrated on cultures



- where the limiting substrate is changed from carbon to nitrogen and vice versa. *Journal of Biomedicine and Biotechnology*, 2010.
- López C., D. C., Barz, T., Körkel, S., and Wozny, G. (2015). Nonlinear ill-posed problem analysis in model-based parameter estimation and experimental design. *Computers & Chemical Engineering*, 77:24–42.
- Marin, G. and Yablonsky, G. (2011). *Kinetics of Chemical Reactions*. Wiley.
- Marquardt, W. (2004). Model-based experimental analysis: A systems approach to mechanistic modeling of kinetic phenomena. In *Proceedings, 6th International Conference on Foundations of Computer-Aided Process Design*, volume 11.
- Marquardt, W. (2005). Model-based experimental analysis of kinetic phenomena in multiphase reactive systems. *Chemical Engineering Research and Design*, 83(6):561–573. 7th World Congress of Chemical Engineering.
- Marvin, W. A., Rangarajan, S., and Daoutidis, P. (2013). Automated generation and optimal selection of biofuel-gasoline blends and their synthesis routes. *Energy & Fuels*, 27(6):3585–3594.
- Mavrovouniotis, M. L. (1992). Synthesis of reaction mechanisms consisting of reversible and irreversible steps. 2. formalization and analysis of the synthesis algorithm. *Industrial & Engineering Chemistry Research*, 31(7):1637–1653.
- Mavrovouniotis, M. L. (1995). Symbolic and quantitative reasoning: Design of reaction pathways through recursive satisfaction of constraints. In Stephanopoulos, G. and Han, C., editors, *Intelligent Systems in Process Engineering Part I: Paradigms from Product and Process Design*, volume 21 of *Advances in Chemical Engineering*, pages 147–186. Academic Press.
- Mavrovouniotis, M. L. and Stephanopoulos, G. (1992). Synthesis of reaction mechanisms consisting of reversible and irreversible steps. 1. a synthesis approach in the context of simple examples. *Industrial & Engineering Chemistry Research*, 31(7):1625–1637.
- Miller, C. E., Tucker, A. E., and Zemlin, R. A. (1960). Integer programming formulation of traveling salesman problems. *J. ACM*, 7:326–329.
- Murabito, E., Simeonidis, E., Smallbone, K., and Swinton, J. (2009). Capturing the essence of a metabolic network: A flux balance analysis approach. *Journal of Theoretical Biology*, 260(3):445–452.
- Niklas, J., Schröder, E., Sandig, V., Noll, T., and Heinzle, E. (2011). Quantitative characterization of metabolism and metabolic shifts during growth of the new human cell line age1. hn using time resolved metabolic flux analysis. *Bioprocess and biosystems engineering*, 34(5):533–545.
- Öncan, T., Altinel, İ. K., and Laporte, G. (2009). A comparative analysis of several asymmetric traveling salesman problem formulations. *Computers & Operations Research*, 36(3):637–654.

- Orman, A. and Williams, H. P. (2006). A survey of different integer programming formulations of the travelling salesman problem. *Optimisation, Econometric and Financial Analysis*, 9:93–108.
- Orth, J. D., Thiele, I., and Palsson, B. Ø. (2010). What is flux balance analysis? *Nature biotechnology*, 28(3):245–248.
- Otarod, M. and Happel, J. (1992). Studies of the structure of chemical mechanisms. *Chemical Engineering Science*, 47(3):587–592.
- Padberg, M. and Sung, T.-Y. (1991). An analytical comparison of different formulations of the travelling salesman problem. *Mathematical Programming*, 52(1-3):315–357.
- Palsson, B. (2015a). *Systems Biology: Constraint-based Reconstruction and Analysis*. Cambridge University Press.
- Palsson, B. Ø. (2015b). Optimization. In *Systems Biology: Constraint-based Reconstruction and Analysis*, pages 298–311. Cambridge University Press.
- Pataki, G. (2003). Teaching integer programming formulations using the traveling salesman problem. *SIAM REV*, 45:116–123.
- Pennaz, E. J. (2011). Conceptual design of biorefineries through the synthesis of optimal chemical reaction pathways. Master’s thesis, Texas A & M University.
- Portela, R., Richelle, A., Dumas, P., and von Stosch, M. (2019). Time integrated flux analysis: Exploiting the concentration measurements directly for cost-effective metabolic network flux analysis. *Microorganisms*, 7(12):620.
- Prinz, O. and Bonvin, D. (1994). Monitoring chemical reaction systems using incremental target factor analysis. *IFAC Proceedings Volumes*, 27(2):339–344.
- Qian, H. and Beard, D. A. (2005). Thermodynamics of stoichiometric biochemical networks in living systems far from equilibrium. *Biophysical Chemistry*, 114(2–3):213–220.
- Qian, H., Beard, D. A., and Liang, S.-d. (2003). Stoichiometric network theory for nonequilibrium biochemical systems. *European Journal of Biochemistry*, 270(3):415–421.
- Rodrigues, D., Billeter, J., and Bonvin, D. (2018). Maximum-likelihood estimation of kinetic parameters via the extent-based incremental approach. *Computers & Chemical Engineering*.
- Santos-Marques, J., Georgakis, C., Mustakis, J., and Hawkins, J. M. (2019). From dynamic response surface models to the identification of the reaction stoichiometry in a complex pharmaceutical case study. *AIChE Journal*, 65(4):1173–1185.
- Sarin, S. C., Sherali, H. D., and Bhootra, A. (2005). New tighter polynomial length formulations for the asymmetric traveling salesman problem with and without precedence constraints. *Operations research letters*, 33(1):62–70.
- Savinell, J. M. and Palsson, B. Ø. (1992). Optimal selection of metabolic fluxes for in vivo measurement. i. development of mathematical methods. *Journal of theoretical biology*,

- 155(2):201–214.
- Schellenberger, J., Que, R., Fleming, R. M., Thiele, I., Orth, J. D., Feist, A. M., Zielinski, D. C., Bordbar, A., Lewis, N. E., Rahmanian, S., et al. (2011). Quantitative prediction of cellular metabolism with constraint-based models: the COBRA Toolbox v2.0. *Nature protocols*, 6(9):1290.
- Schilling, C. H., Edwards, J. S., Letscher, D., and Palsson, B. Ø. (2000a). Combining pathway analysis with flux balance analysis for the comprehensive study of metabolic systems. *Biotechnology and bioengineering*, 71(4):286–306.
- Schilling, C. H., Edwards, J. S., and Palsson, B. Ø. (1999). Toward metabolic phenomics: analysis of genomic data using flux balances. *Biotechnology progress*, 15(3):288–295.
- Schilling, C. H., Letscher, D., and Palsson, B. Ø. (2000b). Theory for the systemic definition of metabolic pathways and their use in interpreting metabolic function from a pathway-oriented perspective. *Journal of Theoretical Biology*, 203(3):229–248.
- Sellers, P. (1984). Combinatorial classification of chemical mechanisms. *SIAM Journal on Applied Mathematics*, 44(4):784–792.
- Seo, H., Lee, D.-Y., Park, S., Fan, L., Shafie, S., Bertók, B., and Friedler, F. (2001). Graph-theoretical identification of pathways for biochemical reactions. *Biotechnology Letters*, 23(19):1551–1557.
- Sherali, H. D. and Adams, W. P. (1990). A hierarchy of relaxations between the continuous and convex hull representations for zero-one programming problems. *SIAM Journal on Discrete Mathematics*, 3(3):411–430.
- Sherali, H. D. and Driscoll, P. J. (2002). On tightening the relaxations of miller-tucker-zemlin formulations for asymmetric traveling salesman problems. *Operations Research*, 50(4):656–669.
- Srinivasan, S., Billeter, J., and Bonvin, D. (2012). Extent-based incremental identification of reaction systems using concentration and calorimetric measurements. *Chemical Engineering Journal*, 207–208(0):785–793. 22nd International Symposium on Chemical Reaction Engineering (ISCRE 22).
- Taccari, L. (2015). *Mixed-integer programming models and methods for bilevel fair network optimization and energy cogeneration planning*. PhD thesis, Dipartimento di Elettronica, Informazione e Bioingegneria - Politecnico di Milano.
- Taccari, L. (2016). Integer programming formulations for the elementary shortest path problem. *European Journal of Operational Research*, 252(1):122–130.
- Thiele, I. and Palsson, B. Ø. (2010). A protocol for generating a high-quality genome-scale metabolic reconstruction. *Nature protocols*, 5(1):93.
- Tick, J. (2007). P-graph-based workflow modelling. *Acta Polytechnica Hungarica*, 4(1):75–88.
- Vercammen, D., Logist, F., and Van Impe, J. (2014). Dynamic estimation of specific fluxes

- in metabolic networks using non-linear dynamic optimization. *BMC systems biology*, 8(1):1–22.
- Vertis, C. S., Oliveira, N. M., and Bernardo, F. P. (2015). Systematic development of kinetic models for systems described by linear reaction schemes. In Krist V. Gernaey, J. K. H. and Gani, R., editors, *12th International Symposium on Process Systems Engineering and 25th European Symposium on Computer Aided Process Engineering*, volume 37 of *Computer Aided Chemical Engineering*, pages 647–652. Elsevier.
- Voll, A. and Marquardt, W. (2012). Reaction network flux analysis: Optimization-based evaluation of reaction pathways for biorenewables processing. *AIChE Journal*, 58(6):1788–1801.
- Wiechert, W. (2001). 13c metabolic flux analysis. *Metabolic engineering*, 3(3):195–206.
- Wikipedia (2021). Minimum spanning tree — wikipedia, the free encyclopedia. [https://en.wikipedia.org/wiki/Minimum\\_spanning\\_tree](https://en.wikipedia.org/wiki/Minimum_spanning_tree). Online; accessed 2-June-2021.
- Willis, M. J. and von Stosch, M. (2016). Inference of chemical reaction networks using mixed integer linear programming. *Computers & Chemical Engineering*, 90:31–43.
- Willis, M. J. and von Stosch, M. (2017). Simultaneous parameter identification and discrimination of the nonparametric structure of hybrid semi-parametric models. *Computers & Chemical Engineering*, 104:366–376.
- Wong, R. T. (1980). Integer programming formulations of the traveling salesman problem. In *Proceedings of the IEEE international conference of circuits and computers*, pages 149–152. IEEE Press Piscataway NJ.
- Yugi, K., Nakayama, Y., Kinoshita, A., and Tomita, M. (2005). Hybrid dynamic/static method for large-scale simulation of metabolism. *Theoretical Biology and Medical Modelling*, 2(1):1–11.

# Chapter 4

## Methodology Description

*“As for everything else, so for a mathematical theory:  
beauty can be perceived but not explained.”*

– Arthur Cayley (1821–1895)

Kinetic models of chemical reactions play an important role in the optimization, control and design of chemical processes. In this context, systematic methodologies that incorporate experimental reaction data are sought in order to obtain robust and accurate models. The proposed methodology follows a step-by-step approach, where parts of the model are identified incrementally, keeping the model uncertainty under control and avoiding manipulating nonlinear models in the initial phases. In this sense, the information obtained in each stage is used in the subsequent ones, gradually increasing the complexity of the model.

Three main aspects of the systematic methodology for the development of chemical reaction models can be emphasized as significant differences when compared to the existing reaction systems modeling approaches:

- The methodology spans all feasible structural models in order to guarantee that the best topology is identified, including nonlinear reaction networks.
- The incorporation of invariant relationships in the data regularization procedure is considered to increase data accuracy, allowing better performance in model identification.
- A systematic method for identifying the kinetic expressions of every reaction component that (i) is superstructure-based, (ii) incorporates qualitative and quantitative analyses, (iii) uses information criteria, is proposed.

The methodology, see Figure 4.1, comprises seven steps and takes, as input, reaction data consisting of measurements of chemical species obtained in a batch experiment. The output of the methodology, obtained at the end of the sixth step, is an optimal model

based on first principles laws. The methodology exhaustively explores the generation of reaction networks and makes the most of the experimental data to select plausible structures. The elucidation of the reaction network is decoupled from the kinetic laws expressions, ensuring more certainty about the full model development, and guaranteeing that all structures of reaction networks have been spanned. The methodology converges to a full kinetic model: reaction network and kinetic laws for each chemical reaction. If no unique solution is found, further experiments are proposed to complete the model elucidation. Each methodology step is described next.

**Step 1** This consists of a data reconciliation procedure regarding the mass conservation phenomenon in closed systems and other time-invariant relationships previously identified. Smoothed and continuous concentration profiles are obtained using orthogonal collocation on finite elements. The finite elements typically are cubic polynomials of Lagrange with the roots of Legendre. In addition to conservation relationships, several constraints are also imposed, namely continuity equations between elements in the function value, first and second derivatives. The reconciliation procedure is iterative, where shape constraints are incrementally added in order to avoid undesired profiles oscillations. These shape constraints consist of inequalities equations that establish monotonous behavior that can be observed through the profiles trends. The polynomials are simultaneously fitted minimizing the squared difference between the predicted values and experimental data, subject to the invariant and shape constraints, in an optimal regression procedure. At the end of Step 1, the reconciled data is obtained together with the concentration derivatives continuous profiles.

**Step 2** In this phase, the data analysis is performed to characterize the subspace spanned by the data vectors, and thus, to elucidate its dimension. First, a discrete set of the previously reconciled data is collected in the *variant form*, *i.e.*, time concentration derivatives, or time cumulative concentration changes, of every observed species are collected forming a data matrix in the variant form. The singular value decomposition (SVD) of the data matrix provides decoupled information about *dynamic* and *structural* characteristics of the reaction system, through abstract vectors that form orthonormal bases for the four fundamental subspaces of the matrix. At this phase, we are only interested in the structural information of data since the subspace spanned by the row data vectors roughly corresponds to the subspace spanned by the transposed stoichiometric vectors that compose the reaction network. In this sense, through the singular values analysis and more sophisticated techniques applied to them, the rank of the data matrix can be established (considering the model uncertainty), elucidating the number of linearly independent vectors that are required to explain the observed compositional changes in the reaction system, *i.e.*, the network dimension. At this phase the number of linearly independent invariant relationships is also confirmed by the identification of the dimension of the data null space. Once the data variant subspace is characterized, the superstructure of the reaction net-

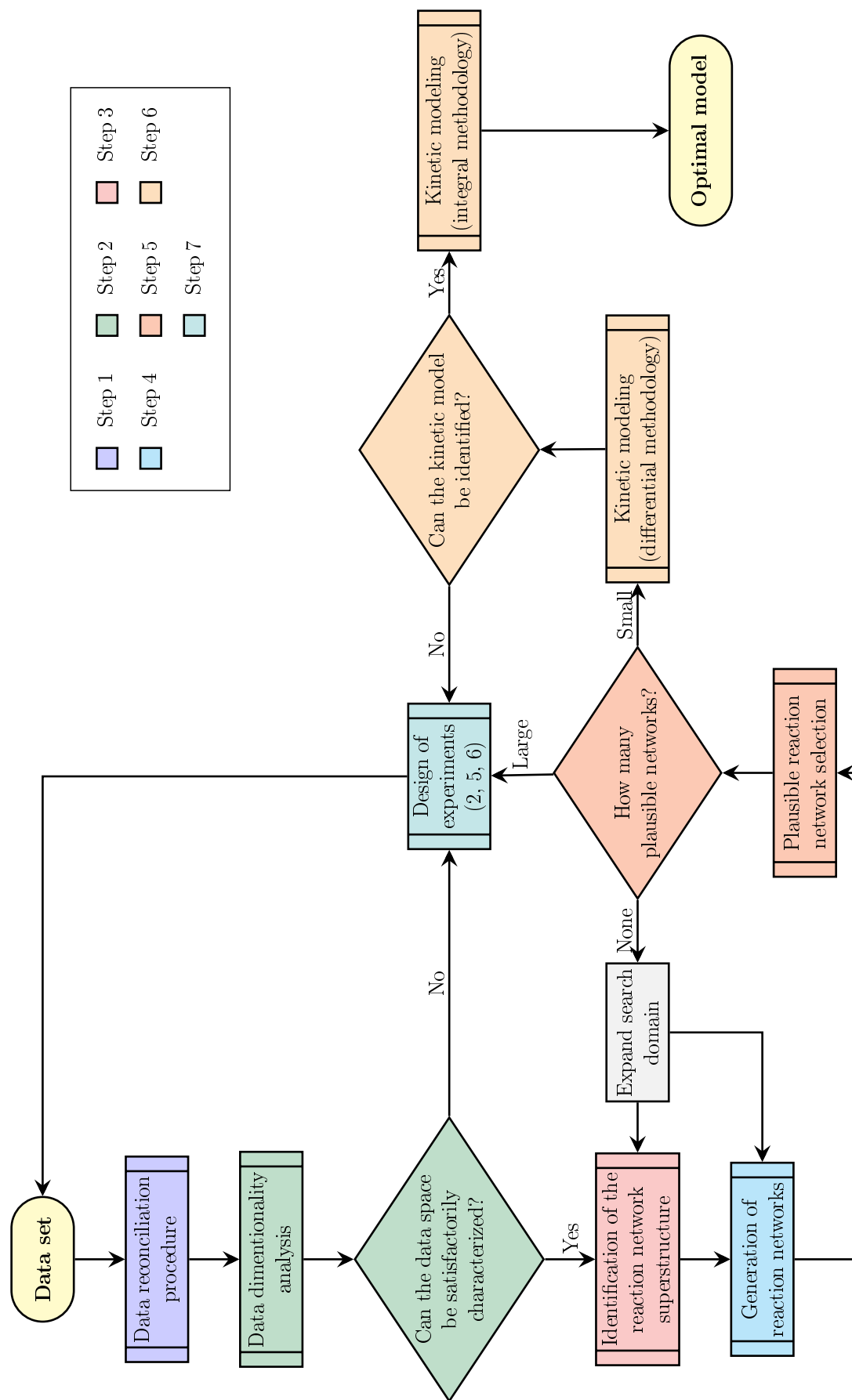


**Figure 4.1** Flowchart of the systematic methodology for the incremental development of chemical reaction models.

works can be constrained to belong to that space, allowing the generation of network structures that are consistent with the observed compositional changes. When the rank of the data is unidentifiable, *i.e.*, it is not clear the linear independence among the data matrix column vectors due to the presence of great collinearity among them and/or the existence of a gray distribution of singular values with similar magnitudes, the *design of additional experiments* may be considered in order to clarify the real dimension of the data characteristic subspaces, by (i) improving the data matrix condition number and its collinearity index, and consequently, increasing model identifiability from data, and (ii) elucidating more invariant relationships in time that could not be observed in the original dataset, assisting in the identification of the model structure. This can be achieved by assessing whether or not the magnitude of smaller singular values increases in the presence of additional datasets with different initial conditions. Moreover, additional data from experiments designed for that purposes can turn the modeling task in a well-posed regression problem in later steps of the methodology.

**Step 3** This addresses the reaction network superstructure generation. For this task, several sub-steps are followed: (i) the generation of chemical reactions, or equivalently, reaction vectors composed by species stoichiometric coefficients; (ii) the target vector/factor analysis, and; (iii) the reaction thermodynamic analysis. The *generation of chemical reactions* in sub-step 3(i) is achieved using MILP, where the number of participating species is minimized subjected to invariant constraints, such as elemental conservation. The complete enumeration of feasible reaction vectors is achieved using integer cut equations that forbid repeated and equivalent solutions. After obtained the entire list of potential reaction vectors, ensuring the formation of all observed species, the target reaction vector analysis is performed in sub-step 3(ii) in order to *verify whether that reaction vectors lie to the data variant subspace*. This is done by evaluating the error of projection of individual target vectors in the data variant subspace identified in the Step 2. The ideal situation is when all reaction vectors completely span the data subspace. However, in the presence of data with great uncertainty, the individual component vectors respected to reactions that produce residual species may be hard to be identified in that data subspace, presenting great projection errors. In those cases, the procedures of data reconciliation and analysis (Steps 1 and 2) can be reconsidered in order to well characterize the data subspace by finding (and imposing) more time invariants and, therefore, decreasing data uncertainty. Nevertheless, when the problem persists and no additional experiments can be done, the next methodology steps must be followed with special attention to those problematic/unidentified reaction vectors. This means that unidentified reaction vectors are not excluded, they must continue as candidate reaction vectors, since they can be required to explain the origin of residual species in a consistent network structure. Once the reaction vectors that are consistent with the data are identified, the thermodynamic analysis is performed in sub-step 3(iii) to elucidate the *energetically feasible net flux direction* of every chemical reaction.



The net flux direction is energetically feasible when the Gibbs free energy change, related to the respected reaction extent, is negative. Therefore, at the end of this step, the data consistent and energetically feasible superstructure of the reaction network is obtained.

**Step 4** During this step, the generation of reaction networks is considered using MILP formulations, where binary variables indicate whether a reaction vector (from the superstructure) participates in the final reaction network. Although the number of linearly independent chemical reactions is fixed (it is a constant value equal to the rank of data previously elucidated), the artificial objective function consists of minimizing the reaction network complexity, that is measured by the number of constituent chemical reactions. Integer cut equations are used to enumerate all reaction networks that are linear combinations of each other, *i.e.*, several bases composed by reaction vectors that (approximately) span the same data subspace. The formulation is generic and can also be applied to chemical systems with more than one initial reactant. Furthermore, the incorporation of precedence constraints is needed for nonlinear chemical systems to avoid generating structurally inconsistent nonlinear networks. The generation of networks can be expressed as a combinatorial optimization problem, consisting a NP-complete problem inserted in the constraint programming field.

**Step 5** In this step the generated reaction networks are validated using the reconciled data, according to a plausibility criterion. This criterion consists of selecting (meaningful) networks that conduct to positive reaction rates as solutions of the linear mass balance equations, where the species concentration derivatives vector is described by a set of positive coordinates (reaction rates) in the row space defined by the reaction vectors that make up the stoichiometric matrix. The structures that pass this phase are classified as plausible networks, or in a vectorial space perspective, they are plausible bases. Note that, the generated reaction networks already were (i) set of bases that are consistent with data, (ii) linear combinations of each other, and now, after passing the plausibility test, they are a special subset once they conduct to positive coordinates that build the derivative vector. Thus, the derivative vector lies to the positive orthant of the stoichiometric matrix row space, it is a linearly dependent vector that is written by the sum of positive coefficients (reaction rates) times the respective reaction vectors that form the plausible basis. If none plausible structure can be found, the expansion of the search domain is considered by (i) generating more complex chemical reactions (reactions that contain more participating species), thus going back to Step 3, and/or (ii) increasing the number of chemical reactions in the networks in Step 4. When the number of plausible reaction networks is significant, (more than 5), the design of experiments can be proposed to discriminate the true reaction structure of the chemical system in Step 7.

Instead generating data consistent structures to later identify the ones that are plausible, the implicit generation of reaction networks can be considered when in-

corporating the mass balance equations in the MILP formulation to generate only plausible reaction network structures. This consists of the union of Steps 4 and 5. The implicit generation of reaction networks can be advantageous for large problem sizes, *i.e.*, chemical systems with more than ten chemical species, since it can avoid a lot of computational effort associated with the explicit generation of reaction networks.

**Step 6** This last step involves the kinetic modeling task. Individual reaction rate profiles are analyzed in order to elucidate the kinetic expressions (based on first principles), *e.g.*, power mass law, chemical adsorption, enzymatic, etc. The kinetic expressions are proposed based on the correlation found between the reaction rate and the reactant species concentration. At this phase, some important system phenomena can be observed, for example, if there are (i) inhibition (observed through delay in the rate profiles) and (ii) reversible chemical reactions. The individual fit of the kinetic models is performed minimizing the squared difference between the observed reaction rates (calculated through the species fluxes) and the model counterpart (given by the kinetic expression). At this phase, information criterion is used for establishing a balance between model complexity (number of parameters) and fit quality. If more than one candidate kinetic expression presents a good fit agreement, additional experiments can be proposed to discriminate them.

For large problem sizes, the implicit generation of reaction networks can be even more restrictive by considering the simultaneous identification of plausible structures with established kinetic expression for each reaction component. The basic idea here is to find a good correlation of the every reaction rate with the species concentration of the respective reactant, starting from a pre-specified superstructure of kinetic laws based on first principles. This consists of the union of Steps 4, 5 and 6 (initial phase).

Although the reaction network and the kinetic expressions were elucidated using the previously described incremental approach based on the differential method, the validation of the entire kinetic model is performed using the integral method. This latter consists in a simultaneous fine tuning of the model parameters when minimizing the squared difference between concentration data and predicted (integrated) model values. On the downside, this simultaneous approach configures a nonlinear optimization regression problem, where the results obtained may be local optimal solutions, very sensitive to their initial guesses. However, on the topside, this final tuning is free of bias allowing the achievement of optimal parameters in the maximum likelihood sense. The solution (parameters values) obtained by the incremental method is used as initial guess value for the regression variables. At the end of this phase, parameters confidence intervals are computed confirming the robustness of the proposed methodology when tight intervals are obtained, even in the presence of originally noisy datasets (data with great uncertainty). Finally, the best reaction model (reaction network and kinetic expressions) that describes the experimental data is developed.

# Chapter 5

## Step 1 — Data Pre-processing

*“The journey of a thousand miles begins with one step.”*

– Lao Tzu

### Contents

---

5.1	Step 1 motivation . . . . .	134
5.2	Regularization methods . . . . .	135
5.2.1	Filter-based approaches . . . . .	136
5.2.2	Tikhonov regularization . . . . .	137
5.2.3	Sparse regression using MILP . . . . .	138
5.2.4	Smoothing splines . . . . .	139
5.2.5	Dynamic Response Surface Methodology with additional constraints . . . . .	143
5.2.6	Comparative analysis of regularization methods . . . . .	145
5.3	Continuous approximation of concentration data . . . . .	146
5.3.1	Orthogonal Collocation on Finite Elements . . . . .	147
5.3.2	Step 1 formulation . . . . .	147
5.3.3	Step 1 flowchart . . . . .	151
5.3.4	Application example . . . . .	151
	Bibliography . . . . .	155

---

Data pre-processing (DPP) methods are used to treat and validate data in order to identify and correct data mistakes, *i.e.*, to correct measurements in industrial processes. Inaccurate process data can easily lead to poor decisions, which may negatively influence many parts of the process (Mah et al., 1976). Hence, the use of DPP techniques increases the

overall accuracy of data, turning data more interpretable and leading to accurate insights about the chemical system under analysis.

The available experimental data constitute the essential support for the development of kinetic models that describe the dynamic behavior of the chemical system under study. In this work it is assumed that the results of one or more experimental tests are available for analysis, containing temporal concentration profiles of the various chemical species present in the system (tests in transient state). Usually, these profiles are characterized by measurements of concentrations in a discrete set of points and contain errors inherent to the analytical method used. In addition, the range of sampling intervals is high in many cases, however, interpolation techniques can be used to estimate concentrations at intermediate times.

Without affecting the scope of the developed methodology, it is assumed that all essential variables are measured to determine the time-concentration profiles of all species present in the system and some of these species can be determined by difference in the closing of the corresponding system mass balance. Additionally, mass balances (global or partial) provide a good test for validating the quality of the data obtained.

Since the developed methodology to model chemical reaction systems presented in this thesis is supported by the differential method, having good estimates of species fluxes and reaction fluxes is crucial to the successful identification of the model structure. Consequently, the main effort of the first step of the methodology is associated with the calculation of good estimates of concentration derivatives. In this chapter, a novel DPP method is presented supported on orthogonal collocation on finite elements, including the use of material conservation and profile shape constraints, for the obtainment of smoothed and reconciled time-concentration profiles.

This chapter is organized as follows. Section 5.1 presents a contextualization of the theme, framing where the pre-processing of data is applied for the identification of chemical reaction models. In Section 5.2 several data regularization methods are presented for continuous (or quasi-continuous) approximation of concentration data and consequently estimation of species concentration derivatives. This last section presents the state of the art of Step 1, including a simplified comparison of the previously exposed methods where the aspects that are essential for the development of Step 1 are highlighted. In Section 5.3, the proposed DPP method is described, presenting the theoretical concepts involved, the developed formulation and an application example that considers the experimental data related to the catalytic hydrogenation of succinic acid.

## 5.1 Step 1 motivation

In the application of incremental modeling strategies, the differential and the integral methods have been considered for classical analysis of reaction data and kinetic model identification (Levenspiel, 1998), as it was previously presented in Section 3.1.2. The

differential method offers the advantages of being able to (i) directly calculate the reaction rates once the derivatives of the concentration (or number of moles) time profiles are differentiated and (ii) more easily identify the kinetic expression that best correlates each individual reaction rate as a function of the respective reactant species. However, the computation of concentration derivatives usually introduces errors in the estimates of the reaction rates, which can be substantial if adequate procedures are not used (Varah, 1982; Yeow et al., 2003). In contrast, the integral method can become less sensitive to errors in specific concentration measurements, especially when the conversions become significant, but still may lead to biased concentration estimates.

Hence, the need of DPP methods is verified in the context of reaction model identification, especially DPP methods in which time-invariant constraints are incorporated ensuring conservative relationships among chemical species profiles. These kind of pre-processing data methods are called *data reconciliation* methods. The use of time-invariant relationships decreases the uncertainty originally present in the concentration measurements, enabling the obtaining of reconciled smoothed (continuous) profiles with more confidence on which the model structure identification will be based. Hence, the use of data reconciliation methods results in more accurate predictions, either for the calculation of reaction rates or extents in the differential and integral methods, respectively, during incremental kinetic model development.

## 5.2 Regularization methods

*“In God we trust, all others bring data.”*

– William Edwards Deming (1900-1993)

The estimation of the derivatives of the concentration profiles from experimental data is known to be an ill-posed problem, due to the sparsity and noise contamination of the measurements (Michalik et al., 2009). Perhaps the differentiation of the noise-corrupted concentration measurements is the major limitation in the application of the full incremental approach, since small errors in concentration data might lead to large errors in its derivatives estimates with respect to time, which can compromise the model identification task. Consequently, diverse regularization techniques have been tried to obtain solutions to similar but related problems, which enforce additional smoothness assumptions on the solutions obtained. A common goal of these techniques is to deal only with well-posed problems, which provide solutions as close as possible to the solution of the original problem, but are less sensitive to small changes in the input data (Hansen, 1992). Methods such as the use of filter-based approaches (Section 5.2.1), Tikhonov regularization (Section 5.2.2), sparse regression using MILP (Section 5.2.3), the continuous approximation of the discrete points by smoothing splines (Section 5.2.4), and response surface methodologies with additional constraints to enforce smoothness of the obtained profiles for model

approximation of discrete data from optimal design of experiments (Section 5.2.5), followed by differentiation of the resulting numerical solution, have been reported.

Although regularization techniques allow to obtain meaningful results even for ill-posed problems, the estimated derivatives are always biased and the bias introduced propagates to the following incremental steps of model identification. Hence, a common tradeoff in these approaches is the amount of bias introduced in the estimates of the derivatives produced (which is dependent on the particular technique used), versus the amount of regularization achieved. Different methods for choosing the regularization parameter are known, such as the discrepancy principle, the generalized discrepancy principle, the quasi-optimality criterion, the generalized cross validation, the L-curve criterion and the perturbation bound methods (Hansen, 1992).

### 5.2.1 Filter-based approaches

The filter-based approaches consist of an alternative to continuous curve approximation in order to smooth experimental data through its filtering. This allows the regularization of discrete profiles, approximating them to “quasi-continuous” profiles. This procedure can be coupled with the detection and removal of *outliers*, which could significantly influence the shape of the obtained curves. Some of these filtering methods can also be used to solve problems of lack of information corresponding to unmeasured values. The Savitzky-Golay methodology provides a filtering approach that consists of using local least squares regressions, considering a moving window that covers the entire horizon to be filtered (Savitzky and Golay, 1964). Similarly, the LoESS - *Local Regression* technique is a filtering method also based on a moving horizon, where it is possible to differentiate the weights of the various experimental points in the regression window. An important and significant advantage of these two filtering methods lies in the fact that these procedures allow not only the calculation of the “smoothed” values of the function, but also the direct calculation of their smoothed derivatives at the regression points.

Since these filtering methods use a fixed length regression window, a compromise between the *filtering capacity* and the *fidelity* to the original data appears in their application. In general, with the order of the regressor polynomial being fixed, the larger the size of the window used, *i.e.*, the more points are included in each regression, the greater the smoothness of the resulting curve, and the lesser the ability to approximate rapid variations in the model profile, which may result in loss of information relevant to the system under study. This difficulty can be overcome by using adaptive windows or nonlinear regressors, as is the case with *SuperSmoother* (Givens and Hoeting, 2012). The choice of adjustable parameters in the filtering methods (the degree of the regression polynomial and the dimension of the moving window), as well as the estimation of the uncertainties of the approximation is usually made through statistical methods of model validation such as, for example, cross-validation, preventing also the *overfitting* of the optimal parameters of the filtering model. In this case, cross-validation methods can be used, such as

leave-one-out, and  $k$ -fold, among others (Moore, 2006).

### 5.2.2 Tikhonov regularization

Alternatively to filter-based approaches, the ridge regression has been used for data regularization (Michalik et al., 2009). The ridge regression is a particular case of Tikhonov regularization method in which the regression coefficients are shrunk by imposing a penalty on their size (Hastie et al., 2013). The common objective function of that problem is

$$\min_{\boldsymbol{\beta}} \phi(\lambda) = (\mathbf{y} - \mathbf{X} \cdot \boldsymbol{\beta})^T (\mathbf{y} - \mathbf{X} \cdot \boldsymbol{\beta}) + \lambda \boldsymbol{\beta}^T \cdot \boldsymbol{\beta} \quad (5.1)$$

where  $\mathbf{y} \in \mathbb{R}^m$  is the vector of target values that is written as a linear combination the predictors  $\mathbf{x}_j \in \mathbb{R}^m$  for  $j = 1, \dots, n$  that compose the columns of the predictor matrix  $\mathbf{X} \in \mathbb{R}^{m \times n}$ , through the vector of coordinates  $\boldsymbol{\beta} \in \mathbb{R}^n$ , *i.e.*,  $\mathbf{X}$  maps  $\boldsymbol{\beta}$  to  $\mathbf{y}$ . The model parameters  $\boldsymbol{\beta}$ , or the regression coefficients, are tuned when minimizing  $\phi$  in (5.1), where besides the least squares term  $(\mathbf{y} - \mathbf{X} \cdot \boldsymbol{\beta})^T (\mathbf{y} - \mathbf{X} \cdot \boldsymbol{\beta})$  in the objective function, the  $\ell_2$ -norm of  $\boldsymbol{\beta}$  is minimized weighted by the positive regularization factor  $\lambda$ . In that case, the ridge regression solution is simply

$$\hat{\boldsymbol{\beta}} = (\mathbf{X}^T \cdot \mathbf{X} + \lambda \mathbf{I})^{-1} \cdot \mathbf{X}^T \cdot \mathbf{y} \quad (5.2)$$

where  $\mathbf{I}_n$  is the identity matrix with squared dimension  $n$ . In (5.2), it is observed that a positive constant  $\lambda$  is added to the diagonal of  $\mathbf{X}^T \cdot \mathbf{X}$  before inversion, turning the problem nonsingular (even if  $\mathbf{X}^T \cdot \mathbf{X}$  is singular). When considering the SVD of  $\mathbf{X}$ <sup>1</sup>, it is possible to write (after some simplification) the response vector  $\mathbf{X} \cdot \hat{\boldsymbol{\beta}}$  as

$$\begin{aligned} \mathbf{X} \cdot \hat{\boldsymbol{\beta}} &= \mathbf{U} \cdot \boldsymbol{\Sigma} \cdot (\boldsymbol{\Sigma}^2 + \lambda \mathbf{I})^{-1} \cdot \boldsymbol{\Sigma} \cdot \mathbf{U}^T \cdot \mathbf{y} \\ &= \sum_{j=1}^m \mathbf{u}_j \frac{\sigma_j^2}{\sigma_j^2 + \lambda} \mathbf{u}_j^T \cdot \mathbf{y} \end{aligned} \quad (5.3)$$

where  $\mathbf{u}_j$ ,  $j = 1, \dots, m$  are the columns of  $\mathbf{U}$ . Notice that like in the least squares procedure, the ridge regression computes the coordinates of the response variable  $\hat{\mathbf{y}}$  with respect to the complementary orthogonal subspaces concerning the column ( $\mathbf{u}_j$ ,  $j = 1, \dots, R$ ) and left null ( $\mathbf{u}_j$ ,  $j = R + 1, \dots, m$ ) spaces of  $\mathbf{X}$  in which  $R$  is the matrix rank of  $\mathbf{X}$  ( $R \leq n < m$ ), and those coordinates  $\frac{\sigma_j^2}{\sigma_j^2 + \lambda} \mathbf{u}_j^T \cdot \mathbf{y}$  for  $j = 1, \dots, m$  are being shrunk by the factor  $\frac{\sigma_j^2}{\sigma_j^2 + \lambda}$  since  $\lambda > 0$  and, consequently,  $\frac{\sigma_j^2}{\sigma_j^2 + \lambda} \leq 1$ . This means that the coordinates respected to smaller  $\sigma_j$  suffer a great amount of shrinkage, approximating the  $j$  model direction component to the null point (origin) of the linear space  $\mathbb{R}^m$ .

---

<sup>1</sup>For more information about SVD and the use of SVD to solve linear systems of equations, see Section 2.2.3 and Section 2.4.2, respectively.

Yeow et al. (2003) have proposed a regularization method to smooth concentration data supported on Tikhonov regularization. The proposed approach converts time-concentration data,  $c(t) = f(t)$ , into concentration-concentration change rate data,  $dc(t)/dt = f(c(t))$ , in which the concentration change rate is given by the first derivative of species concentration with respect to time. Using Tikhonov regularization, the minimization of both components: (i) the squared residues in concentration data regarding the difference of measured species and its model predicted counterpart and (ii) the second derivative estimate of the adjustable variable weighted by a regularization factor ( $\lambda$ ), is performed depending on that  $\lambda$  value that is set before the adjustment. The authors cite the Morosov Principle to choose a suitable value for  $\lambda$  parameter, in which the average and the maximum deviation among model prediction and experimental data must be comparable to the magnitude of data uncertainty while ensuring that the resulting reaction rate curve is sufficiently smooth, concluding that as long as  $\lambda$  is of the appropriate order of magnitude, small changes in that parameter (within this range) do not greatly affect the final results. The proposed method does not require information related to the kinetic expressions and the reaction network, *i.e.*, no structural information regarding the species interconnections must be known (or proposed) for the regularization procedure. After obtained the regularized and smoothed data, a greater understanding of the dynamics of the system could be acquired through the behavior of the concentration change rate profiles, thus allowing in a postpone phase a direct adjustment of kinetic parameters when comparing candidate rate expressions with the smoothed concentration change rates.

Whether through Tikhonov regularization or ridge regression, a large  $\lambda$  will give a smooth  $f(t)$  but at the expense of the goodness of fit of the kinetic data and vice versa. Moreover, as  $\lambda$  approximates zero, the problem becomes ill-conditioned, *i.e.*, the determinant of the design matrix tends to zero. Hence  $\lambda$  is responsible to introduce a sufficient amount that makes the design matrix better conditioned, increasing its smaller singular values. On the one hand, the Tikhonov regularization decreases the probability of modeling model components that, previously, could be unidentifiable (perhaps, noise contributions) which passed as insignificant when its coordinate is weighted by the  $\frac{\sigma_j^2}{\sigma_j^2 + \lambda}$  constant (as shown in (5.3)), but, from another point of view, this procedure increases the possibility of discarding low reaction extents that in practice are of the same magnitude of the measurement uncertainty, simultaneously ensuring enhanced numerical properties for the regression procedure.

### 5.2.3 Sparse regression using MILP

Recently, Willis and von Stosch (2017) proposed the use of MILP for performing sparse regression, where parameter regularization is considered using the entire set of candidate model variables and controlling model complexity, leading to an improved predictive performance since overparameterization is avoided. In this case the objective function is



given by

$$\min_{\beta} \phi(\lambda) = \|\mathbf{y} - \mathbf{X} \cdot \beta\|_1 + \lambda \|\beta\|_0 \quad (5.4)$$

where the  $\ell_1$ -norm of the residuals (model prediction error) plus the weighted/penalized  $\ell_0$ -norm of the variables vector are minimized. The regularization parameter  $\lambda$  may be determined using information criteria for model selection or cross-validation strategies. The authors transform (5.4) in a MILP formulation using auxiliary (continuous positive) variables to compute the absolute instantaneous residues and binary variables to compute the carnality of the active parameters in  $\beta$  vector. These binary variables are correlated with the respected  $\beta$  using Big-M constraints, such that they are set one when  $\beta$  is different of zero, and set zero otherwise, ensuring regression model sparsity.

Hence, this linear formulation considers the least absolute error as alternative to the least square error as considered by ridge and least squares regression for data parameterization, which is more robust towards outliers, *i.e.*, the  $\ell_1$ -norm is insensitive to outliers in the dataset. However, an improved MILP formulation is considered for increasing the smoothness of the formulation, turning the problem easier to solve by considering a slack variable  $z \in \mathbb{R}_0^+$  in the objective function. The  $\|\beta\|_0$  (given by the sum of binary variables) pass to be replaced by  $z$ , and an additional constraint

$$\|\beta\|_0 - z \leq 0 \quad (5.5)$$

is imposed, enabling the MILP to violate the constraint, if no alternative solution can be found thereby promoting a more efficient search. Notice that  $z = \|\beta\|_0$  when  $\phi$  is minimum.

In addition, the authors have shown that when considering a relaxation of the binary variables, enabling them to be continuous variables between  $[0,1]$  interval, the problem approaches to the least absolute shrinkage and selection operator (LASSO) regression, that is much easier to solve since it is solvable in polynomial time using linear programming rather than NP-hard optimization problem with the MILP formulation. In this case the LASSO is performed using  $\ell_1$ -norm regularization, where the parameter penalization term is given by the sum of absolute parameter estimates times the regularization factor, and the model approximation term is the total absolute model prediction error.

With the proposed computational approach, Willis and von Stosch (2017) showed that sparse regression/regularization using MILP can be efficiently and accurately solved for problems with significant input dimension ( $> 50$ ), presenting parsimonious model structures.

### 5.2.4 Smoothing splines

One of the most common ways of approximating continuous functions is to use approximation polynomials called *splines*. These polynomials are defined in finite subdomains of the

approximation domain, having different continuity properties at the ends of these intervals (called knots, or nodes). Since each of these polynomials is continuous and has continuous derivatives at all points in the subdomain where it is defined, and the continuity of these approximating functions (and their derivatives) is also ensured at the transition points, this approach seems to be naturally appropriate for the desired function.

In a generic scenario, the total time interval of a dataset is divided into  $n$  intervals  $[t_0, t_1], [t_1, t_2], \dots, [t_{n-1}, t_n]$ , in which  $S_i$  is the polynomial regarding the interval  $[t_i, t_{i+1}]$ . In this way,  $n$  polynomials will be obtained, from  $S_0$  to  $S_{n-1}$ . The polynomial  $S_{i-1}$  and  $S_i$  interpolate the same point  $t_i$ , so  $S_{i-1}(t_i) = S_i(t_i)$ , for every  $i = 1, \dots, n-1$ , making  $S$  continuous across the domain. Considering the use of cubic polynomials, in total it will, then, presents  $4n$  coefficients relative to each cubic element. In each sub-interval  $[t_i, t_{i+1}]$  there are two interpolation conditions:  $S_{i-1}(t_i) = S_i(t_i)$  and  $S_i(t_{i+1}) = S_{i+1}(t_{i+1})$ , accounting for a total of  $2n$  restrictions. The continuity in the 1st derivative is given between each extreme  $S'_{i-1}(t_i) = S'_i(t_i)$ , accounting for  $n-1$  conditions. The same occurs for the continuity restrictions in the 2nd derivative, accounting for more  $n-1$  conditions. Therefore, there are  $4n-2$  conditions to determine  $4n$  coefficients, resulting in two degrees of freedom in this interpolation approach of class  $C^2$  (with continuous derivatives up to the 2nd order) (Kincaid and Cheney, 1991). Some variations in these cubic spline interpolation formulations are also known. For example, the *natural spline* is characterized by fixing the 2nd derivative of the start point ( $t_0$ ) and the end point ( $t_n$ ) equal to zero, which means that the function becomes linear at the extremities of the considered horizon. Another variation consists of the use of *B-splines* (basis splines), where in each interval the resulting polynomial is a linear combination of basis splines of the same degree and smoothness, being stable numerically (de Boor, 2001).

Regardless of the chosen methodology, the approximation through the *spline* function can result in oscillatory curves within the intervals, even obeying all previous continuity restrictions. To solve this problem, it is usual to apply tension on the curves so that “the curve stretches”, removing these oscillations. This technique is called in the literature as *spline under tension*, in which it is intended to limit the variations of the 2nd derivative of the function.

de Boor (2001) also proposes the use of smoothing splines. This formulation is widely used in data processing, including statistical analysis, and can be found in data filtering formulations. Here a compromise is established between a very smooth curve, but eventually more distant from the experimental points, and a curve more faithful to the data, but with greater oscillations, through the minimization of the objective function

$$\min \phi(p) = p \sum_{k=1}^n \left( \frac{y_k - f(x_k)}{\delta_k} \right)^2 + (1-p) \int_0^{t_n} f''(x_k)(t)^2 dx, \quad (5.6)$$

where  $p \in [0,1]$  is a penalty term (smooth factor) that controls the amount of smoothing introduced,  $\delta_k, k = 1, \dots, n$  are weights ( $\delta_k^{-2}$ ) of each respective point  $y_k$ ,  $f(x_k)$  represents

the model predicted (smoothed) value of  $y_k$ . When  $y_k$  is a vector of concentrations (the most common situation), problem (5.6) is usually solved separately for each component in  $y$ , which means that the corresponding parameter  $p$  can also be selected separately for each concentration profile. When  $p \rightarrow 0$  the function converges to a straight line (maximum smoothing of the curve) at each interval, approaching a linear least squares formulation since no second derivative can be tolerated. When  $p \rightarrow 1$  the function converges to the interpolating spline (de Boor, 2001).

de Boor (2001) describes an algorithm to determine a suitable value for the penalty value. For this purpose a constant  $S$  is considered as an upper bound for the sum of square residues, such that

$$\sum_{k=1}^n \left( \frac{y_k - f(x_k)}{\delta_k} \right)^2 \leq S. \quad (5.7)$$

The algorithm starts with  $p = 0$  and increases  $p$  until the previous condition is met. The constant  $S$  is recommended to be chosen in the interval  $[n - \sqrt{2n}, n + \sqrt{2n}]$  when  $\delta_k$  is an estimation of the standard deviation for  $y_k$ . When  $S = 0$  the function is the natural spline. Increasing  $S$  the interpolating function becomes smoother, distancing from the original data. However, the choice of  $p$  can be made by other techniques, such as the generalized cross validation.

An important feature of this method is that if *natural* splines are considered, for  $p < 1$  an amount of bias is known to be present in the derivative estimates produced. This error tends to be larger at the extremes of the interpolating interval, since the second derivatives of the approximating functions are assumed to vanish there; consequently, the use of boundary corrected smoothing splines is preferred (Huang, 2001). However, the choice of  $p$  still influences the presence of bias in the estimates produced by this method, reviving the question of the choice of most appropriate regularization methods, among alternative approaches.

Notice that (5.6) establishes a combined function that lies in the Sobolev space. This space is defined for functions that present the computation of their  $\ell_2$ -norm (the least squares term) simultaneously with their derivatives up to a given order. In this case, the function (5.6) is defined on an infinite-dimensional Sobolev space. However, it is known that (5.6) has an explicit, finite-dimensional, unique minimizer which is a natural cubic spline with knots at the unique values of the  $x_i$ ,  $i = 1, \dots, n$  (Hastie et al., 2013). Since the solution is a natural spline, we can write it as

$$f(x) = \sum_{j=1}^n N_j(x)\theta_j \quad (5.8)$$

where  $N_j$ ,  $j = 1, \dots, n$  are basis functions that represent the piece-wise polynomials in the  $n$ -dimensional linear space establishing the set of natural splines. Hence, (5.6) can be

written as

$$\min_{\boldsymbol{\theta}} \phi(\lambda) = (\mathbf{y} - \mathbf{N} \cdot \boldsymbol{\theta})^T (\mathbf{y} - \mathbf{N} \cdot \boldsymbol{\theta}) + \lambda \boldsymbol{\theta}^T \cdot \boldsymbol{\Omega}_{\mathbf{N}} \cdot \boldsymbol{\theta} \quad (5.9)$$

where  $\mathbf{y} \in \mathbb{R}^n$  is the response variable,  $\mathbf{N}$  is a square matrix<sup>2</sup> with  $\{\mathbf{N}\}_{i,j} = N_j(x_i)$  for  $j = 1, \dots, n$  basis components and  $i = 1, \dots, n$  spline knots,  $\boldsymbol{\Omega}_{\mathbf{N}}$  is a square matrix of dimension  $n$  with integrated squares of second derivatives, *i.e.*,  $\{\boldsymbol{\Omega}\}_{i,j} = \int N_i''(t)N_j''(t) dt$ ,  $\boldsymbol{\theta} \in \mathbb{R}^n$  is the vector of parameters (polynomial coefficients) that are tuned in this minimization procedure, and  $\lambda \in (0, \infty)$  is a fixed smoothing parameter. Similarly as the  $p$  parameter in (5.6), the  $\lambda$  establishes a tradeoff between the closeness of the function to the data and the function curvature. Hence, when  $\lambda = 0$ ,  $\hat{\mathbf{y}}$  is a function that interpolates data, and, when  $\lambda = \infty$ , the problem consists of a simple least squares line fit. The optimal parameters values are easily calculated through

$$\begin{aligned} \hat{\boldsymbol{\theta}} &= (\mathbf{N}^T \cdot \mathbf{N} + \lambda \boldsymbol{\Omega})^{-1} \cdot \mathbf{N}^T \cdot \mathbf{y} \\ &= \mathbf{S}_{\lambda} \cdot \mathbf{y} \end{aligned} \quad (5.10)$$

for which the predicted response

$$\hat{\mathbf{y}} = \mathbf{N} \cdot \hat{\boldsymbol{\theta}} \quad (5.11)$$

is obtained.

Like in the ridge regression data regularization method, the smoothing splines method *shrinks* basis vectors in order to obtain more well-posed data behavior by the price of introducing bias in the model. If we consider the eigen-decomposition of  $\mathbf{S}_{\lambda}$  (which is a positive semidefinite matrix) such as

$$\mathbf{S}_{\lambda} = \sum_{j=1}^n \sigma_j^2(\lambda) \mathbf{u}_j \cdot \mathbf{u}_j^T, \quad (5.12)$$

where  $\mathbf{u}_j$  and  $\sigma_j^2(\lambda)$  for  $j = 1, \dots, n$  are eigenvectors and eigenvalues of  $\mathbf{S}_{\lambda}$ , and

$$\sigma_j^2(\lambda) = \frac{1}{1 + \lambda \sigma_j^2} \quad (5.13)$$

with  $\sigma_j^2$  the corresponding eigenvalue of the  $\mathbf{K}$  matrix obtained from the *Reinsch* format of  $\mathbf{S}_{\lambda}$  such that

$$\mathbf{S}_{\lambda} = (\mathbf{I} - \lambda \mathbf{K})^{-1} \quad (5.14)$$

where  $\mathbf{K}$  does not depend on  $\lambda$  (but only of  $x$  data), it is possible to assess how the smoothing procedure works.

Therefore the smoothing spline fitted values are a linear combination of the basis vectors

---

<sup>2</sup>We opted to maintain the literature nomenclature for that matrix, but please do not confound with the stoichiometric matrix. In this chapter  $\mathbf{N}$  is referred to a set of basis of natural splines.

$\mathbf{u}_j$  written with weighted coordinates, such that

$$\hat{\mathbf{y}} = \sum_j^n \frac{\mathbf{u}_j^T \cdot \mathbf{y}}{1 + \lambda \sigma_j^2} \mathbf{u}_j = \frac{\mathbf{u}_1^T \cdot \mathbf{y}}{1 + \lambda \sigma_1^2} \mathbf{u}_1 + \frac{\mathbf{u}_2^T \cdot \mathbf{y}}{1 + \lambda \sigma_2^2} \mathbf{u}_2 + \dots + \frac{\mathbf{u}_n^T \cdot \mathbf{y}}{1 + \lambda \sigma_n^2} \mathbf{u}_n. \quad (5.15)$$

Notice that the coordinates of  $\hat{\mathbf{y}}$  in the basis  $\mathbf{U}$  are given by the the inner product of the respective basis vector  $\mathbf{u}_j$  with the experimental data  $\mathbf{y}$  vector weighted by  $\sigma_j^2(\lambda)$ . Hence, the higher the complexity of the basis component  $\mathbf{u}_j$  the more it is shrunk (Hastie et al., 2013), *i.e.*, for model components in which the variances (eigenvalues) are greater, after the smoothing procedure their respective coordinates are approximated to the origin with greater magnitude than for model components with lower variances, since the  $\sigma_j^2(\lambda)$  is lower for  $j$  components with greater  $\sigma_j^2$ .

Moreover, the sum of diagonal elements of  $\mathbf{S}_\lambda$

$$\text{df}_\lambda = \text{trace}(\mathbf{S}_\lambda) = \sum_j^n \sigma_j^2(\lambda) \quad (5.16)$$

is defined as the *effective degrees of freedom* (Hastie et al., 2013). These authors propose an inverse method for determining the smoothing parameter  $\lambda$  by fixing  $\text{df}_\lambda$  and solving numerically  $\text{df}_\lambda = \text{trace}(\mathbf{S}_\lambda)$ . Consequently, several values of  $\text{df}_\lambda$  can be tested and the criterion established through the Fisher ratio of variances can be used (*F*-test) in order to select a good value for lambda with greater confidence. The *F*-test is presented in more detail in the next chapter under a different context: for determining the dimension of the data space. However, since (in this work) the smoothing splines is not the adopted data regularization technique, the methodologies for selecting a good  $\lambda$  value were not explored, although cross-validation is one of them, which is also explored in the next chapter under the context of determining the dimension of the data space, by evaluating the cross validation prediction error for a set of excluded data (test dataset).

### 5.2.5 Dynamic Response Surface Methodology with additional constraints

In the context of data-driven modeling methodologies, the Dynamic Response Surface Methodology (DRSM) has been used as a regularization method for time-resolved measurements from Design of Experiments (DoE) datasets (Santos-Marques et al., 2019; Dong et al., 2019a,b). The original datasets consist of simulated species concentration measurements (corrupted with noise) at three different experimental temperature and several initial conditions, concerning to a pharmaceutical case study. The objective of these works is to, from DRSM data, increase the model identifiability.

The approximating function (5.17) consists of a quadratic model (linear in their parameters), where the dependent (response) variable  $y(\tau)$  is estimated as a function of (i) the

input factors  $x_i, i = 1, \dots, n$  in a DoE design, and (ii) parametric functions  $\beta_q, q = i, ij, ii$ , for  $i = 1, \dots, n$  and  $j = 1, \dots, i - 1$ , described by a linear combination of shifted Legendre polynomials  $P_{r-1}$  of several orders, *i.e.*,  $r = 1, \dots, R$ , as shown in (5.18).

$$y(\tau) = \beta_0(\tau) + \sum_{i=1}^n \beta_i(\tau)x_i + \sum_{i=1}^n \sum_{j=i+1}^n \beta_{i,j}(\tau)x_i x_j + \sum_{i=1}^n \beta_{i,i}(\tau)x_i^2 \quad (5.17)$$

$$\beta_q(\tau) = \sum_{r=1}^R \gamma_{q,r} P_{r-1}(\tau) \quad (5.18)$$

In order to prevent overparametrization, the authors have determined the number of polynomials ( $R$ ) using the Lack-of-Fit (LoF) statistic, where the model with lowest  $R$  value is selected with acceptable LoF (Santos-Marques et al., 2019); or using the Bayesian information criterion (BIC), where the model selected is the one that presents lowest BIC value (Dong et al., 2019a,b). Also, in both works, the coefficients  $\gamma_{q,r}$  that multiply each Legendre polynomial were estimated (and analyzed) using stepwise regression and ANOVA methods in order to assess their significance, thus removing the ones that are insignificant from the model.

Dong et al. (2019a) proposed an enhanced DRSM approach using an exponential transformation of time to a new independent variable  $\theta$ , as shown in (5.19), where a time constant  $t_c$  is determined (simultaneously with the  $R$  value) using BIC, characterizing the slowest dynamics of the process.

$$\theta = 1 - \exp(t/t_c) \quad (5.19)$$

The transformation of time in (5.19) enabled the obtainment of smoother profiles, reducing the undesired oscillatory behaviors that the original DRSM (Santos-Marques et al., 2019) presented in the concentration profiles of many chemical species, in their first derivative profiles, and, consequently, at the computed reaction rate profiles after proposing a reaction network. Moreover, simultaneously with (5.19), Dong et al. (2019a) proposed the use of additional constraints to obtain physically meaningful results, concerning (i) constraints at initial time, forcing the model species concentration to be exactly the same value known from the DoE design, (ii) imposition of positiveness of the first derivative for concentration profiles that start at zero value, ensuring an increasing profile behavior, and (iii) imposition of non-negative DRSM output, ensuring positive predicted species concentration values.

During the application of DRSM, each species profile is adjusted individually and, therefore, the same procedures described above (parameter tuning, model analyzes and use of additional constraints) must be repeated for every species, requiring, on the down side, a high computational effort and time spent for the obtainment of regularized data, especially if there are many chemical species in the reaction system. Also, no concern related to the identification of time-invariant characteristics of the reaction system and their incorporation in the DPP method was presented in these works, in order to increase

the accuracy of the model and, therefore, to enhance its identifiability. Nevertheless, the authors have shown that DRSM enhances the model identifiability from regularized data, even with noise measurements.

### 5.2.6 Comparative analysis of regularization methods

Table 5.1 presents a comparison of the previously discussed data regularization methods. All these methods enable an easy calculation of time-derivatives of the approximated function. The five methods consider the individual approximation of a single response variable, although an adaptation of these methods can be considered for the simultaneous adjustment of several response profiles. In that case, time-invariant constraints should be incorporated in the respected formulation, concerning simultaneous profile adjustments to reconcile data, increasing the accuracy of obtained results.

**Table 5.1** Comparison of previously discussed data regularization methods for incremental identification of chemical reaction models.

Method	Type of approximation	Outliers sensitivity	Critical parameters and key aspects that introduce bias/smooth
Filter-based*	Quasi-continuous	High	Dimension of the moving window and degree of the regression polynomial.
Tikhonov	Continuous	Low	Regularization parameter that penalizes the square $\ell_2$ -norm of parameters vector.
MILP sparse regression	Continuous	Insensitive	Regularization parameter that penalizes the $\ell_0$ -norm of active parameters vector (sum of binary variables).
Smoothing splines	Continuous	Medium	Regularization parameter that penalizes the curvature of the approximating function ( $\approx$ the 2nd time-derivative).
DRSM	Continuous	Medium	Degree of regression polynomial and time constant.

\*Filter-based methods such as Savitzky-Golay and LoESS.

The next section addresses the data regularization method proposed in this work. This approach considers

- continuous approximation of data through base cubic polynomials,

- inclusion of qualitative constraints for modeling trends of profiles (avoiding undesired oscillatory behaviors, *i.e.*, introducing bias to the solution),
- the use of time-invariant constraints for the obtainment of reconciled data with greater accuracy.

The proposed method has proven to present (i) a stable formulation as orthogonal polynomials are used, (ii) ease of implementation, without the need of cross-validators for determining regularization factors; in this case, the shape constraints are iteratively and interactively inserted in the formulation (like in a “puzzle problem”) until the pretended smooth degree is obtained, (iii) an increased ability to identify the model structure from species fluxes estimated with high precision as time-invariant relationships are imposed between species profiles.

### 5.3 Continuous approximation of concentration data

*“Never trust an experiment that is not supported by a good theory.”*

– Jacques Monod

Besides the use of smoothing splines, alternative approximation techniques have also been applied in the solution and optimization of differential-algebraic process models. In particular, orthogonal collocation, has been widely used in the solution of reaction models (Finlayson, 1975). Due to its efficiency and versatility, orthogonal collocation on finite elements has also been proposed for the parametrization of general differential algebraic optimization problems. An important advantage of this approximation method is the existence of strategies for the adaptation of the lengths (and placement) of the elements, resulting in a high-order approximation with relatively few elements (Biegler, 2010). Unseemly related applications, for the qualitative modeling of physical systems and the description of the trends and main features of the process responses observed, have also been developed in the literature (Cheung and Stephanopoulos, 1990; Schaich et al., 2001). These techniques seek to extract a high-level description of the observed behavior, translatable into a group of constraints that can be used to help the posterior identification of quantitative kinetic models (Madár et al., 2003; Villez et al., 2013). The selected combination of features from both contributions, simultaneously with the incorporation of time-invariant constraints, provide an alternative regularization methodology for the estimation of the concentration derivatives, described in this section.

Alternatively, it was tested with the case studies considered the possibility of obtaining concentration derivatives estimates by applying data regularization methods, such as the filter-based approaches described in Section 5.2.1 and smoothing splines in Section 5.2.4. In particular, Savitzky-Golay filtering approaches and the LoESS technique were tested first. The results obtained showed that, although the quality of the estimates improved



significantly compared to the possible results through the application of finite differences, there was still some “noise” in the estimates produced, with a negative impact on the possible conclusions. In view of the results of these tests, we opted instead to use a technique of smooth continuous approximation of the experimental profiles, which would allow to obtain derivatives with less oscillations. In this case, an adaptation of the original smoothing splines formulation was considered by imposing invariant constraints in the simultaneous fit of every species profile, although each one with its regularization parameter. However, the results obtained by the use of smoothing splines were unsatisfactory since the species profiles presented undesired oscillations even with great penalization of the curvature function.

### 5.3.1 Orthogonal Collocation on Finite Elements

Orthogonal collocation can be described as a variant of the weighted residual method, where polynomials are used to approximate a continuous function, at particularly chosen (collocation) data points (Finlayson, 1972). Besides the use of B-splines (Poyton et al., 2006), other equivalent forms of representing the approximating polynomials are possible; a typical choice is to apply the Lagrange polynomial interpolation method to each finite element (Finlayson, 1975; Biegler, 2010), and for convenience, the Lagrange interpolation form is used here. The interpolating stability of the Lagrange form is known based on the roots of Legendre’s orthogonal polynomials (Trefethen, 2013). Considering the use of cubic polynomials, approximations are formed by a linear combination of 4 cubic polynomials orthogonal to each other, which constitute the generator set of the interpolator polynomial in the  $\mathcal{P}_3(\mathbb{R})$  space, of dimension 4.

The chosen collocation points generally coincide with the location of the roots of orthogonal polynomials. Using cubic polynomials, the number of collocation points totals  $3n + 1$ , where  $n$  is the number of finite elements. In this case, there are 2 internal roots in each interval (finite element), and the remain ones coincide with the ends of these intervals. The Figure 5.1 illustrates the location of the roots of orthogonal polynomials of Legendre, used in this work, normalized to the  $x \in [0,1]$  interval. As it can be seen in this figure, at each collocation point, only one of the interpolating polynomials does not cancel out.

### 5.3.2 Step 1 formulation

For the considered case, it is necessary to construct interpolating polynomials  $P_{s,i}(t)$  to describe the time profiles of concentrations of the species, with the index  $s \in \mathbf{sp}$  referring to the chemical species considered ( $s = 1, \dots, n_{\mathbf{sp}}$ ) in the set  $\mathbf{sp}$ , and  $i \in \mathbf{fe}$  relative to the approximating interval ( $i = 1, \dots, n_{\mathbf{fe}}$ ) of the finite elements set  $\mathbf{fe}$ . Using Lagrange’s interpolating form, these approximations can be written as

$$P_{s,i}(x) = \sum_{j \in \mathbf{cp}} a_{s,i,j} l_j(x), \quad \forall s \in \mathbf{sp}; \forall i \in \mathbf{fe} \quad (5.20)$$

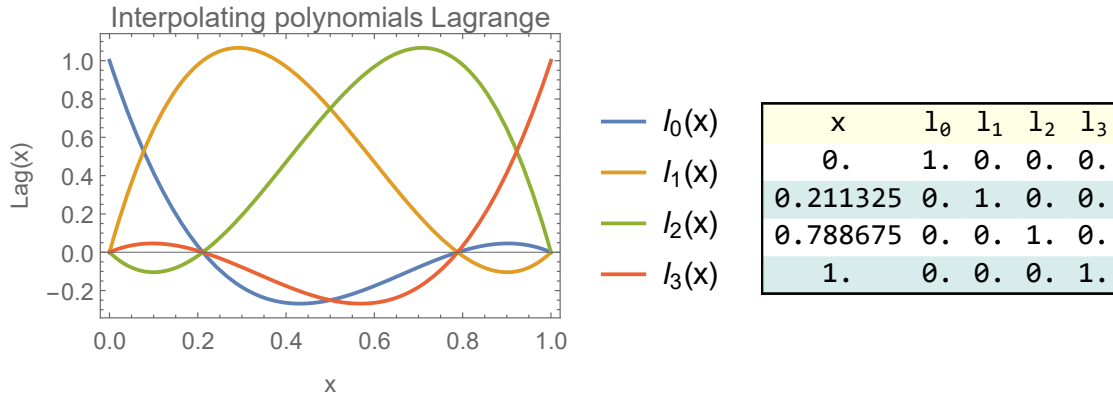


**Figure 5.1** Profiles behavior of the orthogonal polynomials on the left-hand side, and associated roots on the right-hand side.

where  $\mathbf{cp}$  is the set of collocation points in each element, ( $j = 0, 1, 2$  and  $3$ ) including the boundaries,  $x \in [0, 1]$  is the normalized independent coordinate,  $a_{s,i,j}$  is the coefficient to be determined (variable of the problem) and  $l_j(x)$  is the Lagrange interpolating polynomial. Notice that the polynomials  $P_{s,i}(x)$  are being constructed as linear combinations of the respective  $l_j(x)$ . The Lagrange polynomials can be written as

$$l_j(x) = \frac{\prod_{\substack{k=0 \\ k \neq j}}^{n_k} (x - x_k)}{\prod_{\substack{k=0 \\ k \neq j}}^{n_k} (x_j - x_k)}, \quad \forall j \in \mathbf{cp} \quad (5.21)$$

with, in this case,  $n_k = 3$ .

Therefore, cubic polynomials with two interior collocation points inside each element are assumed. The normalized coordinate  $0 \leq x \leq 1$  is defined for each element to locate the collocation points at specific values, corresponding to the normalized roots of orthogonal Legendre polynomials, independently of the lengths of each element. With these definitions, we note that in this initial phase of the incremental model identification where the concentration derivatives are estimated, the model (2.7) is still not known, and only constraints that concern about the system time-invariant relationships can be considered, as shown in eqs. (2.36) and (2.38).

Using the approximation in (5.20) it is possible to consider the determination of the necessary coefficients  $a_{s,i,j}$  by solving an optimization problem

$$\min_{a_{s,i,j}} \phi = \sum_{m \in \mathbf{me}} \sum_{s \in \mathbf{sp}} w_s (c_{s,m} - \hat{c}_{s,m})^2 \quad (5.22)$$

where the quadratic objective function minimizes the total weighted square error in concentration data, where  $\hat{c}_{s,m}$  represents the predicted response (concentration) of species  $s \in \mathbf{sp}$  at the sampling time  $t_m$ , with  $m \in \mathbf{me}$ , the set of measurement instants,  $c_{s,m}$

its experimentally observed counterpart, and  $w_s$  the respective weight of that species in the adjustment procedure. However, no preferences of adjustments among the measured species were considered in the following case studies, *i. e.*,  $w_s = 1, \forall s \in \mathbf{sp}$ . In cases where outliers are presented, at specific instants  $t_m$  the model can not evaluate the function by setting that  $w_{s,m}$  to zero.

The concentrations predicted by the model for each species  $s \in \mathbf{sp}$  use the set of approximations  $P_{s,i}(x)$  defined above, as interpolating functions ( $f_{\text{int}}$ ) in domain  $t$ :

$$\hat{c}_{s,m} = f_{\text{int}}(t_m; \{P_{s,i}(x)\}), \quad \forall s \in \mathbf{sp}; \forall m \in \mathbf{me} \quad (5.23)$$

In the internal collocation points, it is necessary to check exactly the time-invariant restrictions, which in the previous case can be written as

$$\mathbf{A} \cdot \hat{\mathbf{c}}_{j,i} = \mathbf{b}_{\text{in}} \quad \text{or} \quad \mathbf{A} \cdot \hat{\mathbf{c}}'_{j,i} = \mathbf{0}, \quad j = 1,2; \quad \forall i \in \mathbf{fe}, \quad (5.24)$$

where  $\mathbf{A} \in \mathbb{N}^{\text{ni}_{\text{li}}} \times n_{\text{sp}}$  is the matrix of invariant relationships,  $\hat{\mathbf{c}}_{j,i} \in \mathbb{R}^{n_{\text{sp}}}$  is the predicted concentration vector evaluated at the internal collocation points ( $j = 1,2$ ) of every finite element  $i \in \mathbf{fe}$  and  $\mathbf{b}_{\text{in}} \in \mathbb{N}^{\text{ni}_{\text{li}}}$  the vector of conserved amounts. Notice that this same equation can be written in terms of compositional changes (right side of (5.24)), where  $\hat{\mathbf{c}}'_{j,i}$  is the vector of instantaneous concentration derivatives of the corresponding  $\hat{\mathbf{c}}_{j,i}$  vector, that lies in the null space of  $\mathbf{A}$ .

At the ends of the intervals, continuity restrictions are imposed on the approximation functions and their derivatives:

$$P_{s,i}(1) = P_{s,i+1}(0), \quad (5.25a)$$

$$P'_{s,i}(1) = P'_{s,i+1}(0), \quad (5.25b)$$

$$P''_{s,i}(1) = P''_{s,i+1}(0), \quad \forall s \in \mathbf{sp}; i = 1, \dots, n_{\text{fe}} - 1 \quad (5.25c)$$

As in the case of splines, the approximation through orthogonal collocation on finite elements can produce solutions with more oscillation than desired. This behavior can be avoided by converting the objective function (5.22) to the form (5.6), and setting the parameter  $p$  carefully. Alternatively, restrictions can be imposed directly on the signals and relative magnitudes of the derivatives of the approximating functions<sup>3</sup>. For example, the signs of variations in concentrations can be restricted to always be positive in certain finite elements (or collocation points) where a species is produced in net terms, and negative when it is consumed in net terms:

$$P'_{s,i}(x_r) \leq 0 \quad \vee \quad P'_{s,i}(x_r) \geq 0, \quad \forall i \in \mathbf{fe}^*; r = 0,1,2; s \in \mathbf{c}^* \quad (5.26)$$

In these equations the quantities  $x_r$  correspond to the abscissa of the collocation points

<sup>3</sup>As it is more directly applicable, this was the approach used with the case studies considered.

(normalized), and  $\mathbf{c}^*$  designates the group of species to which these restrictions are applied. It is also useful to impose monotonicity restrictions on concentration changes along finite elements, ensuring that profiles in certain areas have monotonous variations (increasing or decreasing), depending on the (net) production or (net) consumption of this species:

$$P'_{s,i}(x_r) \leq P'_{s,i}(x_{r+1}) \quad \vee \quad P'_{s,i}(x_r) \geq P'_{s,i}(x_{r+1}), \quad \forall i \in \mathbf{fe}^*; r = 0,1,2; s \in \mathbf{c}^* \quad (5.27)$$

Similarly for the 2nd and 3rd derivatives:

$$P''_{s,i}(x_r) \leq P''_{s,i}(x_{r+1}) \quad \vee \quad P''_{s,i}(x_r) \geq P''_{s,i}(x_{r+1}), \quad \forall i \in \mathbf{fe}^*; r = 0,1,2; s \in \mathbf{c}^* \quad (5.28)$$

$$P'''_{s,i} \leq P'''_{s,i+1} \quad \vee \quad P'''_{s,i} \geq P'''_{s,i+1}, \quad i = 1, \dots, \mathbf{fe} - 1 \cap \mathbf{fe}^*; s \in \mathbf{c}^* \quad (5.29)$$

These constraints are also linear in the decision variables  $a_{s,i,j}$ , due to the form of the interpolating polynomial (5.20), and can be enforced at all collocation points. Hence the application of this methodology does not require the choice of a particular value of a smoothing parameter and, because it is entirely based on the incorporation of additional observed features in the solution, it has the potential to provide better estimates of its derivatives.

The complete mathematical formulation for the continuous approximation of data by orthogonal collocation can be written as:

$$\min_{a_{s,i,j}} \phi \quad (5.30a)$$

$$\text{s.t. Equations (5.20—5.29)} \quad (5.30b)$$

$$\hat{c}_{s,j,i} \geq 0, \quad \forall s \in \mathbf{sp}, j \in \mathbf{cp}, i \in \mathbf{fe}. \quad (5.30c)$$

This formulation corresponds to a quadratic optimization problem with linear constraints (QP). It should be noted that in this formulation, the residuals of the objective function (5.22) are calculated at the experimental points, using the interpolating polynomials (5.23), with the remaining restrictions being imposed on the considered collocation points.

Note that only one approximation problem is constructed to simultaneously approximate the concentration of all species in the system. Also, and contrarily to the regularization approaches previously described, the presence of the system of equations (5.24) in the QP forces the estimates to be automatically reconciled with the conservation constraints identified *a priori* for the particular chemical system, such as the overall or the elemental mass balances. These constitute significant advantages over the use of other independent and purely numeric smoothing techniques.

The restrictions corresponding to the eqs. (5.26) to (5.29) are incrementally added to the adjustment problem by the modeler, through a qualitative analysis of the trends observed

in the experimental data, and in the eventual need to eliminate oscillations in the profiles, which can vary from case by case, *i.e.*, this procedure cannot be generalized. In general, the first solution of the formulation (5.30) involves only the use of a reduced set of equations of this type, due to its possible interaction with the usual procedures of length adaptation of finite elements for equidistribution of the approximation errors, which must be avoided. Consequently, the continuous profiles will tend to exhibit various oscillations, and the solution will try to interpolate the available data. In a second iteration, after the convergence of the location of the ends of the elements, it is possible to add additional restrictions of the type (5.26—5.29), to eliminate the existence of any oscillations observed in the profiles, although with a reduced impact on the quality of the adjustment produced. These can be intuited from the simple inspection of the approximated profiles, and added interactively to the problem, which needs to be subsequently resolved. In alternative, the qualitative modeling approaches described earlier can also be used to derive the corresponding constraints (Schaich et al., 2001; Villez et al., 2013).

### 5.3.3 Step 1 flowchart

The flowchart of this first step of the proposed methodology is presented in Figure 5.2. Next section addresses the application of the proposed method.

### 5.3.4 Application example

The catalytic hydrogenation of succinic acid (previously presented in Section 1.5), is taken as an illustrative example. Prior assumptions relative to the nature of the reactions in this system indicate that the sum of the concentrations of the C<sub>4</sub> and C<sub>3</sub> should be conserved, establishing the invariant relationship discussed in Section 2.3, presented in Figure 2.20.

The application of the proposed data reconciliation method for this case study is challenging since there is appreciable error in the overall mass balance closure in the original experimental concentration data. This fact may significantly influence the conclusions obtained, since in some regions the amplitude of this uncertainty overlaps with the concentrations registered for some species<sup>4</sup>. Also, the original dataset presents irregular structure since not all species were measured at the same time instants, presenting some species more data than others. In Figure 5.3 the experimental data reported by Deshpande et al. (2002) is plotted in the discrete points, the dashed curves are linear interpolation of the dots used to calculate the error of moles.

The time horizon was divided in ten finite elements with several lengths. Shorter elements are required when greater second derivatives of concentration profiles are occurring, in order to better describe the observed oscillations of the concentration profiles. Since the

---

<sup>4</sup>For example, the THF species shows a slight decrease in the last 2 experimental points registered in Figure 5.3. Given the enormous value of the error in closing the global mass balance in this region, there may be a doubt about whether to classify this species as *terminal* (monotonously increasing concentration) or not.

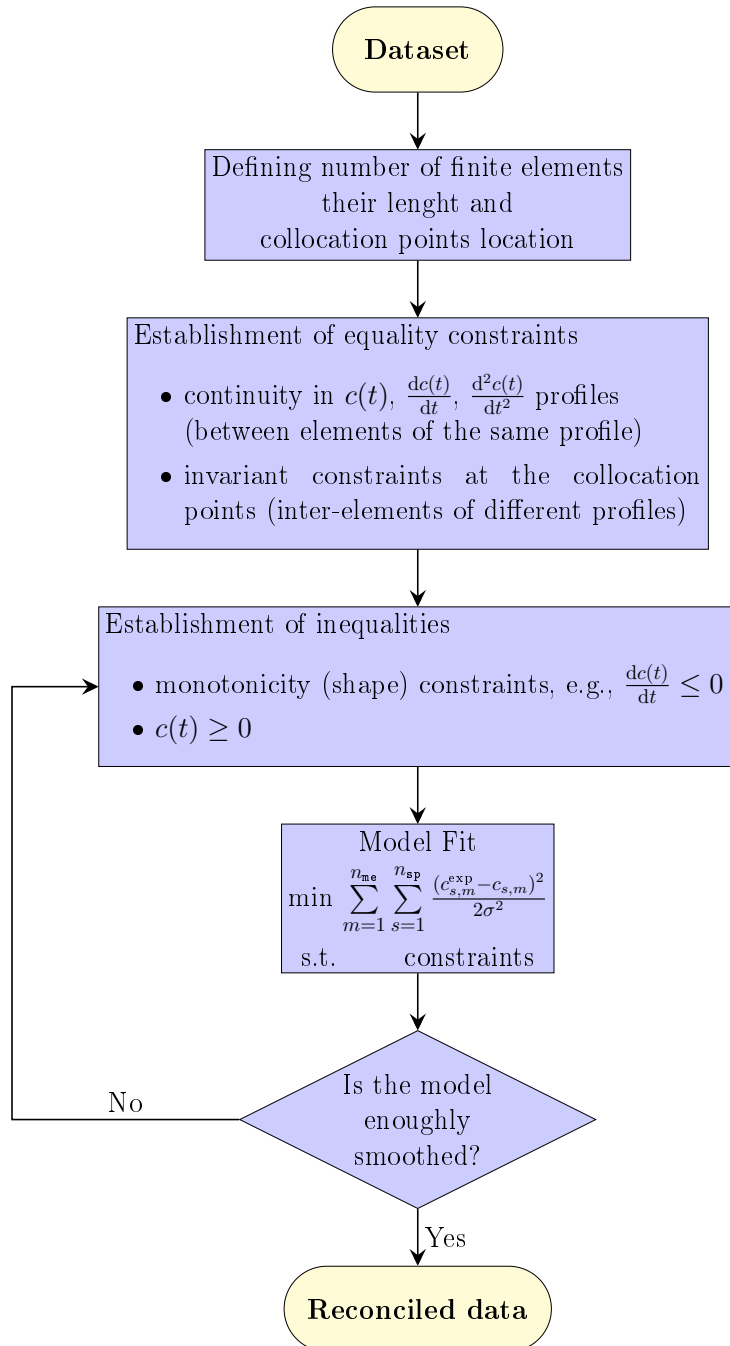


**Figure 5.2** Step 1 flowchart. Schematic overview of the proposed method for data reconciliation supported on orthogonal collocation on finite elements.

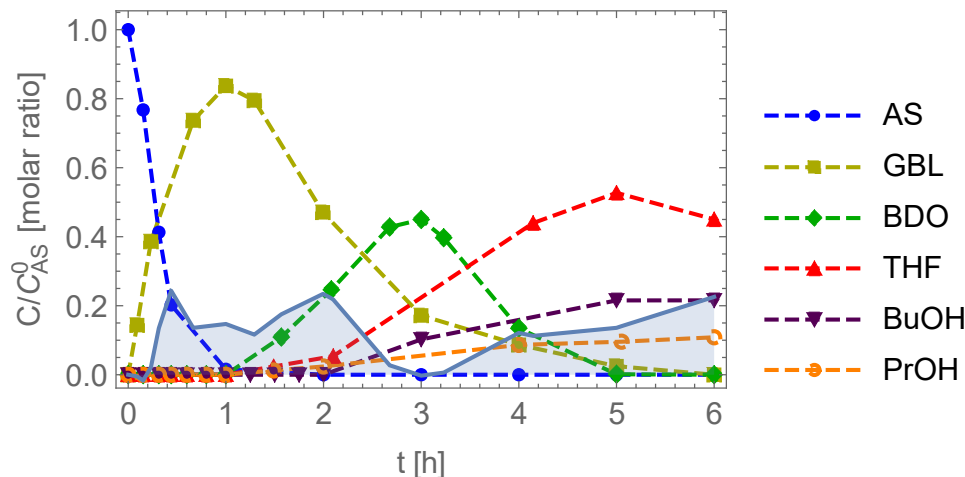


**Figure 5.3** Concentration data for the succinic acid system. The shadowed profile represents the overall mass error.

size of each element is common for every species profile, this criterion must be established accounting a kind of mean curvature. Moreover, the mass conservation relationship was imposed at the collocation points in every finite element, establishing that the amount of moles given by  $AS + GBL + BDO + THF + BuOH + PrOH$  is unchanged.

In this example, each polynomial also has 4 coefficients to be determined, using 10 finite elements; in this case, 240 optimization variables are required since 6 species profiles are adjusted. Equality restrictions total 191 equations (that is, there are a maximum of 49 degrees of freedom in the problem), 593 inequality restrictions were considered. The problem was solved in the **Mathematica**® 12.0, using the function `FindMinimum`. Despite the great uncertainty presented in the original data, the smoothing procedure produced very reasonable results, as can be seen in Figure 5.4. Notice that great disagreements among experimental data and model profiles occur at the zones in which significant mass error are verified. Therefore, due to the equal weighting factors used, in the regions where there is more error, the larger errors observed tend to be equidistributed between the present species, except when the qualitative constraints used in the respective or contiguous elements disallow this behavior.

Additional constraints were required in order to avoid oscillatory profiles behavior; these constraints are related to the qualitative analysis of each individual profile. For example, the first derivative of AS derivative is always negative and increases monotonically; the first derivative of GBL is positive until the end of the third element and negative from the fifth element; and the first derivative of BDO is positive until the end of the third element and increases monotonically until the end of the fourth element, etc. Figure 5.5 presents the individual species profiles with their first and second concentration derivatives.

The same smoothing problem, but without imposing shape constraints, was considered in order illustrate the need of those inequalities during data regularization. The obtained

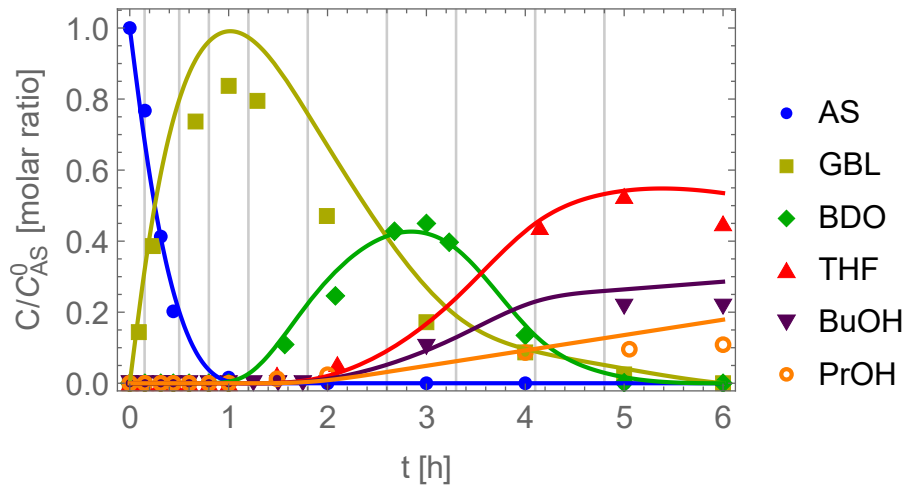


**Figure 5.4** Concentration profiles for the succinic acid system. Vertical lines present the size of the finite elements.

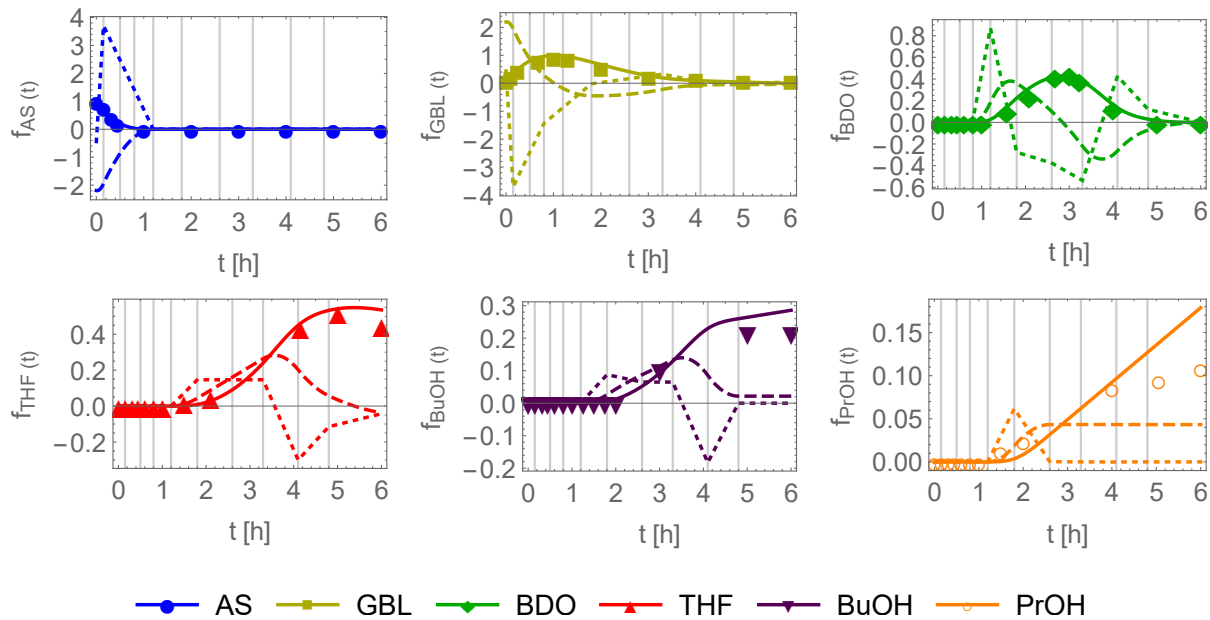


**Figure 5.5** Individual concentration profiles, including their first (dashed profiles) and second (dotted profiles) derivatives for the succinic acid system.

profiles are presented in Figure 5.6. Observe that better agreement of data-model is verified, although presenting undesired oscillatory behaviors. However, the constraints related to the non-negative responses were imposed at the collocation points (unless for AS species after four hours of reaction), simultaneously with the invariant relationship.

The proposed data regularization method based on orthogonal collocation on finite elements enabled the obtainment of smoothed reconciled  $c(t)$  profiles, simultaneously with the achievement of good estimates of smoothed concentration derivatives that will support



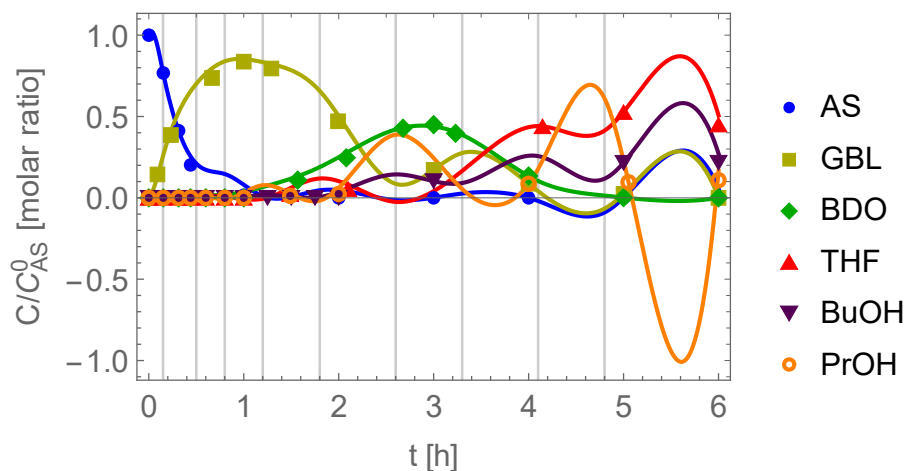


**Figure 5.6** Concentration profiles for the succinic acid system without considering qualitative (shape) constraints.

all the model identification tasks at the next phases. The species first derivative profiles are shown in Figure 5.7.

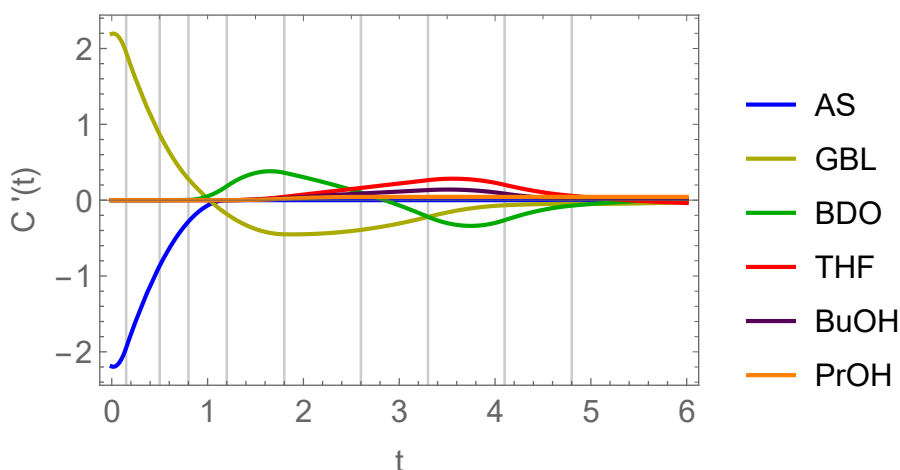


**Figure 5.7** First derivative of species concentration profiles for the succinic acid system.

## Bibliography

- Biegler, L. (2010). *Nonlinear Programming: Concepts, Algorithms, and Applications to Chemical Processes*. Society for Industrial and Applied Mathematics, Philadelphia, PA.
- Cheung, J.-Y. and Stephanopoulos, G. (1990). Representation of process trends — Part I. A formal representation framework. *Computers & Chemical Engineering*, 14(4–5):495–510.
- de Boor, C. (2001). *A Practical Guide to Splines*. Applied Mathematical Sciences. Springer New York.

- Deshpande, R., Buwa, V., Rode, C., Chaudhari, R., and Mills, P. (2002). Tailoring of activity and selectivity using bimetallic catalyst in hydrogenation of succinic acid. *Catalysis Communications*, 3(7):269–274.
- Dong, Y., Georgakis, C., Mustakis, J., Hawkins, J. M., Han, L., Wang, K., McMullen, J. P., Grosser, S. T., and Stone, K. (2019a). Constrained version of the dynamic response surface methodology for modeling pharmaceutical reactions. *Industrial & Engineering Chemistry Research*, 58(30):13611–13621.
- Dong, Y., Georgakis, C., Mustakis, J., Hawkins, J. M., Han, L., Wang, K., McMullen, J. P., Grosser, S. T., and Stone, K. (2019b). Stoichiometry identification of pharmaceutical reactions using the constrained dynamic response surface methodology. *AIChE Journal*, 65(11):e16726.
- Finlayson, B. (1972). *The Method of Weighted Residuals and Variational Principles*. Academic Press, New York, NY.
- Finlayson, B. (1975). *Orthogonal Collocation in Chemical Reaction Engineering*. Marcel Dekker, Inc., New York, NY.
- Givens, G. and Hoeting, J. (2012). *Computational Statistics*. Wiley Series in Computational Statistics. Wiley.
- Hansen, P. C. (1992). Analysis of discrete ill-posed problems by means of the L-curve. *SIAM review*, 34(4):561–580.
- Hastie, T., Tibshirani, R., and Friedman, J. (2013). *The Elements of Statistical Learning: Data Mining, Inference, and Prediction*. Springer Series in Statistics. Springer New York.
- Huang, C. (2001). Boundary corrected cubic smoothing splines. *Journal of Statistical Computation and Simulation*, 70(2):107–121.
- Kincaid, D. and Cheney, E. (1991). *Numerical Analysis: Mathematics of Scientific Computing*. Mathematics Series. Brooks/Cole.
- Levenspiel, O. (1998). *Chemical Reaction Engineering, 3rd Edition*. John Wiley & Sons.
- Madár, J., Abonyi, J., Roubos, H., and Szeifert, F. (2003). Incorporating prior knowledge in a cubic spline approximation application to the identification of reaction kinetic models. *Industrial & Engineering Chemistry Research*, 42(17):4043–4049.
- Mah, R. S., Stanley, G. M., and Downing, D. M. (1976). Reconciliation and rectification of process flow and inventory data. *Industrial & Engineering Chemistry Process Design and Development*, 15(1):175–183.
- Michalik, C., Brendel, M., and Marquardt, W. (2009). Incremental identification of fluid multi-phase reaction systems. *AIChE Journal*, 55(4):1009–1022.
- Moore, A. W. (2006). Cross-validation for detecting and preventing overfitting. <https://www.cs.cmu.edu/~awm/tutorials/overfit10.pdf>. Accessed: 2020-08-01.
- Poyton, A., Varziri, M. S., McAuley, K. B., McLellan, P. J., and Ramsay, J. O. (2006).

- Parameter estimation in continuous-time dynamic models using principal differential analysis. *Computers & chemical engineering*, 30(4):698–708.
- Santos-Marques, J., Georgakis, C., Mustakis, J., and Hawkins, J. M. (2019). From dynamic response surface models to the identification of the reaction stoichiometry in a complex pharmaceutical case study. *AIChE Journal*, 65(4):1173–1185.
- Savitzky, A. and Golay, M. J. (1964). Smoothing and differentiation of data by simplified least squares procedures. *Analytical chemistry*, 36(8):1627–1639.
- Schaich, D., Becker, R., and King, R. (2001). Qualitative modelling for automatic identification of mathematical models of chemical reaction systems. *Control Engineering Practice*, 9(12):1373–1381.
- Trefethen, L. (2013). *Approximation Theory and Approximation Practice*. Other Titles in Applied Mathematics. SIAM.
- Varah, J. M. (1982). A spline least squares method for numerical parameter estimation in differential equations. *SIAM Journal on Scientific and Statistical Computing*, 3(1):28–46.
- Villez, K., Venkatasubramanian, V., and Rengaswamy, R. (2013). Generalized shape constrained spline fitting for qualitative analysis of trends. *Computers & Chemical Engineering*, 58:116–134.
- Willis, M. J. and von Stosch, M. (2017). L0-constrained regression using mixed integer linear programming. *Chemometrics and Intelligent Laboratory Systems*, 165:29–37.
- Yeow, Y., Wickramasinghe, S., Han, B., and Leong, Y.-K. (2003). A new method of processing the time-concentration data of reaction kinetics. *Chemical Engineering Science*, 58(16):3601–3610.



# Chapter 6

## Step 2 — Data Dimensionality Analysis

*“The universe may be a 4-dimensional soap bubble  
in an 11-dimensional space. Who knows?”*

– Christian Klixbull Jørgensen

### Contents

---

6.1	Introduction and chapter’s organization . . . . .	160
6.2	Step 2 overview . . . . .	161
6.3	Effect of noise in the singular values and replicated experiments . . . . .	162
6.4	Determining the model dimension using singular value analysis with empirical and heuristic approaches . . . . .	170
6.4.1	Scree test . . . . .	171
6.4.2	Fractional variances test . . . . .	171
6.4.3	Kaiser test and auto-scaling operation . . . . .	173
6.4.4	Conclusion on the basis of the results obtained . . . . .	175
6.5	Determining the variant space of data by theoretical approaches . . . . .	175
6.5.1	Malinowski test . . . . .	176
6.5.2	Cross-validation . . . . .	181
6.5.3	Hard-thresholding . . . . .	186
6.6	Determining the invariant data space using optimization . . . . .	187
6.6.1	Methodology for evaluating reaction-invariant relationships . . . . .	187
6.6.2	Methodology for evaluating time-invariant relationships . . . . .	188
6.6.3	Application example, discussion of the results obtained and conclusion about the proposed method . . . . .	190
6.7	Comparative analysis of the applied methods . . . . .	193

## 6.1 Introduction and chapter's organization

As previously discussed in the theoretical background in Section 2.4, the identification of the stoichiometry  $\mathbf{N}[nr_{\text{xi}} \times n_{\text{sp}}]$  and/or the invariants  $\mathbf{A}[nin_{\text{li}} \times n_{\text{sp}}]$  from data in the variant form  $\mathbf{D}[n_{\text{to}} \times n_{\text{sp}}]$  is not an easy and simple task in the presence of noisy data, namely concentration measurements with associated uncertainty. The real situation presents mass balances of the type (2.41) with an additional matrix: the error matrix, concerning to data components that the model cannot predict. Clearly, the objective is to maintain that error as low as possible, but without introducing data overfit. Therefore, great effort has been made for the identification of  $\mathbf{N}$  from  $\mathbf{D}$ , presenting good agreement between model and data, as well as accurate and reliable model parameters. Hence, one of the key-problems of modeling chemical reaction systems is to **identify the model dimension**, or in other words, what is the hidden dimension  $nr_{\text{xi}}$  of the data variant space, or even better, what is signal and what is noise in the data. This is the main objective of this methodology step.

This chapter introduces several methods that address this issue. Three methods of the literature are described in more detail, namely the Malinowski test (Malinowski and Howery, 1980; Malinowski, 1989), cross-validation (Wold, 1978; Eastment and Krzanowski, 1982; Krzanowski and Kline, 1995) and the hard-thresholding (Gavish and Donoho, 2014). The comparison of these methods is supported by applying them to a challenging case study. In addition, heuristic methods are also considered for the same purpose.

Since time-invariant vectors span a complementary space where the compositional changes occur<sup>1</sup>, the use of time-invariant relationships can assist and support the identification of  $\mathbf{N}$  from reconciled data  $\mathbf{D}$ , by decreasing data uncertainty and consequently increasing the modeling of real data signal (thus diminishing the likelihood of data overfitting). Moreover, when elucidating  $nin_{\text{li}}$ , the model dimension is consequently determined since  $nin_{\text{li}} = n_{\text{sp}} - nr_{\text{xi}}$ . Due to these facts, in this methodology step, a lot of effort is associated with the identification of time invariants, *i.e.*, with the identification of the number of invariants  $nin_{\text{li}}$  and the subspace spanned by them, so as to support the modeling of the data variant space.

Two approaches can be considered for identifying time-invariant relationships. First, through the trivial computation of the null space of  $\mathbf{N}$ , when the system stoichiometry is known. However, this approach is not practical since  $\mathbf{N}$  is generally unknown. System stoichiometry is often what modelers want to determine or identify. Second, through the assessment of chemical species formula, *i.e.*, from the analysis of the molecular structure of the measured chemical species. In both cases, the aim is to find the least cluster (or

<sup>1</sup>A detailed discussion about this topic is addressed in Sections 2.2 and 2.3.

block) of chemical elements that is common between the measured species, allowing the establishment of meaningful (minimal and positive) conservation relationships. These relationships  $\mathbf{a}_i \in \mathbb{R}^{n_{\text{sp}}}$  for  $i = 1, \dots, n_{\text{sp}} - n_{\text{rx}_{\text{li}}}$  must be validated using experimental data. This means that it is expectable that the square euclidean norms

$$\|\mathbf{D} \cdot \mathbf{a}_i\|_2^2 \equiv (\mathbf{D} \cdot \mathbf{a}_i)^{\text{T}} \cdot \mathbf{D} \cdot \mathbf{a}_i, \quad \forall i \in \text{in} \quad (6.1)$$

present lower amounts, approaching the magnitude of the original data uncertainty.

In this chapter, a new method for identifying the dimension of the invariant space,  $n_{\text{in}_{\text{li}}}$ , from data with low noise content is proposed. In some cases, it is also possible to determine the appropriate invariant relationships that come closest to span the null space of the noisy data with the identified dimension. The method is based on discrete optimization and singular value decomposition of the noisy data matrix, where from an abstract (orthonormal) basis that spans the null space of noisy data, a plausible candidate basis is obtained (formed by the sparsest vectors with positive and integer entries).

This chapter is organized as follows. In Section 6.2, the overall description of Step 2 is presented. In Section 6.3, a study on data with simulated noise is carried out to evaluate the behavior of singular values in the presence of noise. The number of replicated experiments is evaluated so as to determine with confidence the effective model dimension. In Section 6.4, heuristic methods are considered for determining the data variant space dimension. In Section 6.5, the three literature methods (introduced above) for determining the characteristic data variant space are addressed. In Section 6.6 the proposed new methods for determining the invariant relationships are presented: a MILP formulation for computing the sparsest positive null space of the stoichiometric matrix (Section 6.6.1) and a novel method for determining the dimension of the data invariant space (Section 6.6.2). All methods (from Section 6.3 to 6.6) are applied to the Pfizer case study, in order to illustrate all the features of the problem of finding the data dimensionality. Finally, in Section 6.7, the presented methods are compared with key observations presented.

Moreover, the decomposition of data matrix in singular values and vectors is revisited in Appendix I.3.

## 6.2 Step 2 overview

*“We share a philosophy about linear algebra: we think basis-free, but when the chips are down we close the office door and compute with matrices like fury.”*

– Irving Kaplansky (1917–2006) speaking about Paul Halmos (1916–2006)

The Step 2 consists of identifying the data dimension for determining (i) the number of chemical reactions that the model must present  $R = n_{\text{rx}_{\text{li}}}$ , (ii) the number of time-invariant relationships  $n_{\text{in}_{\text{li}}} = n_{\text{sp}} - R$ , and (iii) an orthonormal basis for the data variant

space  $\mathbf{N}_d$ . Regarding the item (ii), this information may be previously known from the data reconciliation step, and therefore, the analysis performed at this phase is used as a validation tool of the previously imposed invariants during data reconciliation.

Figure 6.1 presents the diagram of this step, where firstly the SVD of reconciled data is considered for singular value analysis. At this phase several observations are made from data analysis, such as the quantification of the near linear dependence among its features, the evaluation of how much ill-posed is the problem on hands and the prediction of identifiability problems related to model components and their parameters. The application of several methods for determining model dimension is considered and the comparison of the results obtained is performed, deciding how much of data we expect that the model to explain.

Also, at this phase the validation of  $\text{nin}_{\text{li}}$  time-invariant relationships that is already present at the reconciled data is performed when the model dimension identified corresponds to the difference  $R = n_{\text{sp}} - \text{nin}_{\text{li}}$ . When these numbers do not match, *i.e.*, when the elucidated model dimension  $R$  is lower than  $n_{\text{sp}} - \text{nin}_{\text{li}}$ , more time invariants should be proposed until the numbers matching, implying the repetition of the data reconciliation procedure with additional invariant constraints and the application of the methods for determining model dimension again in iterative procedures.

When the case study under analysis reveals data identifiability problems, presenting a significant amount of data uncertainty, the need of more experiments can be justified in order to clarify the data space dimension. On the other hand, when data is satisfactorily characterized the model dimension is elucidated simultaneously with the time-invariant relationships, allowing the computation of an orthonormal basis of the data variant space.

### 6.3 Effect of noise in the singular values and replicated experiments

*“For even the most stupid of men, by some instinct of nature, by himself and without any instruction (which is a remarkable thing), is convinced that the more observations have been made, the less danger there is of wandering from one’s goal.”*

– Jacob Bernoulli (1655-1705)

A study of the behavior of singular values in relation to adding random noise to data is presented in this section. The objective is to evaluate the number of replicated experiments that allows obtaining (i) certainty/confidence about the expected mean value, and consequently (ii) convergence towards the value of the pure signal without noise. Thus, the model dimension (data variant space dimension) is precisely identified, and consequently also the invariant space dimension that the data would present in the absence of



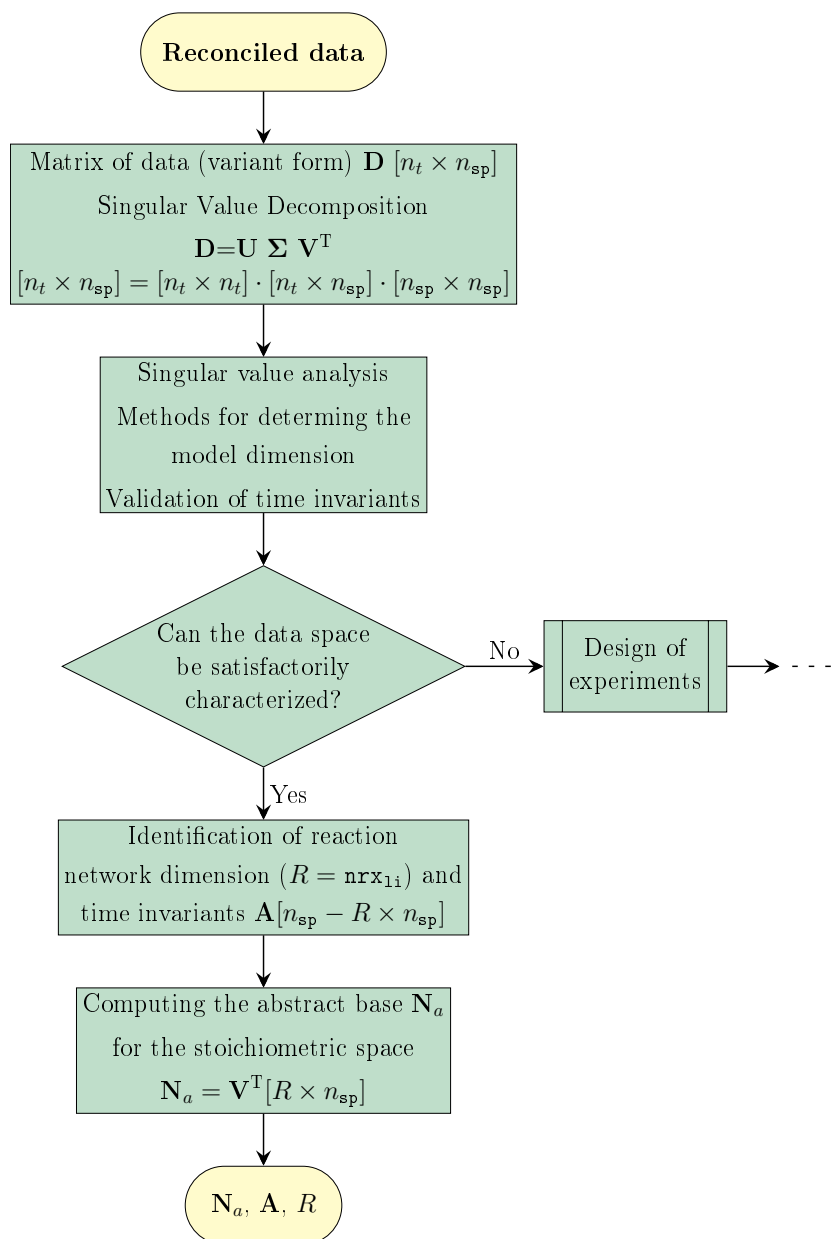


**Figure 6.1** Step 2 flowchart.

noise.

The study is performed using experimental data from the Pfizer case study. The dataset consists of cumulative change in the number of moles of ten species registered in 15 experiments with three temperature values and several different initial conditions. Data was previously reconciled with two invariant relationships. The matrix  $\mathbf{D}_{\Xi}$  of cumulative changes of number of moles has dimension  $[225 \times 10]$  and matrix rank eight. The singular values ( $\sigma^*$ ) of  $\mathbf{D}_{\Xi}$  are shown in Table 6.1. For the practice of this study, we assume that  $\mathbf{D}_{\Xi}$  is free of noise, which is a valid assumption in terms of comparison of noisy singular values with the reference ones that have no noise. Gaussian noise with zero mean and

0.005 standard deviation was systematically added to  $\mathbf{D}_\Xi$  during  $n = 1000$  iterations, such that

$$\tilde{\mathbf{D}}_k = \mathbf{D} + \mathbf{E}_k, \quad \forall k = 1, \dots, n \quad (6.2)$$

where  $\tilde{\mathbf{D}}_k$  and  $\mathbf{E}_k$  are, respectively, the noisy data and the noise matrices with dimension  $[225 \times 10]$  at the replicated experiment  $k = 1, \dots, n$ . The noise (each entry of  $\mathbf{E}$ ) is created through a random function in every iteration. For the sake of simplicity, in (6.2), the subscript  $E$  is omitted in  $\mathbf{D}$  and  $\tilde{\mathbf{D}}$ , and will also be omitted in the remaining of this section. Then, the noisy data of each iteration was appended to a list, forming a list with dimension  $[1000 \times 225 \times 10]$ . Therefore, for every entry  $d_{x,s}$  of  $\mathbf{D}$ , where  $x = 1, \dots, 225$  is the time instant index of the cumulative change in the number of moles of species  $s = A, B, \dots, J$ , a random noise  $\epsilon_{k,x,s}$  is added, forming the noisy entry  $\tilde{d}_{k,x,s}$  of matrix  $\tilde{\mathbf{D}}_k$ . Consequently, a distribution of a thousand values of  $\tilde{d}_{*,x,s}$  is obtained for every  $x = 1, \dots, 225$ , and for every  $s = A, B, \dots, J$ , which assumes the format of normal (Gaussian) distributions since Gaussian noise was considered (*i.e.*, one obtains 2250 Gaussian distributions composed by 1000 noised entries). Figure 6.2 shows the distribution of  $\tilde{d}_{*,x,s}$  for  $s = A$  and  $x = 2$  (*i.e.*,  $t = 1.2$  h).

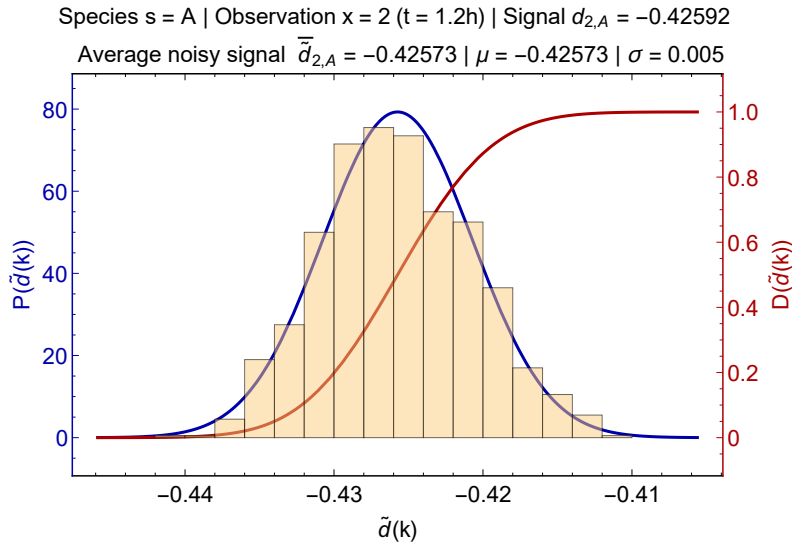


**Figure 6.2** Distribution of  $\tilde{d}_k$  values concerning species  $A$  at 1.2 h for a thousand replicated experiments. The  $\mu$  and  $\sigma$  are the mean and the standard deviation, respectively, concerning the PDF function (blue curve).

In Figure 6.2, the y-axis of the left side concerns to the probability density function (PDF, blue curve) for the respective noisy data entry  $\tilde{d}_k$  (x-axis) obtained, and the y-axis of the right side concerns to the cumulative distribution function (CDF, red curve), which gives the probability that a variate will assume a value  $\leq \tilde{d}$ .

According to a famous citation of James Gleick: “Everything we care about lies somewhere in the middle, where pattern and randomness interlace”, the expected value of a *random* variable  $\tilde{d}$  is a function that turns the probabilities  $P(\tilde{d})$  into a *sure* variable called the

mean of  $\tilde{d}$ , ( $\text{mean}(\tilde{d})$ ) (Lemons et al., 2002). When we consider  $\tilde{d}_{k,x,s}$  which is the random signal value at experiment  $k = 1, \dots, n$  for species  $s$  in observation  $x$ , the average amount  $\bar{\tilde{d}}_{x,s}$  is

$$\bar{\tilde{d}}_{x,s} = \frac{\tilde{d}_{1,x,s} + \tilde{d}_{2,x,s} + \tilde{d}_{3,x,s} + \dots + \tilde{d}_{n,x,s}}{n}, \quad x = 1, \dots, 225; \quad s = A, \dots, J \quad (6.3)$$

and the variance of the average is

$$\text{var}(\bar{\tilde{d}}_{x,s}) = \frac{\sum_{k=1}^n \text{var}(\tilde{d}_{k,x,s})}{n^2}, \quad x = 1, \dots, 225; \quad s = A, \dots, J \quad (6.4)$$

assuming that every  $\tilde{d}_{k,x,s}$  for  $k = 1, \dots, n$ , and the same  $s$  and same  $x$ , is statistically independent. For the sake of simplicity, indexes  $x$  and  $s$  will be omitted in  $\tilde{d}_{k,x,s}$  since the analysis for particular values of  $x$  and  $s$  is also valid for the remaining values, thus in the following text only the experiment subscript will be used *i.e.*,  $\tilde{d}_k$ .

Once it is desirable to decrease the variability in a random variable, considering its average value is a very good reason that meets this need, since the variance of the average  $\bar{\tilde{d}}$  decreases with increasing  $n$  as  $1/n$ , as it is shown in (6.4), *i.e.*, the numerator increases (roughly) with the number of the experiments ( $n$ ) and the denominator increases with the squared of this amount ( $n^2$ ). Since, we are handling replicas (*i.e.*, every experiment was made in the same way), the next equality holds

$$\text{var}(\tilde{d}_1) = \text{var}(\tilde{d}_2) = \dots = \text{var}(\tilde{d}_n) \quad (6.5)$$

and, therefore, the computation of  $\text{var}(\bar{\tilde{d}})$  is simplified to

$$\text{var}(\bar{\tilde{d}}) = \frac{\text{var}(\tilde{d}_1)}{n} \quad (6.6)$$

Hence, averaging is always helpful if the experiments are replicas (Lemons et al., 2002).

In this case, the standard deviation of  $\bar{\tilde{d}}$  can be predicted using

$$\text{std}(\bar{\tilde{d}}) = \sqrt{\text{var}(\bar{\tilde{d}})} = \frac{\text{std}(\tilde{d}_1)}{\sqrt{n}} \quad (6.7)$$

where it can be seen that the standard deviation of the average decreases with the number of terms included in the average. Therefore the average  $\bar{\tilde{d}}$  approaches a random variable whose variance disappears when  $n$  becomes indefinitely large, that is,  $\bar{\tilde{d}}$  approaches the sure value  $\text{mean}(\bar{\tilde{d}}) = d$ , the pure signal (without the random component, noise).

Therefore, considering the distribution presented in Figure 6.2, it is possible to estimate the standard deviation of  $\bar{\tilde{d}}$  using (6.7), which is  $\text{std}(\bar{\tilde{d}}) = 1.58 \times 10^{-4}$ . This indicates

that the  $\bar{\tilde{d}}$  obtained is representative of the expected value since its standard deviation is sufficiently small to infer its accuracy. However, if (instead one thousand) a reduced number of replicas were considered, for example three replicated experiments, the standard deviation of the average value would increase to  $\text{std}(\bar{\tilde{d}}) \approx 0.003$ , which could maintain uncertainty over small singular values. Hence, the number of experiments can be determined in order to increase the accuracy of  $\bar{\tilde{d}}$ , that in turn is more representative than the individual  $\tilde{d}$ , since  $\bar{\tilde{d}}$  shows lower variance.

The comparison of noisy singular values with the true/reference ones was performed considering different  $n$ , *i.e.*, different numbers of replicas. The results obtained are shown in Table 6.1, where the real (pure signal) singular values are represented by  $\sigma^*$  computed through the SVD of  $\mathbf{D}$ , the noisy singular values corresponds to  $\tilde{\sigma}$  computed through the SVD of the average of replicated experiments  $\tilde{\mathbf{D}}_k$  matrices ( $\bar{\tilde{\mathbf{D}}}$ ), and the relative error (RE) among  $\sigma^*$  and  $\tilde{\sigma}$  is computed using

$$\text{RE} = \frac{|\sigma^* - \tilde{\sigma}|}{\sigma^*} \times 100 \quad (6.8)$$

**Table 6.1** Results from the simulation of data with additive Gaussian noise considering several numbers of replicated experiments.

$j$	$\sigma^*$	3 replicas		10 replicas		100 replicas		1000 replicas	
		$\tilde{\sigma}$	RE [%]	$\tilde{\sigma}$	RE [%]	$\tilde{\sigma}$	RE [%]	$\tilde{\sigma}$	RE [%]
1	22.273	22.272	0.003	22.272	0.004	22.273	0.001	22.272	0.002
2	2.719	2.720	0.033	2.719	0.005	2.719	0.014	2.719	0.003
3	1.969	1.966	0.121	1.967	0.062	1.969	0.007	1.969	0.008
4	0.372	0.378	1.452	0.375	0.689	0.373	0.075	0.372	0.046
5	0.283	0.286	0.928	0.284	0.437	0.283	0.100	0.283	0.042
6	0.242	0.240	0.684	0.242	0.049	0.242	0.295	0.242	0.056
7	0.126	0.130	2.911	0.126	0.489	0.126	0.260	0.126	0.039
8	0.075	0.090	19.386	0.079	5.069	0.075	0.291	0.075	0.216
9	0	0.040	$\infty$	0.025	$\infty$	0.008	$\infty$	0.002	$\infty$
10	0	0.039	$\infty$	0.022	$\infty$	0.007	$\infty$	0.002	$\infty$

As can be seen in Table 6.1, in most of the model components directions, the RE decreased with the number of replicas since a better estimate of the  $\bar{\tilde{\mathbf{D}}}$  is obtained, approaching to the pure signal  $\mathbf{D}$  matrix. Also, the lower model components ( $j \geq 6$ ) present greater error of convergence since they are more affected by the noise variability, even considering a high number of replicas. The model components  $j = 9$  and  $j = 10$  are related to the invariant relationships that were lost by data noise addition, showing errors in singular values of the order of magnitude of noise and a mathematical indeterminacy in relation to the RE. On the other hand, the singular values concerned to model directions of lower data variability ( $6 \leq j \leq 8$ ) have decreased with the  $n$ , indicating that these components

have signal even highly contaminated with noise in individual experiments. However, the results are globally pretty good for 10 replicas, since RE is lower than 1% for the first seven model components, and  $\approx 5\%$  for the last one. Hence, the averaging of replicated experiments is filtering the noise, once the noisy singular values are converging to the pure signal. Therefore, replicating experiments aids in determining the model dimension. Figure 6.3 presents the RE for a number of replicas within the range  $n = [1,1000]$ .

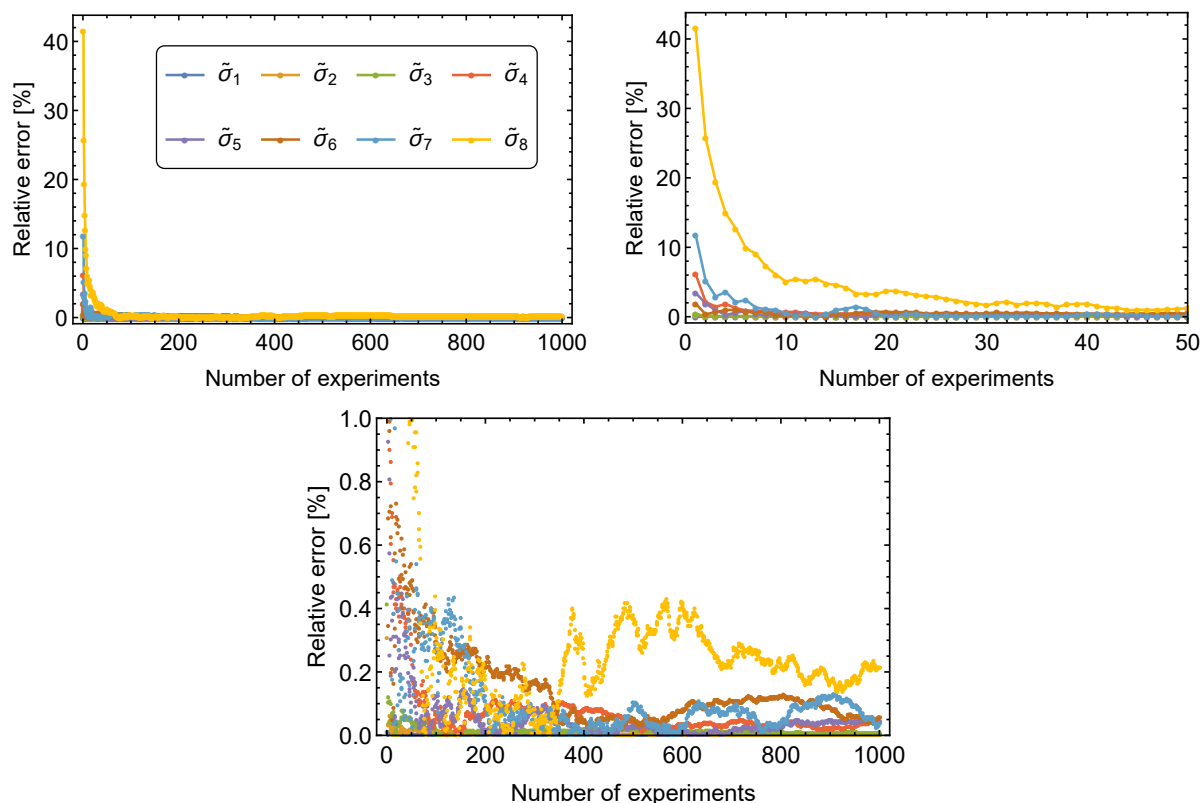


**Figure 6.3** Relative error (RE) of the singular values for a range of experiments between one and a thousand. The top-right plot is zoomed in the x-axis. The bottom-centered plot is zoomed in the y-axis.

As can be seen in Figure 6.3, the RE shows an accentuated drop for few replicated experiments, and tends to stabilize with  $n$ . However, the RE presents fluctuations (it is not monotonous) specially for magnitudes inferior than 1%. This oscillatory behavior is due to the random noise added to original data.

Figures 6.4 and 6.5 present the dataset that composes  $\mathbf{D}$  and  $\tilde{\mathbf{D}}$  for one thousand of experiments, where on the former individual species plots are presented (*i.e.*, individual columns of  $\mathbf{D}$  and  $\tilde{\mathbf{D}}$ ) and on the latter the entire data is shown in a single plot. In these figures at every multiple of 15, a grid line is drawn indicating a new (sub) dataset that concerns to different experimental conditions, for the same reaction system.

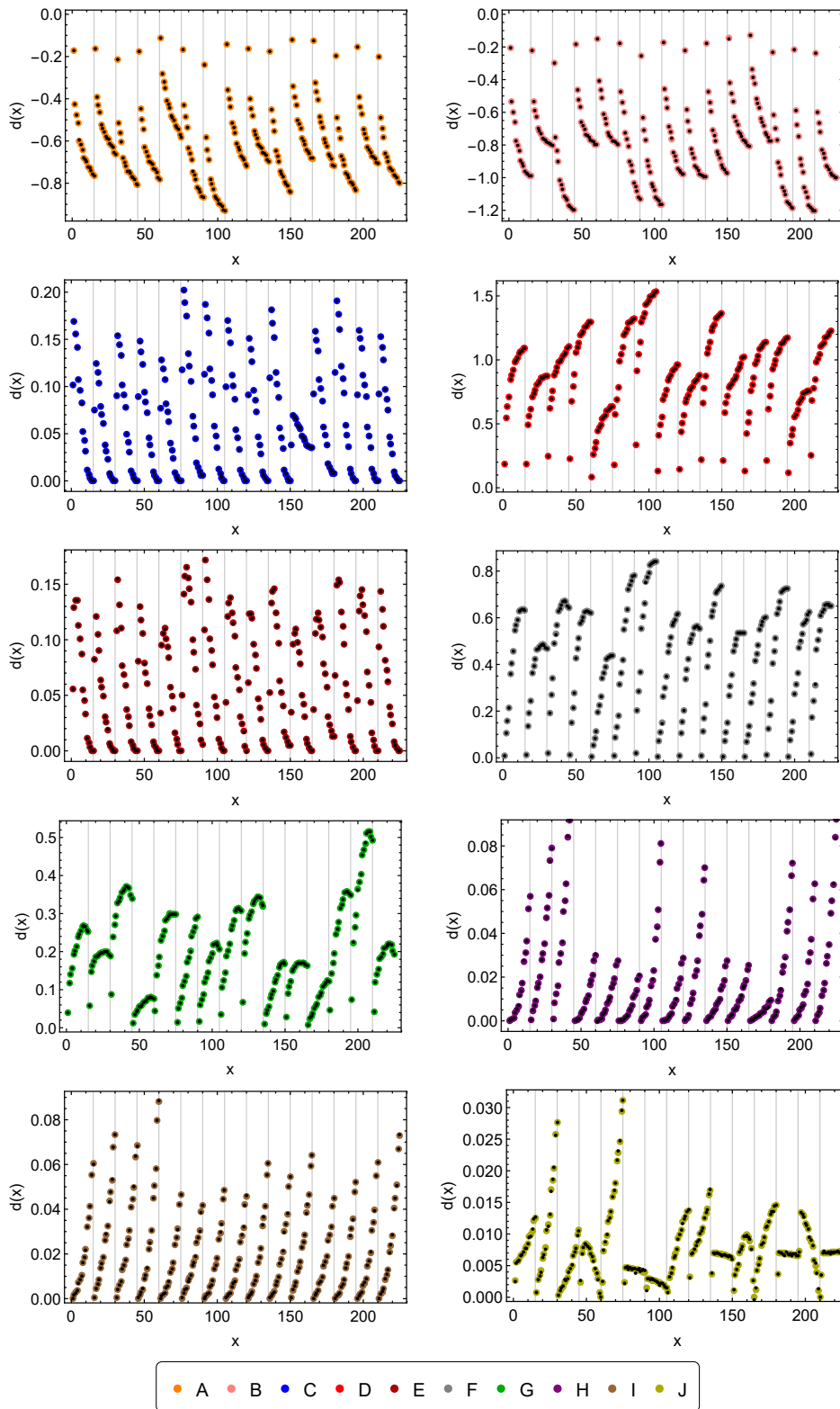


**Figure 6.4** Individual species profiles. Non-black points: true signal of data. Black points: average of noisy data for one thousand of experiments.

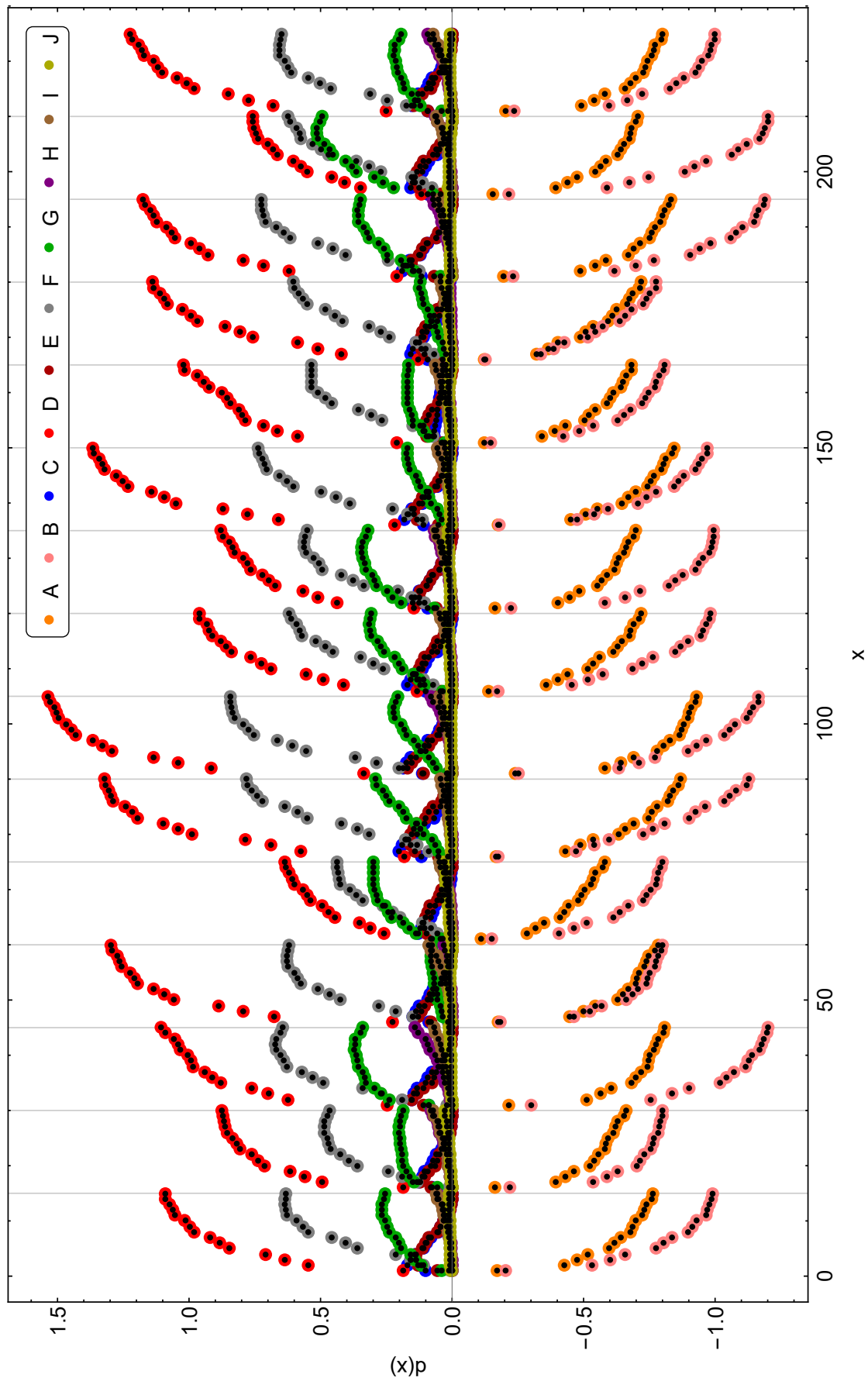


**Figure 6.5** Entire dataset free of noise is presented by non-black dots. Smaller black dots represent the average of each noisy data in one thousand replicas.

## 6.4 Determining the model dimension using singular value analysis with empirical and heuristic approaches

As previously discussed in the introduction of this chapter, experimental data has uncertainty associated, *i.e.*, it includes noise. A common concern of modelers is to maximize the extent of data explained by the model and at the same time avoid the addition of model components that mainly result from noisy data, and thus avoid overfitting. Since SVD decomposes data in directions that can be ordered by decreasing variance, the information it provides can be very useful in determining an adequate model dimension, taking into account that data directions corresponding to the smallest singular values are the most affected by noise.

Hence, one of the most important questions for modeling dynamic systems how many eigenvectors should be considered when projecting data, or where  $\text{SVD}(\mathbf{D})$  should be truncated. The economy SVD format (discussed in detail in Appendix I.1) consists of eliminating the columns of  $\mathbf{U}$  and  $\mathbf{V}$  corresponding to the left and right null spaces of  $\mathbf{D}$ , respectively. However, in this case, the SVD truncation is about “leaving behind” a residual component of the data matrix that we cannot (or don’t want to) explain, such that

$$\mathbf{D} = \mathbf{U} \cdot \boldsymbol{\Sigma} \cdot \mathbf{V}^T = \mathbf{U}_R \cdot \boldsymbol{\Sigma}_R \cdot \mathbf{V}_R^T + \mathbf{E} \quad (6.9)$$

where  $R$  is the model dimension, *i.e.*, the number of principal components selected as model constituent, and  $\mathbf{E}[n_{\text{to}} \times n_{\text{sp}}]$  is the matrix of data residuals to be left behind. The matrices  $\mathbf{U}_R$ ,  $\boldsymbol{\Sigma}_R$  and  $\mathbf{V}_R$  contains the first  $R$  columns of the original ones, *i.e.*,  $\mathbf{U}_R$  and  $\mathbf{V}_R$  contain  $R$  eigenvectors of  $\text{cov}(\mathbf{D}^T)$  and  $\text{cov}(\mathbf{D})$ , respectively, hierarchically ordered by the greatest variance.

This section presents three empirical (*ad hoc*) methods, available in the literature, for determining  $R$ , namely the scree test, the analysis of fractional variances, and the Kaiser test. The application of these methods is considered using the Pfizer case study, using the same noisy dataset studied in the previous section. This dataset concerns to cumulative values of numbers of moles variation with added Gaussian noise (zero mean and 0.005 standard deviation), respecting to batch experiments with ten observed species. The true data dimension, without noise, is known a priori to be eight. The singular value list is shown in (6.10). Figure 6.6 presents the singular values in several scree plots.

$$\boldsymbol{\sigma} = \{22.271, 2.720, 1.964, 0.374, 0.293, 0.251, 0.158, 0.102, 0.083, 0.073\} \quad (6.10)$$

After the application of each method, a short discussion of the obtained results is made, and at the end of this section an overall conclusion is provided.



### 6.4.1 Scree test

The scree test assumes that the relevant information can be distinguished from random noise in terms of singular values and that the magnitude of the random noise variation seems to stabilize linearly with the number of components (Cattell, 1966). The common graphical analysis based on heuristic principles is to plot the  $\log(\sigma_j) = f(j)$  and look for the elbow of the profile, that separates the singular values with greater variance from those with lower variance. However, these heuristic methods can fail if the profile behavior is not sufficiently sharp, or if the data has a similar distribution of singular values to the assumed noise distribution.

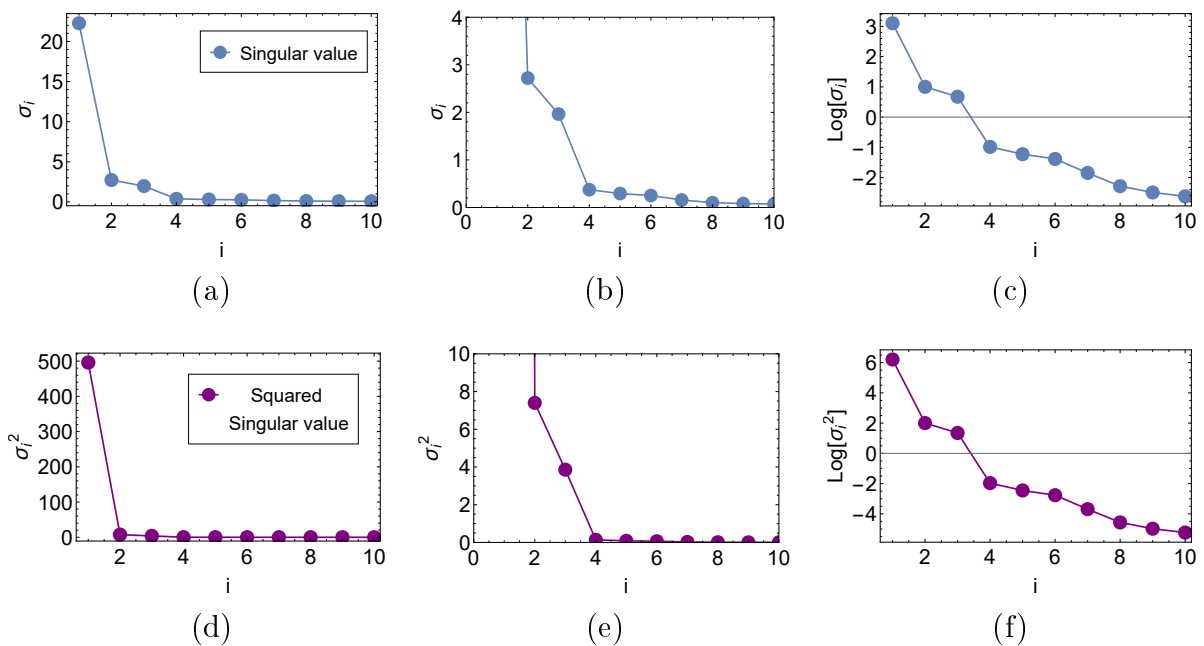


**Figure 6.6** The singular values are plotted in (a), with zoom-in in (b), and with the logarithm of their values in (c). The variances are plotted in (d), with zoom-in in (e), and with the logarithm of their values in (f).

From the visual analysis of the singular values and variances curves in Figure 6.6, it would be not uncommon to decide to truncate the data matrix at the fourth position, *i.e.*,  $R = 4$ , since an elbow can be seen at the fourth component. Nonetheless this result is highly restrictive, leading to the exclusion of true model components. Therefore, it is hard to distinguish between real and noise singular values using only heuristic methods that are supported on visual graphical analysis.

### 6.4.2 Fractional variances test

Another rule of thumb is to choose the first  $R$  eigenvectors such that the sum of their variances (eigenvalues) is up to an amount of the total (a kind of parsimonious criterion), such as 95% or 99%. This high fraction of variation covered by the model must be set

according to the percentage of noise in data (percentage of the noise variance), for example if it is known that data measured has 1% of noise, it is expected that the model describes the entire variation up to about 99% (Bro and Smilde, 2014). However, in many cases this percentage of noise is unknown or imprecise, which hampers the use of this criterion. Also, the uncertainty can be different for each measured variable.

Figure 6.7 presents the fractional variances (variance and total variance ratio) and the respective cumulative curve. The zoom-in plots located at the bottom of this figure show the thresholds (red lines) for two percentages of variation: 99% and 99.9975%, on the left and on the right sides, respectively.

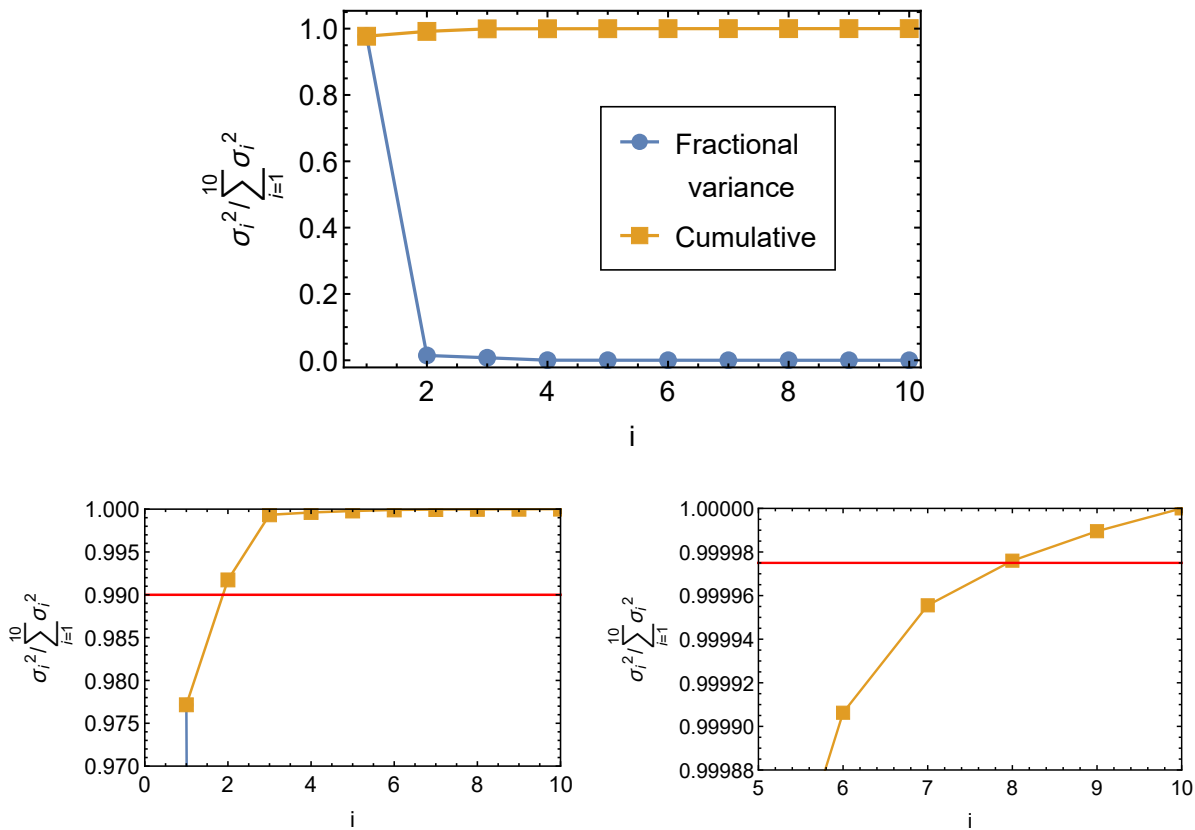


**Figure 6.7** The variances over total variance ratio and its cumulative values are plotted considering a threshold for the retention of 99% of variability on the left figure and 99.9975% on the right figure, indicated by the red lines. The bottom plots are zoomed-in.

On the left-hand-side plot, this heuristic criterion indicates that only a single component should be considered for data with 1% of noise, covering  $\approx 97.7\%$  of the data variation. In this case, the cumulative variance covered by models with more than one eigenvector is greater than 99%, presenting data overfit (explaining noisy components). Therefore, even considering a high limit for explaining the data variability (99% of the total data variance), this amount would be unsatisfactory (not enough) since 7 real components were excluded for this noise level. On the other hand, on the plot at the right-hand side, the red line indicates that seven components (eigenvectors) should be selected as model constituent,

covering 99.9956% of the data variation. The cumulative variance covered by more than seven components is greater than 99.9975%, (which indicates the incorporation of noisy components for data with 0.0025% of noise). The obtained result ( $R = 7$ ) is very close to the real dimension of the 8-component model. This happens due to the consideration of the real noise standard deviation (0.005) for this last threshold establishment, although, even so, the eighth component of the model is left out.

### 6.4.3 Kaiser test and auto-scaling operation

The Kaiser's rule is based on the assumption that if a component has an eigenvalue greater than one, it explains the variation of more than one original variable (Cliff, 1988). This assumption is supported on the fact that autoscaled data presents a variance of one for each variable, and if all variables are orthogonal to each other, then every component in a SVD model would present unitary eigenvalues. This led to the rule of selecting all components with eigenvalues (or singular values) greater than one. However, it has been shown that it is perfectly possible that even components with eigenvalues far below one can be real and significant for data with low noise content. Hence real phenomena can be small in variation, yet accurate (Bro and Smilde, 2014).

For the illustration of this criterion, the autoscaling of data was performed, *i.e.*, the subtraction of the mean of every column and the division of the respective standard deviation was considered for each column concerning original data in two separated steps, such that

$$\mathbf{Y} = \mathbf{D} - \mathbf{1} \cdot \boldsymbol{\mu}^T \quad \text{and} \quad \mathbf{Y}' = \mathbf{Y} \cdot \mathbf{W} \quad (6.11)$$

where in the first operation (mean-centering)  $\mathbf{Y}[n_{t0} \times n_{sp}]$  is the matrix of mean-centered data with the same dimension of  $\mathbf{D}$ ,  $\mathbf{1}[n_{t0} \times 1]$  is a column vector with unitary entries and  $\boldsymbol{\mu}[n_{sp} \times 1]$  is a vector with entries equal to the mean  $\mu_s = 1, \dots, n_{sp}$  of each column  $s$  of  $\mathbf{D}$ , and, in the second operation (scaling)  $\mathbf{Y}'$  is the autoscaled matrix, and  $\mathbf{W}[n_{sp} \times n_{sp}]$  is a square diagonal matrix with entries corresponding to the inverse of the standard deviation of the respective column of  $\mathbf{D}$  (or  $\mathbf{Y}$  since it presents zero mean in every column).

Notice that the autoscaling operation is a data transformation that does not change the structural information contained in the original matrix  $\mathbf{D}$  (Bro and Smilde, 2003). On the one hand, the mean centering works by removing offsets from data regression models, avoiding numerical problems. However, this operation interferes with the signal of each data input and, therefore, no further positive restrictions can be applied. Mathematically, centering is a projection of data onto the null space of  $\mathbf{1}^T$  (for more details, see Bro and Smilde (2003)). On the other hand, the operation of scaling data is usually considered for matrices composed by variables that measure quantities of different nature (*i.e.*, with different physical units), and therefore, when weighting each variable by the inverse of its standard deviation, a normalization is being performed. Consequently, in scaled data, no variable has more variability than the other, *i.e.*, all present the same unity variance, and therefore, variables that before scaling have presented little variation, after scaling,

are modeled with the same significant degree. Scaling can be advantageous for parameter estimate procedures since numerical problems can be avoided, decreasing stiffness and improving solver convergence.

Figure 6.8 shows the Kaiser's criterion, where it can be observed that the exact model dimension is selected for a variance over than unity.

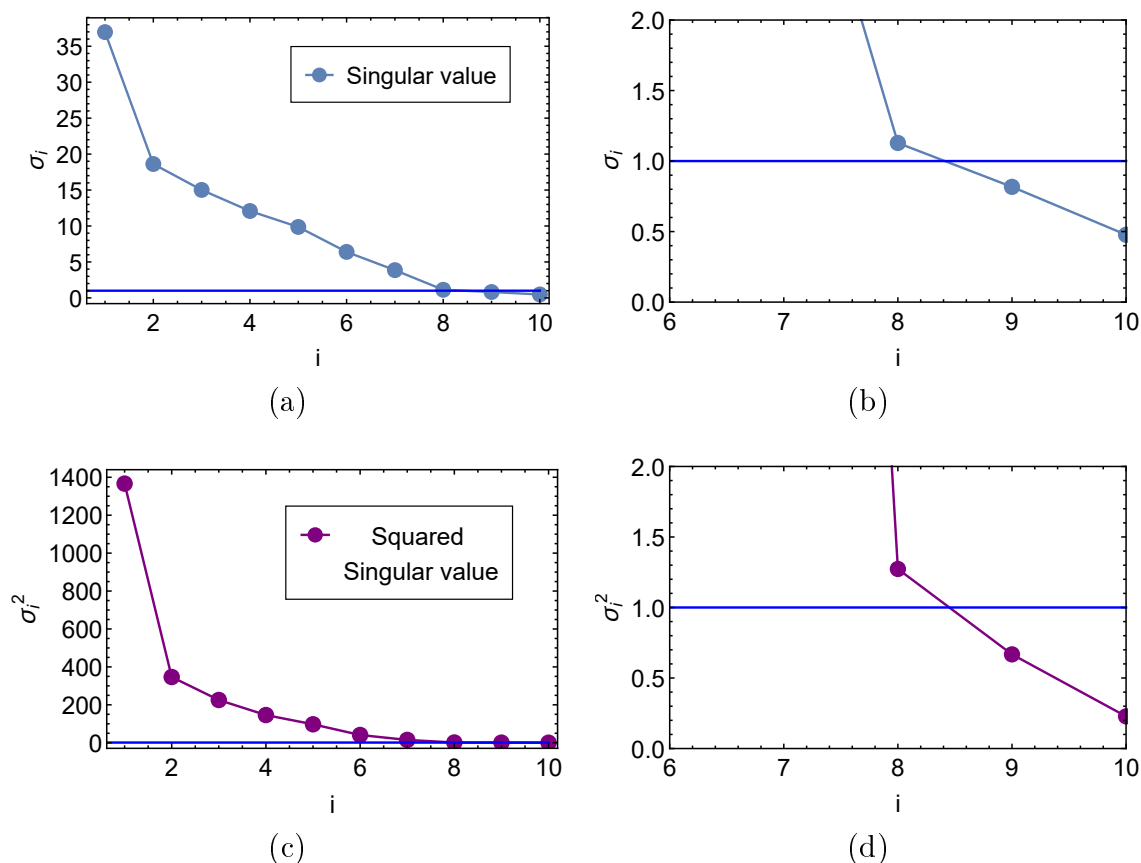


**Figure 6.8** The singular values of autoscaled data are plotted in (a) where the blue line indicates the threshold according to Kaisers' rule, and in (b) with zoom-in. The eigenvalues (variances) of autoscaled data are plotted in (c) and in (d) with zoom-in.

However, this result ( $R = 8$ ) cannot be used for non-autoscaled data. The elucidation of the model dimension must be performed using original data (and not autoscaled data), since it is over the original data that the model identification (network and kinetic parameters) is performed. For modeling chemical reaction systems, it is out of interest eliminating the offset, since the mass balances in (2.41) do not present offsets, *i.e.*, we are modeling Euclidean subspaces with Cartesian coordinates that have their origin in the null dot (these subspaces contain the null vector of the respective dimension, as according to the linear space definition), they are not affine hyperplanes. Moreover, scaling variables is also out of interest since every variable has the same unity, and it is not desirable to level every species variation to the same importance, which is a situation far from the reality of batch chemical systems. In real chemical systems, some species are “more important” than

others when they present greater variation, *i.e.*, when they appear in a more expressive way. Therefore, since there is no need to remove data offsets, and it is not desirable to change the importance of variables in the original data, the data autoscaling is not considered in this work.

Note that when performing mean-centering operations, the originally known percentage (or ratio) of the noise variance in  $\mathbf{D}$  is changed. This can be a problem when the goal is to study the effect of (known) noise on the singular values of the data (including its average information). For example, in Figure 6.7, the first model direction (first eigenvector) contains  $\approx 97.7\%$  of the data variability, including the known Gaussian noise with 0.005 standard deviation ( $25 \times 10^{-6}$  variance). This great amount of data variance captured in this model direction concerns to the mean of the data, since data was not mean-centered in that example. Once the first component (related to the mean) covers 97.7% of the data variation, excluding it by mean-centering would lead to the analysis of the remain 2.3% of the data variability in which the percentage of noise content is unknown, *i.e.*, this 2.3% of data variability would be analyzed as the entire problem in which the noise variance is not anymore  $25 \times 10^{-4}\%$ , but much more higher.

However, mean-centering operation does not change (or affects) the structural information of data since the row space of  $\mathbf{D}$  (or of  $\mathbf{V}^T$ ) is the same with or without mean-centering. This operation only changes the coordinates of each data point (now centered in its mean), *i.e.*, it only interferes in the projection length of every data point in the respective axis of the basis, given by  $\mathbf{U} \cdot \Sigma$ .

#### 6.4.4 Conclusion on the basis of the results obtained

For this case study, from the analysis of singular values, it can be seen that most chemical reactions present low extent, with model components that present variance values comparable to the noise variance, making it difficult to identify the real dimension of the model. Since the singular values most affected by noise are difficult to distinguish, that is, they all have the same range of values, the use of non-heuristic methods is preferable to define  $R$  by adopting a theoretical approach. In this sense, parametric and non-parametric methods are considered in the next section.

### 6.5 Determining the variant space of data by theoretical approaches

In this section three different methods for determining the characteristic space of data in the variant form (dimension and respective linear basis) are presented. These methods include parametric and non-parametric tests, and optimization, namely, the Malinowski test that is supported on the  $F$ -distribution of variance ratios (Malinowski, 1989), the cross-validation method that is based on the evaluation of prediction errors considering

different test sets of data for several candidate model dimensions (Wold, 1978; Eastment and Krzanowski, 1982; Krzanowski and Kline, 1995; Bro et al., 2008), and finally, the hard-threshold method which is based on optimization techniques and noise assumptions (Gavish and Donoho, 2014). The application of these methods is considered using the same case study of Pfizer company.

### 6.5.1 Malinowski test

Malinowski (1989) proposed a parametric test to determine  $R$  within some specified significance level, based on the Fisher variance ratio respected to pools of samples that have normal distributions and are statistically independent. The objective of the  $F$ -test is to test if the variances of two populations are equal, and therefore, the test of hypothesis is performed over samples of these populations. In the context of this section, the main idea of the application of  $F$ -test is to identify the number of *real* eigenvectors that have eigenvalues that are statistically greater than the pooled variance of the noise/random eigenvalues, since the former contain both structural and experimental error contributions and the latter only experimental error (or noise).

As previously discussed in Appendix I.3, (i) each eigenvalue represents the variance in the data accounted for by the associated singular vector/eigenvector, (ii) in the presence of noisy data, only the first  $R$  singular values contain meaningful information in which the signal is greater than the noise contribution, and (iii) therefore, it is over these respective singular vectors that the data variant space must be defined. On the other hand, the remaining  $n_{\text{sp}} - R$  squared singular values are considered purely noise variances, whose respective singular vectors may define the null space of data, or in other words, the time-invariant relationships.

Malinowski (1989) defined the last  $n_{\text{sp}} - R$  squared singular values and their respective singular vectors as the *error eigenvalues* and *error eigenvectors*, considering that they do not contain useful information. In particular, the term “error” for the eigenvalues that are relative to noise variances can be misleading since it is over those respective model directions that the invariant relationships may be identified, aiding the complete identification of the structure of chemical reaction models. Based on the assumption that the last  $n_{\text{sp}} - R$  right singular vectors are referred to time-invariant relationships and not model components with low data variance, the respective last  $n_{\text{sp}} - R$  singular values would had shown zero values if noise was not presented in experimental data. Therefore, it is important to emphasize that in this work, the information contained in the “error” singular vectors is useful. However, it is understandable that the “error” terminology is adopted due to its relation with the error associated with the model responses compared to original noisy data, *i.e.*, the residual terms (as it was presented by the matrix  $\mathbf{E}$  in (6.9)).

Hence, according to the fact that experimental data can be separated in two parcels, (6.9)

can be rewritten as

$$\begin{aligned}\mathbf{D} &= \mathbf{D}_R + \mathbf{D}_0 \\ &= \mathbf{U}_R \cdot \Sigma_R \cdot \mathbf{V}_R^T + \mathbf{U}_0 \cdot \Sigma_0 \cdot \mathbf{V}_0^T\end{aligned}\quad (6.12)$$

where the subscripts “ $R$ ” and “ $0$ ” are referred to the data variant space of dimension  $R$  and to the data null space of dimension  $n_{\text{in}_i} = n_{\text{sp}} - R$ , respectively. Therefore, the squares of the data points can also be divided in the same way, such that

$$\sum_{t=1}^{n_{\text{to}}} \sum_{s=1}^{n_{\text{sp}}} d_{t,s}^2 = \sum_{t=1}^{n_{\text{to}}} \sum_{s=1}^R d_{t,s}^{R^2} + \sum_{t=1}^{n_{\text{to}}} \sum_{s=R+1}^{n_{\text{sp}}} d_{t,s}^{0^2} \quad (6.13)$$

where the superscripts “ $R$ ” and “ $0$ ” are referred to data from matrices  $\mathbf{D}_R$  and  $\mathbf{D}_0$ , respectively.

The same relationship in (6.13) is valid to the eigenvalues, such that

$$\sum_{s=1}^{n_{\text{sp}}} \sigma_s^2 = \sum_{s=1}^R \sigma_s^2 + \sum_{s=R+1}^{n_{\text{sp}}} \sigma_s^2 \quad (6.14)$$

since the sum of eigenvalues is equal to the the sum of squares of the data points  $d_{t,s}$  in the respective matrix, *i.e.*,

$$\sum_{t=1}^{n_{\text{to}}} \sum_{s=1}^{n_{\text{sp}}} d_{t,s}^2 = \sum_{s=1}^{n_{\text{sp}}} \sigma_s^2, \quad \sum_{t=1}^{n_{\text{to}}} \sum_{s=1}^R d_{t,s}^{R^2} = \sum_{s=1}^R \sigma_s^2 \quad \text{and} \quad \sum_{t=1}^{n_{\text{to}}} \sum_{s=R+1}^{n_{\text{sp}}} d_{t,s}^{0^2} = \sum_{s=R+1}^{n_{\text{sp}}} \sigma_s^2 \quad (6.15)$$

Malinowski (1989) proposed a correction (weighting) factor for computing the variance of the  $R$  model component, such that

$$v(R) = \frac{\sigma_R^2}{(n_{\text{sp}} - R + 1)(n_{\text{to}} - R + 1)} \quad (6.16)$$

where each eigenvalue is being weighted in proportion to the amount of information accounted for by it.

The variance of the pool respected to the last  $n_{\text{sp}} - R$  singular vectors,  $v(0)$ , can be calculated from the weighted average of their eigenvalues, such that

$$v(0) = \frac{\sum_{s=R+1}^{n_{\text{sp}}} \sigma_s^2}{(n_{\text{sp}} - R) \sum_{s=R+1}^{n_{\text{sp}}} (n_{\text{sp}} - s + 1)(n_{\text{to}} - s + 1)} \quad (6.17)$$

In this case, the improved statistic test consists of evaluating whether the variance of the component  $R$  is greater than the variance of the pool formed by the last  $n_{\text{sp}} - R$  singular vectors, in order to infer that the model dimension  $R$  is signal, and not noise. For this

purpose the  $F$  value, which is the ratio of these two samples variances, is computed as

$$F(1, n_{\text{sp}} - R) = \frac{v(R)}{v(0)} = \frac{\sum_{s=R+1}^{n_{\text{sp}}} (n_{\text{sp}} - s + 1)(n_{\text{to}} - s + 1)}{(n_{\text{sp}} - R + 1)(n_{\text{to}} - R + 1)} \frac{\sigma_R^2}{\sum_{s=R+1}^{n_{\text{sp}}} \sigma_s^2} n_{\text{sp}} - R \quad (6.18)$$

designed to test the null hypothesis

$$H_0 : v(R)^* = v(0)^* \quad (6.19)$$

against the alternative hypothesis

$$H_a : v(R)^* > v(0)^* \quad (6.20)$$

where the superscript “\*” indicates the variance of the population. Notice that the proposed  $F$ -test is designed to evaluate one individual model component at a time against the remain components that form the pool. Hence, the  $F$  value has only one degree of freedom in its numerator concerning the  $R$  model component against  $n_{\text{sp}} - R$  degrees of freedom in its denominator concerning the discarded pool.

The procedure starts considering the last singular vector as the unique constituent of the pool, and, therefore, the model dimension that is tested in this first iteration is the dimension  $(n_{\text{sp}} - 1)$ th and  $F(1,1)$  is computed using (6.18). The obtained value must be compared to a critical  $F$  value ( $F_c$ ) that is established within some specified significance level, for example  $\alpha = 0.05$ . If the calculated  $F$  is lower than the critical value ( $F < F_c$ ), the null hypothesis in (6.19) is failed to be rejected, and therefore, the  $(n_{\text{sp}} - 1)$ th model component does not present (statistically inferred) variance greater than the (statistically inferred) variance of the  $n_{\text{sp}}$ th component, (*i.e.*,  $v(n_{\text{sp}} - 1)^*$  is not greater than  $v(0)^*$ ). Consequently, the  $(n_{\text{sp}} - 1)$ th dimension is added to the pool of discarded singular vectors, passing now to have a 2-dimensional space, and the procedure starts again for testing the  $(n_{\text{sp}} - 2)$ th model component. This process of testing and adding to the invariant pool is repeated until the variance ratio of the  $R$ th eigenvalue exceeds the tabulated  $F_c$ , marking the division between the vectors that are signal from the vectors that are noise. The  $F$ -test procedure is presented in the diagram of blocks in Figure 6.9.

### Application of the Malinowski test and discussion of the results obtained

The same list of singular values in (6.10) is considered:

$$\sigma = \{22.271, 2.720, 1.964, 0.374, 0.293, 0.251, 0.158, 0.102, 0.083, 0.073\}$$

The obtained results of  $F$ -test are shown in Table 6.2, where the model dimension is identified for  $R = 6$ .

Figure 6.10 presents the  $F$ -distributions for several dimensions of invariant pools, *i.e.*, for different dimensions of deleted singular vectors from the candidate variant data space,



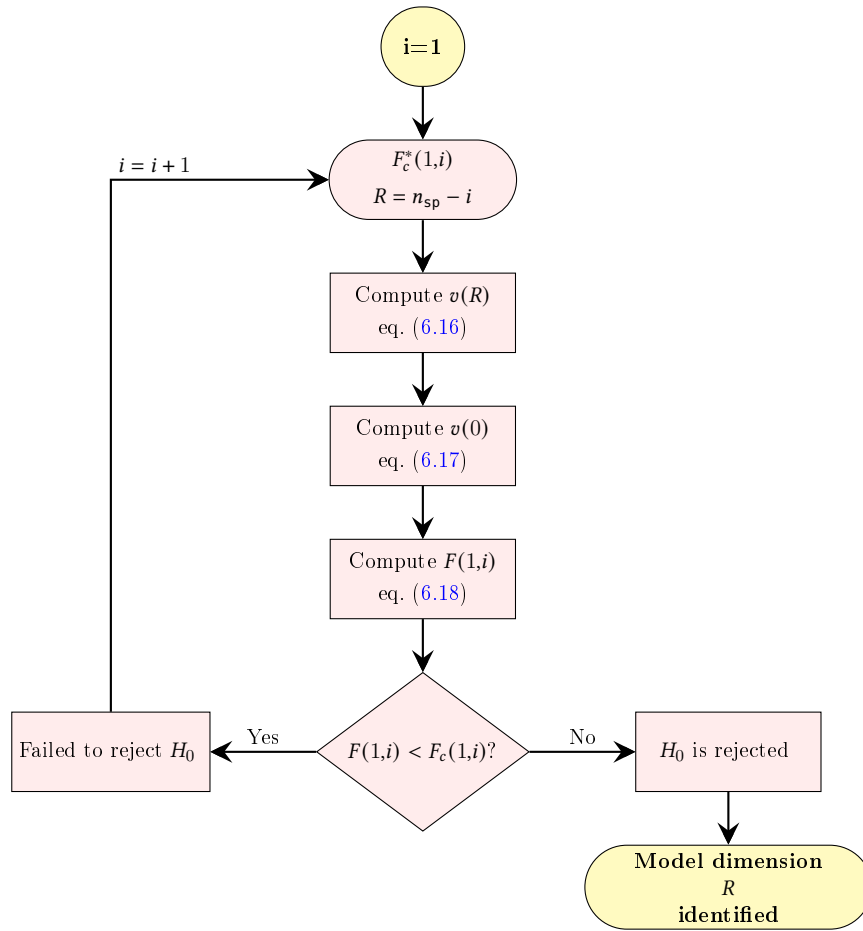
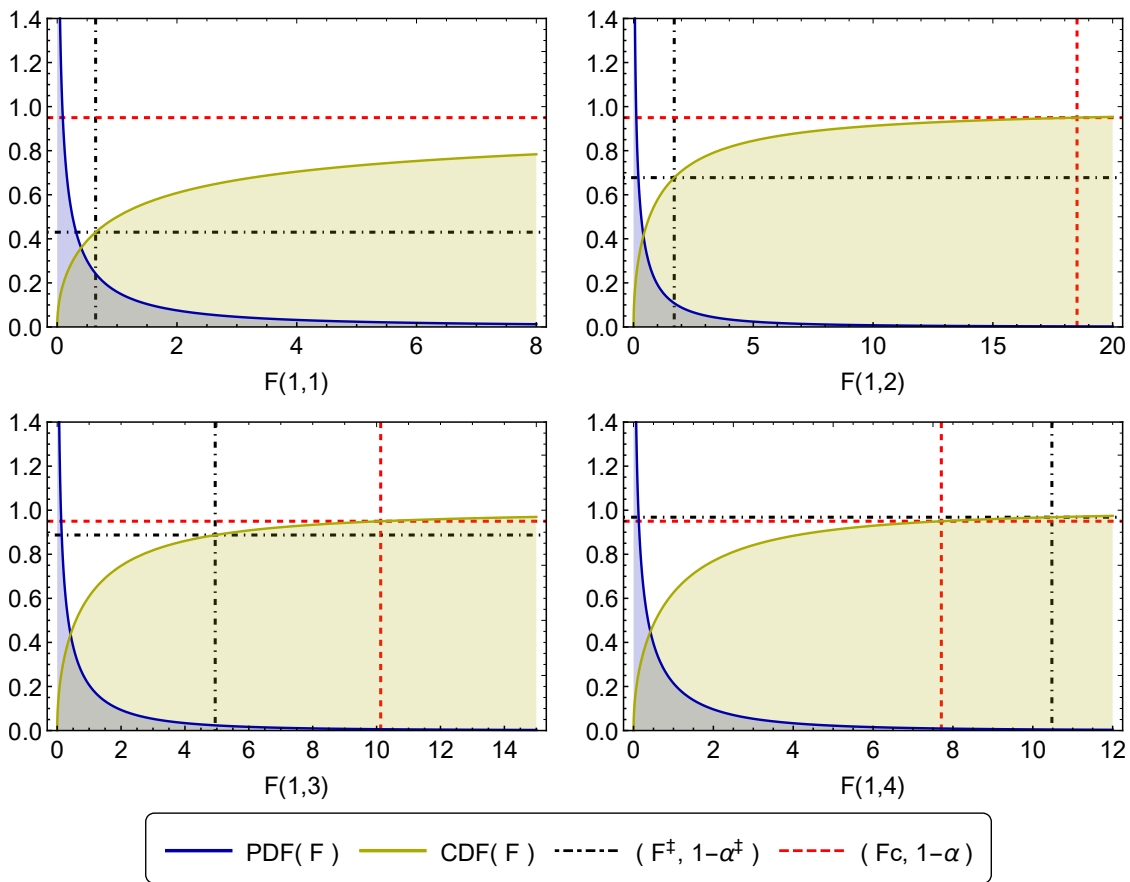


Figure 6.9 F-test diagram.

Table 6.2 F-test results.  $F_c$ : critical  $F$  value for  $\alpha = 5\%$ .  $\alpha^\ddagger$  indicates the percentage of the remain CDF function for each  $F$  observed (cutoff value if that  $F$  was considered critical).

$R$	$n_{sp} - R$	$v(R) \times 10^5$	$v(0) \times 10^5$	$F(1, n_{sp} - R)$	$F_c(1, n_{sp} - R)$	$\alpha^\ddagger$ [%]	$H_0$
9	1	1.580	2.461	0.642	161.448	56.996	Failed to reject
8	2	1.590	0.936	1.699	18.513	32.227	Failed to reject
7	3	2.854	0.577	4.947	10.128	11.260	Failed to reject
6	4	5.717	0.546	10.478	7.709	3.176	Rejected
5	5	6.493	0.674	9.640	6.608	2.671	Rejected
4	6	8.986	0.711	12.635	5.987	1.200	Rejected
3	7	216.277	0.780	277.389	5.591	0.000	Rejected
2	8	367.114	6.600	55.621	5.318	0.007	Rejected
1	9	22044.500	12.936	1704.150	5.117	0.000	Rejected

indicating the respective PDF (probability density function) and CDF (cumulative density function) values. These profiles, in accordance with the results shown in Table 6.2, present  $F < F_c$  until the 3-dimensional pool size (the vertical dashed line is located to the right of the vertical black dotdashed line, as such as the horizontal dashed line is located above of the horizontal black dotdashed line). When the fourth lowest component is scrutinized, the opposite behavior is observed, *i.e.*,  $F > F_c$ . Therefore, this last result indicates that the sixth model component (concerning the sixth greater singular value) is signal (and not noise), *i.e.*, it contains structural information related to the data variability that is greater than the noise variability, and hence, it must not be discarded to the pool of the null space of data.



**Figure 6.10**  $F$ -distributions for several dimensions of invariant pools. The blue and green curves indicate the PDF and CDF values for the respective  $F$  (variances ratio). The red dashed lines indicate  $F_c$  (x-axis) concerning an  $\alpha = 5\%$  (y-axis). The black dotdashed lines indicate the observed  $F$  (x-axis) and the respective  $\alpha^{\dagger}$  (y-axis).

The result obtained  $R = 6$  does not correspond to the real dimension of the model  $R = 8$ . This indicates that the last two real variant data dimensions are of the same magnitude of the noise variance, and therefore, they cannot be identified using the criterion established by the  $F$ -test. Moreover, considering  $R = 6$  as the dimension of the data variant space would lead to the assumption that the data invariant space is 4-dimensional. This

assumption is wrong since no more than two time-invariant relationships exists. Consequently, it is a good idea to look for the establishment of meaningful time invariants in simultaneous with the identification of  $R$  in order to well elucidate the data variant and invariant spaces dimensions. In accordance with this idea, the method proposed in this work looks for the establishment of meaningful time-invariant relationships in the right singular vectors of the experimental data matrix using optimization tools (Section 6.6.2). Next section presents a non-parametric test for the identification of the variant data space dimension.

### 6.5.2 Cross-validation

In this section the cross-validation method is used to identify the data dimension by estimating how much is signal and how much is noise in a dataset. Noise in this case refers to uncontrolled experimental and instrumental variations arising from random processes (Wise and Ricker, 1991). The  $k$ -fold cross-validation is considered. The procedure starts by splitting data in  $k$  groups of randomized data, and one of these groups (at a time) must be removed from the original set of data. The removed dataset is called the *test* or *validation* set with size  $n/k$ , where  $n$  is the number of observations. The remain data is called the *train* set of data that, after removing the test set, presents  $n - n/k$  observations. It is over the train set that the SVD is performed in order to build a principal component (PC) model, in which the number of significant components ( $R$ ) is what we desire to determine. Hence, the PC model is built considering several candidate dimensions. On the other hand, it is over the test set that the prediction error is evaluated using the obtained PC model that was trained without this test set. The procedure of evaluating the prediction error must be repeated for all  $k$  groups of test, and the decision of the model dimension is based on the lowest total prediction error found. Therefore, the goal is to find the number of components for which adding more components does not provide a better description (in an overall least squares sense) of the data not previously included (Bro et al., 2008). The prediction error of the test set in this cross-validation procedure is called PRESS-CV (predicted residual error sum of squares evaluated in a cross-validating approach).

The evaluation of the PRESS-CV, *i.e.*, the identification of the model dimension for which PRESS-CV is minimum, presents a meaningful criterion (with very good performance) for linear models of the type  $\mathbf{y} = \mathbf{X}\mathbf{b}$  in which the residues are computed by the differences  $\mathbf{y} - \hat{\mathbf{y}}$ , *i.e.*, the prediction  $\hat{\mathbf{y}}$  is computed using the predictor variables  $\mathbf{X}$ . On the other hand, the evaluation of PRESS-CV in PC models, as it was originally proposed, does not result in a good criterion, since there are no dependent and independent variables (all variables are treated together), *i.e.*, the error is evaluated by computing the difference  $\mathbf{X} - \hat{\mathbf{X}}$ , where the variables  $\mathbf{X}$  are used to predict  $\hat{\mathbf{X}}$ , and consequently, the residuals from the model of  $\mathbf{X}$  are not independent of  $\mathbf{X}$  *i.e.*, the left-out elements and their predicted values are not independent, and therefore, the PRESS-CV decreases with increasing number of

components and never reaches a minimum (Bro et al., 2008). This result leads to the mistaken conclusion that all components are significant. Or in rare cases the PRESS-CV does reach a minimum, but still tends to overfit and overestimate the optimal model dimensionality (Amoeba, 2014).

In this work two evaluations of PRESS-CV were considered following the CV methods proposed by Wold (1978) and Eastment and Krzanowski (1982); Krzanowski and Kline (1995), respectively. However, both approaches showed an unsatisfactory monotonous decreasing PRESS-CV behavior due to the above presented reason (error dependence on  $\hat{\mathbf{X}}$ ) once the proposed CV methods were applied to PC models. Bro et al. (2008) made a comparison of several CV methods of evaluating PRESS-CV, where two additional methods were presented for PC models in which the described dependence of the error in  $\hat{\mathbf{X}}$  is avoided, namely the *cross-validation by eigenvector* and the *expectation maximization cross-validation*. In this work, the cross-validation by eigenvector is presented.

### Cross-validation by eigenvector

The algorithm is described as follows:

Divide the randomized  $n_{\text{to}}$  rows of  $\mathbf{D}$  in  $n_k$  groups.

(i) For every group  $k = 1, \dots, n_k$ , remove from  $\mathbf{D}$  the  $\frac{n_{\text{to}}}{n_k}$  rows respected to the group  $k$ , forming two matrices:  $\mathbf{D}^{-k} [n_{\text{to}} - \frac{n_{\text{to}}}{n_k} \times n_{\text{sp}}]$  and  $\mathbf{D}^k [\frac{n_{\text{to}}}{n_k} \times n_{\text{sp}}]$  that concerns to the train data and test data matrices, respectively, such that  $\mathbf{D}^{-k} \cup \mathbf{D}^k = \mathbf{D}^2$ .

(ii) Compute the SVD model for  $\mathbf{D}^{-k}$ , resulting in the  $\mathbf{U}$ ,  $\mathbf{\Sigma}$  and  $\mathbf{V}$  matrices of dimensions  $[n_{\text{to}} - \frac{n_{\text{to}}}{n_k} \times n_{\text{to}} - \frac{n_{\text{to}}}{n_k}]$ ,  $[n_{\text{to}} - \frac{n_{\text{to}}}{n_k} \times n_{\text{sp}}]$  and  $[n_{\text{sp}} \times n_{\text{sp}}]$ , respectively.

(iii) For every variable  $s = 1, \dots, n_{\text{sp}}$ , update the  $\mathbf{D}^k$  by removing the entire column concerning the variable  $s$  resulting in a matrix  $\mathbf{D}_*^k [\frac{n_{\text{to}}}{n_k} \times n_{\text{sp}} - 1]$ , and the respective removed column vector  $\mathbf{d}_s^k [\frac{n_{\text{to}}}{n_k} \times 1]$ .

(iii-a) For every candidate model dimension  $R = 1, \dots, n_{\text{sp}}$ , compute the projection matrix without considering the variable component  $s$  that was excluded in (iii).

For this purpose, first select column 1 to  $R$  of  $\mathbf{V}$  from (ii) forming a matrix  $\mathbf{V}_R [n_{\text{sp}} \times R]$ , then update  $\mathbf{V}_R$  by excluding the entire row  $s$  respected to the  $s$  variable excluded in  $\mathbf{D}_*^k$ , resulting in a  $\mathbf{V}_{R*} [n_{\text{sp}} - 1 \times R]$ , and in an excluded vector  $\mathbf{v}_{R,s} [R \times 1]$  (notice that when  $R = 1$ ,  $\mathbf{v}_{R,s}$  is a scalar). The projection matrix  $\mathbf{M} [n_{\text{sp}} - 1 \times R]$  is computed through

$$\mathbf{M} = \mathbf{V}_{R*} \cdot (\mathbf{V}_{R*}^T \cdot \mathbf{V}_{R*})^{-1} \quad (6.21)$$

(iii-b) Predict the score  $\mathbf{T} [\frac{n_{\text{to}}}{n_k} \times R]$  of the excluded variable  $s$  of the test set  $k$  (that we

---

<sup>2</sup>Notice that the superscripts “ $k$ ” and “ $-k$ ” indicate the data matrices referred to the test and train data, respectively, and not to powers of  $\mathbf{D}$ .

want to predict,  $\hat{\mathbf{d}}_s^k$ ) by projecting  $\mathbf{D}_*^k$  onto  $\mathbf{M}$ :

$$\mathbf{T} = \mathbf{D}_*^k \cdot \mathbf{M} \quad (6.22)$$

Notice that  $\mathbf{T}$  is a reconstruction of the  $\mathbf{U}^k \cdot \Sigma^k$  with  $\mathbf{U}^k [\frac{n_{to}}{n_k} \times R]$  and  $\Sigma^k [R \times R]$  concerning to the  $s$  variable that was excluded of the  $k$  test set that is going to be predicted.

(iii-c) Compute the prediction of the excluded variable of the test set  $\hat{\mathbf{d}}_s^k [\frac{n_{to}}{n_k} \times 1]$  by

$$\hat{\mathbf{d}}_s^k = \mathbf{T} \cdot \mathbf{v}_{R,s} \quad (6.23)$$

(iii-d) Compute the error of prediction of the excluded variable component  $\mathbf{e}_s [\frac{n_{to}}{n_k} \times 1]$

$$\mathbf{e}_s = \mathbf{d}_s^k - \hat{\mathbf{d}}_s^k \quad (6.24)$$

(iii-e) Store the sum of squares of the  $\mathbf{e}_s$  entries, *i.e.*, store in a list the scalar  $\mathbf{e}_s^T \cdot \mathbf{e}_s$ .

At the end of the loop defined by (iii-a) to (iii-e), the list of  $\mathbf{e}_s^T \cdot \mathbf{e}_s$  values with dimension  $[1 \times n_{sp}]$  concerns to the sum of square errors in each  $R = 1, \dots, n_{sp}$  candidate model dimension for a single variable  $s$  removed. Repeating the procedure for every variable  $s = 1, \dots, n_{sp}$  from item (iii) to (iii-e), a list of errors is obtained with dimension  $[n_{sp} \times n_{sp}]$  where every row concerns to a different excluded variable. Thus, the sum of rows of this error matrix can be performed indicating the total error for predicting the test set  $k$  for every candidate model dimension  $R = 1, \dots, n_{sp}$  in the new list  $[1 \times n_{sp}]$ . Finally, the entire procedure (i) to (iii-e) must be repeated for every  $k$  test set, and, at the end of this sequence of repeated procedures, it is expected to obtain a list of  $[n_k \times n_{sp}]$  containing in its rows the previous results (the total error for predicting the test set  $k$  for every candidate model dimension  $R = 1, \dots, n_{sp}$ ). Again, regarding this final matrix, the sum of the rows must be computed in order to obtain, finally, the PRESS-CV value for every candidate model dimension  $R = 1, \dots, n_{sp}$ .

Wise and Ricker (1991) and Bro et al. (2008) describe this problem as: “In essence, this is a missing data problem where the missing variable is predicted from the model and the sample observation excluding the one variable.”.

### Application of cross-validation by eigenvector and discussion of the results obtained

The same dataset that has been analyzed in this chapter is considered for the application of cross-validation by eigenvector method. The entire dataset without noise was presented in Figure 6.5. Gaussian noise was added to this data with zero mean and 0.005 standard deviation.

The singular value list of noisy data is

$$\tilde{\sigma} = \{22.271, 2.720, 1.964, 0.374, 0.293, 0.251, 0.158, 0.102, 0.083, 0.073\}$$

while without noise added is

$$\sigma^* = \{22.273, 2.719, 1.969, 0.372, 0.283, 0.242, 0.126, 0.075, 0.000, 0.000\}$$

Hence the true data dimension is eight, and the objective of the application of this method is to identify the true data dimension even in the presence of noise.

The *leave-one-out* (LOO) and the  $k$ -fold CV methods were considered, (actually LOO is a particular case of  $k$ -fold, *i.e.*, LOO happens when  $k$  equals the number of data observations). However, since in practice the matrix  $\mathbf{D}$  is composed by 15 batches when performing the traditional LOO (*i.e.*, taking one-to-one row among 225 rows), no disturbance is expected to be observed since the model will be able to predict the data removed very well. The reason for this expected result is because  $\mathbf{D}$  presents a systematic behavior over time (in the matrix lines) for all chemical species, in which repeated patterns can be seen in every 15 rows of the matrix (*i.e.*, an approximately periodic behavior of data can be observed in the rows of  $\mathbf{D}$ , see Figure 6.5). Therefore, in order to turn effective the CV procedure, for both LOO and  $k$ -fold methods, the test samples were collected following the adopted criterion: when taking one row of the first experiment (line 1 to 15) the same row in the second, and the third, and so on, until the 15th experiment are also collected for test. For example, in the LOO approach, the lines {1, 16, 31, 46, 61, 76, 91, 106, 121, 136, 151, 166, 181, 196, 211} were taken for test in the first procedure iteration, *i.e.*, in every iteration 15-stepped lines are taken for the test dataset. Therefore, in LOO the test set has always dimension [15 × 10]. The same approach was adopted for  $k$ -fold. In this case the randomization of the first 15 rows of  $\mathbf{D}$  was considered first, and then, the division in 5 groups ( $k = 5$ ) of dimension 3 was considered. Therefore, the same 15-stepped lines were taken for the test set, resulting in a test set of dimension [45 × 10] for every  $k$  group. This decision of selecting the same lines in every batch experiment was made intuitively in order to turn effective the CV procedure, since, contrarily, the trained model would still predict very well the test datasets for irregularly spaced (unordered) 45 selected rows of the matrix.

Figure 6.11 presents the PRESS-CV for the adopted approaches of sampling test datasets concerning to LOO and  $k$ -fold approaches. In these plots, a flat behavior of the PRESS-CV curve is observed between the components of the model 3 to 8, indicating that the prediction ability of the model remains approximately indifferent for models with these dimensions. This is an unexpected result, since we would like to see sharp PRESS-CV profiles. If we were taking a more data-driven approach, the choice of the optimal model size would be, probably, 3 components. However, in a more conservative approach, it is preferable to remain with eight dimensions in the model since only from the ninth

dimension that PRESS-CV is sharply increased, showing, clearly, the presence of noise in this dimension.

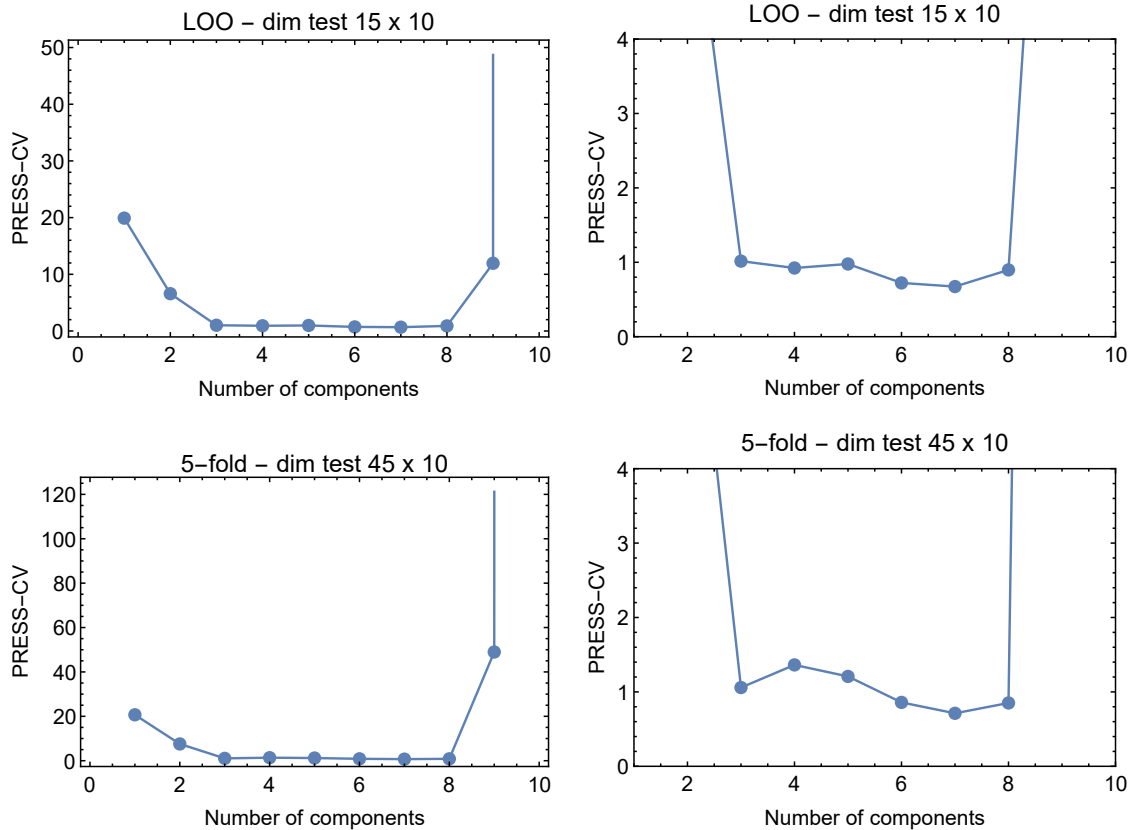


**Figure 6.11** PRESS-CV for LOO and  $k$ -fold cross-validation. Plots zoomed-in on the right-hand side.

Moreover, when looking for the zoomed-in plots of both sampling approaches (specially in the  $k$ -fold approach) slight fluctuations can be observed in the PRESS-CV profiles, decreasing, increasing and decreasing again. This behavior can be explained by the error associated with the sampling method since only one global procedure was performed. If the same global procedure of sampling (for randomized samples of the same size) is repeated many times, a distribution of PRESS-CVs is obtained for every model dimension, and the mean value of these distributions approaches the expected value PRESS-CV, *i.e.*, the real one, if an enough number of repeated procedures is considered. In this case, it is expected that the mean PRESS-CV would not oscillate among model components. However, once the magnitude of the oscillation observed is pretty low, we accept this result as sufficiently significant or representative of the study performed, concluding this analysis. Therefore, from this perspective the PRESS-CV using different sampling techniques for test data did not change much, *i.e.*, the results obtained for LOO and  $k$ -fold, are practically the same, and, adopting a conservative approach the model follows with eight dimensions.

### 6.5.3 Hard-thresholding

Truncation may be seen as a hard threshold on singular values, where values greater than a threshold  $\tau$  are selected, while remaining singular values are truncated (Brunton and Kutz, 2019). Gavish and Donoho (2014) proposed an optimal way to truncate the singular values under the assumption that data is contaminated with Gaussian white noise, providing a principled approach to obtaining low-rank matrix approximations using the SVD. The noisy data  $\mathbf{D}[n \times m]$  can be divided in two matrices

$$\mathbf{D} = \mathbf{D}_{\text{true}} + \gamma \mathbf{D}_{\text{noise}} \quad (6.25)$$

where  $\mathbf{D}_{\text{noise}}$  presents Gaussian properties, *i.e.*, zero mean, unity variance and normal distribution, and  $\gamma$  is a scale factor of that noise that can amplify or decrease it. When the noise magnitude  $\gamma$  is known, there are closed-form solutions for the optimal hard threshold  $\tau$

$$\tau = \lambda(\beta) \sqrt{n} \gamma \quad (6.26)$$

$$\lambda(\beta) = \left( 2(\beta + 1) + \frac{8\beta}{(\beta + 1) + (\beta^2 + 14\beta + 1)^{1/2}} \right)^{1/2} \quad (6.27)$$

where  $\beta = m/n$ , if  $m \leq n$ . Therefore, the  $\tau$  value is only a function of the data matrix aspect ratio  $\beta$  and the noise magnitude  $\gamma$ . To understand how these formulas are derived see (Gavish and Donoho, 2014).

#### Application of hard-thresholding

For the same case study that has been analyzed during this chapter in which the data matrix has dimension  $[225 \times 10]$  and the noise added has magnitude equal to its standard deviation 0.005, the parameters are

$$\beta = 0.044, \quad \gamma = 0.005, \quad \lambda(\beta) = 1.497 \quad \text{and} \quad \tau = 0.112.$$

Figure 6.12 presents the logarithm of the singular values and the hard threshold, indicating that the optimal truncation found is at the seventh dimension.

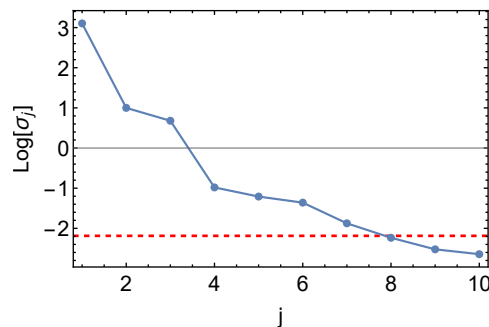


**Figure 6.12** Singular values  $\sigma_j$  and optimal hard threshold  $\tau$  (red dashed line).



## 6.6 Determining the invariant data space using optimization

In this section two MILP formulations for determining invariant relationships are presented. The first concerns to the determination of *reaction invariants* since the conserved relations are obtained using system stoichiometry. The second is related to the identification of *time invariants* since the conserved relations are elucidated from experimental data. However, both reaction and time invariants should span the same space, and ideally they should coincide. Thus, we chose not to distinguish the terms reaction- and time-invariant relationships in the thesis, but in the next sections we separate the two terms to make the description of the formulation under analysis easier to locate.

### 6.6.1 Methodology for evaluating reaction-invariant relationships

As previously discussed in the chapter's introduction, one basic way of computing invariant relationships is by solving the homogeneous equations  $\mathbf{N} \cdot \mathbf{A}^T = \mathbf{0}$ . However, in order to obtain physically meaningful conservation amounts this solution must attend additional constraints: it must present integer and positive entries. The next section presents a MILP formulation for the obtainment of the sparsest positive solutions that span the null space of the stoichiometric matrix.

#### MILP formulation

The conserved amount of a given invariant relationship, defined as  $x_s$ , is a variable of the problem that we want to determine. It must be an integer number assuming an amount as lowest as possible (*i.e.*, with physical meaning), subjected to be part of a vector that lies in the null space of the stoichiometric matrix. Hence, the objective function (6.28a) represents the minimum sum of conserved amounts in species, while the constraint (6.28b) establishes the time invariant relationship, where  $v_{s,j}$  is the stoichiometric coefficient of species  $s \in \text{sp}$  in reaction  $j \in \text{rx}$ .

The complete mathematical formulation for the generation of candidate invariant relationships can be written as an integer programming:

$$\min_{x_s} \quad \phi = \sum_{s \in \text{sp}} x_s \quad (6.28a)$$

$$\text{s.t.} \quad \sum_{s \in \text{sp}} x_s v_{s,j} = 0, \quad \forall j \in \text{rx} \quad (6.28b)$$

$$\sum_{s \in \text{sp}} x_s \geq 1 \quad (6.28c)$$

$$x_s \in \mathbb{N}, \quad \forall s \in \text{sp} \quad (6.28d)$$

In order to enumerate viable solutions and, as far as possible, to obtain linearly independent solutions, integer cuts are added to the formulation in every solver iteration until no other solution can be generated satisfying the imposed constraints. For this purpose, the use of an additional binary variable  $y_s$ , that indicates that species  $s$  is participating in the conserved relationship, is required. For formulating this last condition, BigM-type constraints (Raman and Grossmann, 1991) are considered, as shown in (6.29). The optimal values of  $y_s$  for every feasible solution  $k \in K$  are stored in the parameter  $\text{ccy}(s,k)$  after the first iteration (6.30), to then impose the integer-cut equations (6.31), prohibiting solutions with the same species group from participating in an invariant relationship.

$$y_s M \geq x_s \geq y_s, \quad \forall s \in \text{sp} \quad (6.29)$$

$$y_{s,k} = \text{ccy}_{s,k-1}, \quad \forall s \in \text{sp}, k = 2, \dots, K \quad (6.30)$$

$$\sum_{s \in \text{sp}} \text{ccy}_{s,k} y_s - \sum_{s \in \text{sp}} (1 - \text{ccy}_{s,k}) y_s \leq \sum_{s \in \text{sp}} \text{ccy}_{s,k} - 1, \quad k = 2, \dots, K \quad (6.31)$$

### 6.6.2 Methodology for evaluating time-invariant relationships

The objective of this method is to determine the number of time invariant relationships  $\text{nin}_{\text{li}} = n_{\text{sp}} - \text{nr}_{\text{x}_{\text{li}}}$ , or in other words, the data invariant space dimension, and consequently, identify the number of chemical reactions  $\text{nr}_{\text{x}_{\text{li}}}$  that the reaction network must present in order to span the data variant space. Supported on the SVD of data, the analysis of candidate time-invariant relationships is performed over the right singular vectors respecting data/model component directions with lower variances. Time invariants are quantities that have physical significance, *i.e.*, present positive, integer and (preferably) low magnitude values. On the other hand, the the right singular vectors present rational, positive and negative numbers. Using optimization tools, meaningful time-invariant relationships are searched from the abstract (orthonormal) vectors by linear transformation of bases.

A MILP formulation was developed, where a linear transformation of the abstract matrix that spans the null space of noisy data is performed in order to obtain a new basis composed by sparsest vectors with non-negative numbers between 0 and 1. Each conserved amount in the invariant relationship is associated with a binary variable, through big-M type constraints. Once the most sparse feasible invariant relationships are searched, the objective function consists of the minimization of the total amount given by the sum of the binary variables subjected to few linear constraints. Several null space dimensions are considered with  $1, 2, \dots$  and  $X$  basis vectors, where  $X$  is the number of singular values that presents a magnitude equal of or lower than the data noise variance. Thus, the matrix of invariant relationships with physical meaning is established by interpreting the

obtained results in two procedures: first by transforming the conserved quantities (non-negative numbers between 0 and 1) into fractions, second by finding the least common multiple of these fractions. The program is run for all dimensions of bases, and those that present very high invariant amounts are classified as not plausible to describe the left null space of the stoichiometric matrix. Hence the criterion to identify  $\mathbf{nin}_{\mathbf{i}}$  is established by comparison of the solutions obtained, *i.e.*, by exclusion of the results that present no physical meaning.

Notice that this formulation is based on the assumption that the space spanned by the the abstract basis (the noisy data null space) approaches the left null space of the stoichiometric matrix, since the noise is captured by the singular values, and therefore, their component directions (right singular vectors) still at most close to the the real time-invariant relationships.

### MILP formulation

The orthonormal matrix  $\mathbf{V}^T [n_{\mathbf{sp}} \times n_{\mathbf{sp}}]$  (full rank) that spans row ( $\mathbf{D}$ ) is considered from the SVD ( $\mathbf{D}$ ). The formulation starts by considering only the last row of  $\mathbf{V}^T$  (a single transposed vector of dimension  $[1 \times n_{\mathbf{sp}}]$ ) with  $\mathbf{nin}_{\mathbf{i}} = 1$  in the first iteration, to then increase  $\mathbf{nin}_{\mathbf{i}}$  in one unity by selecting the  $\mathbf{nin}_{\mathbf{i}}$  last rows of  $\mathbf{V}^T$  (obtaining a matrix of dimension  $[\mathbf{nin}_{\mathbf{i}} \times n_{\mathbf{sp}}]$ ) in consecutive problem iterations. The criterion established is that: if the required dimension of the null space is not reached, no meaningful solution can be obtained. On the other hand, if more component vectors are considered than the actual required dimension of the invariant space, no improvement is achieved in the results.

The parameter  $\mathbf{inA}_{i,s}$  is formed through the last  $\mathbf{nin}_{\mathbf{i}}$  rows of the matrix  $\mathbf{V}^T$ , with  $i \in \mathbf{in}$  ( $i = 1, \dots, \mathbf{nin}_{\mathbf{i}}$ ) respected to the candidate *abstract* invariant relationship and  $s \in \mathbf{sp}$  ( $s = 1, \dots, n_{\mathbf{sp}}$ ) to the chemical species. Hence,  $\mathbf{inA}_{i,s}$  is the amount conserved concerning the invariant  $i$  and species  $s$ . These values are rational numbers in which every row vector  $\mathbf{inA}_{i,*}$ ,  $i = 1, \dots, \mathbf{nin}_{\mathbf{i}}$  has unitary length and is orthogonal with the other ones.

The continuous variable  $\tau_i$ ,  $i = 1, \dots, \mathbf{nin}_{\mathbf{i}}$ , establishes the linear transformation of  $\mathbf{inA}_{i,s}$ , such that

$$\sum_{i \in \mathbf{in}} \mathbf{inA}_{i,s} \tau_i = x_s, \quad \forall s \in \mathbf{sp} \quad (6.32)$$

where  $x_s \in [0,1]$ , for every  $s = 1, \dots, n_{\mathbf{sp}}$ , is a continuous variable of the problem that represents the transformed conserved amount regarding the species  $s$ . The entire vector  $\mathbf{x} [n_{\mathbf{sp}} \times 1]$  is a linear combination of the abstract invariant basis. In each solver iteration only a single transformed invariant is obtained, *i.e.*, a single vector  $\mathbf{x}$ . Using integer cuts, in every solver iteration a new vector  $\mathbf{x}$ , that is linearly independent of the previous generated ones, is obtained. The loop of integer cuts stops when  $\mathbf{nin}_{\mathbf{i}}$  vectors  $\mathbf{x}$  are obtained. Those vectors span the same space of the abstract invariant basis.

Big-M type equations are required in order to, on the one hand, set  $x_s = 0$  when the species  $s$  does not contribute to the transformed invariant relationship ( $y_s = 0$ ), and, on the other hand, set lower and upper bounds to  $x_s$  when this species does contribute to the transformed invariant relationship ( $y_s = 1$ ), such as

$$x_s \leq y_s, \quad \forall s \in \text{sp} \quad (6.33)$$

$$x_s \geq y_s \epsilon, \quad \forall s \in \text{sp} \quad (6.34)$$

where  $y_s \in \{0,1\}$  is a binary variable that indicates the species  $s$  as contributor to the invariant phenomenon, and  $\epsilon$  is a small value of the same magnitude of the data uncertainty (noise standard deviation).

Another binary variable  $q_s \in \{0,1\}$  is required in order to ensure the normalization of  $x_s$ . This variable  $q_s$  is set one when  $x_s = 1$ , and is set zero when  $x_s < 1$ :

$$x_s \geq q_s, \quad \forall s \in \text{sp} \quad (6.35)$$

However, it is needed to enforce at least one  $x_s = 1$ :

$$\sum_{s \in \text{sp}} q_s \geq 1 \quad (6.36)$$

We are looking for sparse invariant vectors. For this purpose the objective function consists of the minimization of the number of species contributing to the invariant relationship:

$$z = \sum_{s \in \text{sp}} y_s \quad (6.37)$$

The complete mathematical formulation for the approximation of transformed invariant relationships from abstract null space of noisy data is written as:

$$\min_{\tau, x, y, q} z \quad (6.38a)$$

$$\text{s.t. Equations (6.32—6.37)} \quad (6.38b)$$

$$0 \leq x_s \leq 1, \quad \forall s \in \text{sp}. \quad (6.38c)$$

$$q_s \text{ and } y_s \in \{0,1\}, \quad \forall s \in \text{sp}. \quad (6.38d)$$

### 6.6.3 Application example, discussion of the results obtained and conclusion about the proposed method

The same case study under analysis in this chapter is considered here.

The solution of the problem (6.28) in Section 6.6.1 is presented during the case study

exposure in Section 11.3.2.

In order to test the formulation in (6.38), first we considered the  $\mathbf{V}^T$  from the SVD of the data matrix without added noise, to then consider noisy data. The results were obtained using GAMS® software with the solver CPLEX.

### Data without noise

The matrix  $\mathbf{inA}$  is shown below

$$\mathbf{inA} = \begin{array}{cccccccccc|l} & s=A & s=B & s=C & s=D & s=E & s=F & s=G & s=H & s=I & s=J & \\ \left[ \begin{array}{cccccccccc} -0.075 & 0.346 & 0.213 & 0.256 & -0.005 & 0.211 & 0.058 & -0.785 & 0.194 & -0.249 \\ -0.072 & 0.257 & 0.482 & -0.398 & 0.468 & 0.143 & -0.399 & -0.002 & -0.347 & 0.138 \\ 0.120 & -0.482 & -0.241 & -0.120 & -0.120 & -0.120 & -0.602 & -0.482 & 0.000 & 0.241 \\ 0.356 & 0.021 & 0.251 & 0.126 & 0.126 & 0.126 & 0.147 & 0.021 & 0.482 & 0.713 \end{array} \right. & \begin{array}{l} i=4 \\ i=3 \\ i=2 \\ i=1 \end{array} \end{array}$$

Considering in the first run only the  $i = 1$  abstract row vector of  $\mathbf{inA}$ , the vector  $\mathbf{x}$  obtained was

$$\mathbf{x} = [0.500 \quad 0.029 \quad 0.353 \quad 0.176 \quad 0.176 \quad 0.176 \quad 0.206 \quad 0.029 \quad 0.676 \quad 1.000]$$

which in fractional numbers (with a rest of inferior than 0.005) is

$$\mathbf{x}' = [1/2 \quad 1/34 \quad 5/14 \quad 3/17 \quad 3/17 \quad 3/17 \quad 4/19 \quad 1/34 \quad 17/25 \quad 1]$$

showing an unsatisfactory time-invariant relationship once very high values are presented.

In the second iteration the abstract vectors  $i = 1$  and  $i = 2$  were considered, obtaining the resulting  $\mathbf{x}$  matrix

$$\mathbf{x} = \begin{bmatrix} 0.000 & 0.750 & 0.500 & 0.250 & 0.250 & 0.250 & 1.000 & 0.750 & 0.250 & 0.000 \\ 0.500 & 0.625 & 0.750 & 0.375 & 0.375 & 0.375 & 1.000 & 0.625 & 0.875 & 1. \end{bmatrix}$$

which in fractional numbers is

$$\mathbf{x}' = \begin{bmatrix} 0 & 3/4 & 1/2 & 1/4 & 1/4 & 1/4 & 1 & 3/4 & 1/4 & 0 \\ 1/2 & 5/8 & 3/4 & 3/8 & 3/8 & 3/8 & 1 & 5/8 & 7/8 & 1 \end{bmatrix}$$

showing a very good and satisfactory time-invariant relationships, with physical significance.

In the third iteration the abstract vectors  $i = 1$ ,  $i = 2$  and  $i = 3$  were considered, obtaining the resulting  $\mathbf{x}$  matrix

$$\mathbf{x} = \begin{bmatrix} 0.000 & 0.750 & 0.500 & 0.250 & 0.250 & 0.250 & 1.000 & 0.750 & 0.250 & 0.000 \\ 0.500 & 0.000 & 0.333 & 0.167 & 0.167 & 0.167 & 0.167 & 0.000 & 0.667 & 1.000 \\ 0.566 & 0.000 & 0.211 & 0.402 & 0.000 & 0.151 & 0.522 & 0.120 & 0.911 & 1.000 \end{bmatrix}$$

which in fractional numbers is

$$\mathbf{x}' = \begin{bmatrix} 0 & 3/4 & 1/2 & 1/4 & 1/4 & 1/4 & 1 & 3/4 & 1/4 & 0 \\ 1/2 & 0 & 1/3 & 1/6 & 1/6 & 1/6 & 1/6 & 0 & 2/3 & 1 \\ 9/16 & 0 & 3/14 & 2/5 & 0 & 2/13 & 10/19 & 1/8 & 10/11 & 1 \end{bmatrix}$$

showing satisfactory time-invariant relationships only for the first two lines, The last line of  $\mathbf{x}'$  presents high values that are improbable to describe conserved amounts during the chemical reaction experiment. Therefore, there is no need to continue to the fourth null space dimension since the third dimension is signal, and consequently the fourth is signal too. Thus, without noise in the data, it was possible to correctly identify the invariant relationships.

### Data with noise

The matrix  $\mathbf{inA}$  is shown below

$$\mathbf{inA} = \begin{array}{cccccccccc|l} & \text{s=A} & \text{s=B} & \text{s=C} & \text{s=D} & \text{s=E} & \text{s=F} & \text{s=G} & \text{s=H} & \text{s=I} & \text{s=J} & \\ \left[ \begin{array}{cccccccccc} 0.196 & 0.080 & 0.006 & 0.262 & -0.208 & -0.262 & 0.384 & -0.181 & 0.556 & -0.534 \\ -0.271 & 0.404 & 0.039 & 0.096 & -0.058 & -0.051 & 0.493 & 0.444 & -0.493 & -0.252 \\ 0.121 & -0.151 & -0.244 & 0.238 & -0.537 & -0.495 & 0.090 & -0.220 & -0.346 & 0.369 \\ 0.277 & 0.198 & 0.269 & 0.191 & 0.107 & 0.091 & 0.390 & 0.244 & 0.315 & 0.667 \end{array} \right. & \begin{array}{l} i=4 \\ i=3 \\ i=2 \\ i=1 \end{array} \end{array}$$

Considering in the first run only the  $i = 1$  abstract row vector of  $\mathbf{inA}$ , the vector  $\mathbf{x}$  obtained was

$$\mathbf{x} = [0.416 \quad 0.296 \quad 0.403 \quad 0.287 \quad 0.160 \quad 0.137 \quad 0.585 \quad 0.366 \quad 0.473 \quad 1.000]$$

which in fractional numbers (with a rest of inferior than 0.005) is

$$\mathbf{x}' = [5/12 \quad 3/10 \quad 2/5 \quad 2/7 \quad 3/19 \quad 2/15 \quad 7/12 \quad 4/11 \quad 8/17 \quad 1]$$

showing an unsatisfactory time-invariant relationship once very high values are presented.

In the second iteration the abstract vectors  $i = 1$  and  $i = 2$  were considered, obtaining the resulting  $\mathbf{x}$  matrix

$$\mathbf{x} = \begin{bmatrix} 0.304 & 0.538 & 0.783 & 0.000 & 0.907 & 0.824 & 0.536 & 0.710 & 1.000 & 0.626 \\ 0.449 & 0.561 & 0.800 & 0.152 & 0.764 & 0.690 & 0.712 & 0.726 & 1.000 & 1.000 \end{bmatrix}$$

which in fractional numbers is (with rest lower than 0.005)

$$\mathbf{x}' = \begin{bmatrix} 3/10 & 7/13 & 11/14 & 0 & 10/11 & 14/17 & 7/13 & 5/7 & 1 & 5/8 \\ 4/9 & 9/16 & 4/5 & 2/13 & 13/17 & 9/13 & 5/7 & 8/11 & 1 & 1 \end{bmatrix}$$

showing unsatisfactory time-invariant relationships.

In the third iteration the abstract vectors  $i = 1$ ,  $i = 2$  and  $i = 3$  were considered, obtaining the resulting  $\mathbf{x}$  matrix

$$\mathbf{x} = \begin{bmatrix} 0.486 & 0.000 & 0.232 & 0.242 & 0.011 & 0.000 & 0.248 & 0.017 & 0.512 & 1.000 \\ 0.569 & 0.000 & 0.444 & 0.090 & 0.419 & 0.374 & 0.097 & 0.060 & 1.000 & 1.000 \\ 0.263 & 0.666 & 0.864 & 0.000 & 1.000 & 0.910 & 0.662 & 0.862 & 1.000 & 0.591 \end{bmatrix}$$

which in fractional numbers is (with lower than rest 0.005)

$$\mathbf{x}' = \begin{bmatrix} 13/27 & 0 & 3/13 & 5/21 & 1/90 & 0 & 1/4 & 1/57 & 15/29 & 1 \\ 4/7 & 0 & 4/9 & 1/11 & 5/12 & 3/8 & 1/10 & 1/16 & 1 & 1 \\ 4/15 & 2/3 & 13/15 & 0 & 1 & 10/11 & 2/3 & 13/15 & 1 & 10/17 \end{bmatrix}$$

showing unsatisfactory time-invariant relationships. However, if we compare this result with the previous solution, it can be observed that a worse result is obtained in this iteration, suggesting that the null space dimension is two.

In the third iteration the abstract vectors  $i = 1$ ,  $i = 2$  and  $i = 3$  were considered, obtaining the resulting  $\mathbf{x}$  matrix

$$\mathbf{x} = \begin{bmatrix} 0.252 & 0.000 & 0.133 & 0.118 & 0.000 & 0.024 & 0.103 & 0.122 & 0.000 & 1.000 \\ 0.000 & 0.660 & 0.312 & 0.330 & 0.035 & 0.000 & 1.000 & 0.646 & 0.023 & 0.000 \\ 0.315 & 0.061 & 0.341 & 0.000 & 0.426 & 0.354 & 0.083 & 0.000 & 1.000 & 0.000 \\ 0.410 & 0.000 & 0.376 & 0.000 & 0.451 & 0.391 & 0.014 & 0.000 & 1.000 & 0.414 \end{bmatrix}$$

which in fractional numbers is (with lower than rest 0.005)

$$\mathbf{x}' = \begin{bmatrix} 1/4 & 0 & 2/15 & 2/17 & 0 & 1/41 & 1/10 & 1/8 & 0 & 1 \\ 0 & 21/32 & 4/13 & 1/3 & 1/28 & 0 & 1 & 9/14 & 1/43 & 0 \\ 5/16 & 1/16 & 10/29 & 0 & 3/7 & 5/14 & 1/12 & 0 & 1 & 0 \\ 7/17 & 0 & 3/8 & 0 & 5/11 & 7/18 & 1/72 & 0 & 1 & 5/12 \end{bmatrix}$$

showing unsatisfactory time-invariant relationships. The same analysis performed in the previous solution can be made here, if we compare this result with the second iteration it can be observed that a worse result is obtained in this iteration, suggesting that the null space dimension is two. Therefore, with noise in the data, it was not possible to identify the invariant relationships.

### Discussion of the results obtained and conclusion about the proposed method

Unfortunately, the invariant relationships obtained are still contaminated with noise, and thus, the real conserved amounts are difficult to infer, therefore, noise is a problem. However, the dimension of the null space  $\text{nin}_{\mathbf{I}_i}$  may be elucidated by comparison of the results obtained. This is valuable information not only because  $\text{nr}_{\mathbf{x}_{\mathbf{I}_i}}$  is consequently identified as well, but also (i) to force the identification of  $\text{nin}_{\mathbf{I}_i}$  time invariants by another via, for example, through the assessment of the atomic matrix or structural analysis of molecules, and (ii) to request more elucidative experiments, registering (for example) additional species that could not be measured, and thus assist the process of identifying time invariants.

## 6.7 Comparative analysis of the applied methods

Table 6.3 presents a comparison of the data dimension identification methods discussed above, presenting the type of method, the information needed to carry out the method, the associated computational effort, and a critical observation.

It is difficult to say which will be the best method to identify the model dimension as this result depends a lot on the data itself (of the case study under analysis). However, in the presence of large datasets, the PRESS-CV will be a method that will always perform well with a high probability of being able to elucidate the model dimension correctly. In the

**Table 6.3** Comparison of previously discussed data dimension identification methods.

Method	Type	Requires	CPU effort	Critical observation
Scree-test	Heuristic	SVD (logarithm)	Low	Very dependent on the quality of the data and the system under study.
Fractional variances	Heuristic	SVD and noise level	Low	Need a threshold for the noise level in data.
Kaiser test	Heuristic	SVD and auto-scaling	Low	It has been shown in the literature to be a fallible criterion for several systems.
Replicated experiments	Theoretical/statistics	Repetition of experiences	Medium*	Critical method at the cost of real-life experiences.
Malinowski-test	Parametric	SVD, $F$ -statistics, hypothesis test	Low	Good method, reliable as it is supported by theoretical statistical concepts.
PRESS-CV	Non-parametric	Large datasets	High	Good method, but it needs a lot of data for the result to be representative of reality.
Hard-thresholding	Theoretical	Matrices dimension, noise level	Low	Method supported by deterministic theory and optimization
Reaction invariants	MILP	System stoichiometry	Low	Requires prior knowledge of the system under study.
Time invariants	MILP	SVD of data	Medium	Results lose reliability in the presence of high noise level.

\*Medium for *in silico* experiments and not applicable for real tests.

presence of a lot of data, this method becomes reliable since the chance of sampling bias is small in this case. Furthermore, there is the advantage of constituting a non-parametric method, free from initial assumptions regarding the population. In second place I would recommend the Malinowski test (or  $F$ -test). Certainly, the  $F$ -test is preferable in face of heuristic methods for determining model dimension. The reason for that is the presence of theoretical support given by the parametric method, instead of making decisions on the basis of heuristic and empirical rules.

Furthermore, with the results obtained through the application of the methods to determine  $\text{nr}x_{1i}$ , the message of this chapter is clear: for the identification of the model



dimension, a combined approach of methods to elucidate  $\text{nr}x_{1_i}$  and  $\text{nin}_{1_i}$  should be considered, given that both types of data analyzes are complementary and when carried out together they increase the degree of confidence in the obtained results.

## Bibliography

- Amoeba (2014). Naïve approach to PRESS for PCA. <https://stats.stackexchange.com/questions/93845/how-to-perform-cross-validation-for-pca-to-determine-the-number-of-principal-com>. Accessed: 2020-11-15.
- Bro, R., Kjeldahl, K., Smilde, A. K., and Kiers, H. (2008). Cross-validation of component models: a critical look at current methods. *Analytical and bioanalytical chemistry*, 390(5):1241–1251.
- Bro, R. and Smilde, A. K. (2003). Centering and scaling in component analysis. *Journal of Chemometrics*, 17(1):16–33.
- Bro, R. and Smilde, A. K. (2014). Principal component analysis. *Analytical Methods*, 6(9):2812–2831.
- Brunton, S. and Kutz, J. (2019). *Data-Driven Science and Engineering: Machine Learning, Dynamical Systems, and Control*. Cambridge University Press.
- Cattell, R. B. (1966). The scree test for the number of factors. *Multivariate behavioral research*, 1(2):245–276.
- Cliff, N. (1988). The eigenvalues-greater-than-one rule and the reliability of components. *Psychological bulletin*, 103(2):276.
- Eastment, H. and Krzanowski, W. (1982). Cross-validatory choice of the number of components from a principal component analysis. *Technometrics*, 24(1):73–77.
- Gavish, M. and Donoho, D. L. (2014). The optimal hard threshold for singular values is  $4/\sqrt{3}$ . *IEEE Transactions on Information Theory*, 60(8):5040–5053.
- Krzanowski, W. J. and Kline, P. (1995). Cross-validation for choosing the number of important components in principal component analysis. *Multivariate Behavioral Research*, 30(2):149–165.
- Lemons, D., Langevin, P., and Gythiel, A. (2002). *An Introduction to Stochastic Processes in Physics*. Johns Hopkins Paperback. Johns Hopkins University Press.
- Malinowski, E. R. (1989). Statistical f-tests for abstract factor analysis and target testing. *Journal of Chemometrics*, 3(1):49–60.
- Malinowski, E. R. and Howery, D. G. (1980). *Factor analysis in chemistry*. Wiley New York.
- Raman, R. and Grossmann, I. E. (1991). Relation between MILP modelling and logical inference for chemical process synthesis. *Computers & Chemical Engineering*, 15(2):73–84.

- Wise, B. and Ricker, N. (1991). Recent advances in multivariate statistical process control: improving robustness and sensitivity. In *Proceedings of the IFAC. ADCHEM Symposium*, pages 125–130. Citeseer.
- Wold, S. (1978). Cross-validatory estimation of the number of components in factor and principal components models. *Technometrics*, 20(4):397–405.

# Chapter 7

## Step 3 — Superstructure of the Reaction Network

*“What I cannot create, I do not understand.”*

– Richard Feynman

### Contents

---

7.1	Step 3 overview . . . . .	198
7.2	Generation of chemical reactions . . . . .	199
7.2.1	MILP formulation . . . . .	201
7.2.2	Application example — chemical reaction generation . . . . .	203
7.3	Target factor analysis (TFA) . . . . .	205
7.3.1	TFA critical analysis . . . . .	207
7.3.2	Application example . . . . .	209
7.4	Incorporation of thermodynamic feasibility criteria . . . . .	210
7.4.1	Application example — elucidating the energetically feasible reaction direction . . . . .	212
	Bibliography . . . . .	213

---

Step 3 consists of building the superstructure of the reaction network from a set of observed chemical species. For this purpose, the knowledge acquired from system-theoretical and data analyses in Steps 1 and 2 is required, regarding the properties of linear subspaces observed in experimental data in the variant form and the molecular formula and/or electrical charge of the chemical species, (when these last are available). In other words, the observed variant and invariant relationships are required in this step in order to build candidate reaction vectors for system’s stoichiometry that (i) may span the data variant space, and (ii) respect the observed invariant relationships.

Therefore, the construction of the reaction network superstructure consists of the elucidation of individual chemical reactions that are potential candidates to describe the observed compositional changes occurring in the reaction system. This step must be (i) systematic, ensuring a complete and unique description of the reactions among chemical species, avoiding repeated solutions, (ii) generic, *i.e.*, it can be applied to any chemical system, and (iii) flexible, in the sense that heuristic criteria and knowledge about the chemical system under analysis can also, and should, be incorporated in the formulation.

The next section describes the tasks carried out in this phase. A brief description of the methods to generate chemical reactions found in the literature is also presented, establishing a natural comparison between them and the proposed methodology of Step 3.

## 7.1 Step 3 overview

Smith and Missen (1982); Missen and Smith (1998, 2003) used Gauss-Jordan decomposition of the atomic matrix to find the homogeneous set of solutions that corresponds to stoichiometric balanced chemical reactions, *i.e.*, reactions among chemical species that verify conserved elemental amounts and other invariants such as electric charge, depending on the case study under analysis. An alternative method to generate balanced chemical reactions, also based on the atomic matrix, was developed by Pethő (1990, 1994) and Szalkai (1991, 2000). In this method a simplex is used, represented by a set of linearly dependent vectors which becomes linearly independent when a single vector is omitted. The objective is to find a basis that spans the null space of the unknown stoichiometric matrix. The main limitation of this approach is the difficulty in finding all possible simplexes, which may not be a simple task, requiring additional methods to enumerate all of them and avoid repeated solutions.

In the context of a systematic approach to identify reaction kinetic models, Tsu *et al.* (2019) have used MILP to obtain a set of stoichiometric balanced chemical reactions from observed species (with known molecular formula). The proposed MILP formulation is very similar to the one previously proposed by Vertis *et al.* (2017), in which the reaction stoichiometry is considered using (i) elemental mass balances, (ii) bounds on the stoichiometric coefficients, and (iii) restrictions on the number of species as reactants and products involved in the chemical reaction.

Other criteria, beyond stoichiometric constraints, may also be considered in the optimization procedure for chemical reaction generation, such as the thermodynamic viability of the chemical reaction. The energetic constraints, and the physical property data required for their implementation, can be considered in the reaction generation step either simultaneously with the reaction-invariant restrictions (Beard *et al.*, 2004), or in a *posteriori* phase (Vertis *et al.*, 2017), where these thermodynamic constraints are used to filter the solutions enumerated. Although the simultaneous approach could present an advantage in generating all the solutions that are stoichiometrically consistent with the energetically

feasible direction, it can be negatively influenced by the uncertainty in the physical data used (which needs to be frequently estimated from other properties), *i.e.*, the uncertainty of physical data could lead to the obtainment of solutions that present directions that in the practice could not be identified using that data, leading to the exclusion of the opposite direction that could be also a plausible candidate. However, this solution would need more data to confirm the right direction. Moreover, the nonlinear nature of the thermodynamic equations may require the use of nonlinear programming, while the remaining constraints are usually linear balance equations. For these reasons, the verification of the thermodynamic constraints can be postponed to a later phase, after the enumeration of solutions that satisfy the chemical system's invariants. This is the approach followed in this work.

The Step 3 is composed by three sequential sub-steps (see Figure 7.1) in which (i) a list of chemical reactions is obtained using a MILP to enumerate (through integer cut equations) feasible stoichiometric vectors that verify the identified invariant relationships, to then consider (ii) the assessment of individual reaction vectors from that list using TFA for evaluating whether they lie in the previously characterized data variant space, and, finally, (iii) the energetic analysis of the reaction net flux is performed for each individual stoichiometric vector in order to elucidate the respective thermodynamic feasible direction, based on the negative sign of the Gibbs free energy change.

The formulation (that will be presented in the next section) to generate chemical reactions concerns the same variables and type of constraints as the one proposed in Vertis *et al.* (2017), although it additionally incorporates structural invariant relationships that are previously identified during Steps 1 and 2 of the methodology. These invariant properties do not necessarily match elemental conservation since there may be cases in which not all chemical elements can be verified as constant among the registered species, especially in the absence of species measurements, and therefore, not all of them can be restricted to being preserved.

This chapter presents the description of the method for generating chemical reactions in Section 7.2, followed by the TFA technique presentation in Section 7.3, to then consider, finally, the reaction thermodynamics analysis in Section 7.4. Every sub-step is applied to the succinic acid case study.

## 7.2 Generation of chemical reactions

*“Nature did not invent the wheel.  
No, but nature did invent the catalytic cycle.”*

– Anónimo

Regardless the linear and nonlinear characteristics of the chemical reaction, the adopted reaction generation method is based on integer linear programming, where binary variables

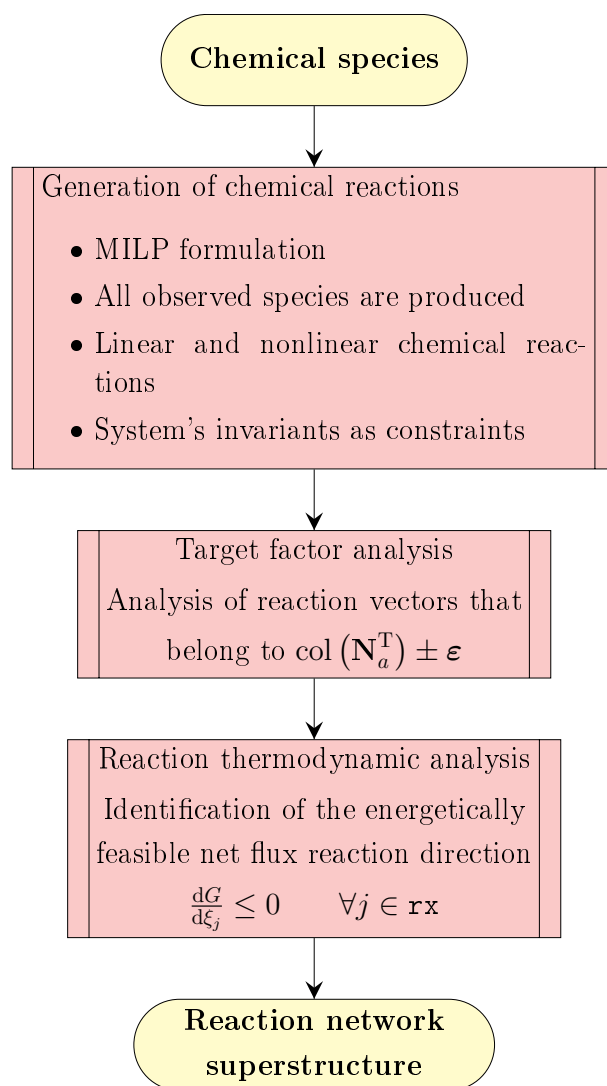


**Figure 7.1** Step 3 flowchart.

are used to decide whether a species is participating in a reaction and integer variables are used to define the species stoichiometric coefficients. The resulting formulation is solved through the enumeration of all feasible solutions using *integer cuts*. In each iteration of the optimization procedure a feasible reaction is generated, completing the enumeration when there is no additional feasible solution in accordance with the formulation constraints. Constraints of several nature can be considered to generate chemical reactions: (i) stoichiometry, the mass (elemental) is conserved in a closed system consisting of a reaction-invariant characteristic; (ii) thermodynamics, chemical reactions far from equilibrium occur in an energetic favorable direction where a negative variation of the Gibbs free energy is verified; (iii) reactivity, chemical physical properties of the molecules involved may be considered, *e.g.*, the collision of more than three molecules is improbable, certain ions must stay in the aqueous phase, etc; and (iv) kinetics.

### 7.2.1 MILP formulation

The observed species  $s \in \mathbf{st}$  are identified and separated into two sets: the representative and non-representative species sets, denoted by  $\mathbf{sp}$  and  $\mathbf{sd}$ , respectively, such that  $\mathbf{sp} \cup \mathbf{sd} \equiv \mathbf{st}$ <sup>1</sup>. Positive integer variables  $\mathbf{nre}_s$  and  $\mathbf{npr}_s$  are used to represent the stoichiometric coefficient of species  $s$  in the reactant and product sides respectively. (7.1) expresses the set of invariants equations considered, where  $a_{s,i}$  is the conserved amount  $i \in \mathbf{in}$  in species  $s \in \mathbf{sp}$ . These invariants, described over the set  $\mathbf{in}$ , always include elemental mass conservation equations, in which the chemical elements  $e \in \mathbf{el}$ , that make up the various species, are a subset of the invariants set ( $\mathbf{el} \subset \mathbf{in}$ ).

$$\sum_{s \in \mathbf{st}} a_{s,i} (\mathbf{nre}_s - \mathbf{npr}_s) = 0, \quad \forall i \in \mathbf{in} \quad (7.1)$$

Binary variables  $\mathbf{yre}_s$  and  $\mathbf{ypr}_s$  are used to denote the existence of the species  $s$  as reactant and as product (respectively) in the reaction. A species cannot simultaneously be reactant and product in the same reaction, (7.2) expresses their exclusive disjunction.

$$\mathbf{yre}_s + \mathbf{ypr}_s \leq 1, \quad \forall s \in \mathbf{st} \quad (7.2)$$

The stoichiometric coefficients are linked to these binary variables through logic constraints, where  $U_s$  represents an upper bound to the stoichiometric coefficient, (7.3) right side. Also, when species  $s$  is selected as reactant or as product, its respective stoichiometric coefficient has to be greater or equal to one, (7.3) left side. The form of these constraints are well known in the literature as big-M. Big-M constraints are frequently used in the development of MILP models (Griva et al., 2009).

$$\begin{aligned} \mathbf{yre}_s &\leq \mathbf{nre}_s \leq \mathbf{yre}_s U_s, \quad \forall s \in \mathbf{st} \\ \mathbf{ypr}_s &\leq \mathbf{npr}_s \leq \mathbf{ypr}_s U_s, \quad \forall s \in \mathbf{st} \end{aligned} \quad (7.3)$$

In order to control the desired linear or nonlinear structure of the chemical reaction, in (7.4), the parameter  $U'$  is set.

$$\sum_{s \in \mathbf{sp}} \mathbf{yre}_s \leq U', \quad \sum_{s \in \mathbf{sp}} \mathbf{ypr}_s \leq U' \quad (7.4)$$

Note that linear chemical reactions,  $U' = 1$ , can occur between (i) two representative species  $s \in \mathbf{sp}$  such as isomerization reaction type, and (ii) two representative species  $s \in \mathbf{sp}$  involving also dependent species  $s \in \mathbf{sd}$ . While nonlinear chemical reactions,  $U' > 1$ , occur between more than two species  $s \in \mathbf{sp}$ , involving or not dependent species  $s \in \mathbf{sd}$ . There is a particular linear case, the *pseudo-linear* chemical reactions. In pseudo-linear reactions, although the stoichiometric coefficients of the representative reactant and

---

<sup>1</sup>The partition of species is considered according to the criterion chosen for representing linear graphs, as previously discussed in Section 2.3.

product species are not the same, their graph representation remain linear, for example the reaction  $2A \rightarrow B$ . Thusly, the bound  $U_s$  in (7.3) has to be tuned depending on the linear reaction type under analysis.

The equation (7.5) ensures the startup of the optimization problem, guaranteeing the achievement of one non null solution.

$$\sum_{s \in \text{st}} y_{\text{re}_s} \geq 1 \quad (7.5)$$

By solving this problem, the chemical reactions can be enumerated establishing any criteria of sorting. In this case, the objective function (7.6) minimizes the variable `ordrx`, establishing a canonical order to sequentially generate chemical reactions with the lowest total mole number first.

$$\text{ordrx} = \sum_{s \in \text{sp}} n_{\text{re}_s} + n_{\text{pr}_s} \quad (7.6)$$

Alternative solutions are enumerated through the incremental inclusion of *integer cuts* in the binary variables that respect the presence of species in the optimal solution. Once obtained the first solution,  $k = 1$  (index of the corresponding solution), the counter `it` is activated, and, the integer cuts are successively added in every  $k$  iteration. The obtained solutions  $k \in \text{it}$  are stored in the parameters `ccres,k` and `ccprs,k` for the use of the next integer cuts. Note that `it` is a dynamic set, with increasing size in every iteration. The program stops when there are not any more solutions that satisfy the imposed constraints. The integer cuts equations ensure, by (7.7), the uniqueness of the generated reactions, and also identify, by (7.8), the reaction in only one aleatory direction. For example, when the reaction  $A \rightarrow B$  is identified, the (i) same reaction, (ii) equivalent reactions (*e.g.*,  $2A \rightarrow 2B$ ), and also, (iii) the reverse one  $B \rightarrow A$  are forbidden to be generated.

$$\sum_s \text{ccre}_{s,k} y_{\text{re}_s} + \sum_s \text{ccpr}_{s,k} y_{\text{pr}_s} - \sum_s (1 - \text{ccre}_{s,k}) y_{\text{re}_s} - \sum_s (1 - \text{ccpr}_{s,k}) y_{\text{pr}_s} \leq \sum_s \text{ccre}_{s,k} + \sum_s \text{ccpr}_{s,k} - 1, \quad \forall k \in \text{it} \quad (7.7)$$

$$\sum_s \text{ccre}_{s,k} y_{\text{pr}_s} + \sum_s \text{ccpr}_{s,k} y_{\text{re}_s} - \sum_s (1 - \text{ccre}_{s,k}) y_{\text{pr}_s} - \sum_s (1 - \text{ccpr}_{s,k}) y_{\text{re}_s} \leq \sum_s \text{ccre}_{s,k} + \sum_s \text{ccpr}_{s,k} - 1, \quad \forall k \in \text{it} \quad (7.8)$$

However, in the next step: generation of reaction networks, each generated reaction must be considered in both individual directions, describing two potential different reactions: one in the forward and another in the reverse directions; unless when the reaction direction, which is energetically feasible, had been previously elucidated based on thermodynamic analysis (Vertis et al., 2017).



The complete formulation for generating both linear and nonlinear chemical reactions can be written as shown in (7.9).

$$\min_{\substack{nre, npr, \\ yre, ypr}} \text{ordrx} \quad (7.9a)$$

$$\text{s.t. eqs. (7.1—7.8)} \quad (7.9b)$$

$$nre_s, npr_s \in \mathbb{N}, \quad \forall s \in \text{st} \quad (7.9c)$$

$$yre_s, ypr_s \in \{0,1\}, \quad \forall s \in \text{st} \quad (7.9d)$$

### 7.2.2 Application example — chemical reaction generation

The catalytic hydrogenation of succinic acid, previously presented in Section 1.5, is taken as an illustrative example for both linear and nonlinear chemical reaction generation. The nine chemical species were divided into representative (**sp**) and non-representative (**sd**) species

- **sp** = {AS, GBL, BDO, THF, BuOH, PrOH}, and
- **sd** = {CH<sub>4</sub>, H<sub>2</sub>O, H<sub>2</sub>},

respecting the species that were measured and were not measured in the experiment, respectively, allowing a linear graph representation of chemical reactions between representative species.

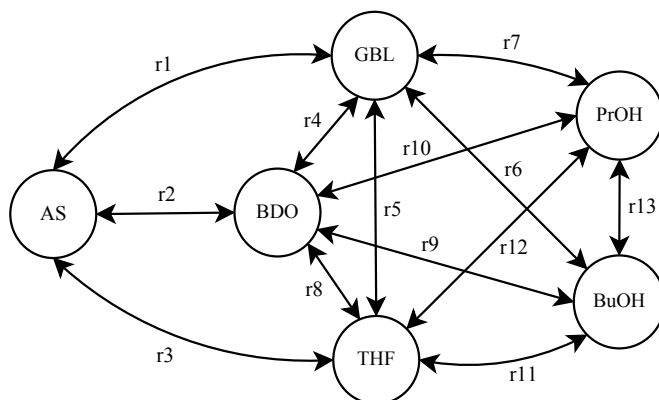
Considering firstly the enumeration of linear chemical reactions, the reaction invariant that can be established between the representative species concerns the relation  $C_4 + C_3 = 1$ , for both sides of every reaction. Moreover, in order to avoid the generation of chemical reactions that are physically improbable to occur, the stoichiometric coefficients of the species  $s \in \text{sd}$  were limited to be lower or equal to 4.

In this case, it was generated 13 linear reactions among the observed species, listed in Table 7.1. The chemical reactions were generated using GAMS® software with the commercial solver CPLEX, considering the formulation (7.9) with integer-cut equations to enumerate all feasible solutions. The total CPU usage was 1.04s. The graph representation of the reactions obtained is shown in Figure 7.2.

The criterion to generate nonlinear chemical reactions is not unique. The maximum reaction complexity to be considered should be intended as a tradeoff between the richness of representation (variety) and the number of combined elementary paths (threshold for the sum of consecutive smaller chemical reactions) required to the description of the chemical system. For example, notice that nonlinear reactions like  $\text{AS} + \text{GBL} \leftrightarrow 2\text{BDO}$  correspond to the sum of linear reactions identified previously, in this case  $r_2 + r_4$  with the resulting balanced equation:  $\text{AS} + \text{GBL} + 6\text{H}_2 \leftrightarrow 2\text{BDO} + 2\text{H}_2\text{O}$ . Once these type of reactions involve the meeting of many molecules, they are not probable to physically occur, and therefore they may be prohibited by controlling the magnitude of stoichiometric

**Table 7.1** Listing of the obtained linear reactions.

$j$	Reaction
1	$\text{AS} + 2 \text{H}_2 \longrightarrow \text{GBL} + 2 \text{H}_2\text{O}$
2	$\text{AS} + 4 \text{H}_2 \longrightarrow \text{BDO} + 2 \text{H}_2\text{O}$
3	$\text{AS} + 4 \text{H}_2 \longrightarrow \text{THF} + 3 \text{H}_2\text{O}$
4	$\text{GBL} + 2 \text{H}_2 \longrightarrow \text{BDO}$
5	$\text{GBL} + 2 \text{H}_2 \longrightarrow \text{THF} + \text{H}_2\text{O}$
6	$\text{GBL} + 3 \text{H}_2 \longrightarrow \text{BuOH} + \text{H}_2\text{O}$
7	$\text{GBL} + 4 \text{H}_2 \longrightarrow \text{PrOH} + \text{CH}_4 + \text{H}_2\text{O}$
8	$\text{BDO} \longrightarrow \text{THF} + \text{H}_2\text{O}$
9	$\text{BDO} + \text{H}_2 \longrightarrow \text{BuOH} + \text{H}_2\text{O}$
10	$\text{BDO} + 2 \text{H}_2 \longrightarrow \text{PrOH} + \text{CH}_4 + \text{H}_2\text{O}$
11	$\text{THF} + \text{H}_2 \longrightarrow \text{BuOH}$
12	$\text{THF} + 2 \text{H}_2 \longrightarrow \text{PrOH} + \text{CH}_4$
13	$\text{BuOH} + \text{H}_2 \longrightarrow \text{PrOH} + \text{CH}_4$

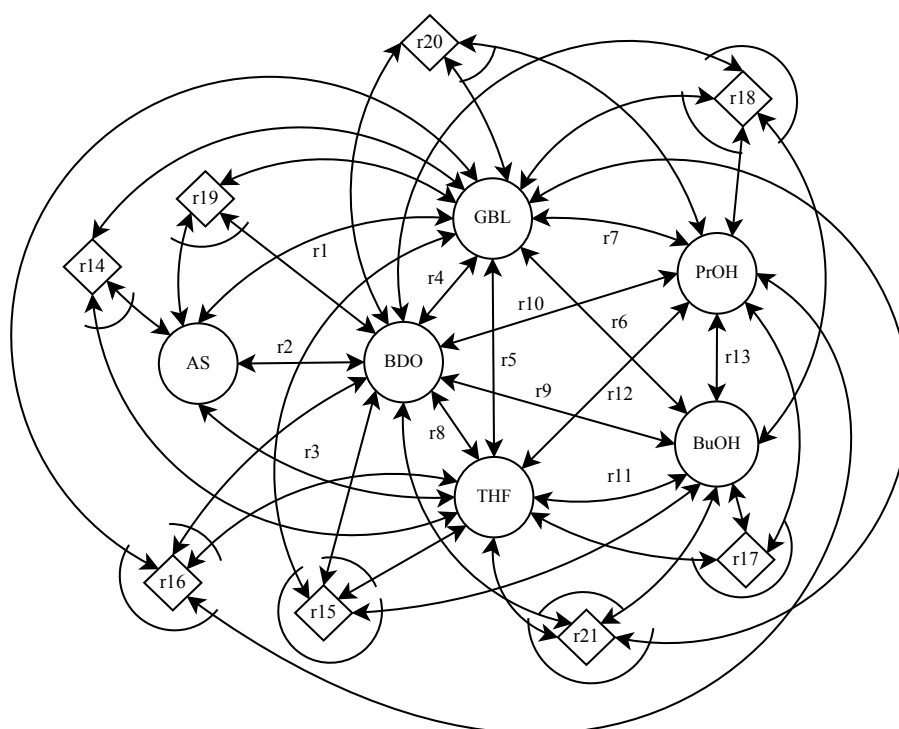
**Figure 7.2** Linear superstructure of reaction networks. The non-representative species are not drawn in the graph.

coefficients and/or the total number of moles in reactant and product reaction sides.

Regarding the generation of nonlinear chemical reactions, the same species division is maintained, although the established invariant is changed to  $C_4 + C_3 = 2$ . Hence, the presence of up to two species  $s \in \mathbf{sp}$  were allowed in both reaction sides. The stoichiometric coefficients of the species  $s \in \mathbf{sd}$  and  $s \in \mathbf{sp}$  were limited to be lower or equal to 4 and 2, respectively. In this case, it was generated 8 nonlinear reactions among the observed species, listed in Table 7.2. The chemical reactions were generated using GAMS® software with the commercial solver CPLEX, considering the formulation (7.9). The total CPU usage was 0.64s. The superstructure of the nonlinear reaction network is presented in Figure 7.3.

**Table 7.2** Listing of the obtained nonlinear reactions.

$j$	Reaction
14	$\text{AS} + \text{THF} \longrightarrow 2 \text{GBL} + \text{H}_2\text{O}$
15	$\text{BDO} + \text{THF} \longrightarrow \text{BuOH} + \text{GBL} + \text{H}_2$
16	$\text{BDO} + \text{THF} \longrightarrow \text{CH}_4 + \text{GBL} + \text{PrOH}$
17	$2 \text{BuOH} \longrightarrow \text{THF} + \text{CH}_4 + \text{PrOH}$
18	$\text{BDO} + \text{BuOH} \longrightarrow \text{GBL} + \text{CH}_4 + \text{PrOH} + \text{H}_2$
19	$\text{AS} + \text{BDO} \longrightarrow 2 \text{GBL} + 2 \text{H}_2\text{O}$
20	$2 \text{BDO} \longrightarrow \text{GBL} + \text{PrOH} + \text{CH}_4 + \text{H}_2\text{O}$
21	$\text{BDO} + \text{BuOH} \longrightarrow \text{GBL} + \text{THF} + 3 \text{H}_2$

**Figure 7.3** Nonlinear reaction network superstructure.

### 7.3 Target factor analysis (TFA)

Supported on linear algebra, the TFA technique has been used by statisticians and mathematicians in order to evaluate the proximity of a target vector to a linear subspace with established dimension in the context of the identification of dynamic models from experimental data using a data-driven approach (Malinowski and Howery, 1980; Malinowski, 1989). The aim is to elucidate whether that vector is a candidate for model constituent when it lies (sufficiently close) in that subspace that is previously characterized using the SVD of data in variant form.

A common metric used in TFA is the *relative error of projection*,  $\varphi$ , which is computed

through ratio of euclidean norms of  $\mathbf{v} - \text{proj}_{\mathbf{S}}\mathbf{v}$  and  $\mathbf{v}$ , as shown in (7.10).

$$\varphi = \frac{\|\mathbf{v} - \text{proj}_{\mathbf{S}}\mathbf{v}\|}{\|\mathbf{v}\|} \quad (7.10)$$

where  $\mathbf{v} - \text{proj}_{\mathbf{S}}\mathbf{v}$  is the error of projection of vector  $\mathbf{v} \in \mathbb{R}^m$  into the characteristic subspace of  $\mathbf{S}[m \times n]$  of dimension  $n$ , with  $m > n$ . This error vector (its norm) is the lowest error in the least squares sense. The error vector gives the projection of  $\mathbf{v}$  into the left null space of  $\mathbf{S}$  of dimension  $m - n$ . The orthogonal projection of vectors in linear subspaces is discussed in more detail in Appendix I.2.

In the context of modeling chemical reaction systems, as previously introduced in the state of the art (Section 3.1.3), TFA (and similar/related techniques) has been used to propose/identify (and/or validate) a reaction network using experimental data (Hamer, 1989; Bonvin and Rippin, 1990; Rastogi et al., 1990, 1992; Fotopoulos et al., 1994; Amrhein et al., 1999; Georgakis and Lin, 2005; Brendel et al., 2006; Bhatt et al., 2012; Santos-Marques et al., 2019; Dong et al., 2019). Hence, in this context, the reaction network is the model to be built, the target vectors are chemical reaction vectors composed by stoichiometric coefficients, and, data is, in general, concentration measurements during batch experiments.

The  $\varphi$  can be easily computed using the SVD of data in the variant format. Remember from (6.9) that the first  $R = \text{nr} \times_{\text{li}}$  columns of  $\mathbf{U}$  and  $\mathbf{V}$  are orthonormal bases for the column and row subspaces of  $\mathbf{D}[n_{\text{to}} \times n_{\text{sp}}]$ , respectively. Thus considering that  $\mathbf{v} = \boldsymbol{\nu}^T[1 \times n_{\text{sp}}]$  is the transposed stoichiometric vector and  $\mathbf{S} = \mathbf{N}_a[R \times n_{\text{sp}}]$  is the abstract basis that spans  $\text{row}(\mathbf{D})^2$ , the equation in (7.10) can be rewritten as

$$\varphi = \frac{\|\boldsymbol{\nu}^T - \boldsymbol{\nu}^T \cdot \mathbf{N}_a^T \cdot \mathbf{N}_a\|}{\|\boldsymbol{\nu}\|} \quad (7.11)$$

According to TFA, one target vector is accepted as model constituent if its error of projection is small. Thus, a threshold related to the truncation error of the data matrix (*i.e.*, to the amount of noise present in the data) must be established to accept or deny a candidate vector. Hence the test of a true stoichiometry is not that it lies exactly on the observed data space from SVD but that it lies “sufficiently close” to it (Fotopoulos et al., 1994). The computation of  $\varphi$  in (7.11) should be repeated until a complete basis that (approximately) spans  $\text{row}(\mathbf{N}_a)$  is obtained, thus validating the obtained network since the stoichiometry and data variant spaces are (approximately) matched.

---

<sup>2</sup>Since the data space dimension  $R$  was identified in Step 2, the abstract basis  $\mathbf{N}_a$  can be computed as the first  $R$  row vectors of  $\mathbf{V}^T$ .

### 7.3.1 TFA critical analysis

Despite its usefulness, several model identification problems can emerge during the application of TFA. These problems are related to the presence of residual species in the reaction mixture. When  $dc_s/dt$  and/or  $\Delta n_s$  are small quantities regarding the species  $s \in \text{sp}$ , *i.e.*, the respective entire columns of the matrices  $\mathbf{D}_R$  and/or  $\mathbf{D}_E$  present small values, one must observe that

- this  $s \in \text{sp}$  species does not significantly contribute to the disagreement of model-data fit, *i.e.*, it hardly influences the data adjustment, since the sum of its squared residuals is marginal.
- two exclusive situations may explain this occurrence, namely when that species  $s$ 
  - is an intermediate component in which the rate of its production is (practically) the same of its consumption in consecutive chemical reactions, thus, hiding or canceling the observation of the species compositional changes, or
  - is a terminal product species that is produced in a very slow reaction rate, configuring a residual species, generally a side-product.
- this  $s \in \text{sp}$  species is greatly influenced by noise, that is, it presents a great uncertainty related to its measurements, depending on the precision of the analytical techniques used to measure this species and, therefore, all calculations that are function of this species are compromised, *e.g.*, the calculations of reaction rates and extents, kinetic parameters, etc.
- this  $s \in \text{sp}$  species is barely identifiable, this means that it is hard to predict its origin, leading to meaningless confidence intervals of kinetic parameters.

In those situations the need of more data is a fact, opening a window of opportunity to design of experiments practices in order to provide specific data that turns the system completely identifiable. Common practices in these problematic situations are (i) the performance of replicated experiments, in which the number of repeated experiments should be calculated in order to eliminate the uncertainty associated with that model component, and (ii) considering the addition of different initial species in new experiments in order to disturb the dynamics of the reaction system, enabling an increase in residual product concentrations and the appearance of decoupled reaction extents.

Notice that small reaction rates and/or extents almost cancel the contribution of a chemical reaction, *i.e.*, of a basic stoichiometric vector that make up the system of coordinates in the data space, meaning that the component  $s$  of the response vector is almost at the origin dot in the row space of the stoichiometric matrix. In that situation, data analysis and statistical tests would lead to the decision of exclusion of this vector component of the model since it is unidentifiable, otherwise, the model parameter that concerns this vector component would present infinite confidence intervals. In this case, the identi-

fication of the model dimension from data analysis using SVD does identify the model dimension that is required to explain the observed data purely supported on a data-driven approach, but it does not necessarily indicate the real model dimension that would be required to describe a mechanistic phenomenon supported on deterministic criteria. When manipulating data with great uncertainty, it is certainly a difficult task to define/elucidate the real model dimension from data analysis, and there is a strong probability that the characteristic data space is being characterized for an incomplete reaction network.

Once we are concerned about developing models in which a feasible reaction network structure is contemplated, more issues must be accounted than data fit quality related topics, such as the need to construct a network in which every species is produced in a consistent sequential fashion, like building a puzzle in which no piece can be left out. Thus, data analysis is elucidative and important in the identification of reaction network models, but it cannot be performed in isolation; the structural information of the network must be also taken into account. This is the approach followed in this work, in which a hybrid methodology is proposed taking as advantage the knowledge acquired from data analysis and, simultaneously taking into account the structural model part supported on deterministic modeling strategies.

In summary, the TFA performs an individual analysis of the stoichiometric target vectors in which it seeks to identify whether these vectors belong to the observed space of the data in order to validate them as a possible model constituent. However, network validation can only be performed when we have the entire set of stoichiometric vectors that forms the stoichiometric matrix. This validation implies the calculation of the coordinates of the vector  $d\mathbf{c}/dt$  or  $\Delta\mathbf{n}$  on a basis of the row subspace of the stoichiometric matrix, and later, the identification of kinetic expressions that correlate the rate with the species concentrations. These coordinates are, respectively, reaction rates or reaction extents, whose values must be positive (and growing monotonous in the latter case). The coordinates close to the origin (practically null) make the contribution of a stoichiometric vector in the model residual in terms of objective function when adjusting data, but in some cases this stoichiometric vector is essential for obtaining a consistent network, even if it is outside the observed data space. Purely data-driven methods do not cover other aspects that play an important role in the task of modeling reaction networks, namely the aspects that guarantee

- the formation of all observed species, networks structurally feasible;
- the presence of positive net reaction fluxes, *i.e.*, of reaction extents that increase monotonically, handling plausible reaction networks;
- coherent feasible structures where a precedence can be established among species;
- reaction thermodynamic viability, *i.e.*, determining the reaction direction in which its reaction flux is energetically feasible.

We propose a methodology that takes the most of information from data analysis using SVD, but also attends to the previous issues list, where the model is incrementally identified from the combination of data-driven and first-principle-based methods, in a hybrid modeling approach. In this sense, TFA is used during this methodology as a tool for evaluating stoichiometric vectors, in order to allow the anticipation of the diagnosis of identification problems that will be faced in the later steps of the methodology. It means that no candidate vector is discarded at this phase, *i.e.*, they are scrutinized and cataloged as, on the one hand, potential problems for parts of the model identification when they present bad projection on data space, and, on the other hand, good candidates for network constituent when they lie in the data variant space.

Finally, it should be noted that time-invariant relationships were identified and incorporated at the data smoothing procedure in the previous methodology steps concerning the data treatment and analysis (*i.e.*, Steps 1 and 2), resulting in the acquirement of reconciled data with minimized noise content. This procedure reduces the chance of facing model identifiability problems from reconciled data since it clarifies the dimension of variant data space, and, consequently, assists the identification of a basis for that space in which compositional changes occur. This means that when facing small singular values from the SVD of reconciled data, they probably are related to model components that should not be discarded. In the Chapter 11, we present a complex case study that addresses this problematic, revealing the impact of the use of invariants during data treatment for model identification.

### 7.3.2 Application example

Following the AS case study, the 21 generated chemical reactions were tested as data consistent.

The dimension of the data variant space is equal to 5, *i.e.*, only one time-invariant is verified in this system concerning to the carbon chain conservation between species  $C_4$  and  $C_3$  type. For more details about this result, see Chapter 6.

The list of singular values of the data matrix is:

$\{1.07997 \times 10^{-3}, 4.19297 \times 10^{-4}, 1.65647 \times 10^{-4}, 1.21314 \times 10^{-5}, 2.96714 \times 10^{-6}, 1.23347 \times 10^{-12}\}$ .

A basis that represents an orthogonal row space of the data matrix of cumulative species molar changes obtained from its SVD in Step 2 is presented in (7.12).

$$\mathbf{N}_a = \begin{bmatrix} -0.857515 & 0.468762 & 0.119974 & 0.151325 & 0.077955 & 0.039498 \\ -0.272265 & -0.747007 & 0.101838 & 0.519320 & 0.264403 & 0.133711 \\ 0.0643277 & 0.189261 & -0.886636 & 0.368726 & 0.171065 & 0.093256 \\ -0.133728 & -0.134091 & -0.138332 & -0.463859 & 0.015854 & 0.854157 \\ 0.0430356 & 0.0421365 & 0.0575293 & 0.435449 & -0.853131 & 0.274980 \end{bmatrix} \quad (7.12)$$

The 21 reaction stoichiometric vectors were individually projected onto the row space of the data matrix and their relative projection errors were calculated using (7.11). Table 7.3 presents the results obtained.

**Table 7.3** List of chemical reactions and respective stoichiometric vectors ( $\nu$ ) and relative projection errors ( $\varphi$ ). The stoichiometric vectors follow the species order AS, GBL, BDO, THF, BuOH and PrOH.

$j$	$r_j$	$\nu^T$	$\varphi \times 10^9$
1	AS $\rightarrow$ GBL	[-1 1 0 0 0 0]	3.148
2	AS $\rightarrow$ BDO	[-1 0 1 0 0 0]	1.169
3	AS $\rightarrow$ THF	[-1 0 0 1 0 0]	9.084
4	GBL $\rightarrow$ BDO	[0 -1 1 0 0 0]	4.318
5	GBL $\rightarrow$ THF	[0 -1 0 1 0 0]	5.936
6	GBL $\rightarrow$ BuOH	[0 -1 0 0 1 0]	2.888
7	GBL $\rightarrow$ PrOH	[0 -1 0 0 0 1]	3.030
8	BDO $\rightarrow$ THF	[0 0 -1 1 0 0]	1.025
9	BDO $\rightarrow$ BuOH	[0 0 -1 0 1 0]	2.457
10	BDO $\rightarrow$ PrOH	[0 0 -1 0 0 1]	3.462
11	THF $\rightarrow$ BuOH	[0 0 0 -1 1 0]	3.482
12	THF $\rightarrow$ PrOH	[0 0 0 -1 0 1]	2.437
13	BuOH $\rightarrow$ PrOH	[0 0 0 0 -1 1]	5.919
14	AS + THF $\rightarrow$ 2 GBL	[-1 2 0 -1 0 0]	1.609
15	BDO + THF $\rightarrow$ BuOH + GBL	[0 1 -1 -1 1 0]	2.157
16	BDO + THF $\rightarrow$ GBL + PrOH	[0 1 -1 -1 0 1]	2.028
17	2 BuOH $\rightarrow$ PrOH + THF	[0 0 0 1 -2 1]	5.427
18	BDO + BuOH $\rightarrow$ GBL + PrOH	[0 1 -1 0 -1 1]	4.490
19	AS + BDO $\rightarrow$ 2 GBL	[-1 2 -1 0 0 0]	4.311
20	2 BDO $\rightarrow$ GBL + PrOH	[0 1 -2 0 0 1]	2.248
21	BDO + BuOH $\rightarrow$ GBL + THF	[0 1 -1 1 -1 0]	2.767

From the results obtained, it is possible to observe that every stoichiometric vector lies in the row space of the data, and, hence, they are good candidates for composing the reaction network. This is not an unexpected result since (i) the data matrix concerns the reconciled data in which the previously identified invariant relationship was imposed as a constraint of the smoothing procedure, and (ii) the stoichiometric vectors also obey that invariant.

## 7.4 Incorporation of thermodynamic feasibility criteria

*“Every good scientific theory is a prohibition:  
it forbids certain things to happen.  
The more a theory forbids, the better it is.”*

– Karl Popper



The analysis of the Gibbs free energy of the system is used as the main criterion to assess the energetic feasibility of the reaction network superstructure. The differential Gibbs free energy variation in a closed system with multiple reactions is

$$dG = -S dT + V dP + \boldsymbol{\mu}^T \cdot d\mathbf{n} \quad (7.13)$$

where  $G$  is the Gibbs free energy,  $S$  is the entropy,  $T$  the temperature,  $V$  the volume,  $P$  the pressure,  $\boldsymbol{\mu}$  is the vector of chemical potentials of the species and  $d\mathbf{n}$  is the differential increment in the species number of moles. Considering the molar balances for a system with multiple chemical,  $d\mathbf{n}$  can be related to the variation in the reaction extents by  $d\mathbf{n} = \mathbf{N}^T d\boldsymbol{\xi}$ . At constant  $T$  and  $P$ , the equation above can be simplified to

$$dG|_{T,P} = (\mathbf{N} \cdot \boldsymbol{\mu})^T \cdot d\boldsymbol{\xi} \quad (7.14)$$

Although  $\mathbf{N}$  appears in this last equation, the Gibbs free energy is a state property, only dependent on the mole number variation, and it does not depend on the structural characteristic of the reaction network (represented by the stoichiometric matrix). At constant pressure and temperature,  $dG < 0$  is a necessary condition for the spontaneity of processes in closed systems.

The contribute for the Gibbs free energy change related to a given reaction extent  $\xi_j$ ,  $j \in r\mathbf{x}$ , corresponding to one entry of the vector  $\mathbf{N} \cdot \boldsymbol{\mu}$ , can be expressed through (Demirel, 2014)

$$\begin{aligned} \left. \frac{dG}{d\xi_j} \right|_{T,P,\xi_{j'}} &= \sum_{s \in \text{st}} (\text{npr}_{s,j} - \text{nre}_{s,j}) \mu_s \\ &= \sum_{s \in \text{st}} (\text{npr}_{s,j} - \text{nre}_{s,j}) \mu_s^0 + RT \sum_{s \in \text{st}} (\text{npr}_{s,j} - \text{nre}_{s,j}) \ln a_s, \quad \forall j \in r\mathbf{x}, j' \neq j \end{aligned} \quad (7.15)$$

where the species chemical potential  $\mu_s$  is expressed in terms of the species activity  $a_s$  and the standard chemical potential  $\mu_s^0$ . The activity can also be computed as  $a_s = \gamma_s c_s$ , where  $\gamma_s$  is the respective activity coefficient. For systems with close to ideal behavior,  $\gamma_s$  can be approximated by unity, and the chemical potential becomes solely a function of the concentration. The standard chemical potential of each species can be calculated at the temperature of the experiment by (Walas, 2013)

$$\frac{\mu_s^0}{T} = \frac{\Delta G_{f,s,T_{\text{ref}}}^0}{T_{\text{ref}}} - \int_{T_{\text{ref}}}^T \frac{1}{T^2} \left[ \Delta H_{f,s,T_{\text{ref}}}^0 + \int_{T_{\text{ref}}}^T C_{p,s}(\theta) d\theta \right] dT, \quad \forall s \in \text{st} \quad (7.16)$$

where  $\Delta G_{f,s,T_{\text{ref}}}^0$  and  $\Delta H_{f,s,T_{\text{ref}}}^0$  are the Gibbs energy and enthalpy changes of formation at the reference temperature, and  $C_{p,s}$  is the heat capacity of species  $s$ , respectively. When  $\Delta H_{f,s,T_{\text{ref}}}^0 \gg \int_{T_{\text{ref}}}^T C_{p,s}(\theta) d\theta$ , the equation above can be further simplified to a Vant'Hoff form.

For systems that are not in equilibrium, the second law of Thermodynamics implies that isolated reactions with a non-zero flux must dissipate energy (Beard et al., 2004). Consequently, the energetically feasible direction of the net flux for a single chemical reaction must occur from the higher to the lower chemical potentials of the species weighted by their respective stoichiometric coefficients (7.15), *i.e.*, the reaction net flux  $j$  is energetically feasible in the direction where  $dG/d\xi_j < 0$ , at isothermal and isobaric conditions. To model chemical reactions that occur between observable species in batch experiments, generally far from global equilibrium, this criterion may be used to identify the feasible flux direction of the individual reactions, thus decreasing the number of networks to be further analyzed.

Given a list of structurally feasible chemical reactions, the evaluation of the energetically feasible directions of their net fluxes can be performed using the global condition  $dG < 0$  and (7.13 – 7.16). At constant  $P$  and  $T$ , and for individual reactions to be included in a reaction network involving only observable species, this condition generally requires that  $dG/d\xi_j < 0$  for each reaction  $j$ , within the reaction extents  $\xi_j$  observed in the system. This requirement might be relaxed if the reactions considered correspond to elementary steps, in a reaction mechanism, where only the global condition  $dG < 0$  needs to be enforced, provided that the steps with positive  $\Delta G$  can be justified within the energy level distributions in the system, in the physical conditions considered.

#### 7.4.1 Application example — elucidating the energetically feasible reaction direction

Consider the same case study, the catalytic hydrogenation of Succinic acid, and the linear chemical reaction generated in Substep 3.1 (Table 7.1). The thermodynamic model parameters, required to calculate the Gibbs free energy changes associated with the individual reactions, are shown in Table 7.4. These values, together with polynomial forms for  $C_{p,s}$  were retrieved from Aspen Properties®.

**Table 7.4** Thermodynamic data - Aspen Properties®.  $\Delta G_f^0$  and  $\Delta H_f^0$  at  $T_{\text{ref}} = 298$  K, and  $\mu^0$  at  $T = 250$  °C. Units in  $\text{kJ mol}^{-1}$ .

$s$	$\Delta G_{f,298}^0$	$\Delta H_{f,298}^0$	$\mu^0$
AS	-697.3	-822.9	-1222.4
GBL	-285.3	-379.0	-500.3
BDO	-278.0	-426.7	-487.7
THF	-79.7	-184.2	-139.5
BuOH	-150.7	-275.1	-280.5
PrOH	-159.9	-254.6	-88.7
CH <sub>4</sub>	-50.5	-74.5	-264.6
H <sub>2</sub> O	-228.6	-241.8	-400.8
H <sub>2</sub>	0	0	-0.1

Figure 7.4 presents the  $dG/d\xi_j$  profiles. As can be observed on first plot, the chemical reactions  $r_4$ :  $\text{GBL} + 2\text{H}_2 \longrightarrow \text{BDO}$  and  $r_5$ :  $\text{GBL} + 2\text{H}_2 \longrightarrow \text{THF} + \text{H}_2\text{O}$  do not achieve a value higher than  $|dG/d\xi_j| \leq 50 \text{ kJ mol}^{-1}$ , indicating that a unique energetically feasible direction cannot be assertively identified. All the others are feasible in the forward direction. Hence reactions  $r_4$  and  $r_5$  and their reverse counterparts are included as candidates in the linear reaction network superstructure (Figure 7.5) together with the remain reactions in the energetically feasible direction. Globally, instead of the original 26 distinct reaction fluxes (Figure 7.2), only 15 were considered as energetically feasible. The generation of reaction networks with this superstructure is considered in the next chapter.

## Bibliography

- Amrhein, M., Srinivasan, B., and Bonvin, D. (1999). Target factor analysis of reaction data: use of data pre-treatment and reaction-invariant relationships. *Chemical Engineering Science*, 54(5):579–591.
- Beard, D. A., Babson, E., Curtis, E., and Qian, H. (2004). Thermodynamic constraints for biochemical networks. *Journal of Theoretical Biology*, 228(3):327–333.
- Bhatt, N., Kerimoglu, N., Amrhein, M., Marquardt, W., and Bonvin, D. (2012). Incremental identification of reaction systems—a comparison between rate-based and extent-based approaches. *Chemical Engineering Science*, 83(0):24–38. Mathematics in Chemical Kinetics and Engineering International Workshop 2011.
- Bonvin, D. and Rippin, D. (1990). Target factor analysis for the identification of stoichiometric models. *Chemical Engineering Science*, 45(12):3417–3426.
- Brendel, M., Bonvin, D., and Marquardt, W. (2006). Incremental identification of kinetic models for homogeneous reaction systems. *Chemical Engineering Science*, 61(16):5404–5420.
- Demirel, Y. (2014). *Nonequilibrium Thermodynamics*. Elsevier Science, Amsterdam, 3rd. edition.
- Dong, Y., Georgakis, C., Mustakis, J., Hawkins, J. M., Han, L., Wang, K., McMullen, J. P., Grosser, S. T., and Stone, K. (2019). Stoichiometry identification of pharmaceutical reactions using the constrained dynamic response surface methodology. *AIChE Journal*, 65(11):e16726.
- Fotopoulos, J., Georgakis, C., and Stenger, H. G. (1994). Structured target factor analysis for the stoichiometric modeling of batch reactors. In *Proceedings of 1994 American Control Conference - ACC '94*, volume 1, pages 495–499 vol.1.
- Georgakis, C. and Lin, R. (2005). Stoichiometric modeling of complex pharmaceutical reactions. In *Proceedings of the Annual AIChE meeting in Cincinnati, OH, November*.
- Griva, I., Nash, S. G., and Sofer, A. (2009). *Linear and nonlinear optimization*, volume

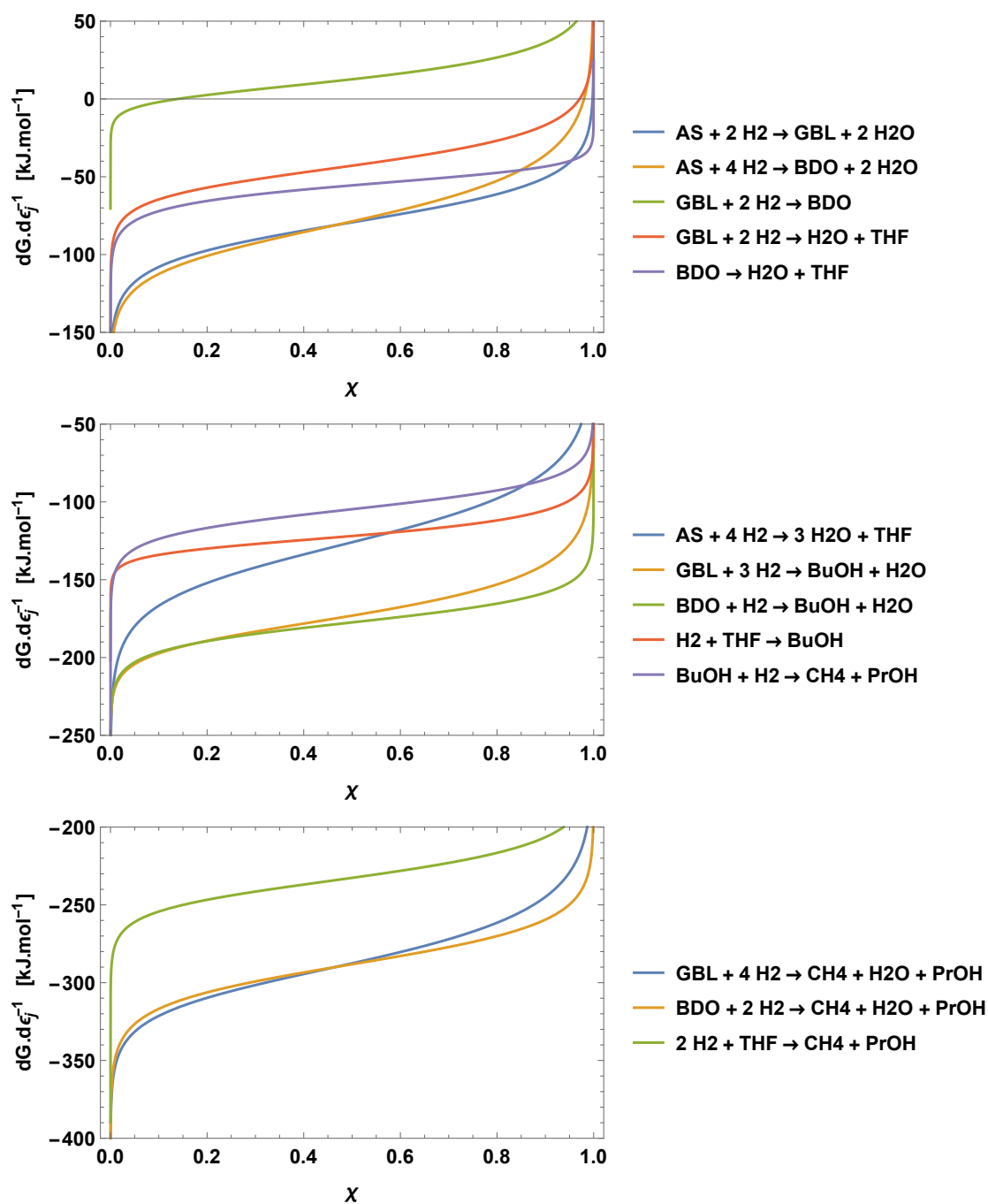


**Figure 7.4** Gibbs free energy changes associated with the individual reactions at isobaric and isothermal conditions.

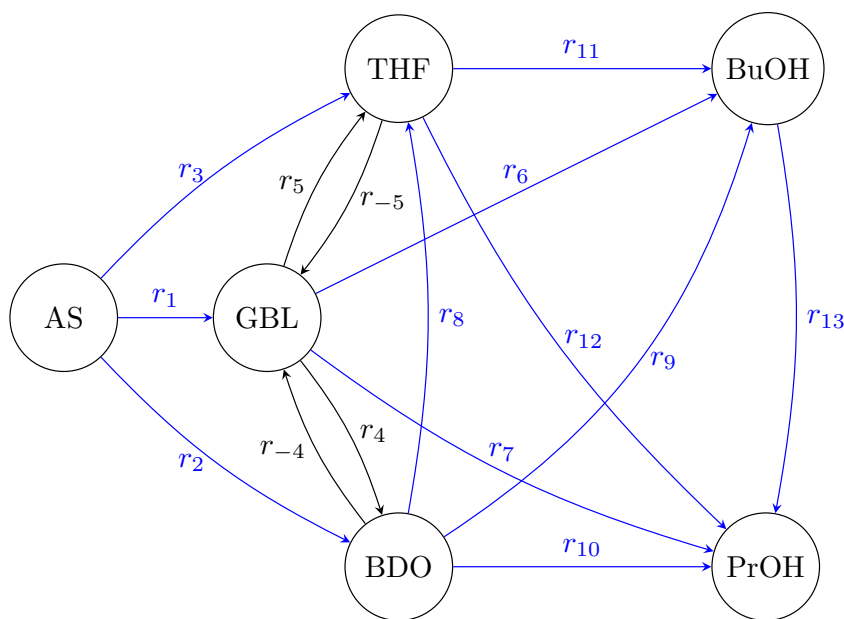


**Figure 7.5** Reaction network superstructure with energetically feasible reaction directions indicated by blue arrows.

108. Siam.

Hamer, J. W. (1989). Stoichiometric interpretation of multireaction data: application to fed-batch fermentation data. *Chemical Engineering Science*, 44(10):2363–2374.

Malinowski, E. R. (1989). Statistical f-tests for abstract factor analysis and target testing. *Journal of Chemometrics*, 3(1):49–60.

Malinowski, E. R. and Howery, D. G. (1980). *Factor analysis in chemistry*. Wiley New York.

Missen, R. W. and Smith, W. R. (1998). Chemical reaction stoichiometry (CRS): A tutorial.

Missen, R. W. and Smith, W. R. (2003). Mass conservation implications of a reaction mechanism. *Journal of Chemical Education*, 80(7):833.

Pethö, Á. (1990). The linear relationship between stoichiometry and dimensional analysis. *Chemical Engineering & Technology*, 13(1):328–332.

Pethö, Á. (1994). Further remarks on the linear relationship between stoichiometry and dimensional analysis. *Chemical Engineering & Technology*, 17(1):47–49.

Rastogi, A., Fotopoulos, J., Georgakis, C., and Stenger Jr, H. G. (1992). The identification of kinetic expressions and the evolutionary optimization of specialty chemical batch reactors using tendency models. *Chemical engineering science*, 47(9-11):2487–2492.

Rastogi, A., Vega, A., Georgakis, C., and Stenger Jr, H. (1990). Optimization of catalyzed epoxidation of unsaturated fatty acids by using tendency models. *Chemical engineering science*, 45(8):2067–2074.

- Santos-Marques, J., Georgakis, C., Mustakis, J., and Hawkins, J. M. (2019). From dynamic response surface models to the identification of the reaction stoichiometry in a complex pharmaceutical case study. *AIChE Journal*, 65(4):1173–1185.
- Smith, W. and Missen, R. (1982). *Chemical reaction equilibrium analysis: theory and algorithms*. Wiley series in chemical engineering. Wiley.
- Szalkai, I. (1991). Generating minimal reactions in stoichiometry using linear algebra. *Hung. J. Ind. Chem*, 19:289–292.
- Szalkai, I. (2000). A new general algorithmic method in reaction syntheses using linear algebra. *Journal of Mathematical Chemistry*, 28(1-3):1–34.
- Tsu, J., Díaz, V. H. G., and Willis, M. J. (2019). Computational approaches to kinetic model selection. *Computers & Chemical Engineering*, 121:618–632.
- Vertis, C. S., Granjo, J. F. O., Oliveira, N. M. C., and Bernardo, F. P. (2017). Systematic generation of chemical reactions and reaction networks subject to energetic constraints. In Espuña, A., Graells, M., and Puigjaner, L., editors, *27th European Symposium on Computer Aided Process Engineering*, volume 39 of *Computer Aided Chemical Engineering*. Elsevier.
- Walas, S. (2013). *Phase Equilibria in Chemical Engineering*. Elsevier Science, Amsterdam.

# Chapter 8

## Step 4 — Generation of Reaction Networks

*“Topology is the property of something that doesn’t change when you bend it or stretch it as long as you don’t break anything”*

– Edward Witten

### Contents

---

8.1	Step 4 contextualization . . . . .	218
8.2	Network complexity and related terminology . . . . .	220
8.3	Sets and common constraints in network generation problems . . . . .	225
8.3.1	Defining sets . . . . .	226
8.3.2	Common constraints . . . . .	226
8.4	Linear reaction networks . . . . .	227
8.4.1	Structural flux analysis (SFA) . . . . .	229
8.5	Nonlinear reaction networks . . . . .	234
8.5.1	Enumeration of reaction networks using ordering constraints . . . . .	235
8.5.2	Enumeration of reaction networks using a tree of states . . . . .	243
8.6	MILP formulations comparison . . . . .	247
	Bibliography . . . . .	252

---

The generation of reaction networks can be approached in several ways. A reaction network must fully explain the production/consumption of each observed species. There are usually many ways to equate the formation of each species in a network, and therefore a systematic approach is needed to enumerate them all. Given this requirement, four MILP

formulations were developed to generate reaction networks using optimization tools that will be presented in this chapter.

Regarding the generation of linear reaction networks, the formulation developed is similar to the one used in single-commodity flow problems, where the mass flow balances of the nodes guarantee the achievement of connected structures using *structural flux analysis*. On the other hand, the remain three formulations conceived to generate nonlinear reaction networks differ with regard to the type of restrictions used for species ordering; they were inspired by attribution (or assignment) problems based on (i) ordering and disjoint constraints, and (ii) state task network. Also, a recursive algorithm is proposed in order to obtain the entire feasible solution set of reaction networks. This algorithm is used as a verification tool, thus, validating the solutions obtained using integer programming (IP). The recursive algorithm is presented in Appendix II.

All formulations can be used to explicitly or implicitly generate networks. The explicit generation of reaction networks ensures the achievement of consistently connected structures, linking every observed chemical species. On the other hand, the implicit generation regards to structural constraints simultaneously with experimental data in order to obtain *plausible* networks that match these data (subjected to positive reaction fluxes), thus constraining even more the generation problem.

The complete enumeration of all possible reaction networks can be achieved either through incremental addition of integer cuts to the formulation (and resolving it) or, more efficiently, through the use of MILP solvers that allow the complete enumeration of all feasible solutions at once. The key idea is to begin from a starting set of nodes (or only one node, depending on the case) and to arrive in the remain nodes contemplated in the superstructure. It is preferable to start with the lowest model complexity that is required to explain the observed data, although in some cases this amount may not be enough, and then, the generation of more complex structures can be considered in an iterative procedure. Moreover, the need of additional experimental data can be observed/identified when the model is unsatisfactory, and, in these cases, optimal experiments can be designed to direct elucidate unclear parts of the structural model.

## 8.1 Step 4 contextualization

In the last decades, many authors have developed formulations based on IP in the context of operational research for several application purposes, involving process (Floudas and Lin, 2005), project (Levy et al., 1963) and transportation (Gavish and Graves, 1978) scheduling problems.

In the context of process scheduling problems, the concept of state task network (STN) was developed. The STN representation of a chemical process consists in a directed graph with (i) circles, called *state* nodes, that represent raw materials, intermediates and/or final products, and (ii) rectangle boxes, called *task* nodes, representing unitary operations such



as reaction, separation (distillation, filtering, extracting, drying, etc.), heating, blending, etc. The directed graph indicates their connection and the scheduled sequence of materials in a chemical process (Floudas and Lin, 2005). The process scheduling problems, from the simplest single-stage single-unit multiproduct processes to the most general multipurpose processes, are inherently combinatorial in nature because of the many discrete decisions involved, such as equipment assignment and task allocation over time. They belong to the set of NP-complete problems.

In project scheduling problems, generally, the time component is the most important factor in which a set of activities must be scheduled in the shortest period of time available. It can involve team decision, *i.e.*, human resource and task allocation, economic problems, etc. Typically, Gantt charts are established showing dependencies and time periods among activities. One of the classical examples that involves ordering constraints is the *Critical Path Method* (CPM). CPM is a simple technique used to analyze, plan and schedule projects. In its essence CPM is used to determine which activities are *critical* on the total project time, and how best to schedule all activities in order to meet a deadline at minimum cost (Levy et al., 1963). The problem begins with a list of activities, their respective time duration, and immediate predecessors. Using inequality constraints the time of the project is determined, establishing an ordered sequence of activities subject to their interrelations. These problems can involve decision variables or not, depending on the need to choose a task among those available. In these cases, binary variables are needed, transforming the linear programming (LP) optimization problem into a mixed-integer linear programming (MILP) problem.

The transportation scheduling problems are also inserted in the field of combinatorial integer optimization problems due to many discrete decisions involved such as paths selection defining routes for an specific purpose, *e.g.*, minimize the route taken to delivery orders. Several examples of transportation scheduling problems were pointed out in Section 3.3.2, including TSP and ESPP.

All these assignment problems are related to finding an optimal graph in which nodes and arcs have different meanings presenting sequences of tasks, activities, operations, cities, etc. Therefore, these scheduling problems can be viewed as a network generation problem. Since the problem of generating *reaction networks* involves the assignment of chemical reactions that consistently link chemical species in a feasible structure, this problem can be handled as an optimization scheduling problem. In this work four assignment-based formulations to generate reaction networks are presented. One is related to process scheduling problems using the STN concept, where every state is characterized through a set of chemical reactions and a set of chemical species. The goal is to build a sequence of states until a complete and feasible reaction network is reached. The remain three formulations are related to transportation scheduling problems, where reaction networks are described as graphs in which chemical species and reactions are represented by nodes and arcs, respectively. In this case, generating a reaction network may pass through determin-

ing a feasible pathway of mass fluxes among species, defining a route in this graph with controlled complexity in a consistently connected structure. The next section presents several parameter definitions that are related to the network complexity and that will be needed in the linear and nonlinear network generation formulations.

## 8.2 Network complexity and related terminology

The problem of generating reaction networks in general starts with the decision of the number of constituent reactions that the network should present, establishing the network complexity. This decision can be supported on data analysis and/or through stoichiometric relationships among observed chemical species. Identifying the model complexity from data analysis consists of determining the linear space dimension of data in the variant form. This data can be formed by time-concentration derivative vectors or cumulative molar changes vectors depending on the method chosen to balance the species mass in batch reaction systems. The singular value analysis can help in elucidating the data dimension by identifying variant and invariant relationships presented during mass transformation (Bonvin and Rippin, 1990; Amrhein et al., 1999; Rodrigues et al., 2015). In other cases parametric and non-parametric statistical methods may be more convenient for determining data dimensionality, such as the *F*-test (Malinowski, 1989) and the cross-validation (Wold, 1978; Bro et al., 2008), respectively. On the other hand, when considering the conserved relationships between the chemical species measured, the dimension of the model can be elucidated by evaluating the dimension of the null space of the matrix of reaction invariants, guaranteeing a feasible number of chemical reactions that connect the known species and preserve the closure of elemental balances and/or other conserved properties (Gadewar et al., 2001; Missen and Smith, 1998, 2003). These topics were considered in methodology Step 2, Chapter 6.

However, identifying the model complexity from data analysis is not an easy task, specially in the presence of noisy, scarce and incomplete datasets. On the other hand, the establishment of stoichiometric relationships requires knowledge about species chemical formula, which can also present some difficulties when unknown (or unobserved) species are present and/or when not all the invariant relationships are known. Consequently, a method capable of generating reaction networks with any complexity is necessary, specially when the dimension of the network cannot be identified in advance. This means that networks of several dimensions can be generated to later identify which one is more adequate to fit the data available, presenting a structure with physical meaning that leads to, for example, positive net reaction rates. Nonetheless, even in the presence of unclear results from previous evaluations of experimental data and system stoichiometry, the application of methods to determine the complexity of the network can be useful when it allows to identify a range of candidate dimensions of the model that must be considered in the network generation step, thus reducing the number of solutions to be generated.

Furthermore, the identification of the model can become uncertain when the data present high uncertainty. Thus, it is advantageous to have a range of possibilities to test and funnel these models based on the available data. These candidate networks can be used for planning additional experiments specifically designed to elucidate uncertain paths that produce residual species. This opens a window of opportunity for the practice of optimal design of experiments.

In the description list below, terminology related to model complexity is introduced; this will be necessary for the developed methods of generating reaction networks.

**nr $x$**  Number of chemical reactions that make up the reaction network and reflects the complexity of the model.

**nr $x_{\min}$**  Minimum number of chemical reactions that explains the production and consumption of every chemical species in the system.

**nr $x_{\max}$**  Maximum number of chemical reactions in the network. This parameter traduces the maximum complexity that the network can present.

**nr $x_{\text{sup}}$**  Number of chemical reactions in the reaction network superstructure.

**nr $x_{\text{li,max}}$**  Maximum number of linearly independent chemical reactions that a reaction network can present. This parameter is given by the matrix rank of the network superstructure stoichiometry. Actually, **nr $x_{\text{li,max}}$**  is related to the number of independent reaction-invariant relations of the chemical system, where the difference between the number of observed species and the independent conserved relations between them gives the number of linearly independent network model components. When these conserved relations are unknown, **nr $x_{\text{li,max}}$**  can assume at most the number of species minus one, since at least the global mass is conserved during the occurrence of chemical reactions among the observed species. For more details see Section 2.3.

**nr $x_{\text{li}}$**  Number of linearly independent chemical reactions in the network; it is computed through the stoichiometric matrix rank.

**DI** Dependence index. This index indicates the number of linearly dependent chemical reactions in the network. It can be computed through  $\text{DI} = \text{nr}x - \text{nr}x_{\text{li}}$ . The **DI** is minimum (**DI $_{\min}$** ) when  $\text{nr}x = \text{nr}x_{\text{li}}$ , and, it is maximum (**DI $_{\max}$** ) when  $\text{nr}x = \text{nr}x_{\max}$  and  $\text{nr}x_{\text{li}} = \text{nr}x_{\min}$ .

**RI** Redundancy index. This index indicates the number of redundant chemical reactions in the network. Redundant chemical reactions describe the species formation that were already produced through other pathway. Nonlinear chemical reactions that simultaneously produce two species in which (i) one already exists and (ii) other is the first appearance in the chemical system, are classified as non-redundant since they bring new information concerning the production of new species in the system.

**CI** Complexity index. It indicates the model complexity in an integer scale, varying between  $[0, \text{CI}_{\max}]$ . It can be computed through  $\text{CI} = \text{nrx} - \text{nrx}_{\min}$ . The **CI** is maximum when  $\text{nrx} = \text{nrx}_{\max}$ .

**nrp** Number of initial representative reactants in the chemical mixture.

The  $\text{nrx}_{\min}$  value can be elucidated using reaction stoichiometrics — through a MILP formulation where  $\text{nrx}$  is minimized in the entire reaction network superstructure, subjected to linear constraints that imply a sequential order of species production through their respective reaction paths. In this formulation binary (decision) variables are used to decide whether chemical reactions are present in the network. The key idea is to obtain the minimum number of chemical reactions that can consistently explain the production of all observed species, starting from  $\text{nrp}$  reactants.

Networks with dimension  $\text{nrx}_{\min}$  ( $\text{CI} = 0$ ) are composed by linearly independent sets of chemical reactions,  $\text{DI} = 0$ , and no redundant paths,  $\text{RI} = 0$ . It means that none chemical reaction can be discarded without turning the network infeasible.

When considering the generation of networks with  $\text{nrx} > \text{nrx}_{\min}$  ( $\text{CI} > 0$ ), these structures can present:

- **DI = 0**: the set of reactions is linearly independent (LI), until reaches  $\text{nrx}_{\text{li}, \max}$ . Networks with **DI = 0** can present:
  - non-redundant chemical reactions, **RI = 0**. Non-redundant LI reactions bring new information to the network, presenting paths that link (at least one) species that were not produced before.
  - redundant chemical reactions, **RI > 0**. Redundant LI reactions are the ones that do not constitute a linear combination of the reactions that form a network with a lower **CI**, but they explain the formation of species that were already produced.
- **DI > 0**: when at least one chemical reaction is described as a linear combination of the remain network reactions. Thus, the set of chemical reactions in this network is linearly dependent (LD). These networks always present redundancies (**RI > 0**), containing reactions that produce the same species through different pathways.

Thus, from another point of view, a network that presents **RI = 0**, necessarily has **DI = 0**.

Reaction networks with  $\text{nrp} = 1$  composed by  $\text{nrx}_{\min}$  chemical reactions ( $\text{CI} = \text{RI} = 0$ ) present all species linked, and therefore, when any reaction is added to these minimal structures, it will configure a redundancy in the respective structure, making this new network with **RI = 1**, whether linear or not. This redundant chemical reaction added (i) turns the entire set of reactions LD in *linear networks* (**DI = 1**), and (ii) can maintain (or not) a LI set of reactions in *nonlinear networks*, *i.e.*, the network dependency index can remain zero (**DI = 0**) or it will increase to **DI = 1** with a LD set. Notice that networks

with  $RI > 0$  present reaction components that could be discarded without breaking the structure with  $nr_{x_{\min}}$ , whether it is linear or not. On the other hand, in most of nonlinear cases, it is possible to generate structures with  $CI > 0$  and  $RI = 0$ , where no chemical reaction can be discarded without resulting in disconnected and infeasible structures. Figures 8.1 and 8.2 present reaction networks with  $DI = 0$  and  $DI = 1$ , respectively, exemplifying different cases of network redundancy.

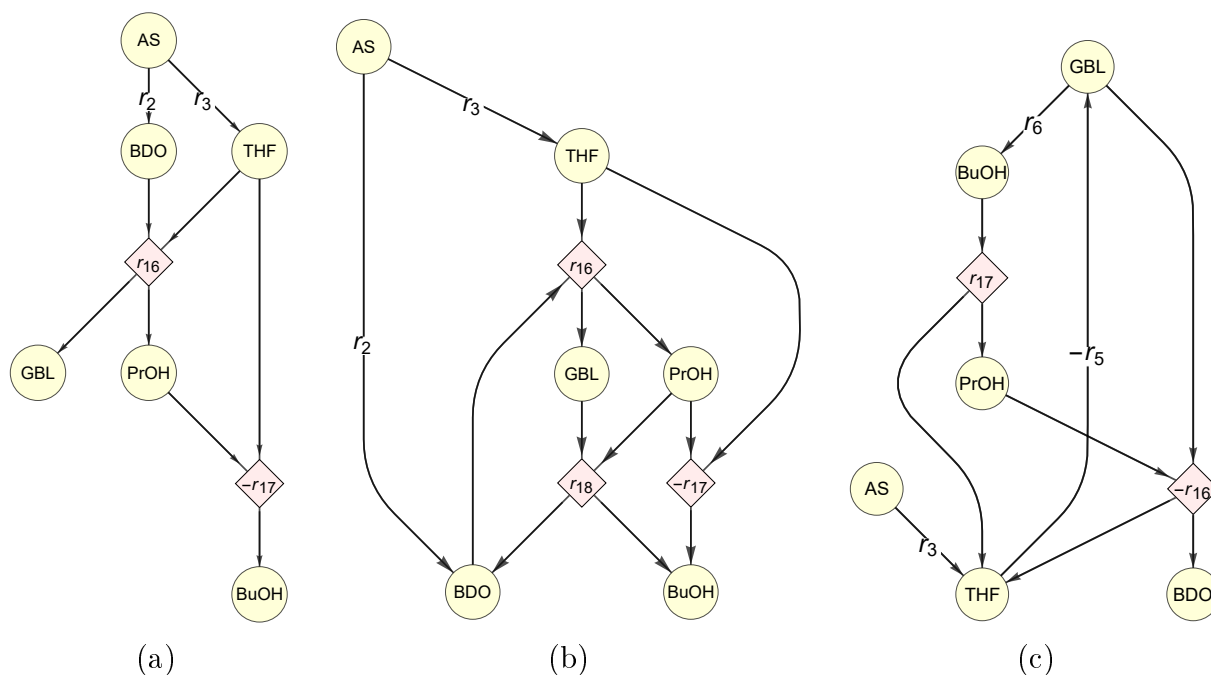


**Figure 8.1** Nonlinear reaction networks with  $DI = 0$ . Networks with (a)  $nr_x = nr_{x_{\min}} = 4$ ,  $CI = RI = 0$ , (b)  $nr_x = nr_{x_{li, \max}} = 5$ ,  $RI = CI = 1$  and (c)  $nr_x = nr_{x_{li, \max}} = 5$ ,  $CI = 1$  and  $RI = 0$ .

In Figure 8.1, when comparing the networks in (a) and (b), it is observed that the network in (b) contains an additional chemical reaction ( $r_{18}$ ) which is linearly independent from the remain reactions but it is redundant since the species BDO and BuOH were previously produced in  $r_2$  and  $-r_{17}$ , respectively. In (b)  $r_{18}$  can be discarded resulting in the same structure presented in (a). In (c) no chemical reaction can be discarded from this structure without turning the network infeasible. Although THF presents more than one origin, the reactions that form it are non-redundant since other (new) species are simultaneously produced.

In Figure 8.2, networks composed by a LD set are presented. When analyzing these networks, it is observed that in (a) there is a redundancy in THF formation through  $r_3$  and  $r_8$  turning the set of chemical reactions linearly dependent, (when removing  $r_8$  the same structure presented in Figure 8.1(a) is obtained), while in (b) the chemical reaction  $r_{15}$  turns the set of chemical reactions LD, (when removing this reaction the same structure presented in Figure 8.1(c) is obtained).

In networks with  $n_{rp} > 1$ , the scenario changes once structures with  $nr_{x_{\min}}$  ( $CI = 0$ ) can

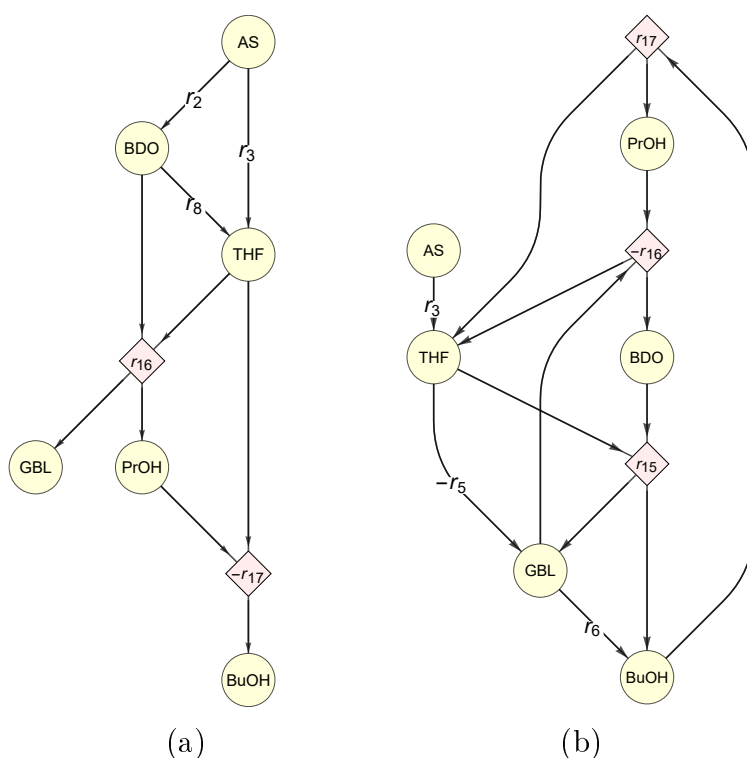


**Figure 8.2** Nonlinear reaction networks with  $\text{DI} = 1$ . The network parameters in (a) are  $\text{nr}x = 5$ ,  $\text{CI} = 1$ ,  $\text{RI} = 1$ ,  $\text{nr}x_{\text{li}} = 4$ . The network parameters in (b) are  $\text{nr}x = 6$ ,  $\text{CI} = 2$ ,  $\text{RI} = 1$ ,  $\text{nr}x_{\text{li}} = \text{nr}x_{\text{li,max}} = 5$ .

present particular sub-networks, *i. e.*, partitioned graphs, with feasible structures that may be plausible to explain experimental data, whether linear or not. In these cases, networks with  $\text{CI} > 0$  can present  $\text{RI} = 0$  (hence  $\text{DI} = 0$ ) in the presence of initial reactant(s) regeneration. See examples in Figure 8.3.

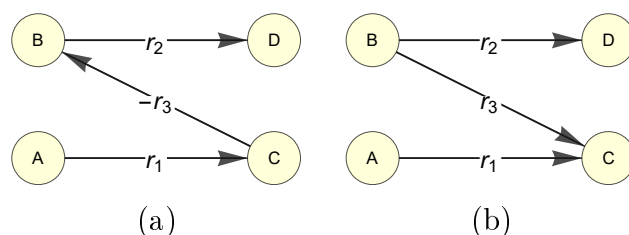


**Figure 8.3** Linear reaction networks with  $\text{nr}p = 2$ ,  $\text{DI} = 0$  and  $\text{CI} = 1$ . Species A and B are initially present in the mixture. Although both structures have the same dimension, they present different redundant index: in (a)  $\text{RI} = 0$  and in (b)  $\text{RI} = 1$ .

Every network complexity that a reaction network can present is illustrated in Figure 8.4. The inner circle represents the set of all networks composed of LI sets of chemical reactions. In this inner circle, networks with  $\text{RI} = 0$  belong to the left half, while networks with  $\text{RI} > 0$  belong to the right half. In the complementary set of the outer circle are all networks composed of LD sets of chemical reactions.

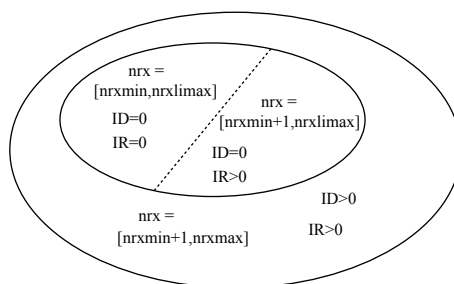


**Figure 8.4** Non-scaled graph illustrating the set of nonlinear reaction networks that can be divided into redundant ( $\mathbf{RI} > 0$ ) and non-redundant ( $\mathbf{RI} = 0$ ) linearly independent ( $\mathbf{DI} = 0$ ), and, redundant linearly dependent networks ( $\mathbf{RI} > 0$ ,  $\mathbf{DI} > 0$ ).

In a perspective of facing easier problems to then consider more complicated ones, first we are interested in analyzing the structures composed by LI non-redundant pathways ( $\mathbf{RI} = \mathbf{DI} = 0$ ), to then consider LI redundant ( $\mathbf{DI} = 0$ ,  $\mathbf{RI} > 0$ ) and, then, if needed consider LD structures ( $\mathbf{DI} > 0$ ). With the formulations presented in the next sections, linear and nonlinear networks with any  $\mathbf{nrp}$  can be generated with the desired  $\mathbf{CI}$ , presenting  $\mathbf{DI}$  and  $\mathbf{RI}$  controlled through (i) constraints that control the incidence of arcs in nodes in linear structures, and (ii) integer-cut equations in nonlinear structures.

The next section presents the definitions of sets that are needed in the following formulations to generate reaction networks as well as the constraints that are common in linear and nonlinear network generation problems.

### 8.3 Sets and common constraints in network generation problems

The generation of linear reaction networks is much simpler and easier to perform, having a direct relationship with the representation of the network in directed graphs where the arcs (which represent the reactions) that connect the nodes (the species) are associated with structural flows that close the mass balances at the nodes. On the other hand, generating nonlinear networks requires much more care, as there is no direct correspondence between chemical reactions and arcs. Thus, there is a need to treat the generation of linear and nonlinear networks separately, and this is the approach adopted in this chapter.

However, in linear and nonlinear network generation problems, some common sets and general constraints compose each formulation, these common aspects are presented in this section.

### 8.3.1 Defining sets

The species stoichiometric coefficients of every chemical reaction, generated in the Step 3, are used in the following routines to generate reaction networks, and auxiliaries sets are defined to map the reactant with product species. The species stoichiometric coefficients are stored in the parameters  $\mathbf{nsr}_{s,j}$  and  $\mathbf{nsp}_{s,j}$ , for  $s \in \mathbf{sp}$ ,  $j \in \mathbf{rx}$ .  $\mathbf{sp}$  and  $\mathbf{rx}$  are the sets of representative species and chemical reactions, respectively.

Additional sets are defined to establish the application domain of several formulation constraints:  $\mathbf{rp} \subset \mathbf{sp}$  and  $\mathbf{pp} \subset \mathbf{sp}$  are the subsets of the initial reactants and reaction products, respectively, such that  $\mathbf{rp} \cup \mathbf{pp} \equiv \mathbf{sp}$ . The subset of nonlinear reactions is denoted as  $\mathbf{rxnl} \subset \mathbf{rx}$ . Auxiliary sets  $\mathbf{exd} \equiv \{\mathbf{exd}_{s,s',j}\}$  and  $\mathbf{exi} \equiv \{\mathbf{exi}_{s,s',j}\}$  are also convenient to denote equations domains. With  $(s,s') \in \mathbf{sp}$ , these control sets can be used to identify flows between two species (reactant and product), concerning to reaction  $j \in \mathbf{rx}$ . These describe the reactions with net mass flows occurring either in the direct or reverse direction (respectively) of the representation used in a particular network. Additionally, for nonlinear reactions the mapping is also done considering the pair reactant/product species, *e.g.*, in the nonlinear reaction  $2A \xrightarrow{\mathbf{rxnl}} B + C$  the mapped pairs are  $(A,B,\mathbf{rxnl})$  and  $(A,C,\mathbf{rxnl})$ .

### 8.3.2 Common constraints

In most of the formulations that will be described in this chapter there are common restrictions related to the assignment of chemical reactions in the network. These restrictions are described in this section so as not to repeat them during descriptions of specific formulations.

Binary variables are used to set the direction of a chemical reaction  $j \in \mathbf{rx}$  in the network:  $\mathbf{yd}_j$  and  $\mathbf{yi}_j$  represent the direct and reverse directions, respectively. Each chemical reaction (associated with its net reaction flux) is considered in a given direction for the purpose of the reaction network generation, as presented in (8.1):

$$\mathbf{yd}_j + \mathbf{yi}_j \leq 1, \quad \forall j \in \mathbf{rx} \quad (8.1)$$

Chemical reactions that present reversible components are identified later by crossing the network obtained with experimental data in order to validate the structure of the network with viable net flow directions.

Binary variables  $\mathbf{yp}_{s,j}$  indicate whether the chemical species  $s \in \mathbf{sp}$  is a product in the reaction  $j \in \mathbf{rx}$ . The parameters  $\mathbf{nsr}_{s,j}$  and  $\mathbf{nsp}_{s,j}$  are used to define eqs. (8.2) and (8.3), linking variables  $\mathbf{yp}_{s,j}$ ,  $\mathbf{yd}_j$  and  $\mathbf{yi}_j$ , and thus, establishing the right direction of the reaction  $j$  in which the species  $s$  is a product:

$$\mathbf{yd}_j = \mathbf{yp}_{s,j}, \quad \forall s, j \in \mathbf{nsp} \quad (8.2)$$



$$y_i = y_{p_{s,j}}, \quad \forall s, j \in \text{nsr} \quad (8.3)$$

When the node  $s$  is not a product of the reaction  $j$ , *i.e.*, the species does not participate in this reaction, the variable  $y_{p_{s,j}}$  is set null, as shown in (8.4):

$$y_{p_{s,j}} = 0, \quad \forall s, j \notin \text{nsr} \cup \text{nsp} \quad (8.4)$$

Enforcing the presence of all species in the network, all products have to be generated at least once as given by (8.5):

$$\sum_{j \in \text{rx}} y_{p_{s,j}} \geq 1, \quad \forall s \in \text{pp} \quad (8.5)$$

The number of chemical reactions in the network,  $\text{nrx}$ , is calculated using binary variables, as in (8.6):

$$\text{nrx} = \sum_{j \in \text{rx}} y_{d_j} + y_{i_j} \quad (8.6)$$

## 8.4 Linear reaction networks

The method proposed to generate linear reaction networks (networks composed solely by linear chemical reactions) is supported on *structural flux analysis* (SFA) over a reaction network superstructure. It consists in a combinatorial discrete optimization problem in which chemical reactions are assigned satisfying linear constraints that ensure the network connectivity with a controlled number of chemical reactions. Through this MILP formulation, linear reaction networks can be generated with (i) different complexities, (ii) more than one initial reactant species, and (iii) parallel and series reaction pathways. If nonlinear reactions are present, additional difficulties associated with the generation of circular networks arise, and other constraints are necessary to ensure consistency on the production of species in a sequential fashion.

In the context of graph theory, as previously discussed in Chapter 3, linear reaction networks can be straightforwardly represented by graphs, where arcs and nodes correspond to chemical reactions and species, respectively (Figure 2.2(a)). Algorithms and formulations that respect to the synthesis of these graphs could be applied to generate linear reaction networks with  $\text{RI} = 0$ . Examples of these algorithms and formulations were presented in Section 3.3. In single- and multi-commodity flow formulations, closing flow balances at each node in the network prevents subtours from being obtained. The same technique is used during SFA. The developed formulation was inspired in the single-commodity flow (SCF) formulation presented by Gavish and Graves (1978) in the context of transportation scheduling problems. Unlike the original SCF, in the proposed SFA formulation (i) it is allowed to leave more than one or no paths from each node and it is not mandatory to return to the initial node, and (ii) the incidence of the node by arcs is controlled through the complexity of the network that we want to obtain and, therefore, cycles are allowed

when desired.

In linear superstructures in which all nodes are connected with each other, *i.e.*, *complete graphs*, the number of undirected arcs is computed using the binomial theorem, where the number of nodes  $n$  choose two, *i.e.*,

$$\binom{n}{2} = \frac{n!}{2!(n-2)!}$$

Since every undirected arc can represent a reaction in both directions, *i.e.*, the direct and the reverse reactions, the number of reactions in the complete linear superstructure corresponds to the double of how many ways it can be chosen two nodes out of  $n_{\text{sp}}$ :

$$\text{nr}x_{\text{sup}} = 2 \binom{n_{\text{sp}}}{2}$$

From these complete linear superstructures, the minimum number of arcs that connects every node is given by the total number of nodes minus one (Meyer, 2000; Marin and Yablonsky, 2011). Each additional arc added to this minimal structure will present a redundancy in this network, making the set of arcs linearly dependent. In other words, linear connected graphs composed by  $n$  nodes and  $n-1$  arcs present the maximum number of linearly independent interconnections among their nodes, without redundant pathways. However, linear reaction networks can present sub-graphs, *i.e.*, disconnected structures, in the presence of more than one (representative) initial reactant, and therefore, the minimal number of chemical reactions ( $\text{nr}x_{\text{min}}$ ) that can be required to explain the observed compositional changes can be inferior to the maximum number of linearly independent chemical reactions in a connected structure. Thus,  $\text{nr}x_{\text{min}}$  must be computed as a function of the number of representative species and initial reactants:

$$\text{nr}x_{\text{min}} = n_{\text{sp}} - \text{nr}p \quad (8.7)$$

The number of chemical reactions ( $\text{nr}x$ ) is related to  $\text{nr}x_{\text{min}}$  by the network complexity index ( $\text{CI}$ ) through:

$$\text{nr}x = \text{nr}x_{\text{min}} + \text{CI} = n_{\text{sp}} - \text{nr}p + \text{CI} \quad (8.8)$$

For linear reaction networks with  $\text{nr}p > 1$ , the minimal structures with  $\text{CI} = 0$  can present sub-graphs with (at most)  $\text{nr}p$  disconnected paths that are allowed to be verified. Some examples of these structures are given in the next section.

The number of linear dependencies in a network can also be controlled through the complexity index for any linear network with  $\text{nr}p$  initial reactant(s) through

$$\text{DI} = 1 - \text{nr}p + \text{CI} \quad (8.9)$$

The  $\text{DI}$  parameter varies between  $[0, \text{DI}_{\max}]$ . In cases where  $\text{nrp} > 1 + \text{CI}$ , the  $\text{DI}$  is considered zero.

Also, the number of redundant chemical reactions in a linear network has bounds given by  $\text{CI}$  in which

$$1 - \text{nrp} + \text{CI} \leq \text{RI} \leq \text{CI} \quad (8.10)$$

the lowest value of parameters  $\text{RI}$  and  $\text{DI}$  is zero. Thus, networks with  $\text{CI} = 0$ , also present  $\text{RI} = 0$ . In the example shown in Figure 8.3, two linear reaction networks with  $\text{CI} = 1$  and  $\text{nrp} = 2$  are presented with different values of  $\text{RI}$ . In (a) there is no redundancy, unlike in (b), where two incident arcs on species C are observed, although both (a) and (b) are composed of linearly independent sets of chemical reactions,  $\text{DI} = 0$ .

In the generation of linear reaction networks, the number of redundant chemical reactions can be controlled constraining the number of incident arcs in a node. Incorporating *a priori* information related to  $\text{RI}$  can be an advantage when avoiding the generation of undesired solutions, saving time and computational effort. For example, when generating networks with  $\text{CI} > 2$ , it may be desirable to generate only structures with products formed by at most two chemical reactions. Thus, linear reaction networks can be generated with the desired  $\text{CI}$  and  $\text{RI}$ , using SFA, this is the next topic.

### 8.4.1 Structural flux analysis (SFA)

Given the graph representation of a linear reaction network superstructure composed by  $\text{nr}_{\text{sup}}$  chemical reactions (directed arcs) and  $n_{\text{sp}}$  representative species (nodes), two additional (fictitious) nodes are considered, the *supersource* and *supersink* nodes, in order to establish SFA, see Figure 8.5. These dummy nodes are responsible for closing the global flow balance, so that the amount injected into the network, through the supersource node, is recovered in the supersink node. This amount is determined through the desired number of chemical reactions that the network should present. In fact, this quantity is related to the number of incident arcs in each node in the final structure.

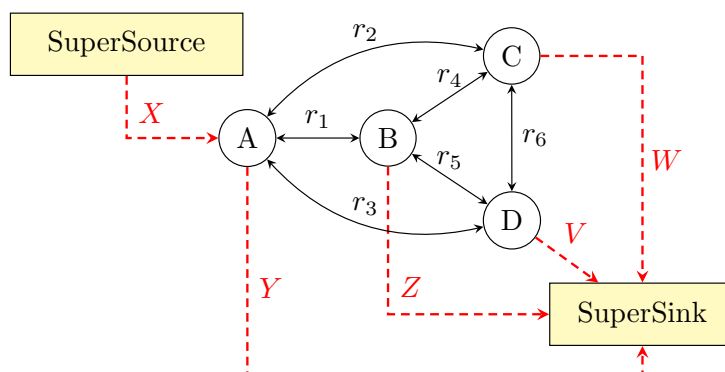


**Figure 8.5** SFA in the superstructure of a linear reaction network. The *supersource* node injects  $X$  units (structural flux) into the superstructure, and the *supersink* node receives  $Y$ ,  $Z$ ,  $V$  and  $W$  units from each node.

In Figure 8.5, the supersource node is only connected to components initially present in the reacting mixture, and it injects  $X$  units in the superstructure, an integer positive amount that equals  $\text{nrx}$ , such that

$$\sum_{s=1}^{n_{\text{sp}}} \text{ss}_s = \text{CI} + n_{\text{sp}} - \text{nrp} \quad (8.11)$$

where  $\text{ss}_s$  is the flux that entry in node  $s \in \text{sp}$  from the supersource node, a variable of the problem when  $\text{nrp} > 1$ . Notice that for non-initially present species, this variable is fixed null:

$$\text{ss}_s = 0, \quad \forall s \in \text{pp} \quad (8.12)$$

and, greater than zero for initial reactant species:

$$\text{ss}_s \geq 1, \quad \forall s \in \text{sp} \setminus \text{pp} \quad (8.13)$$

The supersink node is connected with all species nodes, receiving the amount  $\text{ni}_s$  of node  $s \in \text{sp}$ . The  $\text{ni}_s$  is the node incidence degree, representing the number of incident arcs in the node  $s$ , *i.e.*, the number of reactions in which this species is a product. Binary variables  $\text{yp}_{s,j}$  indicate whether the chemical species  $s \in \text{sp}$  is a product in the reaction  $j \in \text{rx}$  (or not). This variable is related with  $\text{ni}_s$  through:

$$\text{ni}_s = \sum_{j \in \text{rx}} \text{yp}_{s,j}, \quad \forall s \in \text{sp} \quad (8.14)$$

Hence the global flux balance is verified as

$$\sum_{s \in \text{sp}} \text{ss}_s = \sum_{s \in \text{sp}} \text{ni}_s = \sum_{s \in \text{sp}} \sum_{j \in \text{rx}} \text{yp}_{s,j} \quad (8.15)$$

like shown in Figure 8.5, where  $X = Y + Z + W + V$ .

Three examples of linear networks with different complexities are shown in Figure 8.6, where the structural fluxes are indicated above the arcs.

In Figure 8.7 there are three examples of SFA in linear systems with  $\text{nrp} = 2$ , where a system with  $\text{CI} = 0$  presents a single graph partition (two isolated graphs).

The data dimension analysis can always be considered apart from the network generation step, elucidating (when it is possible) the required dimension of the network to explain the observed data. While it is not necessary to determine the network complexity before generating networks, the obtainment of a reduced number of networks with  $\text{nrx}_{\text{li}}$  that are enough to explain the available data may be an advantage, saving time and computational effort during the methodology Steps 4 and 5.

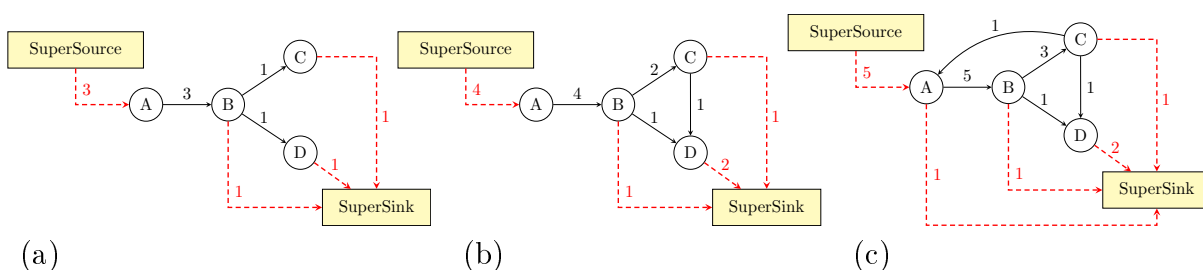


**Figure 8.6** SFA in linear reaction networks with  $n_{rp} = 1$  and  $n_{rx_{\min}} = n_{rx_{li, \max}} = 3$ . The corresponding graph presents (a)  $RI = CI = 0$ ,  $n_{rx} = 3$ , (b)  $RI = CI = 1$ ,  $n_{rx} = 4$  containing a redundant reaction pathway, and (c)  $RI = CI = 2$ ,  $n_{rx} = 5$ , containing two redundant reaction pathways with regeneration of the initial reactant.

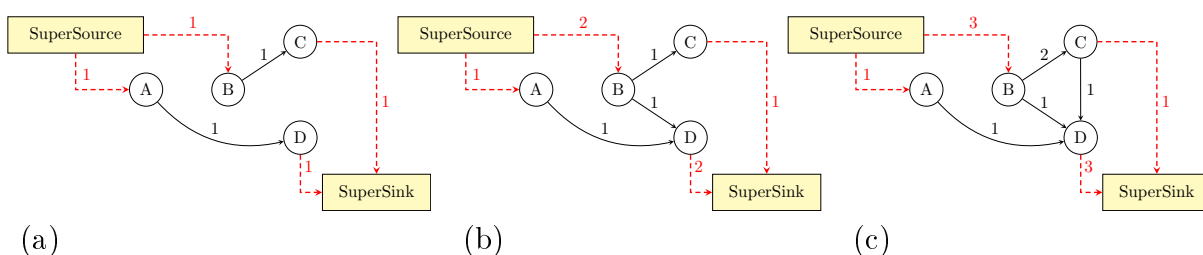


**Figure 8.7** SFA in linear reaction networks with  $n_{rp} = 2$  (species A and B are initial reactant),  $n_{rx_{\min}} = 2$  and  $n_{rx_{li, \max}} = 3$ . The corresponding graph presents (a)  $RI = 0$ ,  $CI = 0$ ,  $n_{rx} = 2$ , with two sub-networks, (b)  $RI = 1$ ,  $CI = 1$ ,  $n_{rx} = 3$ , and (c)  $RI = 2$ ,  $CI = 2$ ,  $n_{rx} = 4$ .

### SFA formulation (FSFA)

The flux balance for every node is given by (8.16), where  $F_{s,s'}$  corresponds to the structural flux from node  $s$  to  $s'$ .

$$ss_s + \sum_{s' \in sp} F_{s',s} - \sum_{s' \in sp} F_{s,s'} - \sum_{j \in rx} yp_{s,j} = 0, \quad \forall s \in sp \quad (8.16)$$

Additional constraints (big-M type) ensure that if a reaction is assigned to the network, the associated structural flux is greater than zero and inferior or equal to  $N$  (right- and left-hand sides of equations 8.17 and 8.18, respectively). On the other hand, when the reaction is not selected as solution constituent, the associated flux must be zero.

$$yd_j N \geq F_{s,s'} \geq yd_j, \quad \forall (s,s',j) \in \text{exd} \quad (8.17)$$

$$yi_j N \geq F_{s,s'} \geq yi_j, \quad \forall (s,s',j) \in \text{exi} \quad (8.18)$$

Regarding the previous restriction in (8.5), all products must be produced at least once, although this production is restricted by an upper limit that is related to the network

redundancy index, as given by (8.19).

$$\sum_{j \in rx} y_{p_{s,j}} \leq RI + 1, \quad \forall s \in sp \quad (8.19)$$

The objective function consists of the minimization of  $nrx$  in (8.6). However, this is an artificial goal since  $nrx$  is a fixed variable depending on the input parameter  $CI$ , which must be set before the network generation.

Formulation (8.20) constitutes a MILP problem with binary and integer variables and linear constraints that can be solved for a global optimal solution.

$$\min_{\substack{F, y_d, \\ y_i, y_p}} nrx \quad (8.20a)$$

$$\text{s.t. eqs. (8.1—8.6, 8.11—8.13, 8.16—8.21)} \quad (8.20b)$$

$$F_{s,s'}, ss_s \in \mathbb{N}_+, \quad \forall s, s' \in sp \quad (8.20c)$$

$$y_{d_j}, y_{i_j}, y_{p_{s,j}} \in \{0,1\}, \quad \forall s \in sp, j \in rx \quad (8.20d)$$

Alternative networks with the same complexity can be enumerated using *integer cut* equations, (8.21). For this purpose, the previous solutions  $i \in it$  (described by the binary variables  $y_{d_j}$  and  $y_{i_j}$ ) are stored in the parameters  $ccrd_{j,i}$  and  $ccri_{j,i}$ . Through the following inequality constraint, the generation of repeated networks is forbidden.

$$\sum_{j \in rx} ccrd_{j,i} y_{d_j} + \sum_{j \in rx} ccri_{j,i} y_{i_j} - \sum_{j \in rx} (1 - ccrd_{j,i}) y_{d_j} - \sum_{j \in rx} (1 - ccri_{j,i}) y_{i_j} \leq \sum_{j \in rx} ccrd_{j,i} + \sum_{j \in rx} ccri_{j,i} - 1, \quad \forall i \in it \quad (8.21)$$

### FSFA - Example 1

In this example, the analysis of the size of the linear network generation problem is performed, evaluating the number of viable solutions. For this purpose, *complete graphs* were considered with a number of nodes varying between three and nine, spanning all networks complexities for linear systems with a single initial reactant.

In Table 8.1 the number of reaction networks obtained is indicated, spanning several RIs. The RI is equivalent to the CI and DI parameters, since the considered examples are linear reaction networks with  $n_{rp} = 1$ . For networks with  $RI = 0$ , the Cayley formula indicates that there are  $n_{sp}^{n_{sp}-2}$  different possible structures (Gross and Yellen, 2005).

Analyzing the results obtained, the number of reaction networks can explode when the number of species is high. To get around this, when many species are present, the follow items can be considered:

**Table 8.1** Problem dimension analysis for linear reaction networks with one initial reactant species. The starting reaction network superstructures are complete graphs with  $n_{\text{sp}}$  nodes. The number of reaction networks grows exponentially with the number of species in the system for the same RI.

$n_{\text{sp}}$	RI	nr <sub>x</sub>	number of reaction networks	$n_{\text{sp}}$	RI	nr <sub>x</sub>	number of reaction networks
3	0	2	3	6	0	5	1 296
	1	3	4		1	6	16 620
4	0	3	16		2	7	96 960
	1	4	63		3	8	339 045
	2	5	84		4	9	787 300
5	3	6	38		5	10	1 269 084
	0	4	125		6	11	1 438 620
	1	5	972		7	12	1 132 720
	2	6	3 190		8	13	592 950
	3	7	5 660		9	14	186 360
	4	8	5 730	10	15	26 704	
8	5	9	3 140	7	0	6	16 807
	6	10	728		1	7	320 400
	0	7	262 144	2	8	1 700 937	
1	8	4 155 143	9	0	8	4 782 969	

- the implicit generation of structures, coupling the Steps 4 and 5 of the proposed methodology, by incorporating experimental data in the formulation to generate only plausible reaction networks (Vertis et al., 2016).
- the incorporation of additional linear constraints, reducing the space of solutions (the most constrained problem). Knowledge about a particular reaction system may be used as constraints for the network generation, *e.g.*, a reaction is known to happen in the system, thus, it can be fixed in the structure.
- the use of additional criteria to limit the reaction network superstructure, *e.g.*, besides stoichiometric constraints, energetic characteristics can be considered to generate chemical reactions stoichiometrically consistent and also energetically favorable. In this case, the net reaction directionality can be elucidated, thus reducing the  $\text{nr}_{\text{x}_{\text{sup}}}$  and, consequently, the number of reaction networks (Vertis et al., 2017).

### FSFA - Example 2

Regarding the AS case study, the superstructure of linear reaction networks (obtained in the previous methodology step) contemplates 15 chemical reactions among 6 representative species, as it was shown in Figure 7.5. From this set of reactions, in the system experimental conditions, 11 mass flux directions were identified as energetically feasible.

AS linear case study characteristics: (i)  $\text{nrp} = 1$ , (ii)  $\text{nrx}_{\text{sup}} = 15$  and  $\text{nrx}_{\text{min}} = 5$ .

The generation of reaction networks was performed in GAMS® with the CPLEX solver, where 144 energetically feasible reaction networks were obtained with  $\text{RI} = 0$ . Examples of these minimal structures are shown in Figure 8.8.

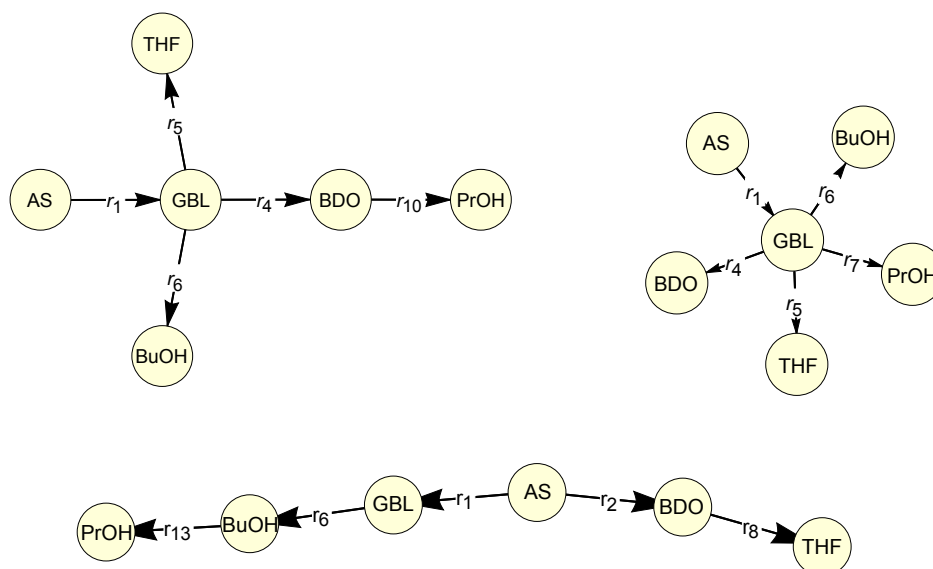


**Figure 8.8** Representation of the 3 first reaction networks generated for AS case study.

However, if the generation of linear structures with  $\text{RI} = 0$  from the network superstructure with 26 chemical reactions (without energetic analysis of net flux directions) would be considered, the number of generated reaction networks increases to 540. Therefore, the number of solutions decreased in 73% when considering the energetic flux analysis for this case study.

## 8.5 Nonlinear reaction networks

Previously, the generation of linear reaction networks<sup>1</sup> was proposed using SFA. SFA guarantees network connectivity by checking the balances of fictitious units that travel through the network, necessarily passing through each node, where the total number of units that enter the network corresponds to the sum of units that leave each visited node (Vertis et al., 2015). However, in general reaction networks may involve chemical reactions with more than one species as reactant and/or as product, namely nonlinear chemical reactions, that can be represented through bipartite graphs (Temkin et al., 1996). The generation of nonlinear networks is more challenging since the presence of

<sup>1</sup>Linear reaction networks are represented by linear graphs where arcs and nodes correspond to chemical reactions and species, respectively. Thus they contain chemical reactions that involve the mass transformation between two representative species.



inconsistencies can appear in nonlinear circular networks when considering only the node balances of structural fluxes as a criterion to generate connected structures, as shown in Figure 8.9. Therefore, the establishment of an order of precedence between nodes is necessary to guarantee the production of species in a sequential way, resulting in a consistently connected network.

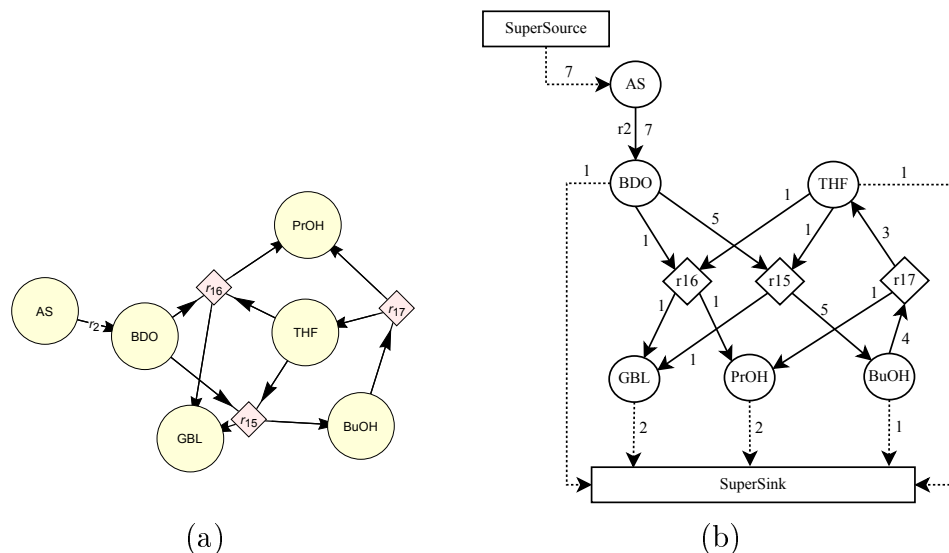


**Figure 8.9** Graph representation of an inconsistent nonlinear reaction network: the THF species is participating as reactant in both  $r_{16}$  and  $r_{15}$  without had been generated before. (a) Inconsistent reaction network. (b) Structural fluxes that satisfy the node balance equations ensuring a connected structure, although allowing nonlinear network inconsistencies.

The precedence among nodes can be imposed through the use of (i) ordering constraints such as MTZ-based constraints in which a position is assigned to each visited node in the network, imposing a sequence of visited nodes in an increasing fashion (Miller et al., 1960; Taccari, 2016), and/or (ii) the concept of a tree of states where binary variables are assigned to several states of the tree that describes a consistently connected network (Kondili et al., 1993; Shah et al., 1993; Maravelias and Grossmann, 2003). Both strategies were studied and adopted to generate nonlinear reaction networks, culminating in the development of three MILP formulations. These formulations are presented in the following sections.

### 8.5.1 Enumeration of reaction networks using ordering constraints

Ordering constraints establish a position (or a theoretical time) of the node along the path, ensuring an increasing order of nodes during the nodes appearance. Miller et al. (1960) were the pioneers in the use of ordering constraints, proposing the most compact formulation in the context of TSP, where the distance traveled by the salesman is minimized subjected to visit a set of cities only once. The development of ordering constraints was motivated in order to avoid undesired subtours in the optimal solutions. They

named these constraints with their surname initials, MTZ, Miller-Tucker-Zemlin. Hence, the MTZ constraints ensure a salesman route that increases his position when visiting next cities, thus establishing a sequential and connected pathway among visited cities using auxiliary variables beyond assignment constraints. The MTZ constraints assume the following format:

$$\begin{aligned} t_1 &= 1, \\ 2 \leq t_i &\leq n, \quad \forall i \neq 1, \\ t_i - t_j + 1 &\leq (n - 1)(1 - y_{i,j}), \quad \forall i \neq 1, j \neq 1 \end{aligned} \tag{8.22}$$

where  $t$  is the position of nodes  $i$  and  $j$  (node alias),  $n$  the number of nodes, and  $y_{i,j}$  the binary variable that assumes one when the path that links nodes  $i$  to  $j$  is assigned to the route. The initial node has the position one. These constraints do not apply to the first node, since in the TSP the salesman route starts and ends at the initial node, and therefore it would be infeasible with (8.22) to assign a directed arc from the last node  $n$  to the first node, closing the circuit. However, as the assignment constraints state that at each node there is a single output arc and a single input arc, the Hamiltonian circuit is perfectly established avoiding subtours by the MTZ constraints.

When  $y_{i,j}$  is equal to one in (8.22), *i.e.*,  $t_j \geq t_i + 1$ , this constraint assumes the same structure as the one proposed in CPM scheduling problems. In CPM there is no decision variables since every activity is already assigned, although their time duration can differ of the unity and thus, the objective here is to schedule these activities without the need to choose one face another. Hence, the CPM scheduling problem is in the field of linear programming, in which ordering constraints without binary variables make up the formulation.

However, MTZ constraints are known to present weak LP relaxations. [Langevin et al. \(1990\)](#); [Padberg and Sung \(1991\)](#); [Gouveia and Pires \(1999\)](#); [Bektaş and Gouveia \(2014\)](#) and other authors have demonstrated a lower polytope projection of the feasible convex hull of solutions from the relaxed LP problem regarding other formulations in the context of TSP. For example, the commodities-based formulations (that uses structural flux analysis) showed larger relaxation value. For more details see Section 3.3.2 in the state of the art of this thesis.

[Haouari et al. \(2013\)](#) presented a stronger formulation than MTZ for ordering constraints, which was obtained using the reformulation linearization technique (RLT), as originally proposed by [Sherali and Adams \(1990\)](#). The RLT is applied in the nonlinear version of MTZ constraints,

$$\begin{aligned} t_j y_{i,j} &= (t_i + 1) y_{i,j}, \quad \forall i, j \\ t_j y_{1,j} &= y_{1,j}, \quad \forall j \end{aligned} \tag{8.23}$$

in which these equations are linearized using auxiliary variables  $\alpha_{i,j}$  and  $\beta_{i,j}$ , such that

$$\alpha_{i,j} = t_j y_{i,j} \quad \text{and} \quad \beta_{i,j} = t_i y_{i,j} \quad (8.24)$$

Then the following equations establish a sequence of nodes through:

$$\begin{aligned} \alpha_{i,j} &= \beta_{i,j} + y_{i,j}, \quad \forall i,j, \\ \sum_{i \neq 1} \alpha_{i,j} - \sum_{i \neq 1} \beta_{j,i} &= 0 \quad \forall j \neq n, \\ y_{1,j} + \sum_{i \neq 1} \alpha_{i,j} - \sum_i \beta_{j,i} &= 0 \quad \forall j. \end{aligned} \quad (8.25)$$

However, with the exception of the arc that closes the circuit from the  $n$  visited node to the starting node, as originally proposed, both eqs. (8.22) and (8.25) do not allow circular structures during the pathway, since it is forbidden the assignment of paths in which arcs go back to any node  $i > 1$  previously visited. In contrast, nonlinear reaction networks can present many cycles. For example, in Figure 8.9 if THF had been produced by BDO or AS, making a consistent network, this reaction network would present a feasible cycle among THF and BuOH species. Therefore, to generate nonlinear networks it is required a formulation that simultaneously allows cycles in its structure and verifies species precedence, ensuring a feasible and consistent network that translates the species consumption and production observed in the chemical reacting system. Attending these needs, two formulations were developed based on MTZ and RLT, respectively. Basically, the key idea of these two formulations is to ensure that every species must be produced before be consumed in *a posteriori* chemical reaction, unless it is an initially present species in the mixture. For this purpose, the time/position in which each species is firstly produced must be specified, verifying that (i) it can only be a reactant if this specific time is reached, (ii) it can be produced again later through other chemical reaction presenting a superior time than that of the first production. In order to implement these requirements, disjoint constraints were used (Grossmann and Ruiz, 2012) identifying when the time of species appearance is minimum. The next sections present the both ordering constrained formulations based on MTZ and RLT (FMTZ and FRLT, respectively) with supporting examples.

### MTZ-based formulation (FMTZ)

The key constraint in this formulation, as shown in (8.26), establishes an order for gradual species production, preventing the cases where a species is a reactant without it had been a product before, unless this species is initial reactant species.

$$T_{\min s} - T_{s',j} + 1 \leq M(1 - y_{p_{s',j}}), \quad \forall s, s', j \in \text{exd} \cup \text{exi} \quad (8.26)$$

where  $T_{\min_s}$  is the minimum theoretical time required to the species  $s \in \mathbf{sp}$  production,  $T_{s',j}$  is the theoretical time that species  $s' \in \mathbf{sp}$  is produced through the reaction  $j \in \mathbf{rx}$ . Notice that (i) the chemical reaction  $j$  occurs among species  $s$  to  $s'$  as mapped on the controlled sets  $\mathbf{exd}$  and  $\mathbf{exi}$  (these sets definitions were presented in Section 8.3.1), (ii) every assigned chemical reaction present, at least, a duration of one unity, and (iii) the  $T_{\min}$  of the initial reactant species is set one. Thus, according to (8.26), when the species  $s'$  is produced in the reaction  $j$ ,  $\mathbf{yp}_{s',j} = 1$ , its production theoretical time  $T_{s',j}$  has to be greater (at least in one unity) than the minimum theoretical time  $T_{\min_s}$  required for the production of the reactant species  $s$ , *i.e.*,  $T_{s',j} \geq T_{\min_s} + 1$ .

Otherwise, when the species  $s'$  is not produced by the reaction  $j$ ,  $\mathbf{yp}_{s',j} = 0$ , the  $T_{s,j}$  has to be equal to the superior bound  $M$  imposed, as shown in (8.27).

$$T_{s,j} \geq M(1 - \mathbf{yp}_{s,j}), \quad \forall s,j \in \mathbf{nsr}_{s,j} \cup \mathbf{nsp}_{s,j} \quad (8.27)$$

Both the  $T_{\min_s}$  and  $T_{s,j}$  can vary between  $[1,M]$ , they are declared as positive variables, although they assume only integer amount since the integrality property holds. The upper bound  $M = n_{\mathbf{sp}} + 1$  is enough to cover the generation of networks with all complexities between  $[\mathbf{nrx}_{\min}, \mathbf{nrx}_{\max}]$ . However, as we are interested in generating networks with  $\mathbf{DI} = 0$ , the superior bound will never cross  $\mathbf{nrx}_{\mathbf{li},\max} + 1$ , and thus, it can be updated to  $M = \mathbf{nrx}_{\mathbf{li},\max} + 1$ .

The variable  $T_{s,j}$  is fixed null for the pairs species/reaction that do not belong to the previously identified parameters  $\mathbf{nsr}_{s,j}$  and  $\mathbf{nsp}_{s,j}$ , as presented in (8.28).

$$T_{s,j} = 0, \quad \forall s,j \notin \mathbf{nsr}_{s,j} \cup \mathbf{nsp}_{s,j} \quad (8.28)$$

The minimum theoretical time  $T_{\min_s}$  required to the production of species  $s$  is constrained to be equal to the lowest production theoretical time  $T_{s,j}$  of the same species  $s$  as a product in reaction  $j$ . This statement is achieved considering disjunctive constraints, as shown in eqs. (8.29) and (8.30):

$$T_{\min_s} \leq T_{s,j}, \quad \forall s,j \in \mathbf{nsr}_{s,j} \cup \mathbf{nsp}_{s,j} \quad (8.29)$$

$$T_{\min_s} \geq T_{s,j} - M(1 - \mathbf{yt}_{s,j}), \quad \forall s,j \in \mathbf{nsr}_{s,j} \cup \mathbf{nsp}_{s,j} \quad (8.30)$$

where the binary variable  $\mathbf{yt}_{s,j}$  is used to identify which reaction  $j$  that produces species  $s$  leads to the minimal  $T_{s,j}$  value. Hence, when  $\mathbf{yt}_{s,j} = 1$ , necessarily  $T_{s,j} = T_{\min_s}$ . On the other hand, when  $\mathbf{yt}_{s,j} = 0$ , both eqs. (8.29) and (8.30) are inactive during optimization, *i.e.*, they are always verified in the optimal solution.

At least one chemical reaction  $j \in \mathbf{rx}$  has to verify  $T_{s,j} = T_{\min_s}$  for every product species  $s \in \mathbf{pp}$ . This is achieved imposing that at least an unique  $\mathbf{yt}_{s,j}$  presents the unity value

for every product species  $s \in \mathbf{pp}$ , as shown in (8.31):

$$\sum_{j \in \mathbf{rx}} \mathbf{y}t_{s,j} \geq 1, \quad \forall s \in \mathbf{pp} \quad (8.31)$$

Notice that this equation dispenses the need to impose the constraint in (8.5), since every product species generation is implicitly ensured through eq. (8.31).

The  $\mathbf{y}t_{s,j}$  is forced to be null when the species  $s$  is not produced via reaction  $j$ , and in simultaneous, it forces  $\mathbf{y}p_{s,j}$  to assume the unity value when  $\mathbf{y}t_{s,j} = 1$ , as shown in (8.32).

$$\mathbf{y}t_{s,j} \leq \mathbf{y}p_{s,j}, \quad \forall s,j \in \mathbf{nsr}_{s,j} \cup \mathbf{nsp}_{s,j} \quad (8.32)$$

Also,  $\mathbf{y}t_{s,j}$  is fixed null when the pair  $(s,j)$  is not mapped in the controlling sets, as presented in (8.33).

$$\mathbf{y}t_{s,j} = 0, \quad \forall s,j \notin \mathbf{nsr}_{s,j} \cup \mathbf{nsp}_{s,j} \quad (8.33)$$

The formulation (8.34) constitutes a MILP with binary and integer variables and linear constraints that can be solved to global optimal solution, generating linear and nonlinear reaction networks with  $\mathbf{nrp} = 1$ .

$$\min_{\substack{\mathbf{y}d, \mathbf{y}i, \mathbf{y}p, \mathbf{y}t, \\ \mathbf{T}_{\min}, \mathbf{T}}} \mathbf{nrx} \quad (8.34a)$$

$$\text{s.t. eqs. (8.1—8.4, 8.6, 8.26—8.33)} \quad (8.34b)$$

$$\mathbf{y}d_j, \mathbf{y}i_j, \mathbf{y}p_{s,j}, \mathbf{y}t_{s,j} \in \{0,1\}, \quad \forall s \in \mathbf{sp}, j \in \mathbf{rx} \quad (8.34c)$$

$$\mathbf{T}_{\min,s}, \mathbf{T}_{s,j} \in \mathbb{R}^+, \quad \forall s \in \mathbf{sp}, j \in \mathbf{rx} \quad (8.34d)$$

When  $\mathbf{nrp} > 1$ , new controlling sets must be established mapping the species  $s \in \mathbf{pp}$  that are produced in specific reaction  $j \in \mathbf{rx}$  from each initial reactant species. For example, if species A and B are initially present in the reacting mixture,  $\mathbf{nsprA}_{s,j}$  and  $\mathbf{nsprB}_{s,j}$  are parameters that maps every reaction  $j$  that produces species  $s$  from reactants A and B, respectively. These parameters are required to impose that every initial reactant must react in the network, through the equations

$$\sum_{(s,j) \in \mathbf{nsprA}} \mathbf{y}p_{s,j} \geq 1 \quad \text{and} \quad \sum_{(s,j) \in \mathbf{nsprB}} \mathbf{y}p_{s,j} \geq 1 \quad (8.35)$$

However when  $\mathbf{nrp} = 1$ , these constraints are not required since the restrictions related to (i) the precedence among species appearance and (ii) the production of every product in the network, eqs. (8.26) and (8.31), respectively, simultaneously ensure that the unique initial reactant is reagent in some assigned reaction(s) in the optimal solution.

In order to enumerate all reaction networks that are LI non-redundant, with complexities between  $[\mathbf{nrx}_{\min}, \mathbf{nrx}_{\mathbf{li}, \max}]$ , the integer cut equations from (8.21) were manipulated to

forbid not only the solutions found in earlier iterations, but also the ones that contain the same basis of chemical reactions. This means that all feasible networks with  $\text{nrx}_{\min}$  are generated first, since  $\text{nrx}$  is being minimized, when passing to the generation of structures with  $\text{nrx} > \text{nrx}_{\min}$ , only the ones with  $\text{RI} = 0$  will be feasible. This is achieved by imposing that at least two chemical reactions are different from the previous solutions. This means that no chemical reactions can be added to previously found solutions, the new solution must contain a different scheme linking each node. For example, if  $\text{nrx}_{\min} = 3$ , when enumerating all feasible networks with 3 reaction components the criterion is always checked since all networks with  $\text{nrx}_{\min}$  are non-redundant LI. However, when considering generating LI networks with  $\text{nrx} > \text{nrx}_{\min}$ , the problem is more restrictive as it does not allow the same combination (observed in previous solutions) of  $\text{nrx} - 1$  binary variables to equal unity. Thus, when  $\text{nrx} = 4$ , the same sets of 3 reactions generated previously cannot be observed as a constituent of the new four-component basis, and so on.

The enumeration of all LI non-redundant networks ( $\text{DI} = \text{RI} = 0$ ) is obtained adding eq. (8.36) to the formulation (8.34).

$$\sum_{j \in \text{rx}} \text{ccrd}_{j,i} y_{d_j} + \sum_{j \in \text{rx}} \text{ccri}_{j,i} y_{i_j} \leq \sum_{j \in \text{rx}} \text{ccrd}_{j,i} + \sum_{j \in \text{rx}} \text{ccri}_{j,i} - 1 \quad \forall i \in \text{it} \quad (8.36)$$

This constraint is active after the obtainment of the first solution in which the parameters  $\text{ccrd}_{j,i}$  and  $\text{ccri}_{j,i}$  store the optimal values of the binary variables related to the chemical reactions in the direct and reverse direction, respectively, for every  $i \in \text{it}$  solver iteration, *i.e.*,

$$\text{ccrd}_{j,i} = y_{d_j} \quad \text{and} \quad \text{ccri}_{j,i} = y_{i_j}, \quad \forall j \in \text{rx}$$

The enumeration of feasible solutions stops when there is no more structures LI non-redundant to be generated.

### FMTZ example

Consider the circular nonlinear reaction network presented on the left side in Figure 8.10. The temporal scale of species production is outlined on the right-hand side of the same figure, where the nodes AS and AS' represent the same species, but with different theoretical production time. In fact the nonlinear chemical reaction  $-r_{14}$ :  $2 \text{GBL} \rightarrow \text{THF} + \text{AS}$  has an arrow coming back to the initial reactant AS. The arrow that close the cycle concerning the  $-r_{14}$  is allowed since the theoretical time of production of the species AS in reaction  $-r_{14}$ ,  $\tau_{\text{AS},-r_{14}} = 3$ , is greater than the theoretical production time of the reactant species GBL,  $\tau_{\min \text{GBL}} = 2$ , thus ensuring the obtainment of a consistent reaction network.

### RLLT-based formulation (FRLLT)

In the RLLT-based formulation, variable substitutions similar to (8.24) were performed in order to turn the MTZ-based formulation (8.34) stronger. For this purpose, the surrogate

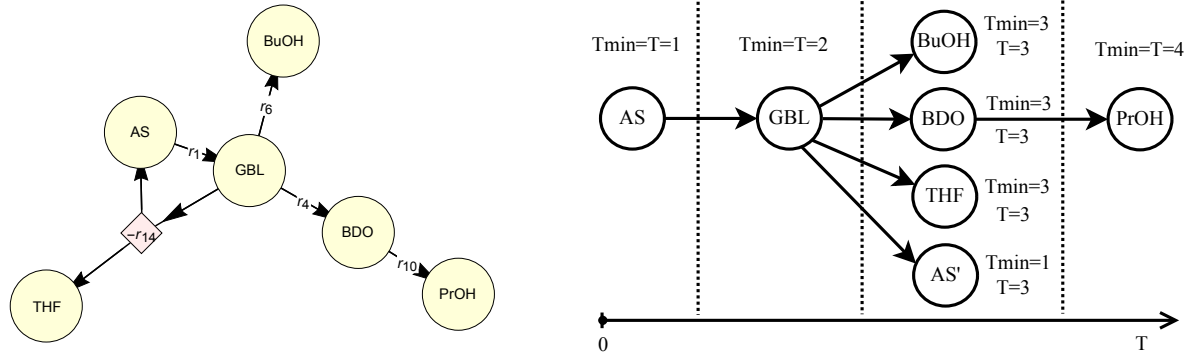


**Figure 8.10** Nonlinear reaction network with a feasible cycle and its respective temporal scale of species production. Notice that this reaction network has  $CI = 1$ ,  $nr_x = nr_{x_{li,max}} = 5$  and  $RI = 0$ ; no chemical reaction can be discarded of this structure without turning it infeasible.

variables  $\alpha_{s,j}$  and  $\beta_s$  were considered to substitute  $T_{s,j}$  and  $T_{mins}$ , respectively, as shown in (8.37):

$$\alpha_{s,j} = T_{s,j} y_{p_{s,j}} \quad \text{and} \quad \beta_s = T_{mins} y_{p_{s,j}} \quad (8.37)$$

Therefore, similarly with (8.26), the precedence among nodes is verified through

$$\beta_s + y_{p_{s',j}} \leq \alpha_{s',j}, \quad \forall s, s', j \in \text{exd} \cup \text{exi} \quad (8.38)$$

where  $\beta_s$  is the minimum position/time of production of species  $s \in \text{sp}$  and  $\alpha_{s',j}$  the position/time of species  $s' \in \text{sp}$  originated through the chemical reaction  $j \in \text{rx}$ . Thus, when  $y_{p_{s',j}} = 1$ , indicating that the product  $s' \in \text{sp}$  is produced in reaction  $j \in \text{rx}$ , the position of  $s'$  has to be greater (at least in one unity) than the first position of its reactant species  $s$ . On the other hand, when  $y_{p_{s',j}} = 0$ ,  $\alpha_{s',j}$  assumes the value of the upper bound  $M$ :

$$\alpha_{s,j} \geq M(1 - y_{p_{s,j}}), \quad \forall s, j \in \text{nsr}_{s,j} \cup \text{nsp}_{s,j} \quad (8.39)$$

where  $M = nr_{x_{li,max}} + 1$ .

Similarly with the previous formulation (8.34), the binary variable  $y_{t_{s,j}}$  is used to identify the reaction  $j$  which produces species  $s$  with the minimal  $\alpha_{s,j}$ . This is achieved using disjunctive constraints, as shown in eqs. (8.40) and (8.41):

$$\beta_s \geq \alpha_{s,j} - M(1 - y_{t_{s,j}}), \quad \forall s, j \in \text{nsr}_{s,j} \cup \text{nsp}_{s,j} \quad (8.40)$$

$$\alpha_{s,j} \geq \beta_s, \quad \forall s, j \in \text{nsr}_{s,j} \cup \text{nsp}_{s,j} \quad (8.41)$$

Thus, when  $y_{t_{s,j}} = 1$ ,  $\alpha_{s,j} = \beta_s$ . The restrictions related to  $y_{t_{s,j}}$  in the previous formulation, eqs. (8.31) to (8.33), are also part of this formulation.

For the purpose of reaction network generation, each chemical reaction can only be considered in a unique direction (direct or reverse), as such it was imposed in (8.1). In this formulation it is established through the following constraints:

$$\mathbf{y}r_{s,j} = \mathbf{y}p_{s',j}, \quad \forall s,s',j \in \text{exd} \cup \text{exi} \quad (8.42)$$

$$\mathbf{y}r_{s,j} + \mathbf{y}p_{s,j} = \mathbf{y}rx_j, \quad \forall s,j \in \text{nsp}_{s,j} \quad (8.43)$$

where the binary variable  $\mathbf{y}r_{s,j}$  indicates that the species  $s$  is a reactant in reaction  $j$ , as such as  $\mathbf{y}p_{s,j}$  indicates the species  $s$  is a product in reaction  $j$ , and  $\mathbf{y}rx_j$  indicates the chemical reaction  $j \in \text{rx}$  assignment in the optimal solution.

The variables  $\mathbf{y}r_{s,j}$  and  $\alpha_{s,j}$  are fixed null for the pairs species/reaction that do not belong to the parameters  $\text{nsr}_{s,j}$  and  $\text{nsp}_{s,j}$ , as presented in eqs. (8.44) and (8.45).

$$\mathbf{y}r_{s,j} = 0, \quad \forall s,j \notin \text{nsr}_{s,j} \cup \text{nsp}_{s,j} \quad (8.44)$$

$$\alpha_{s,j} = 0, \quad \forall s,j \notin \text{nsr}_{s,j} \cup \text{nsp}_{s,j} \quad (8.45)$$

The number of chemical reactions in the network is computed through:

$$\text{nrx} = \sum_{j \in \text{rx}} \mathbf{y}rx_j \quad (8.46)$$

The formulation (8.47) constitutes a MILP with binary and integer variables and linear constraints that can be solved to the global optimal solution.

$$\min_{\substack{\mathbf{y}rx, \mathbf{y}r, \mathbf{y}p, \mathbf{y}t, \\ \alpha, \beta}} \text{nrx} \quad (8.47a)$$

$$\text{s.t.} \quad \text{eqs. (8.4, 8.31—8.33, 8.38—8.46)} \quad (8.47b)$$

$$\mathbf{y}rx_j, \mathbf{y}r_{s,j}, \mathbf{y}p_{s,j}, \mathbf{y}t_{s,j} \in \{0,1\}, \quad \forall s \in \text{sp}, j \in \text{rx} \quad (8.47c)$$

$$\alpha_{s,j}, \beta_s \in \mathbb{R}^+, \quad \forall s \in \text{sp}, j \in \text{rx} \quad (8.47d)$$

When  $\text{nrp} > 1$ , the constraint in (8.48) must be added to (8.47), ensuring that every initial reactant species participates in the reaction network.

$$\sum_{j \in \text{rx}} \mathbf{y}r_{s,j} \geq 1, \quad \forall s \in \text{sp} \setminus \text{pp} \quad (8.48)$$

Thus, at least a single chemical reaction  $j$  with the respective initial reactants as reagent must be verified in the solution when  $\text{nrp} > 1$ .

The enumeration of all LI non-redundant networks ( $\text{DI} = \text{RI} = 0$ ) is obtained adding (8.49)



to the formulation (8.47).

$$\sum_{j \in \text{rx}} (\text{ccrd}_{j,i} + \text{ccri}_{j,i}) \text{yrx}_j \leq \sum_{j \in \text{rx}} \text{ccrd}_{j,i} + \text{ccri}_{j,i} - 1 \quad \forall i \in \text{it} \quad (8.49)$$

This constraint is active after the obtainment of the first solution in which the parameters  $\text{ccrd}_{j,i}$  and  $\text{ccri}_{j,i}$  store the optimal values of the binary variables related to the the chemical reactions in the direct and reverse direction, respectively, for every  $i \in \text{it}$  solver iteration, *i.e.*,

$$\text{ccrd}_{j,i} = \text{yp}_{s,j} \quad \text{and} \quad \text{ccri}_{j,i} = \text{yr}_{s,j}, \quad \forall s, j \in \text{nsp}_{s,j}$$

The enumeration of feasible solutions stops when there is no more structures LI non-redundant.

### 8.5.2 Enumeration of reaction networks using a tree of states

The concept of a tree of states is inspired on the classical scheduling optimization problems involving similar constraints of assignment and state task network problems. In this case the tree contains several states that are organized in sequential levels that grow in depth. Each state is represented by a list of chemical species and a list chemical reactions, that increase in size with the tree level. Every reaction network is sequentially built through the addition of chemical reactions in consecutive states of every tree level. Therefore, as the network of reactions increases in size, the number of states also increases, thus growing the tree in depth. In every solver iteration an unique reaction network (optimal solution) is obtained at the bottom level of the tree forming a linear sequence of states (a single tree branch). When all feasible networks are enumerated, the simultaneous representation of every explored state to obtain the set of feasible solutions forms a tree. For example, consider the linear superstructure presented in Figure 8.11 where 4 chemical species and 12 chemical reactions (direct and reverse components) compose the network domain. The corresponding tree of states for these sets of chemical species and reactions is shown in Figure 8.12.

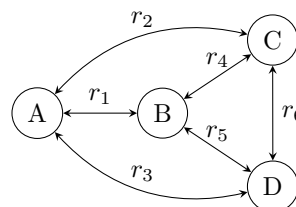
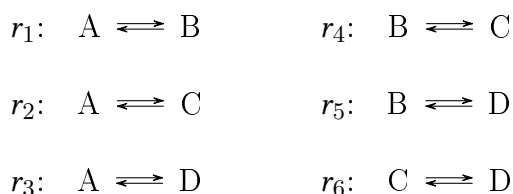


**Figure 8.11** Superstructure of a linear reaction network with 4 representative species and 6 reversible chemical reactions.

Simultaneously with the addition of a *single reaction* in every state, the assignment of *chemical species* is also carried on, corresponding to the species produced in that reaction. The avoidance of inconsistent networks is achieved imposing *preconditions* for every state,

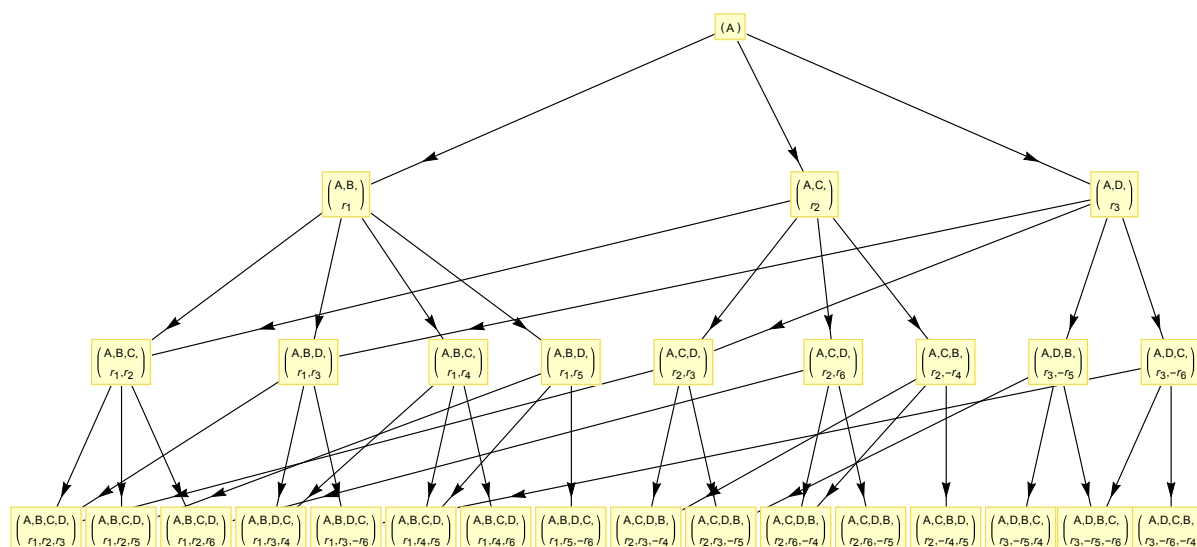


**Figure 8.12** Tree of states respected to the linear network superstructure presented in Figure 8.11. 16 complete states are at the bottom level of the tree, presenting linear reaction networks without redundant pathways.

*e.g.*, to add a chemical reaction in a current state of the tree, the respective reactant species must be available in the previous state.

During the network construction every state is characterized by two lists: (i) the available species, and (ii) the selected chemical reactions. The first tree level, *i.e.*, the initial state, contains only the initial reactant and none chemical reactions. A chemical reaction that verifies the preconditions is added to every consecutive tree level until reach a *complete* reaction network defined as a consistently connected structure where all species have been produced. The objective function consists of the minimization of the chemical reactions in the network, thus networks composed by the minimum number of chemical reactions are the first to be obtained, and then, more complex structures in an increasing sequential order are obtained. The enumeration of them is achieved using integer cut equations that avoid the generation of networks composed by redundant pathways. Next section presents the proposed formulation on the basis of assignment problems (ASP).

### ASP formulation (FASP)

Every state of the tree is disposed in vertical levels  $l \in \text{est}$ , in which  $\text{est}$  constitutes the set of states that are required to obtain a reaction network composed with up to  $\text{nr}_{\text{xi,max}}$  chemical reactions. On the first state,  $l = 0$ , (i) no chemical reaction is allowed to be present, and (ii) only the initial reactant(s)  $s \in \text{rp}$  is/are verified. Thus, the set  $\text{est}$  contemplates the levels  $l = 0, 1, \dots, \text{nr}_{\text{xi,max}}$ . Two binary variables describe each state: the  $\text{y}_{j,l}$  and the  $\text{y}_{s,l}$  that indicate the presence of the reaction  $j \in \text{rx}$  and the species  $s \in \text{sp}$ , respectively, in the level  $l \in \text{est}$  of the tree. The set of chemical reactions  $\text{rx}$  is adapted in this formulation, containing  $n_{\text{rx}}$  reactions in the forward direction plus the

same  $n_{rx}$  reactions in the opposite direction, totaling  $2n_{rx} = n_{rx_{sup}}$  chemical reactions.

To ensure that there are no empty states of chemical reactions, except for the initial state, at least one chemical reaction has to be assigned to every state, as shown by (8.50):

$$\sum_{j \in rx} y_{j,l,j} \geq 1, \quad l = 1, \dots, n_{rx_{li,max}} \quad (8.50)$$

Chemical reactions can only be present in the forward or reverse direction (exclusively) when considered in the solution, as imposed in (8.51):

$$y_{j,l,j} + y_{j,l,j+n_{rx}} \leq 1, \quad \forall l \in est, \quad j = 1, \dots, n_{rx} \quad (8.51)$$

Five constraints (8.52 — 8.56) are related to the precondition imposed to avoid generating inconsistent nonlinear networks. First, the information contained in a certain state must remain in the next ones, that is, the sets of chemical reactions and of species in a certain state must be verified in the next ones. This is achieved through the inequality constraints presented in (8.52) and (8.53), respectively:

$$y_{j,l,j} \leq y_{j,l+1,j}, \quad l = 0, \dots, n_{rx_{li,max}} - 1, \quad \forall j \in rx \quad (8.52)$$

$$y_{s,l,s} \leq y_{s,l+1,s}, \quad l = 0, \dots, n_{rx_{li,max}} - 1, \quad \forall s \in sp \quad (8.53)$$

Second, the controlling sets  $nsr$  and  $nsp$  are used in the remain three constraints (8.54 — 8.56) to ensure network consistency. These equations state that: (i) when the reaction is assigned to the current state, the respective reactant species has to be present in the previous state:

$$y_{j,l+1,j} \leq y_{s,l,s}, \quad \forall l = 0, \dots, n_{rx_{li,max}} - 1, s, j \in nsr \quad (8.54)$$

(ii) when the reaction is assigned in a current state, the product species has to be present in this same state:

$$y_{j,l,j} \leq y_{s,l,s}, \quad \forall l \in est, \quad s, j \in nsp \quad (8.55)$$

and (iii) when the species is present at the current state, at least one chemical reaction which produces this species has also to be there:

$$\sum_{j \in rx} y_{j,l,j} \geq y_{s,l,s}, \quad \forall l \in est, s, j \in nsp \setminus rp \quad (8.56)$$

Ensuring the achievement of a complete reaction networks, every species has to be present in the tree:

$$\sum_{l \in est} y_{s,l,s} \geq 1, \quad \forall s \in sp \quad (8.57)$$

In order to guarantee the assignment of a new chemical reaction to every state until it reaches  $\text{nr}\mathbf{x}_{\min}$ , the number of chemical reactions has to increase in one unity when the number of states increases:

$$\sum_{j \in \text{rx}} y_{j,l,j} + 1 = \sum_{j \in \text{rx}} y_{j,l+1,j}, \quad l = 0, \dots, \text{nr}\mathbf{x}_{\min} - 1 \quad (8.58)$$

In cases where  $\text{nr}\mathbf{x}_{\min} < \text{nr}\mathbf{x}_{l_i, \max}$ , networks composed by  $\text{nr}\mathbf{x}_{\min}$  are firstly generated, and the last  $\text{nr}\mathbf{x}_{l_i, \max} - \text{nr}\mathbf{x}_{\min}$  states are identical, presenting exactly the same variables of the state where  $\text{nr}\mathbf{x}_{\min}$  was reached. When solutions with  $\text{nr}\mathbf{x} > \text{nr}\mathbf{x}_{\min}$  are enumerated, no complete networks can be found at the stage  $l = \text{nr}\mathbf{x}_{\min}$  due to integer cut equations that forbid network redundancies, and thus, in order to obtain a complete network it is necessary to add more chemical reactions until obtain the production of every chemical species in the network.

The objective function is given by the sum of number of chemical reactions selected in every tree level

$$z = \sum_{l \in \text{est}} \sum_{j \in \text{rx}} y_{j,l,j} \quad (8.59)$$

The formulation (8.60) constitutes an integer problem with binary variables and linear constraints that can be solved to global optimum.

$$\min_{y_j, y_s} z \quad (8.60a)$$

$$\text{s.t. eqs. (8.50—8.59)} \quad (8.60b)$$

$$y_{j,l,j} = 0, \forall j \in \text{rx}, l = 0 \quad (8.60c)$$

$$y_{s,l,s} = 0, \forall s \in \text{pp}, l = 0 \quad (8.60d)$$

$$y_{s,l,s} = 1, \forall s \in \text{rp}, l = 0 \quad (8.60e)$$

$$y_{j,l,j}, y_{s,l,s} \in \{0,1\}, \forall s \in \text{sp}, j \in \text{rx}, l \in \text{est} \quad (8.60f)$$

In order to enumerate all reaction networks composed by linearly independent and non-redundant chemical reactions, an integer cut equation (8.61) is iteratively added to the formulation (8.60) after the first solution is obtained until no feasible solution can be generated. For this, the parameter  $\text{ccr}\mathbf{x}_{j,i}$  stores the selected reactions  $j \in \text{rx}$  in the current solution iteration  $i \in \text{it}$ . Thus, after the first solution is obtained, this parameter assumes the optimal value of the  $y_j$  binary variable at the bottom level of the tree:

$$\text{ccr}\mathbf{x}_{j,i} = y_{j,l,j}, \quad l = \text{nr}\mathbf{x}_{l_i, \max}, \quad \forall j \in \text{rx}$$

Equation (8.61) is active in the formulation after the obtainment of the first solution avoiding the generation of solutions that contains the same group of chemical reactions, *i.e.*, at least one chemical reaction must be different of the set of the reactions that

compose the networks previously generated.

$$\sum_{j \in \text{rx}} \text{ccrx}_{j,i} y_{l,j} \leq \sum_{j \in \text{rx}} \text{ccrx}_{j,i} - 1, \quad \forall i \in \text{it}, \quad l = \text{nrx}_{l_i, \max} \quad (8.61)$$

### FASP example

The reaction networks presented in Figure 8.1 (a) and (c), are taken as an illustrative example of the tree of states. The AS nonlinear case study has  $\text{nrx}_{\min} = 4$  and  $\text{nrx}_{l_i, \max} = 5$ . See in Table 8.2 the corresponding distributions of species and chemical reactions in every state of the tree. The objective function for these solutions assume  $z = 14$  and  $z = 15$ , respectively; every reaction network composed by  $\text{nrx}_{\min}$  has  $z = 14$ , while the ones composed by  $\text{nrx}_{l_i, \max}$  have  $z = 15$ .

**Table 8.2** Two branches of the tree concerning to the reaction networks (a) and (c) of Figure 8.1.

Tree level	Network (a) $ys_{l,s}$	$yj_{l,j}$
l=0	{AS}	{ $\emptyset$ }
l=1	{AS, BDO}	{ $r_2$ }
l=2	{AS, BDO, THF}	{ $r_2, r_3$ }
l=3	{AS, BDO, THF, GBL, PrOH}	{ $r_2, r_3, r_{16}$ }
l=4	{AS, BDO, THF, GBL, PrOH, BuOH}	{ $r_2, r_3, r_{16}, -r_{17}$ }
l=5	{AS, BDO, THF, GBL, PrOH, BuOH}	{ $r_2, r_3, r_{16}, -r_{17}$ }
Tree level	Network (c) $ys_{l,s}$	$yj_{l,j}$
l=0	{AS}	{ $\emptyset$ }
l=1	{AS, THF}	{ $r_3$ }
l=2	{AS, THF, GBL}	{ $r_3, r_{-5}$ }
l=3	{AS, THF, GBL, BuOH}	{ $r_3, r_{-5}, r_6$ }
l=4	{AS, THF, GBL, BuOH, PrOH}	{ $r_3, r_{-5}, r_6, r_{17}$ }
l=5	{AS, THF, GBL, BuOH, PrOH, BDO}	{ $r_3, r_{-5}, r_6, r_{17}, r_{-16}$ }

## 8.6 MILP formulations comparison

In Table 8.3 the presented formulations are compared in terms of the number of variables and equations. Notice that the FSFA can only be used to generate linear reaction networks, whereas the remain three formulations (FMTZ, FRLT and FASP) can be used to generate both linear and nonlinear reaction networks. The number of constraints indicated in Table 8.3 does not include integer cut equations.

The four formulations are very similar in terms of the number of binary variables, since

**Table 8.3** Formulations comparison in terms of number of variables and constraints.

MILP formulation	Binary variables	Continuous variables	Constraints
FSFA (8.20)	$2n_{rx} + n_{rx}n_{sp}$	$n_{sp} + n_{sp}^2$	$n_{rx} + 3n_{sp} + 2n_{rx}n_{sp} + 4n_{sp}^2n_{rx} + 1$
FMTZ (8.34)	$2n_{rx} + 2n_{rx}n_{sp}$	$n_{sp} + n_{sp}n_{rx}$	$n_{rx} + n_{sp} + 6n_{rx}n_{sp} + n_{sp}^2n_{rx}$
FRLT (8.47)	$n_{rx} + 3n_{rx}n_{sp}$	$n_{sp} + n_{sp}n_{rx}$	$n_{sp} + 5n_{rx}n_{sp} + 2n_{sp}^2n_{rx}$
FASP (8.60)	$nrx_{li,max}nrx_{sup} + nrx_{li,max}n_{sp}$	—	$nrx_{li,max} + nrx_{li,max}n_{rx} + nrx_{li,max}nrx_{sup} + nrx_{li,max}n_{sp} + 3nrx_{li,max}n_{sp}n_{rx} + n_{sp} + nrx_{min}$

$nrx_{li,max} \leq n_{sp} - 1$  and  $nrx_{sup} = 2n_{rx}$ . However, in terms of number of continuous variables FMTZ and FRLT present a greater amount than FSFA since  $n_{rx} > n_{sp}$ . Regarding the number of constraints, the expression presented in FASP can be approximated to  $3n_{sp} + 3n_{sp}n_{rx} + n_{sp}^2 + n_{sp}^2n_{rx}$ , and therefore, it assumes a greater value when compared to FSFA, FMTZ and FRLT. However, the number of constraints in both FMTZ and FRLT formulations are practically the same.

The IP and MILP formulations presented in this chapter are compared in terms of computational effort considering the number of branch-and-bound nodes, the solver iterations, and the CPU usage to obtain a single and entire set of solutions. The succinic acid case study is taken as an application example to demonstrate both network generation problems: the linear and the nonlinear cases. All results were obtained in Debian Linux operating system, dual processor Intel<sup>®</sup> Xeon, hexa-core, using the software GAMS<sup>®</sup> version 31.1.1 with the commercial solver CPLEX.

Regarding the explicit enumeration of reaction networks with  $RI = 0$  from the nonlinear network superstructure presented earlier in Figure 7.3, it was generated a total of 2921 solutions which correspond to 241 nonlinear reaction networks with  $nrx_{min} = 4$ , 540 linear networks with  $nrx_{min} = nrx_{li,max} = 5$ , and 2140 nonlinear networks with  $nrx_{li,max} = 5$ . Table 8.4 presents the solver performance for the first and last solution obtained, also showing the total CPU usage to obtain the entire set of solutions.

After the first solution obtainment, the integer cut equations are added to the respective formulation, increasing the number of constraints sequentially during the enumeration of alternative solutions. Thus, the last solution is the one with the greatest number of restrictions in the respective formulation, but it does not necessarily represent the most expensive solution in terms of computational effort. In order to assess the solver performance in terms of computational effort the three evaluated parameters were plotted for every obtained solution, as shown in Figure 8.13.

Comparing the results obtained for FMTZ and FRLT, it is possible to observe that both

**Table 8.4** Complete enumeration of linear and nonlinear reaction networks with  $\text{RI} = 0$  from the superstructure presented in Figure 7.3 for the AS case study.

		<b>FMTZ</b>	<b>FRLT</b>	<b>FASP</b>
		First solution		
$i = 1$	Variables	210	243	241
	Equations	371	397	927
	CPU [s]	0.094	0.081	0.117
	Iterations	1389	1011	364
	Nodes	108	67	0
		Last solution		
$i = 2921$	Variables	210	243	241
	Equations	3291	3317	3847
	CPU [s]	9.529	11.012	1.860
	Iterations	45684	62282	9660
	Nodes	4005	3630	800
		Complete enumeration		
	CPU [min]	48.841	57.399	22.058

presented similar performance regarding the generation of a single solution. This result is not unexpected, as both formulations are quite similar in terms of variable types and equations. However, when considering the enumeration of all solutions, FRLT performed worse than FMTZ with a greater computational effort to obtain the same set of optimal solutions. Furthermore, although the number of equations in FASP is higher than in other formulations, FASP showed better solver performance in terms of number of nodes for branch-and-bounding, number of solver iterations, and time taken to reach an optimal solution. Therefore, the FASP is preferable over the FMTZ and FRLT to enumerate nonlinear and linear reaction networks explicitly. This result shows that the comparison of IP and MILP formulations should not be made solely in terms of the number of variables and restrictions, as these indices can lead to misinterpretations and, consequently, to poor choices regarding the most advantageous formulation to be used.

In order to compare the performance of the four formulations presented in this chapter for the explicit generation of linear networks with  $\text{RI} = 0$ , the first 13 linear reactions shown in Table 7.1 (and their reverse components) are considered as the superstructure of reaction networks (Figure 7.2). The results obtained are presented in Table 8.5 and Figure 8.14. It was generated 540 linear networks with  $\text{nr}x_{\min} = \text{nr}x_{\text{li},\max} = 5$ .

Analyzing the results obtained in the explicit generation of linear networks, it can be observed that FMTZ and FRLT presented similar and slightly superior performance to FASP in terms of number of nodes and iterations. However, FSFA presented the lowest computational effort in terms of number of nodes and iterations, despite having the highest CPU usage for the complete enumeration, as can be seen in the three plots shown in Figure 8.14 (orange profile). Nonetheless, regarding the complete enumeration of solutions,

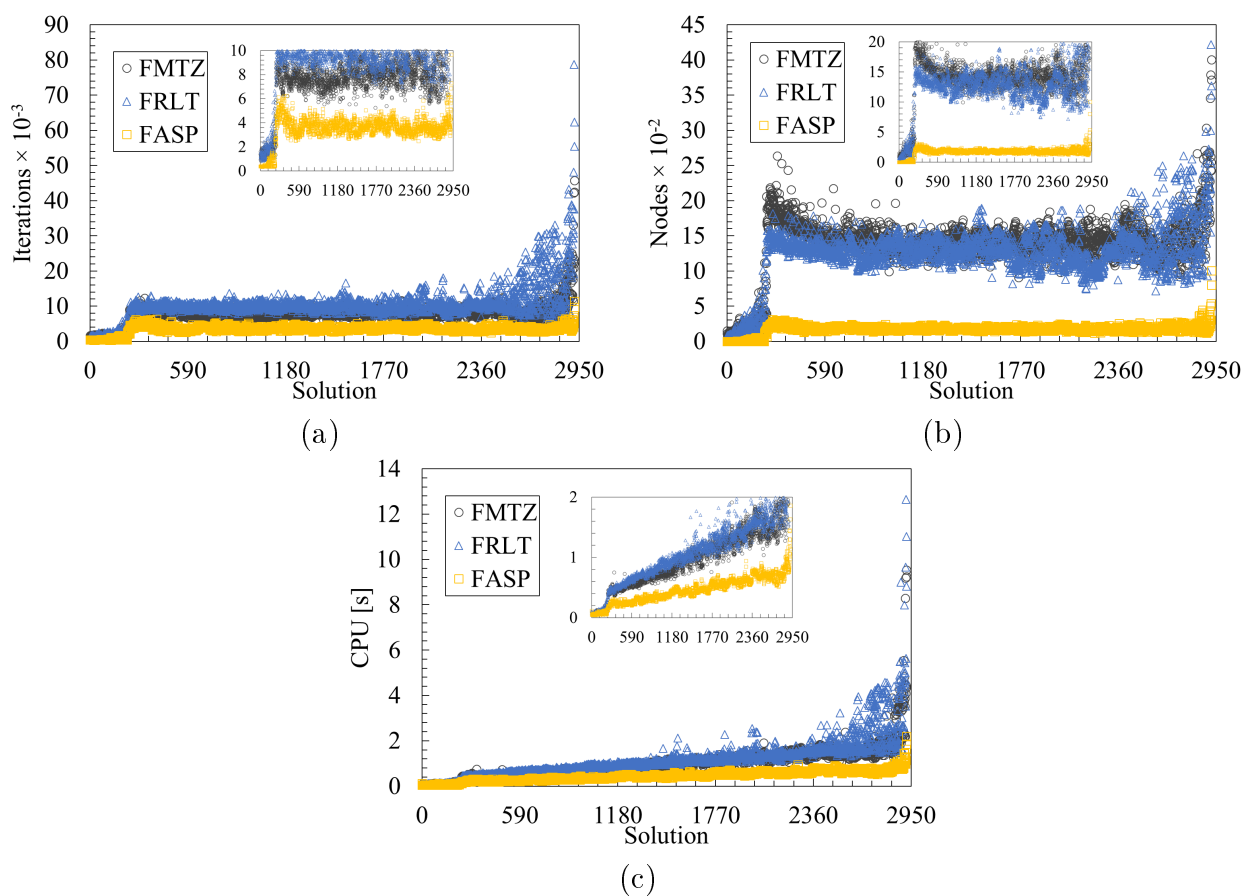


**Figure 8.13** Comparison of formulations performance in the explicit enumeration of linear and nonlinear reaction networks in terms of (a) number of solver iterations, (b) number of branch-and-bound nodes, and (c) CPU usage.

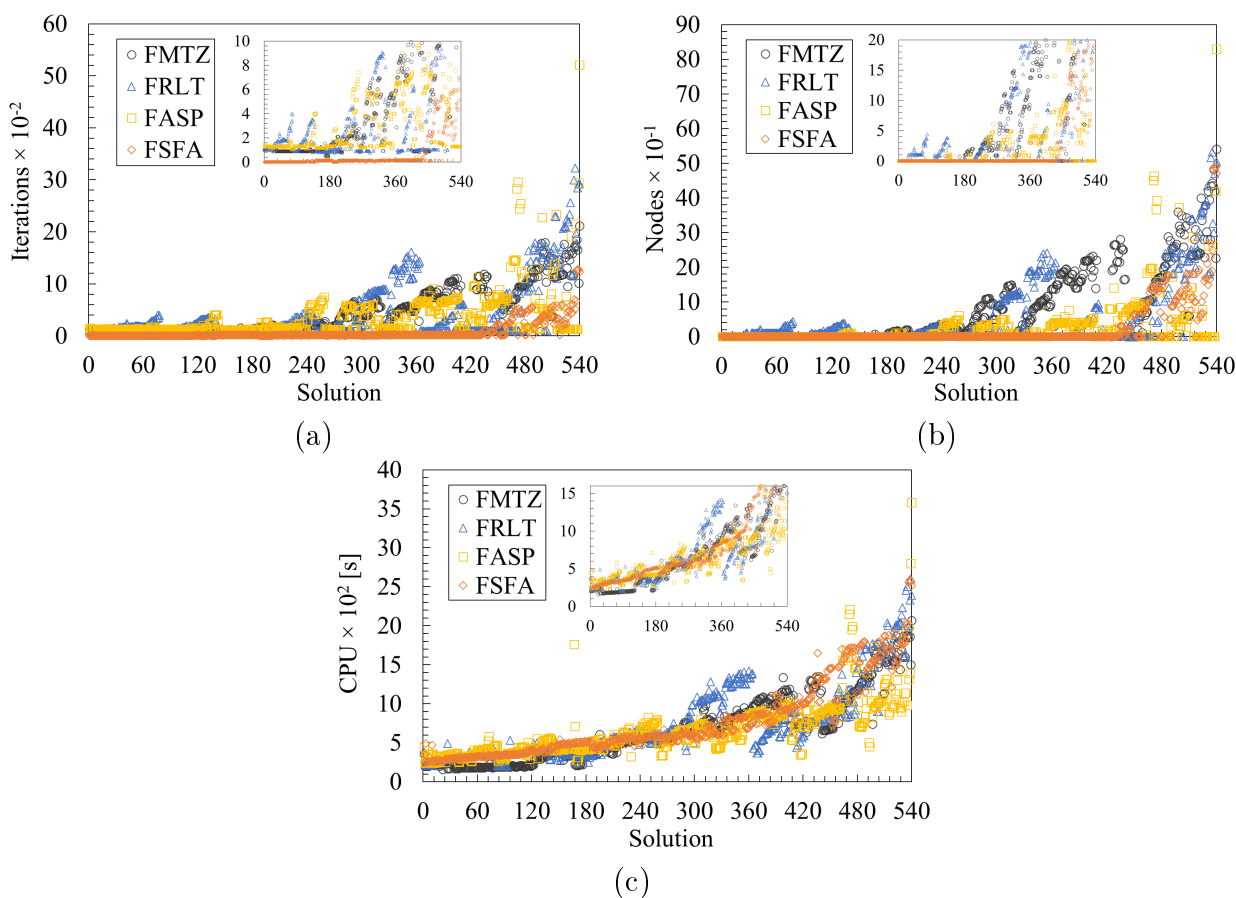
based on the comparison of the four formulations, the difference in terms of CPU usage is in practice negligible and, since FSFA presented better results in solver performance, this is the best formulation indicated to generate linear reaction networks explicitly.

Furthermore, the computational effort to generate linear reaction networks is significantly less than that to generate nonlinear networks (here we speak in seconds, instead of minutes or hours), presenting, as a whole, fewer iterations, branch-and-bound nodes, and CPU usage to achieve a single solution. Therefore, the problem of generating linear networks is much simpler than generating nonlinear structures. This is due to the fact that there is no need to check the precedence in the production of species in linear networks even if cycles were allowed in their structures. In this case, the linear solutions obtained do not present cycles since the generation of networks composed of linearly independent sets of chemical reactions was imposed. In contrast, in nonlinear networks some cases of cycles are allowed while maintaining a non-redundant, linearly independent set of chemical reactions. Thus, in this case, there is a need to impose precedence between species, increasing the complexity of the formulation.



**Table 8.5** Complete enumeration of linear reaction networks with  $RI = 0$  from the superstructure presented in Figure 7.2 for the AS case study.

		FMTZ	FRLT	FASP	FSFA
		First solution			
$i = 1$	Variables	110	123	161	170
	Equations	175	175	527	201
	CPU [s]	0.036	0.038	0.045	0.033
	Iterations	103	100	145	0
	Nodes	0	0	0	0
		Last solution			
$i = 540$	Variables	110	123	161	170
	Equations	714	714	1066	740
	CPU [s]	0.207	0.239	0.358	0.252
	Iterations	2118	2926	5212	1223
	Nodes	541	505	830	471
		Complete enumeration			
	CPU [s]	36.513	40.158	35.954	41.502

**Figure 8.14** Comparison of formulations performance in the explicit enumeration of linear reaction networks in terms of (a) number of solver iterations, (b) number of branch-and-bound nodes, and (c) CPU usage.

## Bibliography

- Amrhein, M., Srinivasan, B., and Bonvin, D. (1999). Target factor analysis of reaction data: use of data pre-treatment and reaction-invariant relationships. *Chemical Engineering Science*, 54(5):579–591.
- Bektaş, T. and Gouveia, L. (2014). Requiem for the miller–tucker–zemlin subtour elimination constraints? *European Journal of Operational Research*, 236(3):820–832.
- Bonvin, D. and Rippin, D. (1990). Target factor analysis for the identification of stoichiometric models. *Chemical Engineering Science*, 45(12):3417–3426.
- Bro, R., Kjeldahl, K., Smilde, A. K., and Kiers, H. (2008). Cross-validation of component models: a critical look at current methods. *Analytical and bioanalytical chemistry*, 390(5):1241–1251.
- Floudas, C. A. and Lin, X. (2005). Mixed integer linear programming in process scheduling: Modeling, algorithms, and applications. *Annals of Operations Research*, 139(1):131–162.
- Gadewar, S. B., Doherty, M. F., and Malone, M. F. (2001). A systematic method for reaction invariants and mole balances for complex chemistries. *Computers & Chemical Engineering*, 25(9–10):1199–1217.
- Gavish, B. and Graves, S. C. (1978). The travelling salesman problem and related problems. *Operations Research Center Working Papers*, 078(78).
- Gouveia, L. and Pires, J. M. (1999). The asymmetric travelling salesman problem and a reformulation of the miller–tucker–zemlin constraints. *European Journal of Operational Research*, 112(1):134–146.
- Gross, J. and Yellen, J. (2005). *Graph Theory and Its Applications, Second Edition*. Textbooks in Mathematics. Taylor & Francis.
- Grossmann, I. E. and Ruiz, J. P. (2012). Generalized disjunctive programming: A framework for formulation and alternative algorithms for minlp optimization. In *Mixed Integer Nonlinear Programming*, pages 93–115. Springer.
- Haouari, M., Maculan, N., and Mrad, M. (2013). Enhanced compact models for the connected subgraph problem and for the shortest path problem in digraphs with negative cycles. *Computers & operations research*, 40(10):2485–2492.
- Kondili, E., Pantelides, C. C., and Sargent, R. W. (1993). A general algorithm for short-term scheduling of batch operations — i. MILP formulation. *Computers & Chemical Engineering*, 17(2):211–227.
- Langevin, A., Soumis, F., and Desrosiers, J. (1990). Classification of travelling salesman problem formulations. *Operations Research Letters*, 9(2):127–132.
- Levy, F., Thompson, G., and Wiest, J. (1963). *The ABCs of the Critical Path Method*. Harvard business review reprint series. Harvard Business Review.

- Malinowski, E. R. (1989). Statistical f-tests for abstract factor analysis and target testing. *Journal of Chemometrics*, 3(1):49–60.
- Maravelias, C. T. and Grossmann, I. E. (2003). New general continuous-time state- task network formulation for short-term scheduling of multipurpose batch plants. *Industrial & engineering chemistry research*, 42(13):3056–3074.
- Marin, G. and Yablonsky, G. (2011). *Kinetics of Chemical Reactions*. Wiley.
- Meyer, C. (2000). *Matrix Analysis and Applied Linear Algebra*. Society for Industrial and Applied Mathematics.
- Miller, C. E., Tucker, A. E., and Zemlin, R. A. (1960). Integer programming formulation of traveling salesman problems. *J. ACM*, 7:326–329.
- Missen, R. W. and Smith, W. R. (1998). Chemical reaction stoichiometry (CRS): A tutorial.
- Missen, R. W. and Smith, W. R. (2003). Mass conservation implications of a reaction mechanism. *Journal of Chemical Education*, 80(7):833.
- Padberg, M. and Sung, T.-Y. (1991). An analytical comparison of different formulations of the travelling salesman problem. *Mathematical Programming*, 52(1-3):315–357.
- Rodrigues, D., Srinivasan, S., Billeter, J., and Bonvin, D. (2015). Variant and invariant states for chemical reaction systems. *Computers & Chemical Engineering*, 73(0):23–33.
- Shah, N., Pantelides, C., and Sargent, R. (1993). A general algorithm for short-term scheduling of batch operations—ii. computational issues. *Computers & chemical engineering*, 17(2):229–244.
- Sherali, H. D. and Adams, W. P. (1990). A hierarchy of relaxations between the continuous and convex hull representations for zero-one programming problems. *SIAM Journal on Discrete Mathematics*, 3(3):411–430.
- Taccari, L. (2016). Integer programming formulations for the elementary shortest path problem. *European Journal of Operational Research*, 252(1):122–130.
- Temkin, O., Zeigarnik, A., and Bonchev, D. (1996). *Chemical Reaction Networks: A Graph-Theoretical Approach*. Taylor & Francis.
- Vertis, C. S., Granjo, J. F. O., Oliveira, N. M. C., and Bernardo, F. P. (2017). Systematic generation of chemical reactions and reaction networks subject to energetic constraints. In España, A., Graells, M., and Puigjaner, L., editors, *27th European Symposium on Computer Aided Process Engineering*, volume 39 of *Computer Aided Chemical Engineering*. Elsevier.
- Vertis, C. S., Oliveira, N. M., and Bernardo, F. P. (2015). Systematic development of kinetic models for systems described by linear reaction schemes. In Krist V. Gernaey, J. K. H. and Gani, R., editors, *12th International Symposium on Process Systems Engineering and 25th European Symposium on Computer Aided Process Engineering*, volume 37 of *Computer Aided Chemical Engineering*, pages 647–652. Elsevier.

- Vertis, C. S., Oliveira, N. M., and Bernardo, F. P. (2016). Explicit and implicit generation of chemical reaction networks through discrete structural optimization. In *7th International Symposium on Design, Operation and Control of Chemical Processes*. PSE Asia. <http://www.pse143.org/PSEAsiaTokyo/>.
- Wold, S. (1978). Cross-validatory estimation of the number of components in factor and principal components models. *Technometrics*, 20(4):397–405.

# Chapter 9

## Step 5 — Plausible Reaction Networks

*“Pathways are concepts, networks are reality.”*

– Uwe Sauer

### Contents

---

9.1	Step 5 overview . . . . .	256
9.2	Reaction rate estimation . . . . .	257
9.3	Selection of plausible reaction networks . . . . .	258
9.3.1	Application example . . . . .	259
9.4	Implicit generation of reaction networks . . . . .	261
9.4.1	Implicit generation of plausible reaction networks . . . . .	262
9.4.2	Implicit generation of plausible reaction networks with simultaneous kinetic model identification . . . . .	266

---

After the treatment of experimental data, the obtained smoothed profiles of chemical species concentration along time can then be combined with the previously generated list of possible reaction networks. Those that are clearly incompatible with the observed profiles must be discarded, while reaction networks considered plausible, according to a well-established criterion, should be selected and analysed in more detail. In this chapter, a methodology to perform this selection is presented, with the criterion of plausibility being that a reaction network must present positive net reaction rates for all chemical reactions and during the entire experiment. Reaction rates are obtained solving the mass balance equations in the rate-based method, as shown in (2.41), with the concentration derivatives calculated from the smoothed concentration profiles.

However, instead of generating network structures to later identify the ones that are plausible, the implicit generation of reaction networks can also be considered when incorporating the mass balance equations constrained to present positive net reaction fluxes in

the formulation to generate reaction networks. Consequently, in that case, only plausible reaction networks structures may be generated. This consists into the union of Steps 4 and 5 of the proposed methodology. Considering the implicit generation of networks can be an advantage for large problem sizes, (*i.e.*, problems that present network superstructures with more than a hundred reaction components), once it can avoid the combinatorial explosion of alternative networks when generating them explicitly, thus, saving computation effort in the generation task and eliminating the filtering step.

Alternatively, if there are “too many” possible reaction networks, the possibility of suggesting to the user to obtain new experimental datasets should be considered, thus allowing a reduction of the size of this set of plausible networks and increasing the ability to discriminate competitive models. However, in another perspective, when further experimental tests cannot be carried out, the modeling of kinetic expressions can help to discriminate the many plausible candidate solutions. In this case, since there are too many networks structures to be considered, the generation step can be repeated but at this time in a more restrictive formulation, where the network is identified simultaneously with the best kinetic model expression for each chemical reaction component with adjusted parameters. This consists of the union of Steps 4, 5 and 6 (initial phase), where the main goal is to find a positive correlation of the reaction rate with its reactant species in simultaneous with the network synthesis, assisting the model structural identification.

This chapter is organized as follows. In Section 9.1, as overview of Step 5 is presented. Then, in Section 9.2, the computation of reaction rate profiles based on the differential method is addressed. Next, in Section 9.3, the metrics used to select plausible reaction networks are presented. Finally, in Section 9.4, the implicit generation of reaction networks is considered, presenting the formulations for the obtainment of plausible structures (i) with positive reaction rates and (ii) with established kinetic models.

## 9.1 Step 5 overview

In Step 5 the generated reaction networks are validated using the pre-treated data, according to the plausibility criterion. The Step 5 flowchart is presented in Figure 9.1. The models that pass this phase are classified as plausible network structures, that may be analyzed in more detail in Step 6. It is preferable that only a small set of network structures pass this phase.

If none plausible structures can be found, the expansion of the search domain is considered by (i) generating more complex chemical reactions (reactions that contain more participating species), thus going back to Step 3, and/or (ii) increasing the number of chemical reactions in the networks in Step 4.

When the number of plausible reaction networks structures is significant, (more than 5), the design of experiments can be proposed to discriminate the true schema of the reaction system in Step 7. This can be done, for example, by carrying out new experiments under

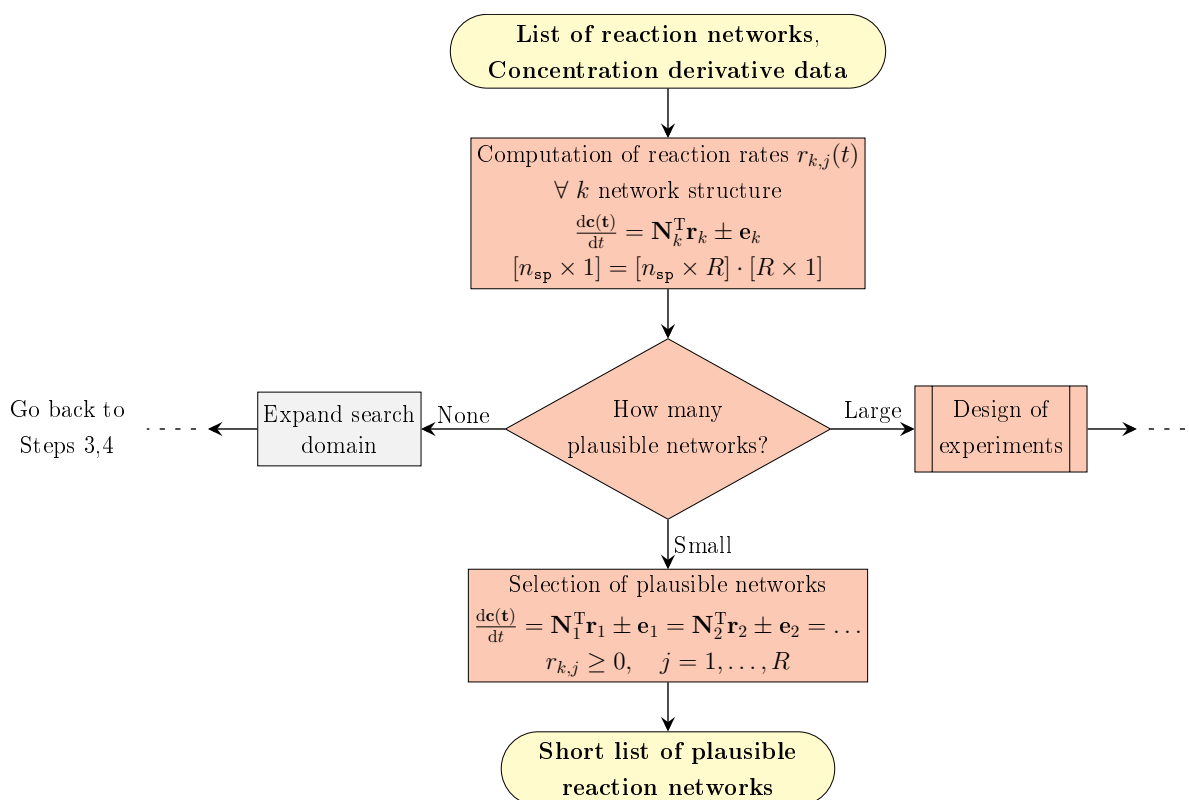


Figure 9.1 Step 5 flowchart.

different operation conditions, or by including other species in the initial reagent mixture, in order to elucidate separately some components of the overall reaction network structure.

## 9.2 Reaction rate estimation

*“It is all about the fluxes.”*

– Jens Nielsen

Consider the species mass balances in a homogeneous batch reactor previously presented in (2.7) and the  $\text{nin}_{\text{li}}$  time-invariant relationships imposed at data reconciliation phase, such that the left side of (2.35) is verified. Thus (2.7) can be replaced by a smaller number of independent mass balances sufficient to fully describe the evolution of the system. These can be written as

$$\frac{d\mathbf{c}_v(t)}{dt} = \mathbf{N}_v^T \cdot \mathbf{r}(t) \quad (9.1)$$

where the subscript “ $v$ ” indicates the reduced form of the concentration vector and the stoichiometric matrix, presenting  $\mathbf{c}_v(t)[n_{\text{sp}} - \text{nin}_{\text{li}} \times 1]$  and  $\mathbf{N}_v[n_{\text{rx}} \times n_{\text{sp}} - \text{nin}_{\text{li}}]$ , respectively. We also denote by  $\mathbf{sv}$  the set of variant species considered in (9.1), such that  $n_{\text{sv}} = n_{\text{sp}} - \text{nin}_{\text{li}}$ . Each entry  $r_j(t)$  of  $\mathbf{r}(t)$  represents the *net flux* of reaction  $j$  in

the reaction network, *i.e.*, the rate of the direct component minus the rate of the reverse component of the reaction.

Since (i) the chemical reactions generated in Step 3 verify the time-invariant relationships that were also imposed during data reconciliation (Step 1), and (ii) the reaction networks generated in Step 4 that form each  $\mathbf{N}$  are composed by a subset of these reactions, where  $\mathbf{N}$  has full row rank with dimension  $n_{\text{rx}_{\text{li}}}$ ,  $\text{row}(\mathbf{N})$  corresponds to  $\text{row}(\mathbf{D})$  as such as  $\text{row}(\mathbf{N}_v)$  to  $\text{row}(\mathbf{D}_v)$ <sup>1</sup>. Thus the reduced system in (9.1) presents a square non-singular matrix  $\mathbf{N}_v$  with dimension  $n_{\text{rx}} = n_{\text{rx}_{\text{li}}} = n_{\text{sv}}$  that can be solved as a linear systems of algebraic equations.

When it is not possible to determine all time-invariant relationships of the system in question and/or impose them during data reconciliation procedure, the linear spaces  $\text{row}(\mathbf{N}_v)$  and  $\text{row}(\mathbf{D}_v)$  may not coincide, resulting in the need of the use of optimization techniques to solve the system in (9.1).

However, it was only necessary to consider a particular reaction network to determine the  $r_j(t)$  for every  $j \in \text{rx}$  reaction rate profile. The analysis of these rate profiles allows the posterior discrimination of the generated reaction networks according to their plausibility. This is the topic of the next section.

### 9.3 Selection of plausible reaction networks

Considering a set of net reaction rates  $\{r_j(t)\}$  with  $j \in \text{rx}$ , a *necessary condition* for its plausibility is that

$$r_j(t) \geq 0, \quad \forall j \in \text{rx}, t \in [t_0, t_f] \quad (9.2)$$

where  $[t_0, t_f]$  represents the time interval that contains the various available experimental points. However, admitting limited experimental errors (*i.e.*, quantifiable data uncertainty), the previous condition is not always strictly obeyed, and consequently the respective reaction networks should not be abandoned.

A simple possibility of eliminating non-plausible reaction networks is to specify a maximum error threshold for checking the inequality in (9.2). In this approach, reaction networks with at least one case  $r_j(t) \leq -\epsilon$ , with  $\epsilon$  representing the chosen cutting level, would be excluded. However, this methodology has the disadvantage of being very sensitive to the choice of the threshold used. Alternatively, this work sought to follow an approach of *maximum likelihood*, where the analyzed reaction networks are ordered according to a growing criterion of violation of the restriction in (9.2) that they present. In this logic, the reaction networks with the least violation of this restriction are located at the top of the list, receiving the most analytical attention. This approach integrates the expectation that, throughout the various experiments carried out, only the reaction

---

<sup>1</sup>Here,  $\mathbf{D}$  is the matrix of time concentration derivatives evaluated at the collocation points in the data reconciliation procedure (the abscissas in which the time invariants were imposed).



networks that can explain all the observed data survive this processing step.

Two metrics are considered respecting different approaches established for the same purpose: to select plausible reaction networks. One is to consider the amount

$$r_{\text{neg},j}(t) = \min\{r_j(t), 0\}, \quad \forall j \in \text{rx}, \quad t \in [t_0, t_f] \quad (9.3)$$

considering the integral

$$\text{irn}_j = \int_{t_0}^{t_f} r_{\text{neg},j}(t) dt, \quad \forall j \in \text{rx} \quad (9.4)$$

given the need to check the previous inequality over a period of time. This makes it possible to define scalar quantities

$$\text{trn}_k = \sum_{j \in \text{rx}} \text{irn}_{j,k} \quad (9.5)$$

for each reaction network  $k$  considered. Thus, the lower the  $\text{trn}$  value obtained, the better the classification of the corresponding reaction network.

The other metric is to directly consider optimization tools, even for perfectly determined systems, solving the following constrained optimization problem

$$\begin{aligned} \min_{\mathbf{r}(t)} \quad & \phi = \int_{t_0}^{t_f} \mathbf{e}(t)^T \cdot \mathbf{w}(t) \cdot \mathbf{e}(t) \\ \text{s.t.} \quad & \mathbf{e}(t) = \frac{d\mathbf{c}_v(t)}{dt} - \mathbf{N}_v^T \cdot \mathbf{r}(t) \\ & \mathbf{r}(t) \geq 0 \end{aligned} \quad (9.6)$$

for each reaction network considered. Thus, the lower the  $\phi$  value obtained, the better the classification of the corresponding reaction network.

In some cases several plausible reaction networks can be found, constituting all of them bases rotations of each other, leading to the same description of the data variant space in different systems of coordinates. Notice that the concentration derivatives vectors lie in the positive orthant of the row space of the stoichiometric matrix. For more detailed discussions about linear spaces and linear system of equations see Sections 2.2 to 2.4.

### 9.3.1 Application example

From the list of 540 linear reaction networks generated concerning the AS case study, 28 reaction networks were identified, selected using the plausibility criterion for a more rigorous analysis. Figure 9.2 shows the  $\text{trn}$  value of all 540 reaction networks, sorted in ascending order. By observing this figure, a cutoff value of  $0.033 \text{ mol L}^{-1}$  was considered. The reactions participating in these 28 best reaction networks are shown in Table 9.1,

with their respective relative frequency.

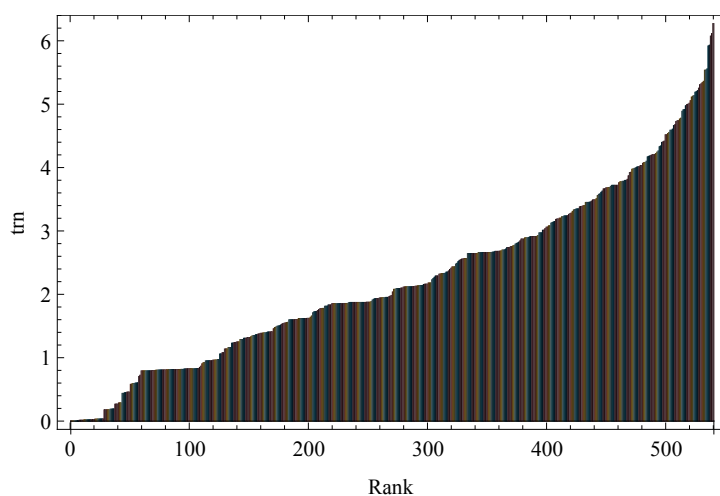


**Figure 9.2** Reaction networks ordered by the plausibility criterion for AS case study.

**Table 9.1** Relative frequency (RF) of reactions in the 28 most plausible reaction networks - case study AS.

$r_j$	RF [%]	$r_j$	RF [%]	$r_j$	RF [%]
$r_1$	100	$r_7$	21.43	$-r_{11}$	21.43
$r_4$	78.57	$r_6$	21.43	$r_{13}$	14.28
$r_8$	57.14	$r_{12}$	21.43	$-r_{13}$	14.28
$r_{10}$	42.86	$-r_{12}$	21.43	$-r_{10}$	10.71
$r_9$	42.86	$r_{11}$	21.43	$-r_9$	10.71

When analyzing the most plausible networks, it appears that the reactions  $r_1$ ,  $r_4$  and  $r_8$  appear quite frequently in the most plausible reaction networks. A qualitative analysis of the temporal profiles of the concentrations of the species involved allows us to confirm that these reactions should be included in the final reaction network.

When considering the reduced list of generated reaction networks with feasible energetic directions previously identified, a reduction of the number of plausible networks was obtained: 12 candidate structures composed by five (non-redundant) chemical reactions pass the plausibility test with zero  $\phi$  value from the 144 generated networks. In all of them the series of three consecutive chemical reactions ( $r_1$ ,  $r_4$  and  $r_8$ ) is verified, *i.e.*,  $AS \rightarrow GBL \rightarrow BDO \rightarrow THF$ , and no definition about the origins of BuOH and PrOH species could be established. Notice that BuOH and PrOH are residual species in this chemical system with great uncertainty related to their measurements. Figure 9.3 presents the limited superstructure of reaction networks indicating the identified chemical reaction occurring in that system (through full arrows) and the plausible ones to be further identified. In this figure the blue colored arrow indicates that the reaction direction was identified as energetically feasible.

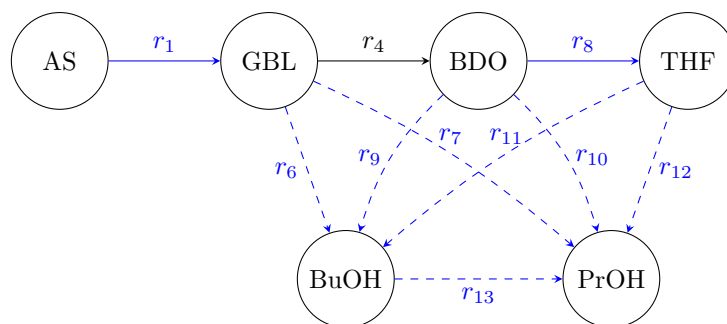


**Figure 9.3** Limited reaction network superstructure. Full arrows: identified chemical reactions. Dashed arrows: still uncertain pathways.

In this case, it is advisable to carry out additional experiments to completely elucidate the reaction network, taking into account the error in closing the total mass balance in this system, described previously. It is recommended to carry out at least 4 additional experiments, starting with the final products until the intermediates, *i.e.*, using a reverse order to that of the reaction network. Experiments can be started, for example, with the BuOH compound, to verify the formation of PrOH and to quantify it. Then the experiment with THF can be carried out, to check if BuOH and PrOH are formed, and if that PrOH formed also comes from THF or not. The next experiment would be to try to hydrogenate BDO; depending on the results obtained, and comparing these results with previous experiences, it will be possible to draw conclusions regarding the origin of the terminal components. Finally, an isolated hydrogenation reaction of GBL may be suggested, to confirm that this compound only gives rise to BDO.

## 9.4 Implicit generation of reaction networks

The implicit generation of reaction networks is a more restrictive problem that attends to the identification of structures subjected to satisfy an additional criterion simultaneously with the original structural constraints. In this section two MILP formulations are presented to generate reaction networks implicitly supported on experimental data information: one considers the plausibility criterion, thus generating structures that present positive reaction rates, and the other addresses the simultaneous identification of the reaction network structure and of the best kinetic expressions concerning each reaction component.

The implicit generation of networks can be an advantage for large problem sizes, *i.e.*, problems that present network superstructures with more than a hundred reaction components, once it can avoid the combinatorial explosion of alternative networks when generating them explicitly, thus, saving computation effort in the generation task and eliminating the filtering step. Notice that in the explicit generation of networks, the feasible solutions are only structurally constrained to be consistent, without the need of using experimental data.

Next sections concern the implicit generation of (i) plausible reaction networks and (ii) plausible networks with simultaneous kinetic model identification. In Chapter 11, the respective formulations are illustrated using the AP and Pfizer case studies.

### 9.4.1 Implicit generation of plausible reaction networks

The implicit generation of reaction networks consists of the identification of plausible network structures that satisfy the mass balance closure subjected to positive reaction rates. This approach differs from the one proposed in the original methodology diagram (Figure 4.1) in which the network identification is performed in two decoupled steps, namely, the generation of reaction networks (explicitly) regarding the structural modeling part in Step 4, followed by the filtering of these feasible structures supported on experimental data using the plausibility criterion in Step 5. In the implicit network generation, these steps are simultaneously performed, thus generating only plausible reaction network structures.

The formulation can be divided into two parts: one involving experimental data and species mass balances, and other containing structural constraints for network building, where continuous and discrete variables, respectively, make up the optimization problem. On the data related part, a linear system of equations with positive (real) constrained variables (plausible reaction rates) is optimally solved using the species concentration derivatives calculated in Step 1. Regarding the structural modeling part, binary variables are used to select chemical reactions from the superstructure of the network using common constraints of explicit generation, ensuring the obtainment of structurally consistent networks. Previously, in Sections 8.5.1 and 8.5.2 two different MILP formulations to explicitly generate networks were described, namely, the MTZ- and the Assignment-based formulations, respectively. Although both can be used in the latter part of the implicit generation, in the next section the MILP formulation based on assignment problem is explained.

#### Assignment-based formulation

This formulation is inspired on the classical scheduling optimization problems involving similar concepts of the assignment problem and state task network, where chemical reactions can be compared to tasks and states to agents. The goal is to propose a schedule of a total fixed amount of tasks (reaction network with fixed dimension equal to  $n$ ), involving every agent, constrained to be structurally feasible and with no task repetition. Since some chemical reactions involve more than one species, precedence constraints among those chemical reactions are required in order to guarantee consistency during the schedule. This is achieved when considering a linear sequence of states that grows in depth, in which every state  $l \in \mathbf{est}$  is characterized by the presence of chemical species  $s \in \mathbf{sp}$  and chemical reaction  $j \in \mathbf{rx}$  through the binary variables  $\mathbf{y} \mathbf{s}_{l,s}$  and  $\mathbf{y} \mathbf{j}_{l,j}$ , respectively. In every state of the tree branch, the number of chemical reactions is increased in one unity when going depth, from the top to the bottom, until reach  $l = n$ . Once in the first state,

$l = 0$ , there is no chemical reactions and only initial reactant species, the total number of tree states is  $n + 1$ .

The objective function in (9.7), minimization of  $\phi$ , consists of minimizing the integral of the absolute error ( $\mathbf{ae}_{s,t,i,k}$ ) profile using Gauss quadrature rule, where  $h$  is the length of finite element  $i \in \mathbf{fe}$ ,  $w$  is the collocation point weight at  $t \in \mathbf{cp}$  and  $k \in \mathbf{ds}$  the dataset index. The absolute error is computed through eqs. (9.8) and (9.9), where its artificial module is estimated from inequalities constraints considering the difference among species concentration derivatives  $d_{s,t,i,k}$  and its predicted values (model parameter and model variable, respectively). The vector of predicted concentration derivatives (*i.e.*, the instantaneous rate of species change vector) is computed through the product stoichiometric matrix times reaction rate vector, which is represented in the algebraic equation format in eqs. (9.8) and (9.9), where  $v_{s,j}$  is the stoichiometric coefficient of species  $s$  in reaction  $j$  and  $\mathbf{cr}_{j,t,i,k}$  the respective instantaneous reaction rate. Since binary variables are used to select chemical reactions as network components from the network superstructure, they must be correlated with the continuous positive variable  $\mathbf{cr}$ , as shown in (9.10), imposing, on the one hand, null reaction rate values when the chemical reaction is discarded, and on the other hand, an upper bound for the reaction rate when it is selected.

$$\phi = \sum_{k \in \mathbf{ds}} \sum_{i \in \mathbf{fe}} \frac{h_i}{2} \sum_{t \in \mathbf{cp}} w_t \sum_{s \in \mathbf{sp}} \mathbf{ae}_{s,t,i,k} \quad (9.7)$$

$$\mathbf{ae}_{s,t,i,k} \geq d_{s,t,i,k} - \sum_{j \in \mathbf{rx}} v_{s,j} \mathbf{cr}_{j,t,i,k}, \quad \forall s \in \mathbf{sp}, t \in \mathbf{cp}, i \in \mathbf{fe}, k \in \mathbf{ds} \quad (9.8)$$

$$\mathbf{ae}_{s,t,i,k} \geq \sum_{j \in \mathbf{rx}} v_{s,j} \mathbf{cr}_{j,t,i,k} - d_{s,t,i,k}, \quad \forall s \in \mathbf{sp}, t \in \mathbf{cp}, i \in \mathbf{fe}, k \in \mathbf{ds} \quad (9.9)$$

$$\mathbf{y}j_{l,j} M \geq \mathbf{cr}_{j,t,i,k}, \quad l = n, \forall j \in \mathbf{rx}, t \in \mathbf{cp}, i \in \mathbf{fe}, k \in \mathbf{ds} \quad (9.10)$$

Equation (9.11) constraints the number of chemical reactions in the network to be equal to  $n$ , at the bottom level (state) of the tree. At least one chemical reaction has to be assigned to every state (unless the initial state,  $l = 0$ ), according to (9.12). The number of chemical reactions has to increase in one unity when the number of states increases, as shown in (9.13). When the chemical reaction is present in a state, it has to be also present in the next state, according to (9.14). The chemical reactions can only, exclusively, be present in the forward or the reverse direction, as defined by (9.15).

$$n = \sum_{j \in \text{rx}} yj_{l,j}, \quad l = n \quad (9.11)$$

$$\sum_{j \in \text{rx}} yj_{l,j} \geq 1, \quad l = 1, \dots, n \quad (9.12)$$

$$\sum_{j \in \text{rx}} yj_{l,j} + 1 = \sum_{j \in \text{rx}} yj_{l+1,j}, \quad l = 0, \dots, n-1 \quad (9.13)$$

$$yj_{l,j} \leq yj_{l+1,j}, \quad l = 0, \dots, n-1, \forall j \in \text{rx} \quad (9.14)$$

$$yj_{l,j} + yj_{l,j+n_{\text{rx}}} \leq 1, \quad \forall l \in \text{st}, j = 1, \dots, n_{\text{rx}} \quad (9.15)$$

Three constraints are associated with the avoidance of inconsistent nonlinear networks. The first one establishes that when the reaction is selected to the current state, the respective reactant species have to be present in the previous state, eq. (9.16). The second constraint establishes that when the reaction is selected, the product species have to be present in the same state, according to (9.17). The last one establishes that when the species are present at the current state, there has to be at least one chemical reaction that produces these species, eq. (9.18).

$$yj_{l+1,j} \leq ys_{l,s}, \quad l = 0, \dots, n-1, \forall s, j \in \text{nsr} \quad (9.16)$$

$$yj_{l,j} \leq ys_{l,s}, \quad \forall l \in \text{st}, s, j \in \text{nsp} \quad (9.17)$$

$$\sum_{j \in \text{rx}} yj_{l,j} \geq ys_{l,s}, \quad \forall l \in \text{st}, s, j \in \text{nsp} \quad (9.18)$$

Equations (9.19) and (9.20) are related to species constraints, establishing, respectively, that every species has to be verified in the tree, and when the species is present in the current state, it also has to be present in the next ones.

$$\sum_{l \in \text{st}} ys_{l,s} \geq 1, \quad \forall s \in \text{sp} \quad (9.19)$$

$$ys_{l,s} \leq ys_{l+1,s}, \quad \forall s \in \text{sp}, l = 0, \dots, n-1 \quad (9.20)$$

Equations (9.7—9.10) concern the former formulation part related to data, equations (9.11—9.20) concern the latter part related to network structure, and, equations (9.21—9.25) are referred to fixed variables in the initial tree state, variable lower bounds and

domains. The entire MILP formulation to generate plausible reaction networks is given by:

$$\min_{\mathbf{y}_s, \mathbf{y}_j, \mathbf{c}_r, \mathbf{a}_e} \phi$$

$$\text{s.t. eqs. (9.7—9.20)}$$

$$\mathbf{y}_{l,j} = 0, \quad l = 0, \forall j \in \mathbf{rx} \quad (9.21)$$

$$\mathbf{y}_{l,s} = 0, \quad l = 0, \forall s \in \mathbf{sp} \setminus \mathbf{rp}, \quad \mathbf{y}_{l,s} = 1, \quad l = 0, \forall s \in \mathbf{rp} \quad (9.22)$$

$$\mathbf{y}_{l,j}, \mathbf{y}_{l,s} \in \{0,1\}, \quad \forall s \in \mathbf{sp}, j \in \mathbf{rx}, l \in \mathbf{st} \quad (9.23)$$

$$\mathbf{c}_{r_{j,t,i,k}} \in \mathbb{R}_0^+, \quad \mathbf{c}_{r_{j,t,i,k}} \geq 0, \quad \forall j \in \mathbf{rx}, t \in \mathbf{cp}, i \in \mathbf{fe}, k \in \mathbf{ds} \quad (9.24)$$

$$\mathbf{a}_{e_{s,t,i,k}} \in \mathbb{R}, \quad \forall s \in \mathbf{sp}, t \in \mathbf{cp}, i \in \mathbf{fe}, k \in \mathbf{ds} \quad (9.25)$$

The network dimension, the scalar  $n$ , is previously elucidated in the data dimension analysis (Step 2), where the variant and invariant relationships are studied assisting the data reconciliation task (Step 1), iteratively.

In order to enumerate the most plausible reaction networks, integer cut equations are added to this formulation forbidding previous solutions to be conceived. For this purpose, the parameter  $\mathbf{ccrx}_{j,i}$  stores the selected reactions  $j \in \mathbf{rx}$  in the current solution iteration  $i \in \mathbf{it}$ . Thus, after the first solution be obtained, this parameter assumes the optimal value of the  $\mathbf{y}_j$  binary variable at the bottom level of the tree:

$$\mathbf{ccrx}_{j,i} = \mathbf{y}_{l,j}, \quad \forall j \in \mathbf{rx}, \quad l = n$$

After the first iteration, the integer cut equation turns active imposing that the combination of binary variables that assume unity values must be different from the previously formed combinations:

$$\sum_{j \in \mathbf{rx}} \mathbf{ccrx}_{j,i} \mathbf{y}_{l,j} \leq \sum_{j \in \mathbf{rx}} \mathbf{ccrx}_{j,i} - 1, \quad \forall i \in \mathbf{it}, \quad l = n \quad (9.26)$$

The number of enumerated solutions (sorted by the increasing  $\phi$  value) can be controlled (i) when establishing a tolerance for the objective function value, *i.e.*, a threshold for  $\phi$ , terminating the solve loop when there is no more solutions that satisfies this constraint, or (ii) when limiting the desired number of solutions to be listed according to the cardinal of the iteration set  $\mathbf{it}$ .

### 9.4.2 Implicit generation of plausible reaction networks with simultaneous kinetic model identification

The implicit generation of plausible reaction networks can also involve the reaction kinetic model identification. In this case the network is obtained simultaneously with the best kinetic expression for each chemical reaction (with adjusted parameters) that fits (at most) experimental data. Hence, the model (reaction network and kinetic expressions) that most closely matches experimental data is obtained. This consists of a finer filtering of reaction networks structures, joining the Steps 4, 5 and the initial phase of Step 6 (supported on differential method) of the incremental methodology to develop chemical reaction models. Incorporating reaction kinetic expressions in the reaction network identification can be an advantage for high dimension case studies, since it allows the reduction of computational effort when decreasing (significantly) the number of models to be generated.

The developed formulation is designed for identifying homogeneous reaction kinetics, maintaining the network generation problem as a MILP. However, networks presenting heterogeneous (nonlinear) kinetics can also be identified, since they can be forced to be adjusted through a combination of straight lines. Actually, the goal is to find a positive correlation of the reaction rate with its reactant species, assisting the network identification task. In cases described by nonlinear kinetics, the resulting linear correlation found will present unreliable kinetic parameters, requiring the application of the entire Step 6 to better identification of the kinetic expression of each model component, regarding the network structure found. On the other hand, in cases described by linear kinetics, one can directly proceed to the final phase of Step 6 for final parameter tuning using as initial guesses the optimal values obtained, regarding the model structure identified.

#### Constructing the superstructure of reaction kinetics

In order to identify the best kinetic expression, ensuring the spanning of all candidate reaction rates that can be described by linear correlations with its parameters, the superstructure of kinetic model expressions must be considered. For this purpose, the possible homogeneous kinetic laws are automatically built based on reactant stoichiometric coefficients. For the most general case where at most two reactant species and tree-molecular reactions make up the reaction network superstructure, several kinetic expressions are considered. For example, for the nonlinear chemical reaction  $2A + B \xrightarrow{-r^1} C$ , five rate expressions can be eligible:

$$\begin{aligned}r_{1a} &= k_{1a}A^2, \\r_{1b} &= k_{1b}A^2B, \\r_{1c} &= k_{1c}AB, \\r_{1d} &= k_{1d}B, \\r_{1e} &= k_{1e}A,\end{aligned}$$



while for the linear reaction  $C \xrightarrow{r_2} D$ , it is considered only one possible rate expression:

$$r_2 = k_2 C.$$

Next section presents the formulation to generate reaction networks with identified kinetic expressions.

### Formulation

When there is available more than one dataset with different experimental temperature, beyond establishing the dataset index  $k \in \mathbf{ds}$  and the set of temperatures  $\mathbf{ts}$  indexed by  $g$ , it is also required to establish a controlling set that links these both sets, named as  $\mathbf{dts}_{g,k}$ , which is only active for the pair temperature  $g$  and data set  $k$  in agreement with data specification.

The objective function has the same equation format used to generate plausible reaction networks, where the integral of the absolute error ( $\mathbf{ae}_{s,t,i,g,k}$ ) profile is minimized using Gauss quadrature rule, as shown in (9.27), where the temperature index is also considered. Note that the number of times that this equation is written still the same as in (9.7), since the controlling set is only active for the matched pairs  $(g,k) \in \mathbf{dts}$ .

$$\phi = \sum_{g,k \in \mathbf{dts}} \sum_{i \in \mathbf{fe}} \frac{h_i}{2} \sum_{t \in \mathbf{cp}} w_t \sum_{s \in \mathbf{sp}} \mathbf{ae}_{s,t,i,g,k} \quad (9.27)$$

The absolute error calculation is performed through an artificial module of  $\mathbf{ae}_{s,t,i,g,k}$ , as shown in eqs. (9.28) and (9.29), where from inequalities constraints, the absolute difference among species concentration derivatives,  $d_{s,t,i,g,k}$  and its predicted values  $\hat{d}_{s,t,i,g,k}$ , is established.

$$\mathbf{ae}_{s,t,i,g,k} \geq d_{s,t,i,g,k} - \hat{d}_{s,t,i,g,k}, \quad \forall s \in \mathbf{sp}, t \in \mathbf{cp}, i \in \mathbf{fe}, g,k \in \mathbf{dts} \quad (9.28)$$

$$\mathbf{ae}_{s,t,i,g,k} \geq \hat{d}_{s,t,i,g,k} - d_{s,t,i,g,k}, \quad \forall s \in \mathbf{sp}, t \in \mathbf{cp}, i \in \mathbf{fe}, g,k \in \mathbf{dts} \quad (9.29)$$

The predicted concentration derivatives involve the computation of reaction kinetic laws instead reaction fluxes (differing from the previous formulation), as shown in (9.30), where  $\nu_{s,j}$  is the species  $s$  stoichiometric coefficient in reaction  $j$ ,  $k_{j,m,g}$  the kinetic parameter (model variable) of reaction  $j \in \mathbf{rx}$ , concerning the rate expression  $m \in \mathbf{km}$  and temperature  $g \in \mathbf{ts}$ , and,  $c_{j,m,t,i,g,k}$  the respective species concentration value. This last model parameter is previously computed according to the reactant species involved in reaction  $j$ , which establishes the kinetic expression  $m$ . For example, the reaction  $A + B \rightarrow C$  has three eligible homogeneous kinetic expressions, where this parameter assumes the species

concentration of (i) A, (ii) B and (iii) the product AB.

$$\hat{d}_{s,t,i,g,k} = \sum_{j \in \text{rx}} v_{s,j} \sum_{m \in \text{km}} k_{j,m,g} c_{j,m,t,i,g,k} \quad \forall s \in \text{sp}, t \in \text{cp}, i \in \text{fe}, g,k \in \text{dts} \quad (9.30)$$

The chemical reactions that were selected as solution must present one (and only one) kinetic rate expression, as shown in (9.31), where  $y_{m_{j,m}}$  is used to select the kinetic model  $m \in \text{km}$  for reaction  $j \in \text{rx}$ . Also, when the chemical reaction is unconsidered, no kinetic model should be selected, equaling to zero both variables  $y_j$  and  $y_m$ .

$$y_{l,j} = \sum_{m \in \text{km}} y_{m_{j,m}}, \quad l = n, \forall j \in \text{rx} \quad (9.31)$$

Since binary variables are used to select reaction kinetic models, they must be correlated with the continuous positive variable  $k$ , as shown in (9.32), imposing, on the one hand, null kinetic parameter values when the reaction model is discarded, and on the other hand, an upper bound for this parameter when it is selected.

$$y_{m_{j,m}} M \geq k_{j,m,g}, \quad \forall j \in \text{rx}, m \in \text{km}, g \in \text{ts} \quad (9.32)$$

The entire MILP formulation to generate reaction networks simultaneously identifying the reaction kinetic expressions is given by the following equations, where equations (9.27—9.30) concern the related data part, eqs. (9.31) and (9.32) are associated to the kinetic model expression selection, equations (9.11—9.22) concern the formulation part related to network structure, and, eqs. (9.33) and (9.35) are referred to variable lower bounds and domains.

$$\begin{aligned} & \min_{y_s, y_j, y_m, k, a_e} \phi \\ & \text{s.t.} \quad \text{eqs. (9.11—9.22, 9.27—9.32)} \\ & y_{l,j}, y_{l,s}, y_{m_{j,m}} \in \{0,1\}, \quad \forall s \in \text{sp}, j \in \text{rx}, l \in \text{st}, m \in \text{km} \quad (9.33) \\ & k_{j,m,g} \in \mathbb{R}_0^+, \quad k_{j,m,g} \geq 0, \quad \forall j \in \text{rx}, m \in \text{km}, g \in \text{ts} \quad (9.34) \\ & a_{e_{s,t,i,g,k}} \in \mathbb{R}, \quad \forall s \in \text{sp}, t \in \text{cp}, i \in \text{fe}, g,k \in \text{dts} \quad (9.35) \end{aligned}$$

# Chapter 10

## Step 6 — Reaction Kinetic Modeling

*“A model that proves very inadequate will be quickly rejected, without contributing much to the genesis and progression of knowledge, while a succession of adjustments to a model that is useful, though not perfect, will lead to an increasingly detailed representation of the phenomenon.”*

– Antoine Danchin

### Contents

---

10.1 Step 6 overview . . . . .	270
10.2 Methodology description . . . . .	271
10.3 Application example . . . . .	278
Bibliography . . . . .	280

---

Posterior to the identification of the plausible reaction networks, and their restriction to a limited set of alternatives, the last step in a methodology for developing kinetic models consists of the identification of the appropriate models for the description of the individual reactions considered, and in the numerical quantification of the corresponding parameters. Since the proposed reaction networks were obtained in a systematic approach, it is expected that, in this final phase, models with a familiar physical-chemical structure can be used. In addition to the correlation between variables, the proposed models must also obey the usual criteria of causality and the law of mass action, in its non-equilibrium form.

In addition to the new information produced, this step should also aid to reduce the number of reaction networks that remain plausible with the available experimental data, ultimately reducing the number of candidates essentially for a single network that can be considered definitive. For this purpose, the need to obtain additional experiments, which allow discriminating between the remaining model structures, can also be considered. In

this sense, the design of new experiments with the aim to the *optimal discrimination of models* (Seber and Wild, 2005) is one of the techniques that can be used to progressively reduce the number of candidates. Similarly, the introduction of *appropriate disturbances* during the experimental tests, (*e.g.*, pulse change of a species concentration) is another way of evaluating the model structure of the system in question. This technique has been used to elucidate the type of causal connectivity, including the local species connection, and the global structure of the reaction network (Vance et al., 2002). Finally, to determine correlations among the identified net reaction rates and the species concentrations, the usual tools of *exploratory data analysis* can be used (Tukey, 1977).

This chapter is organized as follows: in Sections 10.1 and 10.2 a brief introduction and a detailed description of the Step 6 are presented, respectively, and in Section 10.3 the AS case study is considered to illustrate the proposed method.

## 10.1 Step 6 overview

Step 6 comprises two major sequential phases that are supported by different approaches: the differential method and the integral method (DM and IM, respectively). In general, the first phase consists of linear regression procedures, with guaranteed global optima, where the best model structure can be elucidated based on the reaction fluxes calculated from the species concentration derivatives. If no kinetic structures can be found at the end of this step, or even if more than one (or many of them) are viable, additional experiments are needed to elucidate (or discriminate) the model(s). On the other hand, when the kinetic model of the reaction is identified, the true parameters are obtained in a simultaneous nonlinear regression procedure in the last phase, using available concentration data and initial estimates of parameters of the optimal DM solution. This final optimization is susceptible to local optima, although bias-free. The condensed diagram of Step 6 is presented in Figure 10.1.

When more than one dataset with distinct operating conditions is available, the optimal parameters values may be correlated with the experimental temperature through suitable relationships. To this end, two additional sequential approaches are proposed, where the structure of the model with parameters as a function of temperature is elucidated in a first phase and the fine tuning of its energy parameters in a nonlinear regression free of bias is considered in the final phase. During the model structure elucidation, it is identified which and how the parameters (or chemical reactions) are affected by temperature changes, thus, indicating, for example, endo- and exothermic reactions, spontaneous or not. When the results are analyzed, the model that does not present physical-chemical meaning can be discarded, that is, the presence of physically meaningless temperature-parameter correlations can evidence erroneous model structures. Thus, this criterion can be used as an auxiliary tool to discriminate competitive models. In the last phase, nonlinear regressions are part of the problem using the entire concentration data referring to all

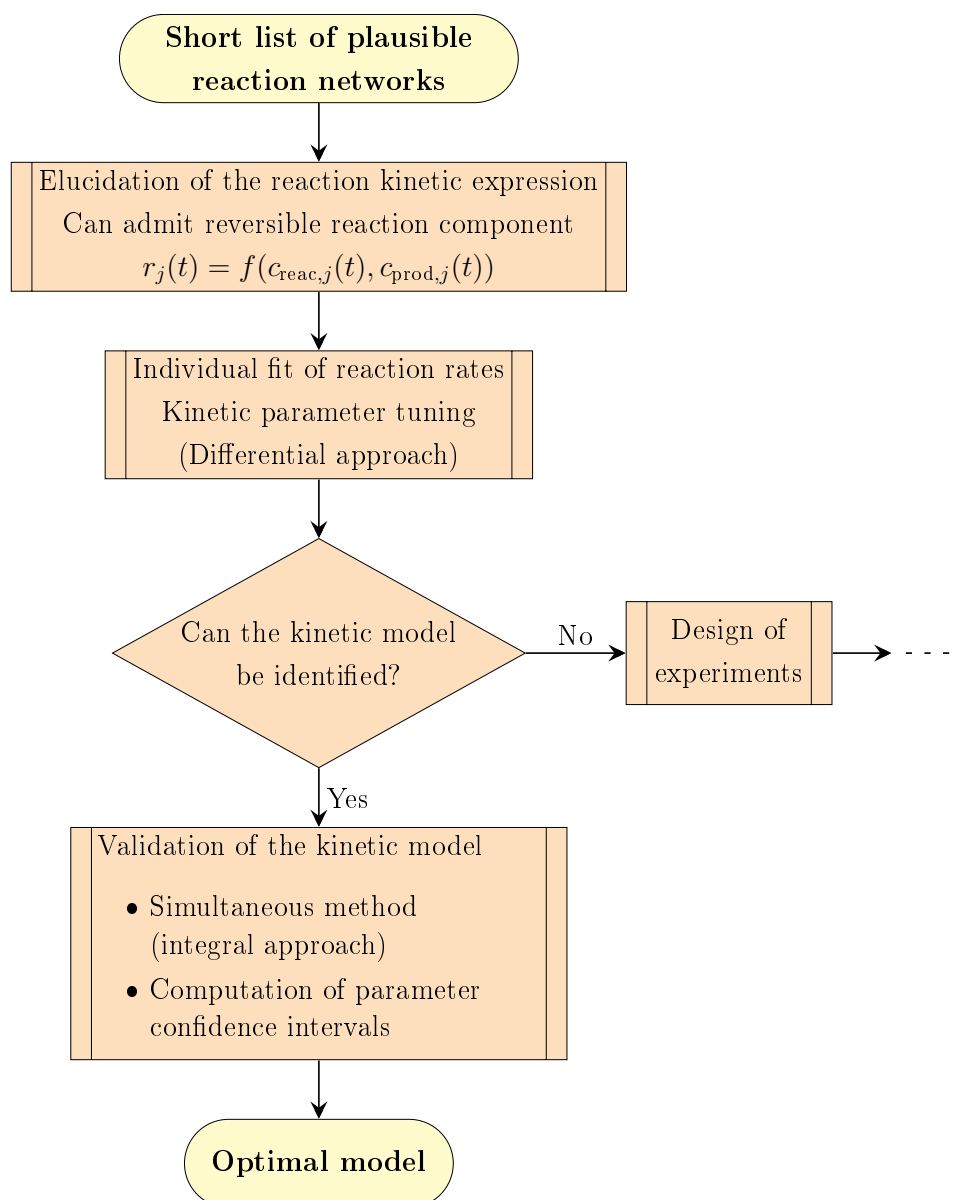


**Figure 10.1** Condensed Step 6 flowchart.

experimental conditions. The final parameters are tuned in an optimization procedure in the maximum likelihood sense, and their statistical metrics are evaluated.

## 10.2 Methodology description

The Step 6 comprises seven sequential sub-steps as shown by the rectangular boxes in Figure 10.2. The description of this step is presented next simultaneously with an illustrative example.

**6.1 Elucidation of potential kinetic expressions** The reaction kinetic laws present particular function shapes that can be observed when correlating the reaction rate

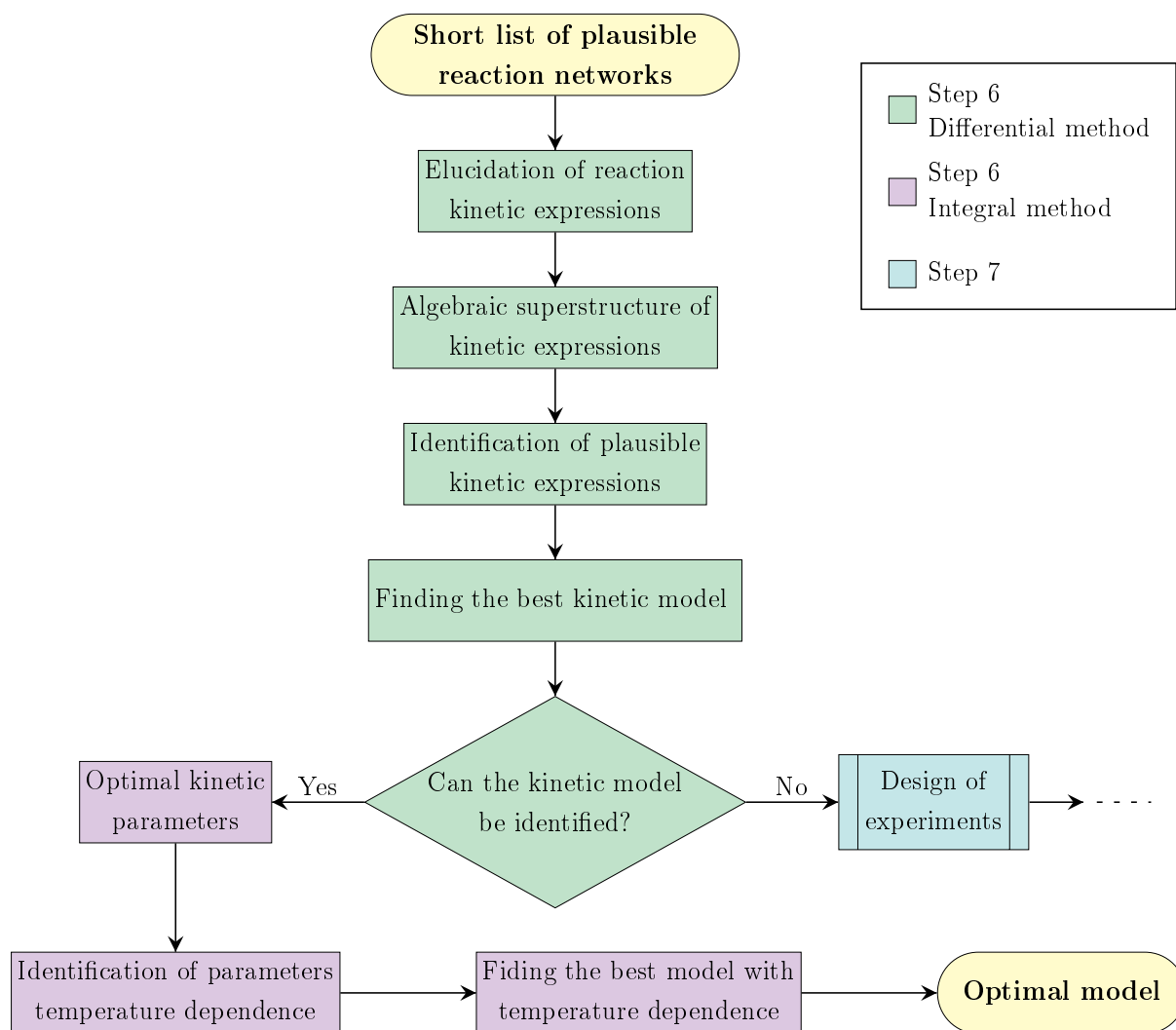


**Figure 10.2** Detailed Step 6 flowchart.

with the respective reactant species concentration. Therefore, after having selected plausible reaction networks (with positive reaction rates), the rate profiles are plotted as a function of their reactant species to elucidate potential kinetic expressions. In this phase, in addition to elucidating the characteristic mathematical expression, one can observe the presence of (i) inhibition (verified when there is a delay in the reaction rate profile), and/or (ii) a reversible component of the reaction.

Consider a chemical reaction,  $A \rightleftharpoons 2B$ , with reversible component between two observed species, as an example to be followed throughout this section. The net reaction rate profile as a function of the normalized concentration of A species is plotted in Figure 10.3. Several mathematical expressions of kinetic models can be proposed to identify which one best describes the behavior of this profile.

**6.2 Algebraic superstructure of kinetic expressions** More than one type of kinetic expression can be eligible to make part of the superstructure. A potential algebraic

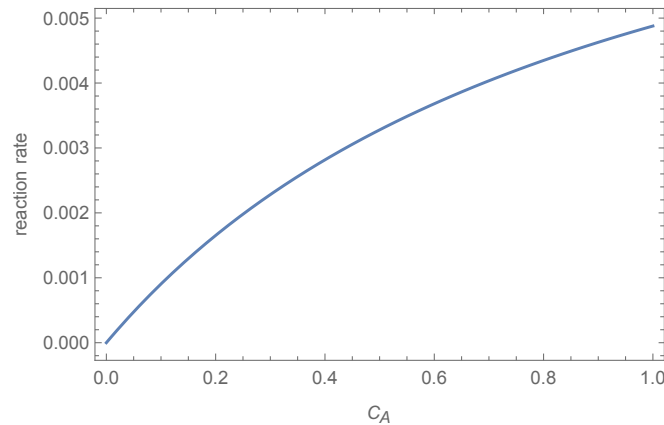


**Figure 10.3** Net reaction rate plotted as a function of  $c_A$ . The concentration is dimensionless (molar ratio) and the reaction rate presents units of molar ratio per time. Chemical reaction:  $A \rightleftharpoons 2B$ .

superstructure of kinetic expressions could be

$$r = \frac{k_d c_A - k_i c_B^2 + k'_d c_A^{0.5} - k'_i c_B}{1 + K_A c_A + K_B c_B}$$

to allow the presence of (i) homogeneous and (ii) heterogeneous kinetics, both with reversible components.

Rearranging the previous equation in a matrix format, a linear system of equations is obtained:

$$r = \begin{bmatrix} c_A & -c_B^2 & c_A^{0.5} & -c_B & -rc_A & -rc_B \end{bmatrix} \cdot \begin{bmatrix} k_d \\ k_i \\ k'_d \\ k'_i \\ K_A \\ K_B \end{bmatrix}$$

The rate of change of  $r(t)$  with respect to its parameters corresponds to the design matrix entries, forming the columns  $\begin{bmatrix} c_A & -c_B^2 & c_A^{0.5} & -c_B & -rc_A & -rc_B \end{bmatrix}$ . Although several kinetic expressions are eligible to be part of the algebraic superstructure, the resulting system must present a design matrix composed of linearly independent column vectors, ensuring that the matrix is non-singular, or in other words, guaranteeing that the model structure can be identified.

**6.3 Identification of plausible kinetic expressions** The individual adjustment of each superstructure of kinetic expressions (one for each chemical reaction of the reaction network) is performed by minimizing the squared error between the model response values and the corresponding reaction rates calculated from the concentra-

tion derivatives and the stoichiometry of the system. This adjustment is restricted to present positive parameters. When the model parameters converge to insignificant values in this procedure ( $k \approx 0$  or  $K \approx 0$ ), the previous structure assumes different forms of kinetic laws. In cases where heterogeneous laws are considered, the adjustment must be performed simultaneously for all reaction components since the adsorption term is common in all reactions. In these multiple response regression problems, the kinetic parameters concerning reversible reaction components can become unidentifiable in some cases. Therefore, the design matrix must be carefully constructed to ensure that it has full rank and that the problem is at most well-posed. Thus, this first constrained regression elucidates the kinetic laws that are plausible solutions when their parameters assume positive values, discarding those that converge to extremely insignificant values ( $k \sim 10^{-8}$ ).

Following the example, a new structure was found indicating that this chemical reaction system is described by a heterogeneous kinetic law with an irreversible chemical reaction, where both species A and B are adsorbed on the catalyst:

$$r = \frac{k_d c_A}{1 + K_A c_A + K_B c_B}$$

**6.4 Best kinetic expression** Once the plausible terms that remain in the full kinetic expression are elucidated, two questions arise at this stage: could this resulting model be overfitting the data? In the presence of a combination of kinetic models as a plausible solution, which will be the best? Through the use of information criteria, such as the Bayesian Information Criterion (BIC) (Schwarz et al., 1978), the model identification is performed parsimoniously by considering a new constraint-free fit for each parcel of the model and computing the corresponding BIC values, through

$$\text{BIC} = m \ln(\text{SSE}/m) + \ln(m)n \quad (10.1)$$

where  $m$  is the number of data points and  $n$  is the number of degrees of freedom (kinetic parameters). Therefore, the best tradeoff between the goodness of fit and the number of parameters is established by the model with the lowest BIC.

In the example, three additional model parcels are considered:

$$r = k_d c_A, \quad r = \frac{k_d c_A}{1 + K_A c_A} \quad \text{and} \quad r = \frac{k_d c_A}{1 + K_B c_B}$$

in addition to the complete structure identified earlier. The best kinetic expression with the lowest BIC value is in this case  $r = k_d c_A / (1 + K_A c_A)$ .

Thus, after the best (parsimonious) structure of the model has been incrementally identified, the differential approach ends here, as shown by the green area of the block diagram in Figure 10.2. Still in Step 6, in the next phase the adjustment of



the kinetic parameters of the model found is considered, adopting procedures based on the IM indicated by the purple area in the diagram. Otherwise, if no structure can be identified, additional experiments are needed to provide more and better data, aiding in the modeling identification task in Step 7 (petrol blue box).

**6.5 Optimal kinetic parameters** The best kinetic expressions established for all chemical reactions in the reaction network are taken to this step, where, finally, the global fit is performed minimizing the squared error between the experimental data (measurements of concentration) and the response variables of the system of ODEs integrated. This step is supported in IM, where parameter adjustment is performed simultaneously for all chemical reactions present in the network in a nonlinear regression procedure. Although this nonlinear regression may face local optima, the procedure is bias-free, and the solution of the differential approach is used as an initial estimate of the parameters to assist the optimization in finding the global optimum. Confidence intervals for each kinetic parameter are also calculated, and the optimal result obtained is the best identified model.

**6.6 Parameters with temperature dependence** When there is more than one dataset with different temperatures, the kinetic parameters can be correlated with the temperature using suitable equations, such as the Arrhenius equations (10.2) and van't Hoff (10.3). In (10.2),  $A_0$  is the pre-exponential factor, a constant for each chemical reaction,  $E_a$  is the reaction activation energy,  $R$  is the universal gas constant and  $T$  the experimental temperature:

$$k = A_0 \exp(-E_a/RT) \quad (10.2)$$

Considering heterogeneous reaction kinetics, at equilibrium, the adsorption parameter  $K$  can be related to the Gibbs free energy change,  $\Delta G$ , through  $\Delta G_{ad} = -RT \ln K$ . Also, under constant pressure and temperature conditions  $\Delta G_{ad} = \Delta H_{ad} - T\Delta S_{ad}$ , where  $\Delta H_{ad}$  and  $\Delta S_{ad}$  are the enthalpy and entropy changes, respectively, in the adsorption reaction. Hence, when considering these both relationships, the following expression arises in a van't Hoff equation form, where the natural logarithm of  $K$  varies linearly with the inverse of temperature:

$$K = \exp(-\Delta H_{ad}/RT + \Delta S_{ad}/R) \quad (10.3)$$

Again, two sequential approaches can be considered to estimate the energy parameters: (i) an approximate method based on linear regression and (ii) a simultaneous (and more rigorous) method where the parameters are fitted in a nonlinear regression procedure (and bias-free), supported by IM, using the previous solution as an initial estimate.

In (i), the energy relationships are linearized by taking the natural logarithm of the

optimal parameters correlated with the inverse of temperature. Thus, the activation energy and the enthalpy of the adsorption reaction can be estimated through the slope of the straight line for the Arrhenius and van't Hoff equations, respectively. Procedure (ii) is covered in the next stage.

Considering the previous example, where the best structure achieved was  $r = \frac{k_d c_A}{1 + K_A c_A}$ , the both  $k$  and  $K$  will be correlated with experimental temperatures through:

$$\ln(k_d) = \ln(A_0) - \frac{E_a}{RT}, \quad \text{and} \quad \ln(K_A) = -\frac{\Delta H_{ad}^0}{RT} + \frac{\Delta S_{ad}^0}{R}$$

The results of this approximate method can elucidate what are (and how) the kinetic parameters sensitive to temperature changes in the system. For example, the horizontal lines indicate that there is no temperature dependence, while the sign of the slope (positive or negative) can indicate endo or exothermic reactions, spontaneous or not, etc. Furthermore, the magnitudes of the values of the adsorption parameters obtained can elucidate the type of adsorption of the reaction when coinciding with pre-established characteristic intervals (from the literature).

**6.7 Parameters with nonlinear temperature dependence** Once the reactions in the system that are sensitive to temperature changes are elucidated, a more rigorous approach can be considered based on the IM. The same integration procedure considered in 6.5 is performed, but instead of adjusting the kinetic parameters (one for each temperature), the energy parameters are adjusted by replacing the respective model expressions that correlate the kinetic constant with the temperature in the mass balance. Thus, through the minimization of squared error between measured concentration data at several temperatures and predicted model species concentrations, the energetic parameters are tuned in the maximum likelihood sense.

Continuing the previous example, considering three datasets  $l = 1, 2, 3$  with different temperatures, the optimization problem can be summarized as shown below. Note that for this simple example, the mass balance is performed for both species  $s = 1, 2 \equiv A, B$ , and with a single chemical reaction  $A \rightarrow 2B$ , where  $\alpha_s$  is the stoichiometric coefficient of the species  $s$  with  $\alpha_A = -1$  and  $\alpha_B = +2$ .

$$\begin{aligned} \min_{\substack{A_0, E_a, \\ \Delta H_{ad}^0, \Delta S_{ad}^0}} & \sum_{l=1}^3 \sum_{s=1}^2 \sum_{t=1}^{n_{to}} e_{s,t,l}^2 \\ \text{s.t.} & \quad e_{s,t,l} = c_{s,t,l} - \hat{c}_{s,t,l} \\ & \quad \frac{d\hat{c}_{s,t,l}}{dt} = \alpha_s \frac{A_0 \exp(-E_a/RT_l) c_{A,t,l}}{1 + \exp(-\Delta H_{ad}^0/RT_l + \Delta S_{ad}^0/R) c_{A,t,l}} \end{aligned}$$

In this formulation,  $\hat{c}$  is the model concentration calculated by solving the ODEs, and  $c$  is the measurement of the experimental concentration.

However, these parameter-temperature correlations, (10.2) and (10.3), have some drawbacks when considering their parameter estimates in a nonlinear multiresponse regression. The format of these equations, as they were originally proposed, generally presents parameters with high correlation, translated by the almost linear dependence between them (high collinearity index), and also, the optimization of the resulting model can present difficult convergence to the optimal solution due to numerical problems, instabilities, and error propagation, consisting of an ill-conditioned nonlinear problem. This kind of disadvantage can be mitigated when considering an adequate reparametrization of the model, thus making the design matrix well conditioned with a lower correlation between the model parameters. Some reparametrizations of the Arrhenius equation have been proposed in the literature, involving the use of scale factors, reference temperatures, and exponential operations (Himmelblau, 1970; Schwaab and Pinto, 2007; Schwaab et al., 2008; Buzzi-Ferraris and Manenti, 2010; Quaglio et al., 2019).

In the next chapter where the case studies are presented, the equations adopted for the reparametrization of (10.2) were:

$$k = \exp \left( \alpha - \frac{\beta 10^4}{R} \left( \frac{1}{T} - \frac{1}{T_{\text{ref}}} \right) \right) \quad (10.4)$$

where  $\alpha = \ln k(T_{\text{ref}})$ ,  $\ln k(T_{\text{ref}}) = \ln A_0 - \frac{\beta 10^4}{RT_{\text{ref}}}$  and  $\beta = E_a 10^{-4}$ . And,

$$k = \exp \left( A_0 - \frac{E_a 10^4}{RT} \right) \quad (10.5)$$

While the reparametrization adopted for (10.3) was

$$K = \exp \left( \frac{\phi 10^2}{R} - \frac{\theta 10^5}{R} \left( \frac{1}{T} - \frac{1}{T_{\text{ref}}} \right) \right) \quad (10.6)$$

where  $\phi 10^2 = \Delta S_{ad}^0 - \frac{\theta 10^5}{T_{\text{ref}}}$ , and,  $\theta = \Delta H_{ad}^0 10^{-5}$ , which is similar to (10.4).

Equations (10.4) and (10.6) suggest almost an autoscaling format of the kinetic parameters, since the inverse of experimental temperature is subtracted from the inverse of reference temperature (like a mean centering), and then, weighted by a factor (scaling operation). Therefore, the advantage of considering this equation format is that from a good initial estimate for  $\alpha$  ( $k(T_{\text{ref}})$  logarithm), it is possible to better estimate the parameter  $\beta$ .

### 10.3 Application example

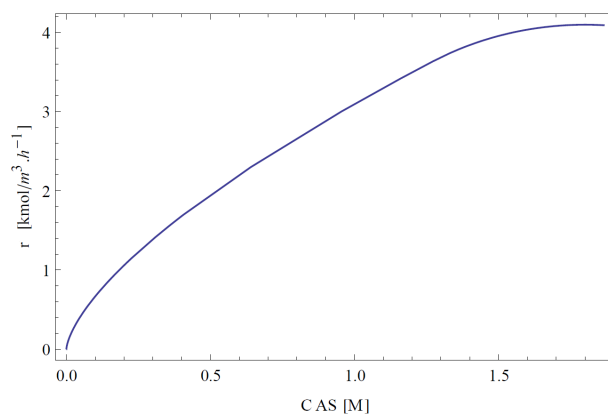
The complete analysis of the AS case study is quite limited by the presence of significant errors identified previously in the closing of the total mass balance to the system. Therefore, the uncertainty in the determination of the concentration profiles is high, and, consequently, it is very difficult to propose a complete reaction network for this case. Due to this fact, only a partial determination of the corresponding kinetic model will be analyzed in this section, considering the sub-steps related to the differential method in which the reaction rates can be individually analyzed.

In Section 9.3.1, the reactions that necessarily integrate the definitive reaction networks were characterized:



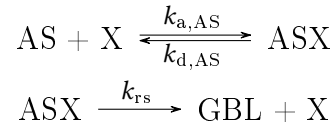
However, taking into account the superstructure of the candidate reaction networks for this system (Figure 9.3), the determination of both  $r_4$  and  $r_8$  rates are dependent on the reaction network considered, since the GBL and the BDO reagents can simultaneously participate as reagents in other parallel reactions, depending on the particular network considered. Consequently, in this case study, only a single kinetic model will be obtained for the first reaction.

Figure 10.4 presents the rate profile of  $r_1$  as a function of reagent concentration obtained using the continuous approximation of the concentration profiles made in Step 1. The behavior shown indicates an approximately linear reaction rate in the intermediate concentration zone, which rapidly tends to a constant value as the reactant concentration increases. This behavior (profile shape) is compatible with an essentially irreversible *Langmuir-Hinshelwood* kinetic response, given that it is a heterogeneous system with the presence of a solid catalyst. As an alternative, the approximation of these data to first-order kinetics was also studied for comparison purposes.



**Figure 10.4** Reaction rate  $r_1$  as a function of AS concentration.

Considering the Langmuir-Hinshelwood kinetics in its simplest form, this model assumes the adsorption of the reactant on the surface of the catalyst, corresponding to the limiting reaction step:



In this equation the constants are relative to adsorption ( $k_a$ ) and desorption ( $k_d$ ) of the reagent AS, and X represents the active sites of the catalyst. The corresponding reaction kinetic model may be written as:

$$r_1 = k_{\text{rs}} \frac{K_{\text{AS}} \text{AS}}{(1 + K_{\text{AS}} \text{AS})} \quad (10.7)$$

where  $K_{\text{AS}} = k_{a,\text{AS}}/k_{d,\text{AS}}$  is the equilibrium constant.

Since the values of  $r_1$  were previously determined, by applying the differential method, the two parameters of this model ( $k_{\text{rs}}$  and  $K_{\text{AS}}$ ) can be determined by linear regression, transforming the previous equation into the form

$$\frac{1}{r_1} = A \frac{1}{\text{AS}} + B \quad (10.8)$$

where:

$$A = \frac{1}{k_{\text{rs}} K_{\text{AS}}} \quad \text{and} \quad B = \frac{1}{k_{\text{rs}}}$$

Figure 10.5(a) shows the transformed experimental data, and the adjustment obtained. In this case, the kinetic parameters  $k_{\text{rs}} = 1.83 \text{ M h}^{-1}$  and  $K_{\text{AS}} = 8.81 \text{ M}^{-1}$ , were obtained using an objective function corresponding to the square residues of the model (10.8). The residual value of the objective function was 15.97, in the units considered. Figure 10.5(b) compares the experimental reaction rates produced by the previous model. As can be seen through these last figures, the adjustment achieved can only be considered reasonable, and other forms of catalytic kinetic models more complex than (10.7) should be investigated. However, this issue was not analyzed in this thesis, once again taking into account the uncertainty in the original experimental data.

Considering the first order kinetics, the reaction rate as a function of AS reagent concentration was approximated to a straight line, as shown in Figure 10.6(a). Through the linear regression between the  $r_1$  data and the AS concentration, considering the linear model  $r_1 = k_1 \text{AS}$ , it was obtained  $k_1 = 2.82 \text{ h}^{-1}$ . The estimate of the total squared error of the regression was in this case  $19.72 \text{ M}^2 \text{ h}^{-2}$ . Figure 10.6(b) compares the experimental reaction rate with that predicted by the linear model. In this case, despite the reaction taking place in a catalytic medium, the 1st order kinetics presents results with similar

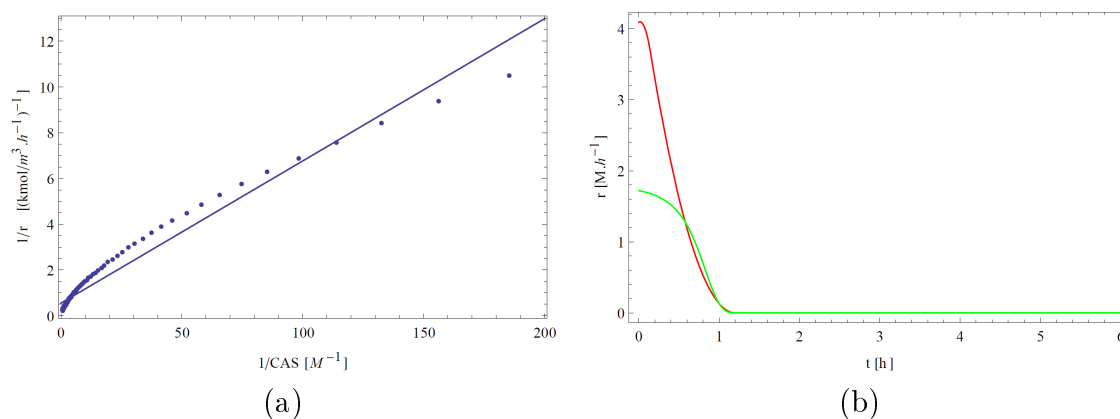


**Figure 10.5** Chemical adsorption kinetics of  $r_1$ . In (a) adjustment of the kinetic model to  $r_1$  (continuous curve), and experimental data considered. In (b) comparison between the model (green curve) and the experimental data (red curve).

quality to the previously considered Langmuir-Hinshelwood kinetic model.

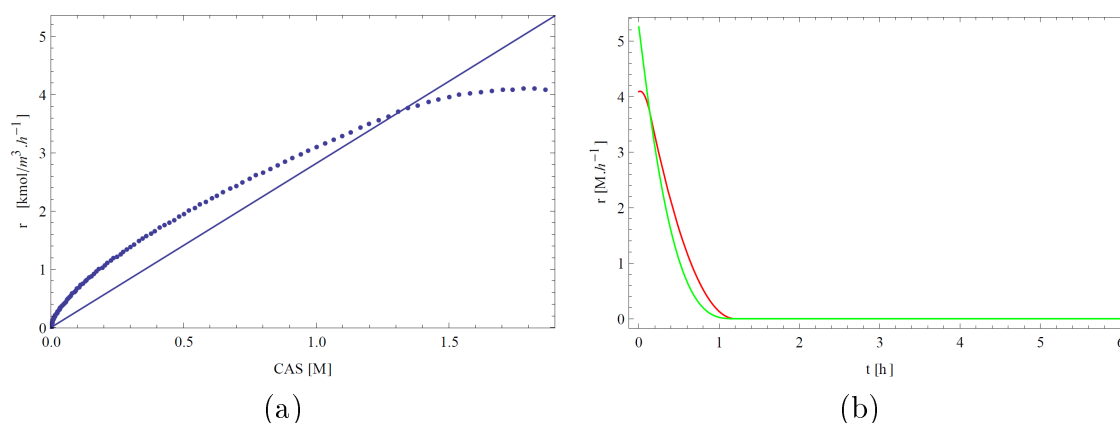


**Figure 10.6** Homogeneous kinetics. In (a) linear approximation of reaction rate  $r_1$ . In (b) comparison between the model (green curve) and the experimental data (red curve).

## Bibliography

- Buzzi-Ferraris, G. and Manenti, F. (2010). Better reformulation of kinetic models. *Computers & Chemical Engineering*, 34(11):1904–1906.
- Himmelblau, D. (1970). *Process analysis by statistical methods*. Wiley.
- Quaglio, M., Waldron, C., Pankajakshan, A., Cao, E., Gavriilidis, A., Fraga, E. S., and Galvanin, F. (2019). An online reparametrisation approach for robust parameter estimation in automated model identification platforms. *Computers & Chemical Engineering*, 124:270–284.
- Schwaab, M., Lemos, L. P., and Pinto, J. C. (2008). Optimum reference temperature

- for reparameterization of the arrhenius equation. Part 2: Problems involving multiple reparameterizations. *Chemical Engineering Science*, 63(11):2895–2906.
- Schwaab, M. and Pinto, J. C. (2007). Optimum reference temperature for reparameterization of the arrhenius equation. Part 1: Problems involving one kinetic constant. *Chemical Engineering Science*, 62(10):2750–2764.
- Schwarz, G. et al. (1978). Estimating the dimension of a model. *Annals of statistics*, 6(2):461–464.
- Seber, G. and Wild, C. (2005). *Nonlinear Regression*. Wiley Series in Probability and Statistics. Wiley.
- Tukey, J. (1977). *Exploratory Data Analysis*. Addison-Wesley series in behavioral science. Addison-Wesley Publishing Company.
- Vance, W., Arkin, A., and Ross, J. (2002). Determination of causal connectivities of species in reaction networks. *Proceedings of the National Academy of Sciences*, 99(9):5816–5821.





# Chapter 11

## Case Studies

*“Out of intense complexities, intense simplicities emerge.”*

– Winston Churchill

### Contents

---

11.1 Isothermal isomerization of $\alpha$ -pinene . . . . .	284
11.1.1 Finding the model structure . . . . .	285
11.1.2 Parameter correlation with temperature . . . . .	290
11.1.3 Parameter fitting in comparison with the Stewart & Sørensen model . . . . .	292
11.1.4 Parameter fitting in comparison with the Box et al. and Tjoa & Biegler models . . . . .	295
11.2 Hydrogenation of maleic acid (MAC) . . . . .	297
11.2.1 Finding the model structure . . . . .	297
11.2.2 Parameter correlation with temperature . . . . .	307
11.3 Pfizer case study . . . . .	316
11.3.1 Data reconciliation . . . . .	316
11.3.2 Analysis of time invariants . . . . .	325
11.3.3 Evaluating the use of invariants in data reconciliation to in- crease model identifiability . . . . .	326
11.3.4 Identifying the true network . . . . .	332
11.3.5 Reaction kinetic expressions . . . . .	337
11.3.6 Parameter correlation with temperature . . . . .	341
Bibliography . . . . .	342

---

This chapter presents the main results obtained from the application of the systematic methodology for modeling chemical reaction systems to several case studies, namely, the thermal isomerization of  $\alpha$ -pinene in Section 11.1, the catalytic hydrogenation of maleic acid in Section 11.2, and the pharmaceutical case study, Pfizer, in Section 11.3. An introduction to these case studies was presented in Section 1.5.

## 11.1 Isothermal isomerization of $\alpha$ -pinene

The thermal isomerization of  $\alpha$ -pinene has been studied for several authors in the field of kinetic modeling. Several datasets were found in the literature, respecting to isothermal batch experiments in the temperature range 189.5–285 °C and with pure initial reactant in liquid phase. In the original articles, the registered experiments consists of ten datasets with different initial and experimental conditions (Fuguitt and Hawkins, 1945, 1947). The entire data shows an irregular structure, presenting in some experiments the absence of particular species measurements, as well as few registers (only one measurement sample and one replica). The pioneer authors commented about the difficulties in measuring some of the residual species, namely the pyronenes<sup>1</sup>. Consequently, they considered the isomers  $\alpha$ - and  $\beta$ -pyronene as a single species in their registers (BP) and an estimate of this species concentration, assuming a linear increase of BP produced with respect to the amount of AP consumed (Fuguitt and Hawkins, 1947).

Fuguitt and Hawkins (1945) have suggested a reaction network, Figure 11.1(a), based on their interpretation from data recovered. The reaction network (a) was used for parameter fitting with different optimization approaches by Box et al. (1973) and Tjoa and Biegler (1991), both considering the same dataset concerning to the isothermal experiment at 204.5 °C with AP initial reactant. In 1981, Stewart & Sørensen proposed another reaction network, Figure 11.1(b), based on the ten datasets and other considerations that allow for a bias-free modeling approach for fitting kinetic parameters correlated with experimental temperature (Stewart and Sørensen, 1981; Stewart et al., 1992). In this work we propose a different reaction network, Figure 11.1(c), that was identified using the systematic methodology to model chemical reaction systems.

The reaction network in (c) differs of (a) and (b) in the BP species origin, once it is produced from AP instead of from AO in a secondary step. Moreover, the identified structure presents a lower number of kinetic parameters than (b), once there is no redundant pathway concerned to the origin of D species.

This case study is presented in separate parts. Section 11.1.1 presents how the model structure was identified. Section 11.1.2 addresses the parameters correlation with temperature. In Section 11.1.3 the model proposed in this work is compared with the proposal

---

<sup>1</sup>The pyronenes presented boiling point between AP and LIM, and refractive index similar with LIM.

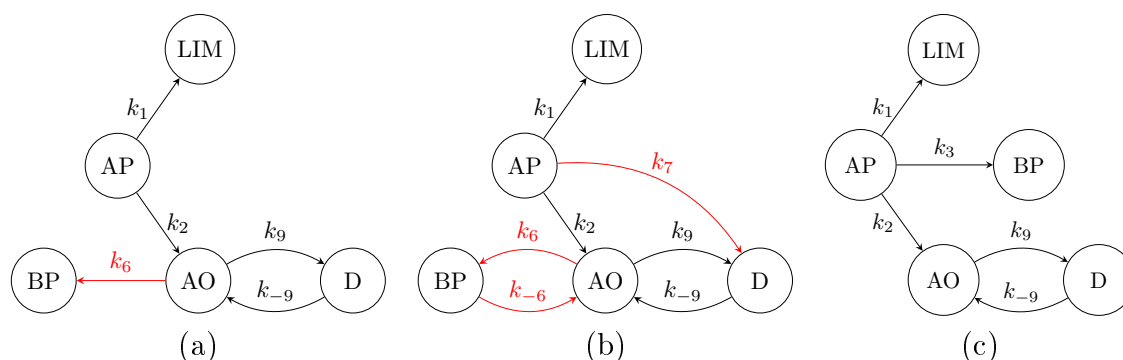


**Figure 11.1** Reaction network proposed by (a) [Fuguitt and Hawkins \(1945\)](#), (b) [Stewart and Sørensen \(1981\)](#) and (c) this work. The red arrows in (a) and (b) indicate chemical reactions that are not present in (c).

by [Stewart and Sørensen \(1981\)](#), while in Section 11.1.4 it is compared with the model proposed by [Box et al. \(1973\)](#) and [Tjoa and Biegler \(1991\)](#).

### 11.1.1 Finding the model structure

From Step 1 to Step 5 of the proposed methodology, the  $\alpha$ -pinene case study was modeled on the basis of two datasets with  $T_1 = 189.5^\circ\text{C}$  and  $T_2 = 204.5^\circ\text{C}$  (datasets #1 and #2), both with AP initial reactant ([Fuguitt and Hawkins, 1947](#)). These datasets are the only ones that contain all species registered, with an enough amount of measurements that enabled the data reconciliation procedure to be well applied resulting in good estimates of species concentration derivatives ([Vertis et al., 2016](#)).

The generation of chemical reactions resulted in 10 linear chemical reactions, listed in Table 11.1. The results were obtained using GAMS® software with the commercial solver CPLEX. The total CPU usage was 0.75 s using the formulation containing integer cut equations to enumerate alternative feasible solutions.

**Table 11.1** Stoichiometric coefficients (nre and npr) and respective linear chemical reactions. Class of reactions: isomerization (1 — 6) and dimerization (7 — 10).

Index	AP	LIM	AO	BP	D	Reaction
1	-1	1	0	0	0	$\text{AP} \rightarrow \text{LIM}$
2	-1	0	1	0	0	$\text{AP} \rightarrow \text{AO}$
3	-1	0	0	1	0	$\text{AP} \rightarrow \text{BP}$
4	0	-1	1	0	0	$\text{LIM} \rightarrow \text{AO}$
5	0	-1	0	1	0	$\text{LIM} \rightarrow \text{BP}$
6	0	0	-1	1	0	$\text{AO} \rightarrow \text{BP}$
7	-2	0	0	0	1	$2 \text{AP} \rightarrow \text{D}$
8	0	-2	0	0	1	$2 \text{LIM} \rightarrow \text{D}$
9	0	0	-2	0	1	$2 \text{AO} \rightarrow \text{D}$
10	0	0	0	-2	1	$2 \text{BP} \rightarrow \text{D}$

Energetic analysis of the 20 reaction fluxes (forward and reverse components) of the listed chemical reactions was considered to identify their energetically viable reaction flux directions (net). The parameter values used to compute the standard potential of the species are shown in Table 11.2. These values, together with polynomial forms for  $C_{p,s}$ , were retrieved from Aspen Properties®. For the BP and D species, the  $\Delta G_{f,s,T_{\text{ref}}}^0$  and  $\Delta H_{f,s,T_{\text{ref}}}^0$  were estimated using the Benson Group contribution method. Figure 11.2 presents the  $dG/d\xi_j$  profiles. As can be observed on the right plot, the chemical reactions relative to the dimerization ( $r_7 - r_{10}$ ) are only feasible in the dimer formation direction. The  $dG/d\xi_j$  of the other chemical reactions do not reach a value higher than  $40 \text{ kJ mol}^{-1}$ , indicating that a unique direction cannot be assertively identified (Wells and Rose, 1986). Hence, reactions  $r_1$  to  $r_6$  and their reverse counterparts are included as candidates in the reaction network superstructure (Figure 11.3). Globally, instead of the original 20 distinct reaction fluxes, 16 were considered as energetically feasible.

**Table 11.2**  $\Delta G_f^0$  and  $\Delta H_f^0$  at  $T_{\text{ref}} = 298 \text{ K}$ , and  $\mu^0$  at  $T = 204.5 \text{ }^\circ\text{C}$ . Units in  $\text{kJ mol}^{-1}$ .

$s$	$\Delta G_{f,298}^0$	$\Delta H_{f,298}^0$	$\mu^0$
AP	216.0	28.3	328.9
LIM	202.1	6.4	319.9
AO	242.4	54.3	355.6
BP	208.8	2.4	332.9
D	240.2	198.3	265.4

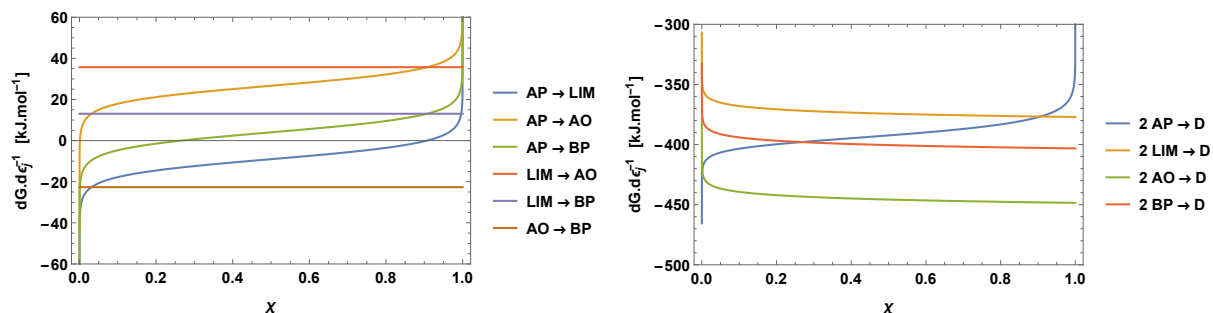


**Figure 11.2** Gibbs free energy variations associated with the individual reactions.

The generation of reaction networks with this superstructure (Figure 11.3) was performed. The number of generated reaction networks (without redundant pathways) decreased from 50 to 16, *i.e.*, a reduction of 68% in the number of structures to be further analyzed. In these solutions, the  $r_9$  reaction ( $2 \text{ AO} \rightleftharpoons \text{D}$ ) is present in all networks, as its occurrence is known in the literature (Fuguitt and Hawkins, 1945). The 16 energetically feasible reaction networks (composed of four chemical reactions) were classified as plausible, since these networks showed positive net reaction rates across the time domain.

However, when considering the list of 50 linear reaction networks generated in Step 4 of the methodology (without considering energetically favorable reaction directions), 31

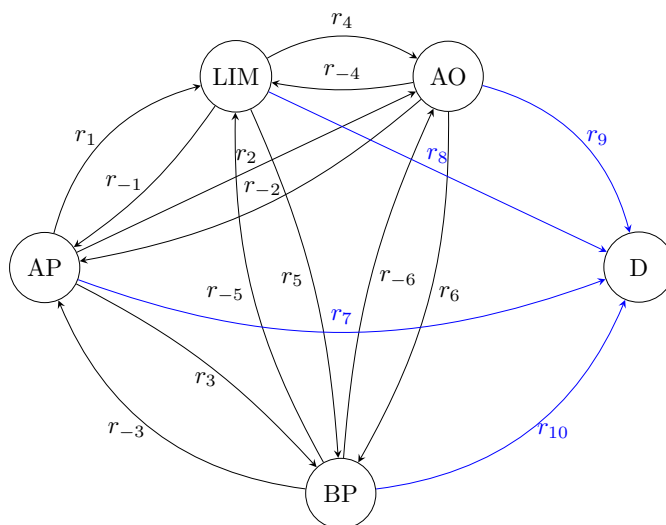


**Figure 11.3** Linear superstructure with energetically feasible directions identified in blue arrows.

and 34 reaction networks were selected as plausible in relation to datasets  $T_1$  and  $T_2$ , respectively, for a threshold  $\phi < 0.005$  established through the qualitative analysis of the results obtained in Step 5. The ranking of these 50 network structures is shown in Figure 11.4, where the networks are displayed (ranked) with increasing  $\phi$  value.

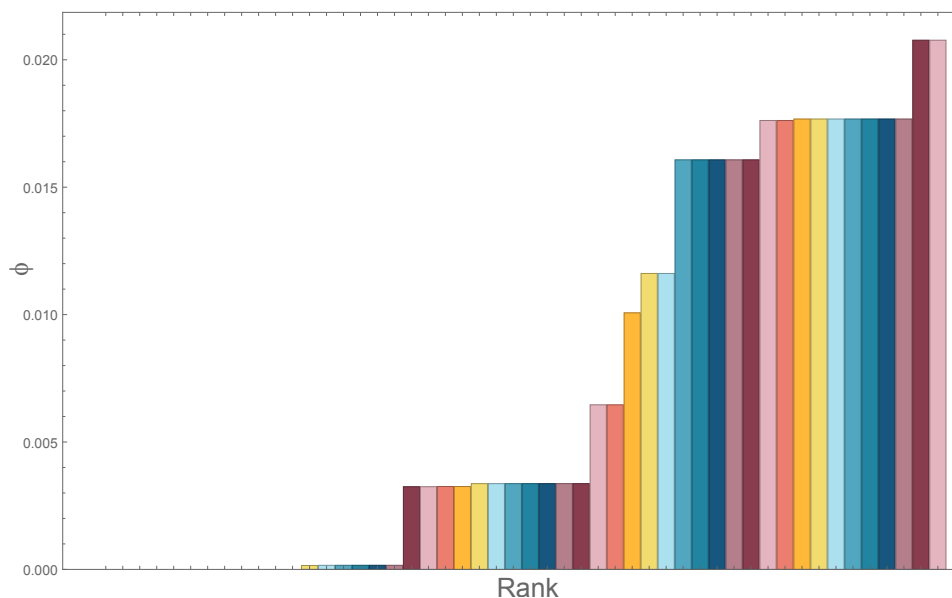


**Figure 11.4** Reaction networks ordered by the plausibility criterion using dataset T2.

When considering the implicit generation of reaction networks, 8 plausible reaction network structures were generated with four positive net reaction rate profiles, see Figure 11.5. The MILP formulation presented in Section 9.4.1 was run in GAMS® software with the commercial solver CPLEX. The total CPU usage was 11.03s.

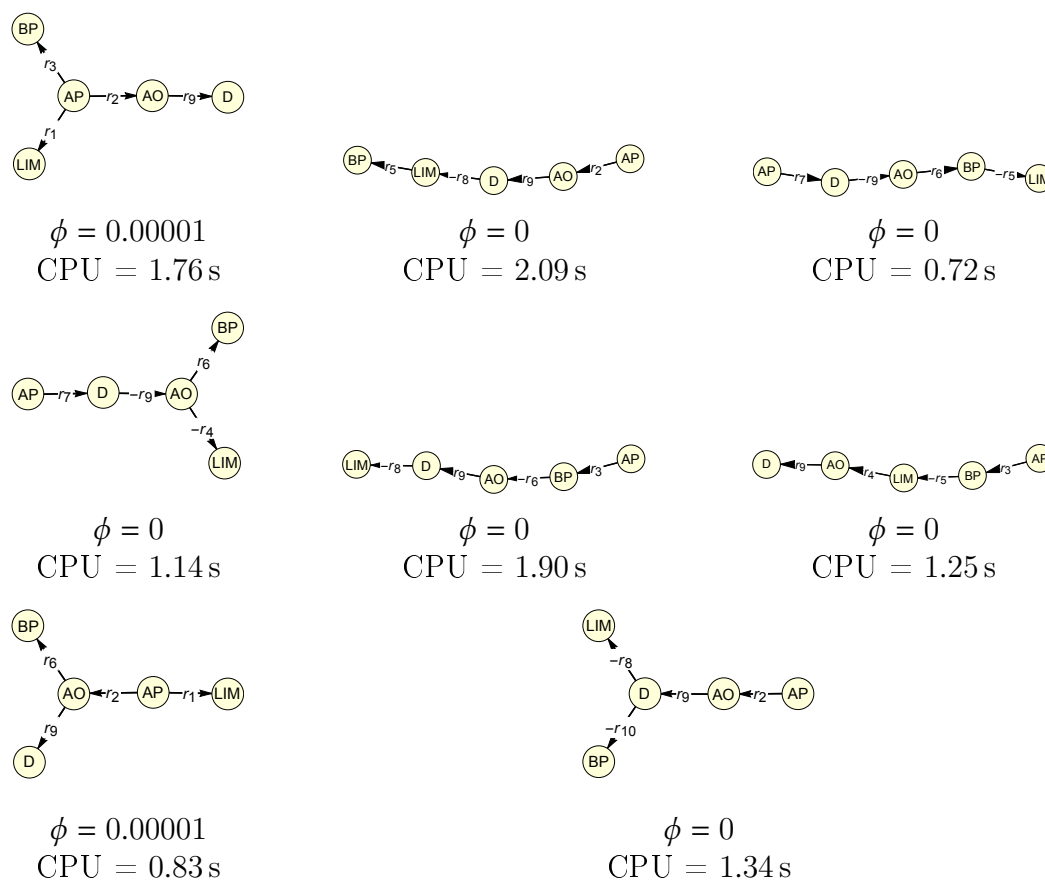


**Figure 11.5** Linear graph representation of the eight plausible structures obtained in the implicit generation of reaction networks. Notice that the 1st and the 7th networks in this figure correspond to the networks (a) and (c), respectively, in Figure 11.1.

After analyzing the individual plots of the net reaction rates as a function of the respective reactant species, the reaction kinetic expressions were proposed considering reversible reaction components. Linear regressions for each network model were performed individually for each chemical reaction, and the best network together with its reaction kinetic expressions could be found (based on the differential method), presenting first and second order homogeneous kinetic laws, with reversible reaction components for  $r_3$  and  $r_9$  (Figure 11.6).

In the final phase of Step 6, where the integral method is performed using the original experimental data, some changes were obtained in the model structure previously identified. Using the  $k$  values from the differential method for every dataset as initial parameter estimates, the differential mass balances (presented above) were numerically solved in a nonlinear regression procedure without constraints. The results obtained are summarized in Table 11.3, where the objective function value (SSE) related to each considered method is also presented. The SSE concerns to molar ratios of species concentrations (dimensionless). For both datasets, the  $k_{-3}$  showed no physical meaning converging to

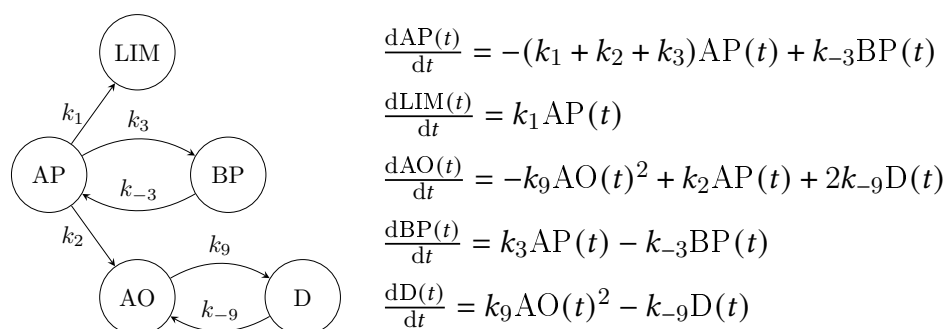


**Figure 11.6** Reaction network identified in Step 5 with 4 chemical reactions. Reversible components of  $r_3$  and  $r_9$  were elucidated during the differential method of Step 6. Species mass balances on the right-hand side.

negative values, and also, it presented (i) a great correlation with its opposite component  $k_3$ , (ii) poor confidence intervals, and (iii) high  $p$ -values (near to one). The same statistical metrics were obtained when considering positive constraint to that parameter. Thus, the reversible component  $r_{-3}$  was excluded of the proposed model as shown Figure 11.1(c), consisting of a reaction network with a smaller number of parameters to be correlated with temperature.

**Table 11.3** Optimal kinetic parameters  $k \times 10^3$  in  $\text{min}^{-1}$  obtained at experimental temperatures  $T_1 = 189.5^\circ\text{C}$  and  $T_2 = 204.5^\circ\text{C}$ . DM: differential method. IM: integral method. CI: confidence intervals. Results related to the reaction networks presented in Figure 11.6 (\*1) and Figure 11.1(c) (\*2).

Parameter		DM <sup>*1</sup>	IM <sup>*1</sup>	CI	$p$ -val	IM <sup>*2</sup>	CI	$p$ -val
$k_1$	$T_1$	0.059	0.058	(0.056, 0.060)	0.000	0.058	(0.056, 0.060)	0.000
	$T_2$	0.220	0.223	(0.220, 0.225)	0.000	0.223	(0.220, 0.225)	0.000
$k_2$	$T_1$	0.033	0.026	(0.024, 0.029)	0.000	0.026	(0.024, 0.029)	0.000
	$T_2$	0.124	0.124	(0.121, 0.127)	0.000	0.124	(0.121, 0.126)	0.000
$k_3$	$T_1$	0.003	0.002	(-0.000, 0.005)	0.081	0.003	(0.001, 0.004)	0.001
	$T_2$	0.112	0.012	(0.009, 0.014)	0.000	0.012	(0.010, 0.014)	0.000
$k_{-3}$	$T_1$	0.002	-0.013	(-0.069, 0.043)	0.645	-	-	-
	$T_2$	0.030	-0.002	(-0.027, 0.022)	0.854	-	-	-
$k_9$	$T_1$	2.138	2.630	(0.497, 4.762)	0.017	2.621	(0.514, 4.728)	0.016
	$T_2$	3.167	4.971	(4.485, 5.457)	0.000	4.969	(4.281, 5.658)	0.000
$k_{-9}$	$T_1$	0.028	0.037	(-0.034, 0.107)	0.304	0.036	(-0.034, 0.105)	0.304
	$T_2$	0.165	0.138	(0.128, 0.147)	0.000	0.137	(0.095, 0.180)	0.000
SSE	$T_1$	0.022	0.012	-	-	0.012	-	-
	$T_2$	0.003	0.001	-	-	0.001	-	-

### 11.1.2 Parameter correlation with temperature

The differential mass balances with the respective  $k$  values replaced using (10.4) result in the next system of equations:

$$\begin{aligned}\frac{dAP(t)}{dt} &= - \left( \exp \left( \alpha_1 - \frac{\beta_1 10^4}{R} \left( \frac{1}{T} - \frac{1}{T_{\text{ref}}} \right) \right) + \exp \left( \alpha_2 - \frac{\beta_2 10^4}{R} \left( \frac{1}{T} - \frac{1}{T_{\text{ref}}} \right) \right) + \right. \\ &\quad \left. \exp \left( \alpha_3 - \frac{\beta_3 10^4}{R} \left( \frac{1}{T} - \frac{1}{T_{\text{ref}}} \right) \right) \right) AP(t) \\ \frac{dLIM(t)}{dt} &= \exp \left( \alpha_1 - \frac{\beta_1 10^4}{R} \left( \frac{1}{T} - \frac{1}{T_{\text{ref}}} \right) \right) AP(t) \\ \frac{dAO(t)}{dt} &= - \exp \left( \alpha_9 - \frac{\beta_9 10^4}{R} \left( \frac{1}{T} - \frac{1}{T_{\text{ref}}} \right) \right) AO(t)^2 + \exp \left( \alpha_2 - \frac{\beta_2 10^4}{R} \left( \frac{1}{T} - \frac{1}{T_{\text{ref}}} \right) \right) AP(t) + \\ &\quad 2 \exp \left( \alpha_{-9} - \frac{\beta_{-9} 10^4}{R} \left( \frac{1}{T} - \frac{1}{T_{\text{ref}}} \right) \right) D(t) \\ \frac{dBP(t)}{dt} &= \exp \left( \alpha_3 - \frac{\beta_3 10^4}{R} \left( \frac{1}{T} - \frac{1}{T_{\text{ref}}} \right) \right) AP(t) \\ \frac{dD(t)}{dt} &= \exp \left( \alpha_9 - \frac{\beta_9 10^4}{R} \left( \frac{1}{T} - \frac{1}{T_{\text{ref}}} \right) \right) AO(t)^2 - \exp \left( \alpha_{-9} - \frac{\beta_{-9} 10^4}{R} \left( \frac{1}{T} - \frac{1}{T_{\text{ref}}} \right) \right) D(t)\end{aligned}$$

Parameter adjustments were obtained using **Mathematica**® 12.0 with the NonlinearModelFit function. The CPU usage was 16 s in a quad core i7 Intel processor. In the first run, the initial estimates of the parameters were considered by computing the logarithm of the optimal values of  $k$  at the reference temperature,  $T_{\text{ref}} = T_2 = 477.65$  K. Although bounds in the  $\beta$  parameters were (initially) considered constraining them to be positive and inferior than  $250 \text{ kJ mol}^{-1}$ , these constraints never got active. No more than three iteration were required to obtain the minimal value of the SSE, totaling 0.023120 in units of squared molar concentration ratios. Table 11.4 presents the adjusted parameters with their confidence intervals. All parameters presented a  $p$ -value lower than  $10^{-6}$ , showing that they have statistical significance. The model simulation for the ten datasets is presented in Figure 11.7 in comparison with the original data reported by Fuguitt and Hawkins (1945, 1947).

**Table 11.4** Kinetic parameters tuned using data reported in Fuguitt and Hawkins (1945, 1947). CI: Confidence intervals,  $k(T_{\text{ref}}) \times 10^3$  in  $\text{min}^{-1}$ ,  $A_0$  in  $\text{min}^{-1}$ , and  $E_a$  in  $\text{kJ mol}^{-1}$ .

$k_j$	$\alpha$	CI	$\beta$	CI	$k(T_{\text{ref}})$	$A_0$	$E_a$
$k_1$	-1.481	(-1.506,-1.454)	16.842	(16.426,17.258)	0.228	$5.960 \times 10^{14}$	168.416
$k_2$	-2.152	(-2.192,-2.110)	17.381	(16.919,17.842)	0.116	$1.184 \times 10^{15}$	173.807
$k_3$	-4.551	(-4.797,-4.304)	20.323	(19.347,21.299)	0.011	$1.773 \times 10^{17}$	203.227
$k_9$	1.379	(1.290,1.468)	8.799	(8.218,9.380)	3.972	$1.666 \times 10^7$	87.990
$k_{-9}$	-2.121	(-2.288,-1.954)	10.405	(8.518,12.292)	0.120	$2.869 \times 10^7$	104.049



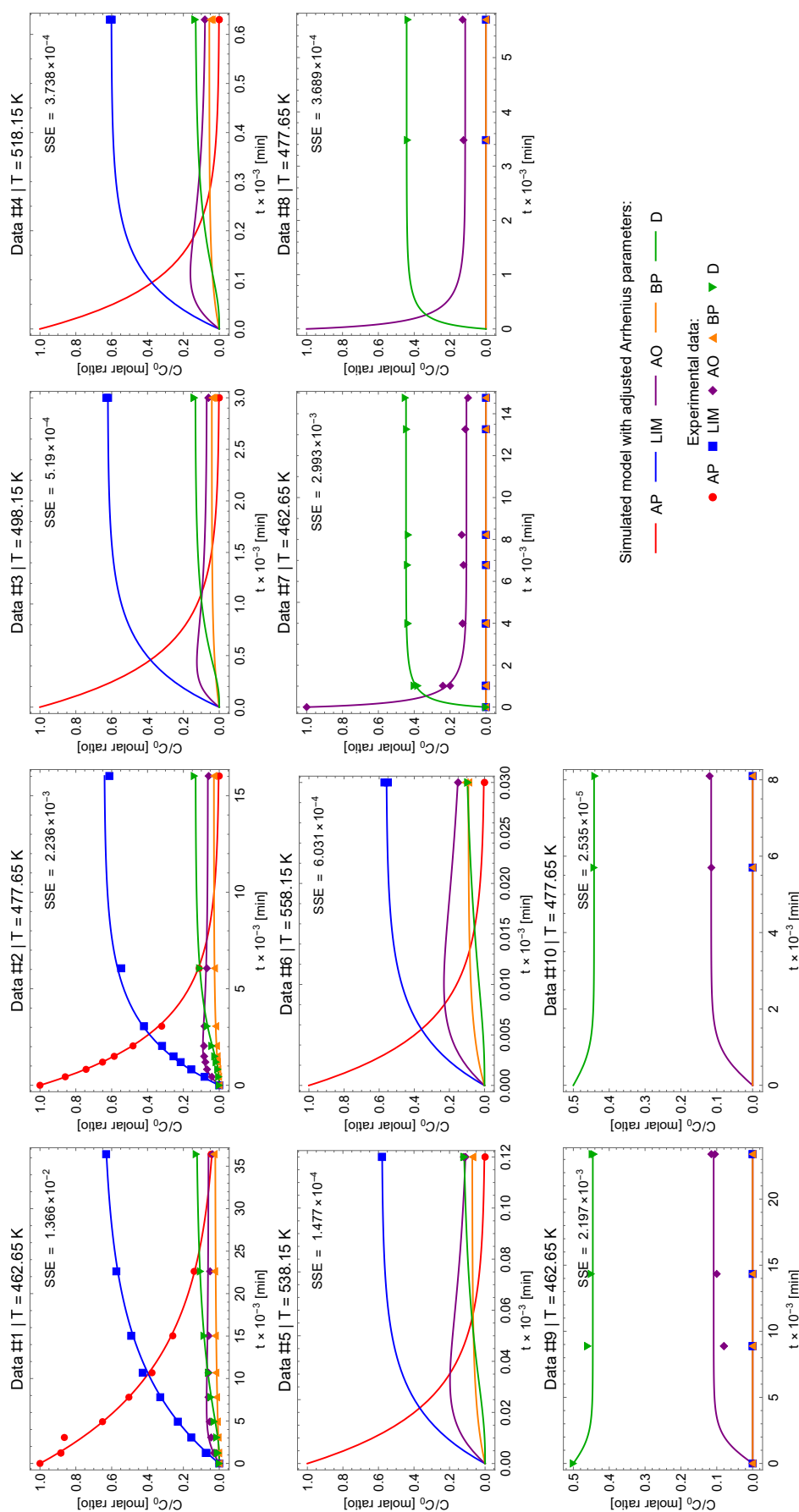


Figure 11.7 Simulation of the developed model in comparison with experimental data reported in Fugitt and Hawkins (1945, 1947).

### 11.1.3 Parameter fitting in comparison with the Stewart & Sørensen model

The 10 data sets presented by [Stewart and Sørensen \(1981\)](#) differ from the original data reported by [Fuguitt and Hawkins \(1945, 1947\)](#) in two respects: (i) the original measurements were equally weighted to verify the overall mass balance and (ii) no related assumptions the BP species was considered<sup>2</sup>, resulting in datasets with measures related to the clustered species (no individual species measurements). Therefore, the species BP is almost never recorded alone, appearing in measurements of clustered species (AP + BP and BP + LIM) so as not to influence/bias the fit of the model parameters. The same datasets reported by [Stewart and Sørensen \(1981\)](#) are considered here.

To adjust the model parameters, the previous ODEs system was numerically solved considering the initial conditions of each data set and the respective temperature of the experiment. In addition, the use of {0,1} weights was necessary to activate and deactivate the contribution of squared residues of species concentrations in the objective function, since the residues of specific responses where no measurements are available should not be evaluated. Furthermore, fictitious species were additionally considered in the regression data matrix representing the summed species. Therefore, an extension of the solution list referring to the response variables of real species was made considering the fictitious species that are computed through the sum of the response variables of the model solved numerically.

The results were obtained using **Mathematica**® 12.0 with the function `NonlinearModelFit`. The CPU usage was 14s in a quad core i7 Intel processor. The initial parameter estimates were considered by computing the logarithm of the optimal values of  $k$  at the reference temperature,  $T_{\text{ref}} = T_2 = 477.65$  K, reported in [Table 11.3](#). The results are presented in [Table 11.5](#). All parameters presented a  $p$ -value lower than  $10^{-9}$ , showing that they have statistical significance. The model simulation for the ten datasets is presented in [Figure 11.8](#) in comparison with Stewart & Sørensen model simulation and experimental data. The SSE is 0.009915.

**Table 11.5** Optimal kinetic parameters. CI: Confidence intervals,  $k(T_{\text{ref}}) \times 10^3$  in  $\text{min}^{-1}$ ,  $A_0$  in  $\text{min}^{-1}$ , and  $E_a$  in  $\text{kJ mol}^{-1}$ .

$k_j$	$\alpha$	CI	$\beta$	CI	$k(T_{\text{ref}})$	$A_0$	$E_a$
$k_1$	-1.484	(-1.505,-1.462)	16.324	(16.000,16.648)	0.227	$1.614 \times 10^{14}$	163.243
$k_2$	-2.168	(-2.199,-2.137)	16.922	(16.575,17.270)	0.114	$3.671 \times 10^{14}$	169.223
$k_3$	-4.677	(-4.920,-4.433)	19.841	(18.796,20.886)	0.009	$4.641 \times 10^{16}$	198.406
$k_9$	1.514	(1.419,1.609)	8.631	(8.137,9.126)	5.543	$1.250 \times 10^7$	86.314
$k_{-9}$	-1.977	(-2.122,-1.833)	10.183	(8.764,11.602)	0.138	$1.894 \times 10^7$	101.831

<sup>2</sup>[Stewart and Sørensen \(1981\)](#) avoided using BP records calculated through a linear approximation proposed by [Fuguitt and Hawkins \(1947\)](#).

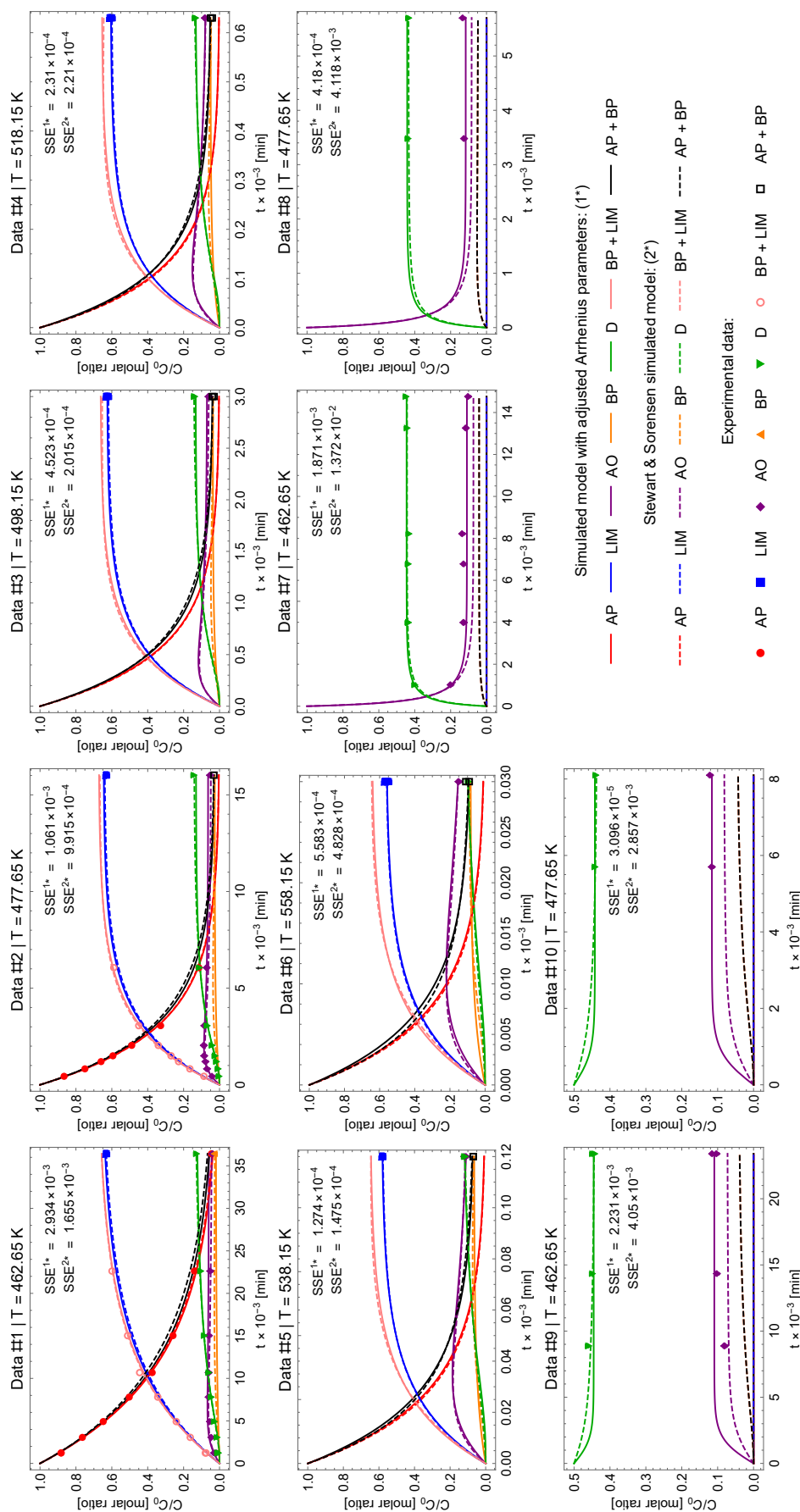


**Figure 11.8** Simulation of the developed model with adjusted parameters in comparison with the simulation of the model proposed by Stewart and Sørensen (1981).

The structural model proposed by these authors consists of the reaction network in Figure 11.1(b). Kinetic expressions take the same format as (10.4) with reparameterized kinetic constants, but no parameter scaling factor  $E_a$  (Stewart and Sørensen, 1981). The simulation of their model was considered, presenting a total SSE of 0.028449. The un-reparameterized parameters values are presented in Table 11.6.

Comparing the model simulations, a very similar goodness of fit (in terms of SSE) is obtained for data sets #1 to #6. On the other hand, the literature model lost quality in the prediction of data sets #7 to #10, showing a poor model-data agreement in relation to the AO profiles. From the simulation of the literature model, it is observed that the species BP is produced when the experiment starts with AO (datasets #7 and #8) or with D (datasets #9 and #10), although no measurements have been recorded for the species BP. This result is in agreement with the structure of the proposed model, since the species BP is formed in parallel with D from the reactant AO in the reaction network (b).

Fuguitt and Hawkins (1945) commented that the experiments regarding datasets #7 to #10 were performed to study the dimerization reaction  $r_9$ , concluding that D is formed from AO in a reversible chemical reaction since an equilibrium relationship was established. They also referred that the AO refractive index (RI) had decreased for experiments heated for longer times, suggesting that the reason for that fact could be the formation of small amounts of other compounds from AO, probably the pyronenes. However, they could not measure any residual species, and, the RI decayed from 1.5412 to 1.5340, not quantitatively justifying (i) the presence of reaction  $r_6$ ,  $\text{AO} \rightarrow \text{BP}$ , and even more, (ii) the presence of its reversible component as proposed by Stewart and Sørensen (1981). Therefore, the reaction network (c) proposed in the thesis is preferable to describe this chemical reaction system since it presents a better ability to predict data with a lower number of parameters when compared to Stewart & Sørensen model.

**Table 11.6** Equivalent kinetic parameters adjusted by Stewart and Sørensen (1981) regarding the reaction network presented in Figure 11.1(b), with  $k(T_{\text{ref}}) \times 10^3$  in  $\text{min}^{-1}$ ,  $A_0$  in  $\text{min}^{-1}$ , and  $E_a$  in  $\text{kJ mol}^{-1}$ .

$k_j$	$k(T_{\text{ref}})$	$A_0$	$E_a$
$k_1$	0.240	$2.179 \times 10^{14}$	164.492
$k_2$	0.128	$1.171 \times 10^{15}$	173.679
$k_6$	0.276	$1.155 \times 10^{12}$	143.101
$k_{-6}$	0.494	$3.554 \times 10^{12}$	145.254
$k_7$	0.006	$8.427 \times 10^{12}$	165.817
$k_9$	4.348	$1.016 \times 10^7$	85.817
$k_{-9}$	0.069	$4.333 \times 10^8$	117.252

### 11.1.4 Parameter fitting in comparison with the Box et al. and Tjoa & Biegler models

Box et al. (1973) and Tjoa and Biegler (1991) studied the reaction kinetic modeling of the  $\alpha$ -pinene isothermal isomerization adopting different optimization strategies. Box et al. (1973) considered a reduced number of response variables from data, namely three linearly independent variables, imposing two time-invariant relationships in the dynamic system: the overall mass balance closure and the linear dependence of BP concentration related to AP consumption, establishing that  $BP = 0.03(100 - AP)$ . In addition to the classic least squares regression procedure, these authors considered minimizing the determinant of the matrix of squared residues related to concentration data using empirical eigenvectors (real eigenvectors from the chosen response variables) and theoretical eigenvectors (orthonormalized vectors that maximize the data variance from the singular value decomposition), finding the parameter values which have the highest posterior density according to the determinant criterion. Tjoa and Biegler (1991) presented another method to parameter estimates based on orthogonal collocation on finite elements, considering as objective function the minimization of SSE using fourth order polynomials on ten finite elements.

Several in common model characteristics were considered in both works: (i) same reaction network structure as originally proposed by Fuguitt & Hawkins, Figure 11.1(a); (ii) parameter estimates supported on dataset #2, (original from Fuguitt and Hawkins (1947)); (iii) first order homogeneous kinetics for all chemical reactions (including dimerizations); (iv) species stoichiometric coefficients equal to unity, *i.e.*, stoichiometric matrix corresponds to an adjacency matrix; (v) parameters tuned using concentration ratios in units of mass (weight percentages). As a result, the model proposed by Tjoa and Biegler (1991) (reaction network, kinetic expressions and optimal parameters values) is exactly the same of one of the proposals by Box et al. (1973), *i.e.*, both works reported the same optimal parameters values regarding the minimization of total SSE problem.

In order to perform the model comparison, the same conditions (ii) to (v) were adopted in this work for parameter fine tuning regarding the network in Figure 11.1(c). The resulting differential mass balances are shown below, where “\*” differs  $k$  from previous models.

$$\begin{aligned}\frac{dAP(t)}{dt} &= -(k_1^* + k_2^* + k_3^*)AP(t) \\ \frac{dLIM(t)}{dt} &= k_1^*AP(t) \\ \frac{dAO(t)}{dt} &= -k_9^*AO(t) + k_2^*AP(t) + k_{-9}^*D(t) \\ \frac{dBP(t)}{dt} &= k_3^*AP(t) \\ \frac{dD(t)}{dt} &= k_9^*AO(t) - k_{-9}^*D(t)\end{aligned}$$

The results were obtained using Mathematica® 12.0 with the NonlinearModelFit function. The CPU usage was 27s in a quad core i7 Intel processor. The optimal parameter

values with their confidence intervals are presented in Table 11.7. All parameters presented a  $p$ -value lower than  $10^{-9}$ , showing that they have statistical significance.

The model simulation is presented in Figure 11.9, in comparison with the literature model simulation (parameter values reported in Table 11.8). Although the number of parameters regarding both reaction networks is the same, the model proposed in this work presents a slightly better data agreement than the model proposed in literature with parameters values obtained using SSE minimization. The simulation of the literature model regarding the optimal parameter values from the minimization of determinant criterion showed worst ability to predict data, especially in predicting BP species. However, the difference in SSE values (14.061 vs. 19.880) does not justify a preference among the candidate reaction networks (a) and (c). Nonetheless, weight concentration ratios (in percentage) were used with kinetic expressions that varies linearly with the weight of reactant species, establishing that reactions occur in an one-to-one weight proportion, according to Lavoisier rules. It is a correct approach from a mathematical and physical point of view, but it does not allow the kinetic model identification, namely the elucidation of the mass action of power laws (in units of moles) that is happening in the system. Furthermore, in this study only a single dataset was considered for parameter adjustment and, therefore, not enough data were used to discriminate the origin of BP species.

**Table 11.7** Optimal parameter values associated with the developed model.

Parameter	$k \times 10^3$ [ $\text{min}^{-1}$ ]	CI
$k_1^*$	0.059	(0.058,0.060)
$k_2^*$	0.027	(0.026,0.028)
$k_3^*$	0.003	(0.002,0.003)
$k_9^*$	0.294	(0.247,0.340)
$k_{-9}^*$	0.046	(0.029,0.062)

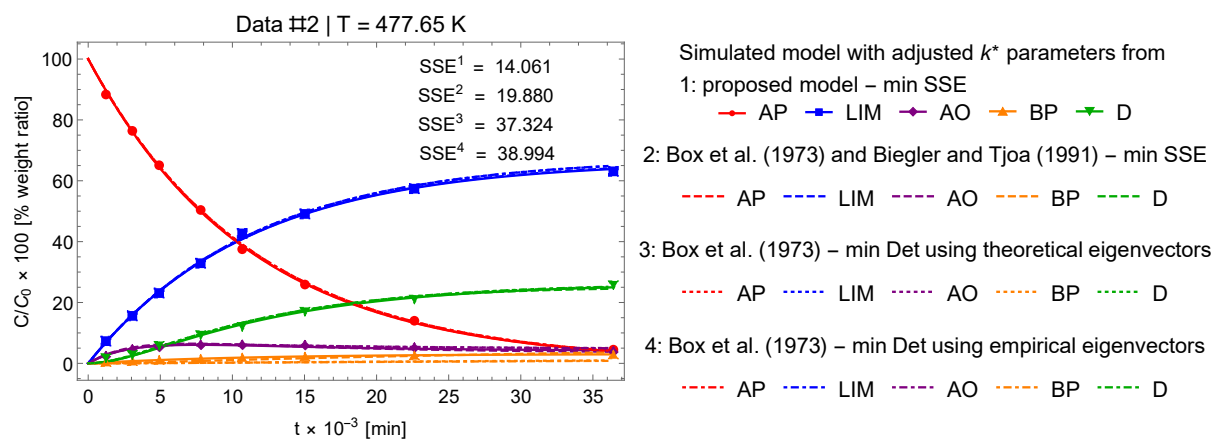


**Figure 11.9** Optimal model simulation in comparison with literature models from Box et al. (1973) and Tjoa and Biegler (1991).

**Table 11.8** Optimal parameter values reported in [Box et al. \(1973\)](#) and [Tjoa and Biegler \(1991\)](#) regarding the reaction network in Figure 11.1(a) and optimization approaches adopted. SSE: minimization of SSE, EE: minimization of determinant matrix using empirical eigenvalues, TE: minimization of determinant matrix using theoretical eigenvalues. Parameters  $k \times 10^3$  in  $\text{min}^{-1}$ .

Parameter	SSE	EE	TE
$k_1^*$	0.059	0.060	0.060
$k_2^*$	0.030	0.028	0.029
$k_6^*$	0.021	0.004	0.005
$k_9^*$	0.275	0.313	0.315
$k_{-9}^*$	0.040	0.057	0.059

## 11.2 Hydrogenation of maleic acid (MAC)

Following the MAC case study introduced in Section 1.5.3, this section presents the results obtained from applying the methodology to this case study, presenting (i) how the model structure was found in Section 11.2.1 and (ii) the correlation of parameters with temperature in Section 11.2.2.

### 11.2.1 Finding the model structure

During the systematic methodology for developing chemical reaction models, the identification of the reaction network was initially performed separately for each data set with different experimental temperatures in order to verify how the model structure behaves under different experimental conditions.

In Step 1, good estimates of species concentration derivatives were obtained for each dataset through the data reconciliation procedure. At this stage, global mass conservation was imposed at each collocation point on each finite element. The profiles of the individual species are shown in Figure 11.10 referring to the T1 dataset, where the vertical lines (on the grid) indicate the finite elements equally distributed in the time horizon, the black dots are the experimental data and the continuous profiles are the optimal results of the data reconciliation procedure. The smoothed profiles obtained are the basis for the identification of the model structure, allowing the selection of plausible reaction networks and expressions of viable kinetic models supported by the differential method.

The data dimension analysis, in Step 2, allowed the data space characterization identifying the need of 4 extents/chemical reactions to describe the concentration changes among the five observed species. This result confirms the prior assumption about only a single time-invariant relationship exists in this system, *i.e.*, the overall mass conservation.

During Step 3, the superstructure of the reaction network (Figure 11.11) was obtained, taking into account (i) the reaction stoichiometry, (ii) the data consistency criterion,

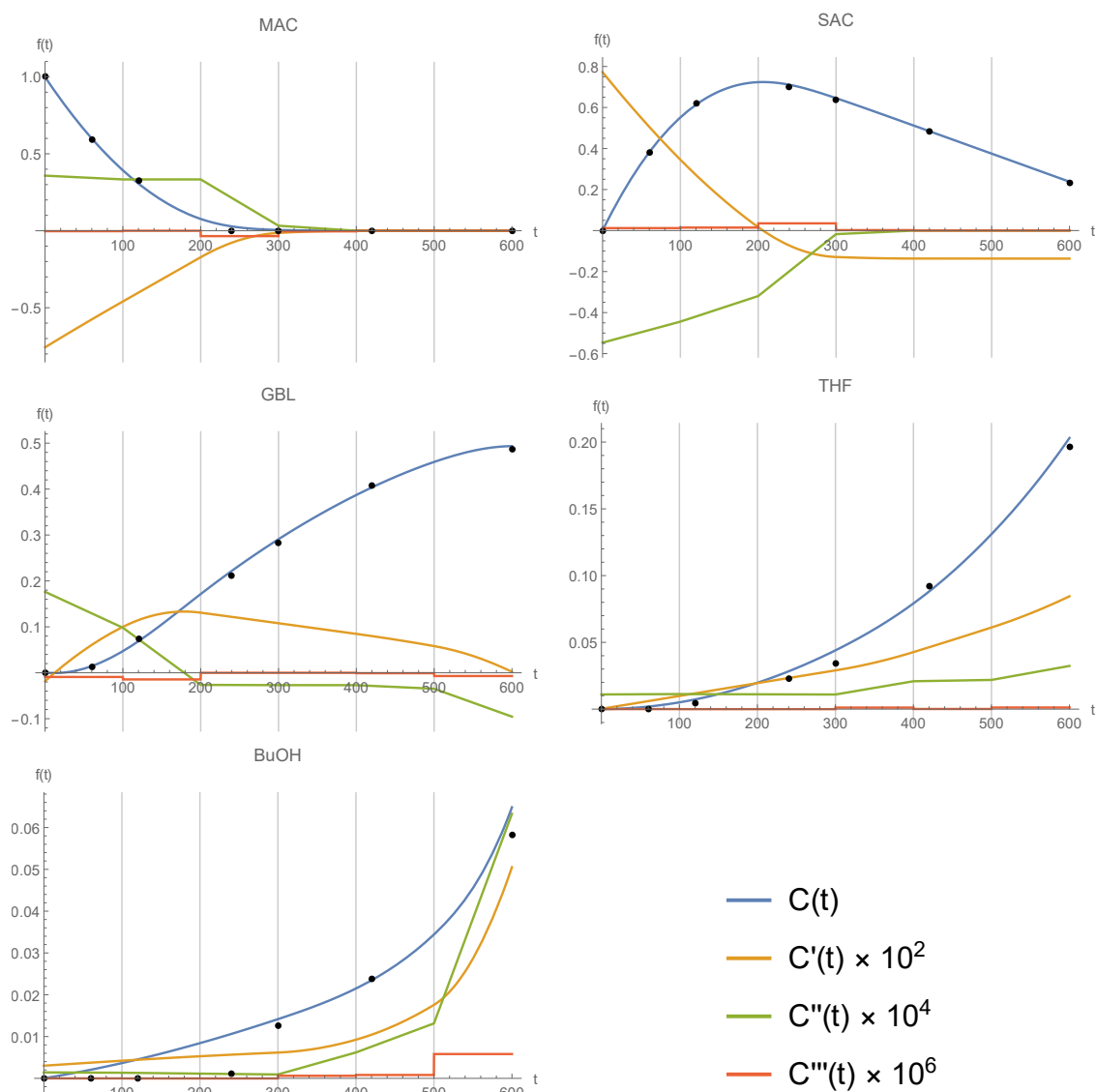


**Figure 11.10** Reconciled data for dataset T1 concerning the MAC case study.

and (iii) the thermodynamics of the reactions. The list of generated chemical reactions is presented in Table 11.9, showing only the observed species. The stoichiometry of this set of chemical reactions spans the data space identified in the previous step. Table 11.10 shows the negative changes of the standard Gibbs free energy at each experimental temperature for each chemical reaction individually, indicating the feasible energetic direction of the respective net reaction flux. For this case study, the amount that contributes to the Gibbs free energy change related to the change in species activities is insignificant when compared to the contribution related to the change in the standard chemical potential of the species. Thus, eq. (7.15) was approximated to

$$\left. \frac{dG}{d\xi_j} \right|_{T,P,\xi_{j'}} \approx \sum_{s \in \text{st}} v_{s,j} \mu_s^0, \quad \forall j \in \text{rx}, j' \neq j$$



**Table 11.9** Target factor analysis. Euclidean norm of the error of stoichiometric vectors projection in the data variant space of dimension four.

$j$	$r_j$	$\ \mathbf{v} - \text{proj}_{\mathbf{S}}\mathbf{v}\  \times 10^{15}$
1	MAC $\rightarrow$ AS	0.631
2	THF $\rightarrow$ BuOH	8.851
3	GBL $\rightarrow$ THF	6.056
4	AS $\rightarrow$ GBL	4.567
5	GBL $\rightarrow$ BuOH	2.901
6	MAC $\rightarrow$ GBL	4.555
7	AS $\rightarrow$ THF	1.741
8	MAC $\rightarrow$ THF	1.749
9	AS $\rightarrow$ BuOH	7.305
10	MAC $\rightarrow$ BuOH	7.296

**Table 11.10** List of stoichiometric balanced chemical reactions with negative standard Gibbs free energy changes at each experimental temperature. Units in  $\text{kJ mol}^{-1}$ .

$j$	$r_j$	$\sum_{s \in \text{est}} \nu_{s,j} \mu_s^0 _{T_1}$	$\sum_{s \in \text{est}} \nu_{s,j} \mu_s^0 _{T_2}$	$\sum_{s \in \text{est}} \nu_{s,j} \mu_s^0 _{T_3}$
1	MAC + H <sub>2</sub> $\rightarrow$ AS	-14.270	-9.132	-3.994
2	THF + H <sub>2</sub> $\rightarrow$ BuOH	-57.330	-55.995	-54.659
3	GBL + H <sub>2</sub> $\rightarrow$ THF + H <sub>2</sub> O	-6.498	-4.887	-3.277
4	AS + 2 H <sub>2</sub> $\rightarrow$ GBL + 2 H <sub>2</sub> O	-48.909	-49.274	-49.639
5	GBL + 3 H <sub>2</sub> $\rightarrow$ BuOH + H <sub>2</sub> O	-63.828	-60.882	-57.936
6	MAC + 3 H <sub>2</sub> $\rightarrow$ GBL + 2 H <sub>2</sub> O	-63.179	-58.406	-53.633
7	AS + 4 H <sub>2</sub> $\rightarrow$ THF + 3 H <sub>2</sub> O	-55.407	-54.161	-52.916
8	MAC + 5 H <sub>2</sub> $\rightarrow$ THF + 3 H <sub>2</sub> O	-69.677	-63.293	-56.910
9	AS + 5 H <sub>2</sub> $\rightarrow$ BuOH + 3 H <sub>2</sub> O	-112.737	-110.156	-107.576
10	MAC + 6 H <sub>2</sub> $\rightarrow$ BuOH + 3 H <sub>2</sub> O	-127.007	-119.288	-111.569

In Step 4, 24 linear reaction networks composed by 4 chemical reactions were generated from the reaction network superstructure in Figure 11.11. Two plausible reaction networks (named S13 and S14) were identified in Step 5, taking into account the three datasets analyzed individually. The S14 network consists of the same structure that was proposed in the literature. The unique difference among S13 and S14 networks is the BuOH precedence: in S13 it is formed from  $r_5$  with GBL as reactant, while in S14 from  $r_2$  with THF as reactant species, see Figure 11.12. It was not possible to elucidate which structure is the real reaction network, as both  $r_2$  and  $r_5$  showed small reaction extents, thus producing residual amounts of BuOH during the three experiments.

However, S13 and S14 were carried out in Step 6 to identify the best kinetic model for this system. Based on the analysis of experimental data and prior knowledge of the literature, LH-type kinetic expressions with one and two active sites in the catalyst were proposed. The algebraic superstructures of these kinetic expressions are shown

in (11.1) and (11.2), where first- and second-order polynomials describe the adsorption phenomenon, respectively.

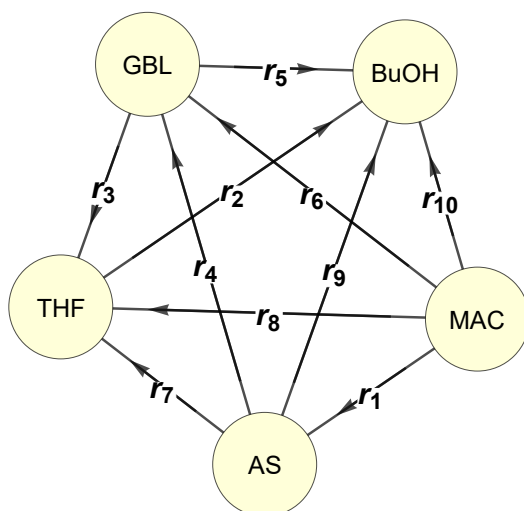


**Figure 11.11** Reaction network superstructure.

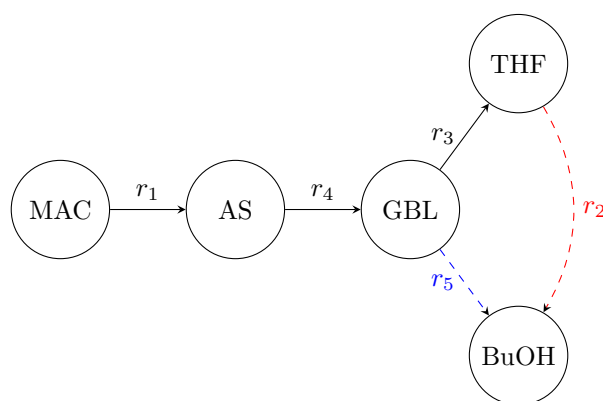


**Figure 11.12** Plausible reaction networks. The reactions  $r_1$ ,  $r_3$  and  $r_4$  belong to both networks,  $r_5$  (blue) to S13 configuring a scheme with parallel pathways and  $r_2$  (red) to S14, a single (in series) pathway. Full arrows: identified chemical reactions. Dashed arrows: plausible reactions that may occur exclusively in the system.

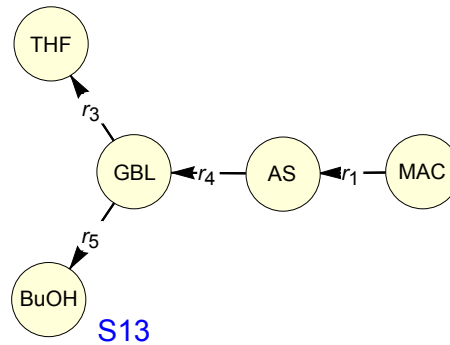
$$r_j = \frac{k'_j C_{\text{reac},j}}{1 + K_{\text{MAC}} \text{MAC} + K_{\text{AS}} \text{AS} + K_{\text{GBL}} \text{GBL} + K_{\text{THF}} \text{THF} + K_{\text{BuOH}} \text{BuOH}}, \quad \forall j \in S \quad (11.1)$$

$$r_j = \frac{k'_j C_{\text{reac},j}}{(1 + K_{\text{MAC}} \text{MAC} + K_{\text{AS}} \text{AS} + K_{\text{GBL}} \text{GBL} + K_{\text{THF}} \text{THF} + K_{\text{BuOH}} \text{BuOH})^2}, \quad \forall j \in S \quad (11.2)$$

The parameter related to hydrogen adsorption  $K_{\text{H}_2}$  is unidentifiable since the  $\text{H}_2$  concentration does not change during the isobaric and isothermal experiment, assuming a gas-liquid equilibrium. Hence,  $\text{H}_2$  contribution in the adsorption phenomenon cannot be evaluated, although equations (11.1) and (11.2) can express this constant term through a simple equation rearrangement.

Multiple response linear regression was considered with all parameters constrained to be positive in the superstructure (11.1). After identified the plausible adsorption terms that remain in the model, parameter estimates without constraints were performed for every potential combination and, BIC values were computed. The same procedures were performed for the nonlinear case when considering the kinetic superstructure (11.2), although with nonlinear regression optimization solvers. These problems were formulated and solved in **Mathematica**® 12.0 software using local and global solvers, such as FindMinimum and NMinimize, respectively. Several optimization methods (stochastic and deterministic) were tested including Interior Point, Newton, Nelder-Mead, Random Search, Simulated Annealing, and Differential Evolution.

Four models have established good tradeoffs between data agreement and number of model parameters. The models associated with (i) reaction network S13 are presented by equations (11.3) and (11.4) in Figure 11.13, and, (ii) reaction network S14, equations (11.5) and (11.6) in Figure 11.14. The four kinetic models presented a single adsorbed species in the catalyst: the initial reactant, even with a different number of active sites on the catalyst. Henceforth the Langmuir-Hinshelwood kinetic models obtained with denominators of 1st and 2nd order will be called LH1 and LH2, respectively. In the following text the four models will be referred as (i) S13LH1, model (11.3); (ii) S13LH2, model (11.4), (iii) S14LH1, model (11.5); and (iv) S14LH2, model (11.6). The acronym SSE, sum (total) of the square error, is used during this section to report the value of the objective function related to the adjustment of the parameters under analysis and, thus, SSE can present different units depending on the adjustment in question.

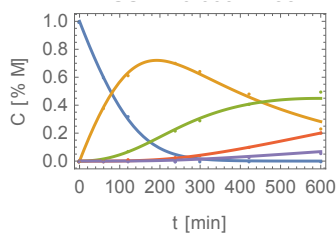


$$\begin{aligned} \frac{d\text{MAC}(t)}{dt} &= -\frac{k_1\text{MAC}(t)}{1 + K_{\text{MAC}}\text{MAC}(t)} \\ \frac{d\text{AS}(t)}{dt} &= \frac{k_1\text{MAC}(t) - k_4\text{AS}(t)}{1 + K_{\text{MAC}}\text{MAC}(t)} \\ \frac{d\text{GBL}(t)}{dt} &= \frac{k_4\text{AS}(t) - (k_3 + k_5)\text{GBL}(t)}{1 + K_{\text{MAC}}\text{MAC}(t)} \end{aligned} \quad (11.3)$$

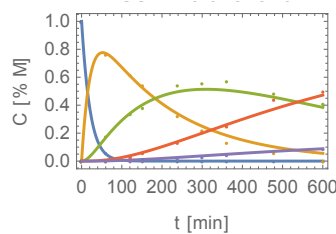
$$\begin{aligned} \frac{d\text{MAC}(t)}{dt} &= -\frac{k_1\text{MAC}(t)}{(1 + K_{\text{MAC}}\text{MAC}(t))^2} \\ \frac{d\text{AS}(t)}{dt} &= \frac{k_1\text{MAC}(t) - k_4\text{AS}(t)}{(1 + K_{\text{MAC}}\text{MAC}(t))^2} \\ \frac{d\text{GBL}(t)}{dt} &= \frac{k_4\text{AS}(t) - (k_3 + k_5)\text{GBL}(t)}{(1 + K_{\text{MAC}}\text{MAC}(t))^2} \end{aligned} \quad (11.4)$$

$$\begin{aligned} \frac{d\text{THF}(t)}{dt} &= \frac{k_3\text{GBL}(t)}{1 + K_{\text{MAC}}\text{MAC}(t)} \\ \frac{d\text{BuOH}(t)}{dt} &= \frac{k_5\text{GBL}(t)}{1 + K_{\text{MAC}}\text{MAC}(t)} \end{aligned}$$

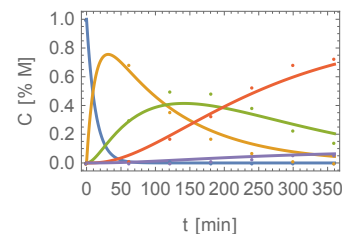
$$\begin{aligned} \frac{d\text{THF}(t)}{dt} &= \frac{k_3\text{GBL}(t)}{(1 + K_{\text{MAC}}\text{MAC}(t))^2} \\ \frac{d\text{BuOH}(t)}{dt} &= \frac{k_5\text{GBL}(t)}{(1 + K_{\text{MAC}}\text{MAC}(t))^2} \end{aligned}$$



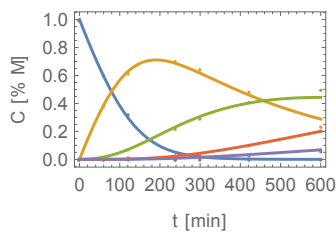
(a) data T1 model (11.3)  
SSE = 0.491



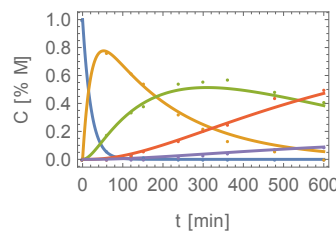
(b) data T2 model (11.3)  
SSE = 2.995



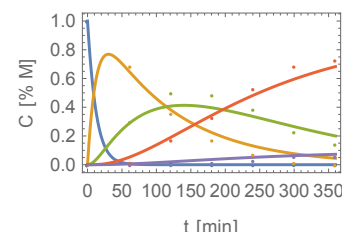
(c) data T3 model (11.3)  
SSE = 5.438



(d) data T1 model (11.4)  
SSE = 0.519

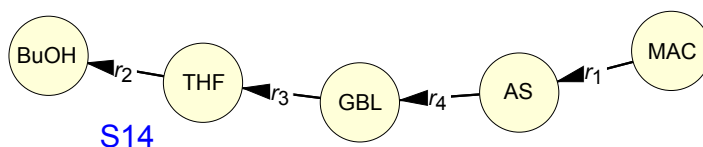


(e) data T2 model (11.4)  
SSE = 2.991



(f) data T3 model (11.4)  
SSE = 6.357

**Figure 11.13** DM results: reaction network S13; models S13LH1 in (11.3) and S13LH2 in (11.4). The plots (a — f) represent the respective simulation of the model with parameters adjusted using DM. SSE  $\times 10^5$  in  $\text{min}^{-2}$  related to the reaction rates adjustment in units of squared molar ratio per time.



$$\begin{aligned}
 \frac{d\text{MAC}(t)}{dt} &= -\frac{k_1\text{MAC}(t)}{1 + K_{\text{MAC}}\text{MAC}(t)} \\
 \frac{d\text{AS}(t)}{dt} &= \frac{k_1\text{MAC}(t) - k_4\text{AS}(t)}{1 + K_{\text{MAC}}\text{MAC}(t)} \\
 \frac{d\text{GBL}(t)}{dt} &= \frac{k_4\text{AS}(t) - k_3\text{GBL}(t)}{1 + K_{\text{MAC}}\text{MAC}(t)} \quad (11.5) \\
 \frac{d\text{THF}(t)}{dt} &= \frac{k_3\text{GBL}(t) - k_2\text{THF}(t)}{1 + K_{\text{MAC}}\text{MAC}(t)} \\
 \frac{d\text{BuOH}(t)}{dt} &= \frac{k_2\text{THF}(t)}{1 + K_{\text{MAC}}\text{MAC}(t)}
 \end{aligned}$$

$$\begin{aligned}
 \frac{d\text{MAC}(t)}{dt} &= -\frac{k_1\text{MAC}(t)}{(1 + K_{\text{MAC}}\text{MAC}(t))^2} \\
 \frac{d\text{AS}(t)}{dt} &= \frac{k_1\text{MAC}(t) - k_4\text{AS}(t)}{(1 + K_{\text{MAC}}\text{MAC}(t))^2} \\
 \frac{d\text{GBL}(t)}{dt} &= \frac{k_4\text{AS}(t) - k_3\text{GBL}(t)}{(1 + K_{\text{MAC}}\text{MAC}(t))^2} \quad (11.6) \\
 \frac{d\text{THF}(t)}{dt} &= \frac{k_3\text{GBL}(t) - k_2\text{THF}(t)}{(1 + K_{\text{MAC}}\text{MAC}(t))^2} \\
 \frac{d\text{BuOH}(t)}{dt} &= \frac{k_2\text{THF}(t)}{(1 + K_{\text{MAC}}\text{MAC}(t))^2}
 \end{aligned}$$

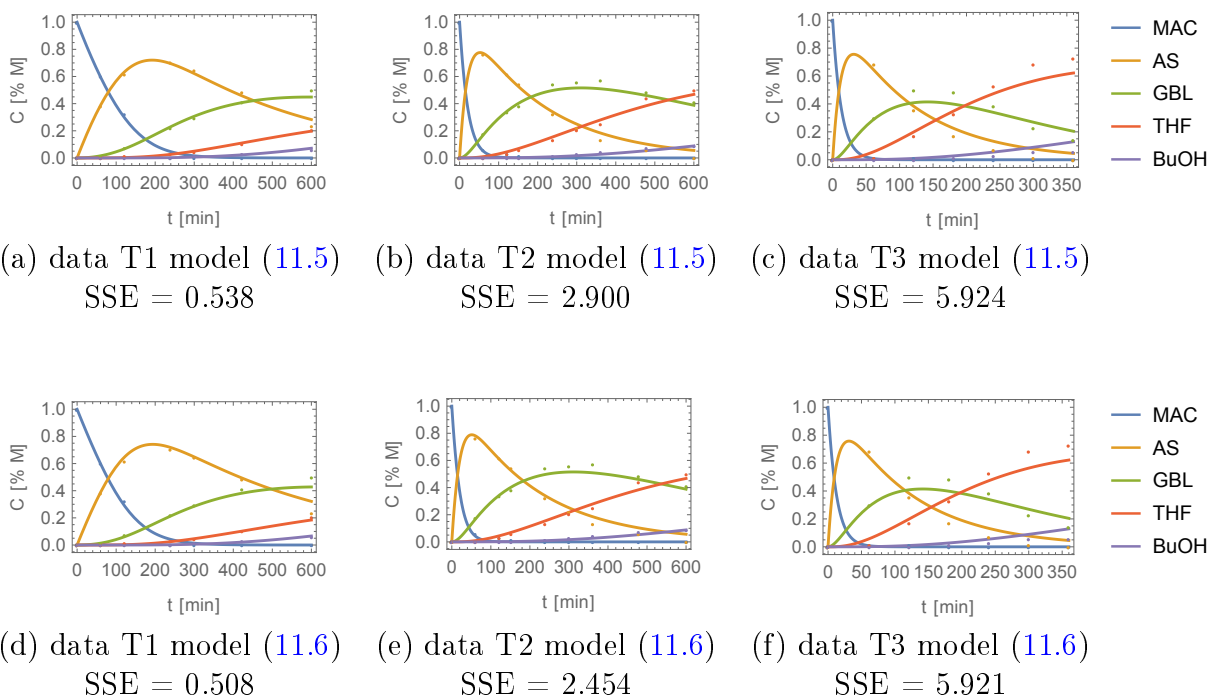


**Figure 11.14** DM results: reaction network S14; models S14LH1 in (11.5) and S14LH2 in (11.6). The plots (a — f) represent the respective simulation of the model with parameters adjusted using DM. SSE  $\times 10^5$  in  $\text{min}^{-2}$  related to the reaction rates adjustment in units of squared molar ratio per time.

All regression procedures so far have been performed by minimizing the SSE between reaction rates based on DM, although model evaluation is done by analyzing the error in the concentration data when simulating the integrated differential models using the fitted

parameters, (see RMSE values at DM columns of Table 11.11). The kinetic expressions LH1 and LH2 presented a similarly satisfactory behavior for both networks S13 and S14, when simulating models with adjusted parameters and evaluating the agreement between the model and the experimental data. Regarding the adjustment performed on the dataset T3, the LH1-type kinetic models converged to 1st order homogeneous kinetics ( $K_{MAC} \approx 0$ ).

Nonlinear regression procedures based on IM, minimization of SSE between model concentration (integrated profiles) and experimental data, were also performed in **Mathematica**® 12.0 software using the same solvers described above and initial parameter estimates given by the optimal solutions obtained with DM. The objective function values are presented in Table 11.11 in comparison with the simulated models from (i) literature, named as Chaudhari (first author), and (ii) DM solutions. The optimal kinetic parameters are presented in Table 11.12 for both DM and IM approaches.

**Table 11.11** Root mean square error (RMSE) in concentration data. Results obtained from DM and IM in comparison with the simulated literature model. Units in rooted mean squared molar ratio, dimensionless.

Model		T1 = 503 K		T2 = 523 K		T3 = 543 K	
		DM	IM	DM	IM	DM	IM
S14	LH1	0.017	0.014	0.027	0.019	0.047	0.029
	LH2	0.022	0.015	0.028	0.019	0.047	0.020
S13	LH1	0.016	0.014	0.027	0.018	0.039	0.028
	LH2	0.018	0.015	0.027	0.018	0.039	0.019
Chaudhari		0.065		0.072		0.042	

**Table 11.12** Optimal kinetic parameters for datasets T1, T2 and T3. DM: differential method and IM: integral method. Units of  $k \times 10^2$  in  $\text{min}^{-1}$  and  $K$  is dimensionless.

Parameters		T1 = 503 K				T2 = 523 K				T3 = 543 K			
		LH1		LH2		LH1		LH2		LH1		LH2	
		DM	IM	DM	IM	DM	IM	DM	IM	DM	IM	DM	IM
S14	$k_1$	1.884	2.254	1.921	2.105	5.081	5.619	5.571	5.595	7.797	5.764	7.908	11.194
	$k_2$	0.176	0.157	0.175	0.152	0.067	0.060	0.067	0.060	0.111	0.039	0.111	0.050
	$k_3$	0.175	0.161	0.173	0.156	0.229	0.218	0.229	0.218	0.688	0.656	0.688	0.688
	$k_4$	0.273	0.284	0.243	0.274	0.501	0.583	0.498	0.581	0.893	1.083	0.893	1.298
	$K_{MAC}$	1.519	2.244	0.636	0.780	0.098	1.000	0.102	0.439	-	-	0.007	1.067
S13	$k_1$	1.888	2.251	1.724	2.105	5.080	5.612	5.092	5.588	7.797	5.809	8.616	11.502
	$k_3$	0.131	0.126	0.131	0.123	0.195	0.193	0.195	0.193	0.629	0.623	0.630	0.645
	$k_4$	0.274	0.284	0.266	0.275	0.501	0.584	0.501	0.583	0.893	1.088	0.897	1.303
	$k_5$	0.044	0.035	0.044	0.035	0.037	0.027	0.037	0.027	0.058	0.040	0.067	0.048
	$K_{MAC}$	1.526	2.238	0.525	0.779	0.098	0.986	0.049	0.433	-	-	0.053	1.089

The IM results show a better data agreement when compared to the DM results, see Table 11.11. This is an expected result since the regression procedure in DM is done with reaction rates, establishing an indirect adjustment of the concentration, while in IM, the

adjustment is performed directly on the concentration measurements. In addition, notice that the former method is biased once the reaction rates are computed from concentration derivatives estimates, while the latter is bias-free. However, the better fit performance in IM does not exclude the need of using DM at all, once the information related to concentration derivatives enables the finding of model structures: reaction network (Step 5) and kinetic expressions (Step 6 initial phase).

The simulations of the models using the optimal parameters obtained through the IM are presented in Figure 11.15. In this figure, similarly to the DM results, the LH1 and LH2 kinetic models do not show significant differences, *i.e.*, the species concentration profiles of the LH1 and LH2 kinetic models respecting the same network are overlapped in all plots, except for the profile of BuOH in the dataset T3. The same result of overlapping profiles is presented when comparing the concentration profiles of networks S13 and S14 with the exception of the BuOH profiles where a notable difference can be observed. This difference happens due to BuOH's origin, where in S13 it is produced from GBL reactant in  $r_5$ , while in S14 network from THF reactant in  $r_2$  chemical reaction. However, note that the concentration of BuOH is much lower (residual) than the other species and therefore the difference between the experimental data and the simulated model profiles does not affect, to the same extent as the other species, the value of the objective function. In addition, in each plot of this figure, the difference between the profiles of the optimal models and the literature model (Chaudhari's model) is evident, where the literature model presented the worst data agreement.

Therefore, it is clear that the common reaction rates in S13 and S14 ( $r_1$ ,  $r_3$  and  $r_4$ ) assume the same value over time, even with the different kinetic expressions of LH1 and LH2 models. To understand the cause of the similar behavior presented by the LH1 and LH2 models, an additional analysis was performed comparing their adsorption terms (denominators). In Figure 11.16 the adsorption terms were plotted as a function of MAC concentration. For LH1-type models, the adsorption terms assume a straight line, where  $K_{\text{MAC}}$  is its slope, while in LH2-type models the  $K_{\text{MAC}}$  is the slope of the squared root of the respective response profile. In Figure 11.16(a) the profiles respecting S14LH1 and S14LH2 are overlapped by S13LH1 and S13LH2, respectively, and in (c) only LH2-type models are presented since for data T3 the models LH1-type converged to homogeneous models (with no adsorption term). From this figure, it can be seen that both LH1- and LH2-type models presented similar straight line profiles, and therefore, the adsorption phenomenon occurs in the same extent for every model. Since the denominators are pretty the same, the numerators are idem in every reaction rate. As long as the initial reagent is present in the reaction mixture the adsorption term influences every chemical reaction in both networks with LH1 and LH2 kinetics, in such a way that this influence is greater in  $r_1 > r_4 > r_3$ . Therefore, there is enough freedom for the quadratic parcel in the denominator of the LH2-type model to converge approximately to a linear parcel in the denominator of the LH1-type model. This means that both models LH1 and LH2 are indiscriminating, or indifferent, since they produce almost the same response.

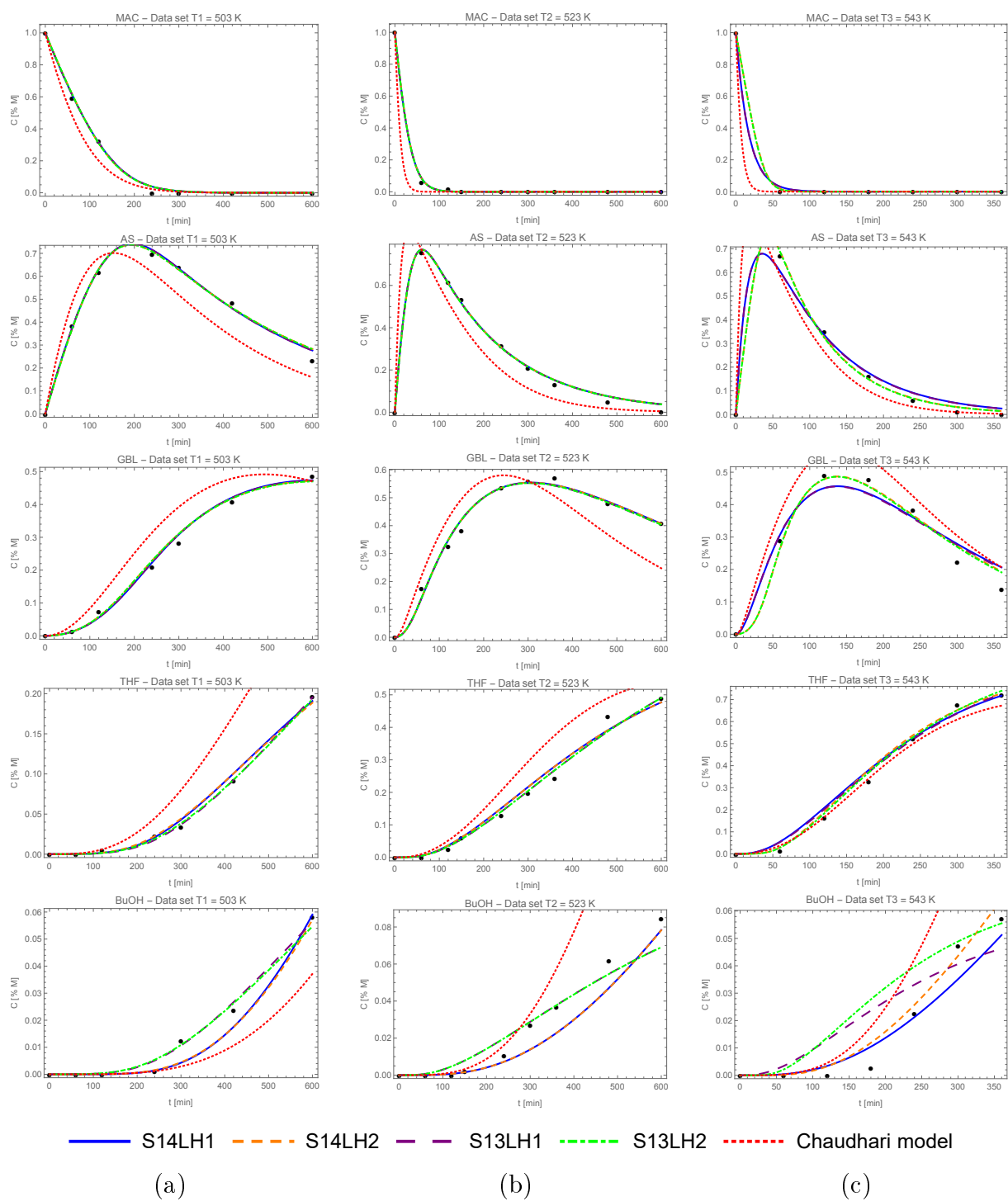


**Figure 11.15** IM results. Experimental data shown by black dots. Comparison of individual species concentration profiles from S13LH1, S13LH2, S14LH1, S14LH2 and literature model. Simulation of models for (a) Data T1; (b) Data T2 and (c) Data T3.



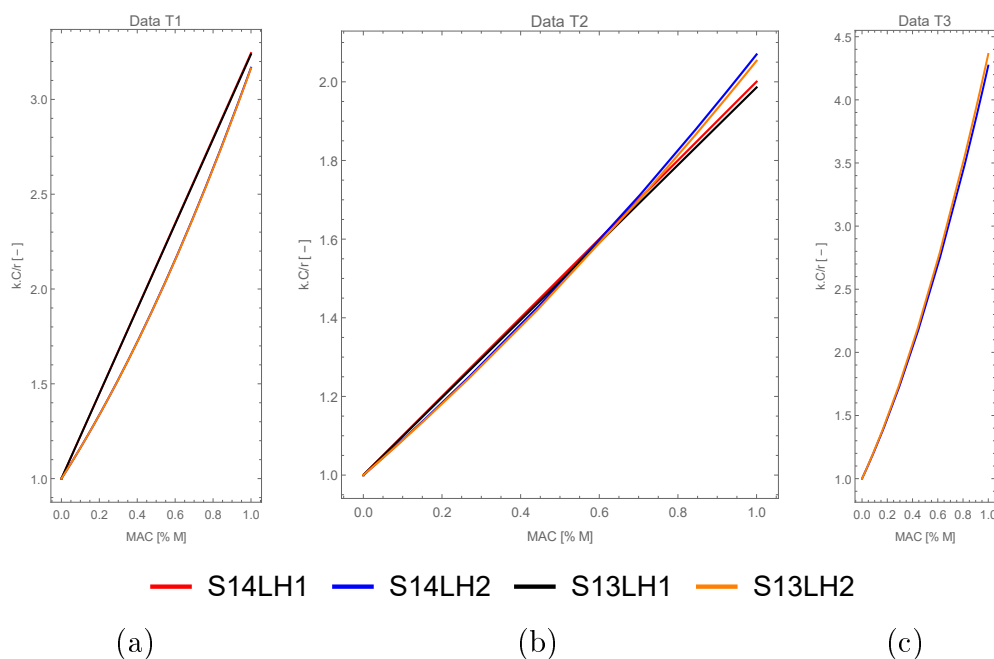


**Figure 11.16** Comparison of reaction kinetic adsorption terms as a function of the initial reactant concentration for S13LH1, S13LH2, S14LH1 and S14LH2 model in (a) dataset T1, (b) dataset T2 and (c) dataset T3.

### 11.2.2 Parameter correlation with temperature

Since there are three sets of data available with different temperatures, it is possible to study the dependence of the parameters on temperature. We hope that based on the correlation found it will be possible to discriminate the candidate models, identifying which one is the true one. Both methods described in Steps 6.6 and 6.7 of Chapter 10 were considered for this case study. During Step 6.6, the natural log of  $k = f(T)$  and  $K = f(T)$  were considered using eqs. (10.2) and (10.3), respectively, to obtain their linear dependence with the inverse of the temperature. The results obtained are presented in Table 11.13 and Figure 11.17.

In Table 11.13, the parameters  $A_0$  related to the reactions  $r_2$  and  $r_5$  (those that produce BuOH) assume approximately null values, with no physical meaning. The estimation of these parameters may lead to problematic solver convergence and stiffness issues in the next full nonlinear regression procedure. Also, many line slopes presented negative values which do not confer realistic results for  $E_a$  parameters. Therefore, regarding the available experimental data for this case study, the proposed linear method of Step 6.6 did not run well, presenting unreliable parameter estimates. First of all, three points for adjusting two variables consists of a very bad regression situation, since the number of points for model regression is very small. Second, no significant variation of  $\ln(k) = f(1/T)$  could be observed in these profiles, suggesting that perhaps for this case study it would be necessary to carry out experiments with a wider range of temperatures to observe that kinetic parameter dependence with experimental temperature. And finally, the regression

**Table 11.13** Parameter values from linear regression. Results concerning the models: (a) S14LH1, (b) S14LH2, (c) S13LH1 and (d) S13LH2; from top to bottom. Parameters  $k \times 10^4$  and  $A_0 \times 10^5$  values in  $\text{min}^{-1} \text{m}^6 \text{kg}^{-1} \text{kmol}^{-1}$ ,  $E_a$  and  $\Delta H$  in  $\text{kJ mol}^{-1}$ ,  $\Delta S$  in  $\text{J mol}^{-1} \text{K}^{-1}$ , and  $K_{\text{MAC}}$  is dimensionless.

	$k_1$	$k_2$	$k_3$	$k_4$	$k_5$	$K_{\text{MAC}}$	
(a)	$T_1$	3.731	0.261	0.266	0.470	-	2.244
	$T_2$	5.248	0.056	0.204	0.544	-	1.000
	$T_3$	2.399	0.016	0.273	0.451	-	-
	$A_0$	0.136	0.000	3.200	2.978	-	-
	$E_a$	-24.238	-157.043	1.152	-2.132	-	-
	$\Delta S$	-	-	-	-	-	-168.962
	$\Delta H$	-	-	-	-	-	-88.369
	(b)	$T_1$	3.486	0.251	0.259	0.454	-
$T_2$		5.225	0.056	0.204	0.543	-	0.439
$T_3$		4.659	0.021	0.286	0.540	-	1.067
$A_0$		2121.750	0.000	8.255	51.006	-	-
$E_a$		16.842	-141.910	5.239	9.997	-	-
$\Delta S$		-	-	-	-	-	29.204
$\Delta H$		-	-	-	-	-	16.719
(c)		$T_1$	3.726	-	0.208	0.470	0.060
	$T_2$	5.241	-	0.181	0.546	0.025	0.986
	$T_3$	2.418	-	0.259	0.453	0.017	-
	$A_0$	0.153	-	34.962	3.153	0.000	-
	$E_a$	-23.733	-	12.144	-1.899	-73.426	-
	$\Delta S$	-	-	-	-	-	-171.529
	$\Delta H$	-	-	-	-	-	-89.647
	(d)	$T_1$	3.485	-	0.204	0.455	0.058
$T_2$		5.219	-	0.180	0.545	0.025	0.433
$T_3$		4.788	-	0.269	0.543	0.020	1.089
$A_0$		3050.170	-	73.085	53.389	0.000	-
$E_a$		18.381	-	15.327	10.182	-60.039	-
$\Delta S$		-	-	-	-	-	31.531
$\Delta H$		-	-	-	-	-	17.925

points did not form a linear trend, showing very close and misaligned values. In conclusion, this method was not able to discriminate between the four candidate models, since the results obtained are not realistic, so we were unable to interpret the results. But even so, the nonlinear correlation of the parameters with the temperature must be considered, because in this case the regression is performed with more data, and therefore a better performance of the method is expected.

During Step 6.7, the nonlinear regression procedure is considered by minimizing the SSE

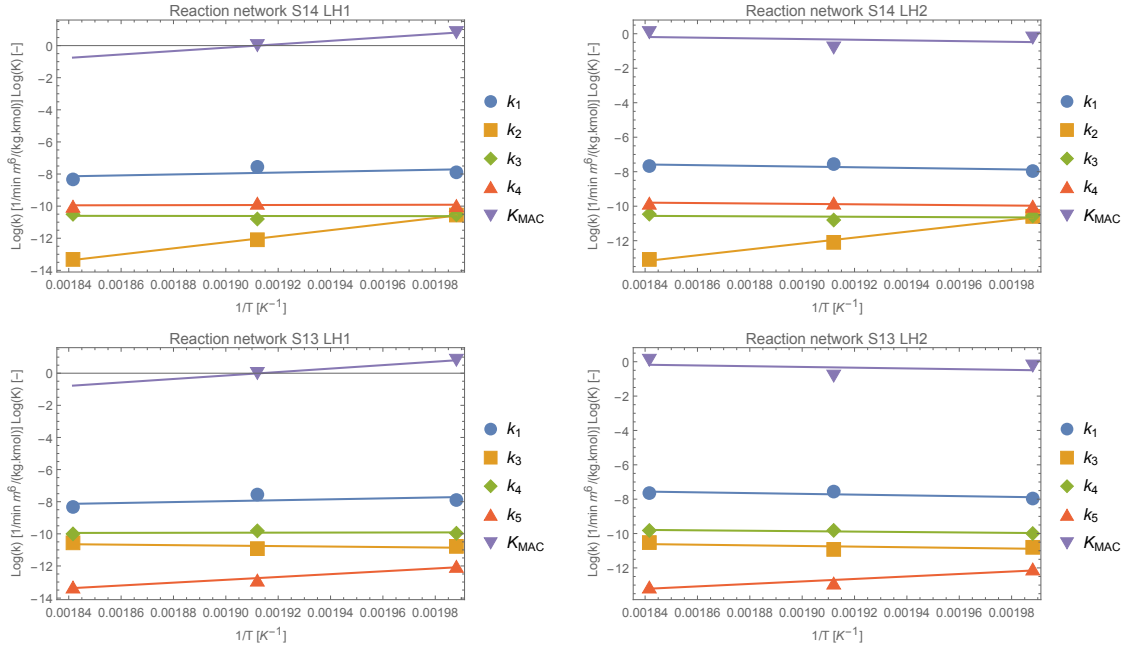


**Figure 11.17** Linear regression results for Arrhenius and van't Hoff parameters tuning. Since the models LH1 converged to homogeneous kinetics at temperature  $T_3$ , there is no experimental point for the adsorption term  $1/T_3$ .

in concentration data concerning the three datasets simultaneously. The reparametrization of kinetic parameters  $k$  and  $K$  (adsorption kinetics) presented in (10.4) and (10.6), respectively, was adopted for this case study. The reparameterized species mass balances assume the generic format as shown in eqs. (11.7) and (11.8), where  $w$  represents the catalyst mass concentration,  $c_{\text{reac},j}(t)$  the reactant species concentration of the respective chemical reaction  $j \in \text{rx}$ ,  $v_{s,j}$  the stoichiometric coefficient of species  $s \in \text{sp}$  in the reaction  $j \in \text{rx}$ ,  $T$  the experimental temperature,  $H_2(T)$  the hydrogen concentration in liquid phase computed using Henry's law for every experimental temperature, and  $T_{\text{ref}}$  the reference temperature, 523 K.

$$\frac{dc_s(t)}{dt} = wH_2(T) \sum_{j \in \text{rx}} v_{s,j} \frac{\exp\left(\alpha_j - \frac{\beta_j 10^4}{R} \left(\frac{1}{T} - \frac{1}{T_{\text{ref}}}\right)\right) c_{\text{reac},j}(t)}{1 + \exp\left(\frac{\phi 10^2}{R} - \frac{\theta 10^5}{R} \left(\frac{1}{T} - \frac{1}{T_{\text{ref}}}\right)\right) \text{MAC}(t)} \quad \forall s \in \text{sp} \quad (11.7)$$

$$\frac{dc_s(t)}{dt} = wH_2(T) \sum_{j \in \text{rx}} v_{s,j} \frac{\exp\left(\alpha_j - \frac{\beta_j 10^4}{R} \left(\frac{1}{T} - \frac{1}{T_{\text{ref}}}\right)\right) c_{\text{reac},j}(t)}{\left(1 + \exp\left(\frac{\phi 10^2}{R} - \frac{\theta 10^5}{R} \left(\frac{1}{T} - \frac{1}{T_{\text{ref}}}\right)\right) \text{MAC}(t)\right)^2} \quad \forall s \in \text{sp} \quad (11.8)$$

Thus, for each model LH1-type (S13LH1 and S14LH1) a system of ODEs is established

from (11.7), as the same for each LH2-type (S13LH2 and S14LH2) from (11.8). For example, the ODEs respecting the S13LH1 model is represented in (11.9).

$$\begin{aligned}
\frac{d\text{MAC}(t)}{dt} &= -\frac{w\text{H}_2(T) \exp\left(\alpha_1 - \frac{\beta_1 10^4}{R} \left(\frac{1}{T} - \frac{1}{T_{\text{ref}}}\right)\right) \text{MAC}(t)}{1 + \exp\left(\frac{\phi 10^2}{R} - \frac{\theta 10^5}{R} \left(\frac{1}{T} - \frac{1}{T_{\text{ref}}}\right)\right) \text{MAC}(t)} \\
\frac{d\text{AS}(t)}{dt} &= w\text{H}_2(T) \frac{\exp\left(\alpha_1 - \frac{\beta_1 10^4}{R} \left(\frac{1}{T} - \frac{1}{T_{\text{ref}}}\right)\right) \text{MAC}(t) - \exp\left(\alpha_4 - \frac{\beta_4 10^4}{R} \left(\frac{1}{T} - \frac{1}{T_{\text{ref}}}\right)\right) \text{AS}(t)}{1 + \exp\left(\frac{\phi 10^2}{R} - \frac{\theta 10^5}{R} \left(\frac{1}{T} - \frac{1}{T_{\text{ref}}}\right)\right) \text{MAC}(t)} \\
\frac{d\text{GBL}(t)}{dt} &= w\text{H}_2(T) \frac{\exp\left(\alpha_4 - \frac{\beta_4 10^4}{R} \left(\frac{1}{T} - \frac{1}{T_{\text{ref}}}\right)\right) \text{AS}(t) - \exp\left(\alpha_3 - \frac{\beta_3 10^4}{R} \left(\frac{1}{T} - \frac{1}{T_{\text{ref}}}\right)\right) \text{GBL}(t) - \exp\left(\alpha_5 - \frac{\beta_5 10^4}{R} \left(\frac{1}{T} - \frac{1}{T_{\text{ref}}}\right)\right) \text{GBL}(t)}{1 + \exp\left(\frac{\phi 10^2}{R} - \frac{\theta 10^5}{R} \left(\frac{1}{T} - \frac{1}{T_{\text{ref}}}\right)\right) \text{MAC}(t)} \\
\frac{d\text{THF}(t)}{dt} &= \frac{w\text{H}_2(T) \exp\left(\alpha_3 - \frac{\beta_3 10^4}{R} \left(\frac{1}{T} - \frac{1}{T_{\text{ref}}}\right)\right) \text{GBL}(t)}{1 + \exp\left(\frac{\phi 10^2}{R} - \frac{\theta 10^5}{R} \left(\frac{1}{T} - \frac{1}{T_{\text{ref}}}\right)\right) \text{MAC}(t)} \\
\frac{d\text{BuOH}(t)}{dt} &= \frac{w\text{H}_2(T) \exp\left(\alpha_5 - \frac{\beta_5 10^4}{R} \left(\frac{1}{T} - \frac{1}{T_{\text{ref}}}\right)\right) \text{GBL}(t)}{1 + \exp\left(\frac{\phi 10^2}{R} - \frac{\theta 10^5}{R} \left(\frac{1}{T} - \frac{1}{T_{\text{ref}}}\right)\right) \text{MAC}(t)}
\end{aligned} \tag{11.9}$$

The four problems were solved in **Mathematica**® 12.0, using the function `NonlinearModelFit`. Parameter initial guesses were considered through the logarithm of the optimal values of  $k$  at the reference temperature,  $T_{\text{ref}} = T_2 = 523$  K reported in Table 11.13. The CPU usage and the objective function value in each regression problem is presented in Table 11.14. Tables 11.15 to 11.18 present the adjusted parameters with its confidence intervals and  $p$ -values concerning the models S13LH1, S14LH1, S14LH1 and S14LH2, respectively. The respective model simulations are presented in Figures 11.18 to 11.21.

**Table 11.14** CPU usage and objective function value, SSE, in squared molar concentration ratio, dimensionless.

	S13LH1	S14LH1	S13LH2	S14LH2
CPU [s]	68	252	527	1345
SSE [-]	0.084	0.093	0.143	0.083

When analyzing the obtained results related to LH1 models for both S13 and S14 networks (Tables 11.15 and 11.16), it is observed that  $\beta$  estimates presented poor confidence intervals and  $p$ -values (nonsignificant statistical test), presenting high uncertainty about their converging values, with the exception of  $\beta_3$  concerning the chemical reaction  $\text{GBL} \rightarrow \text{THF}$ . In contrast, the estimates referring to  $\alpha$  have presented opposite statistical metrics, presenting good confidence intervals and significant  $p$ -values. Also, it can be observed that  $k_{T_{\text{ref}}}$  (from all reactions) have approximately converged to the values that we had obtained in the differential method, confirming that we already had a good estimate of these parameters without assessing their correlation with temperature. When considering

**Table 11.15** Optimal parameter values for S13LH1 model. CI: Confidence intervals,  $k(T_{\text{ref}})$  and  $A_0$  in  $\text{m}^6 \text{kg}^{-1} \text{kmol}^{-1} \text{min}^{-1}$ ,  $E_a$  and  $\Delta H$  in  $\text{kJ mol}^{-1}$ , and  $\Delta S$  in  $\text{J mol}^{-1} \text{K}^{-1}$ .  $p$ -values:  $\alpha_1 \approx 0$ ,  $\beta_1 \approx 1$ ,  $\alpha_3 \approx 0$ ,  $\beta_3 \approx 0$ ,  $\alpha_4 \approx 0$ ,  $\beta_4 \approx 1$ ,  $\alpha_5 \approx 0$ ,  $\beta_5 \approx 1$ ,  $\theta = 0.105$  and  $\phi = 0.302$ .

$k_j$	$\alpha$	CI	$\beta \times 10^2$	CI	$k(T_{\text{ref}}) \times 10^5$	$A_0 \times 10^5$	$E_a \times 10$
$k_1$	-7.854	(-8.105,-7.602)	0.010	(-3.693,3.693)	38.837	38.845	0.010
$k_3$	-10.845	(-10.917,-10.773)	245.207	(1.360,3.544)	1.950	548.524	245.207
$k_4$	-9.954	(-10.010,-9.898)	0.003	(-0.719,0.719)	4.753	4.753	0.003
$k_5$	-13.099	(-13.626,-12.572)	0.025	(-7.757,7.757)	0.205	0.205	0.025
	$\theta$	CI	$\phi$	CI	$\Delta H$	$\Delta S$	
$K_{\text{MAC}}$	-2.999	(-6.639,0.639)	-0.154	(-0.449,0.141)	-299.990	-589.005	

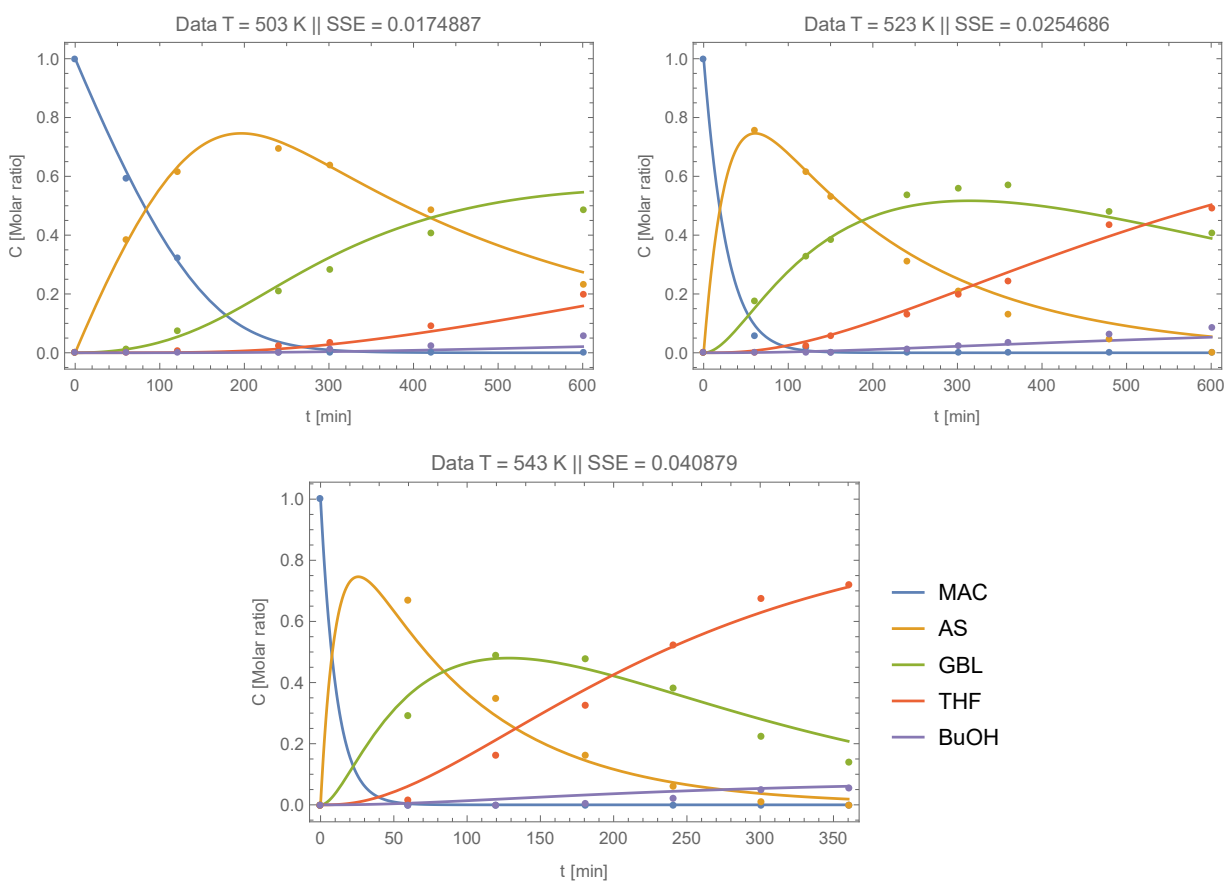


**Figure 11.18** S13LH1 model simulation.

**Table 11.16** Optimal parameter values for S14LH1 model. CI: Confidence intervals,  $k(T_{\text{ref}})$  and  $A_0$  in  $\text{m}^6 \text{kg}^{-1} \text{kmol}^{-1} \text{min}^{-1}$ ,  $E_a$  and  $\Delta H$  in  $\text{kJ mol}^{-1}$ , and  $\Delta S$  in  $\text{J mol}^{-1} \text{K}^{-1}$ .  $p$ -values:  $\alpha_1 \approx 0$ ,  $\beta_1 \approx 1$ ,  $\alpha_2 \approx 0$ ,  $\beta_2 \approx 1$ ,  $\alpha_3 \approx 0$ ,  $\beta_3 \approx 0$ ,  $\alpha_4 \approx 0$ ,  $\beta_4 \approx 1$ ,  $\theta = 0.123$  and  $\phi = 0.325$ .

$k_j$	$\alpha$	CI	$\beta \times 10^2$	CI	$k(T_{\text{ref}}) \times 10^5$	$A_0 \times 10^5$	$E_a \times 10$
$k_1$	-7.857	(-8.120,-7.594)	0.010	(-3.871,3.872)	38.706	38.715	0.010
$k_2$	-13.021	(-14.226,-11.817)	0.029	(-15.366,15.366)	0.221	0.221	0.029
$k_3$	-10.778	(-10.856,-10.699)	244.773	(1.262,3.634)	2.086	580.816	244.773
$k_4$	-9.963	(-10.021,-9.905)	0.004	(-0.745,0.745)	4.709	4.710	0.004
	$\theta$	CI	$\phi$	CI	$\Delta H$	$\Delta S$	
$K_{\text{MAC}}$	-2.999	(-6.830,0.830)	-0.155	(-0.465,0.156)	-299.990	-589.053	

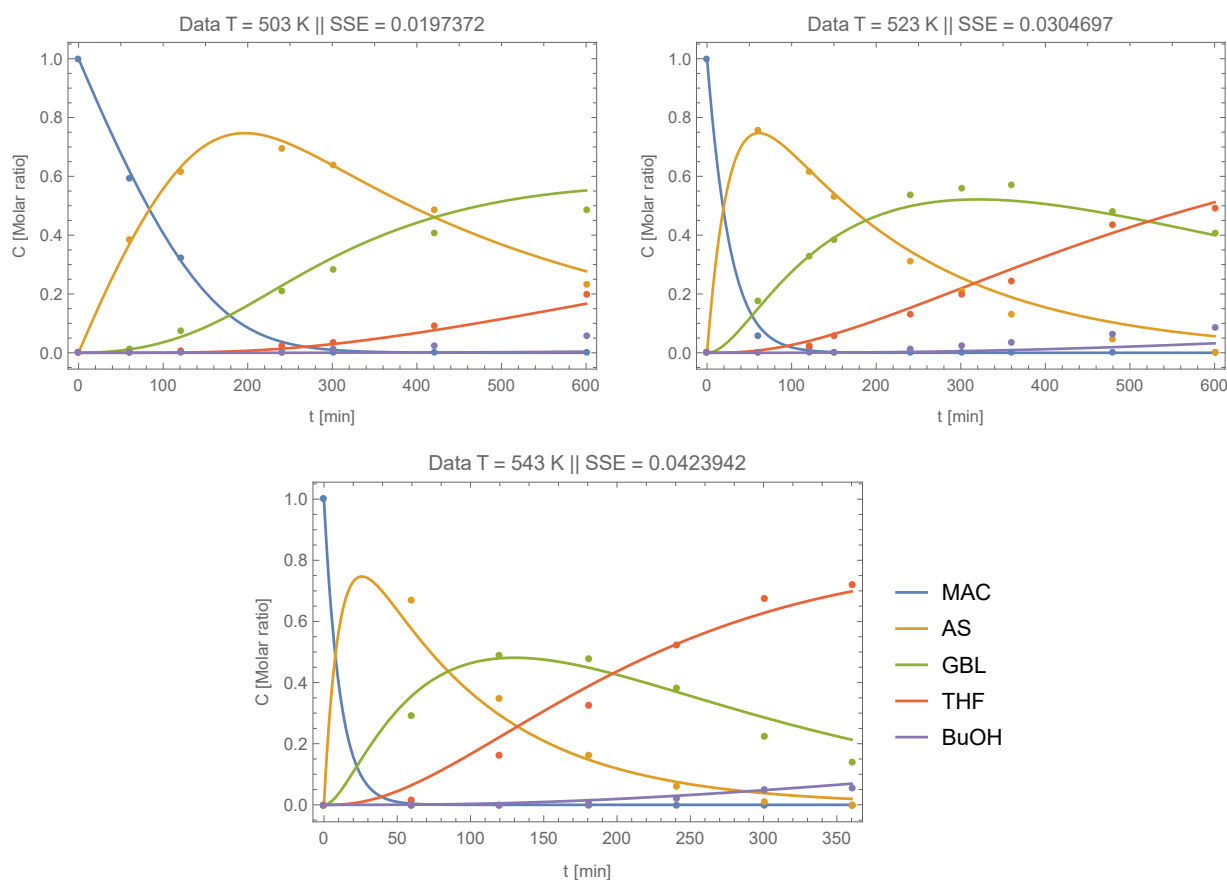


**Figure 11.19** S14LH1 model simulation.

**Table 11.17** Optimal parameter values for S13LH2 model. CI: Confidence intervals,  $k(T_{\text{ref}})$  and  $A_0$  in  $\text{m}^6 \text{kg}^{-1} \text{kmol}^{-1} \text{min}^{-1}$ ,  $E_a$  and  $\Delta H$  in  $\text{kJ mol}^{-1}$ , and  $\Delta S$  in  $\text{J mol}^{-1} \text{K}^{-1}$ .  $p$ -values:  $\alpha_1 \approx 0$ ,  $\beta_1 \approx 0$ ,  $\alpha_3 \approx 0$ ,  $\beta_3 = 0.0004$ ,  $\alpha_4 \approx 0$ ,  $\beta_4 = 0.1511$ ,  $\alpha_5 \approx 0$ ,  $\beta_5 \approx 1$ ,  $\theta = -$  and  $\phi = -$ .

$k_j$	$\alpha$	CI	$\beta$	CI	$k(T_{\text{ref}}) \times 10^5$	$A_0 \times 10^5$	$E_a$
$k_1$	-7.800	(-8.088,-7.512)	9.863	(6.545,13.181)	40.956	$2.90 \times 10^{11}$	98.632
$k_3$	-10.863	(-10.955,-10.772)	2.486	(1.135,3.838)	1.915	582.715	24.863
$k_4$	-10.043	(-10.097,-9.988)	0.567	(-0.211,1.344)	4.350	16.006	5.666
$k_5$	-13.178	(-13.904,-12.451)	0.000	(-10.552,10.552)	0.189	0.189	0.000
	$\theta$	CI	$\phi$	CI	$\Delta H$	$\Delta S$	
$K_{\text{MAC}}$	-0.450	(-0.451,-0.450)	-2.248	(-2.249,-2.248)	-45.040	-310.946	

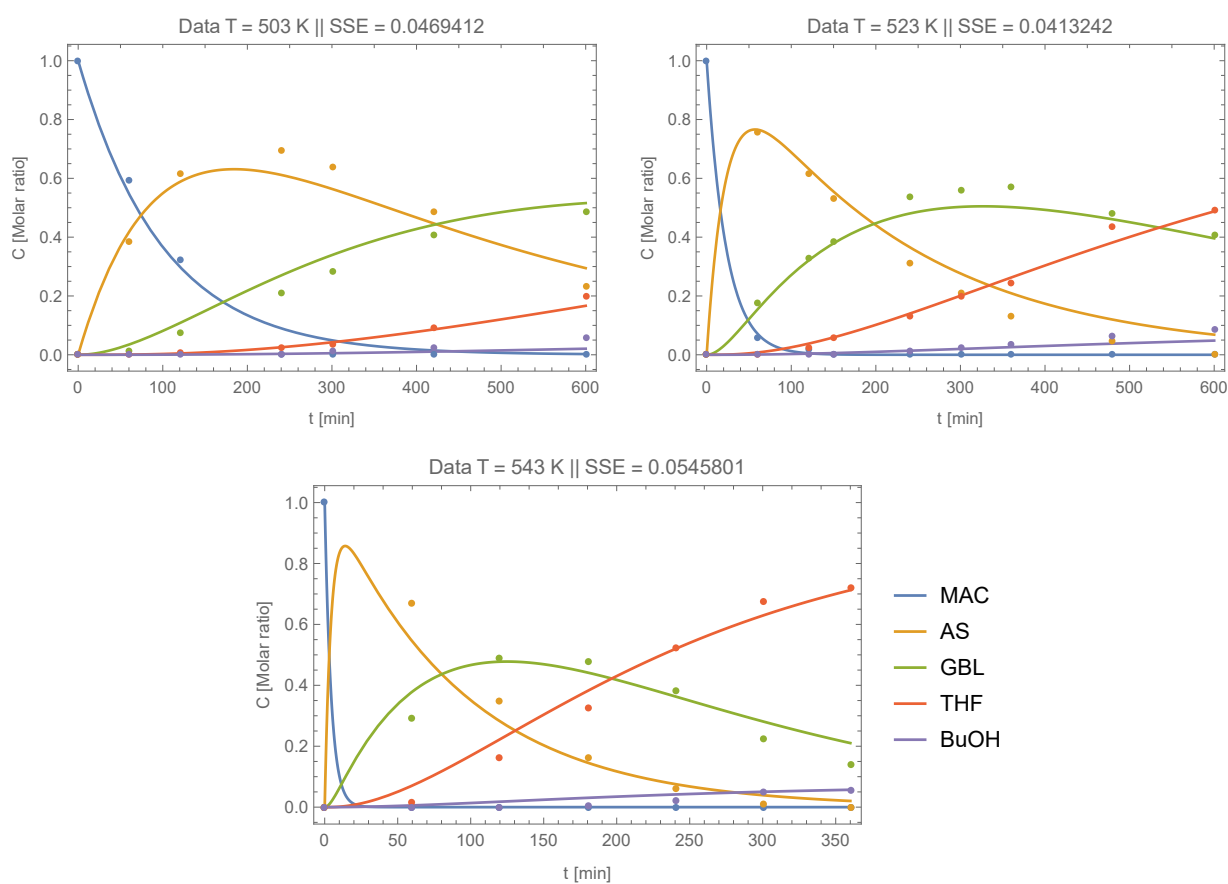


**Figure 11.20** S13LH2 model simulation.

**Table 11.18** Optimal parameter values for S14LH2 model. CI: Confidence intervals,  $k(T_{\text{ref}})$  and  $A_0$  in  $\text{m}^6 \text{kg}^{-1} \text{kmol}^{-1} \text{min}^{-1}$ ,  $E_a$  and  $\Delta H$  in  $\text{kJ mol}^{-1}$ , and  $\Delta S$  in  $\text{J mol}^{-1} \text{K}^{-1}$ .  $p$ -values:  $\alpha_1 \approx 0$ ,  $\beta_1 \approx 0$ ,  $\alpha_2 \approx 0$ ,  $\beta_2 \approx 1$ ,  $\alpha_3 \approx 0$ ,  $\beta_3 \approx 0$ ,  $\alpha_4 \approx 0$ ,  $\beta_4 \approx 0$ ,  $\theta \approx 0$  and  $\phi = 0.342$ .

$k_j$	$\alpha$	CI	$\beta$	CI	$k(T_{\text{ref}}) \times 10^5$	$A_0$	$E_a$
$k_1$	-7.289	(-7.654,-6.924)	14.321	(11.068,17.574)	68.307	$1.37 \times 10^{11}$	143.210
$k_2$	-12.782	(-13.692,-11.872)	0.000	(-11.611,11.611)	0.281	$2.81 \times 10^{-6}$	0.000
$k_3$	-10.773	(-10.847,-10.699)	3.410	(2.286,4.534)	2.096	0.053	34.101
$k_4$	-9.896	(-9.956,-9.835)	2.541	(1.777,3.306)	5.040	0.017	25.415
	$\theta$	CI	$\phi$	CI	$\Delta H$	$\Delta S$	
$K_{\text{MAC}}$	2.169	(1.714,2.624)	-0.028	(-0.085,0.030)	216.923	412.012	

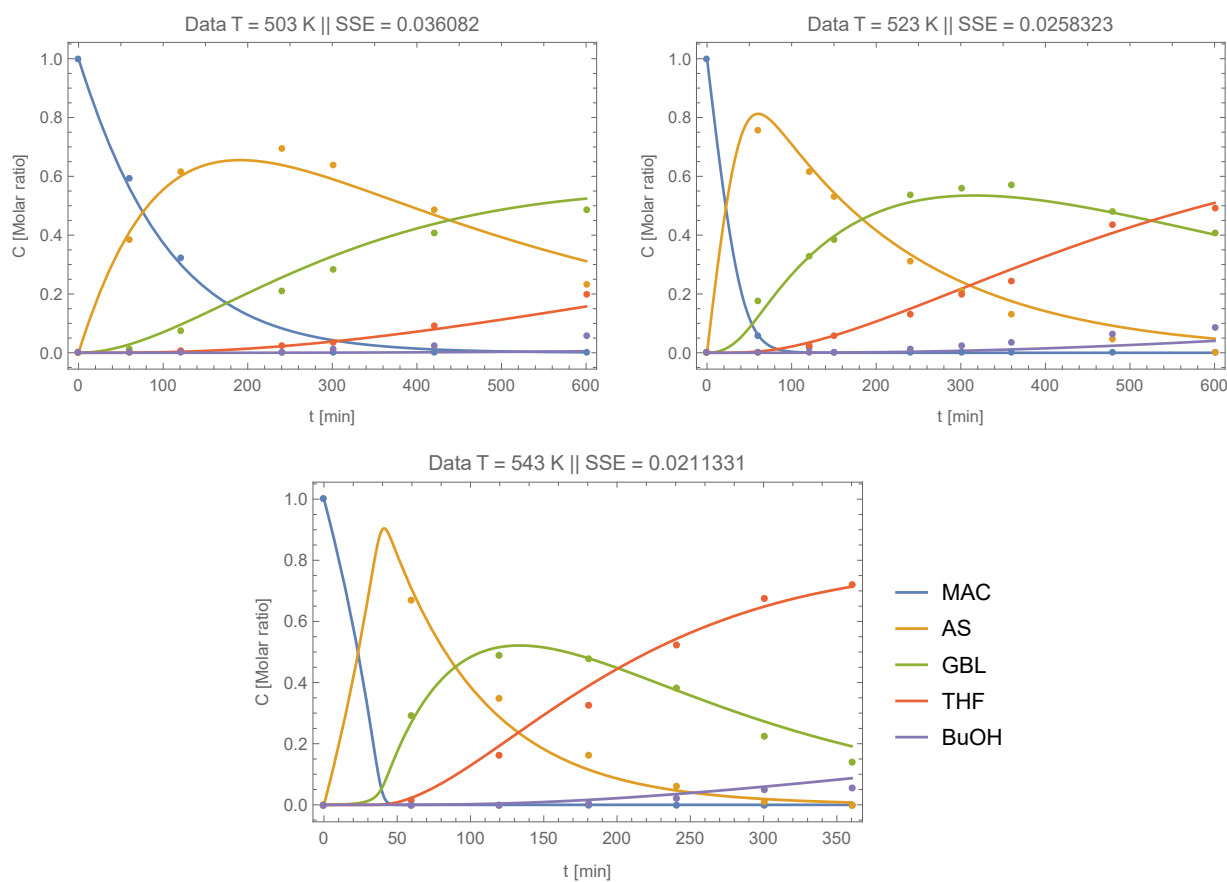


**Figure 11.21** S14LH2 model simulation.



the parameters associated with the adsorption phenomena,  $\theta$  and  $\phi$  presented reasonable confidence intervals and  $p$ -values inferior than 0.35, although  $\theta$  tended to converge to its lower bound (equivalent to an adsorption reaction enthalpy of  $-300 \text{ kJ mol}^{-1}$ ).

When assessing the results obtained for LH2 kinetic models for both S13 and S14 reaction networks in Tables 11.17 and 11.18, the parameters related to Arrhenius equation,  $\alpha$  and  $\beta$ , presented both good confidence intervals and  $p$ -values for every chemical reaction, with exception of the reactions responsible to produce BuOH species ( $r_2$  in S14 and  $r_5$  in S13), where  $\beta$  values showed no statistical significance. The fact that these chemical reactions had small extents and, therefore, the concentration of BuOH is residual in this system (consequently more affected by noise, presenting a significant uncertainty in its measurements), causes a high level of unpredictability associated with the optimal values of the adjusted parameters, confirming the previous analysis based on the results of the approximate method where the linearized functions of  $k$  were considered. When considering the results related to the adsorption component in S14LH2 model, good confidence intervals were obtained for both  $\theta$  and  $\phi$ , although the  $p$ -value for this last parameter rounded 0.3, while for S13LH2 these metrics could not be computed. Also, the enthalpy changes  $\Delta H$  assumed opposite signal values indicating exothermic and an endothermic adsorption processes for S13LH2 and S14LH2 models, respectively.

In reality, the parameters related to the adsorption component are not significant in the overall adjustment since the catalytic hydrogenation of MAC clearly has the homogeneous kinetic component predominating over the chemical adsorption phenomenon. When comparing the several kinetic models, where different species are absorbed on the catalyst, it could be found with confidence that the optimal structure, *i.e.*, the expression that presents the best tradeoff between data fit adjustment and model complexity, consists in the one where only MAC is adsorbed. However, when assessing the MAC species profile, it is observed that MAC is present for a short period of time in the reaction system, especially when the temperature is increased — which makes sense since  $T$  is in the denominator of a negative ratio in Arrhenius equation, thus, the rate of the reaction  $\text{MAC} \rightarrow \text{AS}$  is sped up when increasing  $T$ , *i.e.*,  $k_1$  is increased. Therefore, it can be inferred that the phenomenon of chemical adsorption for this system becomes increasingly negligible with increasing temperature, and that it has a small contribution to the dynamics of the system.

However, concluding this analysis, although the four models showed similar agreement in the goodness of fit to the data, the S13LH2 and S14LH2 models presented parameters with greater statistical significance. Consequently, they are preferable to describe this system. The developed models showed a better fit of the experimental data when compared to the literature model, even presenting less complex structures with a smaller number of parameters associated with the chemical adsorption process. Unfortunately, the available datasets are not enough to discriminate between S13 and S14 networks (where the BuOH species comes from different paths). Additional experiments must be performed in order

to identify the origin of BuOH. The suggestion here is to evaluate, under the same reaction conditions, the THF species alone as the initial reagent and observe if BuOH is formed.

## 11.3 Pfizer case study

The main results obtained through the application of the entire systematic methodology to the Pfizer case study (introduced in Section 1.5.4) are presented in this section. This section is organized as follows. In Section 11.3.1, the data reconciliation results are presented. In Section 11.3.2, the way in which the time-invariant relationships were obtained and selected for this case study is presented. Then, in Section 11.3.3, the use of these conservation relationships in data reconciliation is discussed, considering a comparative study of the reconciled data with different  $n_{in_{\tau_i}}$ , and presenting how they improve the identifiability of the model when applied correctly. In Section 11.3.4, the identification of the reaction network is considered through the Steps 3 to 5 of the proposed methodology. In Section 11.3.5, the identification of the reaction kinetic expressions is considered regarding the true reaction network. Finally, in Section 11.3.6, the parameter correlation with temperature is presented.

### 11.3.1 Data reconciliation

The original data relating to all 17 experiments are presented in Figure 11.22. The set of data presents a regular structure with measurements in every hour in a period of 12 h for every experiment, in which datasets 1, 4 and 14 are replicas. In these figures, the linear interpolation of concentration measurements is presented for all species in the 17 experiments. From the analysis of these plots, it can be observed that regardless of the initial and/or operating conditions, all concentration profiles showed general trends for each chemical species. Thus, these observed trends were implemented in the data reconciliation procedure through shape constraints in order to remove undesired oscillatory behavior from the species profiles. Note that the experimental data related to species H, I, and J, were the most affected by the addition of noise, since these species present residual concentrations.

In order to exemplify the data reconciliation results for this case study, experiments 1, 4 and 14 (replicas) are illustrated in the following figures. Figures 11.23 and 11.24 present the results of reconciling the data without imposing restrictions on form, although time-invariant relationships are verified at all collocation points. The locations of collocation points are shown in the 1st derivative profiles through the gray dots. The time-invariant relationships will be presented in the next section.

After the first data reconciliation procedure, the addition of shape constraints was considered, since the obtained profiles showed unwanted oscillatory behavior. The same shape constraints were applied to each dataset, since the observed trends are the same for all 17 experiments. These profile trends with their respective constraints are summarized

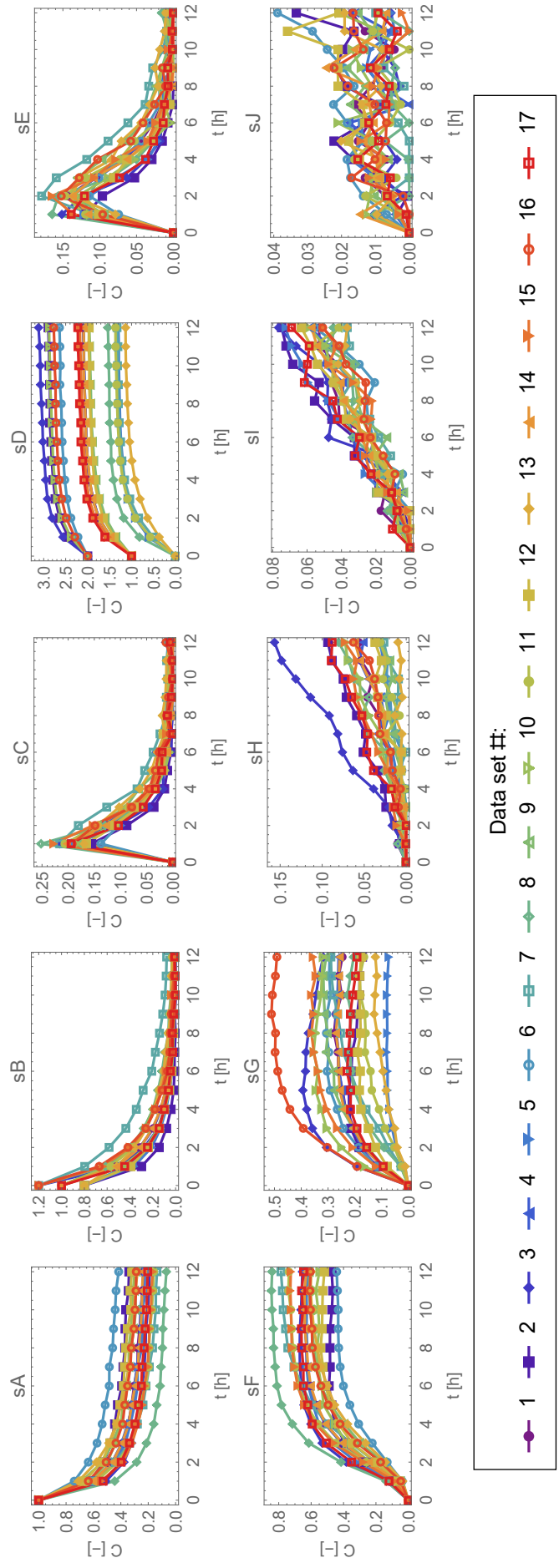
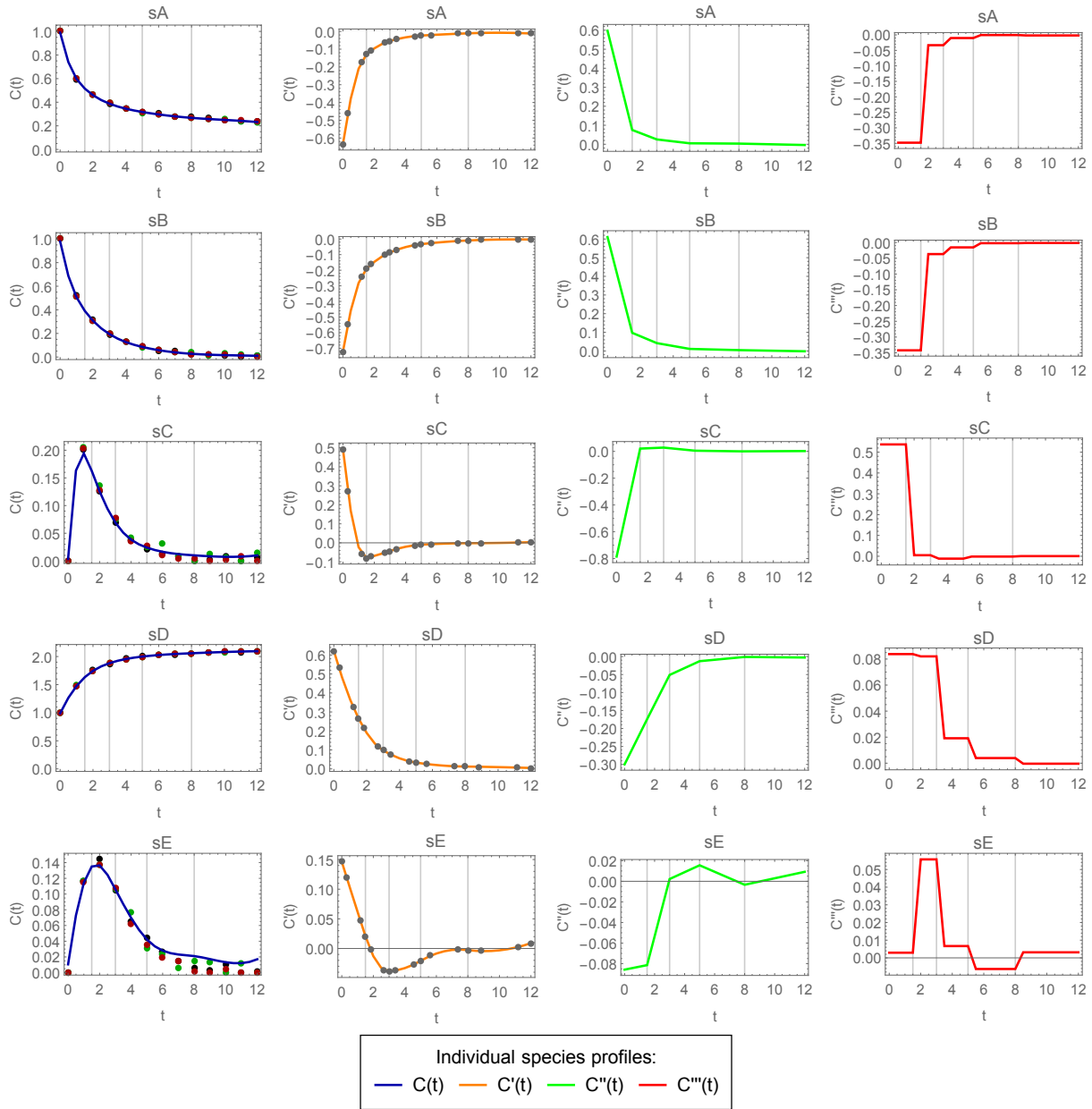


Figure 11.22 Linear interpolation of individual species concentration data regarding the 17 datasets.

in Table 11.19. Figures 11.25 and 11.26 present the smoothed profiles of each individual species, obtained after considering the shape constraints described in Table 11.19.



**Figure 11.23** A to E reconciled species profiles without shape constraints.

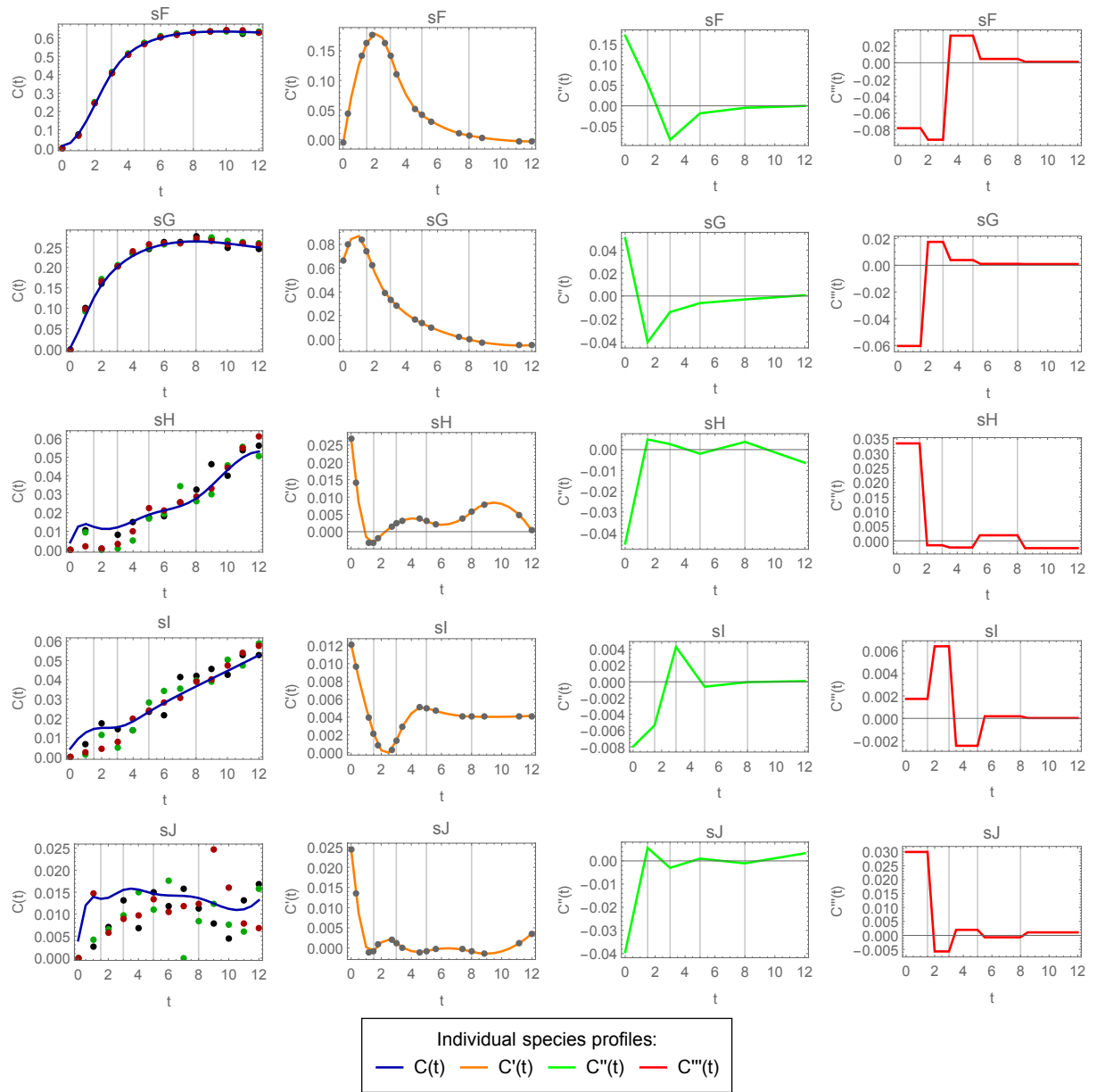


Figure 11.24 F to J reconciled species profiles without shape constraints.

**Table 11.19** Profiles trends from data analysis and respective implemented constraints.  
Abbreviation: c.p.  $\equiv$  collocation point.

Species	Observations	Constraints
A and B	Initial reactants, $C(t)$ decrease in all time domain $C(t)$ decrease in a monotone manner	$\frac{dC(t)}{dt} \leq 0$ $\frac{dC(t)}{dt} _{t_{\text{col}}} \leq \frac{dC(t)}{dt} _{t_{\text{col}+1}}$
C	Intermediate species, $C(t)$ decrease from 3rd c.p. to the end $C(t)$ decrease from 4th c.p. to the end in a monotone way	$\frac{dC(t)}{dt} _{t_{\text{col}} \geq 3} \leq 0$ $\frac{dC(t)}{dt} _{t_{\text{col}} \geq 4} \leq \frac{dC(t)}{dt} _{t_{\text{col}+1}}$
D	$C(t)$ increase in all time domain $C(t)$ increase in a monotone manner Species produced from the beginning	$\frac{dC(t)}{dt} \geq 0$ $\frac{dC(t)}{dt} _{t_{\text{col}}} \geq \frac{dC(t)}{dt} _{t_{\text{col}+1}}$ $\frac{dC(t)}{dt} _{t=0} \neq 0$
E	Intermediate species, $C(t)$ decrease from 6th c.p. to the end $C(t)$ decrease from 7th c.p. to the end in a monotone way Species produced from the beginning	$\frac{dC(t)}{dt} _{t_{\text{col}} \geq 6} \leq 0$ $\frac{dC(t)}{dt} _{t_{\text{col}} \geq 7} \leq \frac{dC(t)}{dt} _{t_{\text{col}+1}}$ $\frac{dC(t)}{dt} _{t=0} \neq 0$
F	Terminal? species, $C(t)$ increase from 1st to the 13th c.p. $C(t)$ increase from 5th c.p. to the end in a monotone way Species not produced from the beginning (in a 2nd, 3rd, etc step)	$\frac{dC(t)}{dt} _{t_{\text{col}} \leq 13} \geq 0$ $\frac{dC(t)}{dt} _{t_{\text{col}} \geq 5} \geq \frac{dC(t)}{dt} _{t_{\text{col}+1}}$ $\frac{dC(t)}{dt} _{t=0} = 0$
G	Terminal? species, $C(t)$ increase from 1st to the 12th c.p. $C(t)$ increase from 3rd to the 12th c.p. in a monotone way Species produced from the beginning	$\frac{dC(t)}{dt} _{t_{\text{col}} \leq 12} \geq 0$ $\frac{dC(t)}{dt} _{3 \leq t_{\text{col}} \leq 11} \geq \frac{dC(t)}{dt} _{t_{\text{col}+1}}$ $\frac{dC(t)}{dt} _{t=0} \neq 0$
H and I	Terminal species (subproducts), $C(t)$ increase in all time domain $C(t)$ increase in a monotone manner Species not produced from the beginning (in a 2nd, 3rd, etc step)	$\frac{dC(t)}{dt} \geq 0$ $\frac{dC(t)}{dt} _{t_{\text{col}}} \leq \frac{dC(t)}{dt} _{t_{\text{col}+1}}$ $\frac{dC(t)}{dt} _{t=0} = 0$
J	Terminal? species (subproduct) Species produced from the beginning	$\frac{dC(t)}{dt} _{t=0} \neq 0$

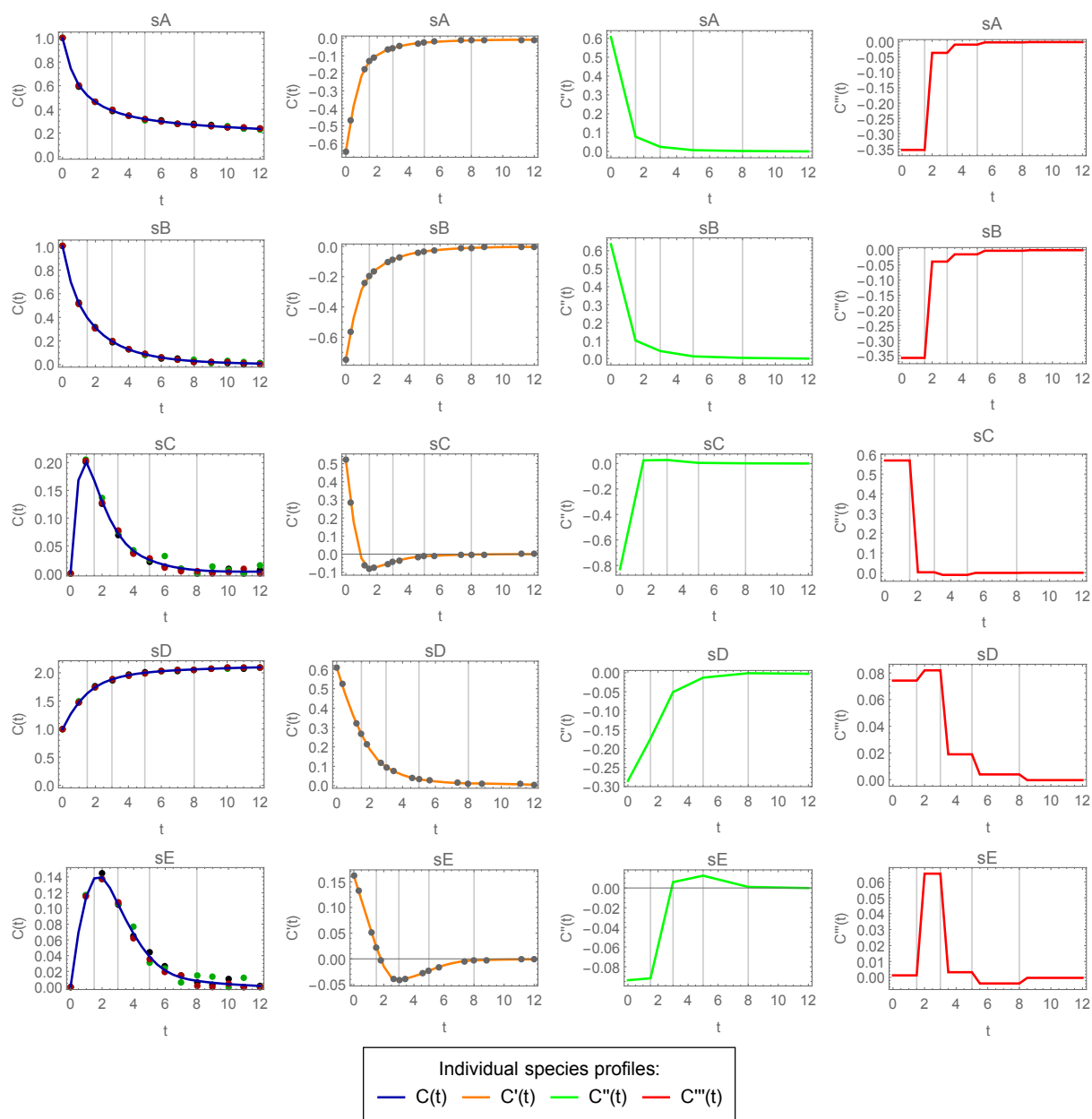
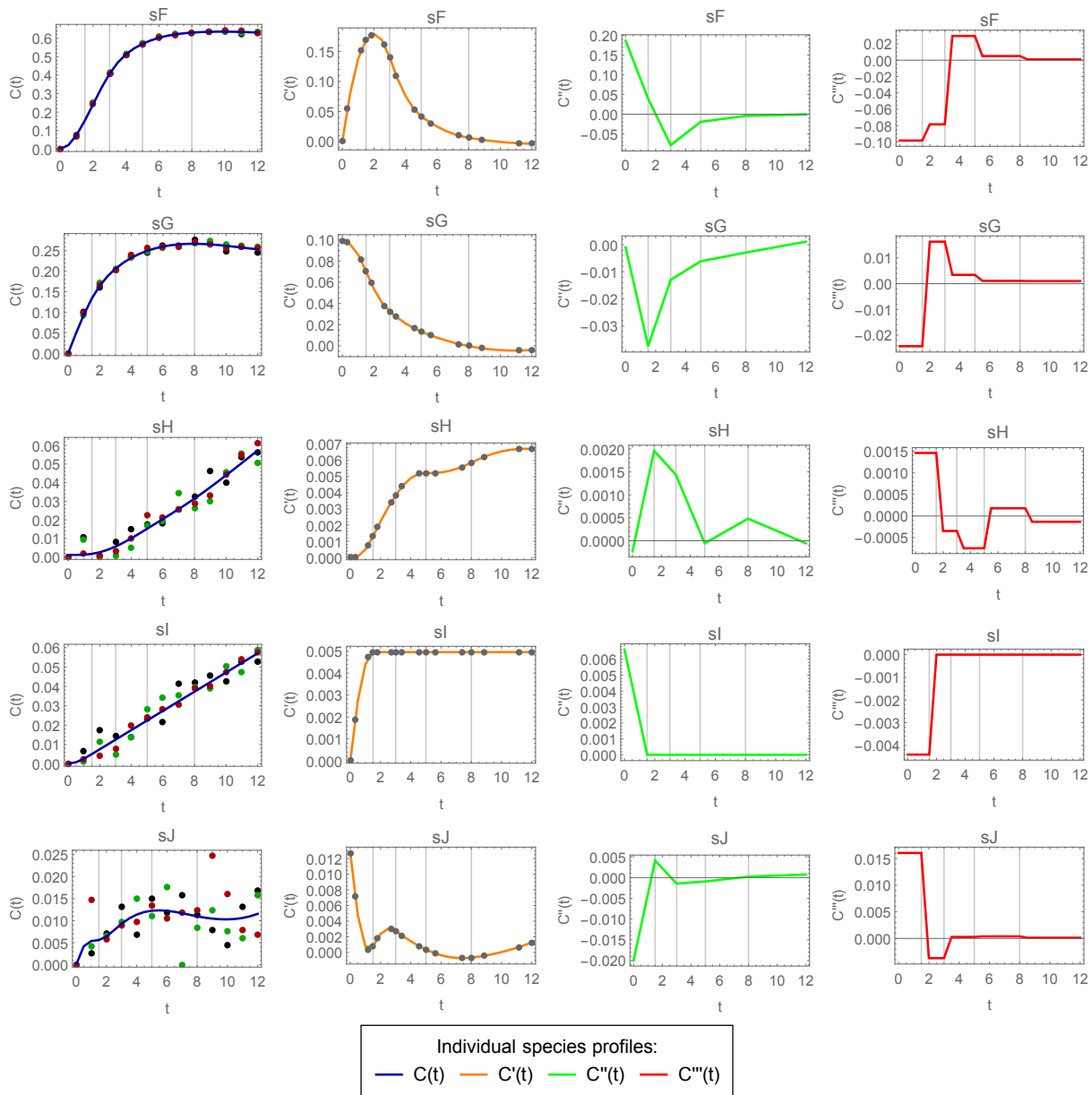


Figure 11.25 A to E reconciled profiles with constraints described in Table 11.19.



**Figure 11.26** F to J reconciled profiles with constraints described in Table 11.19.

However, some species profiles still show undesired oscillatory behavior, mainly in relation to the 1st derivative profiles. Therefore, additional shape constraints were needed to smooth the 1st derivative profiles. Although some species already present smooth profiles in relation to a specific dataset, additional restrictions were imposed on the 2nd derivatives to guarantee the desired degree of smoothness in the other datasets. Therefore, some of these inequality constraints may be inactive in some solutions (datasets). Note that species J is a by-product with negligible extent, therefore it is strongly affected by noise, making it difficult to predict its behavior. Table 11.20 presents the new shape constraints considered after the first iteration. Figure 11.27 presents the final smoothed profiles of each individual species obtained after considering the shape constraints observed from all



data trends (described in Tables 11.19 and 11.20).

**Table 11.20** Profiles trends from previous smooth procedure (2nd iteration) and respective implemented constraints. Abbreviation: c.p.  $\equiv$  collocation point.

Species	Observations	Constraints
A	$\frac{d^2C(t)}{dt^2}$ decrease in a monotone manner in all domain	$\frac{d^3C(t)}{dt^3} _{t_{\text{col}}} \leq \frac{d^3C(t)}{dt^3} _{t_{\text{col}+1}}$
B	$\frac{d^2C(t)}{dt^2}$ decrease in a monotone manner in all domain	$\frac{d^3C(t)}{dt^3} _{t_{\text{col}}} \leq \frac{d^3C(t)}{dt^3} _{t_{\text{col}+1}}$
C	$\frac{d^2C(t)}{dt^2}$ increase in a monotone way from 7th c.p. to end $C(t)$ null in the beginning	$\frac{d^3C(t)}{dt^3} _{t_{\text{col}} \geq 7} \geq \frac{d^3C(t)}{dt^3} _{t_{\text{col}+1}}$ $C(0) = 0$
D	$\frac{d^2C(t)}{dt^2}$ increase in a monotone way in all time domain	$\frac{d^3C(t)}{dt^3} _{t_{\text{col}}} \geq \frac{d^3C(t)}{dt^3} _{t_{\text{col}+1}}$
E	$\frac{d^2C(t)}{dt^2}$ decrease in a monotone way from 10th c.p. to end $\frac{dC(t)}{dt}$ increase in a monotone way from 1st to 3rd c.p. $\frac{dC(t)}{dt}$ increase from the 1st to 3rd c.p. $C(t)$ null in the beginning	$\frac{d^3C(t)}{dt^3} _{t_{\text{col}} \geq 10} \geq \frac{d^3C(t)}{dt^3} _{t_{\text{col}+1}}$ $\frac{d^2C(t)}{dt^2} _{t_{\text{col}} \leq 2} \leq \frac{d^2C(t)}{dt^2} _{t_{\text{col}+1}}$ $\frac{d^2C(t)}{dt^2} _{t_{\text{col}} \leq 3} \leq 0$ $C(0) = 0$
F	$\frac{dC(t)}{dt}$ decrease in a monotone way from the 8th c.p. to the end $C(t)$ null in the beginning	$\frac{d^2C(t)}{dt^2} _{t_{\text{col}} \geq 8} \leq \frac{d^2C(t)}{dt^2} _{t_{\text{col}+1}}$ $C(0) = 0$
G	$\frac{dC(t)}{dt}$ decrease in a monotone way from 5th c.p. to the end $\frac{d^2C(t)}{dt^2}$ increase in a monotone way in all domain $C(t)$ null in the beginning	$\frac{d^2C(t)}{dt^2} _{t_{\text{col}} \geq 5} \leq \frac{d^2C(t)}{dt^2} _{t_{\text{col}+1}}$ $\frac{d^3C(t)}{dt^3} _{t_{\text{col}}} \geq \frac{d^3C(t)}{dt^3} _{t_{\text{col}+1}}$ $C(0) = 0$
H	$\frac{dC(t)}{dt}$ increase in a monotone way from 5th c.p. to the end $C(t)$ null in the beginning	$\frac{d^2C(t)}{dt^2} _{t_{\text{col}} \geq 5} \geq \frac{d^2C(t)}{dt^2} _{t_{\text{col}+1}}$ $C(0) = 0$
I	$\frac{dC(t)}{dt}$ increase in a monotone way in all domain $\frac{d^2C(t)}{dt^2}$ decrease in a monotone way in all domain $C(t)$ null in the beginning	$\frac{d^2C(t)}{dt^2} _{t_{\text{col}}} \geq \frac{d^2C(t)}{dt^2} _{t_{\text{col}+1}}$ $\frac{d^3C(t)}{dt^3} _{t_{\text{col}}} \leq \frac{d^3C(t)}{dt^3} _{t_{\text{col}+1}}$ $C(0) = 0$
J	$\frac{dC(t)}{dt}$ decrease in a monotone way in all domain $C(t)$ increase in a monotone way in all domain $C(t)$ null in the beginning	$\frac{d^2C(t)}{dt^2} _{t_{\text{col}}} \leq \frac{d^2C(t)}{dt^2} _{t_{\text{col}+1}}$ $\frac{dC(t)}{dt} _{t_{\text{col}}} \leq \frac{dC(t)}{dt} _{t_{\text{col}+1}}$ $C(0) = 0$

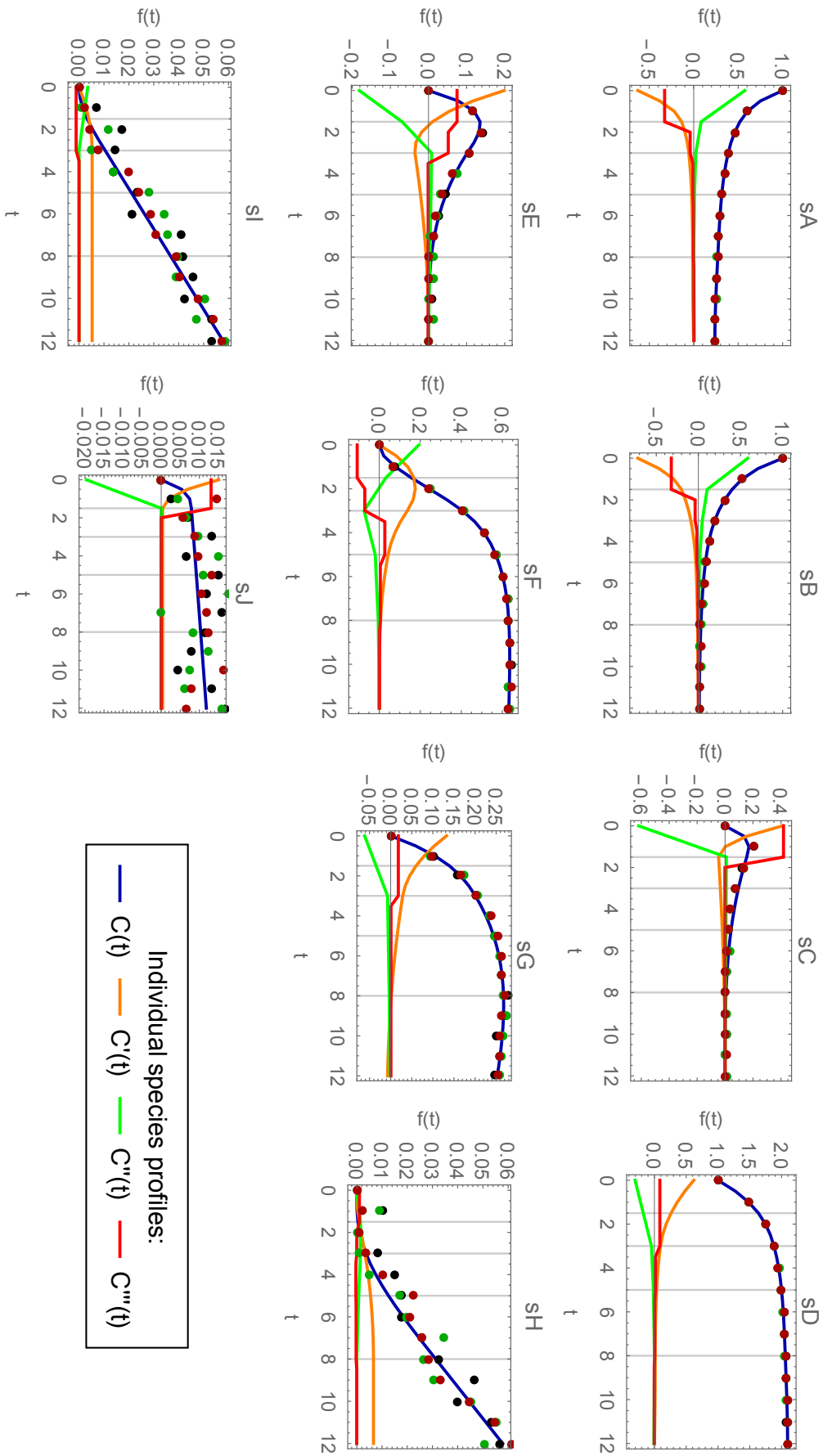


Figure 11.27 Final data reconciliation results.

### 11.3.2 Analysis of time invariants

Obtaining time-invariant relationships was achieved using the known system stoichiometry. However, no information about the nature of the species or their molecular formula is provided by the Pfizer in this example. Consequently, it is impossible to say what these true relationships are, although we can accurately state the space that they span ( $\text{null}(\mathbf{N})$ ) and thus propose a basis that represents the most potential candidate relationships for describing the conserved amounts between molecules. This approach is followed considering the MILP formulation presented in Section 6.6.1.

Hence through the minimization of the  $\ell_1$ -norm of the solution vector that lies in the null space of  $\mathbf{N}$  and is constrained to present integer and positive entries, candidate invariant relationship can be obtained. The enumeration of these solution through integer cut equations ensures a generating set for describing a basis for  $\text{row}(\mathbf{A})$ . Clearly this set contains linearly dependent vectors (see the definition of a generating set in linear algebra), but we are interested in selecting the most plausible vectors that also constitute a basis. Here the criterion of plausible invariant candidates is defined as the compromise between sparsity and vector length ( $\ell_1$ -norm).

A list of four candidates for invariant relationships is shown in Table 11.21, where the last column indicates the vector  $\ell_1$ -norm. The results were obtained using GAMS®.

**Table 11.21** Candidate invariant relationships for the Pfizer example, expressed in terms of the coefficients that involve each chemical species.

	A	B	C	D	E	F	G	H	I	J	Total
<b>inv1</b>	0	3	2	1	1	1	4	3	1	0	16
<b>inv2</b>	1	2	2	1	1	1	3	2	2	2	17
<b>inv3</b>	2	1	2	1	1	1	2	1	3	4	18
<b>inv4</b>	3	0	2	1	1	1	1	0	4	6	19

As can be seen from these results, the most sparse vectors are **inv1** and **inv4** and only two of the four candidate solutions are linearly independent. Since no information regarding the species molecules is known, it is not possible to interpret these quantities strictly as physical amounts. However, since **inv2** presents all values greater than zero and lower than 3, it is a plausible candidate to describe the total mass balance closure. Moreover, **inv1** is also a plausible candidate for a system invariant, like **inv4**, but presents the lowest total amount conserved of these species; thus **inv1** can also be interpreted a true conserved relation. Therefore, in this case we have selected the first two solutions. Any vector that constitutes a linear combination of these two basis vectors could also be a candidate invariant for this system, although these conserved amounts tend to be small and need to be positive, *i.e.*, they may present physical meaning.

An attempt to identify invariants from experimental data, as proposed in formulation (6.38), was performed in Section 6.6.3. Unfortunately, for this case study (regarding the

noisy dataset), the conserved relations could not be satisfactorily elucidated, but  $\text{nin}_{11} = 2$  could be inferred from the analysis of the results obtained.

### 11.3.3 Evaluating the use of invariants in data reconciliation to increase model identifiability

The **inv1** and **inv2** were incorporated at the previously presented data smoothing procedure, resulting in the acquirement of reconciled data with minimized noise content. This procedure reduces the chance of facing model identifiability problems from reconciled data since it clarifies the dimension of the data variant space, and, consequently, assists the identification of a basis for that space in which compositional changes occur. This means that when facing small singular values from the SVD of reconciled data, they probably are related to model components (signal) that should not be discarded.

An assessment of the singular values of the matrix of concentration derivatives collected in every collocation point from the 15 sets of reconciled data, considering (i) no invariant relationship, (ii) only the single **inv1** relationship, and (iii) the both **inv1** and **inv2** relationships, was performed. The obtained singular values ( $\sigma$ ) are presented in Table 11.22.

**Table 11.22** Singular values comparison using data reconciled with 0, 1 and 2 time-invariant relationships. Data variant space concerning concentration derivatives data.

$\sigma_s$	0 invariants	1 invariant	2 invariants
$\sigma_1$	6.689	6.693	6.687
$\sigma_2$	1.865	1.894	1.815
$\sigma_3$	0.880	0.874	0.869
$\sigma_4$	0.519	0.539	0.524
$\sigma_5$	0.162	0.289	0.231
$\sigma_6$	0.141	0.182	0.109
$\sigma_7$	0.108	0.100	0.063
$\sigma_8$	0.066	0.045	0.028
$\sigma_9$	0.028	0.024	$7.71 \times 10^{-12}$
$\sigma_{10}$	0.022	$3.49 \times 10^{-12}$	$2.10 \times 10^{-12}$

Two important observations can be made from the results shown in Table 11.22. Firstly, it is notable that the model direction (component) associated with  $\sigma_{10}$  regarding data reconciled with a single invariant converges to zero, *i.e.*,  $3.49 \times 10^{-12} \approx 0$ , since one dimension of the 10-dimensional variant data space (with zero invariants) is removed when decreasing the degrees of freedom in the data reconciliation procedure by imposing the equality constraint concerning **inv1**, and the same happens for  $\sigma_9$  and  $\sigma_{10}$  in the reconciled data using equality constraints concerning **inv1** and **inv2**. Therefore, the use of invariants decreases the data variant dimension, as previously discussed in Chapter 6. Secondly, and not less important, it is observed that the noise contribution in the singular values is greater in the respective model directions/components with lower variance, for example,

regarding the column of 0 invariants, the noise contribution follows that  $\sigma_{10} > \sigma_9 > \sigma_8 > \dots > \sigma_1$  since the signal-to-noise ratio decreases as the model grows in dimension, *i.e.*, as the signal related to the directions of lower variability decreases. Hence when comparing the  $\sigma_s$  among the columns for the same row of this table, it can be seen that the presented amounts tend to vary more for model components greater than 4. Since the use of invariants in the treatment of data reduces the uncertainty present in the original data, minimizing and/or (at least) optimally distributing the uncertainty (noise) in the reconciled data through optimization, the singular values concerning the last column of this table show greater signal-to-noise ratio than the ones with one and zero invariants, considering the same model component for comparison. For example, the signal-to-noise ratio presented in  $\sigma_8$  with 0 invariants is lower than that with 1 invariant, which in turn is lower than that with 2 invariants. Therefore, concluding this analysis,  $\sigma_9$  and  $\sigma_{10}$  from reconciled data with 0 invariants, as well as  $\sigma_{10}$  from reconciled data with 1 invariant, only exist due to the presence of noise in the original data.

The projection of the true stoichiometric vectors was considered in the data variant space determined from the row space of the instantaneous species concentration derivatives collected at the collocation points, considering reconciled data without, with a single, and with two time invariants. The results of this analysis are shown in Table 11.23. From these results, one can see that the error of projection  $\|\mathbf{v} - \text{proj}_{\mathbf{S}} \mathbf{v}\|_2$ , as well as the relative error of projection  $\varphi$ , decreases when the number of considered equality constraints increases. This observation shows the importance of well determining time-invariant relationships, and of incorporating them in the data reconciliation procedure in order to increase the true model identifiability.

**Table 11.23** TFA results comparison using data reconciled with 0, 1 and 2 time-invariant relationships. \*The metrics in data with 2 invariants are multiplied by  $10^{11}$ .

True reaction network		0 invariants			1 invariant		2 invariants*	
$r_j$	Chemical reaction	$\ \mathbf{v}\ _2$	$\ \mathbf{v} - \text{proj}_{\mathbf{S}} \mathbf{v}\ _2$	$\varphi$	$\ \mathbf{v} - \text{proj}_{\mathbf{S}} \mathbf{v}\ _2$	$\varphi$	$\ \mathbf{v} - \text{proj}_{\mathbf{S}} \mathbf{v}\ _2$	$\varphi$
$r_1$	$A + B \rightarrow C + D$	2.000	0.010	0.005	0.001	0.001	0.143	0.072
$r_2$	$C \rightarrow D + E$	1.732	0.014	0.008	0.012	0.007	0.506	0.292
$r_3$	$E \rightarrow F$	1.414	0.024	0.017	0.026	0.018	0.376	0.266
$r_4$	$B + D \rightarrow G$	1.732	0.017	0.010	0.012	0.007	0.219	0.126
$r_5$	$G \rightarrow D + H$	1.732	0.511	0.295	0.500	0.288	1.868	1.079
$r_6$	$A + F \rightarrow I$	1.732	0.797	0.460	0.765	0.442	1.082	0.625
$r_7$	$2A \rightarrow J$	2.236	0.946	0.423	0.331	0.148	1.302	0.582
$r_8$	$B + J \rightarrow 2E + I$	2.646	1.353	0.511	1.129	0.427	0.561	0.212

Once having the data reconciled with good estimates of concentration derivatives and knowing the stoichiometric relationships among species for this chemical system, the 8 reaction rates could be estimated. The reaction rates for every dataset are presented in Figures 11.28 to 11.30, comparing their behavior when considering 0, 1 and 2 invariants. The most reliable reaction rate profiles are those related to 2 invariants, since the reaction network comprises 8 linearly independent chemical reactions between 10 species, requiring

two invariant relationships.

In order to compute/estimate these reaction rate profiles different methods were considered. On the one hand, when considering reconciled data with 0 and 1 invariant relationships, the reaction rate estimates are performed using optimization since the data dimension is greater than the number of variables, so the problem is to solve a linear system of overdetermined equations for each instant of time using ordinary least squares without constraints, where the

$$\text{SSE}(t) = \left( \frac{d\mathbf{c}(t)}{dt} - \mathbf{N}^T \cdot \mathbf{r}(t) \right)^T \cdot \left( \frac{d\mathbf{c}(t)}{dt} - \mathbf{N}^T \cdot \mathbf{r}(t) \right)$$

is minimized. In the previous equation,  $d\mathbf{c}(t)/dt \in \mathbb{R}^{10}$  is the concentration derivative vector,  $\mathbf{N} \in \mathbb{N}^{8 \times 10}$  the stoichiometric matrix and  $\mathbf{r}(t) \in \mathbb{R}^8$  the reaction rate vector. Note that, in this case, the vector of the derivatives cannot be described as a linear combination of the basis formed by the network stoichiometry since the SSE is not zero. On the other hand, when handling data that verify the same dimension as the number of variables and since the row space of  $\mathbf{D}$  (the matrix of concentration derivatives) is the same row space of  $\mathbf{N}$ , the instantaneous reaction rates are calculated through the simple solve of the linear system of equations

$$\frac{d\mathbf{c}(t)}{dt} = \mathbf{N}^T \cdot \mathbf{r}(t)$$

that is well-determined. Note that  $\mathbf{r}(t)$  is the coordinates vector that build  $d\mathbf{c}(t)/dt$  in the row space of  $\mathbf{N}$ .

As can be seen in Figures 11.28 to 11.30, the use of invariants has impact in the reaction rate profiles and, consequently, in the reaction model identification. The further computations of physical quantities, such as reaction rates and/or reaction extents and their parameters estimates, are more reliable from reconciled data that verify well established time-invariant relationships. The reaction rate profiles that have shown negative values concerning data with 0 and 1 invariant, are less negative, and in some cases change their signal, for data respecting the use of two invariant relationships. The following steps of the methodology are applied using reconciled data with the two invariants identified.

The next sections present two different approaches for a complete identification of the reaction model for this case study. In the first approach (Section 11.3.4), the system stoichiometry is treated as unknown, and the objective is to identify it through the application of Steps 1 to 5 of the methodology. In the second approach (Section 11.3.5), the identification of the reaction kinetics is made through the application of Step 6, regarding the true stoichiometry.

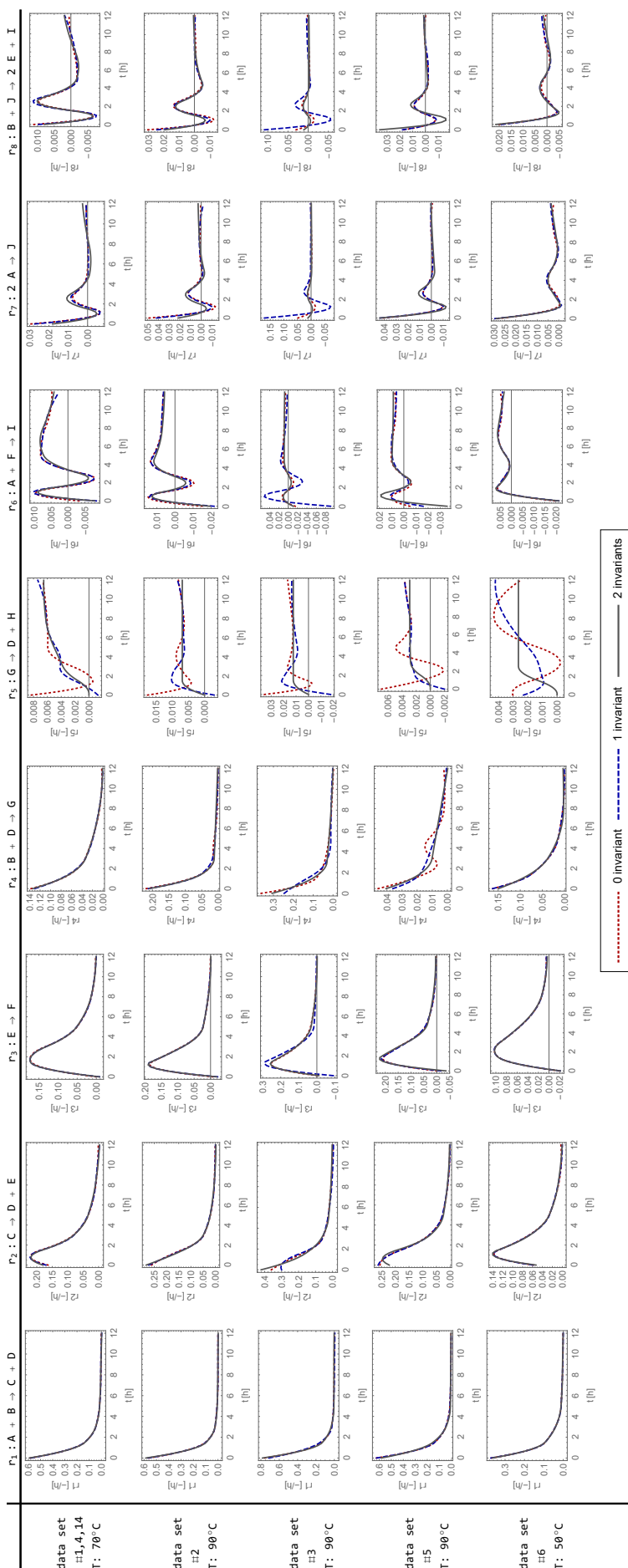


**Figure 11.28** Reaction rates computed using datasets #1, 4 and 14, #2, #3, #5, and #6 with 0, 1 and 2 invariants. Datasets #1, 4 and 14 are replicas.

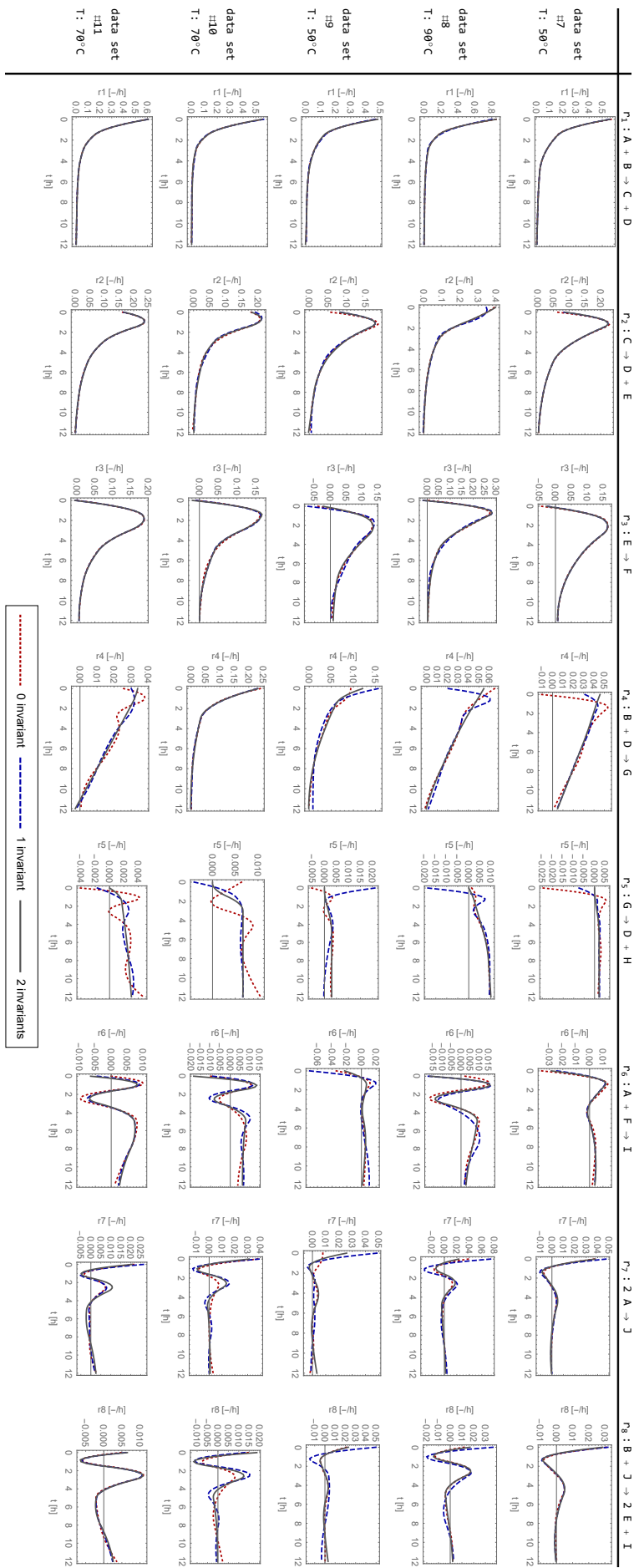


Figure 11.29 Reaction rates computed using datasets #7, #8, #9, #10, and #11 with 0, 1 and 2 invariants.



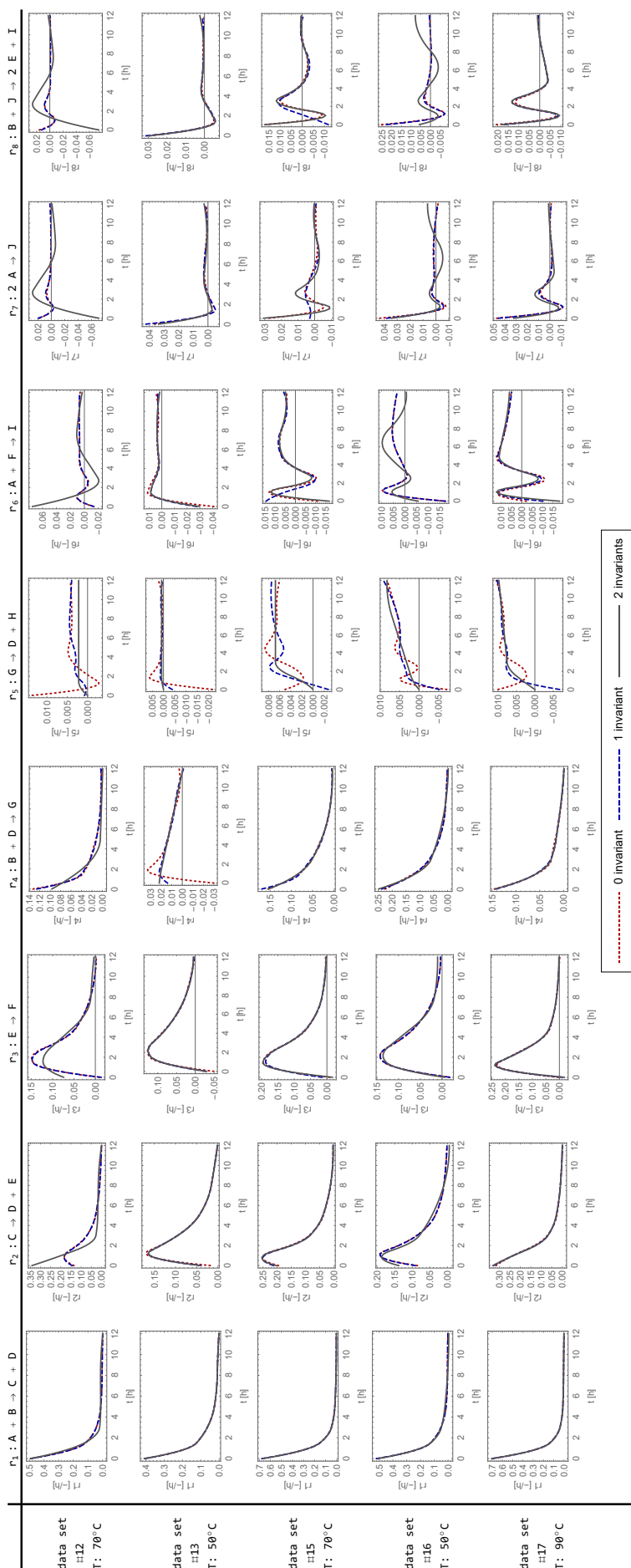


Figure 11.30 Reaction rates computed using datasets #12, #13, #15, #16, and #17 with 0, 1 and 2 invariants.

### 11.3.4 Identifying the true network

During Step 3, 131 chemical reactions were generated using the MILP formulation described in Section 7.2.1. The results were obtained using GAMS® software with the commercial solver CPLEX, with a total CPU usage of 28.93 s. The generated chemical reactions are listed in Table 11.24, sorted with an increasing  $\varphi$  value. The known (true) chemical reactions are highlighted with red color. As can be seen, the stoichiometry lies in the data variant space, presenting an insignificant relative error of projection ( $\varphi \equiv 0$ ). This is not an unexpected result since (i) the matrix of data was built with reconciled data in which the identified time-invariant relationships were imposed as constraints of the smoothing procedure, and (ii) the generated chemical reactions obey the same invariant relationships.

Since there is no information regarding the molecules involved in the system, *i.e.*, the composition of the molecules in terms of number and type of chemical elements is unknown, the Gibbs free energy change could not be evaluated, and therefore, no feasible net flux directions were elucidated for this case study. Consequently, the superstructure of the reaction networks presents a significant number of candidate chemical reactions, presenting 262 directed arcs (131 in the forward direction plus 131 in the reverse direction).

The generation of reaction network structures was considered in Step 4, however, since the dimension of the superstructure is large, the explicit generation exploded presenting more than one billion networks composed by eight chemical reactions. Therefore, the use of implicit generation of reaction networks was necessary for this case study. Firstly, the formulation described in Section 9.4.1 was considered to enumerate a list of the first fifty plausible structures composed by eight chemical reactions. Unfortunately, the true reaction network was not presented in that list. When fixing the true schema as solution of this problem, the objective function value assumed  $\phi = 1.542$ , showing that the positive constraints for some of the reaction rate variables were active in certain time intervals of few experiments. This result shows that even considering the time-invariant relationships in data reconciliation, ensuring that the row space of the basis formed by the true reaction stoichiometries is the same row space of the matrix of concentration derivatives, it does not guarantee the verification of the plausibility criterion in those respective reaction rates. However, other studies were carried on, intensively analyzing the list of plausible structures, for example evaluating the frequency of chemical reactions in that list, with the aim to identify from the implicit generation at least some structural part of the model. Nonetheless, these analyses were not successful since even considering a more restrictive approach to enumerate network structures using the plausibility criterion, the obtained number of plausible candidates still large, and also, no correlation among the plausible reaction rates and the frequency of their appearance in the implicitly generated solutions could be found. Therefore, a more fine network generation approach was further considered, identifying the reaction kinetic expressions simultaneously with the network. For this purpose, the formulation described in Section 9.4.2 was considered, and in this

**Table 11.24** List of generated chemical reactions with the corresponding TFA metrics;  $\|\mathbf{v} - \text{proj}_{\mathcal{S}} \mathbf{v}\|_2$  and  $\varphi$  are multiplied by  $10^{11}$ .

$k$	$r_j$	Chemical reaction	$\ \mathbf{v}\ _2$	$\ \mathbf{v} - \text{proj}_{\mathcal{S}} \mathbf{v}\ _2$	$\varphi$	$k$	$r_j$	Chemical reaction	$\ \mathbf{v}\ _2$	$\ \mathbf{v} - \text{proj}_{\mathcal{S}} \mathbf{v}\ _2$	$\varphi$
1	$r_{90}$	$\text{A} + \text{G} \rightarrow \text{C} + 2\text{D}$	2.646	0.080	0.030	66	$r_{43}$	$\text{B} + \text{F} \rightarrow \text{D} + \text{H}$	2.000	1.106	0.553
2	$r_{34}$	$\text{B} + \text{C} \rightarrow \text{F} + \text{G}$	2.000	0.089	0.045	67	$r_{113}$	$\text{B} + \text{I} \rightarrow \text{C} + 2\text{F}$	2.646	1.501	0.567
3	$r_{21}$	$\text{A} + \text{B} \rightarrow \text{C} + \text{D}$	2.000	0.143	0.072	68	$r_{83}$	$\text{B} + 2\text{E} \rightarrow \text{F} + \text{G}$	2.646	1.538	0.581
4	$r_{131}$	$\text{H} + \text{I} \rightarrow \text{C} + 2\text{F}$	2.646	0.196	0.074	69	$r_5$	$2\text{A} \rightarrow \text{J}$	2.236	1.302	0.582
5	$r_{10}$	$\text{C} \rightarrow \text{D} + \text{F}$	1.732	0.130	0.075	70	$r_{108}$	$2\text{C} + \text{F} \rightarrow \text{G} + \text{I}$	2.646	1.590	0.601
6	$r_{35}$	$2\text{F} \rightarrow \text{D} + \text{E}$	2.449	0.196	0.080	71	$r_{27}$	$2\text{D} \rightarrow \text{E} + \text{F}$	2.449	1.515	0.618
7	$r_{109}$	$\text{D} + 2\text{F} \rightarrow \text{C} + \text{E}$	2.646	0.246	0.093	72	$r_{46}$	$\text{A} + \text{H} \rightarrow \text{C} + \text{F}$	2.000	1.240	0.620
8	$r_{69}$	$\text{A} + 2\text{D} \rightarrow \text{F} + \text{I}$	2.646	0.256	0.097	73	$r_{11}$	$\text{C} \rightarrow \text{E} + \text{F}$	1.732	1.075	0.621
9	$r_{29}$	$\text{A} + \text{C} \rightarrow \text{E} + \text{I}$	2.000	0.210	0.105	74	$r_{84}$	$\text{A} + 2\text{F} \rightarrow \text{D} + \text{I}$	2.646	1.643	0.621
10	$r_{13}$	$\text{B} + \text{D} \rightarrow \text{G}$	1.732	0.219	0.126	75	$r_{111}$	$\text{E} + 2\text{F} \rightarrow \text{C} + \text{D}$	2.646	1.645	0.622
11	$r_{75}$	$\text{B} + 2\text{D} \rightarrow \text{F} + \text{G}$	2.646	0.355	0.134	76	$r_{17}$	$\text{A} + \text{F} \rightarrow \text{I}$	1.732	1.082	0.625
12	$r_{58}$	$\text{A} + 2\text{B} \rightarrow \text{C} + \text{G}$	2.646	0.361	0.136	77	$r_{100}$	$\text{A} + \text{H} \rightarrow 2\text{D} + \text{F}$	2.646	1.661	0.628
13	$r_{56}$	$\text{A} + \text{B} \rightarrow 2\text{D} + \text{E}$	2.646	0.363	0.137	78	$r_{87}$	$2\text{A} + \text{F} \rightarrow \text{E} + \text{J}$	2.646	1.678	0.634
14	$r_{76}$	$2\text{A} + \text{E} \rightarrow \text{D} + \text{J}$	2.646	0.363	0.137	79	$r_{40}$	$\text{B} + \text{E} \rightarrow \text{F} + \text{H}$	2.000	1.283	0.641
15	$r_{81}$	$\text{B} + 2\text{E} \rightarrow \text{C} + \text{H}$	2.646	0.373	0.141	80	$r_7$	$\text{C} \rightarrow 2\text{E}$	2.236	1.451	0.649
16	$r_{33}$	$\text{B} + \text{C} \rightarrow \text{E} + \text{G}$	2.000	0.289	0.144	81	$r_2$	$\text{D} \rightarrow \text{E}$	1.414	0.945	0.668
17	$r_{95}$	$\text{B} + 2\text{F} \rightarrow \text{E} + \text{G}$	2.646	0.411	0.155	82	$r_{15}$	$\text{B} + \text{E} \rightarrow \text{G}$	1.732	1.162	0.671
18	$r_{103}$	$2\text{A} + \text{H} \rightarrow \text{B} + \text{J}$	2.646	0.417	0.158	83	$r_{45}$	$\text{A} + \text{G} \rightarrow \text{H} + \text{I}$	2.000	1.346	0.673
19	$r_{110}$	$\text{B} + \text{I} \rightarrow \text{C} + 2\text{D}$	2.646	0.419	0.158	84	$r_{52}$	$\text{C} + \text{H} \rightarrow \text{E} + \text{G}$	2.000	1.372	0.686
20	$r_{102}$	$\text{A} + \text{H} \rightarrow 2\text{E} + \text{F}$	2.646	0.437	0.165	85	$r_{77}$	$\text{A} + 2\text{E} \rightarrow \text{F} + \text{I}$	2.646	1.828	0.691
21	$r_{42}$	$\text{A} + \text{G} \rightarrow \text{B} + \text{I}$	2.000	0.341	0.170	86	$r_{71}$	$2\text{A} + \text{D} \rightarrow \text{F} + \text{J}$	2.646	1.870	0.707
22	$r_{67}$	$\text{A} + 2\text{D} \rightarrow \text{E} + \text{I}$	2.646	0.509	0.193	87	$r_{59}$	$\text{A} + \text{B} \rightarrow 2\text{E} + \text{F}$	2.646	1.877	0.709
23	$r_6$	$\text{C} \rightarrow 2\text{D}$	2.236	0.440	0.197	88	$r_{97}$	$2\text{C} + \text{E} \rightarrow \text{G} + \text{I}$	2.646	1.964	0.742
24	$r_{23}$	$2\text{C} \rightarrow \text{A} + \text{G}$	2.449	0.541	0.210	89	$r_{91}$	$\text{A} + \text{G} \rightarrow \text{C} + 2\text{E}$	2.646	1.964	0.742
25	$r_{57}$	$\text{A} + \text{B} \rightarrow \text{D} + 2\text{F}$	2.646	0.556	0.210	90	$r_{126}$	$2\text{F} + \text{H} \rightarrow \text{E} + \text{G}$	2.646	2.054	0.776
26	$r_{88}$	$2\text{B} + \text{E} \rightarrow \text{G} + \text{H}$	2.646	0.557	0.211	91	$r_{105}$	$2\text{I} \rightarrow 2\text{D} + \text{J}$	3.000	2.344	0.781
27	$r_{30}$	$\text{A} + \text{C} \rightarrow \text{F} + \text{I}$	2.000	0.424	0.212	92	$r_{72}$	$\text{B} + 2\text{D} \rightarrow \text{C} + \text{H}$	2.646	2.079	0.786
28	$r_{118}$	$\text{B} + \text{J} \rightarrow 2\text{E} + \text{I}$	2.646	0.561	0.212	93	$r_{80}$	$\text{B} + 2\text{E} \rightarrow \text{D} + \text{G}$	2.646	2.107	0.797
29	$r_{24}$	$\text{A} + \text{B} \rightarrow \text{C} + \text{F}$	2.000	0.427	0.213	94	$r_{127}$	$2\text{E} + \text{I} \rightarrow \text{H} + \text{J}$	2.646	2.191	0.828
30	$r_{130}$	$\text{H} + \text{I} \rightarrow \text{C} + 2\text{E}$	2.646	0.639	0.242	95	$r_{14}$	$\text{A} + \text{E} \rightarrow \text{I}$	1.732	1.454	0.840
31	$r_{60}$	$2\text{A} + \text{B} \rightarrow \text{C} + \text{I}$	2.646	0.673	0.254	96	$r_{70}$	$2\text{A} + \text{D} \rightarrow \text{E} + \text{J}$	2.646	2.246	0.849
32	$r_4$	$\text{E} \rightarrow \text{F}$	1.414	0.376	0.266	97	$r_{112}$	$\text{B} + \text{I} \rightarrow \text{C} + 2\text{E}$	2.646	2.250	0.850
33	$r_{85}$	$\text{A} + 2\text{F} \rightarrow \text{E} + \text{I}$	2.646	0.714	0.270	98	$r_{53}$	$\text{C} + \text{H} \rightarrow \text{F} + \text{G}$	2.000	1.740	0.870
34	$r_{73}$	$\text{B} + 2\text{D} \rightarrow \text{E} + \text{G}$	2.646	0.729	0.276	99	$r_{104}$	$2\text{A} + \text{H} \rightarrow \text{C} + \text{I}$	2.646	2.320	0.877
35	$r_{86}$	$2\text{A} + \text{F} \rightarrow \text{D} + \text{J}$	2.646	0.736	0.278	100	$r_{68}$	$\text{B} + \text{C} \rightarrow 2\text{F} + \text{H}$	2.646	2.337	0.883
36	$r_{63}$	$2\text{B} + \text{C} \rightarrow 2\text{G}$	3.000	0.874	0.291	101	$r_{38}$	$\text{C} + \text{D} \rightarrow \text{A} + \text{H}$	2.000	1.789	0.895
37	$r_9$	$\text{C} \rightarrow \text{D} + \text{E}$	1.732	0.506	0.292	102	$r_{116}$	$\text{B} + \text{J} \rightarrow 2\text{D} + \text{I}$	2.646	2.390	0.903
38	$r_{64}$	$\text{A} + 2\text{C} \rightarrow \text{G} + \text{J}$	2.646	0.789	0.298	103	$r_{74}$	$\text{A} + 2\text{E} \rightarrow \text{D} + \text{I}$	2.646	2.392	0.904
39	$r_8$	$\text{C} \rightarrow 2\text{F}$	2.236	0.699	0.313	104	$r_{48}$	$\text{A} + \text{I} \rightarrow \text{D} + \text{J}$	2.000	1.817	0.908
40	$r_{12}$	$\text{A} + \text{D} \rightarrow \text{I}$	1.732	0.542	0.313	105	$r_{54}$	$\text{C} + \text{I} \rightarrow \text{B} + \text{J}$	2.000	1.958	0.979
41	$r_{32}$	$\text{B} + \text{C} \rightarrow \text{D} + \text{G}$	2.000	0.657	0.328	106	$r_{44}$	$\text{B} + \text{F} \rightarrow \text{E} + \text{H}$	2.000	2.021	1.011
42	$r_{25}$	$2\text{C} \rightarrow \text{B} + \text{I}$	2.449	0.816	0.333	107	$r_{18}$	$\text{G} \rightarrow \text{D} + \text{H}$	1.732	1.868	1.079
43	$r_{99}$	$\text{D} + 2\text{E} \rightarrow \text{C} + \text{F}$	2.646	0.882	0.333	108	$r_{37}$	$\text{B} + \text{D} \rightarrow \text{F} + \text{G}$	2.000	2.208	1.104
44	$r_{96}$	$2\text{B} + \text{F} \rightarrow \text{G} + \text{H}$	2.646	0.893	0.338	109	$r_{128}$	$2\text{F} + \text{I} \rightarrow \text{H} + \text{J}$	2.646	2.923	1.105
45	$r_{26}$	$2\text{C} \rightarrow \text{H} + \text{I}$	2.449	0.836	0.341	110	$r_{61}$	$2\text{A} + \text{B} \rightarrow \text{H} + \text{J}$	2.646	2.944	1.113
46	$r_{79}$	$2\text{A} + \text{E} \rightarrow \text{F} + \text{J}$	2.646	0.926	0.350	111	$r_{125}$	$2\text{F} + \text{H} \rightarrow \text{D} + \text{G}$	2.646	2.989	1.130
47	$r_{115}$	$2\text{D} + \text{H} \rightarrow \text{E} + \text{G}$	2.646	0.963	0.364	112	$r_{47}$	$2\text{I} \rightarrow \text{C} + \text{J}$	2.449	2.770	1.131
48	$r_{94}$	$\text{B} + 2\text{F} \rightarrow \text{C} + \text{H}$	2.646	0.982	0.371	113	$r_{51}$	$\text{D} + \text{G} \rightarrow \text{C} + \text{H}$	2.000	2.297	1.148
49	$r_{39}$	$\text{B} + \text{E} \rightarrow \text{D} + \text{H}$	2.000	0.756	0.378	114	$r_{107}$	$2\text{I} \rightarrow 2\text{F} + \text{J}$	3.000	3.459	1.153
50	$r_{89}$	$2\text{C} + \text{D} \rightarrow \text{G} + \text{I}$	2.646	1.032	0.390	115	$r_{66}$	$\text{B} + \text{C} \rightarrow 2\text{E} + \text{H}$	2.646	3.085	1.166
51	$r_{22}$	$\text{A} + \text{B} \rightarrow \text{C} + \text{E}$	2.000	0.802	0.401	116	$r_1$	$\text{B} \rightarrow \text{H}$	1.414	1.650	1.167
52	$r_3$	$\text{D} \rightarrow \text{F}$	1.414	0.570	0.403	117	$r_{50}$	$\text{A} + \text{I} \rightarrow \text{F} + \text{J}$	2.000	2.378	1.189
53	$r_{41}$	$\text{C} + \text{E} \rightarrow \text{A} + \text{H}$	2.000	0.883	0.442	118	$r_{122}$	$2\text{E} + \text{H} \rightarrow \text{F} + \text{G}$	2.646	3.174	1.200
54	$r_{16}$	$\text{G} \rightarrow \text{B} + \text{F}$	1.732	0.787	0.454	119	$r_{36}$	$\text{B} + \text{D} \rightarrow \text{E} + \text{H}$	2.000	2.581	1.291
55	$r_{92}$	$\text{A} + \text{G} \rightarrow \text{C} + 2\text{F}$	2.646	1.213	0.458	120	$r_{114}$	$\text{D} + 2\text{H} \rightarrow \text{B} + \text{G}$	2.646	3.519	1.330
56	$r_{65}$	$\text{B} + \text{C} \rightarrow 2\text{D} + \text{H}$	2.646	1.231	0.465	121	$r_{49}$	$\text{A} + \text{I} \rightarrow \text{E} + \text{J}$	2.000	2.753	1.376
57	$r_{28}$	$\text{A} + \text{C} \rightarrow \text{D} + \text{I}$	2.000	0.954	0.477	122	$r_{101}$	$\text{A} + 2\text{H} \rightarrow \text{C} + \text{G}$	2.646	3.658	1.383
58	$r_{129}$	$\text{H} + \text{I} \rightarrow \text{C} + 2\text{D}$	2.646	1.270	0.480	123	$r_{82}$	$2\text{G} \rightarrow \text{C} + 2\text{H}$	3.000	4.164	1.388
59	$r_{119}$	$\text{B} + \text{J} \rightarrow 2\text{F} + \text{I}$	2.646	1.273	0.481	124	$r_{20}$	$\text{G} \rightarrow \text{F} + \text{H}$	1.732	2.426	1.401
60	$r_{98}$	$2\text{D} + \text{E} \rightarrow \text{A} + \text{H}$	2.646	1.293	0.489	125	$r_{106}$	$2\text{I} \rightarrow 2\text{E} + \text{J}$	3.000	4.206	1.402
61	$r_{62}$	$2\text{A} + \text{C} \rightarrow 2\text{I}$	3.000	1.487	0.496	126	$r_{121}$	$2\text{E} + \text{H} \rightarrow \text{D} + \text{G}$	2.646	3.738	1.413
62	$r_{117}$	$2\text{D} + \text{H} \rightarrow \text{F} + \text{G}$	2.646	1.320	0.499	127	$r_{123}$	$2\text{D} + \text{I} \rightarrow \text{H} + \text{J}$	2.646	4.036	1.526
63	$r_{93}$	$\text{B} + 2\text{F} \rightarrow \text{D} + \text{G}$	2.646	1.356	0.513	128	$r_{124}$	$\text{F} + 2\text{H} \rightarrow \text{B} + \text{G}$	2.646	4.075	1.540
64	$r_{31}$	$2\text{E} \rightarrow \text{D} + \text{F}$	2.449	1.321	0.539	129	$r_{19}$	$\text{G} \rightarrow \text{E} + \text{H}$	1.732	2.800	1.616
65	$r_{78}$	$2\text{B} + \text{D} \rightarrow \text{G} + \text{H}$	2.646	1.433	0.542	130	$r_{120}$	$\text{E} + 2\text{H} \rightarrow \text{B} + \text{G}$	2.646	4.447	1.681
						131	$r_{55}$	$\text{C} + \text{I} \rightarrow \text{H} + \text{J}$	2.000	3.606	1.803

approach, the analyses of the obtained solutions run better.

A list of the first ten implicitly generated reaction networks was obtained with established kinetic expressions using GAMS® software with the commercial solver CPLEX. The true chemical reactions  $r_4$ ,  $r_9$ ,  $r_{13}$  and  $r_{21}$  appear in all 10 solutions presenting the same respective homogeneous kinetic expressions. The unique true chemical reaction that did not appear in those solutions is  $r_{118}$ . The objective function values varied among  $\phi = [8.666, 8.985]$  in those solutions, presenting a CPU usage within [74.4 min, 172.8 min]. The solutions presented great computational effort, even considering a relaxation in the optimization convergence criteria (the absolute and the relative gaps). However, all the obtained solutions converged to the optimal integer solution with normal completion status.

When fixing the reaction binary variables to converge to the true reaction network, the solution presents  $\phi = 13.310$ . At this problem with fixed reactions as solution constituent, the kinetic models converged to the same structure of the best expressions found in Step 6 of the methodology, and presented almost the same parameters values of the ones obtained using DM method in Step 6. These kinetic expressions and respective parameters estimates, are presented in the next section. However, from that list, the only network that will be analyzed here, in more detail, is the one with lowest  $\phi$  value, *i.e.*, the best structure found according to the considered optimization problem. The best structure found is shown in Figure 11.31.

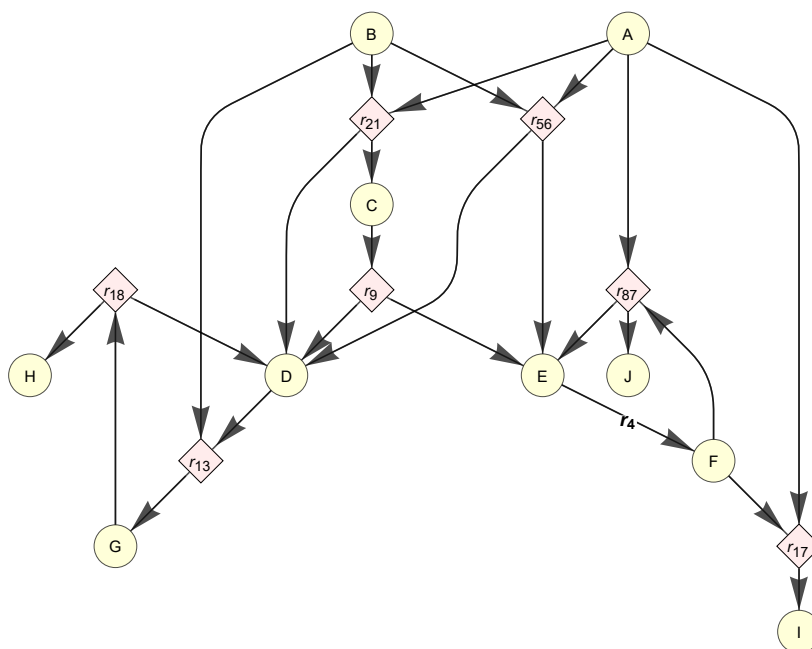
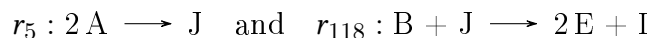


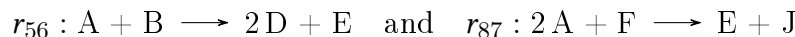
**Figure 11.31** First implicitly generated network structure with simultaneous identification of kinetic models.

This reaction network contains six of the eight true stoichiometries: presenting  $r_4$ ,  $r_9$ ,  $r_{13}$ ,  $r_{17}$ ,  $r_{18}$  and  $r_{21}$  in common with the true network, and presenting  $r_{56}$  and  $r_{87}$  as additional

chemical reactions instead of  $r_5$  and  $r_{118}$ . Notice that



were replaced by



in which one of them forms a set of linearly dependent chemical reactions, *i.e.*, the matrix rank of the stoichiometric matrix, concerning the reaction network in Figure 11.31 composed by eight chemical reactions, is seven. The kinetic expression regarding  $r_{87}$  converged to an homogeneous kinetics of 2nd order as a function of a single initial reactant species (see Table 11.25). Notice that the reaction  $r_5$  can also be described by an homogeneous kinetics of 2nd order as a function of A species, as it will be shown in the next section. However, both  $r_5$  and  $r_{87}$  (i) present small reaction extents in every experiment and (ii) originate the same side-product species J that is substantially affected by the noise. Similar observations happens to  $r_{118}$ , which is a chemical reaction that presents small extents in every experiment, responsible to produce the side-product species I that is also substantially affected by the noise. Therefore, interpreting these results, the obtained optimal model (i) excluded one model component related to  $r_{118}$ , since this component is pretty near to the dot origin in the original network basis, not greatly affecting the value of the objective function, and (ii) added a linearly dependent chemical reaction  $r_{56}$  that fits the data subject to all formulation constraints.

**Table 11.25** List of kinetic expressions identified simultaneously with the reaction network in Figure 11.31, and corresponding parameter estimates  $k$  in  $\text{h}^{-1}$  for every experimental temperature.

$r_j$	Kinetic expression	$k$ at $T = 50^\circ\text{C}$	$k$ at $T = 70^\circ\text{C}$	$k$ at $T = 90^\circ\text{C}$
$r_4$	$k_4E$	0.999	1.239	1.560
$r_9$	$k_9C$	0.803	0.754	0.682
$r_{13}$	$k_{13}BD$	0.097	0.101	0.107
$r_{17}$	$k_{17}AF$	0.024	0.030	0.040
$r_{18}$	$k_{18}G$	0.010	0.020	0.035
$r_{21}$	$k_{21}AB$	0.350	0.444	0.455
$r_{56}$	$k_{56}AB$	0.111	0.217	0.411
$r_{87}$	$k_{87}A^2$	0.007	0.005	0.008

Concluding this analysis, the reaction components that are identifiable, involving species that were weakly affected by noise, are those listed in Table 11.25 that appear in common in both Figure 1.6 and Table 11.26 (with the identified kinetic laws). On the other hand, the remaining reactions can be any as long as, together with the others, they present a consistent network with an acceptable correlation between the reaction rates and the reactant species, since they will not significantly affect the model data adjustment

procedure, *i.e.*, the value of the objective function.

We decided to consider the true network for kinetic modeling of reactions in Step 6, even having already obtained plausible kinetic models with the implicit generation for some reactions of this true network. In this case, we chose to adopt the original reaction labels ( $r_1$  to  $r_8$ ) in order to simplify the notation. The eight true chemical reactions were indexed by the generation number as shown in Table 11.26.

**Table 11.26** True reaction network with corresponding reaction labels numbered according to the reaction generation order.

$r_j$	True chemical reactions	Network graph
$r_{21}$ ( $r_1$ )	$A + B \longrightarrow C + D$	
$r_9$ ( $r_2$ )	$C \longrightarrow D + E$	
$r_4$ ( $r_3$ )	$E \longrightarrow F$	
$r_{13}$ ( $r_4$ )	$B + D \longrightarrow G$	
$r_{18}$ ( $r_5$ )	$G \longrightarrow D + H$	
$r_{17}$ ( $r_6$ )	$A + F \longrightarrow I$	
$r_5$ ( $r_7$ )	$2A \longrightarrow J$	
$r_{118}$ ( $r_8$ )	$B + J \longrightarrow 2E + I$	

### 11.3.5 Reaction kinetic expressions

The 17 datasets were grouped according to their experimental temperature, forming three clusters: data at 70 °C, 50 °C, and 90 °C composed of 7, 5, and 5 datasets, respectively. The reaction kinetic superstructures considered for the 8 chemical reactions are shown in (11.10).

$$\begin{aligned}
 r_1(t) &= k_{1,A}A(t) + k_{1,B}B(t) + k_{1,AB}A(t)B(t) - k_{1,C}C(t) - k_{1,D}D(t) - k_{1,CD}C(t)D(t) \\
 r_2(t) &= k_{2,C}C(t) - k_{2,D}D(t) - k_{2,E}E(t) - k_{2,DE}D(t)E(t) \\
 r_3(t) &= k_{3,E}E(t) - k_{3,F}F(t) \\
 r_4(t) &= k_{4,B}B(t) + k_{4,D}D(t) + k_{4,BD}B(t)D(t) - k_{4,G}G(t) \\
 r_5(t) &= -k_{5,D}D(t) + k_{5,G}G(t) - k_{5,H}H(t) - k_{5,DH}D(t)H(t) \\
 r_6(t) &= k_{6,A}A(t) + k_{6,F}F(t) + k_{6,AF}A(t)F(t) - k_{6,I}I(t) \\
 r_7(t) &= k_{7,A^2}A(t)^2 - k_{7,J}J(t) \\
 r_8(t) &= k_{8,B}B(t) - k_{8,E^2}E(t)^2 - k_{8,I}I(t) - k_{8,E^2I}E(t)^2I(t) + k_{8,J}J(t) + k_{8,BJ}B(t)J(t)
 \end{aligned} \tag{11.10}$$

The best correlation found of  $r = f(C)$  of each reaction superstructure is shown in Figures 11.32 and 11.33, where the corresponding BIC values are reported. The  $k$  values are reported in Table 11.27.

The reaction rates  $r_1$  to  $r_4$  have shown good linear approximation with their reactant species concentration, in Figure 11.32. These chemical reactions are responsible for forming the main chemical products (species C, D, E, F, and G) and occur in more significant proportions than  $r_5$  to  $r_8$ , see Figure 11.33, which are responsible for producing the secondary products (species H, I, and J). These last species are the most affected by noise because they present residual amounts of concentration. Despite producing H,  $r_5$  also produces D to a lesser extent having shown an acceptable linear correlation with the reagent G, in contrast to  $r_6$  to  $r_8$  where the behavior of the rate profiles is more difficult to predict. Thus,  $r_6$  to  $r_8$  have identifiability problems associated with noisy measurements.

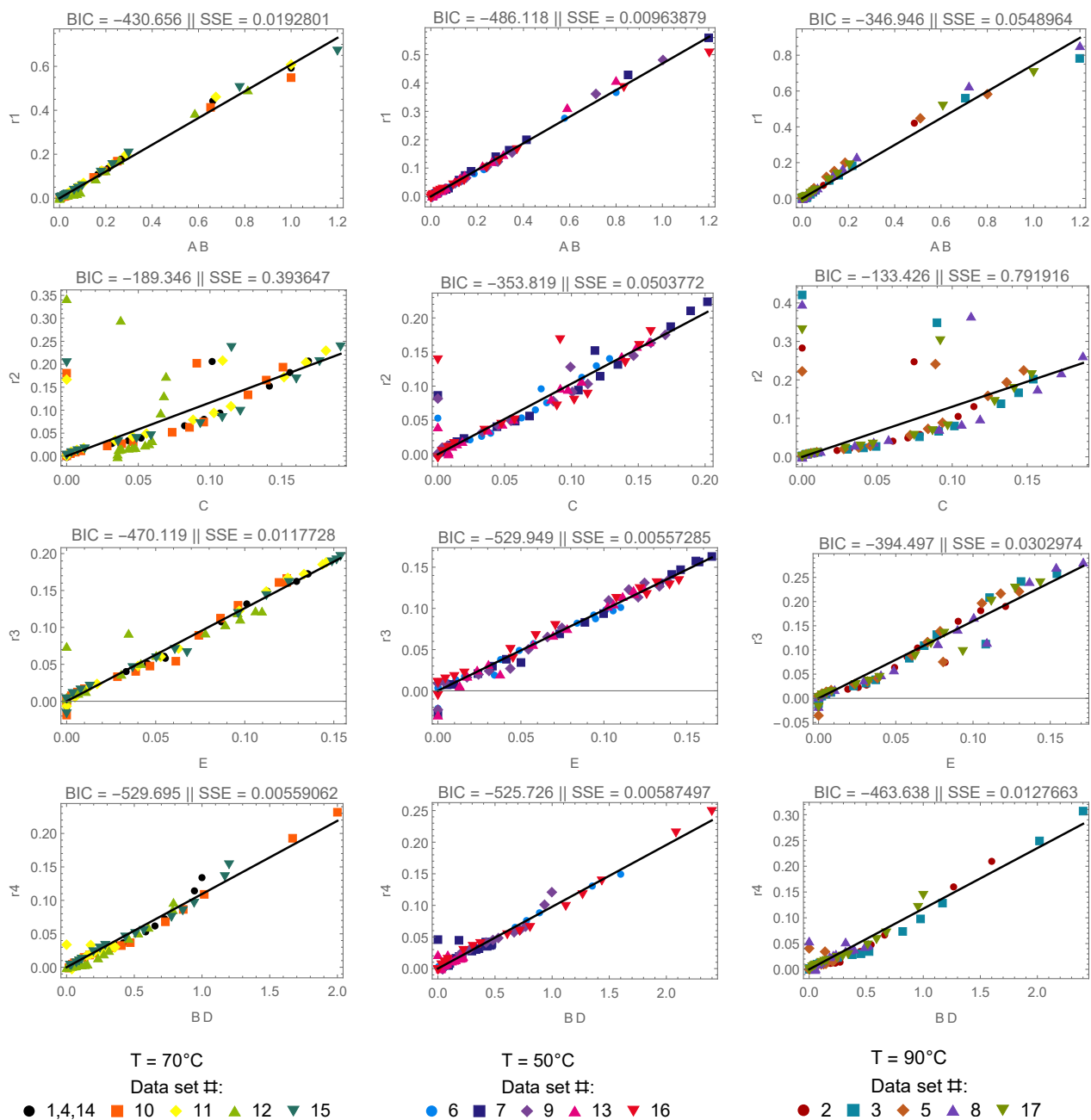


Figure 11.32 Reaction rates  $r_1$  to  $r_4$  as a function of reactant species concentration.



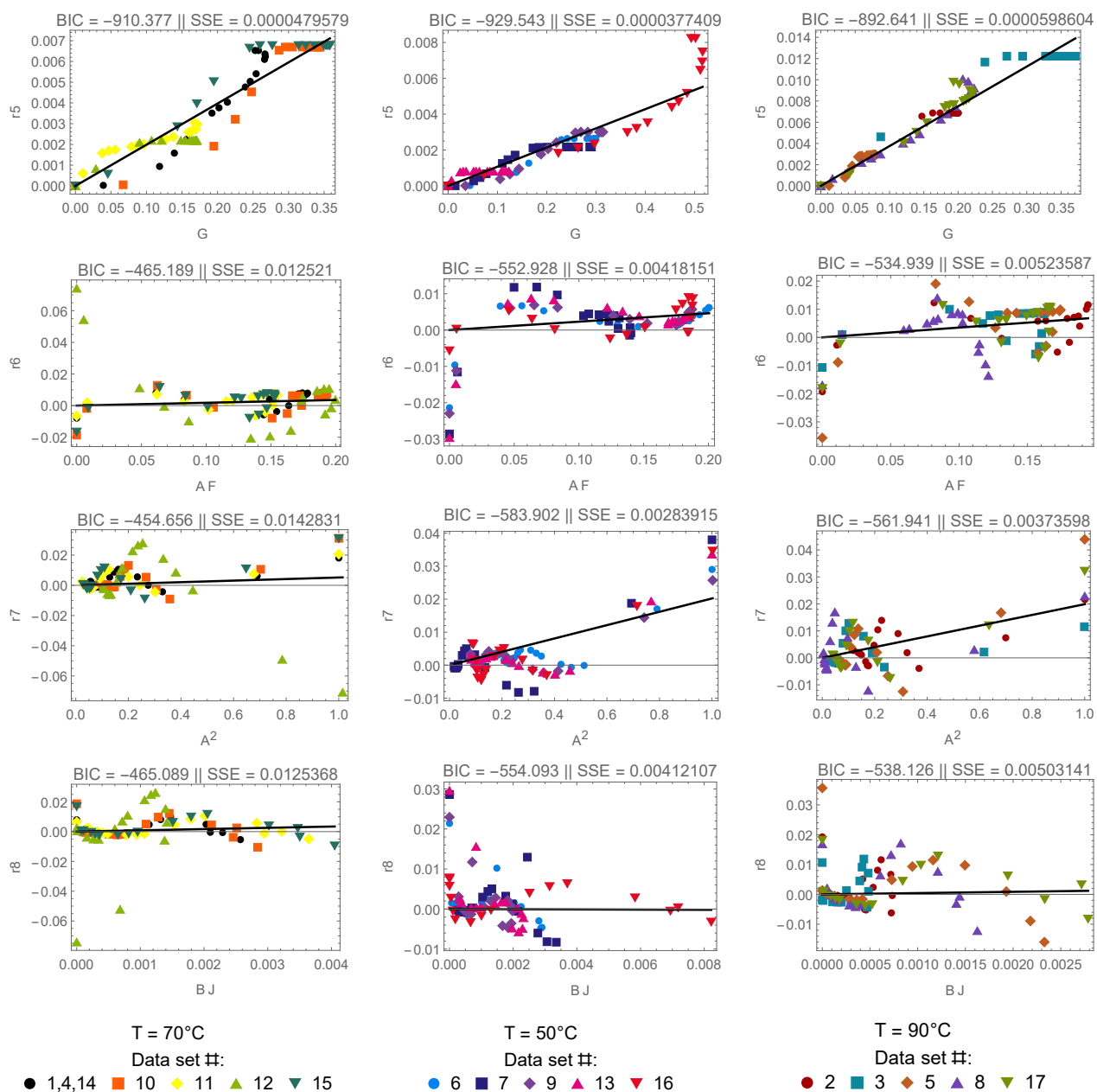


Figure 11.33 Reaction rates  $r_5$  to  $r_8$  as a function of reactant species concentration.

After considering the linear regressions performed individually for each reaction rate in the DM approach, having found the optimal reaction kinetic structures, the IM must be considered for the estimation of bias-free parameters constituting a nonlinear multiple response regression problem for each dataset cluster. In this case, (i) original species concentration measurements (with noise), (ii) the best model structure found, and (iii) the optimal DM solutions as initial parameter estimates, are used. The species mass balances are shown in (11.11). The optimal kinetic parameters with their confidence intervals are presented in Table 11.27, compared to the DM results.

$$\begin{aligned}
 \frac{dA(t)}{dt} &= -k_1A(t)B(t) - k_6A(t)F(t) - 2k_7A(t)^2 \\
 \frac{dB(t)}{dt} &= -k_1A(t)B(t) - k_4B(t)D(t) - k_8B(t)J(t) \\
 \frac{dC(t)}{dt} &= k_1A(t)B(t) - k_2C(t) \\
 \frac{dD(t)}{dt} &= k_1A(t)B(t) + k_2C(t) - k_4B(t)D(t) + k_5G(t) \\
 \frac{dE(t)}{dt} &= k_2C(t) - k_3E(t) + 2k_8B(t)J(t) \\
 \frac{dF(t)}{dt} &= k_3E(t) - k_6A(t)F(t) \\
 \frac{dG(t)}{dt} &= k_4B(t)D(t) - k_5G(t) \\
 \frac{dH(t)}{dt} &= k_5G(t) \\
 \frac{dI(t)}{dt} &= k_6A(t)F(t) + k_8B(t)J(t) \\
 \frac{dJ(t)}{dt} &= k_7A(t)^2 - k_8B(t)J(t)
 \end{aligned} \tag{11.11}$$

**Table 11.27** Optimal kinetic parameters for each dataset cluster. DM: differential method, IM: integral method, and CI: Confidence interval. Parameters  $k$  in  $\text{h}^{-1}$ .

$k_j$	T = 70 °C			T = 50 °C			T = 90 °C		
	DM	IM	CI	DM	IM	CI	DM	IM	CI
$k_1$	0.608	0.654	(0.651, 0.658)	0.468	0.466	(0.463, 0.469)	0.748	0.892	(0.883, 0.900)
$k_2$	1.165	1.251	(1.231, 1.270)	1.035	1.042	(1.022, 1.063)	1.303	1.487	(1.452, 1.522)
$k_3$	1.261	1.307	(1.283, 1.332)	0.981	0.982	(0.961, 1.004)	1.600	1.684	(1.632, 1.736)
$k_4$	0.109	0.111	(0.110, 0.112)	0.098	0.102	(0.101, 0.103)	0.118	0.125	(0.124, 0.127)
$k_5$	0.020	0.021	(0.020, 0.022)	0.011	0.010	(0.009, 0.011)	0.037	0.039	(0.037, 0.040)
$k_6$	0.018	0.029	(0.028, 0.030)	0.023	0.021	(0.020, 0.022)	0.035	0.040	(0.038, 0.041)
$k_7$	0.005	0.010	(0.009, 0.010)	0.020	0.009	(0.009, 0.010)	0.020	0.009	(0.008, 0.010)
$k_8$	0.849	0.476	(0.366, 0.586)	-0.024	0.452	(0.346, 0.557)	0.427	0.361	(0.127, 0.595)

### 11.3.6 Parameter correlation with temperature

The reparametrization of the Arrhenius equation in (10.5) was adopted to estimate the final temperature-dependent parameters, the respective mass balances are shown in (11.12).

$$\begin{aligned}
\frac{dA(t)}{dt} &= -\exp\left(A_{01} - \frac{E_{a1}10^4}{RT}\right)A(t)B(t) - \exp\left(A_{06} - \frac{E_{a6}10^4}{RT}\right)A(t)F(t) - 2\exp\left(A_{07} - \frac{E_{a7}10^4}{RT}\right)A(t)^2 \\
\frac{dB(t)}{dt} &= -\exp\left(A_{01} - \frac{E_{a1}10^4}{RT}\right)A(t)B(t) - \exp\left(A_{04} - \frac{E_{a4}10^4}{RT}\right)B(t)D(t) - \exp\left(A_{08} - \frac{E_{a8}10^4}{RT}\right)B(t)J(t) \\
\frac{dC(t)}{dt} &= \exp\left(A_{01} - \frac{E_{a1}10^4}{RT}\right)A(t)B(t) - \exp\left(A_{02} - \frac{E_{a2}10^4}{RT}\right)C(t) \\
\frac{dD(t)}{dt} &= \exp\left(A_{01} - \frac{E_{a1}10^4}{RT}\right)A(t)B(t) + \exp\left(A_{02} - \frac{E_{a2}10^4}{RT}\right)C(t) - \exp\left(A_{04} - \frac{E_{a4}10^4}{RT}\right)B(t)D(t) + \\
&\quad \exp\left(A_{05} - \frac{E_{a5}10^4}{RT}\right)G(t) \\
\frac{dE(t)}{dt} &= \exp\left(A_{02} - \frac{E_{a2}10^4}{RT}\right)C(t) - \exp\left(A_{03} - \frac{E_{a3}10^4}{RT}\right)E(t) + 2\exp\left(A_{08} - \frac{E_{a8}10^4}{RT}\right)B(t)J(t) \\
\frac{dF(t)}{dt} &= \exp\left(A_{03} - \frac{E_{a3}10^4}{RT}\right)E(t) - \exp\left(A_{06} - \frac{E_{a6}10^4}{RT}\right)A(t)F(t) \\
\frac{dG(t)}{dt} &= \exp\left(A_{04} - \frac{E_{a4}10^4}{RT}\right)B(t)D(t) - \exp\left(A_{05} - \frac{E_{a5}10^4}{RT}\right)G(t) \\
\frac{dH(t)}{dt} &= \exp\left(A_{05} - \frac{E_{a5}10^4}{RT}\right)G(t) \\
\frac{dI(t)}{dt} &= \exp\left(A_{06} - \frac{E_{a6}10^4}{RT}\right)A(t)F(t) + \exp\left(A_{08} - \frac{E_{a8}10^4}{RT}\right)B(t)J(t) \\
\frac{dJ(t)}{dt} &= \exp\left(A_{07} - \frac{E_{a7}10^4}{RT}\right)A(t)^2 - \exp\left(A_{08} - \frac{E_{a8}10^4}{RT}\right)B(t)J(t)
\end{aligned} \tag{11.12}$$

The nonlinear multiple dynamic response problem was solved in **Mathematica**® using the `NonlinearModelFit` function. In the initial iterations the parameters  $E_{a7}$  and  $E_{a8}$  converged to negative values, presenting a result with no physical meaning. Thus, these parameters were set equal to zero in the next iterations, establishing no dependence on temperature, where  $A_{07}$  and  $A_{08}$  are actually  $k$  constant parameters in all datasets. The optimal values of the Arrhenius parameters are shown in Table 11.28. All parameters presented a  $p$ -value lower than  $10^{-6}$ , showing that they have statistical significance. The model simulation with its adjusted parameters is presented in Figures 11.34 to 11.36 for the temperature conditions of 70, 50, and 90 °C, respectively. The global SSE is 0.124, achieved after 9 s of CPU usage.

From the model simulation, one can observe a good model-data agreement for species A to G, and reasonable profile behaviors for H to J, since their original measurements

**Table 11.28** Optimal Arrhenius parameter values:  $A_0$  in  $\text{h}^{-1}$  and  $E_a$  in  $\text{J mol}^{-1}$ .

	$\log(A_0)$	CI	$A_0$	$E_a \times 10^{-4}$	CI
$k_1$	5.112	(5.023,5.202)	166.069	1.579	(1.553,1.604)
$k_2$	3.267	(3.021,3.512)	26.225	0.867	(0.797,0.937)
$k_3$	4.860	(4.565,5.155)	128.981	1.310	(1.227,1.394)
$k_4$	-0.523	(-0.647,-0.399)	0.593	0.473	(0.438,0.509)
$k_5$	7.191	(6.635,7.746)	1326.820	3.156	(2.993,3.320)
$k_6$	1.892	(1.349,2.436)	6.634	1.546	(1.388,1.705)
$k_7$	-4.662	(-4.707,-4.618)	0.009	0	—
$k_8$	-0.806	(-0.976,-0.636)	0.447	0	—

are noisy, presenting observations with random trends. The model simulation for every dataset is presented in Figure 11.37. The proposed methodology of kinetic modeling of chemical reactions (Step 6), from a known reaction stoichiometry, was able to (i) identify the kinetic expression of each chemical reaction and (ii) perform its parameter estimates, describing well the noisy data available in the case study of the Pfizer company.

## Bibliography

- Box, G., Hunter, W., MacGregor, J., and Erjavec, J. (1973). Some problems associated with the analysis of multiresponse data. *Technometrics*, 15(1):33–51.
- Fugitt, R. E. and Hawkins, J. E. (1945). The liquid phase thermal isomerization of  $\alpha$ -pinene. *Journal of the American Chemical Society*, 67(2):242–245.
- Fugitt, R. E. and Hawkins, J. E. (1947). Rate of the thermal isomerization of  $\alpha$ -pinene in the liquid phase. *Journal of the American Chemical Society*, 69(2):319–322.
- Stewart, W. E., Caracotsios, M., and Sørensen, J. P. (1992). Parameter estimation from multiresponse data. *AIChE Journal*, 38(5):641–650.
- Stewart, W. E. and Sørensen, J. P. (1981). Bayesian estimation of common parameters from multiresponse data with missing observations. *Technometrics*, 23(2):131–141.
- Tjoa, I. B. and Biegler, L. T. (1991). Simultaneous solution and optimization strategies for parameter estimation of differential-algebraic equation systems. *Industrial & Engineering Chemistry Research*, 30(2):376–385.
- Vertis, C. S., Oliveira, N. M., and Bernardo, F. P. (2016). Constrained smoothing of experimental data in the identification of kinetic models. In Kravanja, Z. and Bogataj, M., editors, *26th European Symposium on Computer Aided Process Engineering*, volume 38 of *Computer Aided Chemical Engineering*, pages 2121–2126. Elsevier.
- Wells, G. and Rose, L. (1986). *The Art of Chemical Process Design*. Computer-aided chemical engineering. Elsevier.

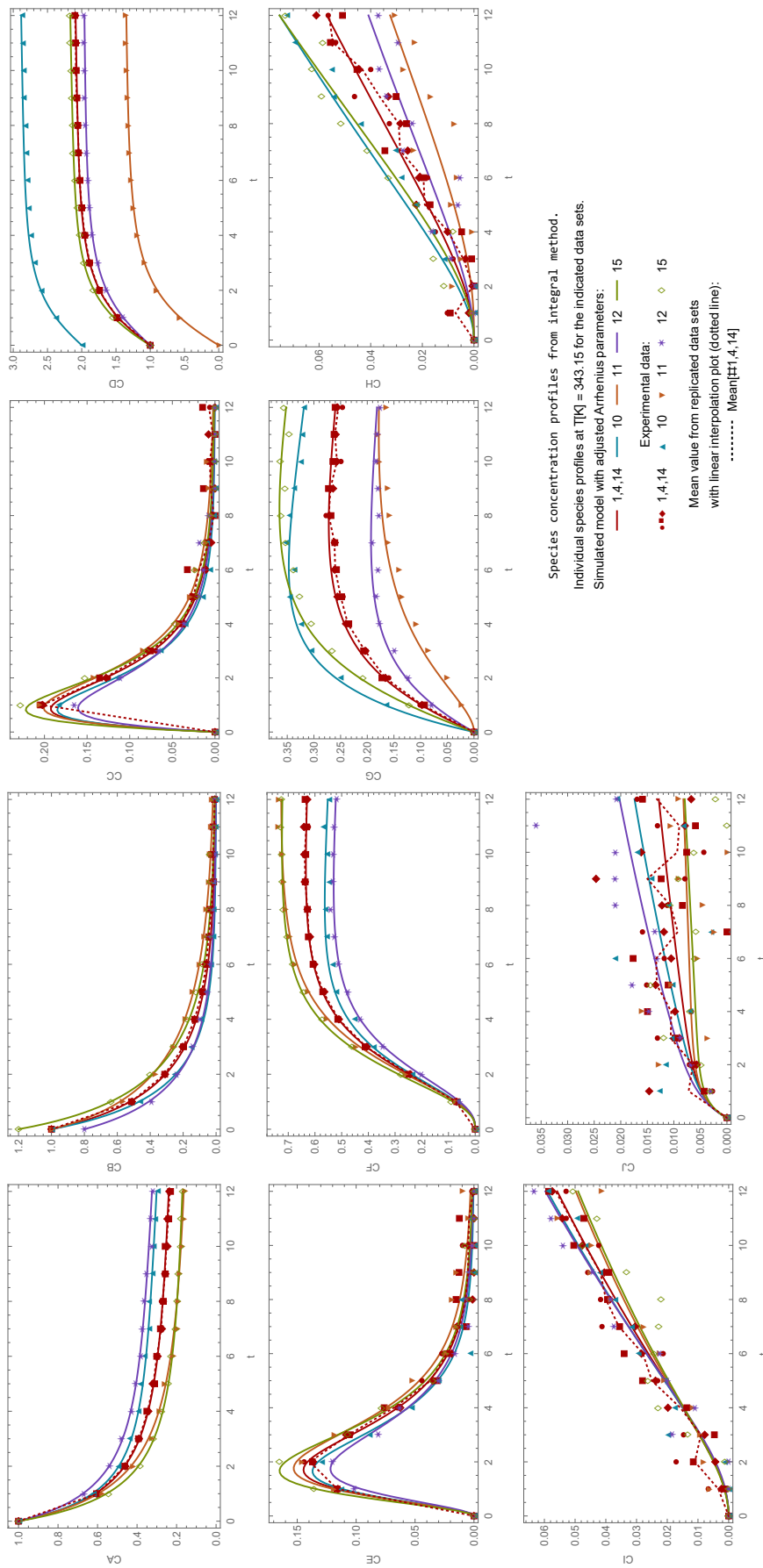


Figure 11.34 Individual species concentration profiles at 70 °C.

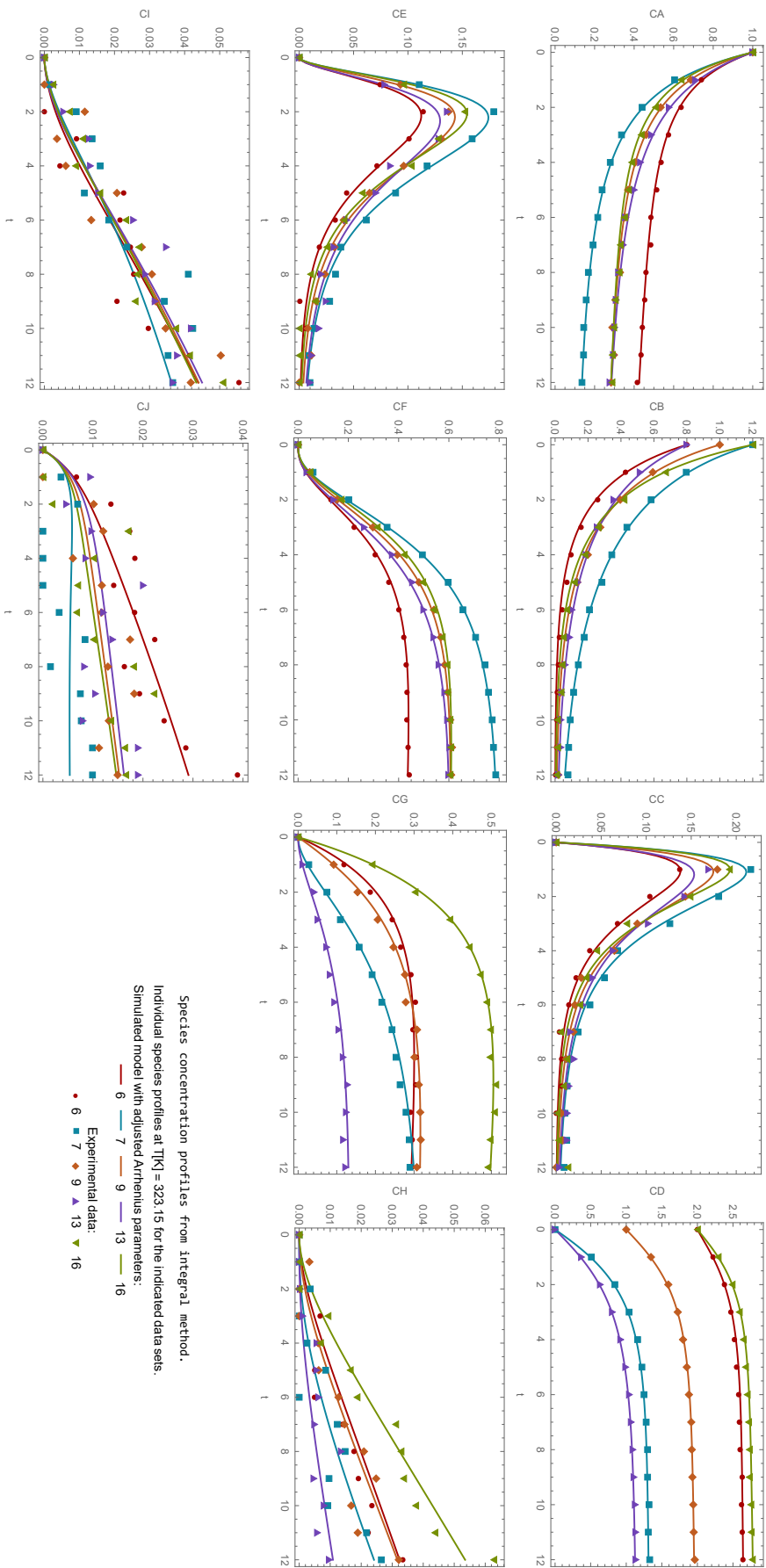


Figure 11.35 Individual species concentration profiles at 50°C.

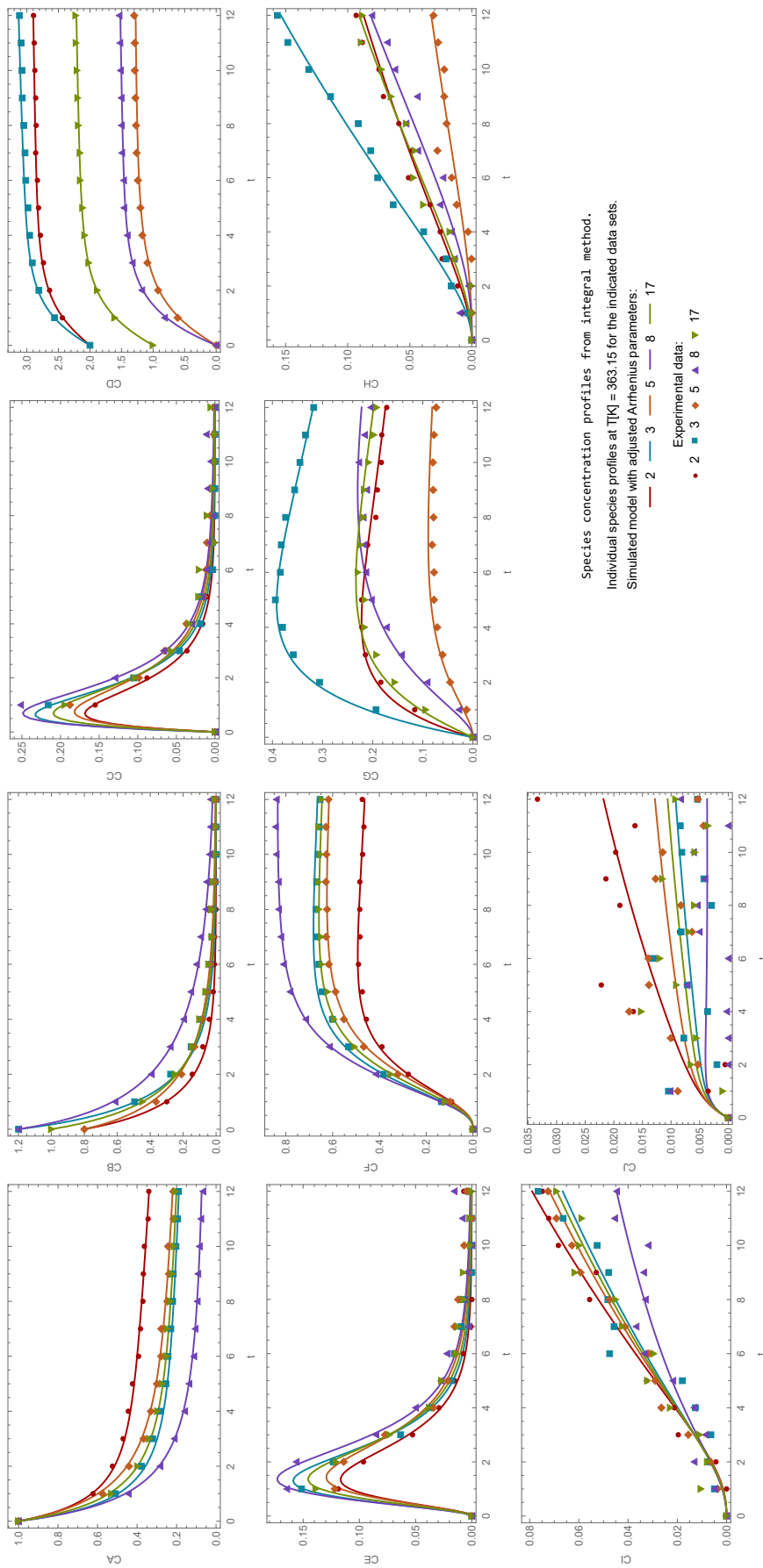
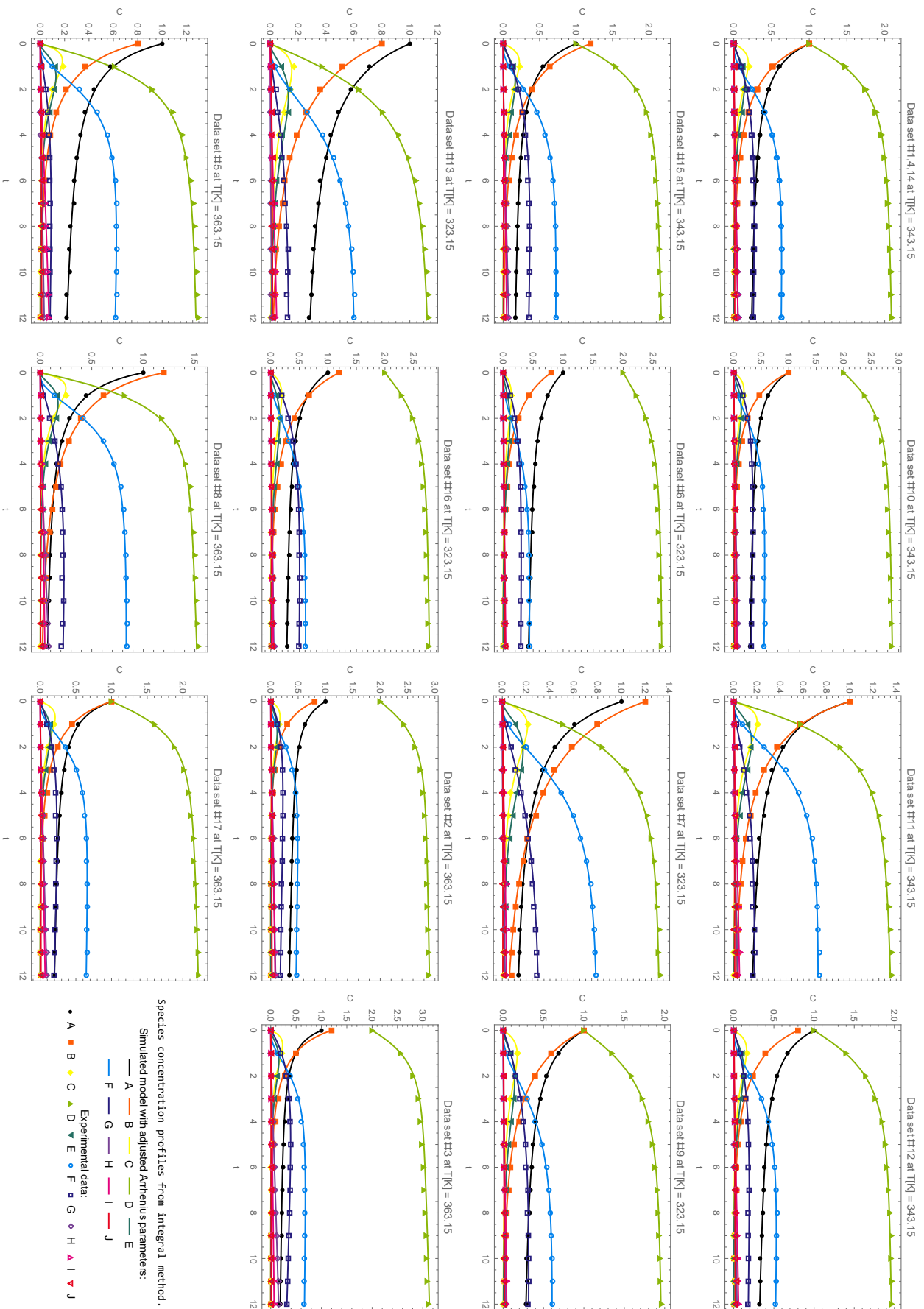


Figure 11.36 Individual species concentration profiles at 90 °C.





# Chapter 12

## Conclusions and Possible Extensions

*“Knowledge gives humility, from humility comes worthiness, from worthiness one gets wealth, from wealth (one does) righteous deeds, from that (comes) joy.”*

– Hitopadesha, 12th-century CE

### Contents

---

12.1 Main methodology attributes and contributions . . . . .	347
12.2 Conclusions related to the case studies . . . . .	349
12.3 Possible extensions of the methodology . . . . .	351

---

### 12.1 Main methodology attributes and contributions

Attending to Problems P1 to P5 listed in the thesis introduction, a systematic methodology was proposed for incrementally build first principles models incorporating experimental data and chemical reaction theoretical knowledge. The methodology contemplates a data processing step that enables obtaining robust estimates of the species concentrations together with their time derivatives to support structural model identification. The time derivatives of these smoothed profiles are then the basis to identify the reaction network that explains/respects the key directions of species compositional changes. Finally, reaction kinetic expressions for each component of the model are individually identified from the respective reaction rates. When parts of the model are not satisfactorily identified, design of experiments is considered in order to elucidate the complete structure of the model under analysis. Therefore, a systematic and generic methodology was developed, allowing the incremental construction of robust models taking full advantage of experimental data and various optimization techniques. The proposed methodology can be used for simplification of dynamic models, transforming complex dynamic models into physical meaningful models, removing redundant elements and identifying time-invariant

relationships. Thus, the obtained model increases process knowledge and facilitates process scale-up, monitoring, control and optimization, which in fact, naturally, may be used for improving safety, product quality and productivity.

The next item list summarizes the main methodology characteristics:

- The identification of the reaction network is uncoupled from the kinetic parameter estimates. The use of the differential method supports the network identification. Basically the model components that constitute the network correspond to key directions of compositional changes. In this sense, the network consists of a basis that spans the data variant space. The methodology spans all plausible bases for that variant space, ensuring that the best structure is found. For elucidating uncertain pathways, or discriminate between candidate network structures, experimental proposals can be suggested based on model information obtained.
- The enumeration of reaction networks is considered using MILP formulations, ensuring linear independence among chemical reactions and feasible connected solutions from a superstructure of reaction networks. These formulations are generic, and they can be applied for synthesis of any process that can be described by graphs. The incorporation of precedence constraints is considered for nonlinear structures synthesis, guaranteeing, beyond connectivity, network consistency. The formulations developed are a contribute to the state of the art. However, it consists of a combinatorial problem that can be computational intensive for large problem sizes.
- The implicit generation of networks that incorporates experimental data in the formulation is considered in order to enumerate plausible solutions that (most) close the species differential mass balance with positive reaction fluxes; or in a more restrictive perspective/outlook, the implicit generation of networks that present good correlations between reaction fluxes and respective reactant species concentration for each reaction model component can be also considered, for avoiding combinatorial problems (explosion) in the explicit network enumeration.
- Data treatment with incorporation of time-invariant relationships is a crucial step of the proposed methodology. It increases data accuracy and enables good estimates of species fluxes, supporting the entire structural model identification.
- The methodology incorporates the use of methods for determining data variant and invariant spaces, and validating them. A novel method for determining the data invariant space dimension supported on SVD was proposed in the thesis.
- The identification of kinetic expressions is performed separately/individually for each model component. It is supported on the differential method and Bayesian information criterion. For reaction kinetic modeling, a systematic methodology is proposed that captures linear correlation among reaction rates (or a surrogate variable/response/dependent variable) and species concentration, identifying the

best kinetic expression that fits data with the lowest number of parameters. After the structure of the model has been identified, the integral method is also considered for obtaining unbiased parameter estimates, according to the maximum likelihood criterion. The obtained solution approaches the global optimum since the initial biased estimates were obtained using the incremental methodology proposed, where the model is developed with great accuracy and robustness.

- In order to support the identification of the model, the need for more experimental data and, consequently, for proposals for additional experiments can happen in three phases of the methodology: during (i) data treatment and data analysis, in order to help the identification of data dimension and time-invariant relationships, (ii) network identification phase, in order to elucidate uncertain reaction pathways (in general for elucidating the origin of residual species), and, finally, (iii) kinetic model development, for discrimination between candidate kinetic expressions. However, it is notable that these experiments are aimed at elucidating specific problems that arise from incomplete/unsatisfactory information, which in turn constitute model results obtained during the application of the methodology. Therefore, these experimental proposals are model-driven, supported on mechanistic information.

Table 12.1 presents an overview of the main contributions of the thesis that are relevant for academia and industrial applications, pointing out their advantages and limitations. Notice that each thesis contribution corresponds to the main objective of a particular methodology step.

## 12.2 Conclusions related to the case studies

The main results obtained from the methodology application to the considered case studies are presented in this conclusion section.

On the basis of the results obtained for AP and MAC case studies, it can be concluded that a systematic development of models is very important for obtaining models of reduced complexity (simpler models) with great confidence that still are highly process descriptive, (when compared to literature model proposals).

The AS case study enabled to conclude that experimental data with high uncertainty may compromise the complete identification of the model structure, requiring additional experiments for allowing a better explanation of the network structure, eventually validating the network proposed in the literature. In addition, regarding the enumeration of reaction networks, this case study has demonstrated that the use of (i) energetic criterion for constraining the network superstructure, enabled a significant reduction of the number of generated networks, saving time and computational effort, and (ii) of precedence constraints is required for generating consistently connected nonlinear reaction networks.

On the basis of the results obtained for MAC case study, it can be concluded that system-

**Table 12.1** Main contributions of the thesis for academia and industrial applications with advantages and limitations.

Main contributions	Advantages and benefits	Disadvantages and limitations
Data processing with incorporation of time-invariant relationships — Step 1.	<ul style="list-style-type: none"> <li>• Increase data accuracy. / Decrease data noise content.</li> <li>• Enable incremental model building and support structural model identification (reaction network and kinetic expressions).</li> <li>• Good estimates of species fluxes.</li> <li>• Smooth and accurate species profiles.</li> </ul>	<ul style="list-style-type: none"> <li>• Hard to be automated due to the need of incorporating qualitative analysis (iterative insertion of profile shape constraints).</li> </ul>
Linear and nonlinear network synthesis (with explicit and implicit graphs enumeration) — Steps 4 and 5.	<ul style="list-style-type: none"> <li>• Generic formulation for any process that can be described by connected structures.</li> <li>• Can generate nonlinear structures verifying precedence constraints (consistently connected structures).</li> <li>• Can incorporate experimental data for network identification without the need of establishing kinetic laws (implicit generation of plausible networks).</li> <li>• Can simultaneously identify the reaction kinetic expression (implicit generation of plausible networks with identified kinetic expressions).</li> <li>• Flexible formulation, can incorporate heuristic and chemistry knowledge.</li> <li>• Can control the linear (in)dependence of chemical reactions/model components.</li> </ul>	<ul style="list-style-type: none"> <li>• Can be computational intensive for large problem sizes.</li> <li>• Needs a pre-specified superstructure of networks.</li> <li>• For implicit enumeration of networks with kinetic model elucidation, it captures the <i>linear</i> correlation among reaction flux and species concentration.</li> </ul>
Systematic reaction kinetic modeling methodology. (Identification of reaction expressions with best balance of data agreement and parameters number). Step 6.	<ul style="list-style-type: none"> <li>• Easily automated, generic and flexible formulation.</li> <li>• Use of information criterion (BIC).</li> <li>• Can incorporate heterogeneous and homogeneous kinetic laws.</li> <li>• Model reparameterization for modeling parameter correlation with temperature.</li> </ul>	<ul style="list-style-type: none"> <li>• Requires the reaction network previously identified, composed by linearly independent reaction components.</li> <li>• The superstructure of kinetic expressions must be linear in its parameters.</li> </ul>
Methodology to validate reaction invariants and determine the data invariant space dimension — Step 2.	<ul style="list-style-type: none"> <li>• Enables model reduction.</li> <li>• Increase model identification.</li> <li>• Full comprehension of the network topology for a better description of the system dynamics.</li> </ul>	<ul style="list-style-type: none"> <li>• Results accuracy dependent of noise level in data.</li> <li>• Needs SVD of the data matrix.</li> </ul>
Superstructure of reaction networks synthesis — Step 3.	<ul style="list-style-type: none"> <li>• Incorporates reaction-invariant constraints.</li> <li>• Flexible, generic formulation.</li> <li>• Incorporates reaction energetic analysis.</li> <li>• Incorporates data analysis (TFA).</li> </ul>	<ul style="list-style-type: none"> <li>• Needs data invariant space basis and/or reaction theoretical invariant relationships.</li> <li>• Needs thermodynamic reaction parameters.</li> <li>• Needs data variant space basis.</li> </ul>

atic methods for reaction kinetic modeling is required for accurate model identification, avoiding overparameterization, and obtaining tight parameter confidence intervals.

The impact on the use of time-invariant relationships in the data reconciliation procedure was demonstrated using data from the pharmaceutical Pfizer company. It was demonstrated that under-dimensioned null spaces have a negative impact on the final quality of the reconciled data obtained, compromising the complete structural identification of the model. Therefore, when properly applied, these conserved relationships reduce the noise-to-signal ratio, and consequently, increase the model identifiability using reconciled data. This is an important contribute of the thesis for the state of the art.

Moreover, the implicit generation of reaction networks were tested considering the AP and Pfizer case studies, showing that it is possible to incorporate experimental data in the network generation phase to structural identification, and thus, consequently, reduce the number of alternative model candidates to be further analyzed, but at the cost of loosing incremental model development.

## 12.3 Possible extensions of the methodology

The improvement of the design of experiments in Step 7 of the methodology is one of the future works that should be considered. Several steps in the methodology may lead to the conclusion that more data is needed, however, at each step the need for more data can have a different reason. For example, in Step 2 additional data may be needed to (i) help in identifying the dimension of the data in the variant form, and (ii) establish the number of invariant relationships over time. In Step 5, additional data may be needed to discriminate plausible reaction network structures, thus elucidating the uncertain origin of residual species, for example. In Step 6, additional data may be needed to identify candidate kinetic expressions that have shown equal data-fitting performance. For these reasons, a more systematic approach to designing experiments should be considered, taking advantage of existing methods in the literature and incorporating new techniques aimed to solve the specific problems described above.

Another future work is to demonstrate the impact of handling reliable models that describe a reaction system for applications after the modeling phase on, for example, optimum design of equipment, monitoring and control of chemical industrial processes, and energy and mass integration of processes. In this scope, the comparison of models must be carried out, together with a sensitivity analysis of the optimal solution obtained in the presence of variations in the model parameters.

Finally, another interesting field for future work is to improve the proposed methodology by incorporating more data-driven approaches, supported on statistical learning techniques, enabling the obtainment of hybrid models. This may require the use of deterministic and empirical modeling strategies for determining (semi) surrogate models that can enable a better description of the chemical reaction process.



# Appendix I

## Basic Concepts

This chapter presents basic concepts that support methods proposed and used in the thesis, namely the Singular Value Decomposition in Appendix I.1, the orthogonal projection of vectors in linear spaces in Appendix I.2, and singular values and eigenvalues related definitions in Appendix I.3.

### I.1 Singular Value Decomposition

The Singular Value Decomposition (SVD) is a matrix factorization technique in which the original matrix, is decomposed in three matrices with particular characteristics. For example, consider an arbitrary matrix  $\mathbf{X} \in \mathbb{R}^m \times n$  which is decomposed as

$$\mathbf{X} = \mathbf{U} \cdot \mathbf{\Sigma} \cdot \mathbf{V}^T \quad (\text{I.1})$$

where  $\mathbf{U}$  is a squared real matrix with dimensions dictated by the number of rows of  $\mathbf{X}$ , *i.e.*,  $\mathbf{U} \in \mathbb{R}^m \times m$ ,  $\mathbf{\Sigma}$  is a diagonal matrix with the same dimensions of  $\mathbf{X}$  with positive entries,  $\mathbf{\Sigma} \in \mathbb{R}_+^m \times n$ , and  $\mathbf{V}$  another squared real matrix with dimensions dictated by the number of columns of  $\mathbf{X}$ , *i.e.*,  $\mathbf{V} \in \mathbb{R}^n \times n$ . Matrices  $\mathbf{U}$  and  $\mathbf{V}$  are *orthonormal*, *i.e.*, they are formed by orthogonal unitary vectors. The inner product of orthonormal vectors is zero. The inner product of an orthonormal vector with itself is unity. Hence  $\mathbf{U}$  and  $\mathbf{V}$  are full rank and

$$\mathbf{U}^T \cdot \mathbf{U} = \mathbf{U} \cdot \mathbf{U}^T = \mathbf{I}_m \quad \text{and} \quad \mathbf{V}^T \cdot \mathbf{V} = \mathbf{V} \cdot \mathbf{V}^T = \mathbf{I}_n \quad (\text{I.2})$$

where  $\mathbf{I}$  is the *identity matrix* with the respective dimensions  $m$  and  $n$ . The  $\mathbf{\Sigma}$  diagonal positive entries are sorted in a decreasing order, *i.e.*,  $\sigma_{1,1} \geq \sigma_{2,2} \geq \sigma_{3,3} \geq \dots \geq 0$ , and the number of  $\sigma_{i,j} : i = j, (i,j) = 1, \dots, \min(m,n)$ , differing zero, establishes the matrix rank,  $R$ , of  $\mathbf{X}$ .

Since only the diagonal entries of  $\mathbf{\Sigma}$  can be different of zero, it is possible to write the

same factorization as a sum of outer products  $\mathbf{u} \otimes \mathbf{v}$  scaled by the respective  $\sigma$ , *i.e.*,

$$\mathbf{X} = \sum_{i=j}^{\min(m,n)} \sigma_{i,j} \mathbf{u}_i \cdot \mathbf{v}_j^T \tag{I.3}$$

where each matrix  $\mathbf{u}_i \cdot \mathbf{v}_j^T, i = j$ , has unitary rank.

However when  $R \leq \min(m,n)$  and  $m \neq n$ , there exists the economy SVD form in which

$$\mathbf{X} = \hat{\mathbf{U}} \cdot \hat{\Sigma} \cdot \hat{\mathbf{V}}^T \tag{I.4}$$

where  $\hat{\mathbf{U}} \in \mathbb{R}^{m \times R}$ ,  $\hat{\Sigma} \in \mathbb{R}_+^{R \times R}$ , and  $\hat{\mathbf{V}} \in \mathbb{R}^n \times R$ .

In cases where  $R < \min(m,n)$ ,  $\mathbf{X}$  contains linear dependencies in  $n - R$  columns and  $m - R$  rows, thus, there exists  $n - R$  null  $\sigma$  diagonal entries, *i.e.*,  $\sigma_i = 0, i = R + 1, \dots, n$ . For notation simplification consider  $\sigma_i \equiv \sigma_{i,j}, i = j$ . Therefore in (I.3) will exists (i)  $n - R$  matrices (multiplied by null values) and (ii)  $m - R$  vectors  $\mathbf{u}$ , *i.e.*,  $\mathbf{u}_i, i = R + 1, \dots, m$ , that are not contributing to  $\mathbf{X}$  formation. In Figure I.1 there is an example where  $R = n < m$  of the economy SVD of  $\mathbf{X}$ .

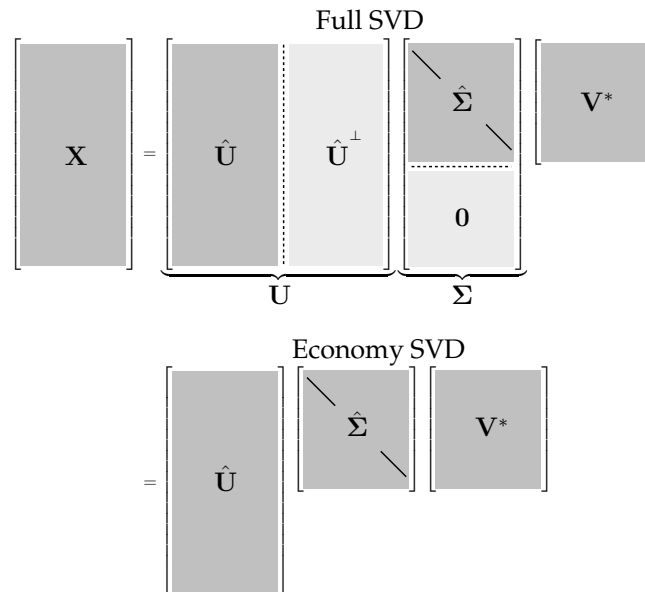


**Figure I.1** Schematic representation of the SVD of  $\mathbf{X}[m \times n]$  and economy SVD of  $\mathbf{X}$  when  $R = n$ , *i.e.*,  $\mathbf{X}$  in non-singular (full rank) in this example. Notice that all diagonal entries are positive,  $\sigma_i > 0, i = 1, \dots, n$ , but once  $m > n$  there exists the economy SVD.  $\mathbf{V}^* \equiv \mathbf{V}^T$  (Brunton and Kutz, 2019). Copyright (2021) by Cambridge University Press.

These  $\mathbf{u}_i, i = R + 1, \dots, m$  and  $\mathbf{v}_j, j = R + 1, \dots, n$  are exactly the vectors that form, respectively, the orthogonal basis of left and right null spaces of  $\mathbf{X}$ . Hence the economy SVD, in (I.4), excludes the components related to the null spaces of  $\mathbf{X}$ . On the other hand, the



components that do contribute to  $\mathbf{X}$  formation, for example in eqs. (I.3) and (I.4), are located at the column and row spaces of  $\mathbf{X}$ , such that  $\mathbf{u}_i$  and  $\mathbf{v}_i, i = 1, \dots, R$  are orthogonal basis for the column and row space of  $\mathbf{X}$ , respectively. These vectors  $\mathbf{u}_i$  and  $\mathbf{v}_i, i = 1, \dots, R$  are named as *left* and *right singular vectors*, respectively, while  $\sigma_i, i = 1, \dots, R$  are the *singular values*  $\mathbf{X}$ . Notice that the left singular vectors multiplies  $\mathbf{X}$  on the left side such that

$$\mathbf{u}_i^T \cdot \mathbf{X} = \sigma_i \mathbf{v}_i^T, \quad i = 1, \dots, R \quad (\text{I.5})$$

while the right singular vectors multiplies  $\mathbf{X}$  on the right side

$$\mathbf{X} \cdot \mathbf{v}_i = \sigma_i \mathbf{u}_i, \quad i = 1, \dots, R \quad (\text{I.6})$$

Therefore the left singular vectors may be viewed as a system of coordinates of the right singular vectors scaled by their respective singular values in the row space of  $\mathbf{X}$ . Similarly the right singular vectors are coordinates of respective left singular vectors weighted by the singular value in the columns space of  $\mathbf{X}$ .

In fact  $\sigma$  translates the importance associated with original data in  $\mathbf{X}$  described on (i) its columns, thus captured in the respective direction  $\mathbf{u}$ , and (ii) its rows, depicted on  $\mathbf{v}$  vectors. Since they are hierarchically sorted in order of decreasing values, the SVD decomposes the original matrix looking for the directions where the variances are largest, and this arrange turns this decomposition unique when all singular values are distinct. When the singular values are degenerated, the uniqueness of this decomposition is no longer valid, although the lack of uniqueness does not affect any of the low-rank approximation properties of SVD (Kambhampati, 2020).

Considering the correlation matrix given by  $\mathbf{C} = \mathbf{X}^T \cdot \mathbf{X}$ , in which  $\mathbf{C}$  is symmetric and positive semi-definite since its entries are obtained from every inner product among column vectors of  $\mathbf{X}^1$ , *i.e.*,

$$\mathbf{C} = \begin{bmatrix} \mathbf{x}_1^T \mathbf{x}_1 & \mathbf{x}_1^T \mathbf{x}_2 & \dots & \mathbf{x}_1^T \mathbf{x}_n \\ \mathbf{x}_2^T \mathbf{x}_1 & \mathbf{x}_2^T \mathbf{x}_2 & \dots & \mathbf{x}_2^T \mathbf{x}_n \\ \vdots & \vdots & \ddots & \vdots \\ \mathbf{x}_n^T \mathbf{x}_1 & \mathbf{x}_n^T \mathbf{x}_2 & \dots & \mathbf{x}_n^T \mathbf{x}_n \end{bmatrix}$$

this matrix can also be obtained through the SVD of  $\mathbf{X}^T \mathbf{X}$  such that

$$\mathbf{C} = \mathbf{V} \cdot \Sigma \cdot \mathbf{U}^T \cdot \mathbf{U} \cdot \Sigma \cdot \mathbf{V}^T = \mathbf{V} \cdot \Sigma^2 \cdot \mathbf{V}^T \quad (\text{I.7})$$

It is possible to see that every right singular vector of  $\mathbf{X}$ ,  $\mathbf{v}_i, i = 1, \dots, R$ , constitutes an *eigenvector* of  $\mathbf{C}$ , *i.e.*,

$$\mathbf{C} \cdot \mathbf{v}_i = \sigma_i^2 \mathbf{v}_i, \quad i = 1, \dots, R \quad (\text{I.8})$$

where  $\sigma_i^2$  is the *eigenvalue* of  $\mathbf{C}$ , corresponding to the squared singular value of  $\mathbf{X}$ .

---

<sup>1</sup>Essentially it guarantees the achievement of nonnegative real eigenvalues.

Similarly, it is also valid for the left singular vectors of  $\mathbf{X}$ ,  $\mathbf{u}_i, i = 1, \dots, R$ , corresponding to the eigenvectors of  $\mathbf{C}^T$ , such that

$$\mathbf{C}^T \mathbf{u}_i = \sigma_i^2 \mathbf{u}_i, \quad i = 1, \dots, R \quad (\text{I.9})$$

Therefore another valid interpretation related to  $\mathbf{U}$ ,  $\Sigma$  and  $\mathbf{V}$  follows the correlation criterion, the columns of  $\mathbf{U}$  and  $\mathbf{V}$  are hierarchically ordered by how much correlation they capture, respectively, in the columns and in the rows of  $\mathbf{X}$ , since the singular values are arranged in descending order by magnitude in  $\Sigma$  (Brunton and Kutz, 2019).

The SVD has many powerful applications in several areas, it can be used to (i) dimensionality reduction of high-dimensional data, (ii) compute the pseudo-inverse of nonsquare matrices, providing solutions to underdetermined and overdetermined linear system of equations, (iii) de-noise datasets, and (iv) to characterize the input and output geometry of a linear map between vector spaces. The items (i), (ii) and (iii) are discussed in Chapter 6 where SVD is used to assess the dimension of noisy experimental data from batch reaction experiments in order to determine the required dimension of the network that will make up the developing model. However, the item (iv) is illustrated in Section 2.2.3 in the context of the stoichiometric matrix.

## I.2 Orthogonal projection

The shortest distance among a vector  $\mathbf{v} \in \mathbb{R}^m$  and a subspace  $\mathbf{S} \in \mathbb{R}^m$  with dimension  $n$  (with  $m > n$ ) is obtained when computing the orthogonal projection of  $\mathbf{v}$  in  $\mathbf{S}$ ,  $\text{proj}_{\mathbf{S}} \mathbf{v}$ , in which this latter is the vector in  $\mathbf{S}$  such that  $\mathbf{v} - \text{proj}_{\mathbf{S}} \mathbf{v}$  is orthogonal to  $\mathbf{S}$  (Meyer, 2000). Therefore, the difference vector  $\mathbf{v} - \text{proj}_{\mathbf{S}} \mathbf{v}$  represents the shortest distance among the vector  $\mathbf{v} \in \mathbb{R}^m$  and the subspace  $\mathbf{S} \in \mathbb{R}^m$  with dimension  $n$  since it is orthogonal to every member of  $\mathbf{S}$ . Notice that  $\mathbf{v} - \text{proj}_{\mathbf{S}} \mathbf{v}$  belongs to the orthogonal complement of  $\mathbf{S}$ , *i.e.*,  $\mathbf{v} - \text{proj}_{\mathbf{S}} \mathbf{v} \in \mathbf{S}^\perp$ , where  $\mathbf{S}^\perp$  is also a subspace of  $\mathbb{R}^m$ , complementary to  $\mathbf{S}$ , with dimension  $m - n$ . In fact, the vector  $\mathbf{v}$  is being written as the sum of the two vector components which lie in both complementary subspaces of  $\mathbb{R}^m$ , *i.e.*,

$$\mathbf{v} = \text{proj}_{\mathbf{S}} \mathbf{v} + \text{proj}_{\mathbf{S}^\perp} \mathbf{v} \quad (\text{I.10})$$

Considering that  $\mathbf{B} \in \mathbb{R}^m \times n$  has full rank matrix in which its  $n$  columns constitute a basis for  $\mathbf{S}$ , it is clear that (i) the vector  $\text{proj}_{\mathbf{S}} \mathbf{v} \in \text{col}(\mathbf{B})$ , *i.e.*, it can be written as a linear combination of the  $n$  column vectors of  $\mathbf{B}$ , and (ii) the vector  $\text{proj}_{\mathbf{S}^\perp} \mathbf{v} \in \text{leftNull}(\mathbf{B})$ , *i.e.*, it belongs to the orthogonal complement of  $\text{col}(\mathbf{B})$ , whose  $m - n$  basis vectors,  $\mathbf{w}_i \in \mathbb{R}^m, i = 1, \dots, m - n$ , satisfy the homogeneous system of equations  $\mathbf{B}^T \cdot \mathbf{w} = \mathbf{0}$ , defining a basis for the left null space of  $\mathbf{B}$  in which  $\text{proj}_{\mathbf{S}^\perp} \mathbf{v}$  is written as a linear combination. Hence,  $\mathbf{B}^T \cdot \text{proj}_{\mathbf{S}^\perp} \mathbf{v} = \mathbf{0}$ . A detailed discussion about the four subspaces that a matrix can present is addressed in Section 2.2.2.

The  $\text{proj}_{\mathbf{S}}\mathbf{v}$  is computed through the sum of individual projections of  $\mathbf{v}$  in each column vector that form a basis that spans  $\mathbf{S}$ , as it is shown in (I.11)

$$\text{proj}_{\mathbf{S}}\mathbf{v} = \frac{\mathbf{v} \cdot \mathbf{b}_{*,1}}{\|\mathbf{b}_{*,1}\|^2} \mathbf{b}_{*,1} + \frac{\mathbf{v} \cdot \mathbf{b}_{*,2}}{\|\mathbf{b}_{*,2}\|^2} \mathbf{b}_{*,2} + \cdots + \frac{\mathbf{v} \cdot \mathbf{b}_{*,n}}{\|\mathbf{b}_{*,n}\|^2} \mathbf{b}_{*,n} \quad (\text{I.11})$$

where  $\mathbf{b}_{*,j}, j = 1, \dots, n$  are column vectors of the matrix  $\mathbf{B} \in \mathbb{R}^{m \times n}$  that form a basis for  $\mathbf{S}$  with dimension  $n$ .

Therefore, simplifying the previous equation, one can simply mention that  $\text{proj}_{\mathbf{S}}\mathbf{v}$  is written (uniquely) as a linear combination of the columns of  $\mathbf{B}$  (full rank matrix), *i.e.*,

$$\text{proj}_{\mathbf{S}}\mathbf{v} = \mathbf{B} \cdot \mathbf{x} \quad (\text{I.12})$$

with  $\mathbf{x} \in \mathbb{R}^n$ , where every element of this vector  $\mathbf{x}$  is  $\frac{\mathbf{v} \cdot \mathbf{b}_{*,j}}{\|\mathbf{b}_{*,j}\|^2}$  of the corresponding  $j = 1, \dots, n$ .

Considering the vector  $\mathbf{v}$  decomposition in (I.10), it is possible to write that

$$\mathbf{B}^T \cdot (\mathbf{v} - \text{proj}_{\mathbf{S}}\mathbf{v}) = \mathbf{0} \quad (\text{I.13})$$

since  $\text{proj}_{\mathbf{S}^\perp}\mathbf{v}$  lies in the left null space of  $\mathbf{B}$ .

Substituting variables from (I.12) in (I.13), it is obtained

$$\mathbf{B}^T \cdot \mathbf{v} - \mathbf{B}^T \cdot \mathbf{B} \cdot \mathbf{x} = \mathbf{0} \quad (\text{I.14})$$

Since  $\mathbf{B}$  has full (column) rank the matrix product  $\mathbf{B}^T \cdot \mathbf{B}$  is invertible, and, therefore, after some mathematical manipulation of the previous equation, the vector of coordinates  $\mathbf{x}$  is calculated through

$$\mathbf{x} = \left(\mathbf{B}^T \cdot \mathbf{B}\right)^{-1} \cdot \mathbf{B}^T \cdot \mathbf{v} \quad \Leftrightarrow \quad \mathbf{x} = \mathbf{B}^+ \cdot \mathbf{v} \quad (\text{I.15})$$

Therefore, the  $\mathbf{x}$  that satisfies (I.12) is obtained using (I.15). This vector corresponds to the optimal solution in the least squares sense. It is the coordinates of  $\text{proj}_{\mathbf{S}}\mathbf{v}$  in the basis  $\mathbf{B}$  that gives the minimum error of projection, satisfying (I.13). Moreover, we see that the pseudo-inverse of  $\mathbf{B}$  is given by

$$\mathbf{B}^+ = \left(\mathbf{B}^T \cdot \mathbf{B}\right)^{-1} \cdot \mathbf{B}^T \quad (\text{I.16})$$

Hence, the projection of  $\mathbf{v}$  into  $\mathbf{S}$  is given by

$$\text{proj}_{\mathbf{S}}\mathbf{v} = \mathbf{B} \cdot \left(\mathbf{B}^T \cdot \mathbf{B}\right)^{-1} \cdot \mathbf{B}^T \cdot \mathbf{v} \quad \Leftrightarrow \quad \text{proj}_{\mathbf{S}}\mathbf{v} = \mathbf{B} \cdot \mathbf{B}^+ \cdot \mathbf{v} \quad (\text{I.17})$$

If we consider the economy SVD( $\mathbf{B}$ ) to compute its pseudo-inverse, after some manipu-

lation of (I.17) we obtain

$$\text{proj}_{\mathbf{S}} \mathbf{v} = \hat{\mathbf{U}} \cdot \hat{\mathbf{U}}^{\text{T}} \cdot \mathbf{v} \quad (\text{I.18})$$

where  $\hat{\mathbf{U}}$  is the orthonormal basis that for  $\text{col}(\mathbf{B})$  without its complementary left null space component (economy format).

However, when considering the same matrix  $\mathbf{B}$ , but at this time having full row rank, as a basis that span the row space of  $\mathbf{S}$ , similarly, the same analysis can be done but now for the complementary row and null spaces of  $\mathbf{S}$ . For example considering  $\mathbf{M}[n \times m] = \mathbf{B}^{\text{T}}$  as a basis whose rows span the row space of  $\mathbf{S}$  of dimension  $n$ , the projection of  $\mathbf{z} \in \mathbb{R}^m$  in  $\mathbf{M}$  is given by

$$\text{proj}_{\mathbf{M}} \mathbf{z} = \mathbf{B}^{\text{T}} \cdot (\mathbf{B} \cdot \mathbf{B}^{\text{T}})^{-1} \cdot \mathbf{B} \cdot \mathbf{z} \quad \Leftrightarrow \quad \text{proj}_{\mathbf{M}} \mathbf{z} = \mathbf{B}^{+} \cdot \mathbf{B} \cdot \mathbf{z} \quad (\text{I.19})$$

If we consider the economy  $\text{SVD}(\mathbf{B}^{\text{T}})$  to compute its pseudo-inverse, after some manipulation of (I.19) we obtain

$$\text{proj}_{\mathbf{M}} \mathbf{z} = \hat{\mathbf{V}} \cdot \hat{\mathbf{V}}^{\text{T}} \cdot \mathbf{z}. \quad (\text{I.20})$$

where  $\hat{\mathbf{V}}$  is the orthonormal basis for  $\text{row}(\mathbf{B})$  without its complementary null space component (economy format).

### I.3 Singular values and eigenvalues — what they mean and how they are related

The Singular Value Decomposition (SVD) is a method of decomposing vectors onto orthogonal axes. Any vector  $\mathbf{d} \in \mathbb{R}^n$  can be expressed in terms of (i) projection directions unit vectors ( $\mathbf{v}_1, \mathbf{v}_2, \dots, \mathbf{v}_n$ ) and (ii) the lengths of projections onto them ( $l_{d1}, l_{d2}, \dots, l_{dn}$ ), such that

$$\mathbf{d} = l_{d1} \mathbf{v}_1 + l_{d2} \mathbf{v}_2 + \dots + l_{dn} \mathbf{v}_n \quad (\text{I.21})$$

Therefore, in this nomenclature,  $\mathbf{v}$  represents the directions onto which the original vector  $\mathbf{d}$  is decomposed, and  $l$  the lengths of projection which informs how much of the vector is contained in each direction of projection.

If instead of only a single vector of  $\mathbf{d}$  we have a matrix  $\mathbf{D} \in \mathbb{R}^m \times n$  in which  $m$  different transposed  $\mathbf{d}$  vectors are displayed at the rows of  $\mathbf{D}$ , this matrix can also be decomposed as

$$\mathbf{D} = \mathbf{L} \cdot \mathbf{V}^{\text{T}} \quad (\text{I.22})$$

where  $\mathbf{L} \in \mathbb{R}^m \times n$  is the matrix containing lengths of projection, and  $\mathbf{V} \in \mathbb{R}^n \times n$  is the matrix containing the decomposition axes. Notice that  $\mathbf{V}$  contains orthonormal columns, *i.e.*, it is composed by unitary and orthogonal vectors, such that  $\mathbf{D} = \mathbf{L} \cdot \mathbf{V}^{-1}$  and  $\mathbf{L} = \mathbf{D} \cdot \mathbf{V}$ .

Hence, every column of  $\mathbf{L}$  contains the lengths of projections of each data point in the

respective coordinate axis  $\mathbf{v}$ , *i. e.*, the first column  $\mathbf{l}_1$  has  $m$  lengths of projection respected to each data point projection onto the axis  $\mathbf{v}_1$ , and so on. If we consider the normalization of these vectors  $\mathbf{l}_1, \mathbf{l}_2, \dots, \mathbf{l}_n$  by dividing each column vector by its respective magnitude  $\sigma$ , such that  $\sigma_1 = \sqrt{l_{d=1,1}^2 + l_{d=2,1}^2 + \dots + l_{d=m,1}^2}$ ,  $\sigma_2 = \sqrt{l_{d=1,2}^2 + l_{d=2,2}^2 + \dots + l_{d=m,2}^2}$ , and so on. We can decompose  $\mathbf{L}$  as the product of two matrices:

$$\mathbf{L} = \begin{bmatrix} l_{d=1,1}/\sigma_1 & l_{d=1,2}/\sigma_2 & \dots & l_{d=1,n}/\sigma_n \\ l_{d=2,1}/\sigma_1 & l_{d=2,2}/\sigma_2 & \dots & l_{d=2,n}/\sigma_n \\ \vdots & \vdots & \ddots & \vdots \\ l_{d=m,1}/\sigma_1 & l_{d=m,2}/\sigma_2 & \dots & l_{d=m,n}/\sigma_n \end{bmatrix} \cdot \begin{bmatrix} \sigma_1 & 0 & \dots & 0 \\ 0 & \sigma_2 & \vdots & \vdots \\ \vdots & \dots & \ddots & \vdots \\ 0 & \dots & \dots & \sigma_n \end{bmatrix} = \mathbf{U} \cdot \mathbf{\Sigma} \quad (\text{I.23})$$

The conventional SVD formula

$$\mathbf{D} = \mathbf{U} \cdot \mathbf{\Sigma} \cdot \mathbf{V}^T \quad (\text{I.24})$$

is equivalent to (I.22), since  $\mathbf{U} \cdot \mathbf{\Sigma} = \mathbf{L}$ . Notice that  $\mathbf{U}$  contains the normalized lengths of projections of each data point in the system of coordinates  $\mathbf{V}$ , and  $\mathbf{\Sigma}$  contains in its diagonal the square root of the sum of squared projection lengths, of all points, onto the respective basis vectors that form  $\mathbf{V}$ . Therefore, the  $\sigma$  values represent how close all the points are to the respective axis of the basis  $\mathbf{V}$ . Hence, the closer the points to a specific axis of projection, the larger the value of the corresponding  $\sigma$ .

Finding a low-dimensional representation of the data that retains as much information as possible, *i. e.*, to project the dataset on the line (or plane, or space) of largest variance, is the main objective of dimensionality reduction. For this purpose, another representation of the data (another set of features that are linear combinations of the original ones) is identified such that the features in this representation have the highest possible variance and lowest possible covariance (Abdullatif, 2019). The covariance can be interpreted as a measure of how accurately one variable can be predicted from another. Notice that features with high variance are more informative and more important, and, in contrast, highly correlated features brings (almost) redundant information since they can be deduced from one to another with little loss of information. The inner (dot) product is a very natural measure for covariance since the more the data deviates from the vector where data is being projected, the larger the angle between the two vectors, and hence the smaller the dot product (Abdullatif, 2019).

The variance along a vector  $\mathbf{x} \in \mathbb{R}^n$  is the average squared deviations of its coordinates from their mean. However, when data is mean-centered, the variance formula is simplified to the average of the inner product  $\mathbf{x}$  to itself, since the mean is zero, such that

$$\sigma^2 = \frac{\mathbf{x}^T \cdot \mathbf{x}}{n} \quad (\text{I.25})$$

where  $n$  is the dimension of  $\mathbf{x}$ . On the other hand, the covariance is a metric established for a pair of vectors, which measures how much they are linearly (in)dependent, *i. e.*, how

much they are correlated. For example consider the vector  $\mathbf{y} \in \mathbb{R}^n$ , the covariance of  $\mathbf{x}$  and  $\mathbf{y}$  is simply  $\text{cov}(\mathbf{x}, \mathbf{y}) = \frac{\mathbf{x}^T \cdot \mathbf{y}}{n}$ . This can be extended to the matrix format, such that

$$\text{cov}(\mathbf{X}) = \frac{\mathbf{X}^T \cdot \mathbf{X}}{n} = \begin{bmatrix} \sigma_x^2 & \text{cov}(\mathbf{x}, \mathbf{y}) \\ \text{cov}(\mathbf{y}, \mathbf{x}) & \sigma_y^2 \end{bmatrix}, \quad (\text{I.26})$$

with  $\mathbf{X} \in \mathbb{R}^{m \times 2}$  containing in its columns the vectors  $\mathbf{x}$  and  $\mathbf{y}$  and  $\text{cov}(\mathbf{X})$  is its covariance matrix of square dimension equal to the number of  $\mathbf{X}$  columns, in this case 2. Notice that  $\text{cov}(\mathbf{X})$  has in its diagonal the variances of each column vector of  $\mathbf{X}$ , and it is symmetrical since  $\text{cov}(\mathbf{x}, \mathbf{y}) = \text{cov}(\mathbf{y}, \mathbf{x})$ .

Regarding a single unit vector  $\mathbf{v} \in \mathbb{R}^n$ , the same relationship in (I.22) can be written as

$$\mathbf{l} = \mathbf{D} \cdot \mathbf{v} \quad (\text{I.27})$$

where  $\mathbf{l} \in \mathbb{R}^m$  is the projection of data  $\mathbf{D}$  on the axis  $\mathbf{v} \in \mathbb{R}^n$ . Therefore, it is easy to find the variance along any axis by projecting the data points on the unit vector representing the line, and then computing the variance of this projection, such that

$$\sigma_v^2 = \frac{\mathbf{l}^T \cdot \mathbf{l}}{n} = \frac{(\mathbf{D} \cdot \mathbf{v})^T \cdot \mathbf{D} \cdot \mathbf{v}}{n} = \mathbf{v}^T \cdot \frac{(\mathbf{D}^T \cdot \mathbf{D})}{n} \cdot \mathbf{v} = \mathbf{v}^T \cdot \text{cov}(\mathbf{D}) \cdot \mathbf{v} \quad (\text{I.28})$$

Therefore, once having  $\text{cov}(\mathbf{D})$ , the problem of data dimension reduction can pass through finding the vector  $\mathbf{v}$  such that  $\sigma_v^2$  is maximum. Moreover, the vector  $\mathbf{v}$  is an eigenvector of the matrix  $\text{cov}(\mathbf{D})$ , since

$$\text{cov}(\mathbf{D}) \cdot \mathbf{v} = \lambda \mathbf{v} \quad (\text{I.29})$$

where  $\lambda$  (scalar) is the eigenvalue corresponding to  $\mathbf{v}$ . Consequently, it is possible to verify from (I.28) and (I.29) that

$$\sigma_v^2 = \mathbf{v}^T \cdot \text{cov}(\mathbf{D}) \cdot \mathbf{v} = \mathbf{v}^T \cdot (\lambda \mathbf{v}) = \lambda \mathbf{v}^T \cdot \mathbf{v} = \lambda \quad (\text{I.30})$$

Therefore, the  $\sigma^2$ , that has been defined in so many ways during this section, *i.e.*, the square of the singular value of the SVD of  $\mathbf{D}$ , the variance of  $\mathbf{l}$ , the covariance of  $\mathbf{l}$  and itself, and the approximation of the squared  $\ell_2$ -norm of  $\mathbf{l}$ , is also the eigenvalue of the covariance matrix of  $\mathbf{D}$ . Consequently, the eigenvector  $\mathbf{v}$  of the covariance matrix that has the largest absolute eigenvalue (largest  $\sigma^2$ ) is the direction of greatest variance<sup>2</sup>. Hence, another valid interpretation related to the SVD follows the correlation (covariance) criterion, since the singular values are arranged in descending order by magnitude in  $\Sigma$ , the columns of  $\mathbf{U}$  and  $\mathbf{V}$  are hierarchically ordered by how much correlation they capture in the columns and in the rows of  $\mathbf{D}$ , respectively (Brunton and Kutz, 2019).

---

<sup>2</sup>In the end of Appendix I.1, we present the same analysis but considering the  $\text{cov}(\mathbf{D}^T)$ , and its associated eigenvalues and eigenvectors.

## Bibliography

- Abdullatif, H. (2019). You don't know svd (singular value decomposition). <https://medium.com/@abdullatif.h>. Accessed: 2020-10-01.
- Brunton, S. and Kutz, J. (2019). *Data-Driven Science and Engineering: Machine Learning, Dynamical Systems, and Control*. Cambridge University Press.
- Kambhampati, S. (2010 (accessed April 25, 2020)). *On the uniqueness of Singular Value Decomposition*. <http://rakaposhi.eas.asu.edu/s10-cse494-mailarchive/msg00030.html>.
- Meyer, C. (2000). *Matrix Analysis and Applied Linear Algebra*. Society for Industrial and Applied Mathematics.





## Appendix II

# Generation of reaction networks without using MILP

### II.1 Recursive algorithm to generate the tree of states

Inspired on STN concept, a recursive formulation was developed to generate all feasible reaction networks composed by linearly independent sets of chemical reactions from a network superstructure. The reaction networks are gradually built in every recursion in which a state of the tree is obtained, attending to constraints related to consistency among species production and linear independence of the set of chemical reactions. With this formulation, a single reaction network can be obtained in few recursions. However, the goal is to obtain all feasible reaction networks, and therefore, to build the *tree of states*.

The tree of states is recursively built spanning the linearly independent space of chemical reactions. Similarly with the previous FASP, a state is defined by two lists, one composed by species and other by reactions. In Figure II.1 a flowchart of the proposed algorithm is shown, in which two starting points are presented: (i) the initial state composed by the initial reactant(s) and an empty set of reactions, and (ii) a list of chemical reactions that compose the network superstructure.

According to the flowchart in Figure II.1, when evaluating, from the list of chemical reactions of the superstructure, which chemical reactions (i) can be consistently appended to the reference state, *i.e.*, reactions in which the reactant(s) is/are present in the reference state, ensuring precedence among species production (thus avoiding the generation of inconsistent networks, see example in Figure 8.9), and, (ii) individually appended to the reference state maintain the set linearly independent, a list of potential reactions to be appended to the reference state is obtained. When this list is not empty, *i.e.*, the dimension of the list is greater than zero, one reaction from this list is appended to the reference state configuring a new state formed by the (i) list of species that now contains the product species of the appended reaction plus the species that were earlier presented, and, (ii)

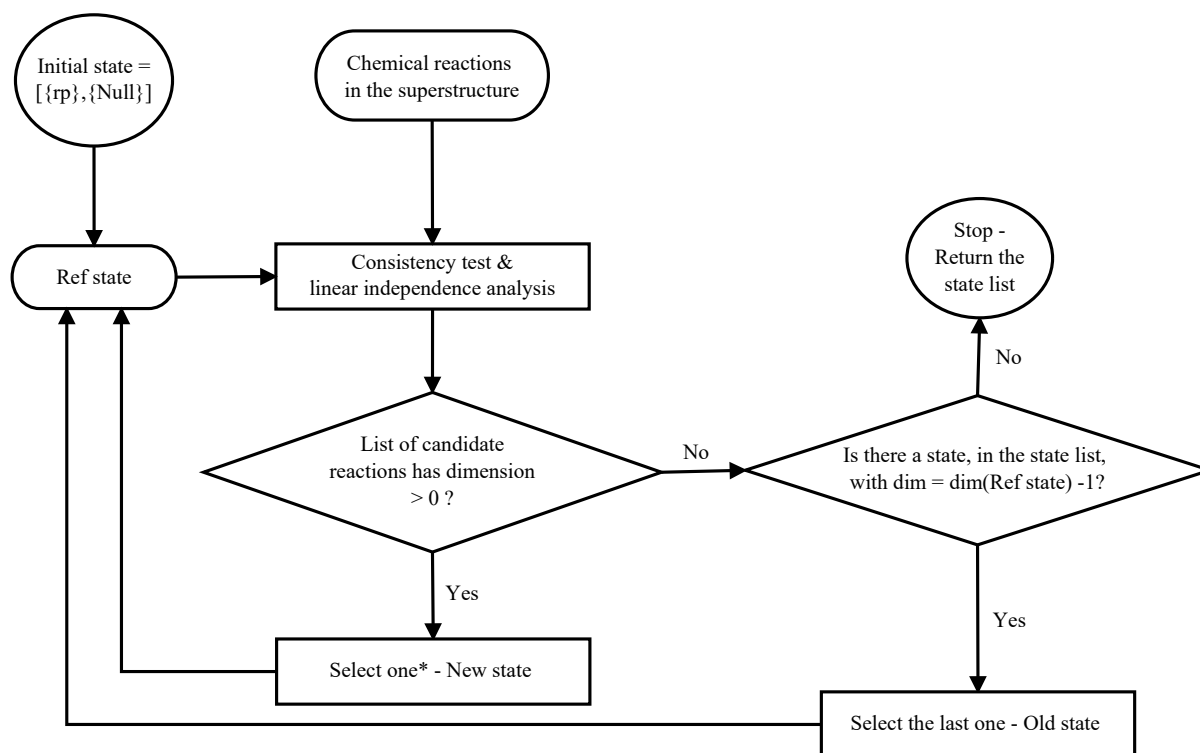


**Figure II.1** Recursive algorithm flowchart for the generation of consistent and linearly independent reaction networks. (\*) The criterion to select one chemical reaction to the new reference state is set according to the adopted search strategy.

list of reactions that now contain the reaction selected. On the other hand, if there is no chemical reaction from the initial list that satisfies the previously described criteria, the algorithm searches for the nearest previous state, that contains a lower dimension of the chemical reactions set, and it starts again the consistency test and linear independence analysis for this reference state. Finally, when there is no more states in which chemical reactions can be added satisfying the imposed criteria, the tree of states is completed.

In short, in each recursion one reaction is added to the reference state maintaining the sub-network consistent and linearly independent. If the  $nr_{li, \max}$  is reached, the algorithm uses the last evaluated reference state with a lower network dimension to continue adding independent and consistent chemical reactions. Therefore, all LI reaction networks can be obtained using this recursive formulation. The non-repetition of states is ensured by forbidding the selection of reactions that conduct to previous states already built/visited. Every built state is saved in a “dejavu” list.

The state is called complete when it consists of a reaction network with  $DI = 0$ . In Figure 8.12, there are 16 complete states at the bottom level of the tree. The adopted strategy to span all states can involve the search in depth or in width over the tree of states, and it can also follow a greedy criterion. For example, from the list of candidate reactions, the one that produces more species is selected, like an heuristic guide procedure.

Thus, the complete states would be found faster. However, as we are concerned in finding all complete states, this kind of greedy procedure does not present advantages. In the previous described approach the search strategy is done in depth, and no preference related to the list of candidate chemical reactions is imposed.

### II.1.1 Pseudo-code

The pseudo-code is presented in the following algorithms (1) and (2).

---

#### Algorithm 1 List of consistent and LI chemical reactions

---

**Require:** estref, stocMat, listrx, listest

**Ensure:**  $\text{reac} \in \text{estref} \wedge \text{rank}(\text{est}) > \text{rank}(\text{estref})$

```

for rx= 1, rx ≤ Length[stocMat], rx++, do
  line=stocMat[[rx]];
  est= AppendTo[estref,line];
  if reac[line] ∈ reac[estref] ∧ rank(est)>rank(estref) ∧ est ∉ listest then
    AppendTo[listrx,line]
  end if
end for
return listrx

```

---



---

#### Algorithm 2 Tree of states

---

**Require:** estref, stocMat, listest

rxad= Call[Algorithm 1,{estref, stocMat, listest}];

**if** rxad =  $\emptyset$  **then**

**if** listest[[-1]] =  $\emptyset$  **then**

**return** listest

**else**

    est=listest[[-1]];

**end if**

  Call[Algorithm 2,{est, stocMat, listest}];

**else**

  rxad = First[rxad];

  est= AppendTo[estref,rxad];

  listest= AppendTo[listest,est];

  Call[Algorithm 2,{est, stocMat, listest}];

**end if**

---

### II.1.2 Example

Considering the tree of states obtained for the nonlinear AS case study, it presented 10269 states in which 8739 are complete states with  $\text{nrX}_{\text{li,max}} = 5$  containing the set of LI redundant and non-redundant networks, and, 241 are complete states with  $\text{nrX}_{\text{min}} = 4$ . The results were obtained using **Mathematica** software.

The linear AS case study presented 902 states, in which 540 are complete ones, located at the bottom of the tree. The tree of states is presented in Figure II.2.

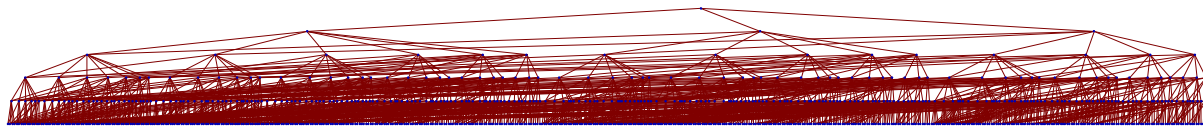


**Figure II.2** Representation of the tree of states containing the linear reaction networks for case study AS at the bottom level of the tree.

## II.2 Another application example

The catalytic reaction of toluene with benzyl alcohol over sulfated zirconia is considered in this section (Ardizzone et al., 2006).

### II.2.1 Toluene case study

The catalytic reaction of toluene with benzyl alcohol over sulfated zirconia was considered (Ardizzone et al., 2006). This case study involves 6 chemical species: toluene (TOL), benzyl alcohol (BzOH), dibenzyl ether (BzOBz), dibenzyl toluene (D), benzyl toluene (M) and water (H<sub>2</sub>O). The water component is not an abundant chemical species since the reactions occur in cyclohexane solvent. Besides nonlinear chemical reactions, two initial reactants are present in the system with high level of purity, they are TOL and BzOH (Figure II.3).

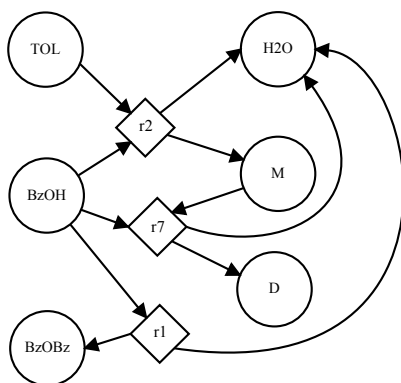


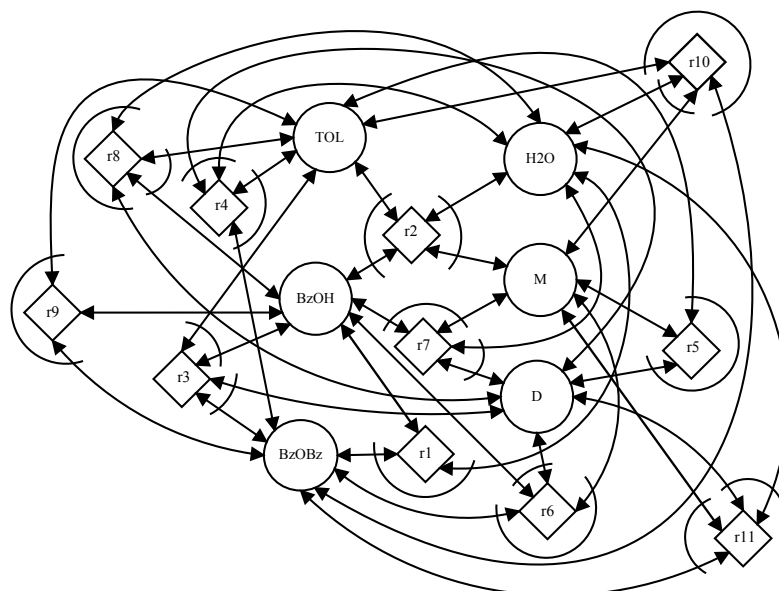
**Figure II.3** Reaction network proposed by Ardizzone et al. (2006).

The chemical reactions are listed in Table II.1. These reactions were obtained considering the formulation to generate chemical reactions presented in the previous work (REF - parte1). The reaction network superstructure is shown in Figure II.4.

TOL case study characteristics:

**Table II.1** Stoichiometric coefficients of the nonlinear chemical reactions — Toluene case study.

Index	TOL	BzOH	BzOBz	D	M	H <sub>2</sub> O	Reaction
1	0	-2	1	0	0	1	$2 \text{ BzOH} \rightarrow \text{BzOBz} + \text{H}_2\text{O}$
2	-1	-1	0	0	1	1	$\text{TOL} + \text{BzOH} \rightarrow \text{M} + \text{H}_2\text{O}$
3	-1	1	-1	0	1	0	$\text{TOL} + \text{BzOBz} \rightarrow \text{BzOH} + \text{M}$
4	-1	0	-1	1	0	1	$\text{TOL} + \text{BzOBz} \rightarrow \text{D} + \text{H}_2\text{O}$
5	-1	0	0	-1	2	0	$\text{TOL} + \text{D} \rightarrow 2 \text{ M}$
6	0	-1	1	-1	1	0	$\text{BzOH} + \text{D} \rightarrow \text{BzOBz} + \text{M}$
7	0	-1	0	1	-1	1	$\text{BzOH} + \text{M} \rightarrow \text{D} + \text{H}_2\text{O}$
8	-1	-2	0	1	0	2	$\text{TOL} + 2 \text{ BzOH} \rightarrow \text{D} + 2 \text{ H}_2\text{O}$
9	-1	2	-2	1	0	0	$\text{TOL} + 2 \text{ BzOBz} \rightarrow 2 \text{ BzOH} + \text{D}$
10	-2	0	-1	0	2	1	$2 \text{ TOL} + \text{BzOBz} \rightarrow 2 \text{ M} + \text{H}_2\text{O}$
11	0	0	-1	2	-2	1	$\text{BzOBz} + 2 \text{ M} \rightarrow 2 \text{ D} + \text{H}_2\text{O}$

**Figure II.4** Superstructure for the generation of nonlinear reaction networks — Toluene case study. The diamond nodes represent the reaction events and their linking arcs map the pair of species in each side of the reaction.

- Rank of  $N_{\text{sup}}$  is 3, networks with  $\text{nr}x_{\text{li,max}} = 3$  have  $\text{RI} = 0$ ,
- $\text{nr}x_{\text{sup}} = 22$ ;  $\text{nr}x_{\text{max}} = 11$  and  $\text{nr}x_{\text{min}} = 2$ .

The Figure II.5 presents the first 3 nonlinear reaction networks obtained for this case study.

Considering the algorithms (1 and 2), using the **Mathematica** software, the number of states obtained was 123 in approximately 4s. The tree of states is presented in Figure II.6. The number of complete networks with LI redundant and non-redundant chemical reactions obtained was 104, from this set 2 are composed by  $\text{nr}x_{\text{min}} = 2$  and 121 by  $\text{nr}x_{\text{li,max}} = 3$ . Note that from these 121 LI networks with  $\text{nr}x_{\text{li,max}} = 3$ , 67 are LI

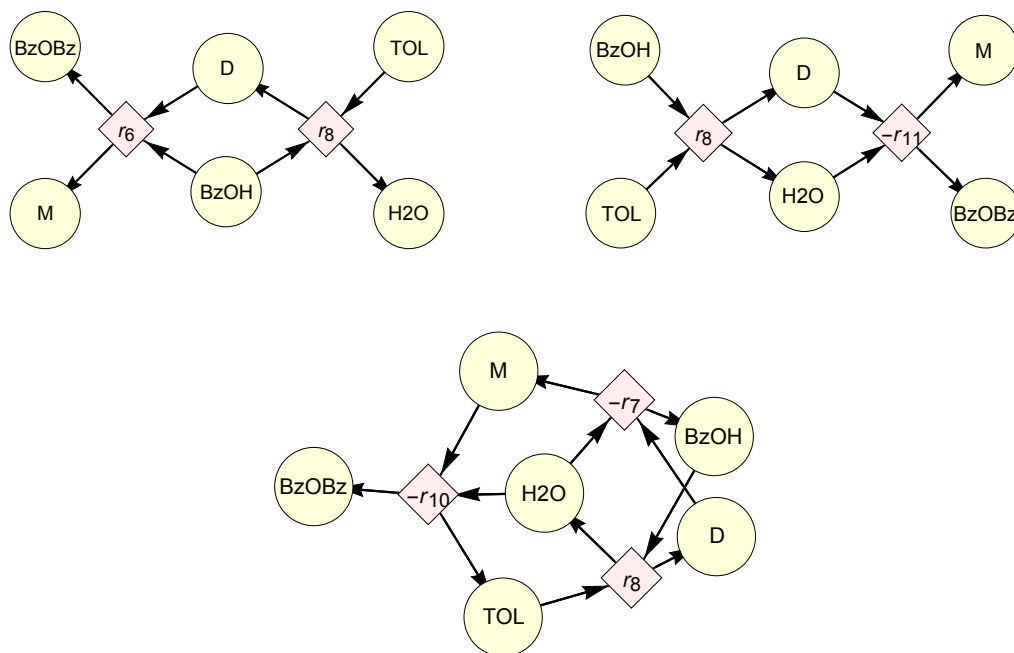


**Figure II.5** First 3 nonlinear reaction networks obtained — Toluene case study.

non-redundant and 54 are LI redundant.

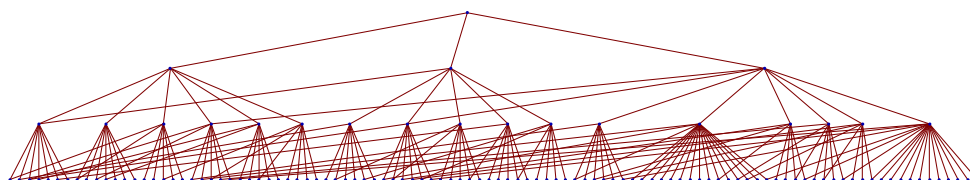


**Figure II.6** Tree of states - Toluene case study.

## Bibliography

Ardizzone, S. A., Beltrame, P., and Zuretti, G. (2006). Kinetics of the reaction of toluene with benzyl alcohol over sulfated zirconia. *Applied Catalysis A: General*, 314(2):240–247.